Subramanian Senthilkannan Muthu
Ali Khadir *Editors*

Membrane Based Methods for Dye Containing Wastewater

Recent Advances

Springer

Sustainable Textiles: Production, Processing, Manufacturing & Chemistry

Series Editor

Subramanian Senthilkannan Muthu, Head of Sustainability, SgT and API, Kowloon, Hong Kong

This series aims to address all issues related to sustainability through the lifecycles of textiles from manufacturing to consumer behavior through sustainable disposal. Potential topics include but are not limited to: Environmental Footprints of Textile manufacturing; Environmental Life Cycle Assessment of Textile production; Environmental impact models of Textiles and Clothing Supply Chain; Clothing Supply Chain Sustainability; Carbon, energy and water footprints of textile products and in the clothing manufacturing chain; Functional life and reusability of textile products; Biodegradable textile products and the assessment of biodegradability; Waste management in textile industry; Pollution abatement in textile sector; Recycled textile materials and the evaluation of recycling; Consumer behavior in Sustainable Textiles; Eco-design in Clothing & Apparels; Sustainable polymers & fibers in Textiles; Sustainable waste water treatments in Textile manufacturing; Sustainable Textile Chemicals in Textile manufacturing. Innovative fibres, processes, methods and technologies for Sustainable textiles; Development of sustainable, eco-friendly textile products and processes; Environmental standards for textile industry; Modelling of environmental impacts of textile products; Green Chemistry, clean technology and their applications to textiles and clothing sector; Eco-production of Apparels, Energy and Water Efficient textiles. Sustainable Smart textiles & polymers, Sustainable Nano fibers and Textiles; Sustainable Innovations in Textile Chemistry & Manufacturing; Circular Economy, Advances in Sustainable Textiles Manufacturing; Sustainable Luxury & Craftsmanship; Zero Waste Textiles.

More information about this series at http://www.springer.com/series/16490

Subramanian Senthilkannan Muthu · Ali Khadir
Editors

Membrane Based Methods for Dye Containing Wastewater

Recent Advances

Editors
Subramanian Senthilkannan Muthu
Head of Sustainability
SgT and API
Kowloon, Hong Kong

Ali Khadir
Islamic Azad University
Tehran, Iran

Contents

About the Editors

Dr. Subramanian Senthilkannan Muthu currently works for SgT Group as the Head of Sustainability, and is based out of Hong Kong. He earned his Ph.D. from The Hong Kong Polytechnic University, and is a renowned expert in the areas of Environmental Sustainability in Textiles & Clothing Supply Chain, Product Life Cycle Assessment (LCA) and Product Carbon Footprint Assessment (PCF) in various industrial sectors. He has five years of industrial experience in textile manufacturing, research and development, and textile testing, and over a decade's of experience in Life Cycle Assessment (LCA), carbon and ecological footprints assessment of various consumer products. He has published more than 100 research publications, written numerous book chapters, and authored/edited over 100 books in the areas of Carbon Footprint, Recycling, Environmental Assessment, and Environmental Sustainability.

Ali Khadir is an environmental engineer and a member of the Young Researcher and Elite Club, Islamic Azad University of Shahre Rey Branch, Tehran, Iran. He has published/prepared several articles and book chapters in reputed international publishers, including Elsevier, Springer, Taylor & Francis, and Wiley. His articles have been published in journals with IF greater than 4, including Journal of Environmental Chemical Engineering and International Journal of Biological Macromolecules. Also, he has been the reviewer of journals and international conferences. His research interests center on emerging pollutants, dyes, and pharmaceuticals in aquatic media, advanced water and wastewater remediation techniques and technology. At present, he is editing other books in the field of nanocomposites, advanced materials, and the remediation of dye—containing wastewaters.

An Introduction to Membrane-Based Systems for Dye Removal

Sana Saif, Tania Saif, Muhammad Arshad Raza, Gulzar Muhammad, Muhammad Mudassir Iqbal, Nabeel Ur Rehman, and Muhammad Ajaz Hussain

Abstract Despite significant contributions to the country's economy and human necessities, the textile industry consumes large quantities of dyes with the discharge of excessive deleterious dye effluents. The wastewater contaminated with dyes if not treated afore discharge poses serious intimidations to the environment and human health. The presence of dyes in untreated wastewater has grown into an emergent apprehension for scientists. Therefore, there is a calamitous prerequisite to discharge wastewater after treatment using different environmentally benign physical, chemical, and biological technologies. The chapter emphasizes the treatment of wastewater dye effluents with membrane-based technologies such as microfiltration, ultrafiltration, nanofiltration, reverse, and forward osmosis. Recent trends in the aforesaid techniques with the benefits and drawbacks have also been reconnoitered in detail. The critical analyses regarding the comparative efficiency of the membrane-based approaches for dye removal from wastewater have been explored systematically. The chapter will widen the industrial applications of membrane-based technology with cost-effectiveness, and performance in the future.

Keywords Wastewater treatment · Dye removal · Membrane-based systems · Membrane technology · Microfiltration · Ultrafiltration · Nanofiltration · Reverse osmosis · Forward osmosis

S. Saif · T. Saif · M. A. Raza (✉) · G. Muhammad (✉) · N. Ur Rehman
Department of Chemistry, GC University Lahore, Lahore, Pakistan
e-mail: arshad.raza@gcu.edu.pk

G. Muhammad
e-mail: mgulzar@gcu.edu.pk

M. M. Iqbal
School of Biochemistry and Biotechnology, University of the Punjab, Lahore 54000, Pakistan

M. A. Hussain
Institute of Chemistry, University of Sargodha, Sargodha, Pakistan

1   Introduction

Water is a crucial element in nearly all activities of humankind. However, the continuously increasing human population is producing tons and tons of wastewater from the industrial sector. The ever-increasing need for water has expedited intense competition and unfair distribution of water among all the sectors. Consequently, developing countries are suffering from a lack of potable water, and agricultural activities are positively affected due to the unavailability of enough water for irrigation and livestock production [1]. Among the industries, the textile industry contributes significantly to economic growth by providing exports, employment opportunities, and industrial production with excessive consumption of water for processing, which led to the production of wastewater. Industrial wastewater consists of a tremendous amount of heavy metals, soluble salts, organic dyes, and suspended materials and is purified using primary, secondary, and tertiary treatments. However, recent studies disclosed that the water treated through the methods described above could not get the effluent quality standards. So, there is a need to develop cost-effective strategies for dye effluent treatment [2, 3].

In this vein, membrane technology has emerged in the last two to three decades due to its benefits in wastewater treatment. The significant reduction in energy requirement, equipment size, and cost-effectiveness are the key features of membrane technology. The membrane technology can be used as a bridging technique between the economic and sustainability gaps. Moreover, it is an easily accessible technique that has proved an environmentally friendly method for wastewater treatment [4]. The most commonly employed membrane processes are microfiltration (MF), ultrafiltration (UF), nanofiltration (NF), and reverse osmosis (RO) [5]. Depending upon the nature of wastewater, there is always space for advancement in energy, efficiency, and technical skill requirements. There are continuous modifications in membrane modules to reduce membrane fouling, a widespread problem in membrane operations. The implementation of membrane technology combined with other forms of technologies such as adsorption or coagulation is being explored in various wastewater treatments [6].

Dyes are highly complex organic compounds that are used for coloring substances. The dyes are expelled into freshwater sources from leather, rubber, textile, cosmetics, and paper. The dye-containing wastewater is highly contagious to the environment and humans. Some of the dyes caused eye irritation, cancer, and skin problems. Therefore, many researchers are continuously developing such separation methods that remove these dyes from industrial wastewater [7]. This chapter focuses on trending membrane technologies for dye removal. The chapter starts with an introduction to membrane filtration for dye removal. Then membrane technologies for dye removal from wastewater such as MF, UF, NF, FO, and RO have been discussed. Recent research work accomplished by researchers to estimate the capability of membranes

in water treatment has also been discussed. Later on, membrane-based bioelectro-chemical cells have been explained. The advantages and limitations of membrane-based systems are also described. Finally, the perspectives toward the development of membrane-based technologies have been addressed.

2 Membrane Technology for Wastewater Treatment

Traditional methods such as bleaching with chlorine, ozonation (ozonization), and the use of H_2O_2/UV cannot remove residual dyes, organic solids, and inorganic salts. Membrane technology is a developing separation technique finding various applications in processing and recycling wastewater. Membrane operations have shown great potential in the rationalization of purification systems. The innate characteristics of higher selectivity, operational simplicity, permeability for specific components, and reasonable stability requirements under a wide range of environmental compatibility and operating conditions have been confirmed in various applications [8]. The preliminary stages remove colloidal particles, suspended materials, and large impurities from wastewater. Secondary biological treatments oxidize organic materials considerably. However, the water still contains dyes and inorganic salts, as indicated by biochemical and chemical oxygen demand. The tertiary treatments usually cannot remove the unwanted substances from the wastewater. Hence, the quality of water remains low. Many techniques have been suggested to remove dissolved solids, dyes, and organic matter. Most of them are not much efficient and cost-effective. A realistic solution, namely, membrane technology was offered in this sense [9].

As the name suggests, membrane technology uses membrane as a barrier to separate dyes and solid materials from wastewater by applying a suitable pressure. The choice of an appropriate membrane technology highly depends on membrane pore size, the shape of the membrane, the composition of the membrane, and the dyes' nature. The pore size decides the removal of salts and other materials. Depending upon the pore size, the membrane technology is classified into four types; MF, UF, NF, and RO [10, 11]. The solids/particles of size up to 500 Å are removed using MF. In contrast, UF removes inorganic salts/organic solids of size up to 30 Å. Similarly, NF eliminates inorganic salts/organic solids of size 10 Å, and RO removes inorganic salts/organic solids of size 1.0 Å. Different membrane techniques operate under other pressure conditions and applied pressure increases due to the decrease in pore size substantially from MF to RO. All these four processes are generally termed as 'Cross-flow Filtration' [12]. Four different configurations of filtration devices are commonly used: tubular module, plate and frame module, hollow fiber module, and spiral wound module. The first two are not employed for water treatment, while the other two are used for both water and wastewater treatment [13].

2.1 Microfiltration

This technique is not usually practiced in wastewater treatment as it exhibits a close resemblance with conventional filtration methods. It is a low-pressure membrane process that separates suspended particles or colloidal matter. The membranes in MF usually have a pore size of 0.1–10 µm, and the filtration is positively affected within 2 bar pressure [14] that caused the restricted implementation of MF in purification processes. The method is mainly employed to remove colloidal dyes while unconsumed auxiliary chemicals, soluble contaminants, and dissolved organic pollutants are easily escaped through the membrane (Table 1). Hence, the technique is seldom used as an independent treatment for the decontamination of wastewater [15]. In hybrid systems, MF is used as a pre-treatment step to complement the connected processes that target soluble components and dyes but fail to remove suspended particulates. However, MF membranes are currently being used as wastewater treatment methods. Reference [16] used the phase inversion method to prepare polyethersulfone membranes and silver nanoparticles by chemical reduction of $AgNO_3$ in an aqueous solution that was impregnated into MF membranes. The membranes with different pore sizes confirmed the presence of silver in the transversal section. The membrane showed antimicrobial activity against *Pseudomonas fluorescens* using the bacterial count method. The membrane was secured to have great potential for water treatment [16]. Reference [17] prepared the graphene oxide quantum dots by the hydrolysis of citric acid. Subsequently, the dots were successfully immobilized into (3-aminopropyl) triethoxysilane functionalized alumina membranes through covalent bonding. The membranes showed improved water permeability with reduced membrane resistance and pure water flux depending upon pore size, surface roughness, and hydrophilicity [17].

2.2 Ultrafiltration Membrane

The membrane separation process is used to separate colloids and macromolecules from a solution; solutes left behind have few thousand Daltons molecular weights [26, 27]. The pore size of UF lies between 0.1 and 0.001 microns and needs low pressure than RO and NF (Fig. 1). Thus, it is more convenient and economical. However, a large pore size can cause low rejection [28]. UF membranes require less energy than water filters to remove suspended matters, macromolecules, and pathogenic microorganisms [29]. The significant use of UF membrane is in the textile industry for the treatment of dyeing effluents. Many studies have shown that a considerable amount of knitting oils and dyes is removed by UF with the reuse and recovery of more than 90% treated dye from wastewater (Table 2). The method has its application in recycling insoluble and high molecular weight dyes (e.g., disperse, indigo), water, and auxiliary chemicals (polyvinyl alcohol). Nonetheless, the limitation is that soluble

Table 1 Synopsis of various studies performed on the applicability of MF in wastewater treatment

Membrane process	Membrane structure	Application in water treatment	References
Tubular ceramic MF membrane	Mullite, mullite–zeolite, mullite–zeolite-activated carbon membrane	Oily wastewater treatment	[18]
Natural MF membrane	Natural cellulose MF membrane	Oil or water nanoemulsion separation	[19]
Modified MF membranes	MF membrane modification with cationic polymer polyethyleneimine	Virus reduction in drinking water	[20]
High flux MF membrane	MF membranes with silver nanoparticles	Disinfection of water	[16]
Flat sheath MF membrane	Hydrophobic hollow fiber MF membranes hydrophilized with polyvinylpyrrolidone and persulfates and functionalized with polyacrylic acids and Fe/Pd nanoparticles	Water purification	[21]
Ceramic MF membranes	Ceramic MF membranes with graphene oxide quantum dots immobilized onto (3-aminopropyl) triethoxysilane functionalized alumina membranes	Enhanced water permeability with high water flux and low membrane resistance	[17]
MF membrane	Nanofibrous composite MF membranes	Removal of the heavy metals and nanoparticles from industrial wastewater	[22]
MF membrane	MF membrane–RO integrated system	Bacterial growth inhibition in wastewater	[23]
MF membrane	Ceramic MF membrane	Oily wastewater treatment	[24]
MF membrane	Fly ash-based MF membranes	Oil–water emulsion treatment	[25]

low molecular weight dyes such as basic, reactive, and acid are not removed by UF [30].

The UF membrane for the treatment of textile wastewater has been investigated to enhance the membrane's performance [42]. In an investigation, innovative modules were engineered for the configuration of flat UF membranes operating under vacuum. Polysulfone membranes were prepared through the phase inversion process at various evaporation temperatures. The membrane effectively removed the contaminants from wastewater. Moreover, textile waste removal efficiency and contamination variation
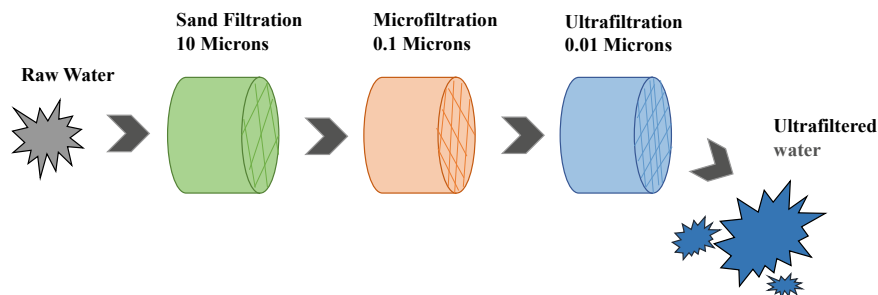
Fig. 1 The wastewater treatment using sand filtration, MF, and UF processes. The particles are removed at each step depending upon the pore size

in the properties were examined [43]. However, traditional polymeric membranes have limitations because of the less resistance to chemicals like organic solvents, the basic or acidic nature of the solutions, and high temperatures [44]. Besides, membrane technology faces membrane fouling and reduction in permeate flux, resulting in impaired performance and economic loss. Here, the need to introduce a hybrid process occurs, where the pre-treatment method, i.e., flocculation, is followed by UF. The evolutions in membrane technology have helped in modifying membranes to show good resistance to fouling by introducing advanced characteristics in the traditional UF membranes [45]. Furthermore, the replacement of polymer membranes with a ceramic membrane in pre-treatment of UF exhibits more excellent permeability rates in addition to other advantageous properties like thermal, chemical, or mechanical stability [44].

Organic dyes present in wastewater are removed by a practical process called Micellar-enhanced ultrafiltration. Different studies have proved the process as a suitable technique for retaining metal ions, organic contaminants, and anions; however, it has no applications on a larger scale or industrial level. The method proceeds by adding a surfactant to an aqueous solution containing pollutants, having a high concentration compared with critical micelle concentration (Fig. 2). Consequently, the micelle formed by the surfactant molecule dissolves inorganic and organic contaminants [46]. Then the micelles having dissolved solutes are rejected during ultrafiltration membrane treatment [28].

Reference [39] prepared an Al^{+3}-doped TiO_2 UF membrane in a modified sol–gel process by utilizing aluminum chloride and butyl titanate as an aluminum source and precursor. A filtration experiment was used (Fig. 3) to investigate Alizarin red-S removal. A layer of TiO_2 sol was formed on a flat homemade Al_2O_3 intermediate followed by heating to acquire the desired membrane. Insertion of Al^{+3} inhibited phase transformation of nano-sized titanium oxide from anatase to avoid the crystallite growth, causing the pore size of at least 3.5 nm of the separation membrane. The membrane showed excellent renewability and a reasonable retention rate for the dye.

Table 2 Summary of various studies in dye removal using UF technique

Membrane process	Membrane structure	Permeate flux L/m^2.h	Applications	References
UF membrane	Hydrolyzed ethanolamine polyacrylonitrile membrane	50–53	The rejection rate for anionic dyes, i.e., 99% for Congo Red, 96% for Methyl Blue, 94% for acid fuchsin	[31]
Composite UF membrane	Polypyrrole/sintered pozzolan membrane	10.3 ± 3	Congo red dye removal up to 98%	[32]
Mixed matrix polysulfone UF membrane	Functionalized boron nitride composite	1253–840 L/m^2.h.bar	Remove dyes from aqueous solution with 98% efficiency	[33]
UF membrane	Polysulphone membrane	133–197.5	Humic acid and photocatalytic dye removal 93.47%	[34]
UF membrane	Palladium nanoparticle-decorated mesoporous Polydopamine/bacterial nanocellulose	137.4	Anionic, cationic, and neutral dyes removal efficiency above 99%	[35]
Polymeric UF membrane	Polyimide UF membrane, Molecular weight 9320 Da	345 and 305.58	Rejection of 98.6% toward Direct Red 23 dye	[36]
Ceramic UF membrane	Bentonite clay Pore size 13 nm	30	Rejection of Direct Red 80 dyes (97%) and Rhodamine B (80%)	[37]
Ceramic UF membrane	Purified natural clay	14–16	Red 80 dyes removal 97–99%	[38]
Tight UF membrane	Al^{+3}-doped TiO$_2$	9.6	Dye removal	[39]
Tubular UF Ceramic membrane	Immobilization of titanium NPs on macroporous clay–alumina support, Pore size 50 nm	70	Rejection of Alizarin Red dye retention rate ≥ 99%	[40]
TiO$_2$ UF membrane	Natural bentonite and micronized phosphate, pore size (1.8 μm)	725 ± 2 L/m^2.h. bar	Dye removal	[41]
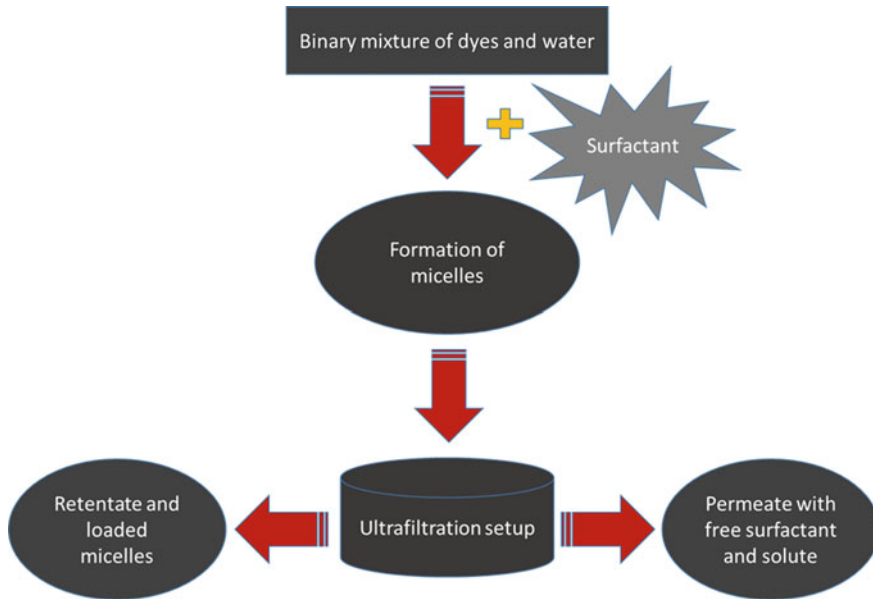
Fig. 2 Schematic representation of Micellar-enhanced UF setup using surfactant for the formation of micelles in dye removal

Reference [37] reported the spin-coating method followed by heating for synthesizing low-cost ceramic UF membrane deposited on perlite support. A tangential filtration experiment was carried out using stainless steel laboratory pilot on three various membrane samples. The membrane removed the cationic dye, i.e., Rhodamine B, and an anionic dye, i.e., Direct Red. The rejection for both dyes was explained by the sieving and electrostatic interactions between dye molecules and membrane surfaces. Consequently, filtration results showed that the ceramic UF membrane was helpful for wastewater treatment regenerated from textile effluents. The setup for UF has been shown in Fig. 4.

2.3 Nanofiltration Membrane

Another developed membrane technology applied for multiple wastewater treatment applications is NF. It was noted that NF is approved to be a promising separation technology to oust previously used techniques, particularly in dye removal [47]. NF membranes have charge and pore size in a range of 0.5–2.0 nm in diameter, making them highly efficient in dye removal (Table 3). The NF membrane-based technology has been placed between RO and UF. Moreover, NF has the advantage over RO and UF regarding relatively low operational cost and osmotic pressure difference,
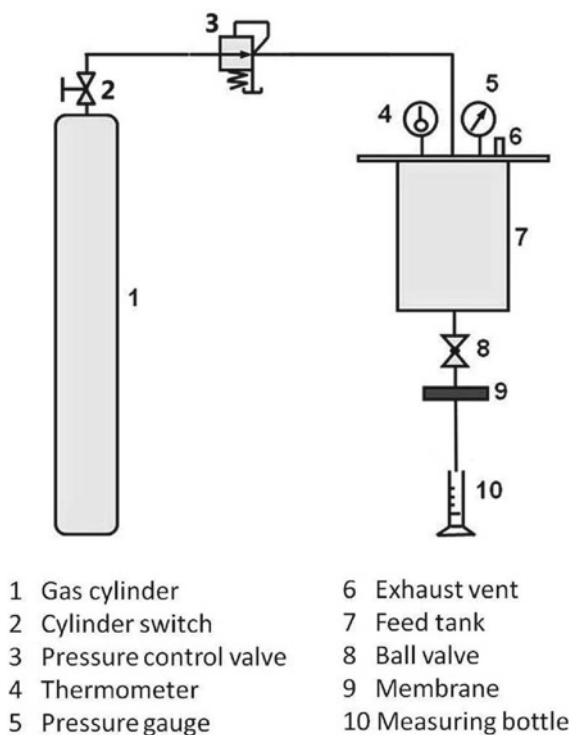
Fig. 3 Schematic diagram of the experimental dead-end apparatus for filtration experiment for determination of water permeability. Reprinted with permission of Elsevier from ref. [39]

and high retention of multivalent salts and permeate flux [28]. A low-pressure range between 500 and 1000 kPa is required for the proper working of NF membrane, enabling low detention of monovalent ions, which increases the opportunity and horizon for reuse and slow brine desertion, thus causing high solute selectivity. The steric and charge repulsion is the reason to cause rejection of species in NF membrane [48].

Other important NF membrane attributes include retaining uncharged dissolved solutes, i.e., organic molecules with a molecular weight greater than 150 Da, high solvent permeability, ease of chemical cleaning, and tendency to stand the high temperature 71 °C, which minimize the energy usage [59]. Zhong et al. prepared two positively charged NF membranes through ultraviolet insertion on sulfonated polyphenylene sulfone under UV exposure. The membrane shows high rejection for positively charged dyes than negatively charged.

Reference [50] reported the use of para-amino benzoate ferroxane nanoparticles as the primary functional nanoparticles through the phase inversion method to enhance the polyethersulfone NF membrane's performance. Later, dead-end permeation experiments (Fig. 5) were performed through a dead-end filtration setup with
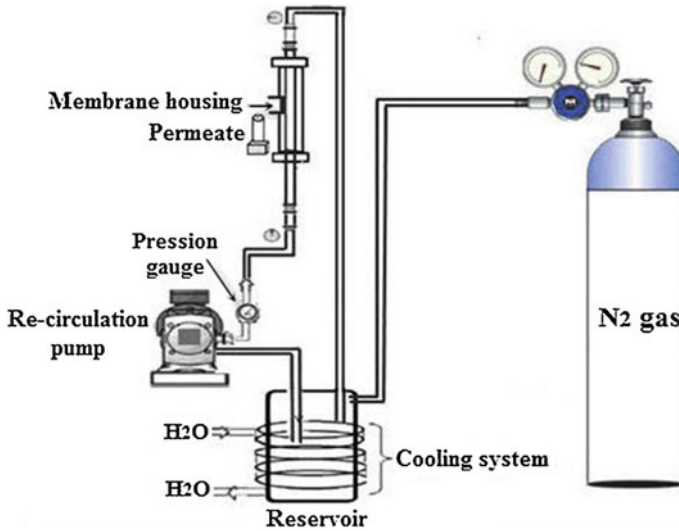
Fig. 4 UF pilot scheme (consisting of the fuel tank; 3L, membrane housing; filtering surface area of 5.3 cm^2, circulation pump, and pressure gauges). Reprinted with permission of Elsevier from ref. [37]

an effective membrane area and volume capacity of 12.56 m^2 and 125 mL, respectively, to assess the membrane permeation performance, dye removal, and antifouling resistance behavior.

Reference [54] investigated that the NF process utilizing a commercial spiral-wound polyamide nanofilter can effectively remove dyes from contaminated water. Different factors, i.e., disperse dye concentration and pH, affect the removal of dyes through polyamide NF membrane in a cross-flow module. The diaphragm pumps were equipped with NF experimental setup, and a feed tank with effluents supply to the system, and a 60 L storage capacity.

2.4 Reverse Osmosis

The semi-permeable spiral wound membrane is used to remove solvated solids, pyrogens, bacteria, colloidal matter at submicron level, organics, and dyes from wastewater RO [60]. The process has industrial usage in removing salts and colors from solutions, supplying deionized water. Moreover, attaining concentration and separation without any change in state, thermal energy, and chemical use benefits this membrane-based process [61]. RO membrane has a tight pore size in comparison to UF membrane, converting hard water into soft water, and they can remove organics, particles, and bacteria by requiring less maintenance. RO system has many applications in groundwater treatment, reclamation of wastewater, distillery spent washes,

Table 3 Different studies using NF technique in dye removal

Membrane	Composition	Permeate flux L/m^2.h	Application	References
Polyamide-based NF membrane	4,4'-Diaminodiphenylmethane, surface roughness, pore size 5.08 nm	36.8	Congo Red dye removal with a rejection rate of 99%	[49]
High flux NF membrane	Para-amino benzoate, ferroxane nanoparticle	64.2 kg/m^{2}h	Dye removal (98.42% for methylene Blue and 99% Direct Red 16)	[50]
Loose NF membrane	Cross-linkage of tannic acid-polyethyleneimine	40.6 L/m^2.hbar^{-1}	Salt and dye mixture Separation	[51]
NF membrane	Polyethyleneimine-modified membrane	–	Dye removal	[52]
Nanofiber composite NF membrane	Coat of calcium alginate hydrogel on electrospun polyhydroxybutyrate/carbon nanotubes nanofiber membrane	150.72	Dye removal	[53]
NF membrane	Polyamide nanofilter membrane	–	Removal of anthraquinone dye from binary solution	[54]
Positively charged loose NF membrane	Polymerization (UV induced) of diallyl dimethyl ammonium chloride on polysulphone NF membrane	60	Dye and salt removal	[55]
NF membrane	Introduction of poly (m-phenylene isophthalamide) hollow fiber substrate in poly (piperazine-amide)	104.13 ± 0.70	97% dye removal efficiency	[56]
NF membrane	Highly permeable polyelectrolyte/UiO-66 NF membrane	102	99.9% rejection of Congo Red dye	[57]
NF membrane	Modification of synthetic polyethersulphone NF membrane with magnetic graphene oxide/metformin hybrid	13.2–33.3	Heavy metals and dye removal	[58]
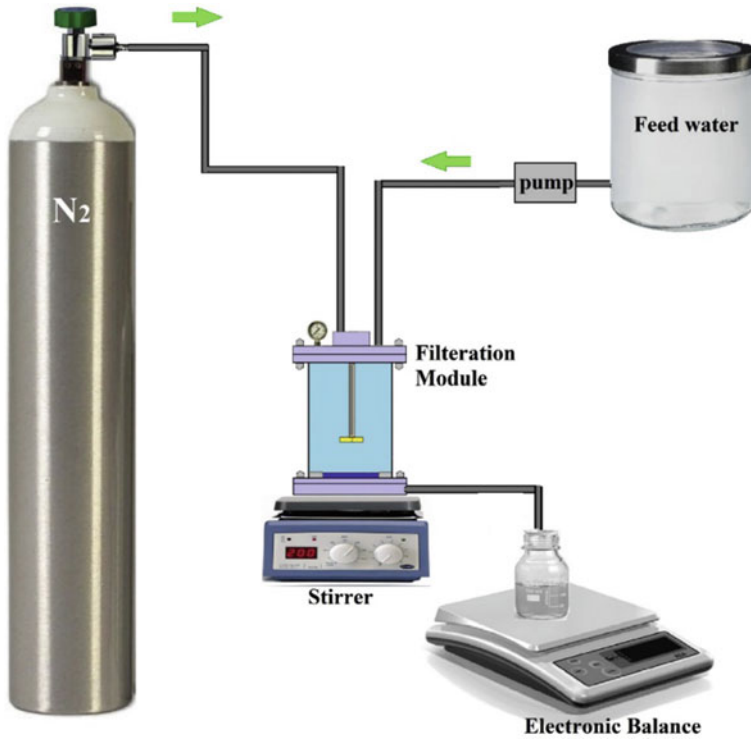
Fig. 5 Schematic diagram of dead-end permeation setup (volume capacity; 125 mL, effective membrane area; 12.56 m^2). Reprinted with permission of Elsevier from ref. [50]

recovery of phenol compounds, seawater RO treatment, and in the beverage industry, which shows their efficiency [62]. RO membranes are expensive and are also prone to fouling thus, affecting the membrane performance. Therefore, trans-membrane pressures ($\geq$2000 kPa) are mandatory to maintain proper permeates flux, which is again very economical [63].

2.5 Forward Osmosis (FO)

Forward osmosis is a built-in phenomenon where the movement of solvent from a low concentration region to a high concentration region occurs through a permeable membrane (Fig. 6) [64]. In the membrane, a highly concentrated draw solution helps establish a concentration gradient to draw water molecules from the feed solution [65]. The method has high efficiency with low brine production and is studied worldwide due to its ability to mitigate water problems; however, recovery of draw solution
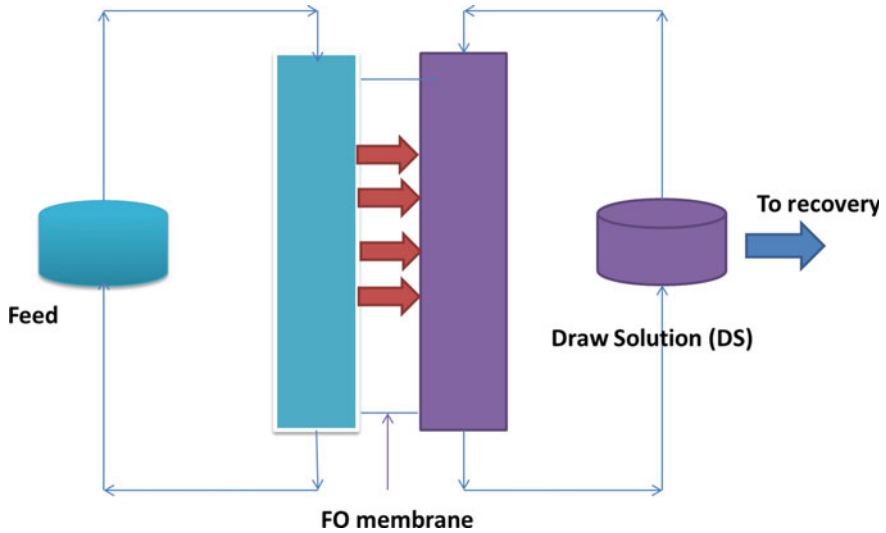
Fig. 6 Illustration of FO membrane carrying water from feed solution to draw solution through the osmotic gradient

for desalination process is expensive; therefore, RO and NF are used for regeneration of draw solution [66].

3 Membrane-Based Bioelectrochemical Cells

Bioelectrochemical systems utilize microbial catalysts for the treatment of wastewater. However, clean water production using aforesaid stand-alone systems is very challenging. To meet the challenges, membrane-based technologies for treating wastewater, like forward osmosis, pressurized filtration (e.g., UF), electrodialysis (ion-exchange membranes), have been integrated into bioelectrochemical systems (Fig. 7). New systematic arrangements such as microbial desalination cells (MDCs), pressurized filtration-microbial cells (PF-MFCs), and osmotic microbial fuel cells (OsMFCs) are developed as a result of the integration [67]. The systems such as OsMFCs and MDCs have been developed to remove salinity. Desalination technology based on ion-exchange methods, i.e., electrodialysis and bioelectrochemical techniques, was combined to form MDCs, desalinating water and producing energy from wastewater [68]. Similarly, forward osmosis was hybridized with the bioelectrochemical system to create OsMFCs [69]. Finally, pressurized filtration systems (dynamic membranes, UF, and MF) have been combined with bioelectrochemical systems to form PF-MFCs for cleaning wastewater [70].
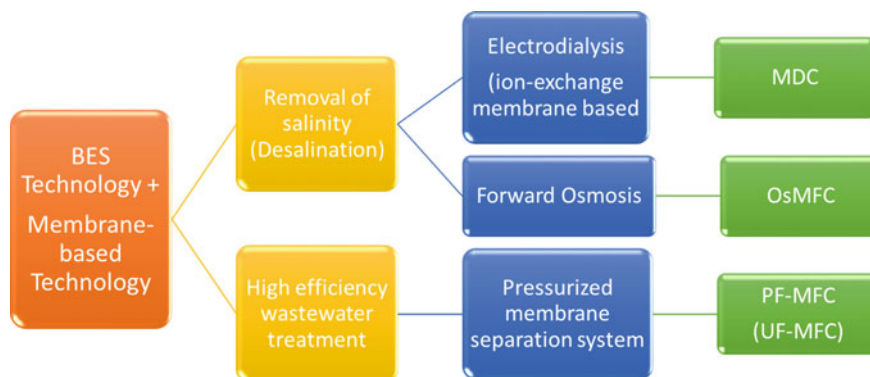
Fig. 7 A precise description of a bioelectrochemical system together with membrane-based technologies for desalination and water treatment

3.1 Microbial Desalination Cell

In MDCs, a supplementary chamber is added between the cathode and anode chambers, usually not present in the conventional MFCs to desalinate saline water [68]. Anion and cation exchange membranes separate the compartments in the MDCs. Degradation of organic compounds into protons and electrons takes place in an anode chamber. Transfer of the electrons into the cathode electrode is done through external circuits that are then used to reduce electron acceptors present in the cathode chamber. Simultaneously, as an electron system, to balance the microbial desalination cell system's net electric charge, the cations and anions present in the chamber are transferred to cathode and anode chambers across cation and anion exchange membranes, respectively. Bacteria play a crucial role in understanding the transfer of electrons. They are employed to oxidize organic matter present in wastewater and convert chemically stored energy in organic matter into electrical current. The desalination of water takes place without using any external energy source, and simultaneously, electricity is generated through MDCs (Fig. 8) [71].

3.2 Osmotic Microbial Fuel Cell

The ability of MFCs to clean water has been improved by combining the MFC system with the FO process. The integrated system is composed of cathode and anode chambers, just like conventional two-chambered MFC. Still, in OsMFC, a forward osmosis membrane is used to divide the chamber instead of an ion-exchange membrane (Fig. 9). In OsMFCs, the anode in the anode chamber is provided with electrochemically active bacteria supplied within organic wastewater of low conductivity
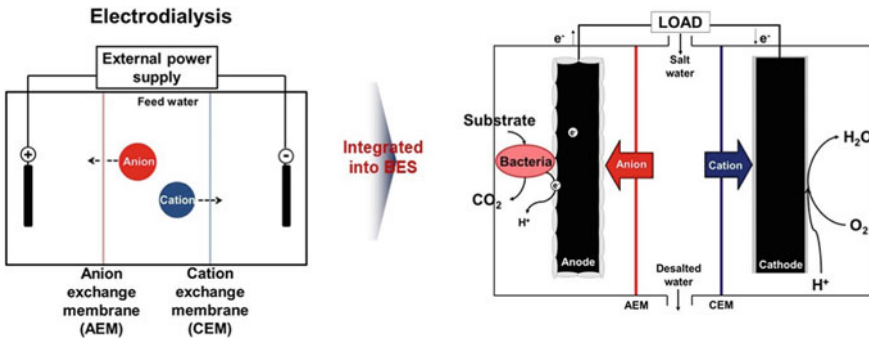
Fig. 8 Schematic diagram of microbial fuel cell for desalination without requiring any external energy source. Reprinted with permission of Elsevier from [67]
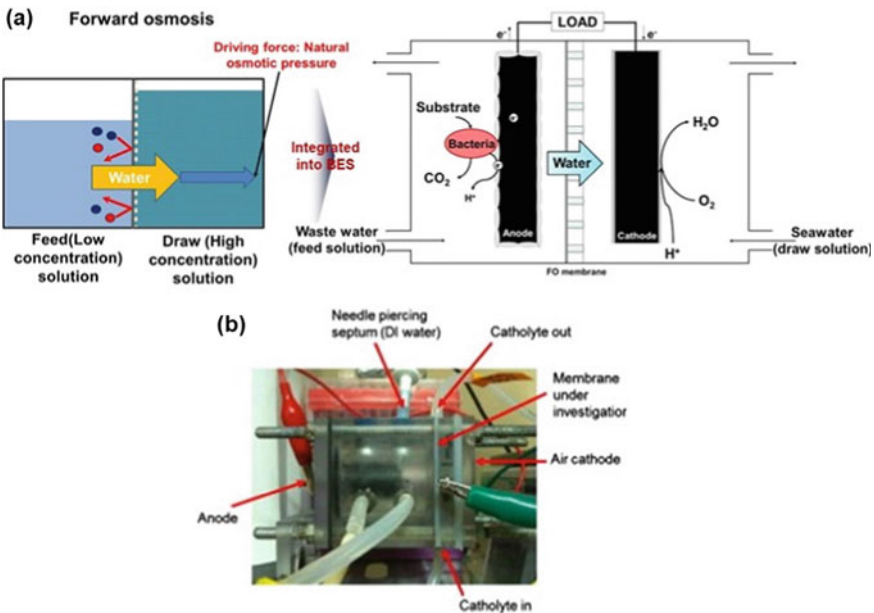
Fig. 9 Schematic diagram of osmotic microbial fuel cell combined with forward osmosis process to strengthen MFCs ability to clean water. Reprinted with permission of Elsevier from ref. [67]

than feed solution. A highly concentrated saline solution is supplied to the electrode within the cathode chamber, usually referred to as draw solution. The applications of OsMFCs include either reuse of water by additionally requiring reconcentration and recycling of draw solution or desalination of water [69].

Pressurized membrane filtration
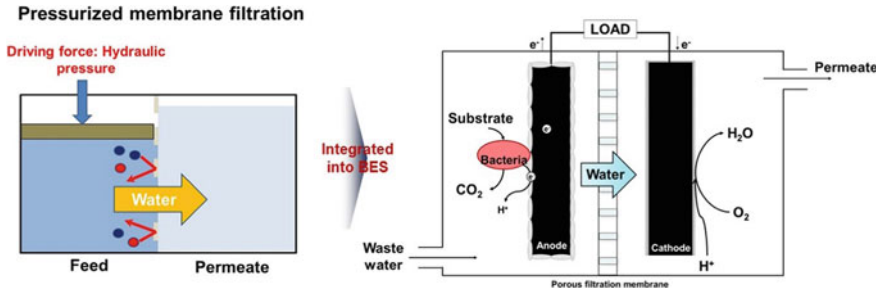
Fig. 10 Schematic diagram of pressurized filtration–microbial fuel cell representing water permeation due to applied pressure. Reprinted with permission of Elsevier from ref. [67]

3.3 Pressurized Filtration–Microbial Fuel Cells

According to the configuration of reactors and type of filtration membrane installed, PF-MFCs have been known as bioelectrochemical membrane reactor [72], MFC membrane reactor [73], UF microbial fuel cell, electrochemical membrane bioreactor, and anaerobic membrane electrochemical bioreactor [74]. However, they all have the same principle. Except for the filtration membrane, a basic PF-MFC configuration is the same as that of a traditional MFC (Fig. 10). Hence, the integration of filtration membrane into microbial fuel cell forming pressurized filtration–microbial fuel cell (PF-MFC) has developed to produce high-quality effluents. Wastewater treated by electrochemically active bacteria is provided to the anode compartment after passing through the porous membrane, such as UF membrane, MF membrane, and dynamic membranes. Low hydraulic pressure is required for wastewater treatment. PF-MFCs can remove the volatile suspended solids, bacteria, viruses, and nitrogen. Hence, a better quality effluent is produced through the cell than conventional MFCs [75].

4 Advantages and Limitations of Membrane-Based Methods

The membrane-based processes surpass the traditional methods used for wastewater treatment in most aspects such as desalination and purification. The methods exhibit a higher efficiency level than conventional methods and are easy to handle and can produce a good quality yield. Moreover, the membranes operate at ambient temperature without changing the composition of the product. The water desalination process is successfully employed using membrane-based techniques such as RO or electrodialysis. The use of either RO or electrodialysis depends on the water quality, desalination capacity, and energy cost. For surface water treatment,

Table 4 Advantages and disadvantages of bioelectrochemical systems integrated with membranes

System	Advantages	Disadvantages
Membrane desalination cell	• Function of desalination • Less carbon footprint • Less excess sludge production • High flexibility of different types of modified MDCs	• Lack of scale-up study • Removal of water from draw solution requires post-treatment • Membrane fouling • Ions accumulation • Expensive
Osmotic microbial fuel cell	• Use for desalination • Facilitate transport of proton across FO membrane through osmotic water flux • Less excess sludge production • Controllable reverse solute flux • Usage of naturally produced osmotic pressure	• No scale-up study • Expensive • Ions accumulation in anode effluents • Membrane fouling • Unfavorable nitrogen crossover across anion exchange membrane
Pressurized filtration–microbial fuel cell	• Effluent quality is high • Less carbon footprint • Nitrogen removal capability • Less fouling as compared to membrane bioreactor • Less excess sludge production	• No scale-up study • Membrane fouling • Hydraulic pressure is required for the operation • Construction cost is high

membrane methods replace carbon adsorption, flocculation, sand bed filtration, and biological treatment. Although membranes are mostly costly, the quality of water provided is way better. However, traditional methods combined with membrane methods can result in cost-effective treatment technologies.

In chemical or petrochemical industries, the implementation of membrane-based methods does not get long-term reliability. Sometimes, it behaves as an expensive pretreatment due to membrane fouling and concentration polarization resulted from interaction with water constituents. Moreover, membranes are not mechanically robust and can be destroyed easily on a slight malfunction in membrane function. However, in the last few years due to advancements in the RO processes, especially for seawater, desalination has improved the overall performance of membranes by enhancing chemical and thermal stability and reducing operational errors (Table 4).

5 Conclusions

In the last few decades, membrane-based technology has emerged as an evolutionary technique for wastewater treatment. The reduction in energy requirement, cost-effectiveness, and equipment size makes it sustainable and more economical

and provides the best alternative for conventional membrane-based methods. The most commonly employed membrane processes such as microfiltration, ultrafiltration, nanofiltration, reverse osmosis, and forward osmosis have extensive desalination and wastewater treatment applications. Moreover, membrane-based technology integrated with bioelectrochemical systems utilizing microbial catalysts for cleaning water is more encouraging for wastewater treatment. However, membrane fouling and sensitivity is a significant limitation in the membrane technologies, and more developments are demanding to overcome the limitations. Despite the limitations, membrane technology development can still be considered a revolutionary leap, with further future advancement and systematic improvements. It will soon be regarded as the most crowning achievement in wastewater treatment technologies.

References

1. Santhosh C, Velmurugan V, Jacob G, Jeong SK, Grace AN, Bhatnagar A (2016) Role of nanomaterials in water treatment applications: a review. Chem Engr J 306:1116–1137
2. Muhammad G, Mehmood A, Shahid M, Ashraf RS, Altaf M, Hussain MA, Raza MA (2020) Biochemical methods for water purification. In: Methods for bioremediation of water and wastewater pollution. Springer, Cham, pp 181–212
3. Altaf M, Yamin N, Muhammad G, Raza MA, Shahid M, Ashraf RS (2021) Electroanalytical techniques for the remediation of heavy metals from wastewater. In: Water pollution and remediation: heavy metals. Springer, Cham, pp 471–511
4. Adeleye AS, Conway JR, Garner K, Huang Y, Su Y, Keller AA (2016) Engineered nanomaterials for water treatment and remediation: costs, benefits, and applicability. Chem Eng J 286:640–662
5. Erkanlı M, Yilmaz L, Culfaz-Emecen PZ, Yetis U (2017) Brackish water recovery from reactive dyeing wastewater via ultrafiltration. J Clean Prod 165:1204–1214
6. Greenlee LF, Lawler DF, Freeman BD, Marrot B, Moulin P (2009) Reverse osmosis desalination: water sources, technology, and today's challenges. Water Res 43(9):2317–2348
7. Van't Hul J, Racz I, Reith T (1997) The application of membrane technology for reuse of process water and minimisation of waste water in a textile washing range. J Soc Dye Colour 113(10):287–294
8. Metcalf L, Eddy HP, Tchobanoglous G (1991) Wastewater engineering: treatment, disposal, and reuse, vol 4. McGraw-Hill, New York
9. Cheremisinoff NP (2001) Handbook of water and wastewater treatment technologies. Butterworth-Heinemann, UK
10. Ravanchi MT, Kaghazchi T, Kargari A (2009) Application of membrane separation processes in petrochemical industry: a review. Desalin 235(1–3):199–244
11. Ashraf RS, Abid Z, Shahid M, Rehman ZU, Muhammad G, Altaf M, Raza MA (2021) Methods for the treatment of wastewaters containing dyes and pigments. Water Pollut Rem Org Pollut 2021:597–661
12. Fane AT, Wang R, Jia Y (2011) Membrane technology: past, present and future. In: Membrane and desalination technologies. Springer, pp 1–45
13. Baker RW (2010) Research needs in the membrane separation industry: looking back, looking forward. J Membr Sci 362(1–2):134–136
14. Werber JR, Deshmukh A, Elimelech M (2016) The critical need for increased selectivity, not increased water permeability, for desalination membranes. Environ Sci Technol Lett 3(4):112–120

15. Torki M, Nazari N, Mohammadi T (2017) Evaluation of biological fouling of RO/MF membrane and methods to prevent it. Eur J Adv Eng Technol 4(9):707–710
16. Ferreira AM, Roque ÉB, Fonseca FVD, Borges CPJD, Treatment W (2015) High flux microfiltration membranes with silver nanoparticles for water disinfection 56(13):3590–3598
17. Gu Q, Ng TCA, Zain I, Liu X, Zhang L, Zhang Z, Lyu Z, He Z, Ng HY, Wang JJASS (2020) Chemical-grafting of graphene oxide quantum dots (GOQDs) onto ceramic microfiltration membranes for enhanced water permeability and anti-organic fouling potential. 502:144128
18. Jafari B, Abbasi M, Hashemifard SAJJoCP (2020) Development of new tubular ceramic microfiltration membranes by employing activated carbon in the structure of membranes for treatment of oily wastewater 244:118720
19. Hu M-X, Niu H-M, Chen X-L (2019) Zhan H-BJC, Physicochemical SA, Aspects E. Natural cellulose microfiltration membranes for oil/water nanoemulsions separation 564:142–151
20. Sinclair T, Robles D, Raza B, Van den Hengel S, Rutjes S, de Roda HA, de Grooth J, de Vos W, Roesink HJC (2018) Physicochemical sA, aspects e. Virus reduction through microfiltration membranes modified with a cationic polymer for drinking water applications 551:33–41
21. Hernández S, Lei S, Rong W, Ormsbee L, Bhattacharyya DJAsc, engineering (2016) Functionalization of flat sheet and hollow fiber microfiltration membranes for water applications 4(3):907–918
22. Liu X, Jiang B, Yin X, Ma H, Hsiao BSJS, Technology P (2020) Highly permeable nanofibrous composite microfiltration membranes for removal of nanoparticles and heavy metal ions 233:115976
23. Park JW, Lee YJ, Meyer AS, Douterelo I (2018) Maeng SKJWr. Bacterial growth through microfiltration membranes and NOM characteristics in an MF-RO integrated membrane system: lab-scale and full-scale studies 144:36–45
24. Rasouli Y, Abbasi M, Hashemifard SAJJoACS (2019) Fabrication, characterization, fouling behavior and performance study of ceramic microfiltration membranes for oily wastewater treatment 7(4):476–495
25. Suresh K, Pugazhenthi G (2016) Uppaluri RJJoWPE. Fly ash based ceramic microfiltration membranes for oil-water emulsion treatment: Parametric optimization using response surface methodology 13:27–43
26. Dutta BK (2007) Principles of mass transfer and seperation processes: PHI Learning Pvt. Ltd.
27. Mulder M, Mulder J (1996) Basic principles of membrane technology. Springer Science & Business Media
28. Ahmad A, Mohd-Setapar SH, Chuong CS, Khatoon A, Wani WA, Kumar R, Rafatullah M (2015) Recent advances in new generation dye removal technologies: novel search for approaches to reprocess wastewater. RSC Adv 5(39):30801–30818
29. Krüger R, Vial D, Arifin D, Weber M, Heijnen M (2016) Novel ultrafiltration membranes from low-fouling copolymers for RO pretreatment applications. Desalin Water Treat 57(48–49):23185–23195
30. Zhang L, Zhang P, Wang M, Yang K, Liu J (2016) Research on the experiment of reservoir water treatment applying ultrafiltration membrane technology of different processes. J Environ Biol 37(5):1007
31. Yun J, Wang Y, Liu Z, Li Y, Yang H, Xu Z-l (2020) High efficient dye removal with hydrolyzed ethanolamine-Polyacrylonitrile UF membrane: Rejection of anionic dye and selective adsorption of cationic dye. Chemosphere 259:127390
32. Derouich G, Younssi SA, Bennazha J, Cody JA, Ouammou M, El Rhazi M (2020) Development of low-cost polypyrrole/sintered pozzolan ultrafiltration membrane and its highly efficient performance for congo red dye removal. J Environ Chem Eng 8(3):103809
33. Singh R, Sinha MK, Purkait MK (2020) Stimuli responsive mixed matrix polysulfone ultrafiltration membrane for humic acid and photocatalytic dye removal applications. Separation and Purification Technology 250:117247
34. Hafeez A, Karim ZA, Ismail AF, Samavati A, Said KAM, Selambakkannu S (2020) Functionalized boron nitride composite ultrafiltration membrane for dye removal from aqueous solution. J Membr Sci 612:118473

35. Gholami H, Gupta P, Gupta R, Rathi P, Morrissey JJ, Singamaneni S (2020) Palladium nanoparticle-decorated mesoporous polydopamine/bacterial nanocellulose as a catalytically active universal dye removal ultrafiltration membrane. ACS Appl Nano Mater 3(6):5437–5448
36. Yang C, Xu W, Nan Y, Wang Y, Chen X (2020) Novel negatively charged nanofiltration membrane based on 4, 4′-diaminodiphenylmethane for dye removal. Separation and Purification Technology 248:117089
37. Saja S, Bouazizi A, Achiou B, Ouaddari H, Karim A, Ouammou M, Aaddane A, Bennazha J, Younssi SA (2020) Fabrication of low-cost ceramic ultrafiltration membrane made from bentonite clay and its application for soluble dyes removal. J Eur Ceram Soc 40(6):2453–2462
38. Ouaddari H, Karim A, Achiou B, Saja S, Aaddane A, Bennazha J, El Hassani IEA, Ouammou M, Albizane A (2019) New low-cost ultrafiltration membrane made from purified natural clays for direct Red 80 dye removal. J Environ Chem Eng 7(4):103268
39. Huang X, Tian C, Qin H, Guo W, Gao P, Xiao H (2020) Preparation and characterization of Al_3+-doped TiO_2 tight ultrafiltration membrane for efficient dye removal. Ceram Int 46(4):4679–4689
40. Oun A, Tahri N, Mahouche-Chergui S, Carbonnier B, Majumdar S, Sarkar S, Sahoo GC, Amar RB (2017) Tubular ultrafiltration ceramic membrane based on titania nanoparticles immobilized on macroporous clay-alumina support: elaboration, characterization and application to dye removal. Sep Purif Technol 188:126–133
41. Bouazizi A, Breida M, Karim A, Achiou B, Ouammou M, Calvo J, Aaddane A, Khiat K, Younssi SA (2017) Development of a new TiO_2 ultrafiltration membrane on flat ceramic support made from natural bentonite and micronized phosphate and applied for dye removal. Ceram Int 43(1):1479–1487
42. Marcucci M, Nosenzo G, Capannelli G, Ciabatti I, Corrieri D, Ciardelli G (2001) Treatment and reuse of textile effluents based on new ultrafiltration and other membrane technologies. Desalin 138(1–3):75–82
43. Koseoglu-Imer DY (2013) The determination of performances of polysulfone (PS) ultrafiltration membranes fabricated at different evaporation temperatures for the pretreatment of textile wastewater. Desalin 316:110–119
44. Barredo-Damas S, Alcaina-Miranda MI, Iborra-Clar MI, Mendoza-Roca JA (2012) Application of tubular ceramic ultrafiltration membranes for the treatment of integrated textile wastewaters. Chem Eng J 192:211–218
45. Simonič M, Lobnik A (2011) The efficiency of a hybrid flocculation/UF process for a real dye-house effluent using hydrophilic and hydrophobic membranes. Desalin 271(1–3):219–224
46. Ngang H, Ooi B, Ahmad A, Lai S (2012) Preparation of PVDF–TiO_2 mixed-matrix membrane and its evaluation on dye adsorption and UV-cleaning properties. Chem Eng J 197:359–367
47. Wang N, Liu T, Shen H, Ji S, Li JR, Zhang R (2016) Ceramic tubular MOF hybrid membrane fabricated through in situ layer-by-layer self-assembly for nanofiltration. AIChE J 62(2):538–546
48. Miner G (2005) Nanofiltration: principles and applications. J Am Water Works Assoc 97(11):121
49. Yang C, Xu W, Nan Y, Wang Y, Hu Y, Gao C, Chen X (2020) Fabrication and characterization of a high performance polyimide ultrafiltration membrane for dye removal. J Colloid Interface Sci 562:589–597
50. Moradi G, Zinadini S, Rajabi L (2020) Development of high flux nanofiltration membrane using para-amino benzoate ferroxane nanoparticle for enhanced antifouling behavior and dye removal. Process Saf Environ Prot 144:65–78
51. Li Q, Liao Z, Fang X, Wang D, Xie J, Sun X, Wang L, Li J (2019) Tannic acid-polyethyleneimine crosslinked loose nanofiltration membrane for dye/salt mixture separation. J Membr Sci 584:324–332
52. Qi Y, Zhu L, Shen X, Sotto A, Gao C, Shen J (2019) Polythyleneimine-modified original positive charged nanofiltration membrane: Removal of heavy metal ions and dyes. Sep Purif Technol 222:117–124

53. Zhijiang C, Cong Z, Ping X, Jie G, Kongyin Z (2018) Calcium alginate-coated electrospun polyhydroxybutyrate/carbon nanotubes composite nanofibers as nanofiltration membrane for dye removal. J Mater Sci 53(20):14801–14820

54. Askari N, Farhadian M, Razmjou A, Hashtroodi H (2016) Nanofiltration performance in the removal of dye from binary mixtures containing anthraquinone dyes. Desalin Water Treat 57(39):18194–18201

55. Liu F, Ma B-r, Zhou D, Zhu L-J, Fu Y-Y, Xue L-x (2015) Positively charged loose nanofiltration membrane grafted by diallyl dimethyl ammonium chloride (DADMAC) via UV for salt and dye removal. React Funct Polym 86:191–198

56. Wang T, He X, Li Y, Li J (2018) Novel poly (piperazine-amide)(PA) nanofiltration membrane based poly (m-phenylene isophthalamide)(PMIA) hollow fiber substrate for treatment of dye solutions. Chem Eng J 351:1013–1026

57. Wang K, Qin Y, Quan S, Zhang Y, Wang P, Liang H, Ma J, Cheng XQ (2019) Development of highly permeable polyelectrolytes (PEs)/UiO-66 nanofiltration membranes for dye removal. Chem Eng Res Des 147:222–231

58. Abdi G, Alizadeh A, Zinadini S, Moradi G (2018) Removal of dye and heavy metal ion using a novel synthetic polyethersulfone nanofiltration membrane modified by magnetic graphene oxide/metformin hybrid. J Membr Sci 552:326–335

59. Yu RF, Lin CH, Chen HW, Cheng WP, Kao MC (2013) Possible control approaches of the Electro-Fenton process for textile wastewater treatment using on-line monitoring of DO and ORP. Chem Eng J 218:341–349

60. Wood AR, Justus K, Parigoris E, Russell A, LeDuc P (2017) Biological inspiration of salt exclusion membranes in mangroves toward fouling-resistant reverse osmosis membranes. FASEB J 31:949

61. Ciardelli G, Corsi L, Marcucci M (2001) Membrane separation for wastewater reuse in the textile industry. Resour Conserv Recycl 31(2):189–197

62. Garud R, Kore S, Kore V, Kulkarni G (2011) A short review on process and applications of reverse osmosis. Univers J Environ Res Technol 1(3)

63. Dasgupta J, Sikder J, Chakraborty S, Curcio S, Drioli E (2015) Remediation of textile effluents by membrane based treatment techniques: a state of the art review. J Environ Manage 147:55–72

64. Ong CS, Al-Anzi B, Lau WJ, Goh PS, Lai GS, Ismail AF, Ong YS (2017) Anti-fouling double-skinned forward osmosis membrane with zwitterionic brush for oily wastewater treatment. Sci Rep 7(1):1–11

65. Suwaileh WA, Johnson DJ, Sarp S, Hilal N (2018) Advances in forward osmosis membranes: altering the sub-layer structure via recent fabrication and chemical modification approaches. Desalin 436:176–201

66. Blandin G, Verliefde AR, Comas J, Rodriguez-Roda I, Le-Clech P (2016) Efficiently combining water reuse and desalination through forward osmosis—reverse osmosis (FO-RO) hybrids: a critical review. Membranes 6(3):37

67. Yang E, Chae K-J, Choi M-J, He Z, Kim IS (2019) Critical review of bioelectrochemical systems integrated with membrane-based technologies for desalination, energy self-sufficiency, and high-efficiency water and wastewater treatment. Desalination 452:40–67

68. Cao X, Huang X, Liang P, Xiao K, Zhou Y, Zhang X, Logan BE (2009) A new method for water desalination using microbial desalination cells. Enviro Sci Technol 43(18):7148–7152

69. Zhang F, Brastad KS, He Z (2011) Integrating forward osmosis into microbial fuel cells for wastewater treatment, water extraction and bioelectricity generation. Enviro Sci Technol 45(15):6690–6696

70. Yuan H, He Z (2015) Integrating membrane filtration into bioelectrochemical systems as next generation energy-efficient wastewater treatment technologies for water reclamation: a review. Bioresour Technol 195:202–209

71. Jacobson KS, Drew DM, He Z (2011) Use of a liter-scale microbial desalination cell as a platform to study bioelectrochemical desalination with salt solution or artificial seawater. Environ Sci Technol 45(10):4652–4657

72. Liu J, Liu L, Gao B, Yang F (2013) Integration of bio-electrochemical cell in membrane bioreactor for membrane cathode fouling reduction through electricity generation. J Membr Sci 430:196–202
73. Malaeb L, Katuri KP, Logan BE, Maab H, Nunes SP, Saikaly PE (2013) A hybrid microbial fuel cell membrane bioreactor with a conductive ultrafiltration membrane biocathode for wastewater treatment. Environ Sci Technol 47(20):11821–11828
74. Katuri KP, Werner CM, Jimenez-Sandoval RJ, Chen W, Jeon S, Logan BE, Lai Z, Amy GL, Saikaly PE (2014) A novel anaerobic electrochemical membrane bioreactor (AnEMBR) with conductive hollow-fiber membrane for treatment of low-organic strength solutions. Environ Sci Technol 48(21):12833–12841
75. Kim KY, Chae KJ, Choi MJ, Yang ET, Hwang MH, Kim IS (2013) High-quality effluent and electricity production from non-CEM based flow-through type microbial fuel cell. Chem Eng J 218:19–23

Technical Aspects of Nanofiltration for Dyes Wastewater Treatment

Alaa El Din Mahmoud, Manal Fawzy, and Mona M. Amin Abdel-Fatah

Abstract Currently, there are many membrane separation technologies that have been attracted growing interest in dyes removal from water streams and wastewater. In this chapter, we focus on nanofiltration (NF). In comparison with the available membrane techniques, NF is deemed to be the most promising technique due to its higher dye rejection, lower energy consumption, and higher antifouling properties. However, the challenge for feasible NF membranes with enhanced permeate flux, selectivity, and higher antifouling properties is remaining in the commonly used polymeric NF membranes. Therefore, numerous methods have been recently adopted by incorporating specific fillers into the polymeric membranes to fill in these gaps. We investigate the recent types of NF modified membranes based on their merits and limitations. Furthermore, the models of spiral wound NF for dyes removal are presented to explain the underlying mechanisms. Hence, this chapter may help the decision-makers to select the suitable membrane technology for the dye treatment removal using NF-based membranes.

Keywords Membrane separation · Textile wastewater · Polymeric nanofiltration · Ceramic nanofiltration · Nano coating · Spiral wound nanofiltration

A. E. D. Mahmoud (✉) · M. Fawzy
Environmental Sciences Department, Faculty of Science, Alexandria University, Alexandria 21511, Egypt
e-mail: alaa-mahmoud@alexu.edu.eg

Green Technology Group, Faculty of Science, Alexandria University, Alexandria 21511, Egypt

National Biotechnology Network of Expertise (NBNE), Academy of Scientific Research and Technology (ASRT), Cairo, Egypt

M. M. A. Abdel-Fatah
Chemical Engineering & Pilot Plant Department, National Research Centre (NRC), Engineering Division, Giza 12622, Egypt

1 Introduction

Water pollution and water shortage are environmental issues that are facing the world. One of the major sources of water pollution is wastewater effluents [33, 39]. Dyes are not only used and discharged in textile industries but also extended to paper, plastics, and other industries which can reach the water bodies to pollute the ecosystem components as well as threaten human health [14, 25].

Annually, almost 10^9 kg of dyes are produced around the world including the textile effluents that are responsible for 17–20% of water pollution [21]. The dyes effluents of textile industries are usually containing high amounts of salts which will produce by-products such as NaCl, Na_2SO_4, $MgCl_2$, and $MgSO_4$ and contribute to the low efficiency of dyes treatment [12, 17]. This can be due to the precipitation of the produced dyes using NaCl in the last step of textile dye production.

Physical and chemical water/wastewater treatment processes have limitations to remove all types and concentration ranges of different pollutants from water [6, 19, 28]. Nowadays, they are combined with membrane technology because it is a practical tool for removing organic pollutants (i.e., dyes) [11]. It is also applicable to implement membrane technology as a separate procedure. Generally, separation membranes possess merits such as flexibility in wide range treatment (pre-/main-treatment), non-hazardous; no additional additives, and low energy requirements results in a lower cost/m^3 treated. Thus, separation membranes are highly recommended with low dissolved components' rejections but with high water permeability. In the market, there are different membrane types with different separation ranges. Table 1 illustrates the four main membrane types with their features.

Table 1 Types of separation membranes with their parameters [1, 29]

Membranes	Microflora tion (MF)	Ultrafiltration (IFF)	Nanofiltration (<NF)	Reverse Osmosis (RO)
Pore size (fim)	0.2–5	0.02–0.2	<0.002	<0.002
Thickness (lim)	10–150	150–250	150	150
Required	0.1–2	2–5	5–15	15–75
pressure (bar)	Low pressure operation	Low pressure operation	High pressure operation	High pressure operation
Solutes retained	Suspended particles, heavy metals, bacteria	Suspended particles, dyes, polymers, viruses, bacteria	Suspended particles, pigments, cations, divalent anions, dyes, sodium chloride, viruses, bacteria	Suspended particles and all dissolved compounds including viruses, bacteria
Separation	Steric exclusion	Steric exclusion	Steric exclusion	Solution-diffusion
Mechanism	Sieving	Sieving	Donnan exclusion, charge effect	

Among the above-mentioned membranes, microfiltration and ultrafiltration membranes are not efficient in trapping dye molecules due to their small sizes. Therefore, RO membranes have been developed that are able to retain dissolved salts, ions and the organic solutes and commercially used in 1970s. Due to using high pressures in RO traditionally resulted in a substantial cost in energy. Hence, Dr. Peter Eriksson referred to a new membrane class named NF in the market application in 1984 which are low-pressure RO membranes, and the first applications were in 1986 (NF born). The first application of NF was as softening membrane instead of lime softening to treat water [5].

In this chapter, we discuss and focus on nanofiltration (NF) membranes which their performances fall between UF (separation is due to size exclusion) and RO (transport by solution-diffusion mechanism) to be the key to trap the dye molecules because of the following reasons:

- The negatively charged surface of NF.
- The size of the pores is ~1 nm.
- Its applicability with the high osmotic pressure of the wastewater which is prohibitive for RO.

NF provides an elegant solution to the dyes treatment problem since NF can fractionate the salts and the organic compounds. It is one of the most effective treatment techniques used for removing ions and organic substances in seawater desalination, industrial wastewater treatment, and drinking water treatment [1]. Furthermore, separate solutes with molecular weights (200–1000 g mol^{-1}) aqueous solutions and is especially applicable for dye removal in wastewater [7, 9, 31, 38, 45].

NF is competitive with routine treatment (physicochemical treatment) and ought to be explored on a case-by-case premise as illustrated below [42].

- More compelling for natural and inorganic removal
- Provide a defensive obstruction against microbes and virus as illustrated in Table 2.
- Ease of operation, coming about in less administrator participation time.
- Greater plausibility of assembly future greatest contaminant levels without extra treatment processes.
- A descending drift in framework capital, operation, and upkeep O&M costs since of nonstop progresses in film technology.
- Overall predominant quality of item water

Furthermore, there are specific advantages of NF over conventional treatment technologies that are comprised in Fig. 1 despite NF cannot reduce or separate soluble impurities. In NF process, the feed water passes through semi-permeable membrane, at which the filtered stream is discharged as permeate and non-filtered portion is rejected as concentrate [1]. First, Eq. 1 can be used to calculate the water flux [12]. After the organic materials removal, chlorine disinfection is strongly recommended for elimination of microbial growth that has been observed in NF systems. The microbial growth can be minimized by using NF membranes with high organic materials removal and low detention of inorganic material and. The NF membrane

Table 2 Nanofiltration impact on various pathogens hindrance that causes diseases

Pathogen type	Pathogen	Disease
Bacteria	*Shigella* spp.	Shigellosis
	Salmonella spp.	Typhoid fever
	Vibrio cholerae	Cholera
	Escherichia coli	Gastroenteritis; respiratory diseases
	Campylobacter spp.	
	Yersinia enterocolifica	
Virus	Enteroviruses	Aseptic meningitis
	Cor antiviruses	Gastroenteritis; respiratory diseases
	Astroviruses	
	Calicivirmes	
	Rotaviruses	Diarrhea
	Hepatitis A virus	Hepatitis A
	Hepatitis E virus	Hepatitis E
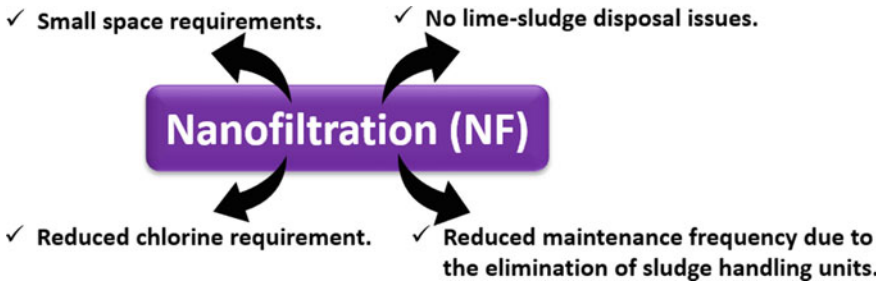
Fig. 1 Advantages of nanofiltration membranes over conventional wastewater treatment technologies

permeance (P) and the rejection of dyes (R) can be estimated and determined using Eqs. 2 and 3, respectively [9].

$$F = \frac{V}{Axt},\qquad(1)$$

$$P = \frac{V}{Axtx\Delta p},\qquad(2)$$

$$R = \left(1 - \frac{C_p}{C_f}\right) \times 100\%,\qquad(3)$$

where *F*: water flux, *P:* membrane permeance, *V:* solution volume (L), *A:* membrane area (m^2), *t:* filtration time (h), and Δp: filtration pressure (bar). *R:* rejection, C_p:

permeate concentration of dyes in water, and C_f: concentration of the feed solution of dyes in water

Other factors should be considered while running NF membranes. For instance, NF membranes are vulnerable to fouling which is related to its hydrophobic nature where the contaminants (dyes) will be aggregated on the membrane surface. This leads to the interaction of hydrophobic foulants to the membrane surface blocking the membrane pores as well as depositing on the membrane surface [32]. Therefore, antifouling resistance behavior is essential to be tested. The antifouling test can be estimated using the powder milk solution filtration test. Its resistance parameter of irreversible (R_{ir}), reversible (R_r), and total fouling (R_t) ratios were calculated by Eqs. 4, 5, and 6. Reference [27] observed that the polyethersulfone (PES) membrane had low fouling resistance around 64.1% R_{ir} and 82.2% R_t owing to poor hydrophilicity.

$$R_{ir} = \frac{J_0 - J}{J_0} \times 100, \tag{4}$$

$$R_r = \frac{J - J_p}{J_0} \times 100 \tag{5}$$

$$R_t = \frac{1 - J_p}{J_0} \times 100 \tag{6}$$

where R_{ir}: ratio of irreversible fouling, R_r: ratio of reversible fouling, R_t: total fouling ratio. J, J_0, and J_p: pure water flux, powder mix solution flux, and second pure water flux, respectively.

In the next sections, we highlight different types of NF membranes and how their performances are differentiated in dyes treatment. Furthermore, we summarize the modules of NF and the used models in the literature.

2 Types of Nanofiltration Membranes and Their Application in Dyes Treatment

NF membrane is composed of cellulose acetate, polysulfone/poly(ether sulfone) or aromatic polyamide [41]. Polyamides which can be made by interfacial polymerization of two multifunctional monomers such as amine and aromatic acid chloride are the most widely used components for modern NF membranes [8, 37]. Nevertheless, the produced polyamide layer is characterized by its rough surface which can lead to high fouling problems [37]. Accordingly, another synthesis method was developed by the reaction of an aliphatic amine monomer such as piperazine with aromatic trimesoyl chloride to form a semi-aromatic poly(piperazine amide). However, as compared to aromatic polyamide membranes, this approach has a lower rejection rate [30].

Recently, NF membranes are also composed of ceramic materials to withstand high temperatures [1]. Ceramic NF membranes provide good performance in the treatment of textile wastewater containing dyes. The reported chemical oxygen demand (COD) rejection ranges of a new developed ceramic NF membrane and other two commercial ceramic NF membranes are 95–97, 86–92, and 79–90, respectively [3]. Since the surface charge is determined by the dissociation degree of functional groups, membrane material could affect charge characteristics [30]. Polyamide layer contains ionizable surface functional groups such as carboxylic acid and amine and thereby causing amphoteric membrane surface [4].

Reference [17] fabricated chitosan nanofiltration membranes with different thickness and they found their efficiencies with six dyes rejections follow 50-4t > 75-4t > 150-4t. It is found that water fluxes obtained by separating methylene blue and brilliant blue solutions (>98%) are higher than those obtained by separating other dyes (methyl red, methyl orange, rose bengal, orange G). The salt rejection follows the order $CaCl_2 > MgSO_4 > Na_2SO_4 > NaCl$. Reference [26] prepared NF membrane with zwitterionic N,N-Bis (3-aminopropyl)methylamine and get high congo red and methyl blue dyes rejections (99.9%) as well as a low NaCl rejection (14.3%).

Submerged hollow fiber NF membrane proved its efficiency in removal of 99.3% color and 91.5% reduction of COD [47]. NF membrane combined with ozonation of the concentrate was utilized for the colored textile wastewater treatment contained organic dyes, NaCl, and copper. The removal of color and copper permeate were > 99% as well as the original water (85%) was reusable [43].

Recently, [13] fabricated Erythritol-based polyester loose nanofiltration membrane with high water permeability that possessed high rejection of dyes and high salts transmission. The rejections of congo red, direct red 23, reactive blue 2 were 99.6%, 95.2%, 99.6%, respectively. Whereas the rejections of Na_2SO_4 and NaCl were 11.0% and 5.6%, respectively.

The performances of two types of NF (neutral and negatively charged) membranes were investigated for the treatment of effluents containing dyes and salt [35]. The results revealed that the dye rejections of the charged membranes are adequate for permeate reuse, while the neutral membranes exhibited lower dye rejection. Reference [27] blended para-amino benzoate ferroxane nanoparticle (PABFNP) with PES nanofiltration membrane to improve its performance. They found that PABFNP membrane has a high rejection for dye (99% for 30 ppm of direct Red 16 and 98.42% for 30 ppm of methylene blue). This may be due to the PES/PABFNPs membranes' high surface hydrophilicity, which allows the dye to adsorb on the membrane surface during the filtration process, resulting in high dye rejection.

Simulated synthetic reactive dyes (reactive black 5 and reactive orange 16) have been separated by polysulfone polyamide NF membrane with operating pressures ranging from 8 to 24 bars and flow velocity of 0.74 m s^{-1} [15]. The NaCl and the color rejections were 20% and 95%, respectively. Decrement of membrane fouling and increasing the color rejection. For further progress, UV-photografting was used to create the same polysulfone NF membrane, and sodium p-styrene sulfonate was used to modify it [16]. The grafted membranes were screened for the removal of five dyes, with dye rejection rates exceeding 90%.

Two advanced treatments: activated sludge process with NF and activated sludge process with ozone or ozone/UV radiation (chemical oxidation) have been compared in order to water reuse in dyeing and printing [40]. The results concluded that NF permeate quality with measured COD less than 50 mg L^{-1}. Furthermore, NF membrane gave high salt rejection and almost complete color removal color value was decreased from 500 to 10 Pt–Co unit and greater removal of COD with 97% have been realized and thus, recycling the permeate to the dye house.

Nanomaterials provide the opportunity to tune the material properties, strength, and surface-volume ratio [2, 22, 23]. Among different nanomaterials, graphene oxide and graphene have rapidly gained research attention in different fields especially water treatment [18, 20, 24]. Nanofiltration membranes coated with Graphene Oxide Quantum Dots (GOQDs) were prepared [46]. Such coating with nanomaterials change the NF surface properties, increasing surface roughness, improving surface hydrophilicity, and electronegativity. These coated NF membranes achieved 97.0% rejection of methyl orange compared to NF membrane alone with 89.2% rejection. Because of the GOQDs coating, the NF membrane surface became more negatively charged. Consequently, the negatively charged dye adsorption on its surface is weakened and increased the dye rejection. On the other hand, the positively charged dyes (methylene blue) is more adsorbed on the GOQDs NF surface and decreased the dye rejection from 76.0 to 71.0%.

3 Modelling and Calculations for Nanofiltration (NF) Membranes

Understanding the fundamentals of NF membrane efficiency is still crucial for the proper selection and operation of industrial systems. NF separations, in comparison to UF and RO systems, are thought to be based on a combination of solution-diffusion and sieving mechanisms, as well as electrostatic activity induced by electrically charged membrane surface groups. NF membranes use steric, Donnan, and dielectric exclusion effects to fractionate low molecular weight solute mixtures at low pressure. The prediction of ionised solute rejection for Charged NF membranes would involve the inclusion of both diffusion and charge repulsion (Donnan exclusion).. Hence, the Nernest–Planck equation (Eq. 7) can be applied for the description of ion transport through the membranes considering solving this equation using approximations for idealized situations.

$$J_i(x) = -D_i \frac{\partial C_i(x)}{\partial x} + \frac{-Z_i F}{RT} D_i C_i \frac{\partial \varnothing(x)}{\partial x} + C_i v(x) \tag{7}$$

where J: Flux is the number of ion moles passing through a unit area per second, D: Diffusion constant, C_i: Concentration, F: Force on a mole of ions, R: Gas constant, and T: Absolute temperature.

Table 3 Characteristic of the four modules of nanofiltration [1, 34]

Characteristics	Plate and frame	Tubular	Spiral wound	Hollow fiber
Packing Density (m^2 nr^3)	30–500	30–200	200–800	500–6000
Required Feed Flow (m^3 nr^2 s^{-1})	0.25–0.50	1.0–5.0	0.25–0.50	-0.005
Ease of cleaning	Good	Excellent	Fair (Poor to good)	Poor
Resistance to fouling	Good	Very good	Moderate	Poor
Relative cost	High	High	Low	Low

Generally, there are four modules of NF. For instance, plate and frame module, tubular module, spiral wound module, and hollow fiber module. Table 3 illustrates characteristics of each module. We summarize the models used in spiral wound module in NF membranes for dyes wastewater treatment in the following section because it is the most used module and popular configuration with relative low cost.

A.   **Solution diffusion model**

The solution diffusion (SD) model has emerged over the past 45 years as the accepted explanation of gas and water transport. SD model is illustrated in Fig. 2, and when estimating the permeate concentration, it takes into account the effects of pressure, recovery, feed stream concentration, solvent, and solute mass transfer coefficients. This method is superior to using percent rejection of a feed stream concentration to estimate permeate concentration, and it is simple enough for most water industry professionals to use [36]. Figure 2 demonstrates the mass balance across the NF membranes for dyes effluents. Mass balance equations for solvent and solute in the membrane module are illustrated in Eqs. 8 and 9.

$$Q_f = Q_C + Q_p \tag{8}$$
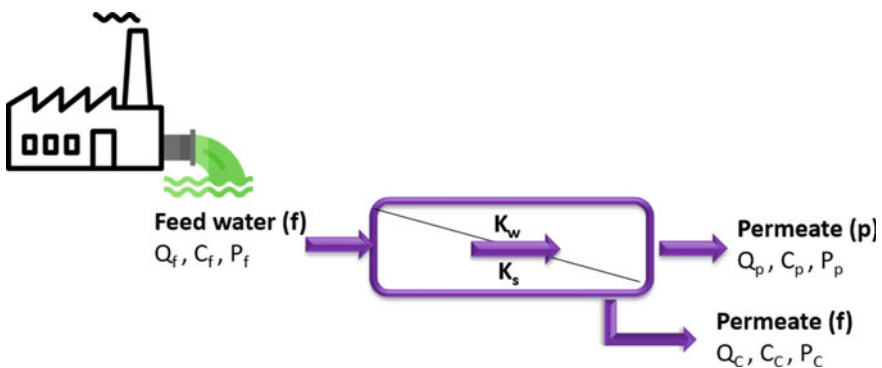
Fig. 2 Mass balance across the nanofiltration membrane system

Table 4 Summary of parameters and equations of spiral wound nanofiltration

Parameters	Equations[a]
Recovery %	$= \frac{Q_p}{Q_f} \times 100$ (10)
Salt Passage, SP %	$= \frac{C_{p\text{TDS}}}{C_{f\text{TDS}}} \times 100$ (11)
Salt Rejection, SR %	$= 100 - (\text{SP})$ % (12)
Membrane surface concentration, (Kg m^{-3})	$C_m = \frac{C_f + C_b}{2}$ (13)
Total Concentrate, ΔC	$= \beta \, x \, (C_m - C_p)$ (14)
Average Osmotic Pressure	$\Delta\pi_m$ (Pa) $= 0.0104 \, (T + 273/293) \, x \, C_m$ (15)
Net Driving Pressure, NDP	$= (\Delta P - \beta) \times \Delta\pi_m$ (16)
Permeate Flux, J_w (L m^{-2} h^{-1})	$= \frac{Q_p}{A} \times 100$ (17)
Salt Transport, Q_s	$= K_s \, x \, A \, x \, \Delta C \, x^* \, \text{TCF}$ (18)

[a]Q_p: Permeate Flowrate, Q_f: Feed Flowrate, C_p: Permeate concentration (Kg m^{-3}), C_f: Feed concentration (Kg m^{-3}), C_b: Bulk concentration (Kg m^{-3}), β: fouling coefficients, T: temperature, ΔP: Transmembrane pressure (kPa), A: Membrane area, K_s: mass transfer coefficient (m s^{-1}), TCF: Temperature correction factor

$$Q_f C_f = Q_C C_f + Q_p C_f \qquad (9)$$

where Q_f: flow rate, C_f: concentration.

We focus in this chapter on the module of spiral wound NF membranes. Their performance can be estimated using the following parameters in Table 4.

B. **Spiegler-Kedem-Kachalsky model (SKK)**

This model was derived from the thermodynamics of irreversible process to explain the salt rejection of a single electrolyte. After that, SKK is extended to include the salt rejection in the existence of a retained organic substance such as dyes in Eq. 19 [44].

$$r_s = \frac{(1 - \sigma_s) \cdot \left(1 + \frac{v \cdot C_D}{c_s}\right)^{0.5}}{1 - \sigma_s \exp\left[\frac{-(1 - \sigma_s) \cdot J}{P_s}\right]} \qquad (19)$$

where r_s: salt rejections, σ_s C_s: salt concentration, C_D: dye concentration, and v: charges number on dye ion.

Furthermore, there is an opposite Donnan effect on dye rejection with the following equation for dye rejection (r_D) in the presence of salt due to concentration polarisation (C_D (m)/C_D) as follows:

$$r_D = 1 - \left(1 - r_D^0\right)\left(1 + \frac{c_s}{\rho . e^{\vartheta . c_s c_D} v . c_D}\right)^{0.5} \tag{20}$$

$$\frac{c_D(m)}{c_D} = \rho . e^{\vartheta . c_s c_D} \tag{21}$$

The separation factor of NF membrane is illustrated by Eq. 22.

$$f = \frac{1 - r_s}{1 - r_D} \tag{22}$$

The SKK is usually employed to predict the removal performance of nanofiltration. It is determined by the solute and solvent fluxes, as well as the chemical potential gradient caused by a concentration or pressure gradient (driving forces) [11]. Therefore, the transportation of solute and solvent is predicted by SKK model regardless the type of solute and solvent (for further information, see [10, 11]). It was found that the rejection of uncharged organics by NF membranes is primarily affected by steric hindrances. Whereas the high rejection of polar organics is due to electrostatic interactions with the charged membrane surface.

4 Conclusions

Nanofiltration membranes (NF) have been applied successfully in dyes rejections with high rates. The functional groups of NF membrane have a role on the efficiency of dyes rejection. The dye removal process is dominated by NF surface charge. However, the polymeric NF membranes revealed no significant variations in the rejection of the negatively and positively charged dyes. Furthermore, the integration of nano-coatings on NF membranes can enhance the performance of the membrane without affecting on the solute rejection significantly. However, there are still technical barriers in the application of NF in dyes effluents treatment such as fouling, insufficient rejection, poor durability, and instability.

References

1. Abdel-Fatah MA (2018) Nanofiltration systems and applications in wastewater treatment. Ain Shams Eng J 9:3077–3092
2. Badr NBE, Al-Qahtani KM, Mahmoud AED (2020) Factorial experimental design for optimizing selenium sorption on Cyperus laevigatus biomass and green-synthesized nano-silver. Alex Eng J 59:5219–5229
3. Chakraborty S, Purkait MK, DasGupta S, De S, Basu JK (2003) Nanofiltration of textile plant effluent for color removal and reduction in COD. Sep Purif Technol 31:141–151
4. Childress AE, Elimelech M (1996) Effect of solution chemistry on the surface charge of polymeric reverse osmosis and nanofiltration membranes. J Membr Sci 119:253–268
5. Conlon WJ, Hornburg CD, Watson BM, Kiefer CA (1990) Membrane softening: The concept and its application to municipal water supply. Desalination 78:157–175
6. El Din MA, Fawzy M (2016) Bio-based Methods for Wastewater Treatment: Green Sorbents. In: Ansari AA, Gill SS, Gill R, Lanza GR, Newman L (eds) Phytoremediation: management of environmental contaminants, vol 3. Springer International Publishing, Cham, pp 209–238
7. Fan H, Gu J, Meng H, Knebel A, Caro J (2018) High-flux membranes based on the covalent organic framework COF-LZU1 for selective dye separation by nanofiltration. Angew Chem Int Ed 57:4083–4087
8. Freger V (2005) Kinetics of film formation by interfacial polycondensation. Langmuir 21:1884–1894
9. Guo D, Xiao Y, Li T, Zhou Q, Shen L, Li R, Xu Y, Lin H (2020) Fabrication of high-performance composite nanofiltration membranes for dye wastewater treatment: mussel-inspired layer-by-layer self-assembly. J Colloid Interface Sci 560:273–283
10. He Q-L, Guo P, Zhao L (2019) Derivation of film theory coupled Spiegler-Kedem-Katchalsky model for membrane separation and purification. arXiv 1912.11753
11. Hidalgo AM, León G, Gómez M, Murcia MD, Gómez E, Gómez JL (2013) Application of the Spiegler–Kedem–Kachalsky model to the removal of 4-chlorophenol by different nanofiltration membranes. Desalination 315:70–75
12. Jin J, Du X, Yu J, Qin S, He M, Zhang K, Chen G (2020) High performance nanofiltration membrane based on SMA-PEI cross-linked coating for dye/salt separation. J Membr Sci 611:118307
13. Jin P, Zhu J, Yuan S, Zhang G, Volodine A, Tian M, Wang J, Luis P, Van der Bruggen B (2021) Erythritol-based polyester loose nanofiltration membrane with fast water transport for efficient dye/salt separation. Chem Eng J 406:126796
14. Katheresan V, Kansedo J, Lau SY (2018) Efficiency of various recent wastewater dye removal methods: A review. J Environ Chem Eng 6:4676–4697
15. Koyuncu I (2002) Reactive dye removal in dye/salt mixtures by nanofiltration membranes containing vinylsulphone dyes: effects of feed concentration and cross flow velocity. Desalination 143:243–253
16. Koyuncu I (2003) Influence of dyes, salts and auxiliary chemicals on the nanofiltration of reactive dye baths: experimental observations and model verification. Desalination 154:79–88
17. Long Q, Zhang Z, Qi G, Wang Z, Chen Y, Liu Z-Q (2020) Fabrication of Chitosan Nanofiltration Membranes by the Film Casting Strategy for Effective Removal of Dyes/Salts in Textile Wastewater. ACS Sustain Chem Eng 8:2512–2522
18. Mahmoud A, Stolle A, Stelter M, Braeutigam P (2018a) Adsorption technique for organic pollutants using different carbon materials, abstracts of papers of the american chemical society. Amer Chem Soc 1155 16th st, NW, Washington, DC 20036 USA
19. Mahmoud AED, Fawzy m, Radwan A (2016): Optimization of Cadmium (CD2+) removal from aqueous solutions by novel biosorbent. Int J Phytoremed 18:619–625
20. Mahmoud AED, Stolle A, Stelter M (2018) Sustainable synthesis of high-surface-area graphite oxide via dry ball milling. ACS Sustain Chem Eng 6:6358–6369
21. Mahmoud AED (2020a) Graphene-based nanomaterials for the removal of organic pollutants: Insights into linear versus nonlinear mathematical models. J Environ Manag 270:110911

22. Mahmoud AED (2020b) Eco-friendly reduction of graphene oxide via agricultural byproducts or aquatic macrophytes. Mater Chem Phys 253:123336
23. Mahmoud AED (2020) Nanomaterials: Green Synthesis for Water Applications. In: Kharissova OV, Martínez LMT, Kharisov BI (eds) Handbook of Nanomaterials and Nanocomposites for energy and environmental applications. Springer International Publishing, Cham, pp 1–21
24. Mahmoud AED, Franke M, Stelter M, Braeutigam P (2020) Mechanochemical versus chemical routes for graphitic precursors and their performance in micropollutants removal in water. Powder Technol 366:629–640
25. Mahmoud AED, Umachandran K, Sawicka B, Mtewa TK (2021) 26—water resources security and management for sustainable communities. In: Mtewa AG, Egbuna C (eds), Phytochemistry, the Military and Health. Elsevier, pp 509–522
26. Mi Y-F, Xu G, Guo Y-S, Wu B, An Q-F (2020) Development of antifouling nanofiltration membrane with zwitterionic functionalized monomer for efficient dye/salt selective separation. J Membr Sci 601:117795
27. Moradi G, Zinadini S, Rajabi L (2020) Development of high flux nanofiltration membrane using para-amino benzoate ferroxane nanoparticle for enhanced antifouling behavior and dye removal. Process Saf Environ Prot 144:65–78
28. Mousazadeh M, Alizadeh SM, Frontistis Z, Kabdaşlı I, Karamati Niaragh E, Al Qodah Z, Naghdali Z, Mahmoud AED, Sandoval MA, Butler E, Emamjomeh MM (2021) Electrocoagulation as a promising Defluoridation technology from water: a review of state of the art of removal mechanisms and performance trends 13:656
29. Obotey Ezugbe E, Rathilal SJM (2020) Membrane technologies in wastewater treatment: a review. 10:89
30. Park M, Snyder SA (2020) Attenuation of contaminants of emerging concerns by nanofiltration membrane: rejection mechanism and application in water reuse, Contaminants of Emerging Concern in Water and Wastewater. Elsevier, pp 177–206
31. Peydayesh M, Mohammadi T, Bakhtiari O (2018) Effective treatment of dye wastewater via positively charged TETA-MWCNT/PES hybrid nanofiltration membranes. Sep Purif Technol 194:488–502
32. Rajabi H, Ghaemi N, Madaeni SS, Daraei P, Astinchap B, Zinadini S, Razavizadeh SH (2015) Nano-ZnO embedded mixed matrix polyethersulfone (PES) membrane: Influence of nanofiller shape on characterization and fouling resistance. Appl Surf Sci 349:66–77
33. Sawicka B, Umachandran K, Fawzy M, Mahmoud AED (2021) 27 - Impacts of inorganic/organic pollutants on agroecosystems and eco-friendly solutions. In: Mtewa AG, Egbuna C (eds), Phytochemistry, the Military and Health. Elsevier, pp 523–552
34. Siddique T, Dutta NK, Roy Choudhury N (2020) Nanofiltration for arsenic removal: challenges. Recent Develop Perspect 10:1323
35. Sójka-Ledakowicz J, Koprowski T, Machnowski W, Knudsen HH (1998) Membrane filtration of textile dyehouse wastewater for technological water reuse. Desalination 119:1–9
36. Sridhar S (2018) Membrane technology: sustainable solutions in water, health. CRC Press, Energy and Environmental Sectors
37. Tang CY, Kwon Y-N, Leckie JO (2009) Effect of membrane chemistry and coating layer on physiochemical properties of thin film composite polyamide RO and NF membranes: II. Membrane physiochemical properties and their dependence on polyamide and coating layers. Desalination 242:168–182
38. Thong Z, Gao J, Lim JXZ, Wang K-Y, Chung T-S (2018) Fabrication of loose outer-selective nanofiltration (NF) polyethersulfone (PES) hollow fibers via single-step spinning process for dye removal. Sep Purif Technol 192:483–490
39. Vambol S, Vambol V, Mozaffari N, Mahmoud AED, Ramsawak N, Mozaffari N, Ziarati P, Khan NA (2021) Comprehensive insights into sources of pharmaceutical wastewater in the biotic systems, Pharmaceutical Wastewater Treatment Technologies. IWA, p 17
40. Van der Bruggen B, Daems B, Wilms D, Vandecasteele C (2001) Mechanisms of retention and flux decline for the nanofiltration of dye baths from the textile industry. Sep Purif Technol 22–23:519–528

41. Van der Bruggen B, Vandecasteele C, Van Gestel T, Doyen W, Leysen R (2003) A review of pressure-driven membrane processes in wastewater treatment and drinking water production. Environ Prog 22:46–56
42. Williams ME (2003) A review of reverse osmosis theory. EET Corporation Williams Engineering Services Company, Inc
43. Wu J, Eiteman MA, Law SE (1998) Evaluation of membrane filtration and ozonation processes for treatment of reactive-dye wastewater. J Environ Eng 124:272–277
44. Xu X, Spencer HG (1997) Dye-salt separations by nanofiltration using weak acid polyelectrolyte membranes. Desalination 114:129–137
45. Ye W, Lin J, Borrego R, Chen D, Sotto A, Luis P, Liu M, Zhao S, Tang CY, Van der Bruggen B (2018) Advanced desalination of dye/NaCl mixtures by a loose nanofiltration membrane for digital ink-jet printing. Sep Purif Technol 197:27–35
46. Zhao G, Hu R, He Y, Zhu H (2019) Physically coating nanofiltration membranes with graphene oxide quantum dots for simultaneously improved water permeability and salt/dye rejection. Adv Mater Interfaces 6:1801742
47. Zheng Y, Yu S, Shuai S, Zhou Q, Cheng Q, Liu M, Gao C (2013) Color removal and COD reduction of biologically treated textile effluent through submerged filtration using hollow fiber nanofiltration membrane. Desalination 314:89–95

Application of Ultrafiltration Membrane Technology for Removal of Dyes from Wastewater

Denga Ramutshatsha-Makhwedzha and Philiswa Nosizo Nomngongo

Abstract Water pollution is normally amplified by wastewater effluent points such as mining activities, textile industries, municipal discharge. Amongst them, textile industries are one of the biggest contributors of various types of dyes in wastewater. Different types of membranes have been used in the treatment of dyes in wastewater such as ultrafiltration (UF), nanofiltration (NF), reverse osmosis (RO) and microfiltration (MF). UF membrane technology has been used as a separation technique for wastewater and purification purpose. This chapter reviews the fundamentals and applications of UF membrane filtration technology for the dye removal in wastewater and their future perspective in UF application.

Keywords Membrane · Ultrafiltration · Wastewater · Dyes · Filtration · Water Pollution · Textile industries

1 Introduction

The global crisis of drinking water is one of the challenges that the humankind is currently facing. The clean water is normally polluted by differing types of wastewater effluents generated from different supply points such as mining activities, textile industries, municipal discharge, etc. [17, 50]. Among them, textile, printing and paper industries and municipal discharge are the most contributing to the presence of different types of dyes in wastewater [17]. Regrettably, most textile industries choose to dispose of their wastewater effluents to the surrounding environment because it is quite difficult to treat this kind of waste [21].

In addition, wastewater quality from textile varies with time and includes various types of solvents, heavy metals, dyes and inorganic salts, the type of process used is important because the chemical concentrations depend on it [20]. Low biodegradability of dyes together with chemicals used in the textile industries makes it difficult

D. Ramutshatsha-Makhwedzha · P. N. Nomngongo (✉)
Department of Chemical Sciences, Doornfontein Campus, University of Johannesburg,
P.O. Box 17011, Johannesburg 2028, South Africa

37

for biological treatment by activated sludge to treat these dyes, and most of them resist aerobic biological treatment and oxidizing agents.

The presence of these chemicals in aquatic environment reduces sun light penetration into the water and afterwards photosynthesis as well as dissolved oxygen that leads to endangering the aquatic microorganism and organism's life [19]. As a result, modern treatment technology is vital, especially if there will be a need to recycle treated wastewater [36].

Different techniques were previously applied for the treatment of dyes in wastewater including electrochemical method [24], filtration [11], adsorption [9], oxidation [22] and chemical coagulation [6]. Membrane filtration can offer a feasible solution in the removal of salt, chemical oxygen demand and dyes from wastewater.

Generally, membranes are responsible for most separation processes such as fractionation, removal and distillation. Their advantages include simple up-scaling, low energy consumption and it has more chances for continuous separation [4].

The industrial membrane processes for water treatment are RO, UF, MF and NF, the main difference being the pore sizes [11]. NF, RO and MF are beyond the scope of this chapter, only UF was covered here. However, the UF membrane technology has been developed for different wastewater purification purposes [36] such as removal of particulates and macromolecules from raw water for drinking water production. The UF membrane filtration uses either concentration gradients or pressure forces to enable separation through semipermeable membranes. In many cases, UF membranes are used for pre-filtration purposes in RO plant to protect the RO membranes. UF is used after the clarification stage, along with MF and NF is used for the mechanical, physical, biological and separation of solids from the treated water. UF is not fundamentally different from MF, but both techniques separate based on particle capture or size exclusion. UF membranes are also described by the molecular weight cut-off (MWCO) of the membrane used and are mainly dead-end mode or applied in cross-flow [5, 51]. In recent decades, the potential of the membrane technology to produce high-quality effluents has led to its growing applications. Industrial polymers are commonly used for UF membrane fabrication such as iron/aluminium hydrolysed precipitate layer [28], polyferric chloride (PFC) [14], powder activated carbon (PAC) [40], graphene oxide (GO)/polyacrylonitrile (PAN) [17], polyphenylsulfone (PPSU)/nano tin oxide (SnO_2) [33] and polysilicate ferric manganese (PSFM) [42], just to name a few. However, this chapter aims at reviewing the application of UF membrane filtration technology for the dye removal from wastewater in the recent 8 years (2012–2020) and suggesting some ways of overcoming membrane challenges. The main subtitles that were discussed in this chapter was classification, sources, occurrence and health effects of dyes and fundamentals of a membrane system in UF. Application of UF membrane, conclusion and future perspectives in UF membrane applications for dye removal from wastewater were also explored.

2 Classification, Sources, Occurrence and Health Effects of Dyes

2.1 Natural Dyes

Dyes are grouped into two main classes: synthetic and natural dyes. Natural dyes are colourants derived from plant sources or parts such as roots, berries, leaves, bark, wood, lichens, invertebrates and minerals [49]. They are cheaper, non-polluting, non-carcinogenic, eco-friendly and easily available.

2.2 Synthetic Dyes

These are man-made dyes introduced in 1856 [2], and they are categorized based on their chemical composition including their methods used on their application in dyeing process. The most known synthetic dyes are cationic (basic), anionic dyes (acidic) and reactive dyes. They are mostly used in various sectors such as textile industries [45], paper industries [46], pharmaceutical [35] and food technology [18], among others. These types of dyes are known to be harmful to the environment as they contain different toxic chemicals when they are discharged into wastewater.

2.2.1 Anionic or Acidic Dyes

Acidic dyes are anionic dyes that are soluble in water and are used in fibres such as wool, nylon and silk using neutral to acid dye baths (e.g.: Methyl orange: MO, Thymol blue: TB, Congo red: CR, acid Fuchsin). MO which is made of sodiene 4-[(4-di-methlylamino) phenlydiazenyl] has benzene sulfonate that when discharged as effluent becomes harmful for living organisms. It is of outmost importance to treat these dyes whilst still in industrial wastewater before it is discharged in the environment [7]. Acid Orange 7 azo dye (AO7) is also one of the important anionic dyes that has chemical formula of $C_{16}H_{11}N_2NaO_4S$. The AO_7 dye has been used for colouring of wool and silk together with synthetic polyamide fibres, and it also consists of an azo group bound to aromatic rings [30]. Not only are they used for textile industries, they are also used for leather dyeing, cosmetic products and as well as papermaking industries [12]. As a result, these industries produce toxic residues that are harmful to the environment because AO7 is a carcinogenic compound that causes severe diseases after ingestion.

2.2.2 Cationic Dyes

Cationic dyes are basic dyes that are water-soluble and are mainly applied to acrylic fibres but find some use for silk and wool (e.g.: Indigo synthetic: IS, Methylene blue: MB, basic Fuchsin) [17]. Cationic dyes pose some disadvantages such as high toxicity, non-biodegradable and causing environmental pollution [7]. MB is a cationic thiazine dye that has the chemical name tetramethythionine chloride. It has a blue colour which makes it a suitable dye to be used in different industries such as plastic, cosmetic, leather and textile industries. The colour of a dye is determined by the ability of the substance to absorb light within the range of 400–700 nm electromagnetic spectrum.

2.2.3 Reactive Dyes

Reactive dyes are mostly used in the textile industry due to their wide variety of high wet fastness, mineral energy consumption, colour shades as well as easy application [27]. The use of reactive dyes among others requires large amount of salt such as 2 kg per kg of fabric to dye the fabric in textile dyeing. The salt is used to promote dye exhaustion, the reaction between the OH groups of the dye and cotton takes place due to the high temperature and alkaline medium [15]. Therefore, reactive dyeing wastewater contains large amounts of dissolved or suspended solids and organic pollutants that contain salt content and high pH, due to dyes that have not reacted which hydrolyse in water following the presence of hydroxyl.

3 Fundamentals of a Membrane System in Ultrafiltration

UF system is an ideal and economical alternative membrane filtration to RO technology, used for wastewater and sewage purification, but both use a semipermeable membrane. This semipermeable membrane helps the system to take out chemicals, infective microorganisms, organic and particulate matters efficiently from the wastewater at low pressure, resulting in a purified potable water source [47]. The primary task of the system is to confiscate the substances which contribute to the colour, taste and odour of water. The employment of a UF membrane system enables one to quickly pull out all such particulates and substances that pollute the water and make it injurious to health. However, in detail, the primary advantages of the UF system are quite long, and in this chapter, only the most key benefits of UF water purification system were discussed. UF does not entail any requirement for power to operate as it can be performed with a normal pressure. Thus, without paying the electric bill or spending any energy, you can get healthy, potable and sanitized water. UF takes out germs and bacteria mercilessly; while other purification systems such as ultra-violet (UV) kills germs, viruses and bacteria in drinking water itself [29], UF is the only system that pulls out the eggs from water, hence ensuring a complete,

safe and drinkable water. The UV systems additionally clean the bodies and eggs of both living and non-living virus and bacterium from the water. UF also removes a large amount of suspended and particulate solids as UF systems are proven to fish out all those matters that contribute to the colour, odour and taste of water. It can quickly cleanse the dirtiest water and make it suitable for drinking [47, 29].

3.1 Advances in Membrane Technology

Membrane technology covers all related engineering and scientific methods for the rejection or transport of substances by the membranes. However, it gives a full explanation on the mechanical separation process of liquid or gas streams [38]. Because of its multidisciplinary nature, membrane technology is also used in wastewater treatments such as domestic or industrial water supply, beverages, biotechnological, chemical, metallurgy, food pharmaceutical and other separation processes [38, 31, 10]. Membrane technology has main advantages such as adjustment of membrane properties, continuous separation under mild conditions, possible hybrid processing and easy up-scaling. Other advantages are its flexibility in system design and generation of high-quality products. The drawbacks of membrane technology are low lifetime, selectivity and flux of the membrane, linear up-scaling, membrane fouling and concentration polarization. Although concentration polarization and membrane fouling are listed as drawbacks, they fortunately form part of a separation process [38]. By applying this technology, therefore, the separation can be uninterruptedly done under normal conditions without the need for additives and with low energy consumption. However, the membrane technology can be used with incorporation of different nanomaterials or combined with other separation techniques, forming a blended process [38].

3.2 UF Membrane Challenges

UF is among well-known pressure-driven membrane separation processes (NF, MF and RO) that is a compact and refined filtration method. It is mostly applied in wastewater treatment, from pre-treatment to post-treatment stages with a capacity of removing solids as small as 0.01 microns, including viruses and silt [11]. However, membrane filtration technologies can have problems without proper care for appropriate pre-treatment, operation and maintenance. UF membranes are typically affected by the following main issues such as membrane fouling that is caused by the deposition of inorganic components, solid particles, membrane scaling, microbiological contaminants, waste stream disposal and increased permeate contamination [23]. However, different ways were developed to overcome UF membrane challenges including the incorporation of inorganic nanomaterials such as nanometre-sized metal oxides (zinc and tin oxides), graphene oxide, silver nanoparticles into a

polymer matrix [41]. Moreover, the incorporation of some nanoparticles is expected to improve the surface properties of the membrane [48]. For example, several metal oxide nanomaterials have shown strong antimicrobial properties by preventing biofouling process through multiple mechanisms that has photocatalytic production of reactive oxygen species [53]. Among these inorganic nanoparticles, tin oxide nanoparticles have attracted a great attention because of their remarkable photo-catalytic behaviour with mechanisms that has been well-established and superhy-drophilicity [53, 37]. In a different work, [32] used UF membrane-incorporated silver nanoparticles, and the results revealed a significant enhancement, due to the incorporation of these nanomaterials, on the destruction effect of bacteria in water source. In addition, many studies show that the existence of these inorganic nano-materials can possibly change the morphology of a membrane to a more porous structure, consequently enhancing and modifying the performance of a membrane by improving mechanical strength, fouling resistance and water permeability [25].

4   Applications of Ultrafiltration Membrane for Removal of Dyes

UF technique has received so much attention in the field of dye effluent treatment [44]. When determining the efficiency for UF in dye removal, two parameters, such as permeate flux (L/m^{2}h) and dye rejection (R%), are calculated using Eqs. (1) and (2).

$$J_p = \frac{V}{S \times t} \tag{1}$$

$$R = \left(1 - \frac{C_p}{C_i}\right) \times 100 \tag{2}$$

where C_i represents the initial feed concentration (Mm), C_p is dye concentration in the permeate (Mm), t is the time difference in hours (h), S is the membrane area (m^2) and V is the volume of permeate (L).

Removal of anionic dye MO has been investigated on the synthesized cationic charged polymer species through the emulsion polymerization that is used as poly-electrolytes in the polyelectrolyte enhanced ultrafiltration (PEUF) [39]. Results showed a complete removal of MO at a concentration up to 50 mg L^{-1} and polymer concentration of 1 g L^{-1}. However, removal decreases when MO concentration increases due to electrostatic repulsion and steric hindrance. Remazol dye removal from wastewater was investigated using micellar-enhanced ultrafiltration membrane (MEUF). This technology involves UF and surfactant combination that has concen-tration with higher surfactant's critical micelle concentration (CMC). The decrease in flux has been observed with increase of filtration time. This was due to the addition

of surfactant in the MEUF system, with observed permeate rejection of Remazol dye concentration of more than 96%, respectively [3].

Reference [13] investigated the removal of MB cationic dye by polyelectrolyte ultrafiltration (PAUF). Results obtained under the optimum conditions of response surface methodology were the following, permeation flux of 71 L/m²h and dye rejection efficiency of 99%, respectively. The major drawbacks encountered were permeation flux decline due to concentration polarization following continuous ultrafiltration. Ultrafiltration membrane has been modified by thermo-responsive poly (N-vinylcaprolactam-titanium oxide-acrylic acid) (VCL-TiO$_2$-AA) polymer and results show high rejection percentage of 97%. The antifouling of the prepared membrane confirms the significant antifouling in nature [43].

Natural coagulant made of combined CF processes with modified-UF membrane was used for the removal of reactive black 5 dye. The pH of the dye solution shows that there were no significant change after the CF coagulant. This avoids unnecessary costs of pH adjustments making CF a good coagulant [8]. The study of ultrafiltration membrane Polyphenylsulfone (PPSU) was conducted on removal of various proteins such as bovine serum albumin (BSA), as well as hazardous dyes like reactive orange 16 (RO-16) and reactive black 5 (RB-5) in aqueous solutions [34]. Modified membranes (PZ-1, PZ-2 and PZ-3) by zeolite ZSM-5 offers outstanding results with good resistance to adsorption of proteins, dyes and also good antifouling ability. Rejection percentages exhibited by higher additive membrane (PZ-3) for reactive dyes are 90.81% for RB-5 and 82.84% RO-16. Addition of ZSM-5 in membrane contributed to better removal of dye due to its hydrophilic and adsorptive nature [34].

5 Conclusion and Future Perspectives in UF Membrane Applications for Dye Removal from Wastewater

There is an unending list of dyes pertaining to UF membrane in wastewater treatment where permeate reflux could range between 53 and 266.81 L/m²h. This chapter summarizes some of the paramount ones that are used, their removal and initial feed concentrations, challenges, as well as some cited examples. However, membrane sensitivity to toxicity and membrane fouling are the major restrictions of the membrane technology. The study of modified membranes by zeolite ZSM-5 offers outstanding results with good resistance to adsorb dyes, proteins and good antifouling ability. The micellar-enhanced ultrafiltration membrane (MEUF) which involves UF, and surfactant combination has contributed to increase in filtration time together with increased dye rejection of 96%.

In the treatment of wastewater sources, the single UF technology is not very effective due to some drawbacks such as membrane fouling and scaling, but when combined with other processes, it can show good performance. Removal of dye solution from aqueous solution is still a major challenge. More investigations still need to be carried out on the treatment of textile effluents and scaling up for pilot

Table 1 Applications of UF membrane systems in wastewater treatment [8 years ago: 2012–2020]

Polymer	Filler	Names of dyes	Initial feed concentration (mg/L)	Removal achieved	Permeate flux (L/m²h)	References
–	Ceramic	Black 5	50	79.80	266.81	[1]
PSS	–	Methylene blue	50	Rejection efficiency 99.0%	71.50	[13]
–	Alumina	Direct Red 80	100	Rejection rate of 99.6%	230.20	[26]
–	TiO$_2$	Black 5 dye	10	100%	875	[8]
PEI	–	Acid-Orange 7	83	Rejection efficiency 99.2%	108.4	[12]
Cellulose	–	Methyl Orange	50	>90%	147	[39]
PAN-ETA	–	Methyl Blue	100	96%	53	[52]
–	Chitosan	Direct blue	–	89%	131	[16]

Foot note [PSS]: polystyrene sulfonate, [PEI]: Polyethylenimine, [PAN]: Polyacrylonitrile

effluent. Confidently, this chapter is useful because it provides good information to carry out the application of membrane technology in future and their challenges in wastewater treatment.

References

1. Alventosa-deLara E, Barredo-Damas S, Alcaina-Miranda MI, Iborra-Clar MI (2012) Ultra-filtration technology with a ceramic membrane for reactive dye removal: Optimization of membrane performance. J Hazard Mater 209–210, 492–500. https://doi.org/10.1016/j.jhazmat.2012.01.065
2. Arora J, Agarwal P, Gupta G (2017) Rainbow of natural dyes on textiles using plants extracts: sustainable and eco-friendly processes. Green Sustain Chem. https://doi.org/10.4236/gsc.2017.71003
3. Aryanti N, Sandria FKI, Putriadi RH, Wardhani DH (2017) Evaluation of micellar-enhanced ultrafiltration (MEUF) membrane for dye removal of synthetic Remazol dye wastewater. Eng J 21(3):23–35. https://doi.org/10.4186/ej.2017.21.3.23
4. Baker RW (2012) Membrane technology and applications. Mem Techn Appl. https://doi.org/10.1002/9781118359686
5. Basile A, Pereira Nunes S (2011) Advanced membrane science and technology for sustainable energy and environmental applications. In: Advanced Membrane Science and Technology for Sustainable Energy and Environmental Applications. https://doi.org/10.1533/9780857093790
6. Bazrafshan E, Alipour MR, Mahvi AH (2016) Textile wastewater treatment by application of combined chemical coagulation, electrocoagulation, and adsorption processes. Desalinat Water Treatment. https://doi.org/10.1080/19443994.2015.1027960

7. Bello K, Sarojini BK, Narayana B, Rao A, Byrappa K (2018) A study on adsorption behavior of newly synthesized banana pseudo-stem derived superabsorbent hydrogels for cationic and anionic dye removal from effluents. Carbohydrate Poly 181(December):605–615. https://doi.org/10.1016/j.carbpol.2017.11.106

8. Beluci N, de CL, Mateus GAP, Miyashiro CS, Homem NC, Gomes RG, Fagundes-Klen MR, Vieira AMS (2019) Hybrid treatment of coagulation/flocculation process followed by ultrafiltration in TiO_2 -modified membranes to improve the removal of reactive black 5 dye. Sci Total Environ 664:222–229. https://doi.org/10.1016/j.scitotenv.2019.01.199

9. Cai Z, Sun Y, Liu W, Pan F, Sun P, Fu J (2017) An overview of nanomaterials applied for removing dyes from wastewater. Environ Sci Pol Res https://doi.org/10.1007/s11356-017-9003-8

10. Castro-Muñoz R, Gontarek E, Figoli A (2019) Membranes for toxic- and heavy-metal removal. In: Current Trends and Future Developments on (Bio-) Membranes: Membranes in Environmental Applications. https://doi.org/10.1016/B978-0-12-816778-6.00007-2

11. Chollo MN (2014) 3(July):1–144. Retrieved from http://hdl.handle.net/10321/1388

12. Cojocaru C, Clima L (2020) Polymer assisted ultrafiltration of AO_7 anionic dye from aqueous solutions: experimental design, multivariate optimization, and molecular docking insights. J Mem Sci 604(January):118054. https://doi.org/10.1016/j.memsci.2020.118054

13. Dasgupta J, Singh A, Kumar S, Sikder J, Chakraborty S, Curcio S, Arafat HA (2016) Poly (sodium-4- styrenesulfonate) assisted ultrafiltration for methylene blue dye removal from simulated wastewater: optimization using response surface methodology. J Environ Chem Eng 4(2):2008–2022. https://doi.org/10.1016/j.jece.2016.03.033

14. Dong H, Gao B, Yue Q, Rong H, Sun S, Zhao S (2014). Effect of Fe (III) species in polyferric chloride on floc properties and membrane fouling in coagulation-ultrafiltration process. Desalinat. https://doi.org/10.1016/j.desal.2013.12.018

15. Erkanlı M, Yilmaz L, Çulfaz-Emecen PZ, Yetis U (2017) Brackish water recovery from reactive dyeing wastewater via ultrafiltration. J Clean Product 165:1204–1214. https://doi.org/10.1016/j.jclepro.2017.07.195

16. Fradj A, Ben, Boubakri A, Hafiane A, Hamouda S, Ben (2020) Removal of azoic dyes from aqueous solutions by chitosan enhanced ultrafiltration. Results in Chemistry, 2. https://doi.org/10.1016/j.rechem.2019.100017

17. Fryczkowska B (2018) The application of ultrafiltration composite GO/PAN membranes for removing dyes from textile wastewater. Desalinat Water Treat, 128(November):79–88. https://doi.org/10.5004/dwt.2018.22599

18. Galaup C, Auriel L, Dubs J, Dehoux C, Gilard V, Poteau R, … Collin F (2019) Blue wine, a color obtained with synthetic blue dye addition: two case studies. Eu Food Res Tech https://doi.org/10.1007/s00217-019-03295-z

19. Hammami A, Charcosset C, Ben Amar RR (2017) Performances of continuous adsorption-ultrafiltration hybrid process for AO_7 dye removal from aqueous solution and real textile wastewater treatment. J Mem Sci Tech. https://doi.org/10.4172/2155-9589.1000171

20. Hassani H, Mirzayee R, Nasseri S, Borghei M, Gholami M, Torabifar B (2008) Nanofiltration process on dye removal from simulated textile wastewater. Int J Environ Sci Tech. https://doi.org/10.1007/BF03326035

21. Karisma D, Febrianto G, Mangindaan D (2018) Removal of dyes from textile wastewater by using nanofiltration polyetherimide membrane. IOP Conf Series: Earth Environ Sci. https://doi.org/10.1088/1755-1315/109/1/012012

22. Khatri J, Nidheesh PV, Anantha Singh TS, Suresh Kumar M (2018). Advanced oxidation processes based on zerovalent aluminium for treating textile wastewater. Chem Eng J. https://doi.org/10.1016/j.cej.2018.04.074

23. Koyuncu I, Sengur R, Turken T, Guclu S, Pasaoglu ME (2015) Advances in water treatment by microfiltration, ultrafiltration, and nanofiltration. In: Advances in Membrane Technologies for Water Treatment: Materials, Processes and Applications. https://doi.org/10.1016/B978-1-78242-121-4.00003-4

24. Kumar PS, Joshiba GJ, Femina CC, Varshini P, Priyadharshini S, Karthick MA, Jothirani R (2019) A critical review on recent developments in the low-cost adsorption of dyes from wastewater. Desalin Water Treat 172:395–416

25. Liang S, Xiao K, Mo Y, Huang X (2012) A novel ZnO nanoparticle blended polyvinylidene fluoride membrane for anti-irreversible fouling. J Mem Sci. https://doi.org/10.1016/j.memsci.2011.12.040

26. Liu Y, Zhu, W, Guan K, Peng C, Wu J (2018) Freeze-casting of alumina ultra-filtration membranes with good performance for anionic dye separation. CeramicsInt 44(10):11901–11904. https://doi.org/10.1016/j.ceramint.2018.03.160

27. Lykidou S, Karanikas E, Nikolaidis N, Tsatsaroni E (2017) Synthesis, characterization and ultrafiltration of reactive dyes. Application by exhaustion and/or ink-jet printing—II. Textile Res J 87(6):694–707. https://doi.org/10.1177/0040517516636004

28. Ma B, Yu W, Liu H, Yao J, Qu JH (2013) Effect of iron/aluminum hydrolyzed precipitate layer on ultrafiltration membrane. Desalinat 330:16–21. https://doi.org/10.1016/j.desal.2013.09.019

29. Mackenzie D (2020) Ultraviolet light fights new virus. Eng. https://doi.org/10.1016/j.eng.2020.06.009

30. Mancuso A, Sacco, O, Sannino D, Pragliola S, Vaiano V (2020) Enhanced visible-light-driven photodegradation of acid orange 7 azo dye in aqueous solution using Fe-N co-doped TiO_2. Arab J Chem 13(11):8347–8360. https://doi.org/10.1016/j.arabjc.2020.05.019\

31. Mehariya S, Lovine A, Casella P, Musmarra D, Chianese S, Marino T, … Molino A (2019) Bio-based and agriculture resources for production of bioproducts. In Current Trends and Future Developments on (Bio-) Membranes: Membranes in Environmental Applications. https://doi.org/10.1016/B978-0-12-816778-6.00012-6

32. Mollahosseini A, Rahimpour A, Jahamshahi M, Peyravi M, Khavarpour M (2012) The effect of silver nanoparticle size on performance and antibacteriality of polysulfone ultrafiltration membrane. Desalinat. https://doi.org/10.1016/j.desal.2012.08.035

33. Nayak MC, Isloor AM, Inamuddin, Prabhu, B, Norafiqah NI, Asiri AM (2019) Novel polyphenylsulfone (PPSU)/nano tin oxide (SnO_2) mixed matrix ultrafiltration hollow fiber membranes: fabrication, characterization and toxic dyes removal from aqueous solutions. Reactive Function Polym 139(March):170–180. https://doi.org/10.1016/j.reactfunctpolym.2019.02.015

34. Nayak MC, Isloor AM, Moslehyani A, Ismail N, Ismail AF (2018) Fabrication of novel PPSU/ZSM-5 ultrafiltration hollow fiber membranes for separation of proteins and hazardous reactive dyes. J Taiwan Ins Chem Eng 82, 342–350. https://doi.org/10.1016/j.jtice.2017.11.019

35. Pereira FAR, Sousa KS, Cavalcanti GRS, França DB, Queiroga LNF, Santos IMG, Jaber M (2017) Green biosorbents based on chitosan-montmorillonite beads for anionic dye removal. J Environ Chem Eng. https://doi.org/10.1016/j.jece.2017.06.032

36. Petrinić I, Bajraktari N, Hélix-Nielsen C (2015) Membrane technologies for water treatment and reuse in the textile industry. Adv Mem Technol Water Treat: Mater, Process Appl https://doi.org/10.1016/B978-1-78242-121-4.00017-4

37. Rahimpour A, Jahanshahi M, Mollahosseini A, Rajaeian B (2012) Structural and performance properties of UVassisted TiO_2 deposited nano-composite PVDF/SPES membranes. Desalinat. https://doi.org/10.1016/j.desal.2011.09.026

38. Saleh TA, Gupta VK (2016) An overview of membrane science and technology. Nano Poly Mem. https://doi.org/10.1016/b978-0-12-804703-3.00001-2

39. Schwarze M, Seo D, Bibouche B, Schomäcker R (2020) Comparison of positively charged polymer species and cationic surfactants for methyl orange removal via polyelectrolyte and micellar enhanced ultrafiltration. J Water Process Eng 36(2019):101287. https://doi.org/10.1016/j.jwpe.2020.101287

40. Shao S, Cai L, Li K, Li J, Du X, Li G, Liang H (2017) Deposition of powdered activated carbon (PAC) on ultrafiltration (UF) membrane surface: influencing factors and mechanisms. J Mem Sci 530:104–111

41. Som C, Wick P, Krug H, Nowack B (2011) Environmental and health effects of nanomaterials in nanotextiles and façade coatings. Environ Int https://doi.org/10.1016/j.envint.2011.02.013

42. Tang L, Xiao F, Wei Q, Liu Y, Zou Y, Liu J, Chow C (2019) Removal of active dyes by ultrafiltration membrane pre-deposited with a PSFM coagulant: performance and mechanism. Chemo 223:204–210. https://doi.org/10.1016/j.chemosphere.2019.02.034
43. Tang L, Xiao F, Wei Q, Liu Y, Zou Y, Liu J, Chow C (2019) Removal of active dyes by ultrafiltration membrane predeposited with a PSFM coagulant: Performance and mechanism. Chemo 223:204–210. https://doi.org/10.1016/j.chemosphere.2019.02.034
44. Tran TT, Van, Kumar, SR, Lue SJ (2019) Separation mechanisms of binary dye mixtures using a PVDF ultrafiltration membrane: donnan effect and intermolecular interaction. J Mem Sci 575(June 2018):38–49. https://doi.org/10.1016/j.memsci.2018.12.070
45. Unugul T, Nigiz FU (2020) Preparation and characterization an active carbon adsorbent from waste mandarin peel and determination of adsorption behavior on removal of synthetic dye solutions. Water, Air, and Soil Pol https://doi.org/10.1007/s11270-020-04903-5
46. Wang H, Han S, Wang J, Yu S, Li X, Lu L (2020) Preparation and synthetic dye decolorization ability of magnetic cross-linked enzyme aggregates of laccase from Bacillus amyloliquefaciens. Bioprocess Biosyst Eng. https://doi.org/10.1007/s00449-020-02481-8
47. Wang W, Yue Q, Li R, Bu F, Shen X, Gao B (2018) Optimization of coagulation pre-treatment for alleviating ultrafiltration membrane fouling: the role of floc properties on Al species. Chemo. https://doi.org/10.1016/j.chemosphere.2018.02.114
48. Wang XM, Li XY, Shih K (2011) In situ embedment and growth of anhydrous and hydrated aluminum oxide particles on polyvinylidene fluoride (PVDF) membranes. J Mem Sci. https://doi.org/10.1016/j.memsci.2010.11.038
49. Waring DR, Hallas G (eds) (2013). The chemistry and application of dyes. Springer Science & Business Media
50. Ye CC, Zhao FY, Wu JK, Weng XD, Zheng PY, Mi YF, Gao CJ (2017) Sulfated polyelectrolyte complex nanoparticles structured nanoflitration membrane for dye desalination. Chem Eng J. https://doi.org/10.1016/j.cej.2016.08.122
51. Youcai Z, Ziyang L (2016) Pollution control and resource recovery: municipal solid wastes at landfill. In: Pollution Control and Resource Recovery: Municipal Solid Wastes at Landfill
52. Yun J, Wang Y, Liu Z, Li Y, Yang H, Xu Z, Liang (2020) High efficient dye removal with hydrolyzed ethanolamine-Polyacrylonitrile UF membrane: Rejection of anionic dye and selective adsorption of cationic dye. Chemo 259:127390. https://doi.org/10.1016/j.chemosphere.2020.127390
53. Zhang M, Zhang K, De Gusseme B, Verstraete W (2012) Biogenic silver nanoparticles (bio-Ag_0) decrease biofouling of bio-Ag_0/PES nanocomposite membranes. Water Research. https://doi.org/10.1016/j.watres.2012.01.015

Progression and Application of Photocatalytic Membrane Reactor for Dye Removal: An Overview

Ayushman Bhattacharya and Selvaraj Ambika

Abstract Globally, textile industries are one of the rapidly growing industrial sectors that are not only contributing significantly towards the economy but are also generating an extensive variety of dyes as pollutants that vitiates the natural ecosystem. The increasing toxicity and recalcitrant nature of the industrial dye effluents are emerging concerns that require immediate attention. Treatment of dye-enriched water bodies and industrial effluents with advanced, economical, sustainable and efficacious technology is the need of the hour. The heterogeneous photocatalysis, an advanced oxidation process (AOP), is a novel and sustainable process that ensures photocatalytic degradation of dyes by generating reactive and oxidizing free radicals under ultraviolet (UV) and visible irradiation. Besides, integrating the membrane separation process with heterogeneous photocatalysis results in a holistic approach—photocatalytic membrane reactor (PMR). The PMR is reported to aid in (i) achieving higher pollution removal efficiency with complete detoxification and (ii) abating the membrane fouling. Coupling the fact of necessity to treat dye-contaminated water and the effective application of PMR, this chapter aims to elucidate the properties and classification of dyes, photocatalytic reaction mechanism and membrane fabrication methods. Also, the chapter conveys comprehensive information and fundamental understanding of different configurations and applications of Photocatalytic Membrane Reactor (PMR) with major emphasis on recent advancements.

Keywords Photocatalytic Membrane Reactor · Auxochrome · Chromophore · Dye Sensitization · Membrane Fabrication · Photocatalysis · Dye Removal

A. Bhattacharya · S. Ambika (✉)
Department of Civil Engineering, Indian Institute of Technology, Hyderabad, India
e-mail: ambika@ce.iith.ac.in

1   Introduction

Dyes are organic compounds that persist as an environmental pollutant and are muta-
genic, carcinogenic and toxic, and can endorse biomagnification [40]. Augmented
production, production and utilization of dyes generates a huge amount of dye-
contaminated water from industries. Industries mainly responsible for the discharge
of dyes are textile industries (54%), dyeing industries (21%), pulp and paper industry
(10%), paint and tanning industry (8%), dye concocting industry (7%), revealing
textile industry as the major polluter [55]. The incomplete removal of dyes in treat-
ment processes, due to the recalcitrant nature, reinforced their presence in surface
water and groundwater and is becoming a matter of great concern worldwide [33].
This further has adversely affected the environment and the health of mankind.
Besides, the existence of dyes in the aquatic ecosystem impedes the photosynthetic
activity which eventually lowers the dissolved oxygen and thereby posing a threat to
aquatic species. Conventional treatment methods for the treatment of organic contam-
inants are adsorption, biological treatment and coagulation–flocculation-based phys-
iochemical treatment. The coagulation-flocculation has limited application due to
the lower decolourization efficiency for the reactive and vat dyes along with higher
sludge generation, and operational cost [25]. In the case of adsorption, pollutants are
trapped in the high surface area of the adsorbents and exhibit higher colour removal
efficiency from wastewater comprising of dyes. Generally, activated carbon is used
as an adsorbent as it is cheap, but possess poor reusability and generates secondary
waste that needs supplementary treatment. In the case of biological treatment, soluble
organic dyes are easily degraded, whereas non-soluble dyes, containing heterocyclic,
polyaromatic hydrocarbons (PAHs), and polychlorinated biphenyls (PCBs) in their
structure, are resistant to the biological process. In addition, biological processes
require large land and suitable operating conditions as the bacterial populations are
very sensitive. Hence, there is a need for a robust treatment technique that over-
comes the above-said limitations and results in the complete eradication of dyes
from aqueous solution.

Advanced oxidation process (AOP) such as heterogeneous photocatalysis involves
the usage of semiconductor particles for the generation of highly oxidative radi-
cals under UV–Visible irradiation. This oxidizes and degrades the non-selective
organic pollutants and transforming them into mineralized products [60]. Though
the precious photocatalyst particles are efficient, due to the huddle in collecting
these particles for reuse, the process becomes resource-intensive and costly. This
compels attaching the particles to a template without compromising the function. In
the arena of wastewater and water treatment, the application of membranes is one of
the promising separation techniques which holds the advantages of enhanced erad-
ication of pollutants, tailor made to have a broader range of pollutants removal and
energy-efficient. Microfiltration (MF), Nanofiltration (NF), Reverse osmosis (RO)
and ultrafiltration (UF) are the generally employed membrane technologies [71]. The
challenges associated with the conventional membranes include membrane fouling
and the inability to degrade pollutants [70].

To synergize the benefits of photocatalysis and membrane-based treatment techniques, and to overcome the drawbacks, the photocatalyst particles can be attached on the membrane surface which results in photocatalytic membrane reactor (PMR). This PMR fosters photocatalysis of dyes and separation of products in one step with strict adherence to the green chemistry principle. Furthermore, the integration of the processes vanquishes the associated challenges of single treatment units. Having understood the importance of PMR in dye removal from the aqueous medium, this chapter outlines the properties and classification of dyes in use, mechanism of photocatalytic reactions and membrane fabrication methods. Correspondingly, the chapter discusses the different configurations and applications of Photocatalytic Membrane Reactor (PMR) with major emphasis on recent advancements.

2 Dyes Classification

Dyes are the unsaturated organic compounds that contain auxochromes and chromophores. Electronic properties of the chromophore molecules like double or triple bond-containing carbon–carbon, carbon–oxygen, nitrogen-nitrogen and carbon–nitrogen atoms influence the colour imparted by the dyes to the solution and are liable for the absorption of light in the UV visible spectrum that leads to excitation of electrons. The compound appears to be coloured when two conditions are fulfilled (i) chromophore molecules should be linked with a conjugated system, inducing bathochromic shift and (ii) the light absorption should take place in the visible spectrum (400–800 nm) [29]. Therefore, depending upon the structure of the dye molecule and the light absorption in UV visible spectrum, the chromophore molecules will cede the colour to the dyes. Based on the above understanding, Fig. 1a infers that chromophore molecules linked with aromatic ring generate colour, whereas no colour was produced when chromophore molecules were placed between methyl groups as shown in Fig. 1b. Both the wavelength and intensity of absorption vary when the covalent saturated group, i.e. auxochromes (NH$_2$, OH, COOH, SO$_3$, halogen, etc.) gets bonded with the chromophore [9, 24]. Auxochrome does not produce colour but modifies the light absorbing ability of the chromophore resulting in the colour
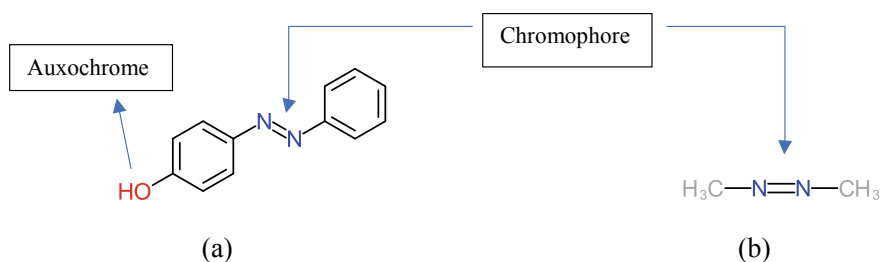

(a)   (b)

Fig. 1 **a** 4-Hydroxyazobenzene (Gurses et al. 2016) **b** Azomethane (Colourless) [29]

intensification of the dye, and therefore, they are known as colour enhancing group [59], (Gurses et al. 2016). Besides, the presence of auxochrome enhances the solubility of the dye and its affinity towards the fibre [55]. In aromatic dye structure, presence of electron donors like hydroxyl, carboxylic and nitrite group assists in electrophilic attack due to increase in electron density on the phenyl ring because of resonance effect causing higher photodegradation rate, whereas presence of chloro group reduces the photodegradation rate and renders the aromatic structure inactive due to their electron withdrawing tendency. Studies have revealed that the presence of any functional group that induces lower solubility of the dye molecules, depresses the rate of photodegradation. That is why higher alkyl chains are responsible for lowering of photodegradation rate [32].
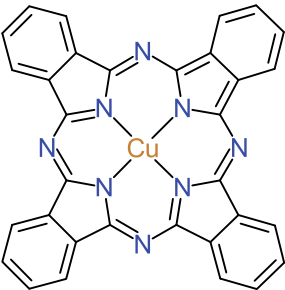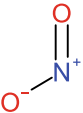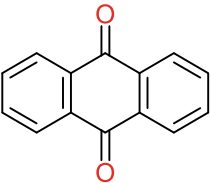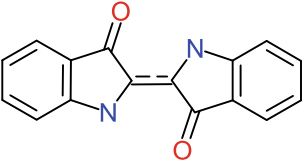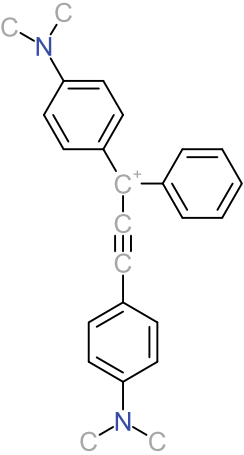
The dyes can be classified based on two features (i) chemical structure, more specifically on the chromophore grouping and (ii) applications [9, 10]. On the basis of chromophore grouping, dyes are categorized as azo dyes, indigo dyes, anthraquinone dyes, phthalocyanine dyes, xanthene dyes, phthalein dyes, nitrated and nitrosated dyes, oxazine, polymethinic dyes, acridine, diphenylmethane and triphenylmethane dyes as shown in Table 1. Among them, azo dyes are commonly employed in industrial applications and are non-biodegradable [13, 67]. Azo dyes comprise of double bond nitrogen atoms $(-N = N -)$ and are classified as mono-azo, di-azo, tri-azo and poly azo depending upon the number of $(-N = N -)$ bonds in the structure. The Van der Waals force of attraction between fibres and azo dyes gets fortified due to the presence of aromatic rings [48]. The area near the chromophore region is the attacking site for the photodegradation of azo dyes resulting in the cleavage of azo bonds either symmetrically or asymmetrically [11].

Furthermore, based on the application, dyes are classified as water-soluble and insoluble as follows.

a. Water Soluble Dyes
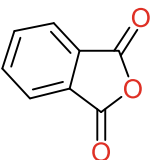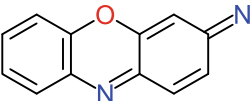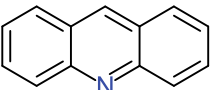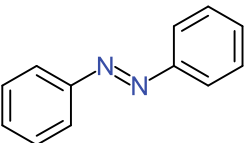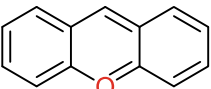
- Acid or Anionic dyes: These dyes are majorly utilized in the dyeing of fibres consisting of an amino group (NH_2) such as silk, polyamide and wool. Most of these dyes falls under the class of azo dyes and anthraquinone dyes.
- Basic or cationic dyes: These dyes possess the ability of directly imparting colour to the anionic sites-linked fibres. These dyes comprise of various chromophore groups falling under the class of azo, anthraquinone, triarylmethane, diarylmethane, anthraquinone.
- Reactive Dyes: It comprises of two vinylsulfone reactive groups and chromophore groups made from anthraquinone and azo dyes. Because of their stability, processing conditions and their greater ability to form covalent bonds with the fibres, reactive dyes are broadly used in the dyeing of cotton, silk and wool fibres.
- Direct or substantive dyes: For cellulose fibres, these dyes possess greater affinity and are significantly used for colouring paper products. Its chromophore grouping majorly includes azo and phthalocyanine.

Table 1 Dyes Classification based on Chromophore group [9, 10, 52, 54]

S. no.	Class	Chromophore
1	Phthalocyanine	
2	Nitro	
3	Anthraquinone	
4	Indigo	
5	Diphenyl Methane	

(continued)

Table 1 (continued)

S. no.	Class	Chromophore
6	Phthalein	
7	Oxazine	
8	Acridine	
9	Azo	
10	Xanthene	

b. Insoluble Dyes in Water

- Vat dyes: These dyes exhibit higher propinquity for cotton, rayon, silk, wool, cellulosic fibres and linen. Primarily possess solubility in hot water while few possess solubility in presence of sodium carbonate. Examples: Indigo carmine, Vat Yellow 1, Vat Black 25.
- Sulphur dyes: These dyes have similar use to vat dyes, contains sulphur-linked molecules produced from desulphurization of organic compounds, and are higher molecular weight dyes. Examples: Sulphur black and Sulphur blue 15.
- Disperse dyes: These are azo structure-based dyes and are mainly used for the dyeing of prefabricated fibres like polyamide and polyester with a suitable dispersing agent in the solution. Nano-sized disperse dye particles show good stability in the high-temperature dyeing process. Examples: Red Disperse 60, Blue disperse 7.

3   Dye Degradation Using Photocatalytic Membrane Reactor

3.1   Mechanism of Photocatalysis in Dye Removal from Aqueous Solution

The mechanism of the photocatalytic reaction is explained by considering TiO_2 as a photocatalyst. The photocatalytic reaction commences with Ultraviolet/Visible light irradiation having energy greater than the bandgap energy (E_g) of the TiO_2 photocatalyst (3.2 eV for anatase and 3.0 eV for rutile) [34, 69]. Upon irradiation, electrons present in the valence band absorb the energy, gets excited and migrates to the conduction band, leaving behind holes in the valence band. Photogenerated electrons then move to the catalyst surface and reduce the O_2 molecules present in the aqueous aerated solution or adsorbed O_2 molecules on the Ti(III) surface and convert them to superoxide radical (O_2^-) that can eliminate an extensive variety of dyes and can inactivate microorganisms. Oxygen molecule acts as an electron scavenger, and in its absence or shortage, photocatalytic reaction efficiency declines due to higher recombination of electrons and holes [3]. The recombination of charge species, i.e. electrons and holes results in the dissipation of heat [17].

Correspondingly, photogenerated holes take part in the oxidation reaction with H_2O and OH^- and converts them to hydroxyl radical ($OH^{\cdot}$) that acts as a strong oxidant and is responsible for the mineralization of organic compounds. Dye molecules adsorbed on the TiO_2 surface or are near to the catalyst surface are attacked by $OH^{\cdot}$ non-selectively [2]. Superoxide radicals and protons react and produce hydroperoxide radicals ($HO_2^{\cdot}$) that exhibit greater potential for the generation of $OH^{\cdot}$, and this generated $OH^{\cdot}$ produces the same effect as like $O_2^{\cdot-}$ [3, 41]. The pollutant concentration, irradiation time, loading of photocatalyst, presence of O_2, pH of the aqueous solution, wavelength and irradiation intensity are the major factors that influence the photocatalytic reactions [45]. The reactions involved in the photocatalytic process are as follows.

$$TiO_2 + h\nu \rightarrow e^- + h^+ \tag{1}$$

$$H_2O + h^+ \rightarrow OH^{\cdot} + H^+ \tag{2}$$

$$OH^- + h^+ \rightarrow OH^{\cdot} \tag{3}$$

$$Ti(IV) + e^- \rightarrow Ti(III) \tag{4}$$

$$Ti(III) + O_2 \rightarrow Ti(IV) + O_2^{\cdot-} \tag{5}$$

$$O_2{}^{\cdot-} + H^+ \rightarrow HO_2{}^{\cdot} \tag{6}$$

$$HO_2{}^{\cdot} + HO_2{}^{\cdot} \rightarrow H_2O_2 + O_2 \tag{7}$$

$$H_2O_2 + e^- \rightarrow OH^{\cdot} + OH^- \tag{8}$$

$$H_2O_2 + O_2{}^{\cdot-} \rightarrow OH^{\cdot} + OH^- + O_2 \tag{9}$$

$$O_2{}^{\cdot-} + DyeMolecules \rightarrow H_2O + CO_2 \tag{10}$$

$$OH^{\cdot} + DyeMolecules \rightarrow H_2O + CO_2 \tag{11}$$

$$e^- + h^+ \rightarrow Heat \tag{12}$$
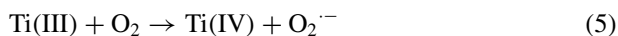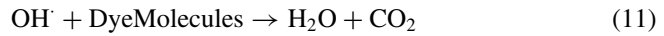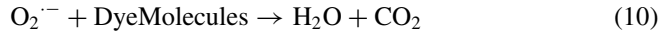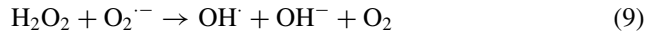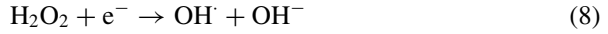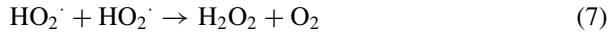
Based on the above understanding of radical's generation and structural properties of dyes, an example of a possible photodegradation pathway of Acid Orange 7 dye is illustrated in Fig. 2.

3.1.1 Dye Sensitization

Generally, dyes are capable of absorbing visible light. Upon irradiation of visible light, dye molecules located at TiO_2/solution interface get excited. From the excited dye molecules (Dye*), electrons are ejected to the conduction band of TiO_2 and lead to the evolution of cationic dye radicals (Dye$^+$). The electron then participates in the redox reaction producing superoxide radicals ($O_2{}^{\cdot-}$) which in turn fosters the generation of hydroxyl radicals (O H$^{\cdot}$) that oxidizes the cationic dye radicals, and mineralized end products are formed [2] (Refer Fig. 3). To ensure effective ejection of an electron from the excited dye molecule (Dye*) to the conduction band of TiO_2, adsorption of dye molecules onto the TiO_2 surface should be strong enough. Adsorption of dye molecules can be influenced by varying the pH value of the solution as it alters the surface charge of the photocatalyst [34, 50]. The TiO_2 photocatalyst demonstrates a positive surface charge at pH less than 6.8 facilitating anionic dye attraction and cationic dye repulsion, whereas it exhibits opposite behaviour when pH is greater than 6.8 [34]. Therefore, it is evident that pH plays an important role in dye sensitization. Also, pH is one of the influential parameters in deciding the dye degradation efficiency. Therefore, the later section briefly discusses the performance of different configurations of photocatalytic membrane reactors for dye removal at varying pH values.

$$Dye + hv \rightarrow Dye^* \tag{13}$$

Fig. 2 Photodegradation pathway of Acid Orange 7 dye [63]
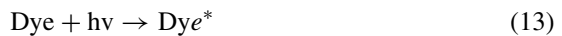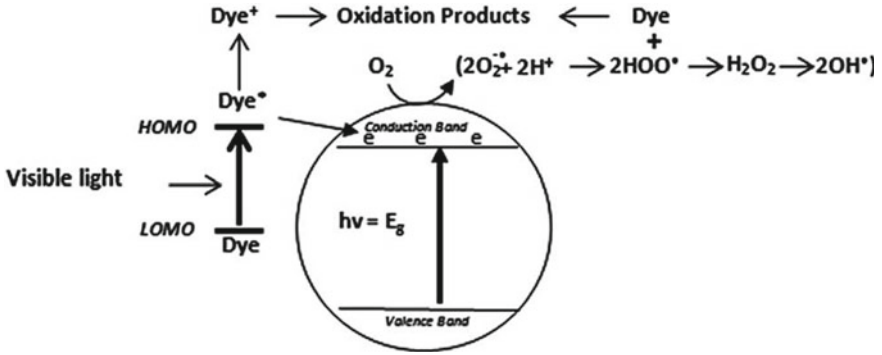
Fig. 3 Schematic illustration of Dye Sensitization [2]

$$Dye^* + TiO_2 \rightarrow Dye^+ + TiO_2^- \tag{14}$$
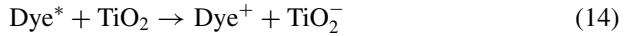
3.2 Design of Photocatalytic Membrane Reactor (PMR)

The designing of a photocatalytic membrane reactor is one of the salient aspects that govern the dye removal efficiency and requires a fundamental understanding of material properties, membrane configuration and synthesis, pollutant behaviour, chemical formulation and reaction kinetics. The photocatalytic membrane reactor has gained widespread attention due to the photocatalytic reaction occurring at the surface of the membrane, which doubles the benefits by inhibiting the aggregation of photocatalysts, thus maintain the process, and lowering the membrane fouling tendency during the treatment processes. Furthermore, the photocatalytic membrane reactor operates in the continuous mode, and the membrane acts as a barrier that eases the separation of products, controls the mass transport, offers effective reaction time and contact area and improves photocatalyst recycling [8]. The generally employed membranes in PMR are MF, UF and NF [33]. The basic components controlling the performance of PMR are the light source, photocatalyst material and reactor design that includes the substrate material of membrane, and configuration of PMC. This section focuses on the characteristics and selection of substrate materials for the photocatalytic membrane along with their fabrication methods.

3.2.1 Substrate Material of Photocatalytic Membrane

The substrate material requires to provide chemical, mechanical, and thermal stability, high surface area and roughness to hold photocatalytic particles and flexibility in adding the functional groups. Generally, chemical composition and structure

influence permeability and selectivity of the membrane. Besides, morphology such as surface and cross-section makeup get altered when photocatalysts are introduced into the membrane matrix. Hence, based on these, the substrate material will be selected for the preparation of the membrane. Inorganic, organic and metallic materials are generally used in the photocatalytic membrane synthesis. The common organic material used for the membrane fabrication is polymers which include polyethylene terephthalate, polyamide, polyvinylidene fluoride, polyethersulfone, polyurethane, polyacrylonitrile and polytetrafluoroethylene. The resultant membrane is reported to be porous and having high surface roughness to offer high performance in dye removal. For instance, [23] demonstrated the intensification of membrane surface roughness with the increment of graphene oxide (GO) loading in graphene-dispersed polysulfone-mixed matrix membrane (PSf/GO). The study witnessed that the hydrophilic GO exhibits a higher affinity towards water, leading to fast migration of GO-dispersed N-methyl-2 pyrrolidonene solvent into non-solvent water during the phase inversion process. This resulted in the formation of a sphere or nodule of polymer that was attributed as a surface roughness (mean fit = 2.35 μm) which further increased the membrane porosity.

Considering the damages associated with the irradiation, and redox reactions due to the direct interaction of membrane with the reaction environment, inorganic ceramic materials such as Al_2O_3, TiO_2, SiO_2, ZrO_2 are the most viable substrate materials compared to polymeric materials. Furthermore, the ceramic membrane possesses higher chemical, mechanical, and thermal stability, a long life span and demonstrates good antifouling properties but is expensive comparatively [6, 26].

The dye removal studies carried out using different varieties of the membrane substrate material in PMR are compiled in Table 2.

3.2.2   Fabrication of Photocatalytic Membrane

Designing and modification in coherence with advancement towards commercialization of photocatalytic membrane reactor requires a deeper understanding of membrane fabrication methods. Therefore, this section emphasizes the mechanism, operation, components and governing factors involved in the different membrane fabrication methods that are prevalent or are recently developed.

Dip Coating

The dip-coating is one of the easiest and widely used methods for immobilizing photocatalyst particles onto the membrane surface [4]. The dip-coating method encompasses immersion of a membrane substrate at a specific speed into the coating solution containing photocatalyst particles. On the membrane surface, the complete deposition of particles is ensured by providing full penetration of the substrate material at an optimum speed for its complete wetting, sufficient contact time and then withdrawing at a constant speed. This is followed by evaporation of solvent leading to the development of a thin film on the surface [57, 61]. The morphology and the thickness of the deposited film are greatly influenced by the viscosity, density, surface

Table 2 Removal of pollutants using different varieties of the membrane

S. no.	Membrane type	Pollutant removal	References
1	Cr_2O_3-enriched geopolymer-based photocatalytic membrane (Cr_2O_3/GPCM)	Basic Green Dye	[14]
2	Ag_3PO_4/Graphene Oxide/3-aminopro-pyltriethoxysilane/PVDF composite membrane	Rhodamine B and Methylene Blue	[14]
3	N-vinylcaprolactam-TiO_2-acrylic acid (VCL-TiO_2-AA) polymer nanocomposite modified polysulfone ultrafiltration membrane	Methylene Blue	[58]
4	AgCO@UiO/Graphene Oxide membrane	Rhodamine B, Methylene Blue, Methyl Red	[68]
5	N-doped TiO_2–ZrO_2/TiO_2 composite ultrafiltration membrane	Methyl Orange	[14]
6	Meso-tetrakis (1-methylpyridinium-4-yl) porphyrin-immobilized sulfonated polysulfone/polyethersulfone blend membrane (TMPyP@SPSf/PES)	Rhodamine B	[65]
7	Cadmium sulphide/polymethyl methacrylate nanocomposite membrane (CdS/PMMA)	Rhodamine B	[28]
8	TiO_2-coated polyvinylidene fluoride flat sheet membrane (PVDF)	Reactive Blue 19	[51]
9	g-C_3N_4/TiO_2 composite photocatalyst/polyacrylic acid/polytetrafluoroethylene ultrafiltration membrane (CNTO/PAA/PTFE UFM)	Methylene Blue	[16]
10	Composite membrane -Polysulfone/Nitrogen, Palladium co-doped TiO_2	Eosin Yellow degradation	[38]
11	Multi-wall carbon nanotubes/Ag_3PO_4/polyacrylonitrile (PAN) ternary composite fibre membrane	Rhodamine B	[66]
12	Graphene oxide/polyacrylonitrile composite membranes (GO/PAN)	Indigo, Methylene Blue, Thymol Blue, Congo Red	[22]
13	Acrylonitrile butadiene styrene/polyurethane blend membrane (ABS/PU)	Disperse Yellow 23, Disperse Red 60, Disperse Yellow 23, Disperse Blue 183, Vat brown 55, Vat blue 66 and Vat red 10	[42]

(continued)

Table 2 (continued)

S. no.	Membrane type	Pollutant removal	References
14	$TiO_2/\alpha\text{-}Al_2O_3$ porous membrane	Methylene Blue	[43]
15	Polysulfone/Titanium dioxide/Multi-walled carbon nanotubes mixed matrix Membranes (PSF/TiO_2/MWCNT)	Acid Black 1	[35]
16	Polyvinylidene fluoride/meso-TiO_2 hybrid membrane	Methyl Orange	[64]

tension and evaporation conditions of the coating solutions along with the immersion time, withdrawn speed, dip-coating cycle and substrate surface characteristics. Various dip coating methods so far followed are direct solution dipping, multi-layered dip coating, photo-based, spin-based, sol–gel-based and vacuum-based methods. The dip-coating method can be operated continuously and is usually employed for ceramic membrane preparation [18]. The availability of quality photocatalyst powder in the photocatalytic membrane to the dyes is the vital deciding factor that controls the removal efficiency. For example, TiO_2-coated polyvinylidene fluoride (PVDF) membrane was fabricated using dip coating with a contact period of 5–60 min. It was observed that membrane porosity declined with an increase in contact period due to aggregation of TiO_2 photocatalyst particles leading to blockage of pores. In addition, the dye removal efficiency escalated from 57.09% to 86.1% with an increment in photocatalyst loading from 0.1 to 1 g/L because of the increase in active sites [51].

Spin Coating

In this method, on the surface of the planar membrane substrate, thin and uniform polymer films are deposited. The various steps involved in the spin coating method are deposition, spin-up, spin-off and evaporation. Initially, the substrate is placed on the revolving base known as a spinner. Either at static or at a slow speed of revolving spinner, the deposition of the photocatalytic solution takes place on the centre of the substrate's surface, and this is known as deposition step. At the spin-up step, the deposited solution spreads radially outward due to centrifugal force exhibited by the high-speed revolving spinner. In spin-off step, accumulation and ejection of the solution takes place due to its outward flow towards the perimeter. The last step involves thinning up the solution due to evaporation, leaving behind the photocatalyst film on the surface of membrane. Various factors influencing the film thickness are evaporation rate, angular velocity, volatility and diffusivity of the solvent along with the solution concentration and its viscosity [20]. The advantage of the spin coating method is that it is applicable for organic, inorganic and organic–inorganic solution mixtures [49].

Electrospinning and Electrospraying

Using electrospraying and electrospinning, the photocatalytic membrane itself can be created or the coating of photocatalyst on the membrane can also be achieved.

The basic principle here is—a high electric field is applied on a blend solution that produces photocatalyst (or membrane substrate and photocatalyst) nanofibres which gets settled on a collector. In case of photocatalyst coating, the membrane substrate will be placed on the collector. The key components of the electrospinning setup are (i) syringe with a needle containing the solution, (ii) high voltage power source and (iii) flat or drum type collector. Initially, the syringe is filled with blend solution, and the metallic needle is applied with high voltage to produce an electric field to vanquish the surface tension of the solution leading to the development of cone-shaped droplet at the needle tip. The syringe pump then constantly pushes the solution, producing ultrafine fibre that gets collected on the collector or the surface of membrane.

The electrospinning are of different configurations such as melt, single-spinneret, multi-spinneret and co-axial [62]. Nano-fibres of polymers, metals, composites and ceramics can be produced by this method. Electric field intensity, solution viscosity and flow rate, polymer concentration, air humidity and work distance influence the electrospinning process [31]. Electrospraying and electrospinning only differ in the quantum of polymer chain entanglements and their presence in the solution. Simply, by lowering the polymer chain entanglements in the solution, structure of regular nanofibres can be transformed to beaded nanofibres and to particles under identical electrospinning conditions [39]. The membrane fabricated using electrospinning demonstrates higher surface area to volume ratio and higher permeability due to its immense control on the cross-linking and regularity.

Vacuum Filtration

Vacuum Filtration allows the photocatalyst particles deposition onto the membrane surface physically. By controlling the concentration of the photocatalyst particles and pressure of the vacuum, different loads of photocatalyst particles can be deposited onto the membrane surface. The large thickness and higher density membrane can be achieved using this method. The uniformity in coating largely depends on the downstream vacuum pressure. This method requires well-dispersed photocatalytic particles, else a non-uniform photocatalytic membrane will be formed due to aggregation of particles. Various photocatalyst particles used in the fabrication of photocatalytic membrane are MoS_2 nanosheets, graphitic carbon nitride and graphene using this method [15].

Phase Inversion

Under controlled conditions, phase inversion refers to the phase transformation of the stable thermodynamic polymer solution from liquid to a solid phase. In other words, precipitation of a polymer from a layer of casting solution involves a change to the solid phase from the solution phase of the polymer by suitable manipulation of the environment. Various techniques of phase inversion are precipitation by immersion in a non-solvent, precipitation by cooling and precipitation by evaporation [21, 27].

In case of immersion in a non-solvent, the cast solution comprising of a membrane substrate (and photocatalyst) in a solvent is immersed in a coagulation tank consisting of non-solvent. The membrane (with the photocatalyst) is precipitated due to the migration of material from the solvent to the non-solvent side. This results in the

formation of a dense ultrathin skin (containing the photocatalyst) at the exposed surface. This dense layer depresses the rate of migration of solvent inside the surface which further lowers the precipitation and forms larger pores. This results in the formation of an asymmetric membrane comprising of dense ultrathin skin layer with porous substructure. Symmetric membranes can also be fabricated by this method by controlling the migration rate of the solution.

In precipitation by cooling method, on any desired surface, the solution containing membrane substrate material (and photocatalyst) and solvent is casted and allowed to cool. The solubility of the solution decreases as the layer cools and formation of a film matrix takes place. Polymeric membranes prepared by this method are polypropylene, polyethylene, polysulfone, polyvinylidene fluoride. In the case of precipitation by evaporation, solvent or mixture of the solvent evaporates from a cast solution, due to which solubility of the solution decreases and precipitation of the solution material occurs. Dense anisotropic membranes with or without photocatalyst can be obtained by this method [21].

3.2.3 PMR Configurations

The photocatalytic membrane process is the compilation of advanced oxidation process with the separation process. To get the most efficiency on the dye removal, the configuration of the PMR is vital. The configurations of PMR are mainly categorized into two (i) photocatalyst in suspension inside the membrane reactor (ii) photocatalyst implanted or immobilized on the membrane surface inside the reactor. The active surface area available for the pollutants is more in the suspended catalyst system as compared to the immobilized catalyst ensuring higher photocatalytic performance for the former and a portion of loss in photoactivity at the latter case. Furthermore, the drawback of the suspended catalyst reactor is the difficulty in recovering or removing the particles after the decontamination of wastewater, whereas an immobilized catalyst reactor eliminates this requirement [44, 46]. Correspondingly, photocatalyst in immobilized mode should be stable and must exhibit strong adhesion with the membrane material. Impregnation of catalyst within the membrane has better reusability and recoverability at nominal cost [44]. Reference [65] fabricated a mesotetrakis (1-methylpyridinium-4-yl) porphyrin-immobilized sulfonated polysulfone/polyethersulfone blend membrane (TMPyP@SPSf/PES) for the degradation of Rhodamine B and Methylene blue dye under visible light (300 W), and has observed the degradation efficiency upto 98.3% and 99.1% for Rhodamine B and Methylene blue dye, respectively.

The studies on PMR for the removal of dyes used varieties of PMR configurations as follows. Figure 4a represents the suspended photocatalyst PMR with the light source placed above the membrane matrix, whereas in Fig. 4b, light source is placed above the feed chamber. Moreover, light source can also be placed both above the feed chamber and membrane matrix. Also, a light source can be placed inside the feed solution using immersed lamps. Figure 5 represents the PMR with photocatalyst embedded on and within the membrane.
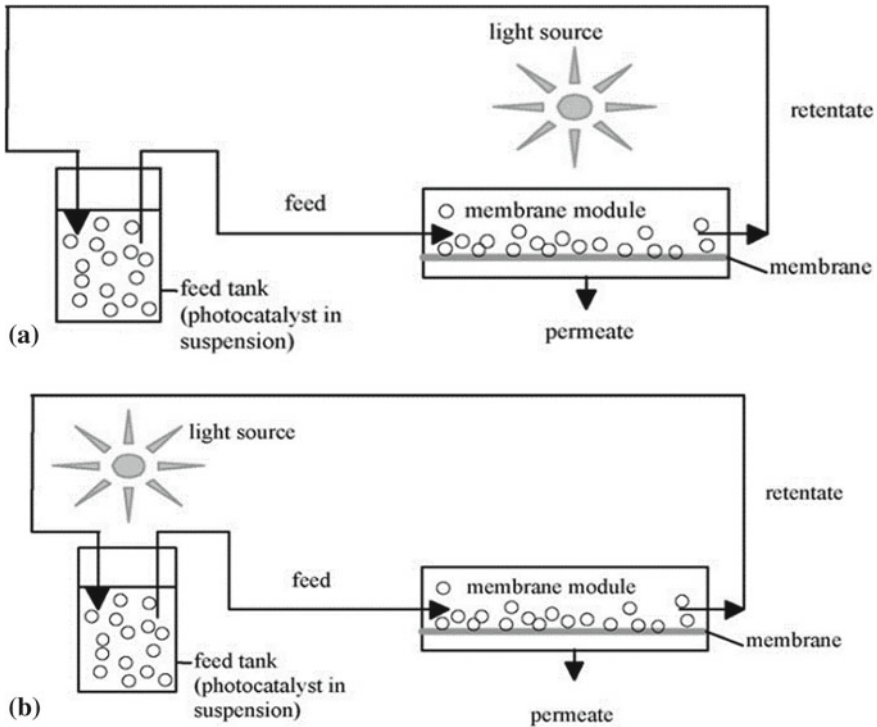
Fig. 4 Suspended PMR **a** Illumination of Membrane Matrix **b** Illumination of Feed Tank [46]

Slurry-Based Photocatalytic Reactor

Slurry-Based Photocatalytic Reactor offers larger interaction between the contaminants and the photocatalyst suspended in the slurry, and are coupled with membrane matrix for separation purposes. Depending upon the configuration, two types of slurry-based photocatalytic reactor are (i) Split-type (ii) Integrated Type. In the case of Split-type, photocatalytic oxidation and membrane separation take place in different chambers as shown in Fig. 6a), whereas both occur in the same chamber in the case of Integrated type [37]. [12] conducted an experiment for the eradication of Disperse Red 73 (DR73) dye from the textile industry effluents using TiO_2 suspended photocatalytic reactor combined with hollow fibre micro-filtration membrane module under ultraviolet irradiation (24 W UV Lamp). Measurement of the percentage of dye degradation was based on the efficiency of Chemical Oxygen Demand (COD) removal. The analysis revealed that the COD removal efficiency elevates from 70 to 90% with an increase in TiO_2 loading from 0.5 g/L to 2 g/L after 180 min of treatment due to an increase in photocatalytic activity as active site increases (Refer Fig. 6b).

Reference [19] carried out an experiment for the elimination of reactive black 5 dye using an integrated type slurry-based photocatalytic reactor built by immersing
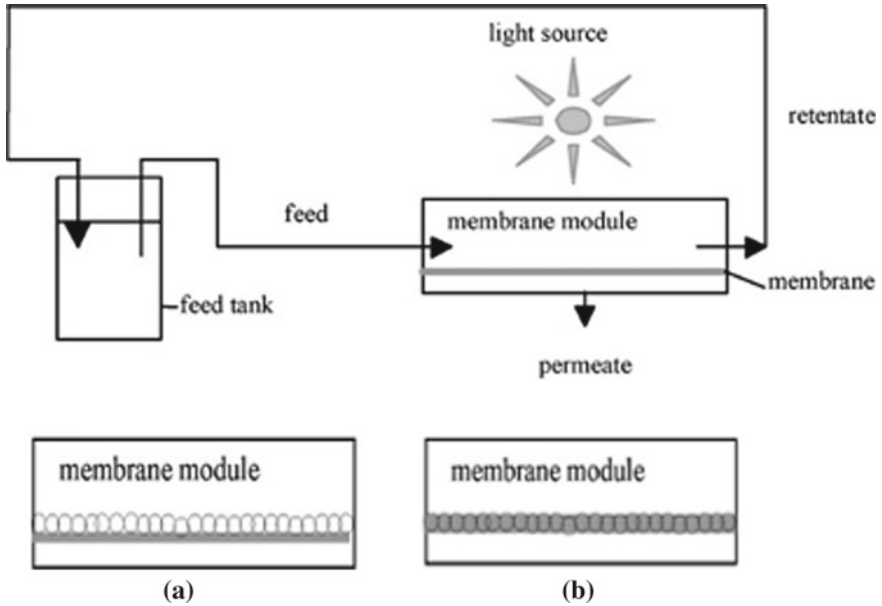
Fig. 5 Immobilized PMR **a** Embedded on the Membrane **b** Within the Membrane [46]
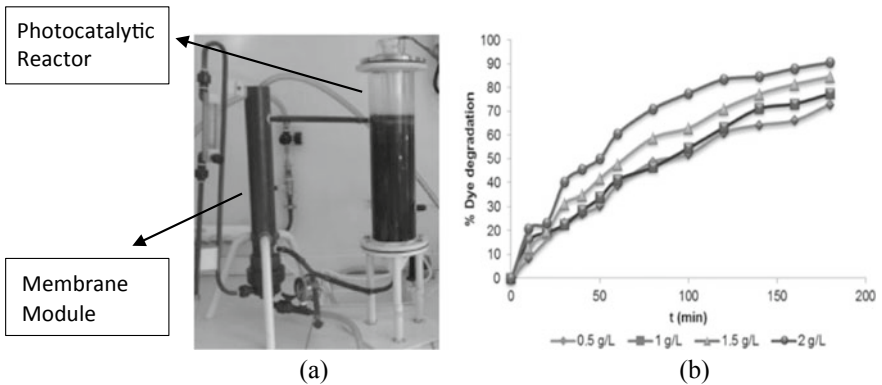
Fig. 6 Split-type Photocatalytic Membrane Reactor **a** Experimental Setup **b** % Dye Degradation Versus time (in min) [12]

a flat polytetrafluoroethylene (PTFE) membrane module into a TiO_2-based slurry photocatalytic reactor as illustrated in Fig. 7a. The membrane module was positioned at the middle of the container and in between the two Ultraviolet lamps (15 W each). Furthermore, a magnetic stirrer was used for mixing the solution along with the air diffuser for continuous aeration. Measurement of % dye degradation was based on COD and Total Organic Carbon (TOC) removal. Experimental results reveal
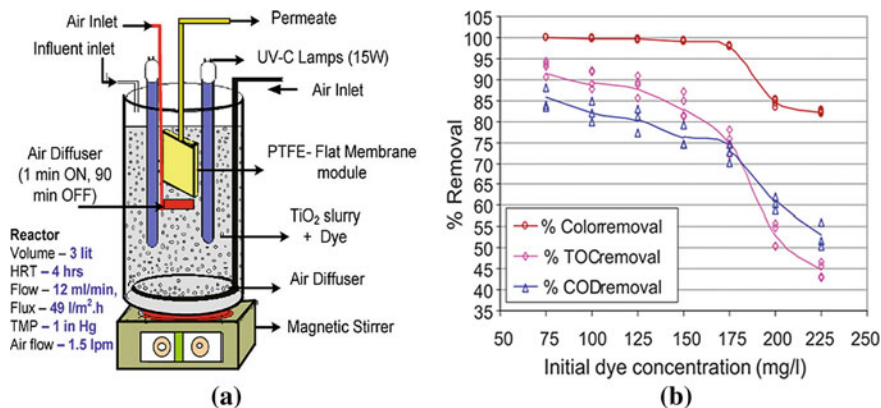
Fig. 7 Integrated Slurry PMR **a** Experimental Setup **b** % Removal versus Initial Dye Concentration [19]

that under continuous flow PMR having a detention period of 4 h, the percentage removal of TOC, COD and colour decreases from 92 to 46%, 82 to 56%, 99.3 to 83%, respectively, with the surge in initial concentration of dye (Refer Fig. 7b). This is because a higher initial concentration of dye intensifies the colour of the solution thereby affecting the depth of the UV light penetration. Moreover, due to constant light intensity and irradiation time, the energy available for the radical generation declines with mounting dye concentration as dye molecules absorb the photon flux.

Immobilized Photocatalytic Membrane Reactor

In this configuration, the membrane not only acts as a selective barrier for the pollutants, but also serves as a support for the photocatalyst [45]. Based on the integration of the photocatalyst, the immobilized PMR are categorized into three types, (i) Membrane coated with photocatalyst (ii) Blending of photocatalyst with the membrane (iii) Self-Photocatalytic membrane.

Membrane Coated with Photocatalyst

Coating techniques like magnetron sputtering, dip-coating, chemical vapour deposition (CVD) and atomic layer deposition (ALD) and electrospinning and electrospraying are used for the synthesis of photocatalytic membranes [37]. A laboratory-scale experiment was carried out by [5] for methylene blue removal using nanofibre membranes deposited with titania nanoparticles. The membrane was fabricated using electrospinning and electrospraying. The study incorporates two cases, i.e. batch process and continuous process for the deposition of nanoparticle and nanofibre as demonstrated in Fig. 8. It was observed that the percentage degradation of methylene blue after 90 min of treatment under UV irradiation (0.6mW/cm^2) is 65.48% for batch process and 99.6% for continuous process, inferring that the batch process membrane fabrication is less efficient as compared to the continuous process because of the
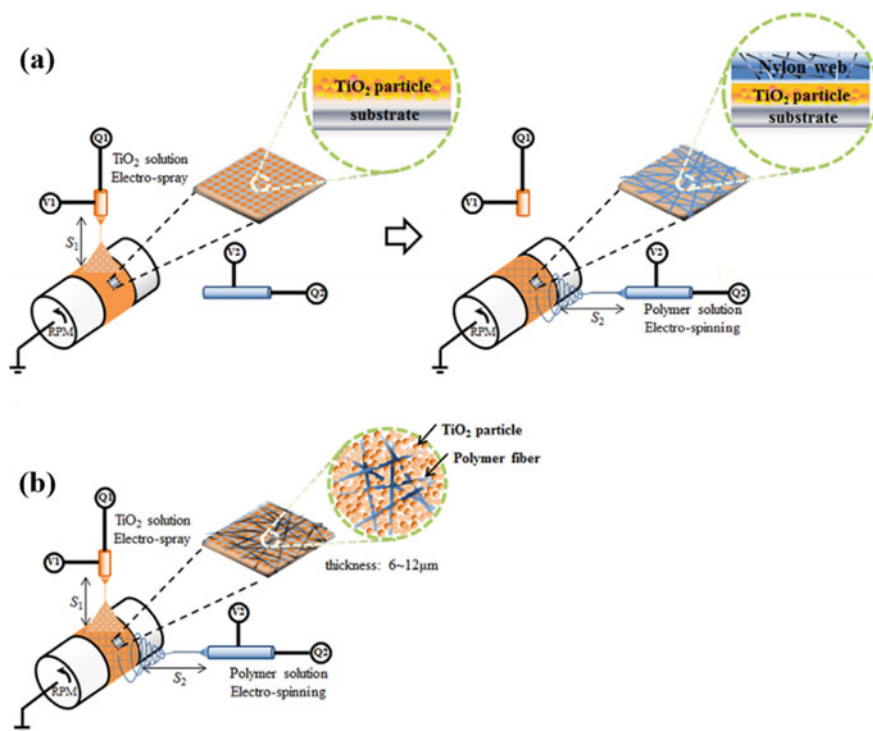
Fig. 8 Photocatalytic membrane fabrication method **a** batch process and **b** continuous process [5]

reduction in photoactive interfacial area due to bilayer deposition of nanoparticles and nanofibres.

Photocatalytic activity of TiO_2-coated Polyvinylidene fluoride membrane synthesized by sol–gel method was tested for the Reactive Black 5 (RB5) dye degradation under ultraviolet illumination (UV-C, 15 W). The TiO_2 particles in this experiment were synthesized at specific pH value 1, 1.25, 1.5 and have found percentage degradation of 54.58, 98.77 and 30.12% for Reactive Black 5 dye in 5 h at pH value of 1.5, 1.25, 1, respectively. This is because of higher photocatalytic activity at pH 1.25, because of high sol density compared to pH 1.5 and due to origination of more favourable TiO_2 crystal type at pH 1.25 than pH 1 [36].

Blending of Photocatalyst with the Membrane

Wet spinning, nonsolvent-induced phase separation (NIPS), electrospinning and sintering are the methods used for the synthesis of these types of membrane. The major advantage of these types of membranes is that the leaching of photocatalyst gets curtailed. Optimizing the proportion of the photocatalyst and the membrane precursors can help us to get the required stability and reactivity of the membrane [37]. Reference [53] carried out an experiment to investigate the effect of photocatalytic

dye degradation under varying experimental conditions like irradiation time, initial concentration of dye and pH using zinc oxide-blended cellulose acetate-polyurethane (CA-PU/ZnO) membrane prepared using solution dispersion blending method for removal of Reactive Red (RR 11) and Reactive Orange (RO 84) dyes. Moreover, in this experiment, ZnO nanoparticles were synthesized by sol gel method. Figure 9 illustrates the experimental setup in which funnel contains the prepared membrane with dye solution and at different time intervals (10–60 min) kept under the sunlight. It was found that with increase in illumination time, the degradation efficiency of dye escalates and reaches its peak after 40 min and then remains constant. Therefore, illumination time of 40 min is kept fixed for the study. It was also observed that at pH value 7, higher degradation efficiency of RR11 and RO84 dyes was achieved by CA-PU/ZnO membrane. Neutral pH is well suited for better performance, because at low pH, ZnO reacts with acids to produce salts, whereas it forms complexes after reacting with base at high pH value. Correspondingly, analysis discovered that the dye degradation efficiency declined with increase in initial dye concentration from 50 to 250 mg/L because generation of hydroxyl ion decreases as active sites of the photocatalyst gets shrouded with the dye molecules.

Reference [1] utilizes the Metal–organic frameworks (MOFs) for the photocatalysis and demonstrated the photocatalytic degradation of methylene blue dye over 5 h under dark, ultraviolet ($\lambda = 253.7$ nm, 6 W) and visible irradiation ($\lambda > 420$ nm, 6 W) using Polysulfone-Blended NH_2-MIL125 (Ti) membrane with MOF/PSf percentage composition of 0, 0.2, 0.5 and 1 wt% and fabricated through phase inversion method.

The NH_2-MIL125(Ti) is a metallic organic form with cyclic $Ti_8O_8(OH)_4$ oxo clusters and 2-aminoterephthalate ligands and exhibit greater adsorption affinity towards visible light due to the presence of amino-functionalized structure. For the analysis, membrane polymeric strip (8 cm x 8 cm) was suspended in 100 mL of methylene blue solution having concentration 10 ppm (Refer Fig. 10). At an interval of 60 min, 2 mL
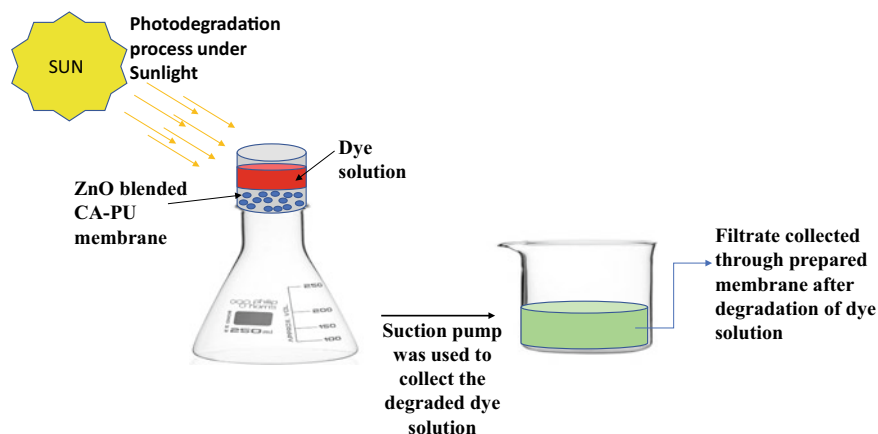
Fig. 9 Experimental Setup for Dye Degradation using CA-PU/ZnO membrane [53]
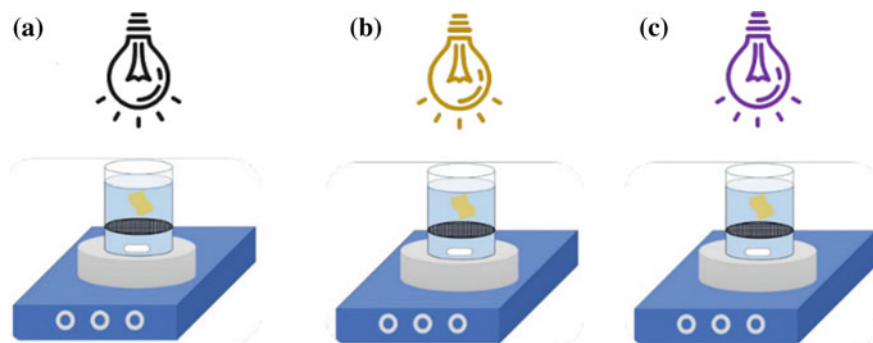
Fig. 10 Experimental Setup in **a** dark, **b** Visible light and **c** UV light [1]

aliquots of the dye solution are withdrawn with a disposable syringe and were monitored using UV–Vis Spectrophotometer. Higher dye removal percentage was found in NH_2-MIL125(Ti)/PSf membrane with composition 1% (in weight) under all three conditions, i.e. dark, visible as well as ultraviolet irradiation. NH_2-MIL125(Ti)/PSf membrane with composition 0, 0.2, 0.5 and 1 wt% showed 30.840, 36.779, 44.203, 49.268% dye removal, respectively, under visible irradiation, whereas under ultraviolet irradiation, they showed 38.538, 48.846, 52.076 and 56.076% dye removal, respectively. This is due to the fact that with increasing concentration of NH_2-MIL125 (Ti), the density and the quantity of membrane pores got enlarged gradually. Furthermore, under dark conditions, due to the adsorption dominance in the dye degradation, NH_2-MIL125(Ti)/PSf membrane with composition 0, 0.2, 0.5 and 1 wt% showed 26.145, 27.389, 31.592 and 37.881% dye removal, respectively.

Self-Catalytic Membrane

These membranes are constructed with a pure photocatalyst through electrochemical anodization, and do not necessitate any immobilization step as required in the coated or blended membrane and can act as antifouling membranes. These membranes possess higher hydrophilicity, anatase crystallinity and surface area and significantly lowers the tendency of photocatalyst leaching [6, 37]. Fabrication of TiO_2 membrane using electrochemical anodization of titanium metallic substrate is widely used, as anodization favours the growth of TiO_2 nanotube from the oxidized Titanium electrode in the presence of fluoride ions in an aqueous electrolytic solution [30, 37].

4 Selected Case Studies

This section delineates the recent pilot-scale studies undertaken by the researchers for dye removal. The following case studies intend to develop a framework and to understand the characteristics and behaviour of different reactor setups.

4.1 Photocatalytic Membrane Bioreactor (PMBR)

Reference [56] experimented to explore the efficiency of tungsten oxide with graphene oxide alginate beads (WO_3/GO) for the photocatalytic degradation of dye using hollow fibre polyethersulphone membrane bioreactor under visible irradiation. Modified Hummer Method was used for the Graphene Oxide synthesis. Synthesis of tungsten oxide involves the usage of tungsten oxide powder, polyvinylpyrrolidone, sodium alginate and calcium chloride bath. Textile wastewater was pumped with a flowrate of 6.7L/h into the photocatalytic reactor having a contact time of 3 h. At the bottom surface of the photocatalytic reactor, an aerator was placed for homogenous mixing of the solution. Furthermore, from the top of the photocatalytic reactor, visible light of 500 W was immersed, reaching ¾th of the tank. The wastewater after photocatalysis passes to the membrane bioreactor (refer Fig. 11). In membrane bioreactor, a hydraulic retention time of 10 h and mixed liquor suspended solid concentration of 8000 mg/L was maintained. The experiment was run twice using both tungsten oxide (WO_3) as well as tungsten oxide (WO_3) with graphene oxide (GO) alginate beads in the photocatalytic reactor. Under the catalyst loading of 500 mg/L and reaction time of 3 h, the analysis of the photocatalytic reactor effluent revealed that a higher percentage of colour and COD removal was found in the case of WO_3/GO, i.e. 25 and 44%, respectively, whereas in the case of WO_3, it was 21 and 36%, respectively. The higher efficiency of WO_3/GO is because graphene oxide acts as an electron acceptor, and it lowers the recombination of electrons and holes resulting in a higher dye degradation efficiency. The effluent from the membrane bioreactor shows 76% COD and 70% colour removal due to higher biomass growth ensuing integrated PMBR improves the degradation efficiency.
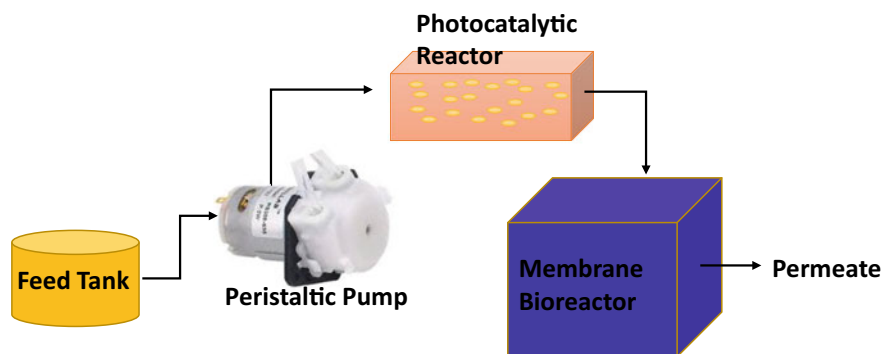
Fig. 11 Experimental Setup of Photocatalytic Membrane Bioreactor (PMBR)

4.2 C-TiO$_2$-CFA/PAN Photocatalytic Membranes

Reference [47] demonstrated the removal of golden yellow and methyl orange textile dyes using novel polyacrylonitrile membrane supported carbon-doped titanium dioxide-coal fly ash nanocomposite (C-TiO$_2$-CFA/PAN). Optimization of photocatalyst along with the effect of pH, photocatalyst loading (0%, 1%, 1.5% and 2% C-TiO$_2$-CFA), initial dye concentration was also evaluated. The carbon-doped titanium dioxide-coal fly ash nanocomposite was synthesized by sol–gel method and through phase inversion technique, immobilized on polyacrylonitrile membrane. Scanning electron microscope analysis reveals the fabricated membrane to be asymmetric with a thin top layer and porous sub-layer. Optimization of photocatalyst for degradation of dyes with different ratios of C-TiO$_2$: CFA is illustrated in Fig. 12.

Figure 12 infers that the optimum proportion of C-TiO$_2$:CFA is 4:1 having a degradation efficiency of 70.5% for Methyl Orange and 93.8% for Golden Yellow dye in 180 min. The degradation efficiency of 90.30% for methyl orange and 89.90% for golden yellow was achieved by using photocatalyst loading of 2%C-TiO$_2$-CFA/PAN, ensuing increase in photocatalyst loading leads to increment in photocatalytic dye degradation. Also, it was noticed that the degradation efficiency declines with the rise in initial dye concentration because of solution opacity as illustrated in Fig. 13. Furthermore, higher photocatalytic activity was observed at lower pH. This is because the TiO$_2$ photocatalyst surface exhibits a positive charge, and methyl orange and golden yellow dye under acidic conditions exhibit zwitterionic structure, because of
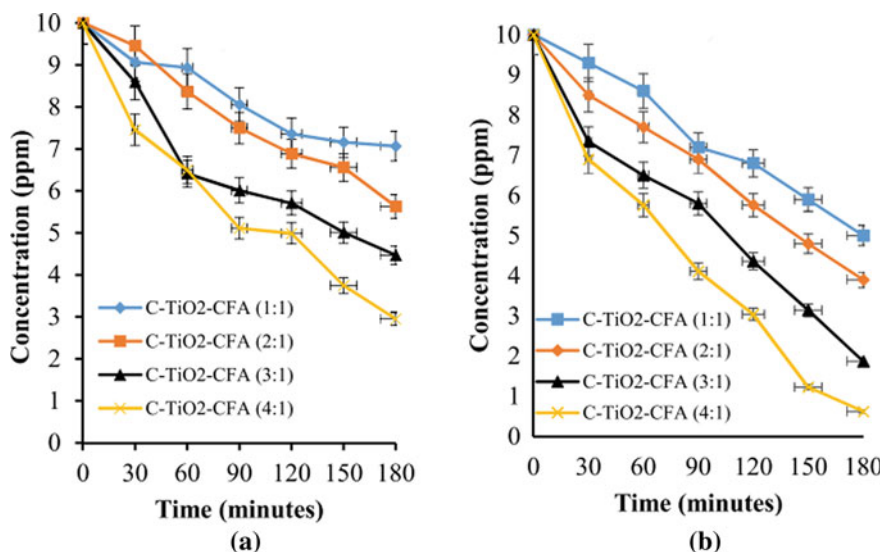
Fig. 12 Degradation of **a** Methyl Orange **b** Golden Yellow dye with different proportion of C-TiO$_2$:CFA [47]
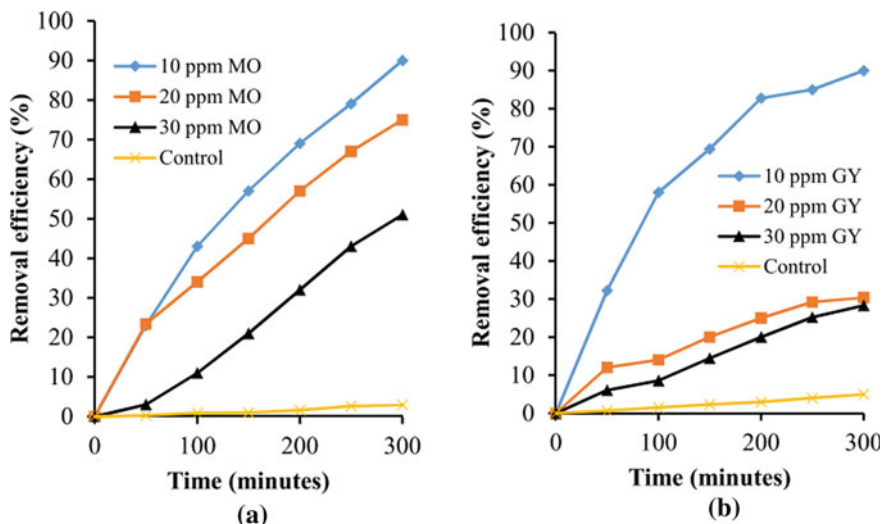
Fig. 13 Removal Efficiency (%) versus Time with increase in initial dye concentration **a** Methyl Orange **b** Golden Yellow dye [47]

which adsorption of dyes on the photocatalyst surface is enhanced leading to a higher rate of photodegradation of dyes.

4.3 Solar Photocatalytic Membrane Reactor with Fe^{3+}-Doped ZnO/polyester

Reference [7] investigated the photocatalytic degradation of Reactive Blue 5 (RB5) dye using Fe^{3+}/ZnO/polyester-based solar PMR. The experiment was performed in a borosilicate glass container comprising of 100 ml of RB5 dye solution (30 ppm), $5 cm^2$ swatch of Fe^{3+}/ZnO/PMR and ZnO/PMR with 60 mg as an average catalyst loading and 30 Mm of H_2O_2 concentration at pH 7 with D65 cool artificial daylight tubes (72 W) under 30–35 °C. Results reveal that untreated dye, i.e. blank showed no change in concentration with time. Fe^{3+}/ZnO/PMR showed maximum dye degradation efficiency in 180 min treatment because doping of Fe^{3+} with ZnO reduces the bandgap resulting in a higher rate of hydroxyl radical generation (refer Fig. 14). Also, the higher photocatalytic activity of Fe^{3+}/ZnO/PMR was observed due to its ability to harvest a visible spectrum of irradiation along with an increased rate of dye adsorption due to higher surface roughness and hydrophilicity.
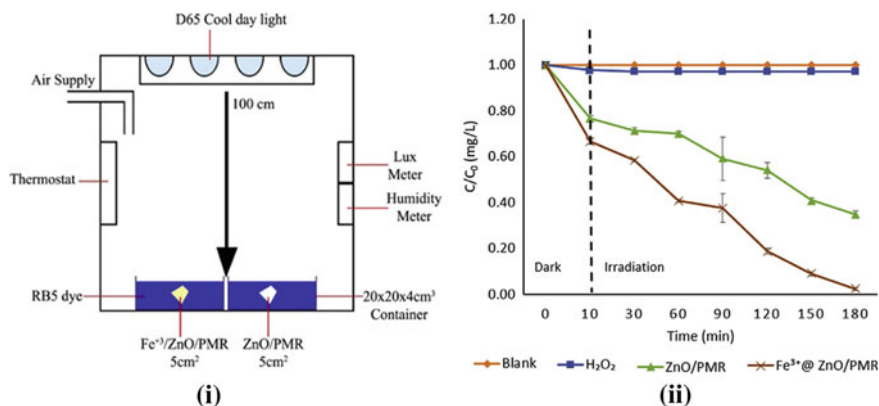
Fig. 14 (i) Experimental Setup of Fe^{3+}/ZnO/polyester-based solar PMR (ii) Degradation of Reactive Blue 5 Dye with time [7]

5   Conclusion

The photocatalytic membrane reactor is gaining widespread recognition due to its broad-spectrum applicability and inherent advantages like low operational cost, low membrane fouling, anti-bacterial properties and efficient degradation of dye effluents. Due to several drawbacks associated with the suspended catalyst system, immobilization of photocatalyst has significant importance in practical applications. Excessive photocatalyst loading reduces the photocatalytic activity due to solution opacity. Commercial application of photocatalytic membrane technology should be promoted by performing pilot-scale experiments or projects. Studies should focus on the discovery of novel visible light-responsive photocatalyst for the elimination of organic contaminants and their suitable recovery/reuse method. Furthermore, an investigation should also be made for the development of advanced membrane material to ensure its stability under UV irradiation and to lower the membrane resistance, and concentration polarization.

References

1. Ahmadi A, Sarrafzadeh MH, Mohamadi M, Mahdigholian Z, Hosseinian A (2020) Investigation on polysulfone blended NH2-mil125 (Ti) membrane for photocatalytic degradation of

methylene blue dye. J Water Environ Nanotechnol 5:234–245. https://doi.org/10.22090/jwent.2020.03.004

2. Ajmal A, Majeed I, Malik RN, Idriss H, Nadeem MA (2014) Principles and mechanisms of photocatalytic dye degradation on TiO_2 based photocatalysts: a comparative overview. RSC Adv 4:37003–37026. https://doi.org/10.1039/c4ra06658h

3. Al-Mamun MR, Kader S, Islam MS, Khan MZH (2019) Photocatalytic activity improvement and application of UV-TiO_2 photocatalysis in textile wastewater treatment: a review. J Environ Chem Eng 7.https://doi.org/10.1016/j.jece.2019.103248

4. Alias NH, Nor NAM, Mohamed MA, Jaafar J, Othman NH (2020) Photocatalytic materials-based membranes for efficient water treatment. Handbook of Smart Photocatalytic Materials. INC. https://doi.org/10.1016/b978-0-12-819051-7.00007-5

5. An S, Lee MW, Joshi BN, Jo A, Jung J, Yoon SS (2014) Water purification and toxicity control of chlorophenols by 3D nanofiber membranes decorated with photocatalytic titania nanoparticles. Ceram Int 40:3305–3313. https://doi.org/10.1016/j.ceramint.2013.09.104

6. Argurio P, Fontananova E, Molinari R, Drioli E (2018) Photocatalytic membranes in photocatalytic membrane reactors. Processes 6.https://doi.org/10.3390/pr6090162

7. Ashar A, Bhatti IA, Ashraf M, Tahir AA, Aziz H, Yousuf M, Ahmad M, Mohsin M, Bhutta ZA (2020) Fe3+ @ ZnO/polyester based solar photocatalytic membrane reactor for abatement of RB5 dye. J Clean Prod 246.https://doi.org/10.1016/j.jclepro.2019.119010

8. Basile A, Sylwia Mozia, Raffaele Molinari (2018) Current trends and future development on bio membranes photocatalytic membranes and photocatalytic membrane reactors, Elsevier

9. Benkhaya S, M'rabet S, El Harfi A (2020) A review on classifications, recent synthesis and applications of textile dyes. Inorg Chem Commun 115:107891. https://doi.org/10.1016/j.inoche.2020.107891

10. Berradi M, Hsissou R, Khudhair M, Assouag M, Cherkaoui O, El Bachiri A, El Harfi A (2019) Textile finishing dyes and their impact on aquatic environs. Heliyon 5.https://doi.org/10.1016/j.heliyon.2019.e02711

11. Bilal M, Rasheed T, Iqbal HMN, Yan Y (2018) Peroxidases-assisted removal of environmentally-related hazardous pollutants with reference to the reaction mechanisms of industrial dyes. Sci Total Environ 644:1–13. https://doi.org/10.1016/j.scitotenv.2018.06.274

12. Buscio V, Brosillon S, Mendret J, Crespi M, Gutiérrez-Bouzán C (2015) Photocatalytic membrane reactor for the removal of C.I. disperse red 73. Materials (Basel). 8:3633–3647. https://doi.org/10.3390/ma8063633

13. Chang MW, Chung CC, Chern JM, Chen TS (2010) Dye decomposition kinetics by UV/H2O2: Initial rate analysis by effective kinetic modelling methodology. Chem Eng Sci 65:135–140. https://doi.org/10.1016/j.ces.2009.01.056

14. Chen H, Zhang YJ, He PY, Li CJ, Li H (2020) Coupling of self-supporting geopolymer membrane with intercepted Cr(III) for dye wastewater treatment by hybrid photocatalysis and membrane separation. Appl Surf Sci 515:146024.https://doi.org/10.1016/j.apsusc.2020.146024

15. Chen X, Hu Y, Xie Z, Wang H (2018) Membranes 71–96.

16. Chi L, Qian Y, Guo J, Wang X, Arandiyan H, Jiang Z (2019) Novel g-C3N4/TiO2/PAA/PTFE ultrafiltration membrane enabling enhanced antifouling and exceptional visible-light photocatalytic self-cleaning. Catal Today 335:527–537. https://doi.org/10.1016/j.cattod.2019.02.027

17. Chong MN, Jin B, Chow CWK, Saint C (2010) Recent developments in photocatalytic water treatment technology: a review. Water Res 44:2997–3027. https://doi.org/10.1016/j.watres.2010.02.039

18. Cui Z (2015) Encyclopedia of membranes. Encycl Membr, 1–2.https://doi.org/10.1007/978-3-642-40872-4

19. Damodar RA, You SJ, Ou SH (2010) Coupling of membrane separation with photocatalytic slurry reactor for advanced dye wastewater treatment. Sep Purif Technol 76:64–71. https://doi.org/10.1016/j.seppur.2010.09.021

20. Fakirov S (2016) Nano-size polymers: preparation, properties, applications. Nano-Size Polym Prep Prop Appl, 1–399.https://doi.org/10.1007/978-3-319-39715-3

21. Figoli A, Marino T, Galiano F (2016) Polymeric membranes in biorefinery. Membr Technol Biorefining https://doi.org/10.1016/B978-0-08-100451-7.00002-5

22. Fryczkowska B (2018) The application of ultrafiltration composite GO/PAN membranes for removing dyes from textile wastewater. Desalin Water Treat 128:79–88. https://doi.org/10.5004/dwt.2018.22599

23. Ganesh BM, Isloor AM, Ismail AF (2013) Enhanced hydrophilicity and salt rejection study of graphene oxide-polysulfone mixed matrix membrane. Desalination 313:199–207. https://doi.org/10.1016/j.desal.2012.11.037

24. Gürses A, Açıkyıldız M, Güneş K, Gürses MS (2016) dyes and pigments: their structure and properties. In: Dyes and pigments. springer briefs in molecular science. Springer, Cham. https://doi.org/10.1007/978-3-319-33892-72

25. Holkar CR, Jadhav AJ, Pinjari DV, Mahamuni NM, Pandit AB (2016) A critical review on textile wastewater treatments: Possible approaches. J. Environ Manag 182:351–366. https://doi.org/10.1016/j.jenvman.2016.07.090

26. Horovitz I, Horovitz I, Gitis V, Avisar D, Mamane H (2020) Ceramic-based photocatalytic membrane reactors for water treatment—where to next? Rev Chem Eng 36:593–622. https://doi.org/10.1515/revce-2018-0036

27. Hołda AK, Vankelecom IFJ (2015) Understanding and guiding the phase inversion process for synthesis of solvent resistant nanofiltration membranes. J Appl Polym Sci 132:1–17. https://doi.org/10.1002/app.42130

28. Hussien MSA, Mohammed MI, Yahia IS (2020) Flexible photocatalytic membrane based on CdS/PMMA polymeric nanocomposite films: multifunctional materials. Environ Sci Pollut Res 27:45225–45237. https://doi.org/10.1007/s11356-020-10305-1

29. IARC monographs on the evaluation of carcinogenic risks to humans (2010) IARC Monogr Eval Carcinog Risks to Humans 93:9–38. https://doi.org/10.1136/jcp.48.7.691-a

30. Iglesias O, Rivero MJ, Urtiaga AM, Ortiz I (2016) Membrane-based photocatalytic systems for process intensification. Chem Eng J https://doi.org/10.1016/j.cej.2016.01.047

31. Jose Varghese R, Sakho EHM, Parani S, Thomas S, Oluwafemi OS, Wu J (2019) Introduction to nanomaterials: synthesis and applications. Nanomater. Sol Cell Appl 75–95. https://doi.org/10.1016/B978-0-12-813337-8.00003-5

32. Kiwaan HA, Atwee TM, Azab EA, El-Bindary AA (2020) Photocatalytic degradation of organic dyes in the presence of nanostructured titanium dioxide. J Mol Struct 1200. https://doi.org/10.1016/j.molstruc.2019.127115

33. Koe WS, Lee JW, Chong WC, Pang YL, Sim LC (2020) An overview of photocatalytic degradation: photocatalysts, mechanisms, and development of photocatalytic membrane. Environ Sci Pollut Res 27:2522–2565. https://doi.org/10.1007/s11356-019-07193-5

34. Konstantinou IK, Albanis TA (2004) TiO_2-assisted photocatalytic degradation of azo dyes in aqueous solution: kinetic and mechanistic investigations: a review. Appl Catal B Environ 49:1–14. https://doi.org/10.1016/j.apcatb.2003.11.010

35. Koutahzadeh N, Esfahani MR, Arce PE (2016) Sequential use of UV/H_2O_2-(PSF/TiO_2/MWCNT) mixed matrix membranes for dye removal in water purification: membrane permeation, fouling, rejection, and decolorization. Environ Eng Sci 33:430–440. https://doi.org/10.1089/ees.2016.0023

36. Kristine N, Cruz O, Uy G, Senoro DB, You S, Lu S (2014) Journal of the Taiwan Institute of Chemical Engineers Dye degradation and antifouling properties of polyvinylidene fluoride/titanium oxide membrane prepared by sol–gel method. J Taiwan Inst Chem Eng 45:192–201

37. Kumari P, Bahadur N, Dumée LF (2020) Photo-catalytic membrane reactors for the remediation of persistent organic pollutants—a review. Sep Purif Technol 230:115878. https://doi.org/10.1016/j.seppur.2019.115878

38. Kuvarega AT, Khumalo N, Dlamini D, Mamba BB (2018) Polysulfone/N, Pd co-doped TiO_2 composite membranes for photocatalytic dye degradation. Sep Purif Technol 191:122–133. https://doi.org/10.1016/j.seppur.2017.07.064

39. Lavielle N, Hebraud A, Schlatter G, Lind T-M, Rossi RM, Popa A (2013) Straightforward approach for fabricating hierarchically structured composite membranes. ACS Appl Mater Interfaces 5:10090–10097
40. Lellis B, Fávaro-Polonio CZ, Pamphile JA, Polonio JC (2019) Effects of textile dyes on health and the environment and bioremediation potential of living organisms. Biotechnol Res Innov 3:275–290. https://doi.org/10.1016/j.biori.2019.09.001
41. Leong S, Razmjou A, Wang K, Hapgood K, Zhang X, Wang H (2014) TiO2 based photocatalytic membranes: a review. J Memb Sci 472:167–184. https://doi.org/10.1016/j.memsci.2014.08.016
42. Mandegari M, Fashandi H (2017) Untapped potentials of acrylonitrile-butadiene-styrene/polyurethane (ABS/PU) blend membrane to purify dye wastewater. J Environ Manage 197:464–475. https://doi.org/10.1016/j.jenvman.2017.04.026
43. Mastropietro TF, Meringolo C, Poerio T, Scarpelli F, Godbert N, Di Profio G, Fontananova E (2017) Multistimuli Activation of TiO2/α-alumina membranes for degradation of methylene blue. Ind Eng Chem Res 56:11049–11057. https://doi.org/10.1021/acs.iecr.7b02778
44. Mohamad Said KA, Ismail AF, Karim ZA, Abdullah MS, Usman J, Raji YO (2020) Innovation in membrane fabrication: Magnetic induced photocatalytic membrane. J Taiwan Inst Chem Eng 113:372–395. https://doi.org/10.1016/j.jtice.2020.08.014
45. Molinari R, Argurio P, Bellardita M, Palmisano L (2017) Photocatalytic processes in membrane reactors, comprehensive membrane science and engineering.https://doi.org/10.1016/B978-0-12-409547-2.12220-6
46. Mozia S (2010) Photocatalytic membrane reactors (PMRs) in water and wastewater treatment. A Rev Sep Purif Technol 73:71–91. https://doi.org/10.1016/j.seppur.2010.03.021
47. Mpelane A, Katwire DM, Mungondori HH, Nyamukamba P, Taziwa RT (2020) Application of novel c-tio2-cfa/pan photocatalytic membranes in the removal of textile dyes in wastewater. Catalysts 10:1–17. https://doi.org/10.3390/catal10080909
48. Muhd Julkapli N, Bagheri S, Bee Abd Hamid S (2014) Recent advances in heterogeneous photocatalytic decolorization of synthetic dyes. Sci World J.https://doi.org/10.1155/2014/692307
49. Norrman K, Ghanbari-Siahkali A, Larsen NB (2005) Studies of spin-coated polymer films. Annu Reports Prog Chem Sect C 101:174–201. https://doi.org/10.1039/b408857n
50. Park H, Kim HI, Moon GH, Choi W (2016) Photoinduced charge transfer processes in solar photocatalysis based on modified TiO2. Energy Environ Sci 9:411–433. https://doi.org/10.1039/c5ee02575c
51. Penboon L, Khrueakham A, Sairiam S (2019) TiO2 coated on PVDF membrane for dye wastewater treatment by a photocatalytic membrane. Water Sci Technol 79:958–966. https://doi.org/10.2166/wst.2019.023
52. Rajeshwar K, Osugi ME, Chanmanee W, Chenthamarakshan CR, Zanoni MVB, Kajitvichyanukul P, Krishnan-Ayer R (2008) Heterogeneous photocatalytic treatment of organic dyes in air and aqueous media. J Photochem Photobiol C Photochem Rev 9:171–192. https://doi.org/10.1016/j.jphotochemrev.2008.09.001
53. Rajeswari A, Vismaiya S, Pius A (2017) Preparation, characterization of nano ZnO-blended cellulose acetate-polyurethane membrane for photocatalytic degradation of dyes from water. Chem Eng J. Elsevier B.V. https://doi.org/10.1016/j.cej.2016.10.124
54. Rauf MA, Hisaindee S (2013) Studies on solvatochromic behavior of dyes using spectral techniques. J Mol Struct 1042:45–56. https://doi.org/10.1016/j.molstruc.2013.03.050
55. Samsami S, Mohamadi M, Sarrafzadeh MH, Rene ER, Firoozbahr M (2020) Recent advances in the treatment of dye-containing wastewater from textile industries: overview and perspectives. Process Saf Environ Prot 143:138–163. https://doi.org/10.1016/j.psep.2020.05.034
56. Sathya U, Keerthi P, Nithya M, Balasubramanian N (2020) Development of photochemical integrated submerged membrane bioreactor for textile dyeing wastewater treatment. Environ Geochem Health 0123456789. https://doi.org/10.1007/s10653-020-00570-x
57. Schneller T, Waser R, Kosec M, Payne D (2013) Chemical solution deposition of functional oxide thin films. Chem Solut Depos Funct Oxide Thin Film 9783211993:1–796. https://doi.org/10.1007/978-3-211-99311-8

58. Singh R, Sinha MK, Purkait MK (2020) Stimuli responsive mixed matrix polysulfone ultra-filtration membrane for humic acid and photocatalytic dye removal applications. Sep Purif Technol 250:117247.https://doi.org/10.1016/j.seppur.2020.117247

59. Su CXH, Low LW, Teng TT, Wong YS (2016) Combination and hybridisation of treatments in dye wastewater treatment: A review. J Environ Chem Eng 4:3618–3631. https://doi.org/10.1016/j.jece.2016.07.026

60. Subramaniam MN, Goh PS, Lau WJ, Ng BC, Ismail AF (2018) Development of nanomaterial-based photocatalytic membrane for organic pollutants removal. Advanced nanomaterials for membrane synthesis and its applications. Elsevier Inc.https://doi.org/10.1016/B978-0-12-814503-6.00003-3

61. Tang X, Yan X (2017) Dip-coating for fibrous materials: mechanism, methods and applications. J Sol-Gel Sci Technol 81:378–404. https://doi.org/10.1007/s10971-016-4197-7

62. Tijing LD, Woo YC, Yao M, Ren J, Shon HK (2017) 1.16 Electrospinning for membrane fabrication: strategies and applications. Compr Membr Sci Eng 1:418–444. https://doi.org/10.1016/b978-0-12-409547-2.12262-0

63. Viswanathan B (2017) Photocatalytic degradation of dyes: an overview. Curr Catal 7:99–121. https://doi.org/10.2174/2211544707666171219161846

64. Wang M, Yang G, Jin P, Tang H, Wang H, Chen Y (2016) Highly hydrophilic poly(vinylidene fluoride)/meso-titania hybrid mesoporous membrane for photocatalytic membrane reactor in water. Sci Rep 6:1–10. https://doi.org/10.1038/srep19148

65. Wang M, Zhang Y, Yu G, Zhao J, Chen X, Yan F, Li J, Yin Z, He B (2020) Monolayer porphyrin assembled SPSf/PES membrane reactor for degradation of dyes under visible light irradiation coupling with continuous filtration☆. J Taiwan Inst Chem Eng 109:62–70. https://doi.org/10.1016/j.jtice.2020.02.013

66. Wu XQ, Shen JS, Zhao F, Shao ZD, Zhong LB, Zheng YM (2018) Flexible electrospun MWCNTs/Ag$_3$PO$_4$/PAN ternary composite fiber membranes with enhanced photocatalytic activity and stability under visible-light irradiation. J Mater Sci 53:10147–10159. https://doi.org/10.1007/s10853-018-2334-0

67. Zangeneh H, Zinatizadeh AAL, Habibi M, Akia M, Hasnain Isa M (2015) Photocatalytic oxidation of organic dyes and pollutants in wastewater using different modified titanium dioxides: a comparative review. J Ind Eng Chem 26:1–36. https://doi.org/10.1016/j.jiec.2014.10.043

68. Zeng H, Yu Z, Shao L, Li X, Zhu M, Liu Y, Feng X, Zhu X (2020)Ag2CO3@UiO-66-NH2 embedding graphene oxide sheets photocatalytic membrane for enhancing the removal performance of Cr(VI) and dyes based on filtration. Desalination 491:114558.https://doi.org/10.1016/j.desal.2020.114558

69. Zhang L, Mohamed HH, Dillert R, Bahnemann D (2012) Kinetics and mechanisms of charge transfer processes in photocatalytic systems: A review. J Photochem Photobiol C Photochem Rev 13:263–276. https://doi.org/10.1016/j.jphotochemrev.2012.07.002

70. Zhang X, Wang DK, Diniz Da Costa JC (2014) Recent progresses on fabrication of photocatalytic membranes for water treatment. Catal Today 230:47–54. https://doi.org/10.1016/j.cattod.2013.11.019

71. Zheng X, Shen ZP, Shi L, Cheng R, Yuan DH (2017) Photocatalytic membrane reactors (PMRs) in water treatment: configurations and influencing factors. Catalysts 7. https://doi.org/10.3390/catal7080224

Fibrous Membranes for Water Purification: Focusing on Dye Removal

Muhammad Mudassir Iqbal, Gulzar Muhammad, Muhammad Arshad Raza, Muhammad Shahbaz Aslam, Muhammad Ajaz Hussain, and Zahid Shafiq

Abstract Synthetic dyes from textile and other manufacturing industries in the wastewater are harmful due to their toxic, mutagenic, and cancer-causing nature, thus compelling for agile development of necessary processes to purify wastewater efficiently. Being a significant step of industrial wastewater purification, the removal of synthetic dyes is always challenging due to complex and stable aromatic molecular structures, hence the prime focus of current research. The techniques such as biodegradation, photocatalytic degradation, Fenton reagent, adsorption, and absorption are either less effective or costly with operational problems. Recent research reveals that fibrous membranes offer high-throughput performance to remove dyes from contaminated water. The chapter will cover the recent advancements in developing novel strategies for active, economical, and facile removal of synthetic dyes from wastewater using fibrous membranes. Different types of dyes and innovative methods for synthesis and modification of fibrous membranes are also discussed in detail. The chapter's core focus is to investigate the underlying mechanisms of dye removal using fibrous membranes for wastewater treatment.

Keywords Fibrous membranes · Dye · Nanofibers · Photodegradation · Electrospun · Wastewater · Polyaniline · Polydopamine · Chitosan · Dextrin · Polyacrylonitrile

M. M. Iqbal (✉) · M. S. Aslam
School of Biochemistry and Biotechnology, University of the Punjab, Lahore, Pakistan

G. Muhammad (✉) · M. A. Raza
Department of Chemistry, GC University Lahore, Lahore, Pakistan
e-mail: mgulzar@gcu.edu.pk

M. A. Hussain
Institute of Chemistry, University of Sargodha, Sargodha, Pakistan

Z. Shafiq
Institute of Chemical Sciences, Bahauddin Zakariya University, Multan, Pakistan

Abbreviations

ßCD	ß-Cyclodextrin
BET	Brunauer–Emmett–Teller
ChNW	Chitin nanowhisker
CMF	Cellulose micro-fibrils
CNFs	Carbon nanofibers
cPAN	Carbonaceous polyacrylonitrile
CR	Congo red
FTIR	Fourier Transform infrared spectroscopy
KCC-1	High-surface area silica nanospheres
kDa	Kilo Dalton
LDH	Layered double hydroxide
MB	Methylene blue
MfSNPS	Methyl functionalized mesoporous silica nanoparticles
MMMs	Mixed matrix membranes
MO	Methyl orange
MOF	Metal–organic frame work
NFMs	Nanofibrous membranes
NMP	*N*-Methylpyrrolidinone
p(GMA)	Poly(glycidyl methacrylate)
PANI	Polyaniline
PAEK-COOH	Carboxylated poly (arylene ether ketone)
PAN	Polyacrylonitrile
PDA	Polydopamine
PEI	Polyethylenimine
PEO	Polyethylene oxide
PIM-1	Polymer of Intrinsic Microporosity
PTFE	Polytetrafluoroethylene
PVA	Polyvinyl alcohol
PVDF	Polyvinylidene fluoride
RCF	Regenerated cellulose films
SEM	Scanning electron microscopy
SPET	Poly(ethylene terephthalate)
TGA	Thermogravimetric analysis
UV–vis	Ultraviolet–Visible
XRD	X-ray diffraction
ZIF	Zeolitic imidazolate framework

1 Introduction

Dyes are an intricate class of contaminants in wastewater harmful to both health and the environment. Industries are endlessly introducing the dyes [26, 54]. Intractability and property of dyes to impart visible and undesirable color to water are now a significant issue for the environment [1]. The development of agile, efficient, and economical water purification systems to eliminate harmful dyes from wastewater is critically important [6, 34, 45, 71]. Dyes employed during dyeing and printing processes of yarn and fabrics are discharged from the textile industry into wastewater. There are various strategies available for the rejection of dyes from industrial discharge water. Examples of dye rejection strategies include biological degradation by activated sludge, adsorption on activated carbon or membranes. No technique yet encompasses the removal of all the dyes from contaminated water. Cost-effectiveness, size of rejection plant, and operation complexity are limiting factors to practice an effective dye removal process from wastewater [15].

Purification of wastewater by adsorption is economical, easy to handle, and practical [4]. Rejection of dyes from wastewater by adsorption is a premium method among versatile techniques practiced currently. Different materials remove the dyes from contaminated water to cut environmental toxicity and encourage salvage practice of water and chemicals [63]. Organic nanofibrous membranes perform brilliantly in contaminated water remediation and recently are noticed extraordinarily [87]. Covalent organic frameworks, evolving materials in the textile discharge treatment, offer potential perviousness and consistent channel structure [58]. Cellulose microfibers find various applications owing to advantages of biological origin, sustainability, and easy availability in abundance [44]. Polyaniline (PANI) and modified forms adsorb dyes through cationic nature and show potential dye rejection from wastewater [63]. Metal–organic framework (MOF) is the focus of current research in wastewater purification. The expensive and time-requiring step during recycling after adsorption is to filter or centrifuge the metal MOF nanoparticles from suspension. The photocatalytic ability of MOF nanofibrous composite membranes eliminates this step. During the regeneration, the fibrous membranes easily separate from the suspension [24]. Modification with specific functional groups increases the capabilities of nanofibrous membranes for dye rejection from contaminated water. Polyacrylonitrile (PAN) nanofibers modified with protein show the ability to confiscate cationic dyes from contaminated water [26].

This chapter starts with an introduction to fibrous membranes employed for dye removal from wastewater. The introduction follows a discussion on the features of fibrous membranes and factors affecting the efficiency and adsorption ability of nanofibrous structures. The parameters which require optimization to achieve maximum efficiency and adsorption capacity are also discussed. The methods for the preparation of fibrous membranes are also introduced. In the next part of the chapter, fibrous membranes are arranged and discussed according to the type of constituent polymer and the modification. Novel strategies and methods for the fabrication, modification, and characterization of various nanofibrous materials recently used

in dye rejection are discussed in detail in this part of the chapter. Dye rejection from contaminated water, mostly industrial discharge water, is the prime focus of discussion. This part of the chapter provides insight into the underlying principles and mechanisms in the fabrication, modification, and adsorption/desorption processes. In this part of the chapter, regeneration and recyclability of the nanofibers are also explored. This chapter also provides the reader a comparison of the dye removal efficiency and adsorption capacity of various nanofibers. In the last, future horizons of fibrous membranes for dye removal are discussed.

2   Features of Fibrous Membrane

The membranes for removing dyes from wastewater rely on adsorption phenomena on nanofibers. The efficiency for dye adsorption is determined by important structural and functional features of nanofibers constituting the membrane. The nature of functional groups on nanofibers controls the type of dye adsorbed by the membrane. The fibrous membranes interact with the dye through electrostatic interactions, hydrogen bonding, or hydrophobic interactions. Figure 1 illustrates the interactions of Congo red (CR) with nonwoven polystyrene/PANI. The functional groups on nanofibers are modified by decoration the membranes with various molecules like enzymes, proteins, nanoparticles, and natural and synthetic polymers [1, 3, 4, 8, 37, 60].

The average diameter of nanofibers constituting the membrane is significant as it affects the surface area available for dye adsorption. A direct relation is observed between dye adsorption capacity and the average fiber diameter [87]. The average
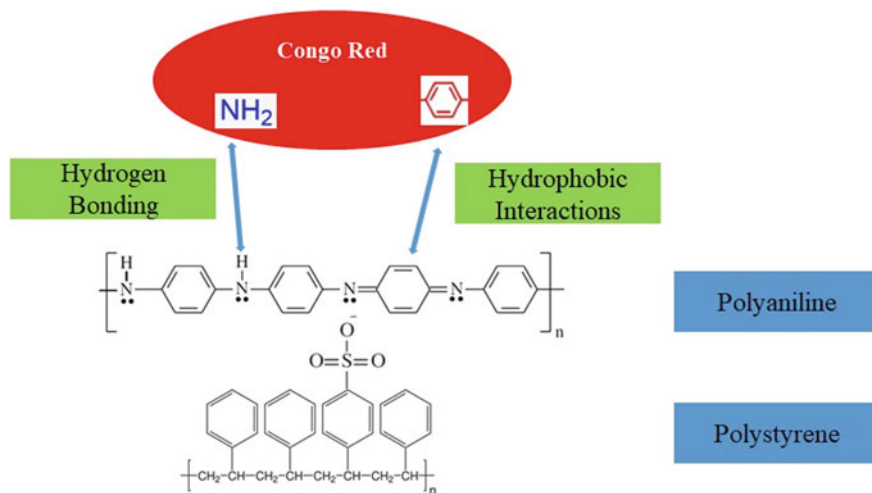
Fig. 1 Congo Red dye is adsorbed on fibrous membranes by hydrophobic interactions (via benzene ring) and hydrogen bonding (via amino group)

pore size and nature of the membrane affect dye adsorption on the membrane [83]. Larger pore size and layered structure increase dye adsorption on the membrane [72]. Reliable techniques and methods characterize the morphological characteristics of fibrous membranes. Elemental analysis, X-ray diffraction (XRD), Brunauer–Emmett–Teller (BET), Fourier Transform infrared spectroscopy (FTIR), EDEX zeta potential, porosity and ion exchange capacity, Energy-dispersive spectrometry, Scanning electron microscopy (SEM), Transmission electron microscopy (TEM), Thermogravimetric analysis (TGA), and Vibrating sample magnetometer are widely used to investigate the structural and morphological characteristics of fibrous membranes [18, 24, 40, 44].

Functional characteristics of fibrous membranes include dye adsorption capacity, dye desorption ability, and recyclability. Membranes with higher adsorption capacity in minimum time, flux volume, and pressure are desired. The adsorbed dye is de adsorbed to regenerate the membrane. Desorption of dye takes place by changing the conditions of adsorption. Alkalies, acids change the pH and weaken the electrostatic interaction between dye and adsorbent. Organic solvents are also useful in the desorption process. The membranes with higher desorption capacity and recyclability are desired. Antifouling and self-cleaning membranes perform excellently in industrial wastewater treatment [36, 56].

3 Factors Affecting Efficiency of Fibrous Membrane for Dye Removal

Initial dye concentration, pH, flow flux, flow time, flow volume, and diffusion rate significantly affect dye's adsorption on the membrane nanofibers during a dye removal process. The parameters are optimized to achieve maximum adsorption capacity in minimum time. Estimating optimum values for operational parameters, in a dye adsorption strategy, through response surface methodology or other available statistical tools reduces time and cost.

4 Methods of Fibrous Membrane Fabrication

Various methods are available for the fabrication of nanofibers used in dye removal from wastewater. Recently employed methods include electrospinning, sol–gel method, calcination and liquid phase deposition, one-pot method, solvent casting/progen leaching method, and non-solvent induced phase inversion process [37, 51]. Among all the nanofiber fabrication methods, electrospinning is widely used to prepare nanofibers. Electrospinning fabricates membranes of uniform pore size with increased surface area [19]. The processes of electrospinning and solvent casting are illustrated in Fig. 2.
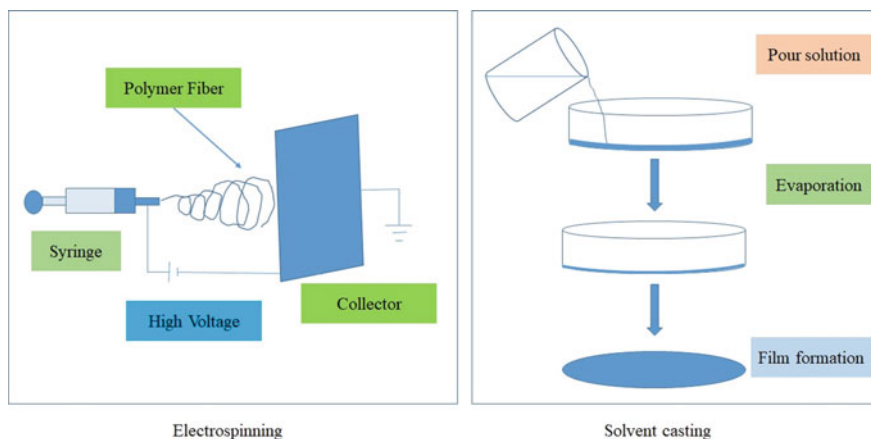
Fig. 2 The processes of electrospinning and solvent casting for preparation of fibrous membranes

5 Organic Polymer Membrane

5.1 Polyacrylonitrile Composite Membrane

Silk fibroin/PAN removes the dye from wastewater. Double-layer filters are synthesized with different compositions of PANI/TiO$_2$. The electrospinning method is used to fabricate these membranes. SEM reveals ultra-fine fibers arranged in mats in the double-layer filters. Beads are not formed in the structure. The Silk fibroin/PAN double-layer filters show high-tensile strength fibers. Anionic reactive black (HFGR) dye removal from aqueous media takes place through adsorption on fibers. The experiment is performed in a dead-end stirred cell filtration device. PANI/TiO$_2$ concentration, pH, and dye concentration affect dye's adsorption [5]. PAN/CaCO$_3$ nanofiber is fabricated using the solvent casting/progen leaching method and subsequently aminated with triethylenetetramine for dye adsorption from an aqueous solution. The nanofiber morphology is investigated by SEM, illustrated in Fig. 3. The functional group modification of nanofibers is investigated by FTIR shown in Fig. 4. Dye removal by the nanofibrous membrane is illustrated in Fig. 5. The optimum conditions for dye removal from wastewater are optimized, and an adsorption model is build using response surface methodology shown in Fig. 6 [51].

Flux and selectivity are essential contrasting features of adsorbents. An inexpensive gradient hybrid membrane is fabricated from oxidized multiwall carbon nanotubes forming a functional layer by electrospray. Ultra-thin PAN layer is fabricated in the middle supported on polypropylene nonwoven fibers. Based on gradient structures, the membrane shows excellent flux under low pressure and removes indigo dye with high removal ratio of 98% [89]. PAN nanofibers' double metal modification shows combined features of ultrathin fiber diameter, greater surface area, and
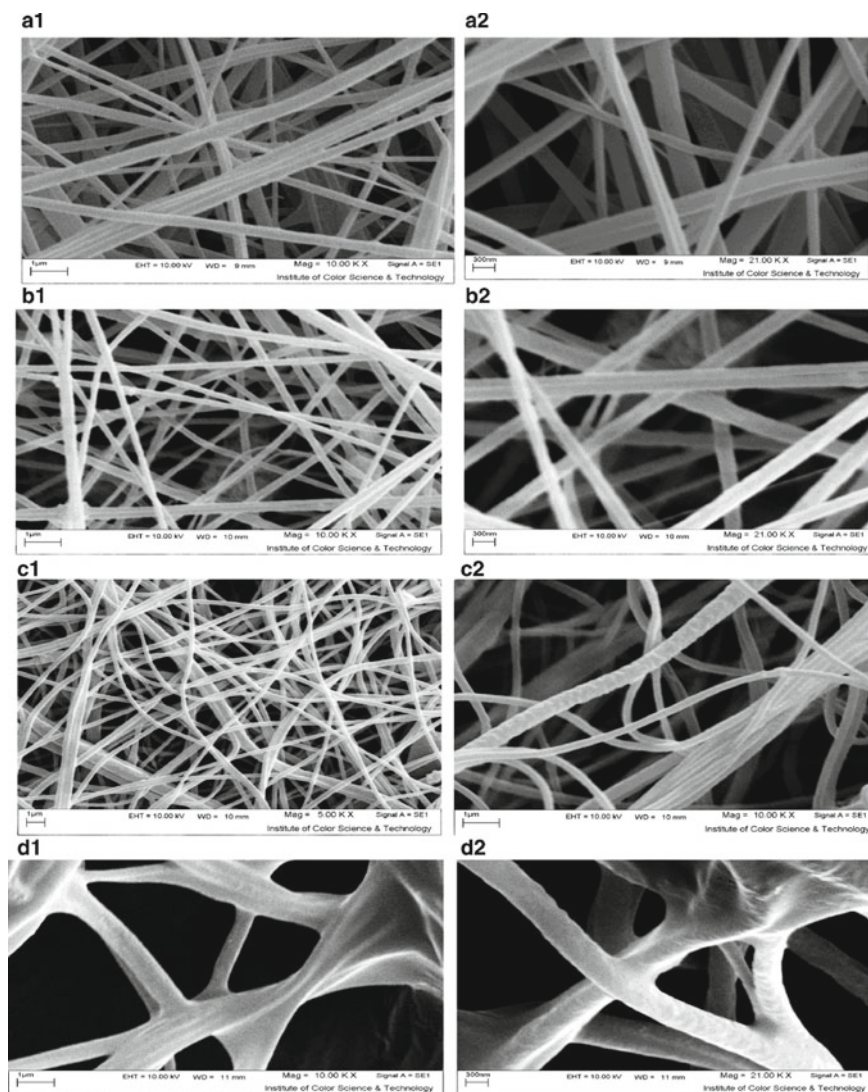
Fig. 3 SEM images showing the morphology of PAN nanofibers and PAN nanoporus fibers before and after functionalization with CaCO₃ or amine. **a**(1,2) Pure PAN nanofibers, **b**(1,2) PAN/CaCO₃ nanofibers, **c**(1,2) nanoporous PAN nanofibers, and **d**(1,2) Aminated nanoporus PAN nanofibers. (Reprinted with permission of Elsevier from [51])

increased porosity. The fibrous membrane releases hydroxyl radicals when irradiated with light and offers excellent dye degradation capacity through photocatalytic activity. Reactive blue 19, reactive red 195, and acid orange 7 are shown to degrade by the membrane's photocatalytic activity. The membrane is reusable [91].
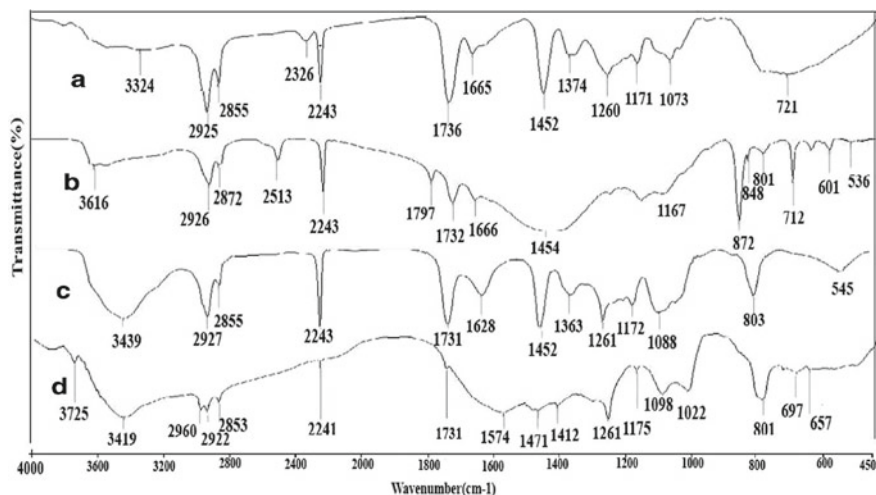
Fig. 4 Fourier transform infrared (FTIR) spectra of the nanofibers shows changes in functional groups during modification of PAN nanofibers. Stretching of carbonyl group disappears due to calcination. And new peaks of calcite appear. Similarly, bending due to amine group and decreased intensity of peak of nitrile group **a** pure PAN nanofiber **b** CaCO$_3$/PAN nanofiber **c** nanoporous PAN nanofiber **d** Aminated nanoporus PAN nanofiber. (Reprinted with permission of Elsevier from [51])

5.2 Polyvinylidene Fluoride Nanofibers

Treatment of PVDF with carbon dioxide plasma by electrospinning decreases hydrophobicity. Carbon dioxide plasma-treated PVDF rejects crystal violet dye efficiently. Phase inversion and solvent casting for PVDF fabrication are disadvantageous due to less surface area and membrane pore size. In contrast, the electrospinning method produces uniform pore size with an increased surface area. FTIR results show the introduction of negatively charged carboxylate groups on PVDF membrane after treatment with carbon dioxide plasma. The introduction of carboxylate groups in PVDF increases rejection capacity to crystal violet due to significant electrostatic interaction with dye [19]. Core–shell-like structures are synthesized from PVDF nanofibers and polypyrrole particles with help of polydopamine (PDA). Initially, PVDF/dopamine nanofibers are synthesized by electrospinning. The addition of Tris-HCl solution initiates the polymerization of dopamine into polydopamine. Pyrrole polymerizes on fibrous membrane through oxidation with the help of FeCl$_3$. Nitrogen-containing groups on the surface of the core–shell-like structure increase surface area and solubility in water. Composite nanofibers show excellent adsorption of methylene blue (MB) and CR [48].

Electrospinning PVDF with chitin nanowhisker (ChNW) introduces functional groups in the membrane used to remove the indigo carmine dye. ChNW are hydrophilic biopolymers containing two functional groups, while PVDF is hydrophobic. PVDF and ChNW ratio (15%:1%) gives a combination of hydrophobic
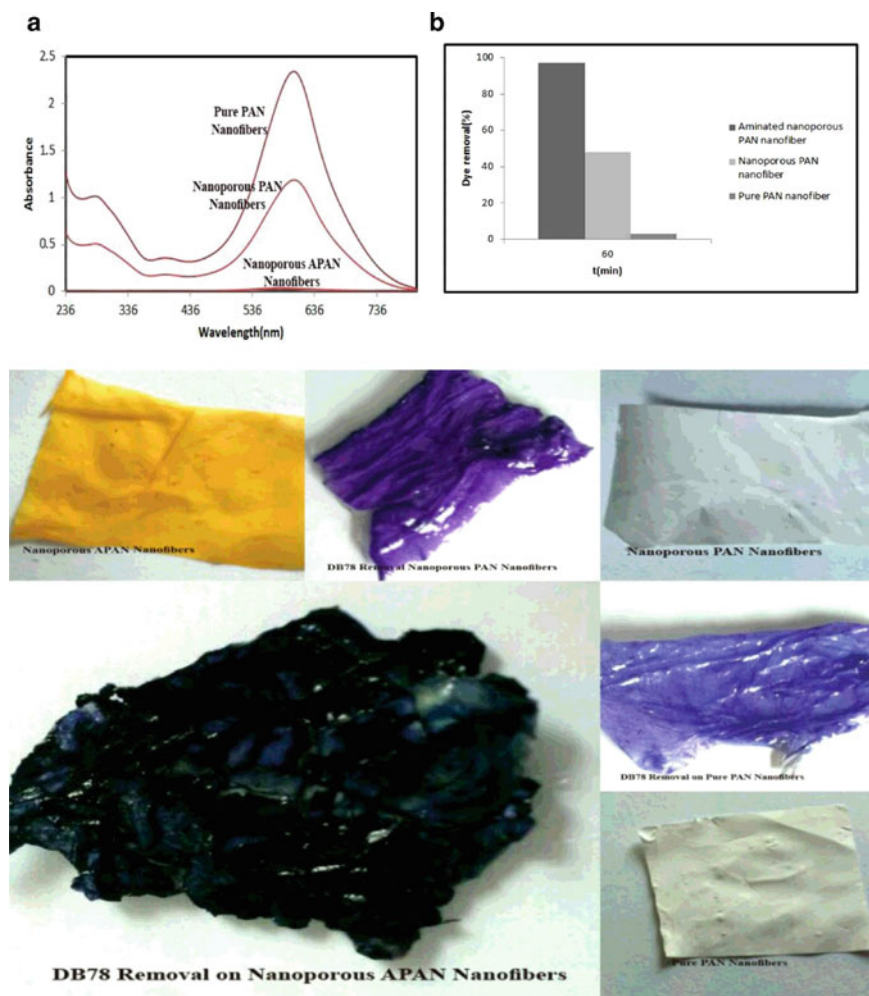
Fig. 5 Use of nanofibers and nanoporus nanofibers to remove dye a Ultraviolet–Visible (UV–vis) absorption spectra of nanofibers and nanoporus nanofibers, **b** Column chart showing dye removal efficiency of nanofibers, Direct Blue 78 (DB78) removal by PAN nanofibers ($C = 80$ mg/L, $V = 250$ mL, $t = 60$ min, $T = 25$ °C). (Reprinted with permission of Elsevier from [51])

and hydrophilic functional groups. ChNW increases the contact angle of PVDF membrane and enhances the dye rejection capacity to IC. The novel idea of combining PVDF and ChNW is further extendable to the rejection of proteins, especially hormones and viruses, from wastewater [20]. Membrane distillation provides long-term and trustworthy water purification system. Polytetrafluoroethylene (PTFE)/PVDF are flat sheet membranes. Membranes are synthesized by using phenomena of evaporation of solvent through heat. Methyl functionalized mesoporous silica nanoparticles (MfSNPS) are used to modify PVDF/PTFE membranes.
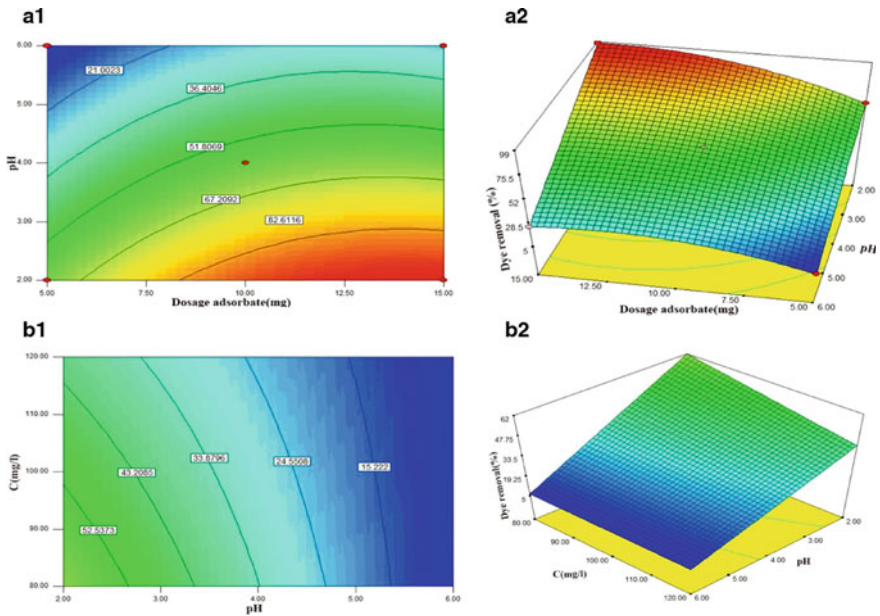
Fig. 6 **a**(1,2) The effect of adsorbent dosage and pH on dye removal by PAN nanofibers, and **b**(1,2) ($V = 250$ mL, $t = 60$ min, $T = 25\ °C$). (Reprinted with permission of Elsevier from [51])

Important surface characteristics of membranes include morphology, water repulsion, and pore size. Lab experiments with feed water solution and permeate solution give a stable and pure water output through MfSNPS/PVDF/PTFE membranes. MfSNPS/PVDF/PTFE membranes show the ability to remove CR dye from an aqueous solution with 99% efficiency [30].

Metal salts with different anions are used to synthesize hybrid membranes from PVDF. Novel PVDF and layered double hydroxide (LDH) composite membrane PVDF@LDH is synthesized by combining the method of electrospinning and hydrothermal treatment. Anions (NO_3^-, Cl^-, SO_4^{2-}) affect the structure and charging extent of LDHs implanted on the surface of PVDF nanofibers. Sulfate ions allow the creation of the hierarchical structure of hybrid fibers. PVDF@CoAl-LDH offers dye adsorption of ~621 mg/g for MO. The composite membrane shows more than 90% dye rejection even after three adsorption and desorption cycles [55]. PVDF-calcium alginate nanofiltration membranes are innovative and offer high flux permeation for dye rejection. The membrane is fabricated by electrospinning PVDF with sodium alginate solution. $CaCl_2$ crosslinks the polymer. Field emission SEM equipped with energy-dispersive spectrometry attenuated total reflectance-FTIR, and X-ray photoelectron spectroscopy is used to characterize the features of the composite membrane. The membrane shows ~99% rejection of MB and higher rejection of seven dyes. The membrane also offers antifouling efficiency to bovine serum albumin and bacteria [56].

5.3 Polyaniline Membrane

PANI is an economical and efficient polymer for the adsorption of dyes from polluted water. Amino groups in PANI acquire positive charge after accepting hydrogen ion. Adsorption of dyes on PANI takes place through mechanisms of different types of interactions. PANI shows more affinity toward anionic dyes. Modified PANI with the increased surface also shows an affinity for cationic dyes. Modified PANI shows enhanced adsorption capacity, porosity, number of binding sites, interaction due to functional group modification, and ion exchange features [63].

Conducting polymers are widely used for wastewater purification. One drawback of conducting polymers is an aggregation of the polymer. Polystyrene/PANI membranes produced by electrospinning are capable of removing dyes from wastewater. Introduction of PANI into nonwoven polystyrene fabricates nonwoven polystyrene–PANI mates. Investigations with contact angle measurements, SEM, FTIR, and UV–vis spectroscopy provide knowledge about composite membranes' characteristics. Interaction time, pH, and initial dye concentration affect adsorption of CR dye and azo dye on the nonwoven polystyrene–PANI membrane. Nonwoven polystyrene–PANI membrane shows the excellent capability to reject CR efficiently from wastewater. The membrane shows recycling ability for 13 cycles of adsorption/desorption without a decrease in dye adsorption capacity on the membrane. The membranes show the application's capability in compact filtration units to achieve fast removal of dye from wastewater [21].

Polyethylene oxide (PEO)/PANI hybrid membranes are inexpensive and novel. Combining PEO with PANI increases the dye adsorbing efficiency of PEO more than two times. The scheme for the fabrication of composite membranes is shown in Fig. 7 while SEM images in Fig. 8 demonstrate surface morphology of the composites. The composite membrane maintains 99% adsorption up to eight cycles of adsorption and desorption. PEO/PANI shows an ability to adsorb methyl orange (MO) dye efficiently. The composite membrane is also applicable for the crossflow filtration unit. The MO and PEO/PANI interaction is illustrated in Fig. 9 [54].

5.4 Polydopamine Membrane

Polyethylenimine (PEI) and PDA are coated on the surface of polyphenylene sulfide. PDA acts like glue in a molecular modification of fibers. Coating increasing stability, the property of polyphenylene sulfide membrane surface to interact with water and life of nanofiber. Besides, the crosslinking of catechol and amino in coating increases resistance to acids. The coated membrane shows more than 99% dye rejection of methyl blue and rhodamine B. The membrane shows dye rejection even after three adsorption–desorption cycles. Additionally, the surface-modified membrane shows the potential for good flux recovery. The membrane also exhibits antifouling property [88]. Chitin nanocrystals are decorated with DA and graphene oxide. DA-Chitin
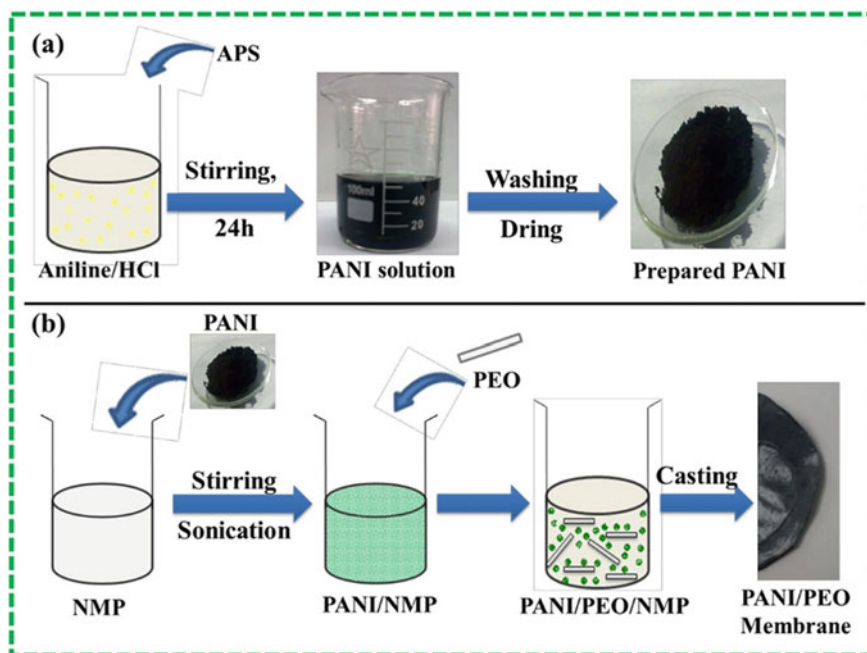
Fig. 7 Scheme the synthesis of **a** PANI powder **b** PANI/PEO composite membrane. *N*-methylpyrrolidinone (NMP). Briefly the PANI is prepared by mixing reactants followed by washing. Then PANI and NMP are stirred to obtain nanofibers and membrane is obtained by casting. APS: Ammonium persulfate; PEO: Polyethylene oxide; PANI: Polyaniline. (Reprinted with permission of Elsevier from [54])

nanocrystals/graphene oxide fabrication is facilitated by vacuum filtration. DA-Chitin nanocrystals proportion in membrane affects hydrophilicity of membrane. Novel membrane shows a high capacity to remove MB (99.3%) and CR (98.3%) from wastewater with recyclability and regeneration properties. The membrane also shows antifouling property [66].

Membranes modified to carry catalytic oxidation take another advantage of the decrease in fouling problem. The surface of polypropylene is modified with PDA and zeolitic imidazolate framework (ZIF), ZIF-67 using local association of monomers to fabricate PDA/ZIF-67/polypropylene hybrid membrane. The fabrication process of PDA/ZIF-67/polypropylene is illustrated in Fig. 10. The crossflow filtration process for wastewater remediation is illustrated in Fig. 11. The membrane rejects dye using visible light and peroxymonosulfate activation simultaneously. Surface decoration of polypropylene with PDA and ZIF-67 increases the adsorption of dye more than two times. The surface decorated membrane shows high efficiency in physical filtration, photocatalysis, peroxymonosulfate catalysis. The mechanism for photocatalysis by PDA/ZIF-67/polypropylene is illustrated in Fig. 12. The membrane also shows recyclability, anti-fouling, and self-cleaning properties for
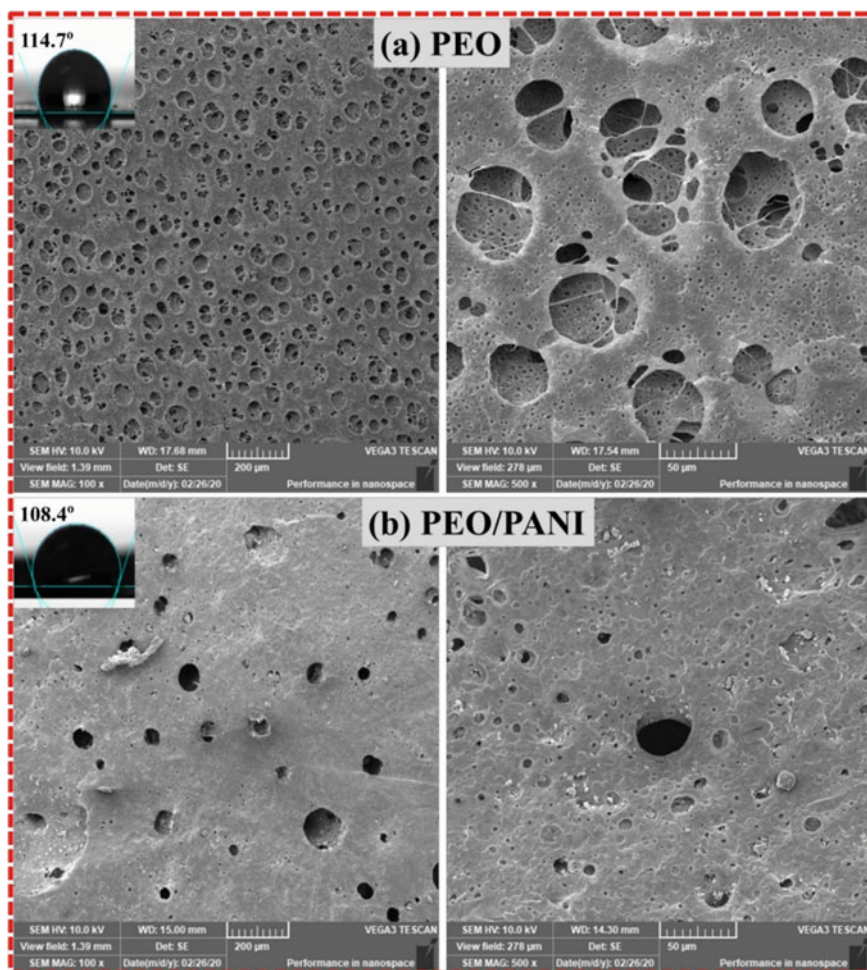
Fig. 8 SEM images and contact angle of **a** pure PEO and **b** PEO/PANI composite membrane. PEO: Polyethylene oxide; PANI: Polyaniline. (Reprinted with permission of Elsevier from [54])

the dye rejection process. The foulants transferred to membrane surface contribute to the high antifouling property of membranes. Sulfate ions and oxide ions help in dye degradation by the membrane [36].

5.5 Polyethylenimine Membrane

Catechol (Cc) implanted PEI nanohybrid membrane is cost-effective and easily fabricated. Surface decorated nanohybrid membrane contains hydrophilic amino
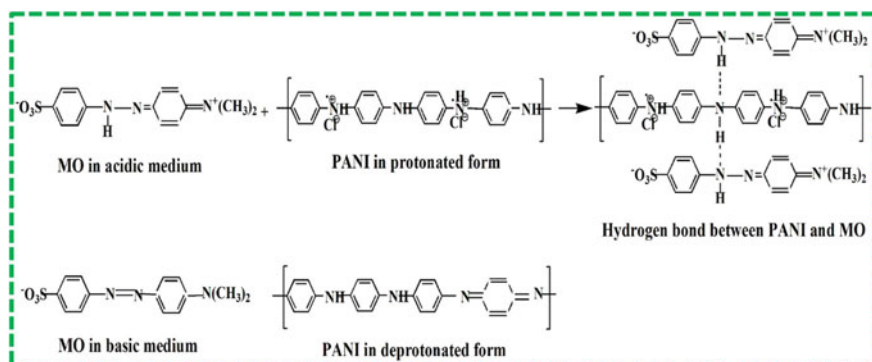
Fig. 9 Effect of acidic and basic pH on chemical structure of MO dye and PANI. The proposed chemical interaction between MO dye and PANI. (Reprinted with permission of Elsevier from [54])
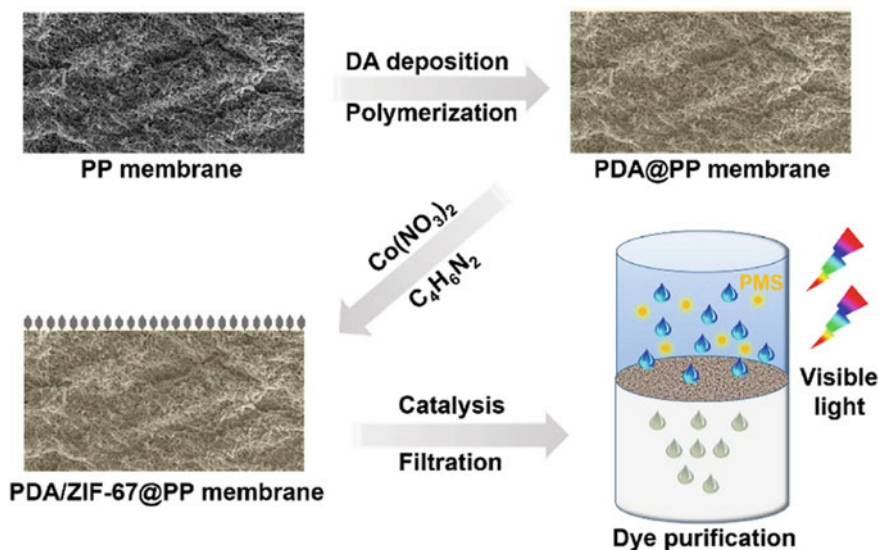
Fig. 10 Fabrication and application of PDA/ZIF-67@PP membrane in dye wastewater remediation. Polypropylene membrane is factionalized with DA and ZIF-67 in two steps. The functionalized membrane removes dye from wastewater through photocatalysis. DA: Dopamine. (Reprinted with permission of Elsevier from [36])

groups in nature and shows high oil-repellent property underwater. Hence, membrane is useful for the separation of dyes and oils and surfactants from oil emulsions during purification steps. The membrane is resilient to alkalies and allows selective control of dye and surfactant rejection. The membrane shows high efficiency for more than 30 regeneration cycles of rejection and recovery. The surface decorated membrane shows the potential of high efficiency in wastewater purification
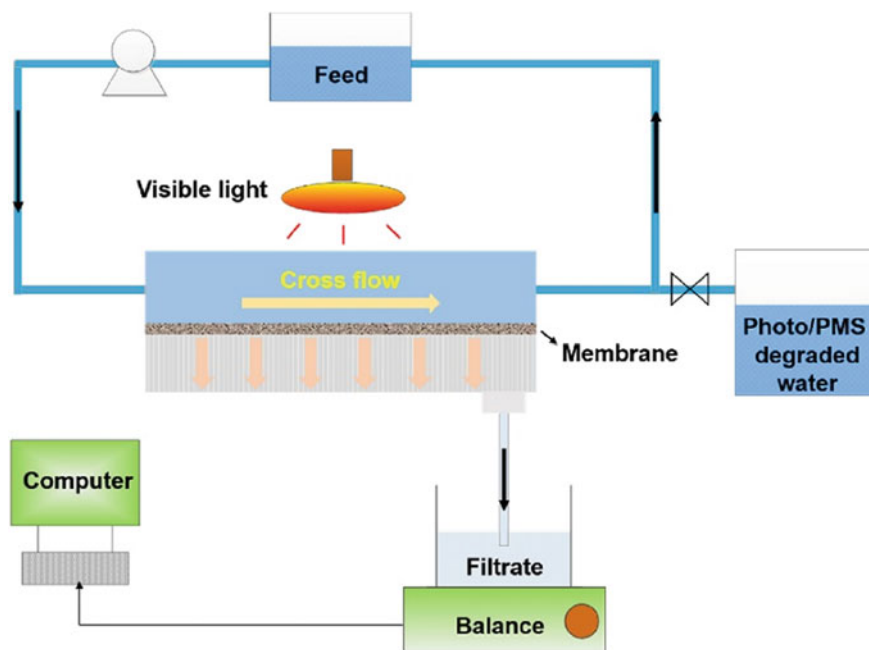
Fig. 11 Crossflow filtration apparatus applied for photodegradation of dye from wastewater. The wastewater, feed contaminated with dye flows on surface of membrane and decontaminated water is collected as filtrate. PMS: Peroxymonosulfate. (Reprinted with permission of Elsevier from [36])

[43]. Hybrid nanofibrous membrane fabricated from modified polyethylenimine (m-PEI) and PVDV through electrospinning show adsorption of MO ~633 mg/g. The composite membrane comprising nanofibers shows a porous structure. The fibrous membrane requires an alkaline solution for regeneration and is recyclable. Film diffusion and intra-particulate diffusion are factors affecting dye's adsorption onto nanofibers [50].

5.6 Polyvinyl Alcohol Membrane

Nanofiber membranes implanted with ZnO nanoparticles on PVA and konjac glucomannan nanofibers are fabricated through electrospun and heat-mediated crosslinking. The resultant membranes are multifunctional and show a capacity to filter air, kill bacteria, and adsorb dyes. Besides, the nanofibrous membrane possesses catalytic activity aided with light. The nanofibrous membrane show high efficiency in dye adsorption for methyl orange aided with photocatalytic activity. The membrane also shows less resistance to flow [46]. PVA/chitosan/silica composite nanofiber (PCSCN) fabricated by electrospinning shows potential adsorption
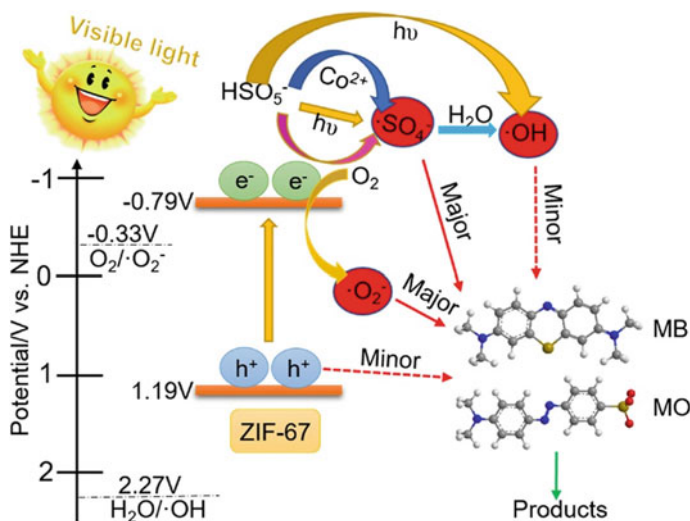
Fig. 12 Proposed mechanism of dye degradation with peroxymonosulfate activated by visible light. ZIF-67 acts as photocatalyst and activates PMS. The reactive species generated by PMS cause degradation of dyes. PMS: Peroxymonosulohate; NHE: Normal hydrogen electrode. (Reprinted with permission of Elsevier from [36])

capacity (322 mg/g) of direct red 80 (DR80) from wastewater. The adsorbent shows maximum adsorption at 2.0 pH, ~2 g dosage, and ~16 mg/L dye concentration [52].

PVA/starch hydrogel nanofibrous membrane is synthesized using electrospinning. Thermal treatment is used to crosslink polymers. PVA/starch hydrogel is used for the rejection of MB dye from aqueous solutions. MB is desorbed from the membrane by passing 5% (v/v) HCl. The membrane shows a maximum adsorption capacity of 400 mg/g. The membrane is suitable for parting MB (cationic dye) and MO (anionic dye). The property is attributed to the stability and tensile strength of membrane fibers [59]. Copolymer PVA/PAA fabricated by electrospinning is coated with PDA. PDA contains functional groups that increase the adsorption of dye on the adsorbent. Membranes fabricated by electrospinning show high specific surface area. The nanofibrous membrane shows an adsorption capacity of 1146.6 mg/g for MB and good recyclability [90].

5.7 Polymers of Intrinsic Microporosity

PIM-1 shows the high binding capability to neutral molecules and are auspicious fibers for decontamination. Due to its nonpolar nature, PIM-1 does not interact with cationic and anionic dyes. Functional group modification of PIM-1 increases the adsorption properties of nanofibers. Borane dimethyl sulfide complex modifies nitrile groups of PIM-1 fibrous membrane (PIM-FM) to amine groups. The fibrous

membrane AM-PIM-FM is obtained with amine modification. For control application, PIM-1 dense membrane (PIM-DM) is also modified. SEM analysis shows that the average diameter of microfiber does not change during conversion. PIM-1 thick membrane and fibrous membrane both are insoluble in organic solvents. The fibrous membranes are useful for the adsorption of anionic dyes, such as methyl orange from wastewater, by electrostatic interactions between amine and anionic dye. The amino-modified membrane shows increased capacity to remove anionic dye from water compared to PM-1 dense membrane used as control. The membrane is investigated for continuous adsorption/desorption and batch adsorption studies to filter anionic dyes from wastewater [75]. Ultrafine fibers of PIM-1 are fabricated by electrospinning method from hydrolyzed PIM-1. Hydrolysis of PIM-1 takes place in the presence of sodium hydroxide base. After hydrolysis, PIM-1 is washed and electrospun. Uniform and bead-free fibers are obtained using PIM-1 with different degrees of hydrolysis. Thus, the adsorbent removes MB from water by a simple filtration process without deriving force [74].

5.8 Miscellaneous Organic Membranes

Polyvinyl chloride membranes synthesized by electrospinning are treated with solvent and heat to remove cationic dye through adsorption. Initial concentration of dye and temperature of the solution affect dye adsorption on fibrous membranes. The membranes contain long and ultrafine fibers when polyvinyl chloride is subjected to electrospinning at a concentration of 10% (w/v) in a solvent containing tetrahydrofuran dimethylformamide. Solvent treatment increases the tensile strength of fibers from 0.67 to 7.87 Mega Pascal. The equilibrium sorption capacity of membrane increases with temperature and initial dye concentration [99].

Clavibacter michiganesis is immobilized on polycaprolactone and polylactic acid nanofibrous webs fabricated by electrospinning. The adsorbent removes setazol blue BRF-X from textile effluents in 48 h from initial concentrations of 50, 100, and 200 mg/ml. The integration of bacteria on nanofibrous webs is investigated by SEM, imaging, and optical density analysis. The adsorbent is reusable for five cycles [73].

Copolymer poly(dimethyl diallyl ammonium chloride-acrylamide) is subjected to electrospinning with cellulose acetate to manufacture hybrid nanofiber membranes. The adsorbent thus produced shows rejection of acid black 172 from contaminated water. An increase in the proportion of copolymer to 40 wt% enhances the adsorption capacity of adsorbent to 192 mg/g. There is a direct relation with the average fiber diameter in the hybrid adsorbent [87]. In a simple two-step method, the polymeric salicyl active esters are deposited on fibrous membranes and then modified with functional groups. Nanocomposites are used to remove organic dye from wastewater. SEM evaluates nanocomposite fibers' structure, while the surface characteristics are analyzed by nitrogen adsorption/desorption isotherm. FTIR is used to study the contact angle and modification of functional groups. Fibrous nanocomposites show selective adsorption of anionic dyes from the mixture of cationic and anionic

dyes and regeneration abilities. Kinetic models and isotherm models investigate the adsorption of dyes on nanofibers. The nanocomposite shows maximum adsorption of methyl blue. Cost-effective synthesis of salicyl active esters, excellent adsorption, and regeneration ability make these fibrous membranes useful in research and water purification applications [94].

Poly (L-lactic acid) nanofibers are synthesized using the plasma etching technique. Plasma etching technique is a simple, emerald, and efficient method for the fabrication of nanofibers and generates active binding sites on the surface of fibrous membranes. Poly (L-lactic acid) nanofibers synthesized by plasma etching efficiently adsorb the MB dye. The adsorption takes place by electrostatic forces of attraction. Initial dye concentration and plasma etching time both affect the adsorption properties of fibrous membranes. Chemical adsorption kinetics of dye on the fibrous membrane is pseudo-second order, and Langmuir model explains the isotherm data [6]. Tight membranes for ultrafiltration are synthesized from carboxylated poly (arylene ether ketone) (PAEK-COOH) using a non-solvent-induced phase inversion process. PAEK-COOH is a condensation polymer of 2-[bis(4-hydroxyphenyl)methyl] benzoic acid and 4,4′-bisfluorodiphenyl ketone. Polymer shows thermal stability with a decomposition temperature of 360 °C. The hydrophilic nature of a tight membrane is determined by the angle of contact. PAEK-COOH tight ultrafiltration membranes show 99.8% adsorption of CR dye from 100 ppm solution at 0.4 megapascal pressure. The membranes are applicable to separate dye from dye and salt mixtures as membranes allow monovalent ions to pass through. Membrane shows a molecular weight cut-off value of 9.260 kDa and hence allows monovalent ions to pass through. Divalent ions are slightly rejected. The membrane also shows antifouling properties and anti-dye adsorption characteristics for bovine serum albumin. The membrane offers an ability to reject CR, coomassie brilliant blue, direct red 23, and Evans blue from dye permeate flux [42].

Porous membrane with catalytic ability in the presence of light is fabricated by electrospinning PTFE/PVA/zinc acetate dehydrate. Later PVA is removed from the membrane. PTFE is a substrate to support ZnO. ZnO particles act as photocatalysts in photocatalytic porous membranes. ZnO photocatalyst particles are formed by the decomposition of zinc acetate dehydrate present in porous membranes. Porous membranes are flexible, chemically stable, and possess surface area with high specificity. Homogenous immobilization of ZnO particles on the surface reduces cluster formation and settling of ZnO particles from suspension. Experiments with vacuum membrane distillation and photodegradation reveal that PTFE/ZnO membranes show the ability to remove dyes and slat both simultaneously. Other PTFE/ZnO membranes exhibit self-cleaning ability when fouled membranes are treated with UV radiation. PTFE/ZnO membranes show the broad-spectrum potential in water purification for dye removal [25].

Capable composite cationic exchange adsorbent fibrous membranes are fabricated to remove chlorazole black E dye from wastewater. Bromoacetyl bromide is an atom transfer radical polymerization (ATRP) initiator and modifies functional groups in cellulose films. Regenerated cellulose films (RCF) are implanted with poly(glycidyl methacrylate) p(GMA) through surface-initiated ATRP (SI-ATRP). H_3PO_4 and

H_2SO_4 are used to modify RCF-g-p(GMA) into RCF-g-p(GMA)–PO_3H_2 and RCF-g-p(GMA)–SO_3H, respectively. The fabrication process of RCF-g-p(GMA)–PO_3H_2 and RCF-g-p(GMA)–SO_3H and subsequent adsorption of chlorazole black E on nanofibers are illustrated in Fig. 13. FTIR, SEM, and analytical procedures characterize the morphology and structure of the modified fibrous membrane. Factors that affect adsorption include a dose of adsorbent, pH, ionic strength, initial concentration of dye, and exposure time. Both membranes show maximum rejection at acidic pH. The adsorption process of chlorazole black E dye on both membranes follows pseudo-second-order kinetics and adsorption equilibrium correlates with Langmuir and Freundlich isotherm. Modified RCF shows an ability to regenerate the membranes for ten cycles of adsorption and desorption of dye from wastewater [8].

To fabricate sulfonated poly(ethylene terephthalate) (SPET) nanofibrous membranes, SPET is electrospun with trifluoroacetic acid/dichloromethane in solution. SPET nanofibers show a diameter of 300 nm–1 μm. Factors affecting adsorption of C.I. Basic blue 3 dye on SPET membrane include concentration, voltage used, pressure, and time for filtration. A dead-end recirculation ultrafiltration setup carries the filtration. The effect of pressure on adsorption of basic blue 3 dye on SPET membrane is significant while operating time is less. Dye equilibrium sorption fits Langmuir and Freundlich isotherms [11]. Polyethersulfone nanofibrous membranes bearing negative charges are fabricated employing the single-step electrospun method. Sodium
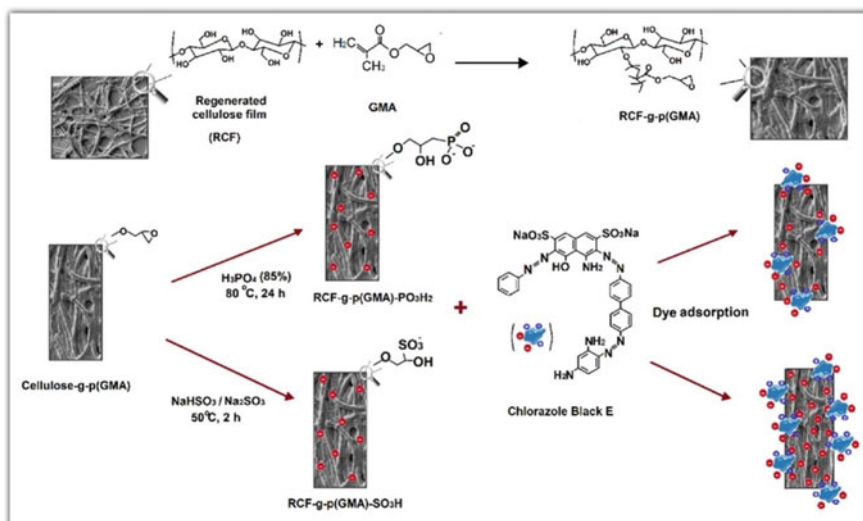
Fig. 13 Modification of cellulose-g-p(GMA) into RCF-g-p(GMA)–PO_3H_2 and RCF-g-p(GMA)–SO_3H and dye adsorption. GMA is grafted on regenerated cellulose films and then epoxy group on RCF-g-pGMA is modified into phosphate and sulfonic acid group. The anionic groups in membrane interact with the dye molecules. GMA: Glycidyl methacrylate; g: grafted. (Reprinted with permission of Elsevier from [8])

styrene sulfonate and acrylic acid are electrospun in polyethersulfone solution. Functional groups are produced through crosslinking and copolymerization. Afterward, negatively charged polyethersulfone nanofibrous membranes (NFMs) are fabricated by direct electrospinning. NFMs are investigated for adsorption of different dyes by batch method at different pH values. NFMs show adsorption of cationic dye, MB efficiently. NFMs show the potential of industrial applications for wastewater purification from dyes [12].

Two methods, electrospinning and in-situ crosslinking, are combined in a novel strategy to fabricate NFMs. Poly ([2-(methacryloyloxy)-ethyl] Trimethyl ammonium chloride) (PMETAC) produces crosslinked polymer in a solution of polyethersulfone. NFMs carry positively charged groups of quaternary ammonium in the polymer of PMETAC and show the capacity to adsorb negatively charged dyes from wastewater. NFMs adsorb CR dye with an adsorption capacity of 208 mg/g and are reusable. NFMs adsorb 100% dye from wastewater for the first time and show an ability to adsorb 96.5% dye in the third cycle of adsorption. NFMs show multi-functionality in wastewater treatment by dye rejection and killing bacteria [45].

6 Metal–Organic Frame Work (MOF)

Metals coordinated to organic ligands show an increased ability to absorb dye. Separation of MOFs from solutions for practical use is difficult. Immobilization of MOFs on fibrous membranes is a novel approach to improving the adsorption of dye and separating the resulting MOFfrom water. Zeolite imidazole framework is immobilized on PAN membranes through electrospinning. The resulting fibrous membrane retains 92% adsorption capacity after four regenerating cycles. Zeolite imidazole framework immobilized on PAN membranes show excellent adsorption of malachite, CR, and Basic fuschin. Easy synthesis, adsorption behavior, and easy purification make such fibrous membranes applicable for industrial use [27]. Iron immobilized on a fibrous membrane in the presence of hydrogen peroxide removes crystal violet dye up to 50 mg L-1 from wastewater. Iron nanoparticles of 50–150 nm size are immobilized on polyester membrane through amine or thiol groups. Iron immobilized to the polyester membrane through thiol removes up to 98.87% dye in 22 min. Chemical oxygen demand analysis shows 78% decrease in toxicity. The membranes are reusable seven times [60].

Hydrazine hydrate and hydroxylamine are used in different ratios to modify PAN nanofibrous membranes' surface, subsequently coordinated with Fe^{3+} ions. Fe^{3+} ions help in the adsorption of azo dye and Reactive Red 195 (RR 195) and oxidation by photocatalysis. The ratio of hydrazine hydrate and hydroxylamine affect the surface characteristics of nanofibrous membrane–Fe complexes. The adsorption of dye takes place through pseudo-second-order kinetics. The dye removal efficiency of MOF is due to the increased photocatalytic rate constant and adsorption of dye in greater quantity. The nanofibrous membranes are reusable [35]. MOF (NH_2–MIL-125) are nanofibrous composite membranes with photocatalytic abilities and reduce the step

of centrifugation or filtration during regeneration of fibrous membranes and are easily separated from suspension. MOF (NH_2–MIL-125) are well characterized composite membranes. Investigation with X-ray diffraction (XRD), SEM, FTIR, TGA,BET, and UV–Vis techniques provide morphological and mechanical information of MOF. MOF adsorbs MB and sodium fluorescein through steric hindrance [24]. Chitosan is a natural polysaccharide. Chitosan/PVA nanofibers are synthesized by electrospinning. ZIF-8/chitosan/PVA bionanocomposite is fabricated by coating MOF, ZIF-8 on chitosan/PVA nanofiber. The adsorbent shows the capability to adsorb malachite green. Artificial neural networks and surface response methodology are used to estimate the initial concentration of dye statistically. Among three coated membranes distinguished by the number of coating cycles, chitosan/PVA coated with ZIF-8 for two cycles shows maximum adsorption capacity [53].

MOFs work by trapping dyes through simple filtration practice. Less MOF loading quantity, resistance by polymer-forming coating, and greater flow flux result in less adsorption ratio and MOFs capacity. Increased adsorption ratio and ability and greater flux are significant challenges for an efficient filtration process. Nanofibers of zeolitic imidazolate framework, ZIF-8 are fabricated through an in situ coating of aramid microfibers and silk microfibers adsorption of dyes. ZIF-8 shows potential adsorption of organic dyes, including coomassie brilliant blue, congo red, malachite green, and methylene blue. Hierarchical microstructures in nanofiber membrane permit high rejection, high flux and large volume filtration applicable for industrial uses [47]. Composite MOF aerogel is fabricated by implantation of zinc nanoparticles on crosslinked cellulose. Materials obtained from biomass are cost-effective, promising, and green. ZIF-67 forms a coating on the cellulose matrix. The composite membrane shows an adsorption capacity of 617 mg/g for MO. The adsorption capacity is four times greater than unmodified cellulose [79]. MOF nanofibrous mats are fabricated for dye rejection. PAN is mixed with 2-methylimidazole and electrospun. Then ZIF-8 nanocrystals are fabricated PAN nanofibers. Mats consisting of nanofibers reject MB and malachite green from an aqueous solution. The adsorbent shows a fast adsorption rate for methylene blue, reaching 1531 mg/g, and degrade MB with ultraviolet radiation irradiation [92].

Polyester membranes are successfully modified by introducing amine or thiol groups and zerovalent iron nanoparticles are implanted on the membrane. Polyester membranes are subjected to plasma treatment before functionalization. The membranes remove dyes and bacteria from contaminated water by a Fenton-like process. Investigations show iron nanoparticles ranging 50–150 nm in size are implanted on fibrous membranes. Fenton-like efficiency of four differently modified membranes derived from polyester to remove crystal violet dye is investigated in the presence of H_2O_2. Polyester nonwoven fibers modified with thiol group and implanted with iron nanoparticles show maximum dye rejection ~98% in 22 min [60]. Zerovalent iron nanoparticles are embedded on the plasma-treated polyester nanofibers before or following modified with polyamidoamine dentrimer, 3-(aminopropyl) triethoxysilane or thioglycerol for dye rejection from wastewater by Fenton-like catalytic process. The adsorption capacity and other parameters affecting

dye rejection by the adsorbent are optimized with statistical modeling and experimental design. The statistical investigation shows that pH greater than 5 decreases the dye rejection; however, an active concentration of hydrogen peroxide increases dye rejection until equilibrium is established [61].

Using PAN fibrils' hydrophilic nature, AgBr/Br Schottky junction is formed on the surface, creating thin films. Electrospinning and wet chemical method are used to synthesize novel PAN/AgBr/Ag fibrous membrane to remove contaminants from wastewater through photodegradation. The membranes show a stable porous structure and mechanical strength. Hence, efficiently filter Disperse red 1 dye and other contaminants from wastewater [71]. Copolymer beads are synthesized from 2-hydroxyethyl-methacrylate and methyl methacrylate using $FeCl_3$. Co-precipitation of Fe^{2+} ions with beads containing Fe^{3+} ions takes place at basic pH with heating. The resulting beads possessing magnetic properties are implanted on p(GMA). The reaction of implanted p(GMA) with ammonia converts epoxy groups into amino groups. Surface area measurements, electron spin resonance, Mossbauer spectroscopy, and SEM are performed to investigate hybrid beads' morphology and structure. P(GMA) implanted and amine group-containing beads adsorb the highest amount of reactive green-19 dye at pH 3.0. The adsorption follows pseudo-second-order kinetics. An acidic dye is removed from wastewater takes advantage of the flexibility of implanted chains. There is no change in beads' initial adsorption capacity by changing the condition of adsorption [7].

Electrospinning and sol–gel methods are combined to fabricate mesoporous nanofibers for dye removal from wastewater. Carboxylated Mn_2O_3 polymers of acrylic acid are investigated by microscopic and specific surface area analysis. Silica and Mn_2O_3 are deposited on the nanofibril surface. Deposition of Mn_2O_3 on polymer increases the diameter of fibers but decreases pore size; hence, a mesoporous filter is obtained. The average surface roughness of the polymer increases after polymerization of the monomer. XRD analysis confirms the grafting of silica on Mn_2O_3 nanofiber surface. The dye adsorption rate on nanofibers is affected by adsorbent dose, pH, inorganic anions, and dye concentration. The kinetics of dye adsorption follows a pseudo-second-order model [9].

7   Cyclodextrin (CD) Modified Membrane

Cyclodextrin offers an advantage for enhancing the efficiency of membranes in two ways. Cyclodextrin helps in the adsorption of organic compounds through the complex formation and increases nanofibers' surface area. PAN nanofibers are electrospun with β-cyclodextrin (β-CD) to introduce functional groups in nanofibers. Although β-CD increases PAN's dye rejection ability from 15.5 to 24% overall, less efficiency of PAN/β-CD membranes is because β-CD is soluble in water and is lost during the filtration process. A polycondensation reaction crosslinks β-CD into β-CD polymer and solves the solubility problem. PAN/β-CD polymer shows an ability to

reject dye with higher efficiency from aqueous solutions. X-ray diffraction analysis reveals that β-CD forms inclusion complexes with dye molecules [16].

Microfibers are obtained from hydroxypropyl-β-CD and benzoxazine in a solution using dimethylformamide through electrospun. Microfibers are crosslinked by thermal treatment. Uniform microfibers are synthesized with a composition of hydroxypropyl-β-CD (120%) and benzoxazine (25%) by weight/volume. The microfibers are water-insoluble. However, the thermal treatment causes changes in the morphology of fibers. Citric acid decreases the deformation in the morphology of nanofibers. Electrospinning helps in crosslinking and increases resistance to heat. The morphology of microfibers in water and different organic solvent is investigated by SEM. Both MB and MO show interaction with cyclodextrin. However, crosslinked hydroxypropyl-ßCD and benzoxazine show selective adsorption of MB, a cationic dye, through electrostatic interactions. The anionic dye shows less electrostatic interaction to microfibers. The cationic dye can be easily removed from microfibers in a water showing regenerative capability [14].

β-CD functionalizes high surface area silica nanospheres (KCC-1) grafted with NH_2 groups. Treatment with toluene followed by 3-aminopropyltriethyloxysilane introduces NH_2 groups in KCC-1 structure. Functional modification of KCC-1 is confirmed with FTIR. SEM and TEM provide knowledge about the morphology of fabricated nanoadsorbents. KCC-1-NH-β-CD shows the ability to remove malachite green from aqueous solutions with high efficiency [1]. β-CD/glutaraldehyde/PVP nanofibrous membrane is fabricated by electrospinning and shows an ability to adsorb MO dye from wastewater. Implantation of β-CD in crosslinked polymer increases the adsorption capacity of nanofibrous membranes. The membranes are investigated for structural features by ATR-FTIR, XRD, SEM, and UV spectroscopy [86].

8 Cellulose Membrane

Membranes based on cellulose materials are cost-effective. Cations are introduced in cellulosic materials employing quaternary ammonium. The membranes are characteristics investigated by FTIR-ATR spectroscopy. The membranes show adsorption of acid, direct, reactive, and cationic dye efficiently. Cotton linters and fabric containing positively charged functional groups show the potential to remove various dyes from wastewater. The membranes are easily regenerated by the bleaching process and retain a good capacity to adsorb dyes [15]. Sustainable carboxylated cellulose membranes reject dyes from contaminated water. 2,2,6,6-etramethylpepridine-1-oxyl introduces carboxyl groups to cellulose via oxidation. Structural and morphological features of filter membrane e characterized by ATR, TGA and SEM investigations. Carboxylated cellulose filter membranes show potential mechanical characteristics and tensile strength. XPS and elemental mapping investigations show carboxylated cellulose filters adsorb potential MB dye (76.9 mg/g) with high flux at low pressure. The excellent dye rejection property of carboxylated filters depends upon the internal micro-nano-scaled structure. The internal micro-nanostructure facilitates

the adsorption of dye. Dye rejection at low pressure indicates that gravity facilitates filtration. Cellulosic fabric filters packed in spiral-wound cartridges are investigated, with wastewater contaminated with dyes and metals simultaneously for remediation. Carboxylated cellulosic fabric filters show a ten times greater capacity to treat contaminated water than cellulosic fabric filters [34].

Cellulose micro-fibrils (CMF)-based membranes implanted with Fe_3O_4 nanoparticles are magnetic and mediate catalysis. HKUST-1/Fe_3O_4/CMF membranes show magnetic and catalytic activity for application in dye rejection from wastewater. CMF disperses MOF crystals (HKUST-1) and Fe_3O_4 nanoparticles and increases the catalytic feature of HKUST-1/Fe_3O_4/CMF. TEM, BET, XRD, FTIR, TGA, and energy-dispersive spectrometry investigate properties of nanofibers. The vibrating sample magnetometery technique confirms the presence of Fe_3O_4 nanoparticles on the surface of CMF. The porous morphology of MOF facilitates the increased adsorption capacity of HKUST-1/Fe_3O_4/CMF. Novel membranes show high efficiency in rejection of MB from wastewater due to larger surface area and catalytic nature with advantages of regeneration, sustainability, and recycling [44]. Copper oxide nanoparticles implanted on the cellulose oxidized with 2,2,6,6, tetramethylpiperidin-1-oxyl increases dye rejection capacity and anti-pathogenic activity. SAXS and QCMD confirm the formation of nanoparticles. The carboxylated cellulose nanolayers act as a substrate and adsorb the metal ions. Cu_2O/TOCNF composite membrane is investigated for UV irradiated MB rejection from aqueous solutions [82]. Highly porous cellulose acetate nanofibers are implanted with silver nanoparticles. The resulting adsorbent shows potential adsorption efficiency in removing Rhodamine B from wastewater, indicating that silver nanoparticles do not affect the adsorption of dye from aqueous solutions. Further silver nanoparticles increase the bactericidal capability of the adsorbent. The adsorbent is applicable to remove dye from wastewater [84].

9   Chitosan Composite Membrane

Chitosan is abundant, biocompatible, able to form films, and possesses polar functional groups for the adsorption of organic molecules. Chitosan/hydroxyapatite is a porous membrane. Sponge-like intrinsic morphology and an outer surface that supports adsorption of dyes from wastewater. Porous chitosan/hydroxyapatite membrane shows four times more adsorption capacity as compared to nonporous one. The adsorbent thus fabricated shows 98% dye rejection in a duration of fewer than 15 min. The procedure of fabrication membrane is facile and easy. The adsorbent is reusable for five cycles at 150 mg L-1 dye concentration [76]. Chitosan (β-(1→4)-linked D-glucosamine and N-acetyl-D-glucosamine) and clay are chemically modified to fabricate chitosan/clay composite. Chitosan/clay composite removes direct rose from an aqueous solution. The formation of composite nanofibers increases the adsorption ability of chitosan. Higher pH allows maximum dye adsorption on the composite adsorbent. The adsorption of direct rose on chitosan/clay follows

pseudo-second-order kinetics and the Redlich–Peterson model. 0.1 M HCl regenerates chitosan/clay adsorbent and elutes the dye. The composite shows ability to remove 87% dye from diluted solution [29].

Chitosan is coated on cellulose acetate/pol(yhydroxybutyrate-co-hydroxyvalerate) fiber layers to synthesize a three-layer composite membrane. Chitosan is used as a substrate, while acetate/pol(hydroxybutyrate-co-hydroxy valerate) acts as a fence. Glycerol content affects the mechanical strength and filtration efficiency of the membrane. The membrane shows a dye adsorption capacity of 188.52 for dispersed dye [95, 96]. Microfibriller cellulose coated with chitosan or ZnO/chitosan is investigated for adsorption efficiency of MO. Coated microfibrillar cellulose fabricated by simple method show the ability to remove MO dye from an aqueous solution. XRD and SEM images show the formation of a thick layer of chitosan over microfibrillar cellulose with a concentrated solution of chitosan. However, treatment with a dilute solution of chitosan results in the wrapping of individual microfibrillar cellulose microfibers. The photodegradation ability of ZnO/chitosan-coated microfibrillar cellulose further increases in the presence of ultraviolet radiation. The adsorption of dye an adsorbent takes faster in the ultraviolet radiation. Maximum dye adsorbed on ZnO/chitosan-coated microfibrillar cellulose is 42.8 mg/g [28].

Composite electrospun nanofibrous membranes, chitosan/PVA/SiO_2 are affinity membranes. Composite membranes show increased mechanical and filtration characteristics. SiO_2 gives strength to the fibrous membrane and increases water flow and adsorption of dye on microfibers' surface. The initial concentration of SiO_2 affects fiber thickness, morphology, pore size, and permeability of affinity membranes. The fibrous membranes show the ability to remove 98% Red 23 dye from an aqueous medium [22]. Chitosan is used to modify palygorskite to fabricate adsorbent for reactive dye. The fabricated adsorbent shows increased adsorption of dye compared to unmodified palygorskite [69]. Crosslinked chitosan–tripolyphosphate/nanotitania composite membrane removes methyl orange dye from aqueous solutions. The efficiency of membrane for removal of dye is analyzed by performing a statistical analysis experiment, the response surface methodology using Box–Behnken design. The parameters optimized in this analysis include TiO_2 initial concentration, dose, pH of the solution, and temperature. 50% TiO_2 initial concentration, 0.09 g dose, 4.0 pH of the solution, and 40 °C temperature gives dye removal efficiency of approximately 87% [2].

Chitosan nanoparticles implanted fibrous membranes are fabricated and investigated to reject negatively charged dyes for purification of contaminated water. Chitosan nanoparticles implanted on cationic fibrous carrier remove anionic dye through adsorption. Activated polyethylene terephthalate fibers are used for the immobilization of chitosan nanoparticles. The modified nanofibrous membrane shows the potential rejection ability of dye rejection 300–1050 mg/g for different dyes. The adsorption capacity of the adsorbent depends upon the type of dye. Negatively charged phthalocyanine dyes of various molecular sizes, nature, and number of ionic groups are investigated for dye rejection by the novel adsorbent. Intra-particle diffusion limits the overall reaction as a rate-determining step, and the adsorption is a

pseudo-second-order reaction. pH also affects the adsorption of dye on the adsorbent, and with maximum capacity in the pH range of 2–8. The chitosan-modified cationic fibrous carrier readily regenerates in alkaline solution [41]. For the fabrication of chitosan/alginate foams, ternary acetic acid/water/tetrahydrofuran are employed as solvents during lyophilization process. The composite membrane shows interconnected pores and appropriate structure fitting for dye adsorption. The foam offers water repelling nature and adsorbs MB (1488.1 mg/g). The adsorbent also shows potential adsorption capacity for acid black-172. The adsorption takes place through chemisorptions and depends upon the weight ratio of chitosan and alginate [97].

10   Modification of Membrane with Protein

Nanofibers are modified with protein for the rejection of cationic dyes from wastewater. Modification with hydrolysis introduces carboxylic groups to PAN nanofibers. Bovine serum albumin purified from laboratory wastes couples with P-COOH to fabricate P-COOH-BSA nanofibrous membranes. Investigations with equilibrium dissociation constant show capability of P-COOH-BSA nanofibers to remove toluidine blue O (TBO) with 434.78 mg/g at alkaline pH. Dye rejection with BSA modified nanofibers follows pseudo-second-order kinetics and fits Langmuir isotherm model. The BSA modified nanofibers are easily regenerated using a high concentration of sodium chloride solution or 50% glycerol, and dye rejection capacity is sustained up to 97% for five cycles [26]. Novel keratin protein-based adsorbent is fabricated from merino wool fibers. The hierarchical microstructure of wool fibers is exposed by controlled hydrolysis of cuticle cells, forming a protective coating on fibers' surface. The adsorbent shows a high adsorption capacity of 294 mg/g for Rhodamine B dye in the presence of 3.5% acetic acid. The hydrolyzed wool fibers contain amine and carboxylic groups involved in the interaction of adsorbent with the dye molecules. The Amine group is capable of accepting hydrogen ions and deprotonation [81].

11   Laccase Immobilized Membrane

Laccase immobilized on polypropylene chloride film fabricated on fibrous polymer pGMA show the ability to remove procion green HG4, brilliant blue G, and crystal violet. The morphology of polypropylene films fabricated on pGMA is characterized by SEM and FTIR. The amount of enzyme immobilized on film and the activity of the enzyme provides an idea about the intact structure of the immobilized enzyme. Experiments show an increase in thermal stability, shelf life, and activity in the immobilized enzyme. MALDI-TOF-MS and kinetic studies show that immobilized laccase possesses the ability to remove dyes from textile wastewater with excellent efficiency [3]. Laccase is implanted on a hybrid membrane fabricated from zeolite like geopolymer. The composite membrane is prepared by a simple, fast method

of cyclic adsorption. The membrane shows more than 99% crystal violet removal with 93% efficiency in 8-h filtration in a flow-through procedure. The membrane is cheaper and durable [93].

12 Biomass-Based Membrane Adsorbents

Leaves of *Posidonia cieanica* (L.) adsorb dye from the textile industry's wastewater. Temperature, pH, and pretreatment of leaves affect the adsorption of e on the biological fibrous material. Leaves of *Posidonia ocieanica* (L.), a seagrass found in the Mediterranean, are economical, available, and renewable biomaterial. An increase in temperature increases the adsorption of dye on biomaterial. At pH 5.0, the biomaterial removes the maximum dye from wastewater. Treatment of fibers with H_3PO_3 and HNO_3 increases the efficiency of fiber for dye adsorption. Adsorption is explained by Lagergren first-order and pseudo-second-order models. Freundlich isotherm model explains the equilibrium data of adsorption [64]. Rice flour and graham flour contain biodegradable natural carbohydrate polymers. Polymeric adsorbents from rice flour and graham flour encapsulate methyl orange dye and show dye rejection capability. The pH of a solution significantly affects the rejection of dye by biodegradable polymeric adsorbent. Langmuir isotherm fits the adsorption of dye by biodegradable polymeric material. The polymeric adsorbent shows the capability of regeneration for several cycles to treat wastewater [62].

Natural carbohydrate from turmeric powder shows potential ability to encapsulate MB at neutral pH efficiently. The adsorbent adsorbs dye even in the presence of different metal ions. FTIR results show that carbonyl and hydroxyl groups in TP adsorbent stabilize dye encapsulation through electrostatic and stable complexation mechanisms. The dye is desorbed by passing ethanol and remains usable for many adsorption and desorption cycles. The natural carbohydrate-based adsorbent is cost-effective, biodegradable, and shows potential dye rejection applications in textile industry discharge [32]. Plant wastes are used as filler fabricate porous mixed matrix membranes (MMMs) from polyethersulfone through phase inversion. The water vapor-induced phase inversion method is used to manufacture MMMs.

MMMs show adsorption of cationic dyes from wastewater. Banana peel, tea waste, and shaddock peel examples of plant waste material used as fillers. MMMs are characterized for their properties by investigations with techniques of BET, FTIR, SEM, TGA, zeta potential, porosity, and ion exchange capacity. MMMs show a high capacity to adsorb cationic dyes, 1173 mg/g for MB and 1244 mg/g for methyl violet 2B. The cationic dyes adsorb on MMMs through the combined effect of electrostatic and hydrophobic forces and hydrogen bonding. Desorption of dye from MMMs is done with 1 M KSCN in 80% methanol. MMMs are regenerated for three cycles with excellent dye rejection and recovery potentials. And are applicable in a dead-end operation at a larger scale [40]. A dual crosslinked hybrid membrane is synthesized from readily available biomaterials. *Plantago Psyllium* mucilage, eggshell membrane, and alginate are used to crosslink. The membrane shows the

capacity to adsorb negatively charged dye MB and positively charged dye MO from wastewater. The adsorbent adsorbs MB and MO from an aqueous solution of 10 ppm initial concentration at alkaline and acidic pH, respectively [57].

Changes in morphology, structure, flimsiness, and damage by pathogens occur with aging of super wetting materials and decrease wettability, restraining application in challenging processes like separation of oil–water emulsions and dye rejection. Microfibers obtained from the chestnut shell are oleophilic/hydrophobic due to aliphatic and aromatic hydrocarbons in higher quantity and show steady structure. The nanofibers show the ability to adsorb organic Rhodamine B and MB dyes from the oil–water boundary efficiently [65].

Eggshell and its membrane show adsorption of CI reactive yellow 205 dye. The adsorption of dye mainly depends on the membrane's surface area [70]. Carbonized eggshell membrane is implanted with Cadmium sulfide quantum dots–TiO_2 and shows efficient rejection of MB from wastewater. Carbonized eggshell membrane is coated with Cds–TiO_2 followed by heat treatment. The resulting membrane shows dye adsorption. Membrane aslo shows catalytic activity in the presence of sunlight [67]. Chemical modification of eggshell membrane is investigated by FTIR, indicating hydroxyl, carbonyl, and methylene groups. The modified membrane adsorbs CR (98%) from aqueous solution [68].

13 Silica-Based Membrane

Silver nanoparticles are fabricated on silica activated with the amino group through a simple method in the presence of an aqueous solution extracted from *Nigella sativa.* Elemental analysis, FTIR, XRD, TGA, SEM, and EDEX techniques are used to analyze membranes. The membranes efficiently reject indigo carmine from wastewater. The effect of factors is investigated in batch experiments. A 20-min contact time establishes the indigo carmine equilibrium during dye rejection. Membrane adsorbs indigo carmine at a capacity of 73.05 mg/g. The adsorption of indigo carmine on Ag activated silica takes place according to pseudo-first-order kinetics. Gibbs free energy, entropy, and enthalpy data show that indigo carmine's adsorption on Ag activated silica is thermodynamically endothermic and feasible. The membrane surface is stable without significant loss of silver nanoparticles in an aqueous environment and can be recycled, showing the cost reduction [18].

PVA/SiO_2 hybrid membrane is functionalized with cyclodextrin using sol–gel or electrospinning method. Tetraethyl orthosilicate and silylated monochlorotriazinyl-ßCD co-condense in the presence of cetyltrimethyl ammonium bromide in one step. Afterward, electrospun fabricate nanofibers when PVA is added. Cyclodextrin functionalizes the hybrid membrane. The functionalized hybrid membrane shows the potential to adsorb carmine dye efficiently. The membrane can be regenerated by acidification [80]. Functionalized nanofibrous membranes are prepared by sol–gel process, electrospun, calcination, and liquid phase deposition. Iron is implanted

on TiO_2/SiO_2 nanofibers. Nanofibers are fabricated by mixing PVP, ferric chloride hexahydrate, tetraethyl orthosilicate, and titanium *n*-butaoxide in a mixture of dimethylformamide and ethyl alcohol in one pot followed by electrospinning. The mixture of dimethylformamide and ethyl alcohol acts as a solvent. The fibrous membrane is then subjected to calcination. Then molecular imprinting is done by the addition of *o*-phenylenediamine with UV irradiation. The molecular imprinted nanofibers show potential for selective photodegradation of 4-nitrophenol [37]. One-step coaxial electrospinning technique is used to fabricate the flexible core–shell fibrous membranes from silica and alumina. Silica forms the core phase, and alumina comprises the shell phase. Calcination of alumina imparts high adsorption capacity to the membrane and increases the mechanical strength of fibers. The membranes show adsorption of CR and are recyclable [85]. Novel magnesium silicate nanofibers are flexible. Silicate nanofibers are fabricated through hydrothermal reaction and electrospinning of silicon dioxide. MgSiFM is used as a filter membrane and shows a potential adsorption capacity of 609.75 mg/g for MB. The fabrication of silicon-based adsorbent is cost-effective, simple, and facile [95].

14 Carbon Nanofibers (CNFs)-Modified Membrane

CNFs/TiO_2–PAN composite membrane is fabricated by electrospinning method from PAN and CNFs. Investigation with SEM shows PAN nanofibers' diameter implanted with CNFs nanoparticles in the range of 200–260 nm. FTIR confirms the implantation of functional groups in the PAN nanofibers after treatment with CNFs. Treatment of PAN nanofibers with CNFs decreases the contact angle from 38° to 18°. The hybrid membrane also adsorbs metal ions with high efficiency and shows potential for purification of contaminated drinking water [33].

CNFs show potential dye adsorbing properties. In a simple method, filtration and adsorption properties of CNFs are utilized to remove MB from contaminated water. CNFs offer greater surface area, uniform structure, and many active sites than granular activated carbon and carbon nanotubes. Hence, they show more significant potential to adsorb dye from contaminated water. CNFs show a potential to reject MB dye at the flux of 1580 Lm^{-2} h^{-2}. CNFs are highly porous and allow stacking of membranes, hence increased adsorption potential. Potential to adsorb dyes and ability to recycle show CNFs are applicable to industrial wastewater treatment [39]. Oxidative template assembly method is used to fabricate polypyrrole nanofibers and further modified with activated carbon through N-linking resulting in formation of N-activated carbon nanofibers adsorbent for the removal of triphenylmethane and chromotropic acid dyes from wastewater. N-activated carbon nanofibers are used as electrodes in capacitor cells. Capacitive dye removal offers a greater voltage window, good capacitive behavior, and enhanced sustainability required to remove chromotropic dyes [77].

Silver ions trapped in carbonaceous microspheres covalently attached to nanofibers show 100% rejection to MB dye. Silver nanoparticles are implanted by
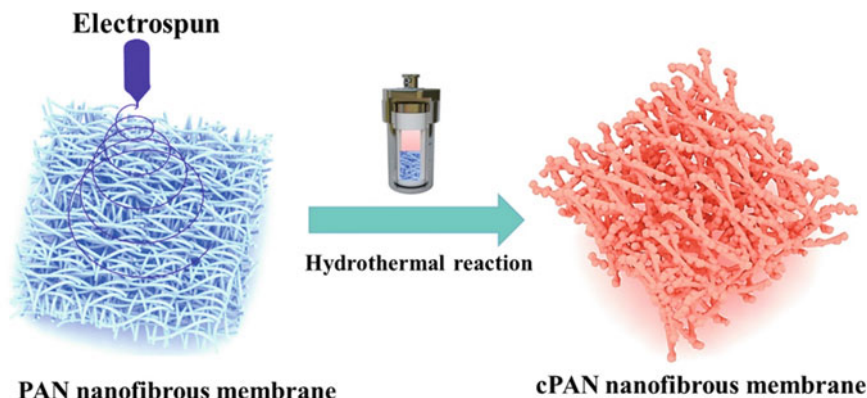
Fig. 14 Schemeforpreparation of the cPAN nanofibrous composite membrane through electrospun and hydrothermal reaction. cPAN: Carbonaceous polyacrylonitrile. (Reprinted with permission of Elsevier from [13])

reduction into the carbonaceous PAN composite nanofibers. The process illustrated in Fig. 14 is used for the synthesis of Ag ions implanted carbonaceous PAN composite nanofibers. The morphology of resulting composite nanofibers is investigated by FE-SEM and TEM techniques. The change in morphology of nanofibers by implantation of Ag is shown in Fig. 15. MB dye adsorbs on fibrous membrane through Fenton-like oxidation of implanted silver nanoparticles. The nanofibrous membranes show potential application for purification of water emulsions due to the presence of superhydrophilic and underwater superoleophobic nature. The process of complex emulsion purification by carbonaceous Ag/PAN composite nanofibers is illustrated in Fig. 16 [13].

A novel dye rejection membrane consists of carboxyl multi-walled carbon nanotubes implanted on bacterial cellulose fibers. After grafting, the material is electrospun, and then chitosan hydrogel is coated on nanofibers. Chitosan acts as a fence layer. The membrane removes direct orange S, Procion Red mx-5B, Stilbene Yellow, and MB with a rejection rate of 90% for dyes molecular weight more than 600 g/mol under 0.5-Pa pressure. The membrane shows antifouling property for both oil and protein [98].

15 Clay-Based Membrane

Palygorskite, sepiolite clinoptilolite are fibrous clay minerals and offer inexpensive removal of dye from wastewater. Clay materials show a large specific surface area and high cation exchange capacity. Clay materials show potential rejection of cationic dye safranin O (SO^+) [78]. Ultrafiltration membranes formed by TiO_2 nanoparticles implanted on bentonite are cost-effective and adsorb anionic
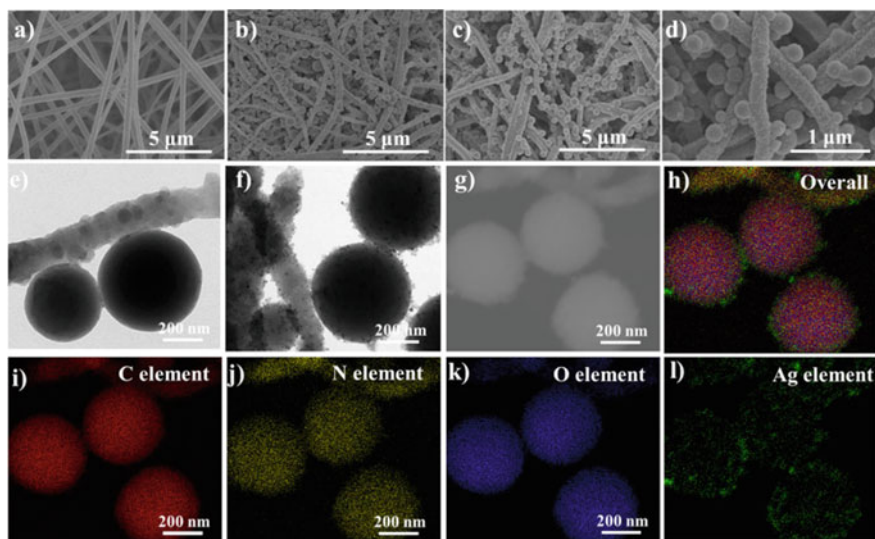
Fig. 15 Morphology characterization of various PAN nanofibers through FE-SEM and TEM. **a–d**: FE-SEM images of PAN, cPAN, cPAN-Ag and magnified view of cPAN-Ag, respectively, d shows implantation of Ag nanoparticles on cPAN nanofibers; **e–g**: TEM images of cPAN cPAN-Ag; g: Dark-field TEM image of cPAN-Ag; **h–l** element mapping results of cPAN-Ag nanofiber. cPAN: Carbonaceous polyacrylonitrile. (Reprinted with permission of Elsevier from [13])
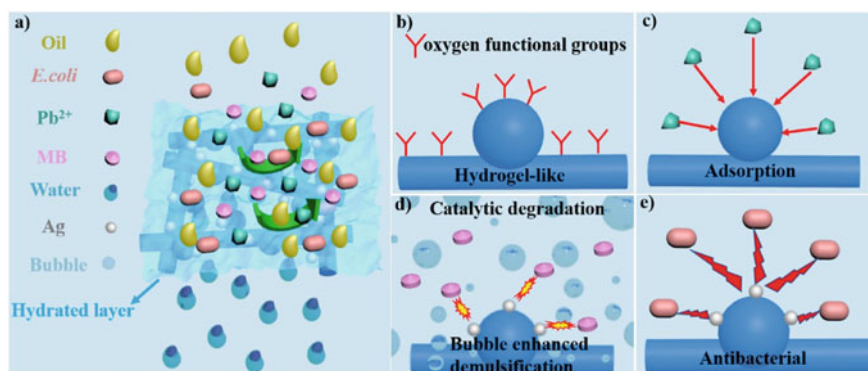
Fig. 16 **a** Purification of complex emulsions by hydrogel-like nanofibrous membranes; **b** The membranes show hydrogel-like properties under water due to oxygenated functional groups; **c** adsorption of lead ions on carbonaceous materials; **d** Organic dyes are degraded by the silver nanoparticles (catalyst)in the presence of H_2O_2 and the bubbles produced in this process demulsify the emulsion; **e** The antibacterial activity of the silver nanoparticles. (Reprinted with permission of Elsevier from [13])

dyes direct 80, acid orange, and cationic dye MB efficiently. After deposition of TiO_2 nanoparticles by the dip-coating method, the layer is heated at a high temperature. TiO_2 nanoparticles adhere to the substrate material. Environmental SEM results show homogenous deposition of TiO_2 nanoparticles [10]. Montmorillonite/chitosan/PVA nanofibrous membranes are fabricated by electrospinning. Novel nanocomposite membranes show the capacity to treat wastewater contaminated with dyes. The affinity membranes allow dye rejection through adsorption of dye, spreading extremely fast throughout the affinity membrane. Implantation of Mt. increases the strength of the electrospun nanofibrous membrane and decreases compaction. The membranes show the ability to remove 95% basic blue 41 along with high flux. The membrane is antifouling and shows the capacity of recycling several times [23].

16   Miscellaneous Membrane Materials

Due to the strong affinity between adsorbed and adsorbing materials, the recycling is difficult. Recycling of adsorbents decreases the expense of the water purification system significantly. The coated adsorbents not only enhance adsorption but are easy to recycle. Modification of coating with iron enhances dye adsorption in the presence of H_2O_2 due to photo-Fenton phenomena. The adsorption capacities at various temperatures and adsorption geometry help decipher the mechanism of adsorption using a statistical physics model. The statistical physics model calculates energy changes during adsorption on iron immobilized fibrous membranes [4]. Gelatin/calcium alginate hybrid nanofibrous membranes fabricated through electrospinning show adsorption of cationic dye MB. The hybrid membrane increases adsorption capacity by decreasing the flow rate. Gelatin combined with alginate increases the mechanical strength of the nanofibrous membrane. Gelatin also increases the recycling ability of alginate-based nanofibrous membrane through positively charged amino groups in gelatin [49].

Fluorene-based covalent organic frameworks show the capacity to reject sky blue A dye from wastewater. The optimum conditions for the effective working of fluorene-based covalent organic framework are investigated by central composition design. Fluorene-based covalent organic shows maximum dye rejection capacity of 299 mg/g (99%) at pH 5.0, 45 °C, and adsorbent dosage 0.005 g in a contact time of 1 h. A cost-effective and movable method based on colorimetry using a mobile phone is developed for in-field analysis of sky blue A rejection in wastewater [58]. Boron nitride ultrathin membranes fabricated by the one-step solvothermal method is innovative and comprise nanofibers of only ~8 nm diameter. Boron nitride membranes are nanonets with the potential efficiency to remove dyes from contaminated water. Boron nitride nanonets show adsorption of MB dye with a capacity of 327.8 mg/g. BN nanonet facilitates ultrafast adsorption of dye on nanofibers. The time required to attain adsorption equilibrium is only 1 minute for boron nitride nanofibers [38]. Hierarchical Al2O$_3$/TiO$_2$ membrane surface shows a great affinity for water, almost

Table 1 Summary of various fibrous membranes used for dye removal from wastewater

Dye	Membrane	References
Methylene blue	Nano-TiO_2 ultrafiltration membrane	[10]
	Polymeric natural carbohydrate of turmeric powder adsorbent	[32]
	Crosslinked *Plantago Psyllium mucilage*, eggshell membrane, and alginate	[57]
	Superhydrophobic/superoleophilic natural fibers	[66]
	Free-standing PVA/PAA membrane	[91]
	Polyethersulfone/plant waste particles mixed matrix membranes	[40]
	Carboxylated cellulose fabric filters	[34]
	PVDF-calcium alginate nanofiltration membranes	[56]

(continued)

0°. The membrane is synthesized by the electrospun method before calcination in the air. Increased water affinity is due to Al_2O_3 heterojunctions spread over the surface of TiO_2. Al_2O_3 heterojunctions increase surface area and hydrogen bonding. The use of adsorption sites under the protection of hierarchical nanostructure increases dye adsorption capability of the nanofibrous membranes up to 98% [17].

Treatment of kraft lignin with glycidyltrimethylammonium chloride introduces positive charge to kraft lignin. Effect of temperature, pH, time, and molar ratio of glycidyltrimethylammonium chloride to lignin are investigated. Ninety percent solubility of lignin in water is achieved with 1wt.% lignin concentration. The cationic material used as flocculent can remove remazol brilliant violet, reactive black, and direct yellow from model contaminated water [31]. Table 1 summarizes various fibrous membranes for dye removal from wastewater.

17 Future Horizons

Nanofibrous membranes show great potential in the dye rejection process. However, the range of dyes removed by a nanofiber is limited. Second, the removal of dye from complex emulsion is difficult, especially in the presence of metals. At present and particularly in future, the cost-effective multifunctional nanofibers with improved dye adsorption capacity and efficiency for a broad range of dyes are critically required. Moreover, in industry, nanofibers capable of maximum performance at industrial parameters like high flux, low pressure, and minimum time are required. The scientists search for novel synthetic and biopolymers and surface modifiers and methods to achieve the above objectives.

Table 1 (continued)

Dye	Membrane	References
	Polymer of Intrinsic Microporosity	[75]
	Magnesium silicate nanofibrous membranes	[95]
	Fibrous chitosan/sodium alginate composite foams	[97]
	Novel boron nitride ultrathin fibrous membrane	[38]
	Carbonaceous nanofibers—50, 100, and 280	[39]
	Cellulose micro-fibrils	[44]
	Gelatin/alginate composite nanofiber membrane	[49]
	Three-dimensional PVDF/starch nanofiber membrane	[59]
	Chitin Nanocrystal Composite Membrane	[66]
	MOF nanofibrous mats	[92]
	Chitosan hydrogel and Bacterial cellulose	[98]
	Polymeric Salicyl Active Esters	[94]
	PVDF/PDA fibrous membrane	[48]
	MOF (NH_2–MIL-125)	[24]
	Poly β-Cyclodextrin/Poly Benzoxazine	[14]
	Plasma-etched PLLA nanofiber membrane	[6]
	Electrospun carbon nanofibers/TiO_2-PAN hybrid membranes	[33]
Methyl orange	Crosslinked chitosan-tripolyphosphate/nanotitania composite	[2]
	Biodegradable natural carbohydrate polymeric adsorbents of rice flour	[62]
	Biodegradable natural carbohydrate polymeric adsorbents of graham flour	
	ZnO/Chitin-microfibriller cellulose mat	[28]
	Crosslinked *Plantago Psyllium mucilage*, eggshell membrane, and alginate	[57]
	Fe-doped TiO_2/SiO_2 nanofibrous membranes	[37]
	Polyethylene oxide/PANI composite membrane	[54]

(continued)

Table 1 (continued)

Dye	Membrane	References
	PEI nanofibrous membrane	[50]
	poly(vinylidene fluoride)@layered double hydroxide	[55]
	β-Cyclodextrin/Glutaraldehyde Crosslinked PVP Nanofibers	[86]
	Cellulose matrix-supported metal–organic framework (MOF) hybrid aerogel (ZIF-67@CA)	[79]
	Amine modified PIM-1 fibrous membrane (AM-PIM-FM)	[75]
Congo red	Modified egg shell membrane	[68]
	Electrospun polystyrene/PANI composite membranes	[21]
	Polymer of Intrinsic Microporosity (PIM-1)	[74]
	Chitin Nanocrystal Composite Membrane	[67]
	Flexible core–shell fibrous membranes for mesoporous alumina-based adsorbents	[85]
	PVDF/PDA fibrous membrane	[48]
	PTFE/PVD	[30]
Crystal violet	Fenton-like functionality of iron immobilized fibrous membranes	[60]
	Fibrous polymer-grafted polypropylene chloride film	[3]
	PVDF electrospun membrane	[19]
	Laccase immobilized composite membrane	[93]
Malachite green	MOF nanofibrous mats	[92]
	β-cyclodextrin functionalized dendritic fibrous nanosilica	[1]
	ZIF-67/PAN Fibrous Membrane	[27]
Azo Dye	Cellulose films with fibrous polymer	[8]
	ZnO/Chitin-microfibriller cellulose mat	[28]
	PAN nanofibrous membrane	[35]
	Iron-modified composite adsorbent coating surface	[4]
	Polystyrene/PANI composite membranes	[21]

Table 1 (continued)

Dye	Membrane	References
Rhodamine B	Mussel-inspired modification of polyphenylene sulfide membrane	[37]
	Superhydrophobic/superoleophilic natural fibres	[66]
	Surface hydrolysed keratin protein fibers	[82]
Indigo carmine	Chitin nanowhisker (ChNW)-functionalized PVDF membrane	[20]
	Cyclodextrin-functionalized mesoporous polyvinyl alcohol/SiO_2	[80]
	Amino-functionalized silica/*Nigella sativa* (black seed) aqueous extract	[18]
Procion green H4G and Brilliant blue G	Fibrous polymer-grafted polypropylenechloride film	[3]
Direct red 80 and acid orange 74	Nano-TiO_2 ultrafiltration membrane	[10]
4-Nitrophenol	Fe-doped TiO_2/SiO_2 nanofibrous membranes	[37]
Direct rose	Chitosan (β-(1 → 4)-linked d-glucosamine and N-acetyl-d-glucosamine) composite	[29]
Acid black 172	Cellulose acetate (CA)/P(DMDAAC-AM) composite nanofibrous membranes	[87]
	Fibrous chitosan/sodium alginate composite foams	[97]
Safranin O	Fibrous clay minerals and zeolites	[78]
Reactive black (HFGR)	Electrospun silk fibroin/PAN	[5]
Reactive green-19	Poly(HEMA-co-MMA) beads	[7]
Sodium fluorescein	MOF (NH_2–MIL-125) nanofibrous hybrid membranes	[24]
Methyl blue	Mussel-inspired modification of polyphenylene sulfide membrane	[88]

References

1. Abbasvash L, Shadjou N (2020) Synthesize of β-cyclodextrin functionalized dendritic fibrous nanosilica and its application for the removal of organic dye (malachite green). J Mol Recognit 33(10):e2850. https://doi.org/10.1002/jmr.2850
2. Abdulhameed AS, Jawad AH, Mohammad AK-T (2020) Statistical optimization for dye removal from aqueous solution by cross-linked chitosan composite. Sci Lett 14(2):1–14. https://doi.org/10.24191/sl.v14i2.9537
3. Arica MY, Salih B, Celikbicak O, Bayramoglu G (2017) Immobilization of laccase on the fibrous polymer-grafted film and study of textile dye degradation by MALDI-ToF-MS. Chem

Eng Res Des 128:107–119. https://doi.org/10.1016/j.cherd.2017.09.023

4. Azha SF, Sellaoui L, Yunus EHE, Yee CJ, Bonilla-Petriciolet A, Lamine AB, Ismail S (2019) Iron-modified composite adsorbent coating for azo dye removal and its regeneration by photo-Fenton process: synthesis, characterization and adsorption mechanism interpretation. Chem Eng J 361:31–40. https://doi.org/10.1016/j.cej.2018.12.050

5. Aziz S, Sabzi M, Fattahi A, Arkan E (2017) Electrospun silk fibroin/PAN double-layer nanofibrous membranes containing polyaniline/TiO_2 nanoparticles for anionic dye removal. J Polym Res 24(9):140. https://doi.org/10.1007/s10965-017-1298-0

6. Bai L, Jia L, Yan Z, Liu Z, Liu Y (2018) Plasma-etched electrospun nanofiber membrane as adsorbent for dye removal. Chem Eng Res Des 132:445–451. https://doi.org/10.1016/j.cherd.2018.01.046

7. Bayramoglu G, Altintas B, Arica MY (2012) Synthesis and characterization of magnetic beads containing aminated fibrous surfaces for removal of Reactive Green 19 dye: kinetics and thermodynamic parameters. J Chem Technol Biotechnol 87(5):705–713

8. Bayramoglu G, Arica MY (2021) Grafting of regenerated cellulose films with fibrous polymer and modified into phosphate and sulfate groups: application for removal of a model azo-dye. Colloids Surf A Physicochem Eng Asp, 126173

9. Berenjian A, Malekania L, Fard GC, Almasian A (2018) Mesoporous carboxylated Mn_2O_3 nanofibers: synthesis, characterization and dye removal property. J Taiwan Inst Chem Eng 86:57–72

10. Bouazizi A, Breida M, Achiou B, Ouammou M, Calvo JI, Aaddane A, Younssi SA (2017) Removal of dyes by a new nano–TiO_2 ultrafiltration membrane deposited on low-cost support prepared from natural Moroccan bentonite. Appl Clay Sci 149:127–135

11. Chegoonian P, Feiz M, Ravandi SAH, Mallakpour S (2012) Preparation of sulfonated poly (ethylene terephthalate) submicron fibrous membranes for removal of basic dyes. J Appl Polym Sci 124(S1):E190–E198

12. Chen S, Du Y, Zhang X, Xie Y, Shi Z, Ji H, Zhao W, Zhao C (2018) One-step electrospinning of negatively-charged polyethersulfone nanofibrous membranes for selective removal of cationic dyes. J Taiwan Inst Chem Eng 82:179–188

13. Ding Y, Wu J, Wang J, Wang J, Ye J, Liu F (2020) Superhydrophilic carbonaceous-silver nanofibrous membrane for complex oil/water separation and removal of heavy metal ions, organic dyes and bacteria. J Membr Sci 614:118491

14. Dogan YE, Satilmis B, Uyar T (2019) Crosslinked PolyCyclodextrin/PolyBenzoxazine electrospun microfibers for selective removal of methylene blue from an aqueous system. Eur Polymer J 119:311–321. https://doi.org/10.1016/j.eurpolymj.2019.08.005

15. Ferrero F, Periolatto M (2012) Functionalized fibrous materials for the removal of dyes. Clean Technol Environ Policy 14(3):487–494

16. Foroozmehr F, Borhani S, Hosseini SA (2016) Removal of reactive dyes from wastewater using cyclodextrin functionalized polyacrylonitrile nanofibrous membranes. J Text Polym 45–52

17. Fu W, Dai Y, Tian J, Huang C, Liu Z, Liu K, Yin L, Huang F, Lu Y, Sun Y (2018) In situ growth of hierarchical Al_2O_3 nanostructures onto TiO_2 nanofibers surface: super-hydrophilicity, efficient oil/water separation and dye-removal. Nanotechnology 29(34):345607. https://doi.org/10.1088/1361-6528/aac9ab

18. Gemeay AH, Aboelfetoh EF, El-Sharkawy RG (2018) Immobilization of green synthesized silver nanoparticles onto amino-functionalized silica and their application for indigo carmine dye removal. Water Air Soil Pollut 229(1):1–17

19. Gopakumar DA, Arumukhan V, Gelamo RV, Pasquini D, de Morais LC, Rizal S, Hermawan D, Nzihou A, Khalil HPSA (2019) Carbon dioxide plasma treated PVDF electrospun membrane for the removal of crystal violet dyes and iron oxide nanoparticles from water. Nano-Struct Nano-Objects 18:100268

20. Gopi S, Balakrishnan P, Pius A, Thomas S (2017) Chitin nanowhisker (ChNW)-functionalized electrospun PVDF membrane for enhanced removal of Indigo carmine. Carbohyd Polym 165:115–122

21. Gorza FDS, Pedro GC, da Silva RJ, Medina-Llamas JC, Alcaraz-Espinoza JJ, Chávez-Guajardo AE, de Melo CP (2018) Electrospun polystyrene-(emeraldine base) mats as high-performance materials for dye removal from aqueous media. J Taiwan Inst Chem Eng 82:300–311

22. Hosseini SA, Vossoughi M, Mahmoodi NM, Sadrzadeh M (2018) Efficient dye removal from aqueous solution by high-performance electrospun nanofibrous membranes through incorporation of SiO_2 nanoparticles. J Clean Prod 183:1197–1206

23. Hosseini SA, Vossoughi M, Mahmoodi NM, Sadrzadeh M (2019) Clay-based electrospun nanofibrous membranes for colored wastewater treatment. Appl Clay Sci 168:77–86

24. Huang J, Huang D, Zeng F, Ma L, Wang Z (2021) Photocatalytic MOF fibrous membranes for cyclic adsorption and degradation of dyes. J Mater Sci 56(4):3127–3139. https://doi.org/10.1007/s10853-020-05473-x

25. Huang Q-L, Huang Y, Xiao C-F, You Y-W, Zhang C-X (2017) Electrospun ultrafine fibrous PTFE-supported ZnO porous membrane with self-cleaning function for vacuum membrane distillation. J Membr Sci 534:73–82. https://doi.org/10.1016/j.memsci.2017.04.015

26. Huong DTM, Chai WS, Show PL, Lin Y-L, Chiu C-Y, Tsai S-L, Chang Y-K (2020) Removal of cationic dye waste by nanofiber membrane immobilized with waste proteins. Int J Biol Macromol 164:3873–3884. https://doi.org/10.1016/j.ijbiomac.2020.09.020

27. Jin L, Ye J, Wang Y, Qian X, Dong M (2019) Electrospinning synthesis of ZIF-67/PAN fibrous membrane with high-capacity adsorption for malachite green. Fibers Polym 20(10):2070–2077. https://doi.org/10.1007/s12221-019-1196-7

28. Kamal T, Ul-Islam M, Khan SB, Asiri AM (2015) Adsorption and photocatalyst assisted dye removal and bactericidal performance of ZnO/chitosan coating layer. Int J Biol Macromol 81:584–590

29. Kausar A, Naeem K, Hussain T, Bhatti HN, Jubeen F, Nazir A, Iqbal M (2019) Preparation and characterization of chitosan/clay composite for direct Rose FRN dye removal from aqueous media: comparison of linear and non-linear regression methods. J Market Res 8(1):1161–1174

30. Khumalo NP, Nthunya LN, De Canck E, Derese S, Verliefde AR, Kuvarega AT, Mamba BB, Mhlanga SD, Dlamini DS (2019) Congo red dye removal by direct membrane distillation using PVDF/PTFE membrane. Sep Purif Technol 211:578–586. https://doi.org/10.1016/j.seppur.2018.10.039

31. Kong F, Parhiala K, Wang S, Fatehi P (2015) Preparation of cationic softwood kraft lignin and its application in dye removal. Eur Polymer J 67:335–345

32. Kubra KT, Salman MS, Hasan MN (2021) Enhanced toxic dye removal from wastewater using biodegradable polymeric natural adsorbent. J Mol Liq, 115468

33. Kumar PS, Venkatesh K, Gui EL, Jayaraman S, Singh G, Arthanareeswaran G (2018) Electrospun carbon nanofibers/TiO_2-PAN hybrid membranes for effective removal of metal ions and cationic dye. Environ Nanotechnol Monit Manag 10:366–376

34. Li C, Ma H, Venkateswaran S, Hsiao BS (2020) Highly efficient and sustainable carboxylated cellulose filters for removal of cationic dyes/heavy metals ions. Chem Eng J 389:123458

35. Li F, Dong Y, Kang W, Cheng B, Cui G (2017) Enhanced removal of azo dye using modified PAN nanofibrous membrane Fe complexes with adsorption/visible-driven photocatalysis bifunctional roles. Appl Surf Sci 404:206–215. https://doi.org/10.1016/j.apsusc.2017.01.268

36. Li N, Chen G, Zhao J, Yan B, Cheng Z, Meng L, Chen V (2019) Self-cleaning PDA/ZIF-67@ PP membrane for dye wastewater remediation with peroxymonosulfate and visible light activation. J Membr Sci 591:117341

37. Li X, Wang J, Li M, Jin Y, Gu Z, Liu C, Ogino K (2018) Fe-doped TiO_2/SiO_2 nanofibrous membranes with surface molecular imprinted modification for selective photodegradation of 4-nitrophenol. Chin Chem Lett 29(3):527–530

38. Lian G, Zhang X, Si H, Wang J, Cui D, Wang Q (2013) Boron nitride ultrathin fibrous nanonets: one-step synthesis and applications for ultrafast adsorption for water treatment and selective filtration of nanoparticles. ACS Appl Mater Interfaces 5(24):12773–12778

39. Liang H-W, Cao X, Zhang W-J, Lin H-T, Zhou F, Chen L-F, Yu S-H (2011) Robust and highly efficient free-standing carbonaceous nanofiber membranes for water purification. Adv Func Mater 21(20):3851–3858. https://doi.org/10.1002/adfm.201100983

40. Lin C-H, Gung C-H, Sun J-J, Suen S-Y (2014) Preparation of polyethersulfone/plant-waste-particles mixed matrix membranes for adsorptive removal of cationic dyes from water. J Membr Sci 471:285–298

41. Lipatova IM, Makarova LI, Yusova AA (2018) Adsorption removal of anionic dyes from aqueous solutions by chitosan nanoparticles deposited on the fibrous carrier. Chemosphere 212:1155–1162. https://doi.org/10.1016/j.chemosphere.2018.08.158

42. Liu C, Mao H, Zheng J, Zhang S (2017) Tight ultrafiltration membrane: preparation and characterization of thermally resistant carboxylated cardo poly (arylene ether ketone)s (PAEK-COOH) tight ultrafiltration membrane for dye removal. J Membr Sci 530:1–10. https://doi.org/10.1016/j.memsci.2017.02.005

43. Liu N, Zhang Q, Qu R, Zhang W, Li H, Wei Y, Feng L (2017) Nanocomposite deposited membrane for oil-in-water emulsion separation with in situ removal of anionic dyes and surfactants. Langmuir 33(30):7380–7388

44. Lu H, Zhang L, Wang B, Long Y, Zhang M, Ma J, Khan A, Chowdhury SP, Zhou X, Ni Y (2019) Cellulose-supported magnetic Fe_3O_4–MOF composites for enhanced dye removal application. Cellulose 26(8):4909–4920

45. Lv C, Chen S, Xie Y, Wei Z, Chen L, Bao J, He C, Zhao W, Sun S, Zhao C (2019) Positively-charged polyethersulfone nanofibrous membranes for bacteria and anionic dyes removal. J Colloid Interface Sci 556:492–502. https://doi.org/10.1016/j.jcis.2019.08.062

46. Lv D, Wang R, Tang G, Mou Z, Lei J, Han J, De Smedt S, Xiong R, Huang C (2019) Ecofriendly electrospun membranes loaded with visible-light-responding nanoparticles for multifunctional usages: highly efficient air filtration, dye scavenging, and bactericidal activity. ACS Appl Mater Interfaces 11(13):12880–12889

47. Lv L, Han X, Mu M, Wu X, Li C (2021) Templating metal-organic framework into fibrous nanohybrids for large-capacity and high-flux filtration interception. J Membr Sci 622:119049

48. Ma F-f, Zhang D, Zhang N, Huang T, Wang Y (2018) Polydopamine-assisted deposition of polypyrrole on electrospun poly(vinylidene fluoride) nanofibers for bidirectional removal of cation and anion dyes. Chem Eng J 354:432–444. https://doi.org/10.1016/j.cej.2018.08.048

49. Ma Y, Qi P, Ju J, Wang Q, Hao L, Wang R, Sui K, Tan Y (2019) Gelatin/alginate composite nanofiber membranes for effective and even adsorption of cationic dyes. Compos B Eng 162:671–677

50. Ma Y, Zhang B, Ma H, Yu M, Li L, Li J (2016) Polyethylenimine nanofibrous adsorbent for highly effective removal of anionic dyes from aqueous solution. Sci China Mater 59(1):38–50

51. Mahmoodi NM, Mokhtari-Shourijeh Z (2016) Preparation of aminated nanoporous nanofiber by solvent casting/porogen leaching technique and dye adsorption modeling. J Taiwan Inst Chem Eng 65:378–389

52. Mahmoodi NM, Mokhtari-Shourijeh Z, Abdi J (2019) Preparation of mesoporous polyvinyl alcohol/chitosan/silica composite nanofiber and dye removal from wastewater. Environ Prog Sustain Energy 38(s1):S100–S109

53. Mahmoodi NM, Oveisi M, Taghizadeh A, Taghizadeh M (2020) Synthesis of pearl necklace-like ZIF-8@ chitosan/PVA nanofiber with synergistic effect for recycling aqueous dye removal. Carbohydr Polym 227:115364

54. Mansor ES, Ali H, Abdel-Karim A (2020) Efficient and reusable polyethylene oxide/polyaniline composite membrane for dye adsorption and filtration. Colloid Interface Sci Commun 39:100314

55. Mei Q, Lv W, Du M, Zheng Q (2017) Morphological control of poly (vinylidene fluoride)@ layered double hydroxide composite fibers using metal salt anions and their enhanced performance for dye removal. RSC Adv 7(74):46576–46588

56. Meng J, Xie Y, Gu Y-H, Yan X, Chen Y, Guo X-J, Lang W-Z (2021) PVDF-CaAlg nanofiltration membranes with dual thin-film-composite (TFC) structure and high permeation flux for dye removal. Sep Purif Technol 255:117739

57. Mirzaei S, Javanbakht V (2019) Dye removal from aqueous solution by a novel dual cross-linked biocomposite obtained from mucilage of Plantago Psyllium and eggshell membrane. Int J Biol Macromol 134:1187–1204

58. Mokhtari N, Afshari M, Dinari M (2020) Synthesis and characterization of a novel fluorene-based covalent triazine framework as a chemical adsorbent for highly efficient dye removal. Polymer 195:122430
59. Moradi E, Ebrahimzadeh H, Mehrani Z, Asgharinezhad AA (2019) The efficient removal of methylene blue from water samples using three-dimensional poly (vinyl alcohol)/starch nanofiber membrane as a green nanosorbent. Environ Sci Pollut Res 26(34):35071–35081
60. Morshed MN, Behary N, Bouazizi N, Vieillard J, Guan J, Le Derf F, Nierstrasz V (2020) Modification of fibrous membrane for organic and pathogenic contaminants removal: from design to application. RSC Adv 10(22):13155–13173
61. Morshed MN, Pervez MN, Behary N, Bouazizi N, Guan J, Nierstrasz VA (2020) Statistical modeling and optimization of heterogeneous Fenton-like removal of organic pollutant using fibrous catalysts: a full factorial design. Sci Rep 10(1):16133. https://doi.org/10.1038/s41598-020-72401-z
62. Munjur HM, Hasan MN, Awual MR, Islam MM, Shenashen MA, Iqbal J (2020) Biodegradable natural carbohydrate polymeric sustainable adsorbents for efficient toxic dye removal from wastewater. J Molecul Liq 319:114356
63. Nasar A, Mashkoor F (2019) Application of polyaniline-based adsorbents for dye removal from water and wastewater—a review. Environ Sci Pollut Res 26(6):5333–5356
64. Ncibi MC, Mahjoub B, Seffen M (2007) Adsorptive removal of textile reactive dye using Posidonia oceanica (L.) fibrous biomass. Int J Environ Sci Technol 4(4):433–440. https://doi.org/10.1007/BF03325978
65. Nine MJ, Kabiri S, Sumona AK, Tung TT, Moussa MM, Losic D (2020) Superhydrophobic/superoleophilic natural fibres for continuous oil-water separation and interfacial dye-adsorption. Sep Purif Technol 233:116062
66. Ou X, Yang X, Zheng J, Liu M (2019) Free-standing graphene oxide-chitin nanocrystal composite membrane for dye adsorption and oil/water separation. ACS Sustain Chem Eng 7(15):13379–13390
67. Pant B, Park M, Kim H-Y, Park S-J (2017) CdS-TiO$_2$ NPs decorated carbonized eggshell membrane for effective removal of organic pollutants: a novel strategy to use a waste material for environmental remediation. J Alloy Compd 699:73–78
68. Parvin S, Biswas BK, Rahman MA, Rahman MH, Anik MS, Uddin MR (2019) Study on adsorption of Congo red onto chemically modified egg shell membrane. Chemosphere 236:124326
69. Peng Y, Chen D, Ji J, Kong Y, Wan H, Yao C (2013) Chitosan-modified palygorskite: preparation, characterization and reactive dye removal. Appl Clay Sci 74:81–86
70. Pramanpol N, Nitayapat N (2006) Adsorption of reactive dye by eggshell and its membrane. Agric Nat Resour 40(6(Suppl)):192–197
71. Qayum A, Wei J, Li Q, Chen D, Jiao X, Xia Y (2019) Efficient decontamination of multi-component wastewater by hydrophilic electrospun PAN/AgBr/Ag fibrous membrane. Chem Eng J 361:1255–1263
72. Saghir S, Fu E, Xiao Z (2020) Synthesis of CoCu-LDH nanosheets derived from zeolitic imidazole framework-67 (ZIF-67) as an efficient adsorbent for azo dye from waste water. Microporous Mesoporous Mater 297:110010. https://doi.org/10.1016/j.micromeso.2020.110010
73. Sarioglu OF, San Keskin NO, Celebioglu A, Tekinay T, Uyar T (2017) Bacteria immobilized electrospun polycaprolactone and polylactic acid fibrous webs for remediation of textile dyes in water. Chemosphere 184:393–399
74. Satilmis B, Budd PM, Uyar T (2017) Systematic hydrolysis of PIM-1 and electrospinning of hydrolyzed PIM-1 ultrafine fibers for an efficient removal of dye from water. React Funct Polym 121:67–75. https://doi.org/10.1016/j.reactfunctpolym.2017.10.019
75. Satilmis B, Uyar T (2018) Amine modified electrospun PIM-1 ultrafine fibers for an efficient removal of methyl orange from an aqueous system. Appl Surf Sci 453:220–229. https://doi.org/10.1016/j.apsusc.2018.05.069
76. Shi C, Lv C, Wu L, Hou X (2017) Porous chitosan/hydroxyapatite composite membrane for dyes static and dynamic removal from aqueous solution. J Hazard Mater 338:241–249

77. Shi K, Zhitomirsky I (2015) Influence of chemical structure of dyes on capacitive dye removal from solutions. Electrochim Acta 174:588–595

78. Sieren B, Baker J, Wang X, Rozzoni SJ, Carlson K, McBain A, Kerstan D, Allen L, Liao L, Li Z (2020) Sorptive removal of color dye safranin o by fibrous clay minerals and zeolites. Adv Mater Sci Eng 2020

79. Song W, Zhu M, Zhu Y, Zhao Y, Yang M, Miao Z, Ren H, Ma Q, Qian L (2020) Zeolitic imidazolate framework-67 functionalized cellulose hybrid aerogel: an environmentally friendly candidate for dye removal. Cellulose 27(4):2161–2172

80. Teng M, Li F, Zhang B, Taha AA (2011) Electrospun cyclodextrin-functionalized mesoporous polyvinyl alcohol/SiO$_2$ nanofiber membranes as a highly efficient adsorbent for indigo carmine dye. Colloids Surf A Physicochem Eng Asp 385(1–3):229–234

81. Tissera ND, Wijesena RN, Yasasri H, de Silva KMN, de Silva RM (2020) Fibrous keratin protein bio micro structure for efficient removal of hazardous dye waste from water: surface charge mediated interfaces for multiple adsorption desorption cycles. Mater Chem Phys 246:122790

82. Valencia L, Kumar S, Nomena EM, Salazar-Alvarez G, Mathew AP (2020) In-situ growth of metal oxide nanoparticles on cellulose nanofibrils for dye removal and antimicrobial applications. ACS Appl Nano Mater 3(7):7172–7181

83. Walker GM, Weatherley LR (2001) Adsorption of dyes from aqueous solution—the effect of adsorbent pore size distribution and dye aggregation. Chem Eng J 83(3):201–206. https://doi.org/10.1016/S1385-8947(00)00257-6

84. Wang K, Ma Q, Wang S-D, Liu H, Zhang S-Z, Bao W, Zhang K-Q, Ling L-Z (2016) Electro-spinning of silver nanoparticles loaded highly porous cellulose acetate nanofibrous membrane for treatment of dye wastewater. Appl Phys A 122(1):40

85. Wang Y, Ding W, Jiao X, Chen D (2014) Electrospun flexible self-standing silica/mesoporous alumina core–shell fibrous membranes as adsorbents toward Congo red. RSC Adv 4(58):30790–30797. https://doi.org/10.1039/C4RA03912B

86. Xiao N, Wen Q, Liu Q, Yang Q, Li Y (2014) Electrospinning preparation of β-cyclodextrin/glutaraldehyde crosslinked PVP nanofibrous membranes to adsorb dye in aqueous solution. Chem Res Chin Univ 30(6):1057–1062

87. Xu Q, Peng J, Zhang W, Wang X, Lou T (2020) Electrospun cellulose acetate/P (DMDAAC-AM) nanofibrous membranes for dye adsorption. J Appl Polym Sci 137(15):48565

88. Xu Y, Li Z, Su K, Fan T, Cao L (2018) Mussel-inspired modification of PPS membrane to separate and remove the dyes from the wastewater. Chem Eng J 341:371–382

89. Xu Z, Li X, Teng K, Zhou B, Ma M, Shan M, Jiao K, Qian X, Fan J (2017) High flux and rejection of hierarchical composite membranes based on carbon nanotube network and ultrathin electrospun nanofibrous layer for dye removal. J Membr Sci 535:94–102. https://doi.org/10.1016/j.memsci.2017.04.029

90. Yan J, Huang Y, Miao Y-E, Tjiu WW, Liu T (2015) Polydopamine-coated electrospun poly (vinyl alcohol)/poly (acrylic acid) membranes as efficient dye adsorbent with good recyclability. J Hazard Mater 283:730–739

91. Yi S, Sun S, Zhang Y, Zou Y, Dai F, Si Y (2020) Scalable fabrication of bimetal modified poly-acrylonitrile (PAN) nanofibrous membranes for photocatalytic degradation of dyes. J Colloid Interface Sci 559:134–142

92. Zhan Y, Guan X, Ren E, Lin S, Lan J (2019) Fabrication of zeolitic imidazolate framework-8 functional polyacrylonitrile nanofibrous mats for dye removal. J Polym Res 26(6):1–11

93. Zhang J, Ding S, Ge Y, Li Z (2020) Enhanced removal of crystal violet in water using a facile-fabricated and environmental-friendly laccase immobilized composite membrane. Process Biochem 98:122–130

94. Zhang X, Li Z, Lin S, Théato P (2020) Fibrous materials based on polymeric salicyl active esters as efficient adsorbents for selective removal of anionic dye. ACS Appl Mater Interfaces 12(18):21100–21113. https://doi.org/10.1021/acsami.0c03039

95. Zhao R, Li Y, Sun B, Chao S, Li X, Wang C, Zhu G (2019) Highly flexible magnesium silicate nanofibrous membranes for effective removal of methylene blue from aqueous solution. Chem Eng J 359:1603–1616

96. Zhao X, Liu Y, Shuai Z, Wang C (2019) Preparation and performance of three-layered struc-
    ture composite membrane for heavy metal ions and hazardous dyes rejection. Polym Eng Sci
    59(S1):E322–E329
97. Zhao X, Wang X, Lou T (2021) Preparation of fibrous chitosan/sodium alginate composite
    foams for the adsorption of cationic and anionic dyes. J hazard Mater 403:124054
98. Zhijiang C, Ping X, Cong Z, Tingting Z, Jie G, Kongyin Z (2018) Preparation and characteriza-
    tion of a bi-layered nano-filtration membrane from a chitosan hydrogel and bacterial cellulose
    nanofiber for dye removal. Cellulose 25(9):5123–5137. https://doi.org/10.1007/s10570-018-
    1914-0
99. Zhu X, Jiang X, Cheng S, Wang K, Mao S, Fan L-J (2010) Preparation of high strength
    ultrafine polyvinyl chloride fibrous membrane and its adsorption of cationic dye. J Polym Res
    17(6):769–777. https://doi.org/10.1007/s10965-009-9368-6

Preparation and Application of Chitosan-Based Membrane: Focusing on Dye Removal

Abubakar Hamisu Mijinyawa, Geeta Durga, and Anuradha Mishra

Abstract Water pollution is caused by the direct discharge of harmful dyes into the environment and is a major global problem. Dyes if present in the water can be toxic to the aquatic organisms and humans. Dyes are recalcitrant in nature, and they can resist attack by heat, light, and microorganisms. Hence, most of the reactive dyes are non-biodegradable and their removal from the aqueous solution is very difficult, and therefore, a necessary measure must be applied in order to tackle the existence of the water pollution problem. Adsorption is a well-known technology that is adopted in the academia and industries for removal of dyes from solution. The adsorption of dyes on adsorbents is a simple and economical procedure that is widely used for large and small-scale removal of dyes. In the current chapter, we reviewed the extraction of chitin from the shells of marine animals, the preparation of chitosan by deacetylation reaction, structure and properties of the chitosan biopolymer. Chitosan films could be prepared by casting technology via dissolution of chitosan in a suitable solvent followed by simple evaporation technique. The chapter highlights that chitosan films have superior physicochemical characteristics than raw chitosan biopolymer; the mechanical strength of reported chitosan films might be as high as 28 MPa. Among the different chitosan films, this chapter has comprehensively presented the discussion on preparation, characterization, and dye removal application of various classes of chitosan composite membranes. The tensile strength of chitosan composite film could reach 35 MPa approximately, thus suggesting the composite films based on chitosan could be considered as good adsorbents for dye removals from water. The maximum adsorption capacity (Q_{max}) of the reviewed composite film could reach 655 mg g^{-1}, but comparatively lower than Q_{max} of chitosan-magnetic cyclodextrin composite by a mammoth difference of 2125 mg g^{-1}. Both of the chitosan-based composites are recyclable through multiple

A. H. Mijinyawa · G. Durga (✉)
Department of Chemistry and Biochemistry, School of Basic Sciences and Research, Sharda University, Greater Noida 201306, India
e-mail: geeta.durga@sharda.ac.in

A. Mishra
Department of Applied Chemistry, School of Vocational Studies and Applied Sciences, Gautam Buddha University, Greater Noida 201312, India

adsorption–desorption cycles. Despite the good adsorption and regeneration and reuse capabilities of chitosan-based composite films, and in order to enhance their dye removal capacities, the present chapter has strongly recommended further works to explore more of magnetic chitosan-based composite membranes with superior adsorptive behaviors for consideration of future practical dye removal application from wastewater. Finally, the characterizations of such adsorbent systems should be comprehensively investigated before and after dye removal to understand the details on mechanism of the removal of dyes from water.

Keywords Water pollution · Chitosan · Chitosan films · Chitosan composite membranes · Tensile strength · Adsorptive behavior · Dyes removal · Maximum adsorption capacity (Q_{max}) · Mechanism · Recycling

Nomenclature

AC	Activated carbon
AFM	Atomic force microscopy
AR	Acid red dye
AO	Acid orange dye
BET	Brunauer-Emmett-Teller
[Bmim] Ac	1-Butyl-3-methylimidazolium acetate
BO	Bezactive Orange
BY	Brilliant yellow
CA	Cellulose acetate
CD	Cyclodextrin
C_e	Equilibrium dye concentration (mg L^{-1})
CNF	Cellulose nanofiber
C_o	Initial dye concentration (mg L^{-1})
CSB	Chitosan/saponin-bentonite composite
CR	Congo red
Da or u	Dalton atomic unit
DD	Degree of deacetylation
DMSO	Dimethyl sulfoxide
[EMIM] AC	1-Ethyl-3-methylimidazolium acetate
FD&C	Food, drugs & cosmetics
FTIR	Fourier Transform infrared spectroscopy
GO	Graphene oxide
ILs	Ionic liquids
IR	Infrared radiation
K	Kelvin
K_c	Equilibrium constant
K_L	Langmuir constant (L g^{-1})
LCTS	Low molecular weight chitosan

MB	Methylene blue dye
MG	Malachite green dye
MgO	Magnesium oxide
MMT	Montmorillonite
MO	Methyl orange
MPa	Megapascals
MWCNTs	Multi-walled carbon nanotubes
MW	Molecular weight (g mol^{-1})
PAA	Polyacrylic acid
PEG	Poly (ethylene glycol)
PZC	Point of zero charge
Qe	Equilibrium adsorption capacity (mg g^{-1})
Q$_{max}$	Maximum or monolayer adsorption capacity (mg g^{-1})
R	Molar gas constant (J mol^{-1} K^{-1})
RB	Reactive blue
R$_L$	Separation factor (dimensionless)
SEM	Scanning electron microscopy
T	Absolute temperature (Kelvin)
TEM	Transmission electron microscopy
TiO$_2$	Titanium dioxide
USD	United State Dollars
W	Weight (gram)
XRD	X-ray Diffraction Analysis
ZnO	Zinc oxide

1 Introduction

Potable water is needed for bulk drinking, agricultural, and industrial applications. Domestic wastes and chemical pollutants are continuously increasing the water pollution burden worldwide, which has today become a critical environmental issue. Combined with the already existing shortage of ground or drinking water, the water pollution is massively increasing water scarcity, especially in the developing countries.

Water purification is a top priority amongst the environmental and industrial chemists and government agencies as well. Biological procedure is a traditional method that is applied by using microbes for the treatment of various domestic, industrial, or sewage pollutants. However, it lacks effectiveness due to the slow nature, low pollutant removal, and high cost of the method. The use of adsorption method using activated carbon has remained the most well-established technology applied both at the academic and commercial or industrial levels. There are large numbers of different adsorbents that have been reportedly adopted for water purification of heavy metals and dyes wastewater [1–3].

Among the class of pollutants, synthetic dyes are known to be highly visible in water, irritant, non-biodegradable, carcinogenic, and mutagenic. Moreover, the dyes have been reported to cause cell inactivation in animals [4]. The two most important components of dyes are chromophore which produces the color and the auxochrome which enhances the affinity of the color of dyes [5]. They (dyes) are commonly classified into anionic, cationic, and nonionic based on the type of charges in their structures.

Notably, the dyes have attracted wide applications in biomedical and industrial fields as coloring agents. Due to the non-biodegradable or recalcitrant nature and toxicity of many dye compounds, their removals from wastewater have remained to be a very difficult task; it is, however, very much necessary to remove dyes from wastewater before being discharged into the environment. Adsorption as advance technology is an effective or robust way for dye removal from the aqueous solution [6].

Despite the bulk of researches and high dye adsorption characteristics possessed by the conventional activated carbons, some conclusions on reasonable answers to the drawbacks of this type of carbons have not yet been made available commercially. The activated carbons are suffering from the high cost of adsorption and regeneration processes, and this has caused a wide restriction of the application of activated carbons at the industrial level. There is also sludge problems that are associated with their use in solution, the removal of which, from surface of treated water, may increase the overall cost of the process.

Activated carbons that are derived from some previously reported low-cost adsorbents including the agricultural solid wastes [7] exhibited similar problems as do the commercial carbons. This kind of wastes themselves require activation in most of the reported studies in order to make them much more effective sorbents for dye adsorption [8], which in turn makes the whole process to be expensive.

Green chemistry area strongly recommends the application of biomaterials in water purification because they are sustainable, low-cost, eco-friendly in nature, and tunable. The use of biomaterials like chitosan in water to remove toxic dyes is a welcomed green practice and being regarded as a new alternative to the use of commercial activated and or similar carbon-based materials.

Chitosan is a well-known derivative of chitin, an animal-based polysaccharide and being a second in abundance apart from the cellulose polymer [9]. It is obtained from the chitin by a chemical deacetylation reaction under alkaline condition [10]. Raw chitosan (Fig. 1) has abundant functional groups, notably, the hydroxyl group or –OH and amino group or $-NH_2$. Hence, chitosan is referred to as the aminopolysaccharide, which gives it a cationic nature due to the positive charge on its nitrogen atoms when in solution.

The adsorptive characteristic of chitosan towards the molecules of dyes depends mainly on these chemical groups and other environmental factors such as the pH of the solution, amount of chitosan or dose, temperature, etc. At a pH value below 6.5, chitosan is protonated and can therefore be used for the adsorption of anionic dyes from water. At the basic pH, the density of negative charges on chitosan increases, and this property makes it useful for adsorption of cationic dyes.
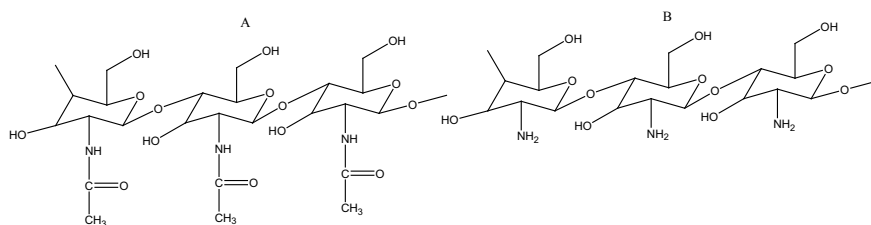
Fig. 1 Chemical structure of **a** chitin and **b** chitosan

Thus, chitosan biopolymer and its derived forms are potentially useful in the adsorption of the molecules of dyes from water [11]. The presence of functional groups in the chitosan, suggests that this biopolymer can be modified to form probably chitosan composite membrane, etc., which may have an improved dye adsorption property in comparison to the raw chitosan.

In this chapter, we firstly describe in brief the preparation and structural properties of chitosan biopolymer and basic principles on membrane systems. Afterwards, we would discuss in comprehensive term the recent advances on preparation and application of chitosan-based membranes, with a clear focus on the chitosan composite membranes that are applicable for dye removal from wastewater. We would pay extreme attention for reviewing on the recent research papers on this topic that were published in the past or within the 10–15 years only. This important chapter would be regarded as a full summary containing great knowledge of various advanced methods that are used in the preparation and characterization of the chitosan composite membranes.

To sum up, the primary objectives of this review are to provide a thorough overview on preparation, physicochemical properties, dye removal, regeneration, and reusability performances of this type of membrane systems, to study the most important interactions that could adequately describe the removal mechanism, and to discuss a direct comparison of adsorption affinities with other reported similar materials. This particular chapter provides a state-of-the-art research documents purposely on the chitosan-based composite membranes for the removal of different kinds of dyes from water. Hence, this chapter will serve as a useful guide for many students and researchers to properly study, to understand, and to conduct/undergo researches in the control of water pollution, especially the dye removals.

2 Chitosan Biopolymer

Naturally, chitosan can be found in the fungal cell wall of aspergillus and mucor. However, the commercially available chitosan polymer is made from chitin that is extractable from the shells of crustaceans and exoskeletons of insects and mollusks

[12]. Chitin is the main component of the marine crustaceans. Chitosan was discovered in the middle of the eighteenth century, but was later little known in 1934 after the verification of its crystalline structure. Herein, we are discussing in detail the common method of preparation and some usual properties of chitosan.

2.1 Preparation of Chitosan from Chitin

Chitin shown in Fig. 1a is a white polysaccharide, hard, crystalline with high molecular weight (MW) distribution, and it is extracted from the shells of shrimp and crab. The biowastes from the crab and shrimp shells are used for the large-scale production of chitin and chitosan.

 The extraction of chitin and preparation of chitosan are stepwise chemical procedures. The extraction of chitin involves the grounding of the shells to obtain some smaller particle sizes; calcium carbonate mineral is removed by treating the grounded shells with the solution of dilute hydrochloric acid followed by stirring under ambient condition [12]. The former process is called demineralization as it involves the removal of mineral contents of the shells. The treatment of the residual material with dilute sodium hydroxide (aqueous solution) helps in the removal of protein from it, which finally yields the raw chitin biopolymer.

 On the other hand, the chitosan is prepared by deacetylation of the extracted chitin using excess of sodium hydroxide solution (normally 40–45% NaOH concentration) and water as a solvent [13, 14]. The chitosan can be separated by filtration method, and then is purified by washing with water several times until the pH of the solution attained neutral state which is then followed by oven drying method. The preparation of chitosan is shown schematically in Fig. 2. The success of the reaction is determined by the parameter called the degree of deacetylation (DD), which is related to the degree of transformation of the chitosan from chitin. The DD, in turn, it depends on the reaction factors viz. the concentration of NaOH, temperature, and time of the deacetylation reaction [15].
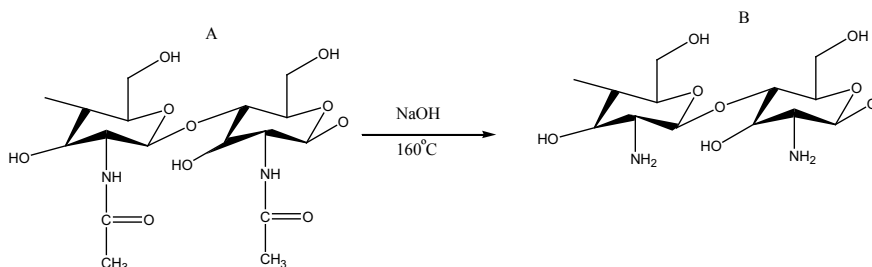
Fig. 2 Chitosan preparation from chitin

2.2 Structure and Properties of Chitosan

Figure 1b depicts the basic structure of chitosan polysaccharide. The chemical name of chitosan is β-(1:4)-linked 2-amino-2-deoxy-β-D-glucopyranose, and it is obtained by transforming the acetamide groups present in the chitin into primary amino groups [16]. This structurally distinguishes chitosan from the initial chitin.

Chitosan is a linear polycation consisting of multiple hydroxylated with amino functional groups in the main structure and plenty of hydrogen bonded structures. The chitosan biopolymer consisted of β-(1:4) linkages of N-acetyl-D-glucosamine and D-glucosamine [17]. In chitosan, the carbon, hydrogen, and nitrogen have elemental compositions of 44.11%, 6.84%, and 7.97%, respectively [14].

Chitosan is renewable and relatively a low-cost polymer, eco-friendly, biodegradable, biocompatible, alkaline stable, film-former, mechanically, and thermally stable. The average MW of chitosan is around 3,800–20,000 Da. A chitin with a degree of deacetylation (DD) of at least 75% is generally classified as a chitosan polymer. The degree of deacetylation enhances greatly the density of positive charge on chitosan, and this property can induce a stronger electrostatic interaction between chitosan and anionic structural matter. The degree of deacetylation for a cationic chitosan with a reasonable good solubility should be within the range of 85–98% [12].

Chitosan has very poor solubility in water [18] owing to the presence of amino groups having pK_a of 6.3–6.6 values. However, it is found soluble in weak acidic media and this particular property may weaken the stability of chitosan film. Some reported dissolution media for chitosan are acetic acid [19], tartaric acid [20], 1-ethyl-3-methylimidazolium acetate [21], etc.

The poor solubility of the chitosan in water has necessitated its chemical modification to obtain various chitosan derivatives with some wider variety of applications. The cross-linking of chitosan with epichlorohydrin, formaldehyde, glutaraldehyde, etc., is one example that is considered as a viable option and is found usually to improve the solubility and mechanical stability of chitosan [22]. The acidic aqueous solutions of chitosan can be useful for the production of chitosan film polymers. The preparation of chitosan membrane is another crucial method for obtaining chitosan derivative with new properties.

Thus, chitin can be extracted from the shells of the marine animals which can be found as wastes from the fishery industries. Chitosan biopolymer is prepared by the deacetylation of chitin using excess NaOH solution. Chitosan has poor solubility in water; hence, its modifications are therefore necessary.

3 Chitosan-Based Membranes

3.1 Definition

The present section would focus on the discussion of solely some reported adsorptive membranes, which are based on chitosan biopolymer. According to an earlier definition, the membrane can be defined simply as semipermeable barrier, which can regulate the transportation of either gaseous or liquid substance between two adjacent phases [23]. The membranes are traditionally used in the separation of gas and for water treatment applications.

3.2 Preparation

Hassan et al. [24] recently highlighted a simple methodology on preparation of a novel biopolymer membrane, for example, chitosan-based film. The simplified scheme for the method of preparation of a biopolymer membrane is given in Fig. 3 as shown below. Inorganic and or organic acids are usually used as the common solvents for dissolving chitosan in order to prepare its corresponding membrane system by the simple evaporation of water molecules.

According to this method, a specified quantity of the biopolymer is dissolved proportionally in its solvent, and then followed by casting on a glass plate, washing, and drying procedures under certain given experimental conditions. Specifically, the polymer solution that is to be casted is obtained after vigorous stirring method for a period of about 24 h at ordinary temperature. [25] dissolved chitosan in an acetic acid solution at 1:1 weight ratio (%) to form a chitosan-based membrane of thickness
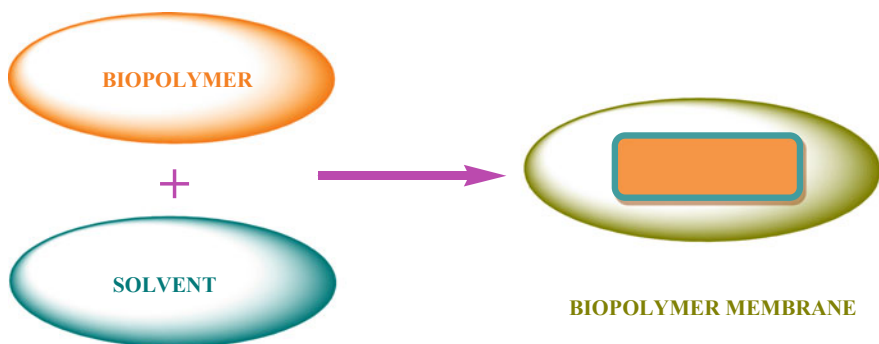

Fig. 3 Common method for the preparation of biopolymer membrane. *Note* The final solution of the biopolymer obtained after stirring is casted on glass plates or petri dishes to form the membrane system, which is being neutralized by the given base, washed several times with water, and then dried

which is around 60 μm. This membrane, according to the authors, was neutralized in a solution of NaOH (0.1 molar concentration) for 10 min followed by excessive washing with distilled water, and finally it was dried.

Cui et al. [19] prepared a chitosan-based membrane by using a combined new binary solvent system involving tartaric acid for pre-treating of the chitosan and 1-ethyl-3-methylimidazolium acetate, i.e., [EMIM] AC for acting as a translucent agent during the preparatory synthesis. Both of the solvents could act simultaneously as dissolution media for chitosan towards the preparation of a smooth and thick chitosan membrane or film. However, the use of the later solvent (an ionic liquid, IL), as the only solvent media for dissolving the chitosan is restricted, owing to the fact that ILs are viscous and not easily recovered at a considerably higher dissolution temperature and lower chitosan concentration.

Nevertheless, the ILs (or the organic salts with melting points equivalent to or below the room temperature) are viewed as desirable green and good solvents for dissolution of biopolymers [26], and have generally attracted some wide applications in the area of material syntheses and catalysis [27].

Certainly, there are drawbacks with regard to the use of both acids and ILs as dissolution medium for chitosan in the formation of a biopolymer membrane. When acids are used, the resultant film also contains residual amount of the acid and this renders a further treatment of the film by using an alkali. This is not a feasible process from the commercial point of view as it may require excess time and money. Hence, another way of dissolving chitosan is indeed a necessary thought.

About a decade ago, [28] proposed a novel method for the development of chitosan film by dissolving the chitosan in the water using carbonic acid or carbon (IV) oxide gas (CO_2). The role of the carbonic acid was to dissolve the chitosan without lowering the pH of the film or final solution, and the CO_2 is eliminated during the process of the film preparation. This new method is shown in Fig. 4. This methodology is different from the one that adopts the use of the common organic acids like acetic acid in which its residual amount may remain in the finally prepared film.

There are two available stages that are involved in the above process. For the stage 1, the CO_2 gas is bubbled into an emulsified form of chitosan in water. The CO_2 reacts with water to form H_2CO_3 acid (pKa = 3.9), which then reacts with chitosan to form the cationic form of chitosan that is soluble in aqueous water. The chitosan film is formed from the stage 2 which is described as follows: During this stage, the H_2CO_3 acid present in the neutral solution of chitosan (pH 6.8) decomposed into the individual CO_2 and H_2O molecules. During the process of evaporation, the molecules of CO_2 evaporated easily along with the water to form the solid chitosan film which contained no remaining acid [28].

3.3 Physicochemical Properties

The groups such as amino, hydroxyl, and acetamide that are present in the structure of chitosan give it some attractive adsorption property [29]. Despite this adsorptive

Aerial Phase CO_2 **(1)**

Aqueous Phase

CO_2 + H_2O ⟶ H_2CO_3

H_2CO_3 ⟵ Chito- NH_2 (gel or Solid)

HCO_3^- + Chito- NH_3^+ (Dissolved)

Aerial Phase CO_2 H_2O **(2)**

Aqueous Phase

CO_2 + H_2O ⟵ H_2CO_3

H_2CO_3 + Chito- NH_2 (Film)

HCO_3^- + Chito- NH_3^+ (Dissolved)
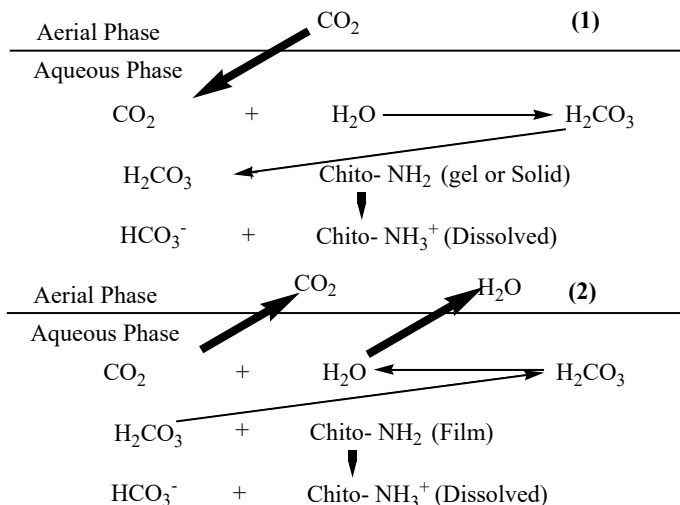
Fig. 4 A novel method for dissolving chitosan using a carbonic acid gas [28]: The chitosan acts as an electron donor (a base) in the reaction

characteristic, chitosan has still some certain major drawbacks which include its low mechanical stability (due to its higher hydrophilicity) and pH sensitive nature. To overcome these inherent problems, scientists have considered the development of chitosan-based membranes or films in the area of dye removal from water [29, 30]. The properties of the film may be dependent upon the several factors which may include the DD of the chitosan, the method of preparation, and type of materials applied in the preparation of the chitosan-based film.

The mechanical strength is a crucial property that can judge the suitability of materials to be either used as effective adsorptive membranes or not. The mechanical strength of chitosan films obtained from its solution is normally found to be in the range 15–18 MPa [31]. However, [19] developed a chitosan-based film by using ethanol as a regenerative solvent, and the maximum strength for this synthesized membrane was determined by the authors to be 24 MPa. The rearrangement and tighter bonding between the curled molecules of chitosan in the film, as a result of the formation of intermolecular hydrogen bonds (upon drying), caused the improvement in the mechanical properties of the resulting chitosan membrane according to the authors.

Chitosan-based membranes have excellent mechanical properties which make them useful for adsorption of the molecules of dyes from water [9, 32]. The tensile strength and elongation at break of reported chitosan films were approximated to be 28 MPa and 64%, and this showed a good mechanical property that could facilitate for easier phase separation of molecules of dyes after their adsorption from water [33, 34]. Thus, the ease of the phase separation property exhibited by the membrane offers it some advantage for the practical/real applications.

The water absorption or swelling degree of chitosan-based films is another significant property that is greatly important in the context of the adsorption of dyes from aqueous solutions, as the porous structures of the films could be expanded after absorption of the water molecules to accommodate the penetration of large molecules of dyes inside the generated pores [22]. Recently, high water absorption (200–900%) behavior has been reported for chitosan-based films [34, 35]. The swelling degree of the chitosan film (500% swelling) does not depend on the temperature of the solution as revealed by [34].

Chitosan film prepared by a ternary solvent method (acetic acid/dioxane/DMSO) exhibited superior water absorbency of around 896 g g^{-1} than the film obtained by using a single solvent or acetic acid alone having the absorbency of 212 g g^{-1} [36]. The micro-nano structural property and the less crystalline or lower amorphous percentages [37] are responsible for such higher water absorbency amount in the chitosan film. The net effect on the film's property was that the surface functional groups are largely exposed for the water absorption purpose.

3.4 Types and Uses of Chitosan-Based Membranes

This section presents some of the various types/classes of novel chitosan-based membranes that are available in the literature along with their respective uses in dye removal application by adsorption phenomenon. They are briefly discussed below one after the other according to their types:

I. *Chitosan blend membrane*: Polymer blending or coating is a simple technique that is applicable in the fabrication of chitosan-based adsorptive membranes. The key to the fabrication of this type of membranes is the consideration of the miscibility of each of the constituent polymers, in order to provide a better interaction among them, resulting in homogenous and much reinforced polymer-based membranes [11]. The introduction of the positively charged chitosan onto a solid polymer support may affect the overall surface charge of the prepared membrane system [38]. The blending of chitosan with polymers, such as cellulose, cellulose acetate (CA), etc., has been considered as an effective traditional way of overcoming the intrinsic shortcomings (low mechanical and chemical stabilities) as possessed by the raw chitosan [39–41]. Solvent casting and deacetylation approach have been successfully applied for the development of biodegradable, miscible, flexible, and water-stable deacetylated cellulose acetate/chitosan blend films for the adsorption of the molecules of acid orange 7 and brilliant yellow dyes [41]. The amount of the positive charge (0.21–0.94 mmolg^{-1}) increased gradually with the increment of the content of the chitosan (6.67–27.3 wt%) in the developed films.

II. *Chitosan porous membrane*: A porous membrane structure can be obtained or prepared by employing the use of chemical additives known as porogens or pore generators (pore-forming agents) through the principal of selective

dissolution mechanism. Porogens that are used in the preparation of chitosan membranes are broadly classified into organic porogens, e.g., poly (ethylene glycol), poly (ethylene oxide), poly (vinyl alcohol), etc., and inorganic porogens, e.g., sodium chloride (NaCl), calcium carbonate ($CaCO_3$), Silica, alumina, etc [11]. The porosity of membranes can be determined by using a Brunauer–Emmett–Teller (BET) method under inert nitrogen atmosphere. The pore structure of the chitosan porous membrane can provide significant reduction in the mass transfer resistance, improved water permeability, and adsorption of molecules of dyes or pollutants. Earlier, a macroporous chitosan film was developed for the adsorption of Congo red dye from water [42]. The authors progressively employed the use of formaldehyde to protect the amino groups in chitosan from being reacted or attacked by the poly (ethylene glycol) or PEG used as porogens during the preparation of the film. The synthesized chitosan porous membrane had exhibited some rough surfaces in comparison to the pure chitosan having a smoothed morphology.

III. *Imprinted chitosan membrane*: Certain polymeric adsorbents may possess some limited adsorptive or binding sites, and this may cause poor ionic selectivity in the specific materials. Imprinting technique can be adopted to overcome the lack of the selectivity of the adsorbents. The imprinting (Fig. 5) is the process by which a target is added during the preparation of the polymer-based membranes in order to introduce some voids on the polymer's background, and the target or the imprinted template is then extracted or washed to obtain the
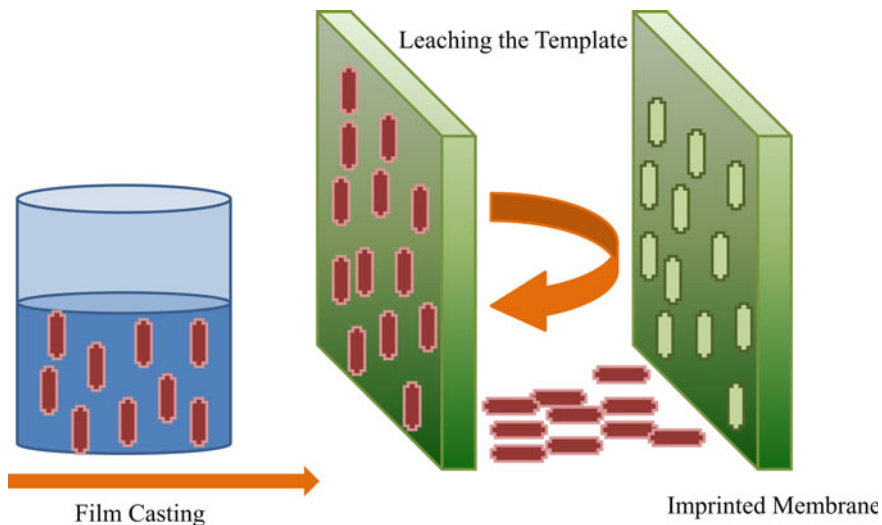
Fig. 5 The imprinted technique for the preparation of imprinted polymer-based membrane. *Note:* The imprinted target or template is casted along with the film, and the template is leached out of the casted film as shown above

active sites or the imprinted polymer specifically to be used for the adsorption of the target template molecules [43, 44].

One of the advantages of the imprinting process is that it increases the selectivity of the membranes through a specialized selective adsorption of the molecules or ions in the aqueous solution (Fig. 6). Chitosan has attractive capacity and potential to be imprinted for the selective sorption of ionic or molecular species [45]. The number of reports on imprinted chitosan-based membranes is very few, and thus, this presents a novel area of research in the development of such membranes for separation purpose.

Recently, a mesoporous imprinted chitosan/titanium dioxide or TiO_2 nanocomposite (approximate surface area and average pore radius were 95 m^2/g and 19 Å, respectively) was synthesized for the highly selective ionic adsorption of Rose Bengal (anionic dye compound) from industrial effluent water (Ahmed et al. 2017). The imprinted chitosan/TiO_2 nanoparticles were prepared through a sol–gel method using the Rose Bengal dye as the template target. The addition of the catalysts such as the tin oxide, and zinc oxide in the synthesis of the imprinted polymer membranes was to facilitate the extraction of the template [46].

IV. *Chitosan composite membrane*: Addition of some particles in the micro or nano level into the structure of matrix or the polymer membrane, inside the matrix or coated on its surface, to produce immiscible mixture with some new properties and applications may result in the formation of polymer composite or nanocomposite membrane as the case it may be [47]. Thus, the formation of
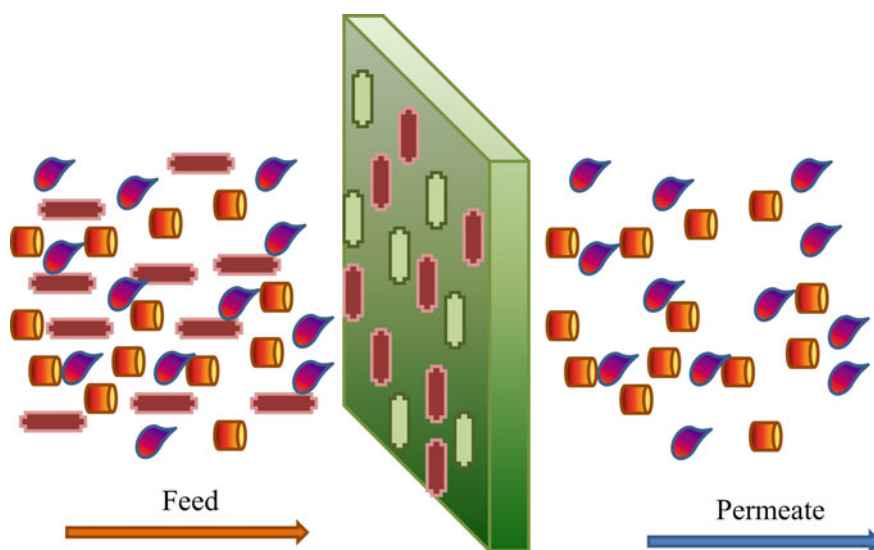
Fig. 6. Selective adsorption of the target ions/or molecule by the imprinted membrane. *Note:* The density or the number of the target (feed side) is being reduced as seen in the permeate site

nanocomposite polymer membrane is simply the combination of the polymeric materials with nanomaterials in order to tailor their structure and physicochemical properties for specific applications such as in the water purification studies. Chitosan displays great potential in the fabrication of polymer-based composite membranes. Various recent literatures had addressed the addition of nanoparticles, such as activated carbon [48], multi-walled carbon nanotubes (MWCNTs) [49, 64], nano clay [50], graphene oxide (GO) [9], titanium dioxide (TiO$_2$) (Ahmed et al. 2017), zinc oxide (ZnO) [51], etc., into the chitosan as the matrix biopolymer to form composites for the removal of different classes of dyes from aqueous solutions.

Most common substances for dissolving chitosan are acids, ionic liquids, carbon dioxide gas, etc. Chitosan-based films are prepared by a solvent casting technology. By this way, the physicochemical properties, such as the mechanical strength of the chitosan, are enhanced. A number of chitosan-based membranes are prepared and reported by various researchers; they are chitosan blend, chitosan porous, imprinted chitosan, chitosan composite membranes, and so on.

4   Chitosan Composite Membranes

In the Sect. 3, the classifications of composite membranes based on the chitosan biopolymer have been briefly introduced by highlighting their methods of preparation and adsorptive applications in the removal of harmful dye molecules from wastewater. Thus, under present section, the various methods of preparation of the chitosan-based composite membranes are going to be well discussed one by one.

4.1   *Chitosan/Activated Carbon Membrane*

Activated carbon or AC is a carbon material that can be prepared by treatment of biowaste, coal, charcoal, coconut shells, or wood, etc., using either physical and or chemical activation methods [8, 52]. The product from the either method is regarded as an activated carbon, which can be used as adsorbent for the adsorption of dyes; its quality or adsorptive property depends on the type of the used biowaste and type of the activation method [53]. The physical method is limited due its requirement of higher temperature and longer time of activation compared to the chemical activation procedure. The activated carbon has typically a porous structure and large specific surface area in the range 500–2,000 m^2 g^{-1} [54]. There are broadly two types of the AC viz. the H-type which has a positive charge when in water and being hydrophobic, and the L-type which assumes negative charge in water and being considered as hydrophilic [5].

Although, the activated carbons have high dye adsorption capacities [5], but their adsorptions can be improved further by composting them with chitosan or biopolymers to form composite membrane (s). The composite may have a possible synergistic high adsorption behavior due to co-existence of both the starting materials. On the other hand, the chitosan in its raw form may have low adsorption affinity for dyes, in particular, the cationic dyes. Its adsorption capacity for removal of different class of dyes can be enhanced by making a composite membrane with the activated carbon due to the synergistic effects. However, there are very limited numbers of or no research works which are available in the literature on chitosan/activated carbon composite membranes that are focused for dye removal studies. Although, the removal of metal ions using chitosan-based activated carbon composite films have been reported earlier [55].

4.2 Chitosan/Carbon Nanotubes Membrane

Carbon nanotubes (CNTs) is being defined as a 1D allotrope of carbon atoms having a rigid cylindrical nanostructure and unique characteristics including its high aspect ratio, chemical stability, ease of functionalization, and so on [56]. The CNTs have since been discovered in the year 1991 by Lijima [57]. According to the number of graphene layers rolling on each atom, the CNTs are categorized broadly into two types, namely, the single-walled CNTs (SWCNTs) and the multi-walled CNTs (MWCNTs).

Functionalizing polymer matrixes with the CNTs by incorporation procedure can provide an enhancement in the separation performance of the composite membranes through an improved water permeability and rejection of pollutants from water on its surface [56, 58]. The CNTs have poor dispersion in polymer matrix due to the smooth surface structure, van-der-Waals, and its π-to-π interactions, and the combined effect is the reduced separation performance of CNTs membrane.

Functionalization or introduction of functional groups on the mouth of the CNTs is considered as a good approach towards the improvement in its properties such as antifouling behavior, mechanical and thermal stabilities, water permeability, pollutants or dyes rejection or adsorption capability [59, 60]. Recent findings have shown that the CNTs have the potential for removal of synthetic dyes by adsorption phenomenon [61]. Their adsorption capabilities are even found to be greater than those for the activated carbons because of the existence of some stronger interactions between the CNTs and the molecule of the dyes in solution [62].

The adsorption capacities of the CNTs can be improved further by functionalizing them with biopolymers such as the chitosan (via a covalent modification) owing to the hydrophilic nature and excellent dispersion of the biopolymers than the CNTs, and this kind of study is attracting great interests from the scientists. It also opens up a new way for the preparation and environmental application of novel biopolymer-based CNTs adsorbents [63].

A magnetic chitosan-graphitized multi-walled carbon nanotubes (designated as CS-m-GMCNTs) was recently being developed by a process called suspension cross-linking method using glutaraldehyde as a chemical cross-linking agent, and was used as adsorbent for the removal of carcinogenic Congo red dye from water by adsorption [49, 64]. The authors have claimed that the synthesized novel adsorbent displays certain advantages for environmental cleanup application such as its excellent dispersion, ease of separation, and high dye adsorption capacity.

4.3   Chitosan/Graphene Oxide Membrane

Graphene oxide or GO is a highly oxidized carbon-based material and a derivative of graphene. GO contains abundant amount of oxygen/or species of oxygen which are available for adsorption between the layers. GO is synthesized by an oxidation method using strong chemical oxidizing agent, example, potassium permanganate or chlorate, etc., forming several oxygen functionalities such as a carboxyl, epoxy, hydroxyl, and so on, and these hydrophilic groups make GO to be well dispersed in water, thus producing some stabilizing effect to GO carbonaceous material [32, 65]. The GO is most successfully prepared from the graphite powder by the Hammers or the newly modified Hammers procedure [66].

Both graphene and its oxidized form, i.e., the graphene oxide have been reportedly used as effective adsorbents for adsorption of anionic and cationic dyes from water [67, 68]. Recovery of GO adsorbent is a problematic issue because it is able to form some stable colloidal particles that may hinder its phase out separation in water. However, immobilization of the GO with biopolymers is used to solve out this drawbacks by forming a GO-based biopolymer composite with the tendency of phase separation and effective adsorption. One example is the amidation reaction between chitosan and carboxyl groups of the GO to form a composite based on chitosan and the GO with a well-dispersed physical characteristics [69].

Recently, chitosan was used to cross-link graphene oxide to yield a framework structure of chitosan/GO composite film (highly swellable in water) to be used as an effective adsorbent for the removal of methylene blue (MB) dye by adsorption method [70]. The average thickness of the synthesized film was around 20–60 μm, and it possessed enhanced negative charge groups when in the ionized state.

4.4   Chitosan/Nano Clay Membrane

Clays are defined as the hydrous aluminosilicate (Al–Si–O–H) minerals that are made up of the colloidal fractions of soils, sediments, rocks, and water molecules, and they may be composed of fine-grained size of minerals and other minerals such as the quartz, carbonate, and oxides of metal. Clays are of several types, amongst them are the pyrophyllite–talc, smectites–montmorillonite, mica–illite, kaolinite, serpentine,

sepiolite, and vermiculite [71]. The common exchangeable ions that are present on the surface of clays include the ions of sodium (Na^+), calcium (Ca^{2+}), magnesium (Mg^{2+}), potassium (K^+), hydrogen (H^+), ammonium (NH_4^+), sulfate (SO_4^{2-}), chlorides (Cl^-), nitrate (NO^{3-}), etc., and the exchange with these ions present on the clays occur so readily without affecting its structural surface [72, 143].

Bentonite and montmorillonite or MMT altogether known as the smectites are the most commonly used nano clay adsorbents in the water purification application. The composition of the bentonite is made up of the MMT and other non-clay minerals [74]. Bentonite has two tetrahedral silicate layers sandwiched in one octahedral sheet of aluminate layer in a ratio of 2:1 with a negative charge on the lattice of the bentonite clay. Thus, it is generally believed that bentonite has greater affinity towards cationic dyes than anionic dyes due to attraction between unlike charges.

Generally speaking, the attraction of the clay minerals to molecules of the cationic dyes is stronger than the attraction to anionic dyes because of the presence of the net negative charge on the surfaces that have a strong affinity for positively charged dyes [75]. For instance, the adsorptions of the clay to Methylene Blue and Malachite Green (cationic dyes) are significantly higher than adsorptions to the molecules of Congo Red and Methyl Orange (anionic dyes), and the main reason for this major difference is as a result of the difference in the surface chemistry of the clay and charges on the dyes. Clays are hydrophilic in nature and therefore not compatible with organic molecules. Hence, the need to modify them has arisen in order to make them compatible with hydrophobic substances.

Modification of clay minerals can be done by acid activation, thermal treatment, and formation of composite membrane [76, 77]. Recently, the group of Zhang (2016) developed a hybrid composite membrane called cross-linked quaternized chitosan/bentonite for adsorption of the anionic Amino black 10B dye from water. The synthesis was done firstly by dispersing the bentonite clay into a quaternized chitosan using a method of the membrane-forming procedure. Secondly, this was followed by cross-linking reaction to make the quaternized material chemically stable. The addition of the clay into a polymer can lead to the development of composite with increased mechanical strength and resistance to heat [78].

A chitosan/saponin-bentonite composite film was developed for the efficient removal of methyl orange dye from wastewater [79]. The saponin is a surface modifying agent, and its addition leads to the surface alteration through the chemical interaction with its two acyl groups [80].

4.5 Chitosan/MgO Membrane

Magnesium oxide (MgO) is a basic oxide that is non-toxic and chemically stable [81]. MgO is an eco-friendly adsorbent with high reactivity and adsorption capability, and it is therefore a promising inorganic compound for water decontamination application. Hydrothermal method is used to prepare an MgO nanostructure with particles that are highly crystalline and homogenous. However, the particles of the MgO obtained from

this method can undergo agglomeration phenomenon [82]. This particular drawback can be tackled by using cetyltrimethylammonium bromide (CTAB) as a soft template to control the morphology of the MgO nanoparticles during the synthesis to prevent its formed particles from being agglomerated.

In the adsorption study, both chitosan and the MgO have certain limitations. Chitosan requires long contact time for dye adsorption. On the other hand, the MgO has lower adsorption, but with much shorter contact time for dye decontamination in comparison to the chitosan [82]. Hence, it may be possible to improve the adsorption behavior of the chitosan via the combination of itself, chitosan, and MgO or the fabrication of novel composite membrane adsorbent having high adsorption and lower contact time for the dyes removal. A chitosan/MgO film was synthesized by solvent casting procedure under mild drying for use as an effective adsorbent in the removal of reactive blue (RB) 19 dye from solution [83].

4.6 Chitosan/Zeolite A Membrane

Zeolite A is an inorganic filler which has the formula $Na_{12} (AlO_2)_{12} (SiO_2)_{12}*27H_2O$. Zeolite A is therefore a synthetic sodium aluminum silicate with a 3D framework of structure, and its cubic microcrystals have rounded corners and edges, and average particle diameter of 3.5 μm [30]. It is used in the household detergents and as catalysts. The structure of Zeolite A can be modified easily, and Zeolite A has been reported to possess some good adsorption properties due to its high specific surface area and ion-exchange capacity [84, 85]. It is therefore used as adsorbent for the dyes removal from aqueous solution. However, Zeolite A has negative charge groups and its application for the removal of anionic dyes is limited due to such observed charge similarity.

While chitosan, on the other hand, can be used for the effective adsorption of anionic dyes because its $–NH_2$ groups are protonated under acidic condition by forming a positively charged biopolymer [84]. There is an extreme scarcity of scientific data on the preparation of composite membranes based on chitosan and the Zeolite A for removal of dyes from the water. A report by [30] discussed the modification of chitosan by Zeolite A that formed chitosan/Zeolite adsorbent for the adsorption of Bezactive Orange 16 from solution [30]. This adsorbent was prepared following a mixing solution method, and the thickness of the obtained colorless film was measured to be 100 μm.

4.7 Chitosan/Zinc Oxide Membrane

Zinc oxide (ZnO) is a chemically stable metallic oxide which is known to be photocatalytic with a wide bandgap of 3.17 eV, biocompatible, non-toxic, and a low-cost compound that have wide range of applications such as in the catalysis [86, 87].

Most scientific reports have focused on the photocatalytic capability of the *n*-ZnO for the water remediation or sequestration of the pollutants from wastewater [89]. Contrarily, the ZnO nanoparticles have been rarely used as adsorbents for the control of dye water pollution [90].

ZnO possess higher specific surface area and strong adsorption affinity, and therefore, it can be applied as a potential adsorbent material for the water treatment application [88]. It is also found to exhibit higher adsorption capacity due to the rapid diffusion and adsorption kinetic rates [91].

Chitosan can be embedded into the ZnO nanoparticles (*n*-ZnO) to suppress the aggregation tendency of the ZnO nanoparticles, and at the same time to increase the number of the adsorptive or active sites on the chemical structure of chitosan [92]. To the best of our ability or knowledge, there are no reports that have been found from the literature on the adsorptive removal of dyes by using the chitosan/ZnO composite membranes only. But, chitosan/ZnO nanocomposite films have been reportedly prepared for other applications [93, 94].

4.8 *Chitosan/Cellulose Nanocrystals Membrane*

Cellulose is an industrial raw material that is useful and being the most abundant polysaccharides that exist naturally. Cellulose is a low-cost polysaccharide which is stable, eco-friendly, and nonpoisonous biomass polymer [95]. The chemical structure of cellulose (Fig. 7) contains multiple hydroxyl groups that can be connected via some strong inter- and intra-molecular hydrogen bonds [27]. These chemical bonds make cellulose hardly to be dissolved in common solvents, and therefore, this limits its further processing and subsequent applications when in the native form. Ionic liquid—a greener solvent like the 1-butyl-3-methylimidazolium acetate ([Bmim] Ac) can dissolve cellulose excellently and satisfactorily [96–98].

Although the chemical structure of the cellulose biopolymer could be modified to produce different derivatives. One of the derivatives of cellulose is the cellulose nanocrystals or the CNCs which can be used as a functional entity or nano-reinforcements in biopolymer membranes for the removal of dyes through electrostatic attraction [3, 99]. Previous publication reported the use of the CNCs as a functional entity in chitosan matrix for the development of chitosan/cellulose nanocrystals
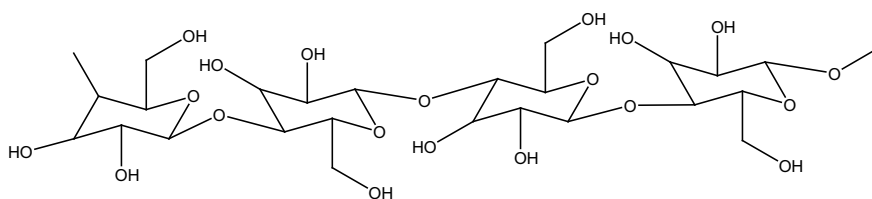

Fig. 7 Structure of cellulose biopolymer

to be used for the removal of targeted dye compounds from water [3]. According to the authors, the increased amount of the CNCs was found to have an incremental effect on the high dye removal efficiency.

4.9   Chitosan/Cellulose Nanofiber Membrane

Cellulose nanofiber (CNF) is an important cellulose-based material which is a by-product of photosynthesis that is produced in abundance from plants or algal biomass. The CNF biopolymer is a sustainable, low-cost polymer and also, it possesses the ease of processing or operation. Unlike the cellulose nanocrystals which is produced by chemical methods like the acid hydrolysis, but the CNF can be prepared by mechanical treatments such as the homogenization, grinding, and or sonication processes [100]. The CNF exhibit unique high surface area and this property could lead to highly reinforced polymeric nanocomposites [101]. Due to its attractive high specific area and biocompatibility, the CNF is often regarded as an ideal adsorbent material for dye adsorption from wastewater.

The corresponding composite of chitosan and CNF is found to have better structural, physical, chemical, and mechanical characteristics. Most recently, the composite film of chitosan and CNF was synthesized by mixing, solution casting, and solvent evaporation, and applied directly for the adsorption of six different types of dyes from water [102]. The four anionic dyes adsorbed onto chitosan/CNF film are methyl orange, eosin, Congo red, and methyl blue, and the two cationic dyes are methylene blue and malachite green. The film exhibited high adsorption and reusable character for methyl orange.

Some of the chitosan composite membranes that are discussed herein are: the chitosan/activated carbons, chitosan/carbon nanotubes, chitosan/graphene oxide, chitosan/nano clay, chitosan/MgO, chitosan/zeolite A, chitosan/zinc oxide, chitosan/cellulose nanocrystals, and chitosan/cellulose nanofiber composites. These types of systems are not being well explored or studied as adsorbents for dye removals; in particular, the membrane systems like chitosan/activated carbon and chitosan/ZnO composites are not being reported from the literature. Interestingly, most of the reviewed chitosan composite membranes exhibited good capacities for the removal of dyes from water by adsorption. Still, further studies in this direction are needed.

5   Methods of Characterization

The primary objective of this section is to present some of the peculiar methods or techniques which are applied in the characterization of chitosan-based composite membranes or films that are specific for dye adsorption study. Focus of the discussion

will be on some of the latest scientific publications that are reported recently on chitosan adsorptive composite membranes.

5.1 Scanning Electron Microscopy (SEM)

The scanning electron microscopy or SEM is being the most frequent microscopic technique that is applied in the characterization of polymeric membrane because of its simpler or easier method of sample preparation [103]. Unlike optical microscopy, the SEM is more sophisticated as it uses electrons as a source of the excitation. Here, a beam of high energy electron interacts with atom of the sample in order to produce signals that can be captured by detectors, thus generating a magnified image of the sample under investigation. The signals that are produced as a result of the interaction can include the secondary electrons, backscattered electrons, and X-rays [104]. Some electron microscopy like the FESEM uses or is linked with an energy-dispersive X-ray spectroscopy (EDS), a quantitative technique that can be used for determination of the elemental composition present in the sample.

SEM or FESEM requires the preparation of sample before the image is taken for subsequent analysis. Generally, the sample needs to be dried with the sole aim to preserve its structure before applying high sputtering temperature or striking its surface with the energetic electrons. Since biopolymers are nonconducting in nature, they must be coated with a thin layer of metals such as the gold or platinum and so on [105]. The SEM technique can be used to produce images with excellent qualities and higher magnification for identification of the structure and surface properties of sample. Earlier study demonstrated that the chitosan-based membrane system possess a uniform or regular surface morphology, especially when prepared by the casting technique [30].

5.2 Transmission Electron Microscopy (TEM)

TEM technique produces sample image with higher resolution than the SEM, although in both the techniques same principle is applied during the analysis of the sample. Structures that cannot be accurately viewed or analyzed with the SEM, can be imaged using the TEM method of analysis. The microstructure and nanoreinforcement in polymer membrane can be studied by using the TEM. This analytical technique or TEM is even more sophisticated than SEM, and hence, there must be an ultrahigh vacuum and an operator who is supposed to be well skilled and should have adequate expertise to operate the TEM machine much effectively [106].

Recent work reported the detailed study on the synthesis, characterization, and application of chitosan/ZnO/GO hybrid nanosized structure. The as-prepared grain bunches of chitosan/ZnO/GO hybrid was demonstrated or analyzed using the TEM

procedure to have some nanosized grains with the size approximated to be found around 5–10 nm [107].

5.3 Atomic Force Microscopy (AFM)

The atomic force microscopy or abbreviated as the "AFM" is a microscopic technique that possesses high resolution capacity for analyzing the topography of the surface of sample by a mapping method using cantilever. The AFM can be used to analyze the composition, mechanical property, and roughness of the surface of a sample [108]. The TEM image of chitosan-based multi-walled carbon nanotubes has been taken by carrying out the AFM test in a scan size of 5 μm by 5 μm. Introduction of the nanotubes as a filler into the matrix has resulted in the increase of the surface roughness of the membrane [56]. This was confirmed by the appearance of the bright sites in the AFM of the membrane due to the existence of nanofiller inside it.

5.4 Fourier Transform Infrared Spectroscopy (FTIR)

The technique of infrared or IR spectroscopy is used to study how matter interacts with light radiation in the electromagnetic region [103]. The IR spectrophotometer comes in different types, the dispersive spectrophotometer which has low reproducibility and Fourier transform infrared (FTIR) spectrophotometer which has higher reproducibility and it is now commonly used in the laboratory for research purpose. Nowadays, the FTIR is the most dominant type of spectrophotometer which enables to record spectra with high signal-to-noise ratio to a depth of 10–20 μm diameters for the samples.

The absorption of IR radiation by a molecule causes molecular vibration due to the bond stretching or bending, and a spectrum is produced which may serve as a fingerprint for identification of the structure of sample. Generally, the IR spectrophotometer can be used in the identification of chemical nature of materials and determination of purity of a particular compound. Table 1 shows the three different regions in the infrared spectrum and their characteristic wavenumbers. In particular, the mid-IR region is used extensively in various applications for qualitative and quantitative analyses of sample analyte [109].

Table 1 Various infrared (IR) regions and their characteristic wavenumbers

S./no.	IR region	Characteristic wavenumbers (cm^{-1})
1	Near-IR	14,000−4,000
2	Mid-IR	4,000−400
3	Far-IR	400−10

Recently, the chemical structure of chitosan/MgO composite film was analyzed by adopting the FTIR spectroscopy [83]. Bands for chitosan biopolymer such as the –N–H stretch and –C–O–C vibrations of chitosan and the Mg-O vibrations of the MgO nanoparticles were identified in the chemical structure of the synthesized nanocomposite film. This clearly showed that molecular interaction might have occurred between the phase of chitosan as the matrix and the MgO particles.

5.5   X-ray Diffraction Analysis (XRD)

The XRD is widely employed in the identification of crystalline, semicrystalline, and or amorphous regions that may be observed in biopolymer membranes [103]. When solid material encounters with some X-ray radiation, a unique XRD pattern is produced which can be used to study the relative crystallinity of the polymeric sample. The beam of the X-ray is focused on the sample at an angle of 2θ, and then a detector records the intensity of the diffracted ray. According to the Bragg's law, the beam of the diffraction by the crystalline phase follows the Bragg's equation (Eq. 1) as shown below:

$$\lambda = 2d * \sin(\theta) \tag{1}$$

where d is the spacing of crystals, λ is the wavelength of the incident rays, and θ is the angle of the diffraction.

The XRD analysis was employed recently for distinguishing the crystalline phases identified in chitosan, GO, and chitosan/GO composite film [70]. The XRD pattern of pure chitosan shows two broad peaks due to its amorphous nature, and that for GO dominantly exhibit high crystallinity as a result of the appearance of one sharp peak. Chitosan/GO film (Fig. 8b) possessed low crystallinity as a result of the reduction of the amorphous phases as observed in its X-ray diffraction pattern. The analysis of the XRD patterns of this composite indicated the exfoliation of the chitosan into the sheets of the graphene oxide with a net increase in the interplanar distance from 0.72 to 0.87 nm.

5.6   Tensile Tests

The tensile test is a physical characterization procedure that can be used for the evaluation of the mechanical properties of biopolymer films. The tensile properties mean the mechanical properties which are caused by the application of regular forces on material. Some of the mechanical properties that are commonly measured for polymer-based films are the elongation at break, Young's modulus, and tensile
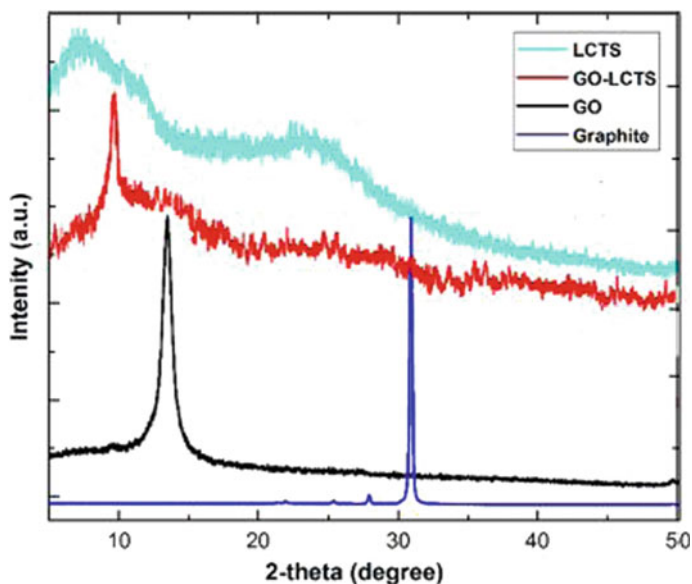
Fig. 8 XRD patters of **a** chitosan (LCTS) and **b** chitosan/GO film (GO-LCTS). LCTS stands for low molecular weight chitosan and GO graphene oxide. (**To take permission from ACS Omega for** https://doi.org/10.1021/acsomega.8b01871)

strength [110]. The tensile versus deformation curve characterizes the tensile capacity for a biopolymer in terms of the listed properties shown in Fig. 9.

The standard methods for tensile testing of materials are the American Society for Testing and Materials [111] for determining the mechanical properties of plastic film with thickness of around 0.25 mm, and the ASTM D638 for testing the mechanical

Fig. 9 A typical tensile behavior in biopolymer film. This curve is termed as the tensile versus deformation curve
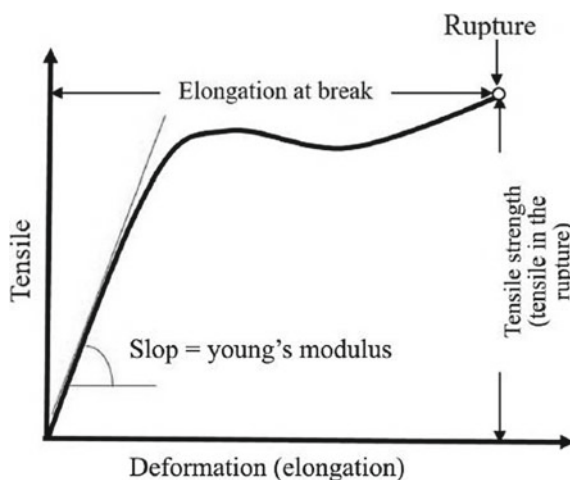
behavior of polymer materials with thickness roughly above 1.00 mm. Earlier, it was found that cross-linking of biopolymers increases the tensile strength, but on contrary, the addition of plasticizers increases the flexibility and deformation at the break, hence a decrease in the tensile strength of biopolymers is observed [113].

The tensile test of chitosan/CNF film was recently performed on a universal testing machine with the specification Model 5576, Instron Instruments, USA at a crosshead speed of 1 mm min^{-1} and gauge length of 40 mm. With the addition of the CNF, the tensile strength of chitosan/CNF film was approximately 35 MPa, in contrast to the strength of chitosan film alone which was around 4.36 MPa [102]. The improvement of mechanical behavior of the chitosan/CNF film may facilitate multiple recycling of the adsorbent due to the possibility of its resistance on the impact of phase separation and adsorption of the dyes.

5.7 Contact Angle

The contact angle or θ as shown in Fig. 10 is that angle between the surface of a solid or film and the tangent to the surface of the liquid (usually water or glycerol, ethylene glycol, etc.) in contact with the solid. The interfacial tensions at the equilibrium is expressed as shown below.

$$\text{Cos } (\theta) = (\gamma_{SV} - \gamma_{SL}) \div \gamma_{LV} \tag{2}$$

where γ_{SV}, $\gamma_{SL,}$ and γLV are the surface tensions at boundaries between solid-to-vapor, solid-to-liquid, and liquid-to-vapor, respectively. For hydrophilic and hydrophilic films, the contact angle covers the values for $\theta < 90°$ and $\theta > 90°$, respectively. The contact angle can be measured by the help of a goniometer instrument in captive bubble mode [115].
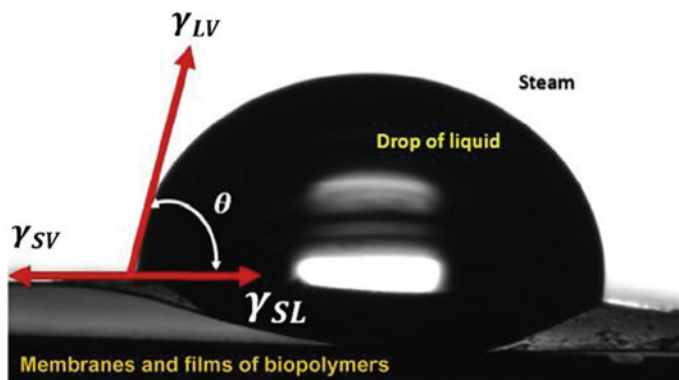

Fig. 10 Contact angle between liquid and the surface of film

The knowledge of the contact angle is vital for evaluating the surface wettability and the resistance of film against water, that is to say, to know whether the film has hydrophilic or hydrophobic nature [114]. In the recent report by Zinadini (2014), the authors reported a static water contact angle of 52.4° for the synthesized carboxymethyl chitosan-coated Fe_3O_4-based membrane; this value meant the prepared membrane has hydrophilic character which can allow it to attract more with the water molecules [10]. This may enhance the penetration of the molecules of dye pollutant in aqueous solution.

5.8 Porosity and Surface Area

The porosity and specific surface area of polymer membranes are usually determined by means of the nitrogen (N_2) adsorption using the Brunauer–Emmett–Teller (BET) method [3]. A cross-linked membrane system consisting of chitosan and cellulose nanocrystals was prepared by casting technology involving simultaneous compression and cross-linking procedures; this membrane was reported to have mean pore sizes and surface area of the magnitude 13 nm and 2.9 m^2g^{-1}, respectively [3]. According to the authors of the publication, the membrane was compacted due to the net influence of the chemical cross-linking using glutaraldehyde solution that lowers the porosity and area. The cross-linking reaction was similarly found to decrease both the pore sizes and surface area of polymer membrane [116, 117].

Most commonly, the chitosan composite membranes are well characterized by employing the use of some modern analytical instrumentations such as the SEM or FESEM, TEM, FTIR, and XRD. Despite the importance of AFM, tensile tests, contact angle, porosity, and surface area measurements, these methods are rarely being presented in most publications for characterizing of chitosan-based membranes. Thus, future studies should focus on a comprehensive characterization of the membrane systems.

6 State-of-the-Art Review on Dye Removals Using Chitosan-Based Membranes

Under this section, we would describe the outcome obtained from the survey of literature on methods and analyses used for the removal of different classes of dyes from water by adsorption onto chitosan films and/or chitosan composite membrane systems along with comparative study with other similar chitosan-based adsorbents.

Adsorption is the physical adherence of gaseous or liquid or ionic pollutant known as the adsorbate, on surface of a solid material known as the adsorbent [118]. The reverse of the adsorption is called the desorption phenomenon. Adsorption is different from absorption phenomenon. Absorption involves the incorporation of

liquid substance into solid matter. Also, there shall be no confusion between the adsorption and sorption processes. Sorption is a general term that is referred to both of absorption and adsorption [119]. Biosorption or bio-adsorption is another term that is often confused in the literature with bioaccumulation, which involves the binding of ions on inactive microorganisms. Biosorption is the sequestration or removal of ions from the solution by microorganisms such as algae, fungi, or bacteria [120]. The microorganisms are collectively referred to as the biosorbent.

6.1 Review on Dye Removals by Adsorption Technology

Synthetic dyes possess several problems from esthetic one to toxic such as mutagenic and carcinogenic environmental issues. The presence of dyes in water and wastewater is undesirable and thus making the water unsafe for drinking and or any other purposes. Dyes are known to have toxic effect to both animals and humans (Mall et al. 2005) [42]. It is therefore compulsory to treat dye-bearing wastewater before being discharged into the surrounding. There are strict regulations imposed by the government to the industries on the compliance or adherence to dye decontamination from wastewater before being released into the environment. Adsorption is the most widely used technology that is available for the dye removal from solution, due to the simplicity and cost effectiveness of the technology [42].

During the adsorption, the molecules of dye get in contact with adsorbent surface via these two important processes or systems viz. the batch adsorption and fixed-bed adsorption [48]. These two systems are found frequently applied in solid–liquid adsorptions and separation processes for lab and large-scale, respectively. Wastewater treatment by adsorption method can be therefore treated discontinuously in batch mode and or continuously in the fixed-bed reactors (Ali et al. 2014). Each of these methods has its own merit and demerit. In the fixed-bed columns, large volume of wastewater can be treated at the industrial scale, but for the batch mode only small or medium size water can be treated at once. However, one of the advantages of the batch mode is its ability to easily adjust and control the adsorption parameters unlike in the fixed-bed mode.

I.   *Dyes removal by using chitosan membranes*

Various state-of-the-art reviews on the chemistry of removal of dyes by adsorption on chitosan membranes would be discussed in the present subsection of the review chapter. With the view of easier understanding in the chemistry or nature of the interactions between dyes and adsorbents, we would also present the structure of the dyes in the discussion in detail. Progress on the modern approach of the dye adsorption would be highlighted with clear emphasis on the chemistry of the applied adsorption and parameters, isotherms, kinetics, and or thermodynamics of the adsorptions in those previously reported studies.

There are several adsorption parameters that are used especially in the batch mode of adsorption for the control of the dye removal process by adsorption. The parameters are commonly optimized by employing the use of traditional or statistical methods of analysis. One of the important parameters is the pH of solution. The pH affects the degree of ionization of dyes in solution, charged groups on adsorbent, and ultimately, the sorption process itself [121]. Other important parameters that are related to the dye adsorption process are the adsorbent dose, contact time, temperature, and ionic strength. The chemistry and or mechanism of dye adsorptions on various kinds of adsorbents are well compiled and reviewed using state-of-the-art publications and are given as follows.

In the removal of Congo red dye, CR (Fig. 11) by adsorption on to a cross-linked membrane of chitosan biopolymer, the optimum pH of adsorption of the CR on chitosan film has occurred within the range of pH 4–6 [42]. The molecule of CR tends to ionize in the aqueous solution and finally forming the $(R-SO_3{}^-)$ groups which are anionic or negative in nature. Under the acidic condition, the electrostatic attraction between protonated chitosan (positively charged) and the negatively charged CR facilitates high removal of molecules of the dye. But, beyond the stated pH above, the CR adsorption decreased due to the presence of large excess of $-OH^-$, that is the competitor ions, thus causing an electrostatic repulsion.

The influence of temperature and thermodynamics of the adsorption was evaluated on the CR adsorption using the prepared chitosan film [42]. The diffusivity of the molecules of dyes increases with increase in the temperature due to the reduction in
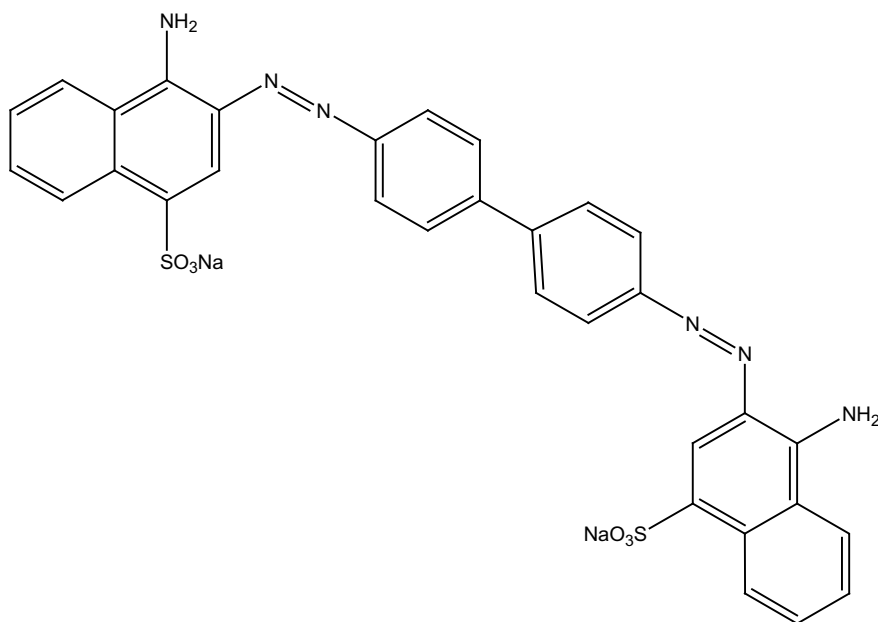
Fig. 11 Chemical structure of Congo red (CR) dye [122]

diffusion resistance [123]. Authors described that as the temperature of adsorption increased from 298 to 318 K, the CR removal efficiency by the film had increased. At high temperatures, the film interacted weakly with the CR dye, consequently, the dye removal efficiency kept still. The negative values for the standard Gibbs free energy (ΔG^0) demonstrated a spontaneous adsorption phenomenon. The van't Hoff equation defines the parameter ΔG^0 as follows:

$$\Delta G^0 = -RT \ln K_c \tag{3}$$

where the R is the molar gas constant and K_c is the adsorption equilibrium constant.

Chitosan film is also used in the adsorption of food dyes from wastewater. Food dyes are those types of dyes that are essentially used to color food-based products such as in the dyeing of chewing gums, juices, sweets, sodas, mustard, etc. [124]. Effluents from the food industries may contain untreated food dyes in the receiving water, and such dyes if found in water are known to create esthetic and carcinogenic harmful effects [125]. Another environmental issue with regard to the discharge of food dyes into water is their ability to cause the reduction of sunlight penetration, thus disturbing the process of photosynthesis in aquatic or marine plants.

Two different food dyes have been recently removed by batch adsorption onto chitosan films [34], the applied model dyes were Acid red 18 (AR 18) with pK_a of 6.4 (Fig. 12) and FD&C blue no. 2 or Indigoid dye with pK_a of 12.2 (Fig. 13). The authors described that the adsorption of the AR 18 on chitosan films was higher than for the corresponding FD&C blue No. 2 dye. The molecular size of the AR 18 dye was lower in comparison to that of the FD&C blue No. 2, hence facilitating an easier

Fig. 12. Chemical structure of Acid red 18 (AR 18) dye [126]
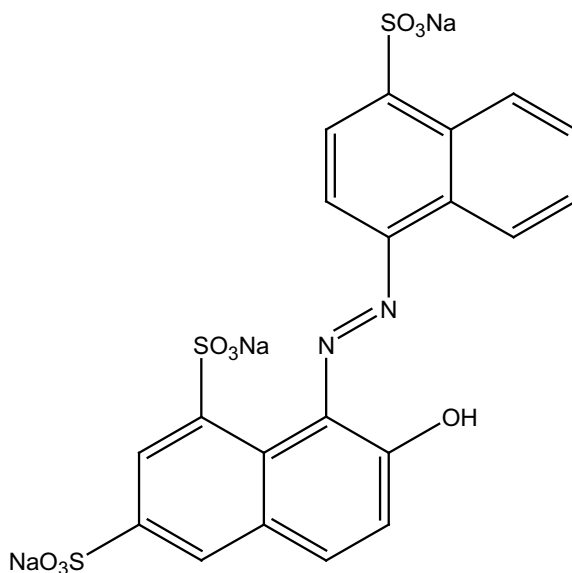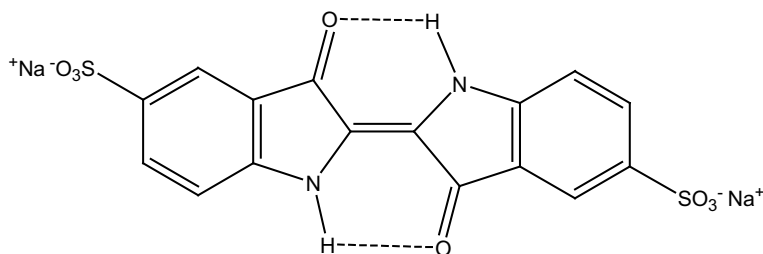
Fig. 13 Chemical structure of FD&C blue No. 2 dye [128]. *Note:* FD&C stands for Food, Drugs, and Cosmetics

diffusion of the dye. The molecules of smaller dye penetrate deeply into the internal pore structure of biopolymer [22].

The adsorption capacities for both AR 18 and FD&C blue no. 2 dyes attained maximum at lower temperatures; the solubility of the dyes increased as temperature of the adsorption increases [22], thus decreasing the adsorption of dyes because the interactions between the dyes and chitosan film became weaker, and conversely the interactions between the dyes and solvent became stronger. The authors analyzed the equilibrium isotherms for the adsorptions of these dyes onto chitosan film. The equilibrium curves for the adsorption of both the AR 18 and FD&C blue no. 2 were described as a type "H," due to the fact that the film possessed some accessible sites for adsorption and hence great affinity towards the modeled dyes [127].

Previously, the removal of another pair of the food dyes had been well demonstrated by adsorption on the chitosan films. The studied food dyes were FD&C red no. 2 or amaranth (Fig. 14) and FD&C yellow no. 5 or tartrazine dye (Fig. 15). The

Fig. 14 Chemical structure of FD&C red no. 2 or amaranth dye [130]
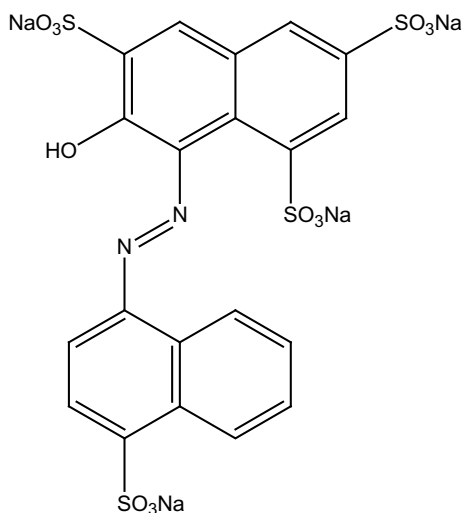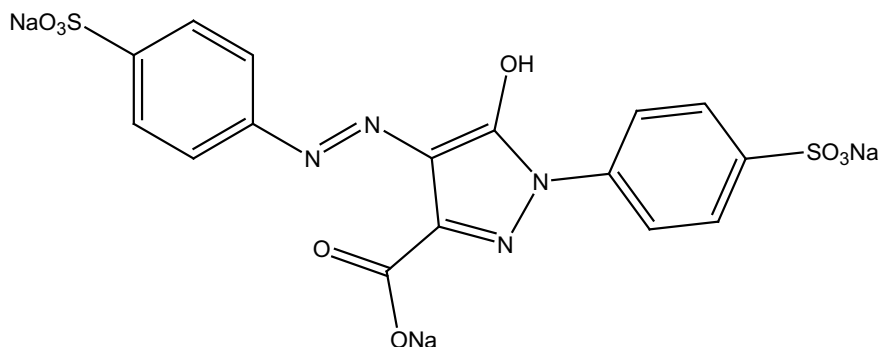
Fig. 15 Chemical structure of FD&C yellow no. 5 or tartrazine dye [130]

adsorption capacities for the two dyes increased with decreasing the magnitude of pH of the solution. Under the acidic condition, the amino groups on chitosan tend to become positively charged via protonation [52], thus bring about an electrostatic interaction between the anionic dyes and the cationic chitosan film. At the pH value 2, swelling degree of chitosan films (700–1200%) increased, and this might also had facilitated the transport and access of the dyes into the sites of the adsorption. Moreover, the FD&C yellow no. 5 with MW of 534.4 g mol^{-1} exhibited the highest adsorption capacity than the FD&C red no. 2 with a larger molecular size, i.e., MW of 604.5 g mol^{-1} [129].

Rêgo et al. [129] analyzed the possible mechanism of adsorption for both the above dyes on chitosan films by examining the FTIR before and after dye adsorptions. Absorption bands of the chitosan film, i.e., before the dye adsorptions (Fig. 16a) in the region of 3300–3100 cm^{-1} were responsible for the stretching vibrations of the N–H and O–H bonds. After the adsorption of both the tartrazine (Fig. 16b) and amaranth (Fig. 16c) dyes, the interactions between each of the dye and the film were same because they have similar structural and functional groups, i.e., the anionic sulfonated groups on each of the dye was similar. According to the authors, the chitosan film (Fig. 17a) adsorbed both dyes due to the presence of S atoms confirmed after the adsorption process (Fig. 17b and c).

II. *Dyes removal by using chitosan composite membranes*

Similarly, the various state-of-the-art reviews on the chemistry of removal of dyes by adsorption on chitosan composite membranes would be discussed in the present subsection of the review chapter. With the view of easier understanding of the chemistry or nature of the interactions between dyes and adsorbents, we would also present clearly the structure of the dyes in the discussion in detail. Progress on the modern approach of the dye adsorption would be highlighted with clear emphasis on the chemistry of the applied adsorption and parameters, isotherms, kinetics, and or thermodynamics of the adsorptions in those previously reported studies.

Chitosan biopolymer is usually modified by converting it to the chitosan membranes or films in order to overcome its intrinsic drawbacks such as the low stability, pH sensitivity, and low adsorption [30, 42, 129, 130].

But still the chitosan membranes are limited due to the possession of lower chemical and mechanical characteristics. To overcome these problems and obtain some products with superior mechanical and adsorptive properties, scientists have nowadays adopted the preparation of chitosan-based composite films as adsorptive membranes for enhanced removal of dye compounds from solution [30, 70, 131].
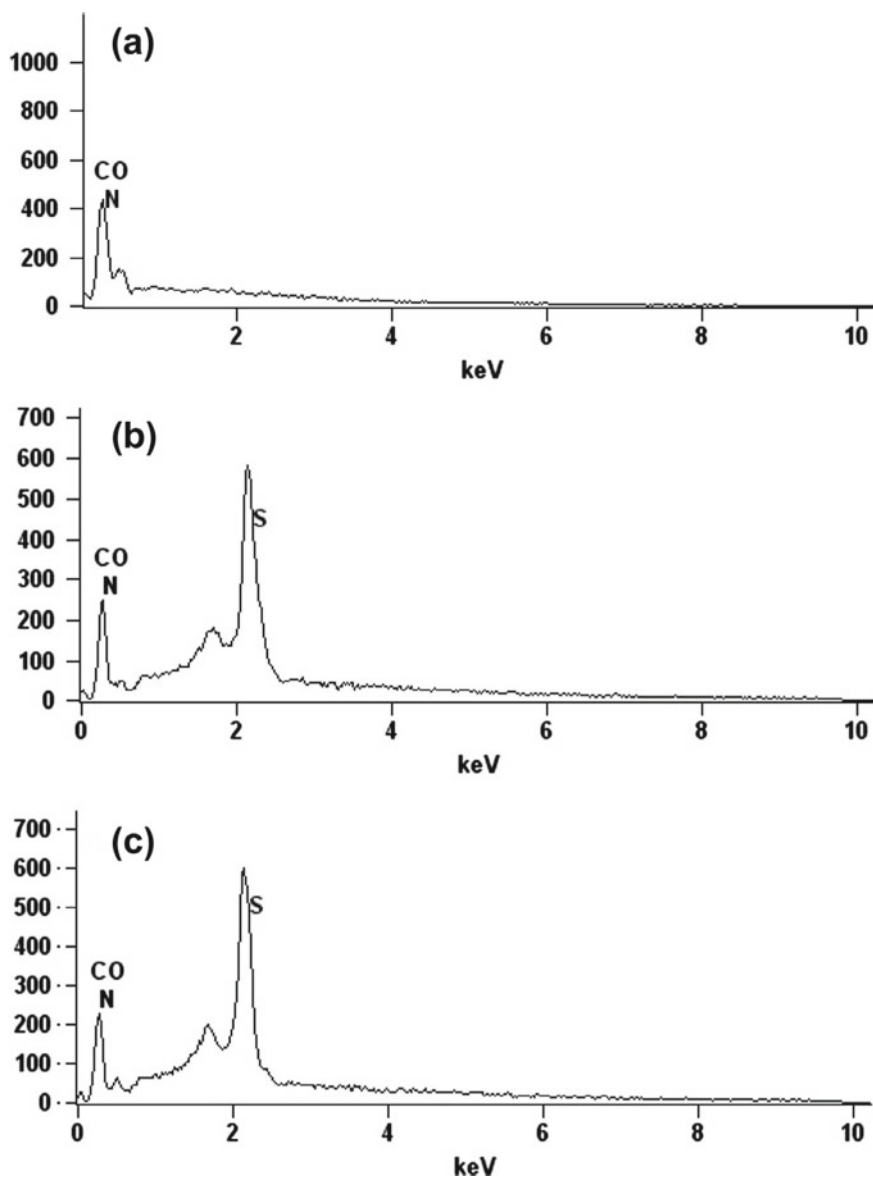
Fig. 17 Elemental composition of chitosan film **a** before the adsorption, **b** after the adsorption with tartrazine dye, **c** after adsorption with amaranth dye [129]. **(To take permission from the Journal of Colloid and Interface Science for** https://doi.org/10.1016/j.jcis.2013.08.051**)**

Fig. 18 Optical photographs: **a** GMCNTs existed in the solution, **b** CS-m-GMCNTs is dispersed in solution, **c** solution of the CR dye, **d** separation of the CS-m-GMCNTs adsorbents from the treated solution of the CR dye by a bar magnet [49, 64]. **(To take permission from the Journal of Appl Surf Sci for the** https://doi.org/10.1016/j.apsusc.2013.09.003**)**

Further, chitosan composite membranes can also be produced with improved dye removal efficiency compared to the chitosan or its corresponding films [83].

The magnetic and cross-linked chitosan-graphitized multi-walled carbon nanotubes (or designated as the CS-m-GMCNTs) was reportedly synthesized and used as an effective adsorbent for the removal of the CR dye (Fig. 11) from the wastewater [49, 64]. The authors described that the dye adsorption reached 263.3 mg g^{-1}, and also the adsorption was temperature-dependent which is spontaneous in nature due to the negative values of the change in the Gibbs free energy. The effectiveness of the CR removal by adsorption on the CS-m-GMCNTs adsorbent could be well ascertained from Fig. 18d.

The sulfonate groups on CR dye dissociated to become negatively charged, and at a pH 6.3, the $-NH_2$ present on the surface of CS-m-GMCNTs were protonated leading to the enhanced CR adsorption through the electrostatic attractions in the aqueous solution. Moreover, in the previous study, the point of zero charge (PZC) of the GMCNTs moiety was reported to be around 4 [132] which meant that at a low pH values, the positive charges or binding sites on the CS-m-GMCNTs adsorbent increased which subsequently got interacted with the anionic CR dye, and hence the high CR dye removal was observed according to the authors' report.

Nešić and co-workers described the adsorption of Bezactive Orange 16 (BO 16) dye on the composite film of chitosan and zeolite A [30]. The BO 16 dye (Fig. 19), MW of 617.54 g mol^{-1}, is an anionic dye and is often applied for the dyeing of cellulosic fibers; its commercial name is Remazol Brilliant Orange 3R. They described that electrostatic interactions was one of the possible mechanism of the adsorption of BO 16 on the film; the adsorption between the positively charged chitosan/zeolite and the molecules of the negative BO 16 dye was maximum at around a pH value of 6 in the aqueous solution. The Langmuir model fitted and adequately predicted the BO
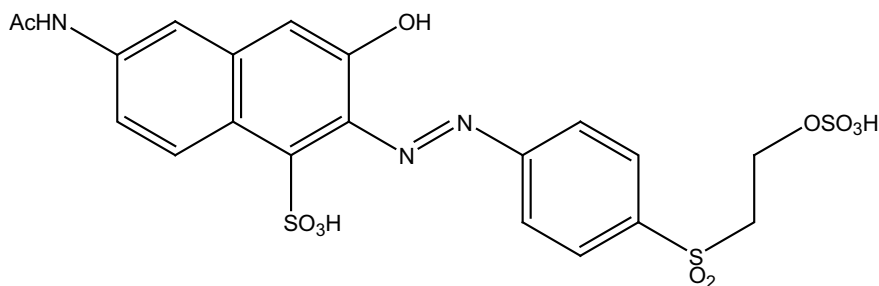
Fig. 19 Chemical structure of Bezactive Orange 16 (BO 16) dye [30]

16 adsorption on chitosan/zeolite film with an adsorption capacity of 305.8 mg g^{-1} value. The Langmuir isotherm model is represented by Eq. 4 as illustrated below.

$$1/Q_e = (1/Q_{max}) + \left[1/\left(Q_{max} * K_L\right)\right] * (1/C_e) \tag{4}$$

where Q_e is the adsorption capacity (mg g^{-1}), C_e is the equilibrium CR dye concentration (mg L^{-1}), and K_L is the Langmuir constant (L g^{-1}). The separation factor, R_L, which is expressed in terms of the K_L, can be defined by Eq. 5 below. The magnitude of the R_L indicates whether the adsorption is favorable ($0 < R_L < 1$), unfavorable ($R_L > 1$), linear ($R_L = 1$), or irreversible ($R_L = 0$) [83, 133].

$$R_L = 1/\left[1 + (K_L * C_o)\right] \tag{5}$$

Sabzevari and co-workers converted GO into the GO-chitosan composite film (swelling degree, 6,500%) by cross-linking it with the chitosan as a biopolymer cross-linker [70]. The formation of an amide linkage formed between the –COOH bond in the GO and –NH$_2$ group in the chitosan supported the formation of the GO-chitosan composite and the cross-linking reaction [134]. The zeta potential of the GO-chitosan film was lower than −30 mV, hence its particles could maintain a stable colloidal solution [136]. According to the authors, the monolayer adsorption of MB dye, MW of 319.85 g mol^{-1} (Fig. 20), on the GO-chitosan film was 402.6 mg g^{-1} (Q_{max}) which exceeded that for the pristine GO material. The GO-chitosan film allowed the
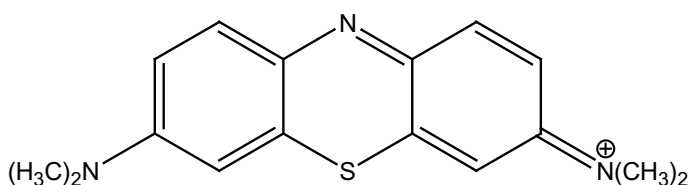
Fig. 20 Chemical structure of Methylene Blue (MB) dye [135]

better dispersion of GO and prevents its aggregation in water, thus leading to high adsorption capacity in the composite.

Earlier, the use of binary blends such as the chitosan/cellulose acetate blends or composite membranes was employed recently to solve the shortcomings of the pure chitosan and was applied for the removal of acid orange 7 (Fig. 21) and brilliant yellow (Fig. 22) dyes from wastewater [131]. The authors developed this membrane by using a mixture of acetic acid and water, casting technology, and deacetylation approach to form the cationic chitosan/cellulose acetate composite membrane. The net positive charge on the surface of the adsorbent was detected by analyzing the curves which were obtained from a potentiometric titration. As described by the authors, the modification of the chitosan/cellulose acetate by deacetylation method removed the acetate group from the film, thus converting the film into much more hydrophilic with the lowest contact angle of 33°.

The researchers described that the adsorptions of both AO 7 and the BY dyes were found to be 9.98 mg g^{-1} (99.8% efficiency) and 9.38 mg g^{-1} (99.7% efficiency), respectively, and their adsorptions on the chitosan/cellulose acetate composite were observed photographically by the authors to be very similar.

The developed chitosan/saponin-bentonite (CSB) composite film was applied for the high adsorption of methyl orange dye from the aqueous solution under the
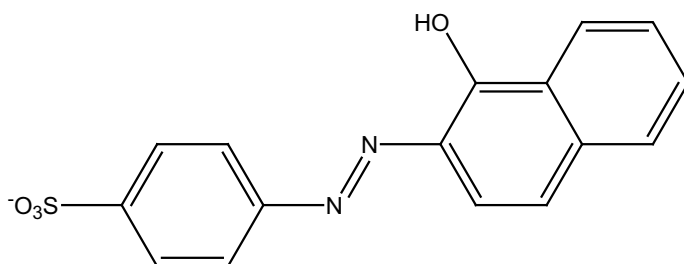
Fig. 21 Chemical structure of acid orange 7 (AO 7) dye [137]
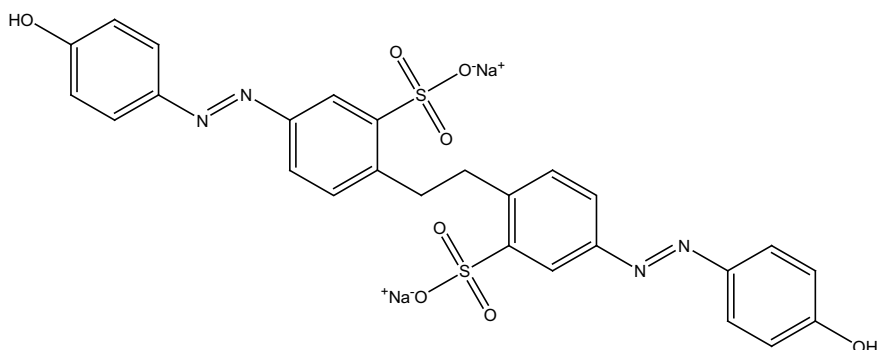
Fig. 22. Chemical structure of brilliant yellow (BY) dye [138]

optimum pH of 4.80–5.30 [79]. The maximum adsorption capacities for the CSB film were investigated by the authors under different temperatures viz. 303, 318, and 333 K, and the corresponding adsorptions were found to be 360.86, 398.98, 641.99 mg g^{-1}, respectively. This showed that the adsorption increased by increasing the temperature, and hence the process was endothermic in nature.

The development of multi-functional adsorbent film based on chitosan biopolymer and MgO nanoparticles was undertaken by Nga and his group for the removal of reactive blue 19 (RB 19) dye (Fig. 23) from the wastewater by adsorption route [83]. Reactive dyes easily form covalent bonds with fibers, have high color stability, solubility, and low degradability, and are also widely applied in the textile industries [52, 139]. After the dyeing process, about 50% of the reactive dyes can be lost, and up to 10–200 mg L^{-1} concentration of the reactive dyes may be found in the wastewater outlets [140, 141].

The adsorption of the AR 19 dye fluctuated over the pH 3–7, but above the pH 7, the dye adsorption on the chitosan/MgO nanocomposite decreased due to the –OH competition with the molecules of the AR dye. They described that under the optimum pH of 7, the maximum adsorption of the AR 19 dye was predominantly due to the electrostatic interactions that occurred between the negatively charged AR dye and the positively charged chitosan/MgO composite film over the pH 3–7 range [83]. The adsorption of the AR 19 dye onto the chitosan/MgO was temperature-dependent, increased with the increase in the temperature, and the Q$_{max}$ of the dye adsorption was determined (from the Langmuir isotherm plot) to be 512.82 mg g^{-1} at 311 K. Accordingly, chemisorption between the counter charges in AR dye and the film controlled the adsorption kinetics.

The improvement in the mechanical properties of membrane adsorbent could promote effectiveness for the dye removal, separation, and recycling studies. The developed and high strength chitosan/CNF film as discussed earlier in the present chapter was employed for the selective adsorption or removal from the aqueous solution of different types of dyes including the methyl orange, MO (Fig. 24), methylene
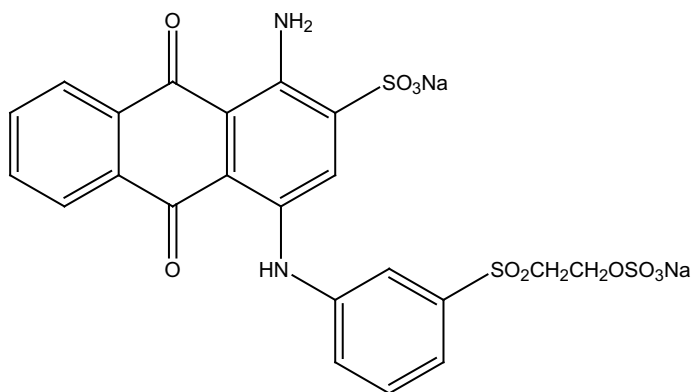
Fig. 23 Chemical structure of reactive blue 19 (RB 19) dye [142]
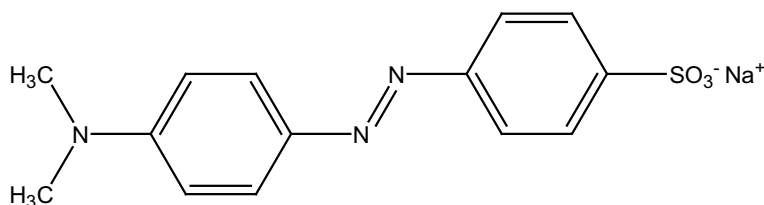
Fig. 24 Chemical structure of methyl orange (MO) dye [138]

blue, MB dye (Fig. 20), malachite green, MG (Fig. 25), and Congo red, CR (Fig. 11) [102].

Both the MO and CR are anionic dyes, while both MB and MG are cationic dyes. And interestingly, according to the authors, the synthesized chitosan/CNF composite selectively adsorbed the different dyes. In the single system dye removal, by comparing the characteristics UV–VIS absorption band of each of the dye before and after the adsorption, the researchers concluded that the chitosan/CNF exhibited efficient adsorption towards the MO dye (Fig. 26a), however, it showed comparatively negligible adsorption towards the MB dye (Fig. 26b). It was speculated by the authors that the rejection of the MB dye by the chitosan/CNF composite was caused by the presence of the chitosan in the composite, which has positive charge on its amino functional groups.

While in the binary system dye removal, mixed solutions of MO/MB dyes were selected by the authors. They demonstrated that the characteristic absorption curve for MO changed drastically (Fig. 26c) after the adsorption process; in contrast, the absorbance for the MB dye was barely changed in the mixture. Similar observation was discussed with the mixture of the MO/MG dyes, while the band for the MG dyes (Fig. 26d) showed insignificant change after the adsorption. Thus, the chitosan/CNF composite film exhibited excellent adsorption selectivity towards the anionic dyes than the cationic dyes due to the electrostatic interactions between the film and the negatively charged dye compounds.

Fig. 25. Chemical structure of malachite green (MG) dye [102]
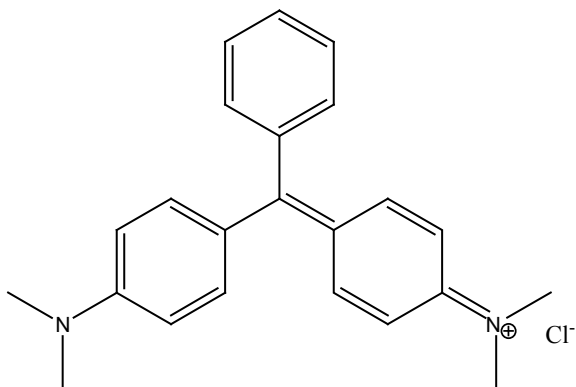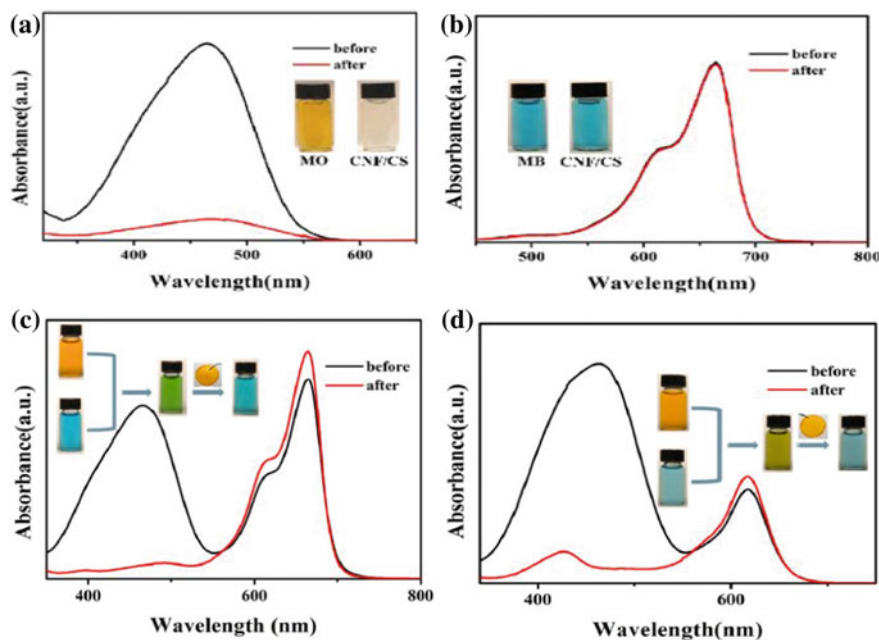
Fig. 26 Absorbance of **a** MO, **b** MB, **c** MO/MB, and **d** MO/MG mixtures, before and after the adsorption process [102]. (**To take permission from the Carbohydrate Polymers for the** https:// doi.org/10.1016/j.carbpol.2020.117473)

Furthermore, the monolayer adsorption (Q_{max}) of MO onto the chitosan/CNF composite was determined by the authors to be 655.23 mg g^{-1}; the Langmuir model as reported by the authors, showed excellent fitting with lower average relative error, thus indicating that the MO was adsorbed on the active sites of the adsorbent. The strong attraction between the composite and the MO dye had attributed to the high adsorption capacity.

6.2 Review on Regeneration and Reusability

Regeneration by desorption process is the separation or detachment of the spent adsorbent material from the contaminant in the solution. It can also be defined as the rapid recycling or recovery of exhausted/or spent adsorbents using feasible techniques or methods. Regeneration of activated carbon is indispensable process. However, for other solid adsorbents, it is also important if necessary. The desorption lowers the operating cost of the adsorption, and it also opens a way for the extraction of the pollutants from solution, and regeneration of the adsorbent for another adsorption cycle [118]. It can also reveal the mechanism of the adsorption. The literature
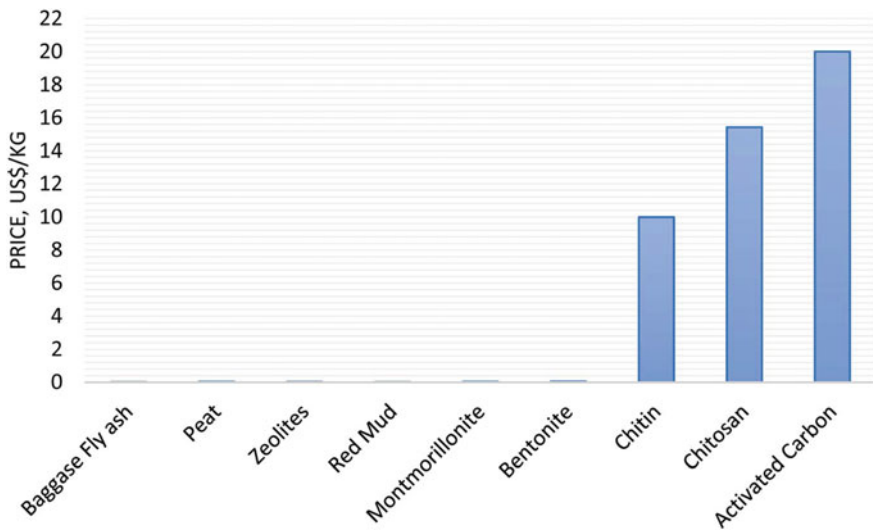
Fig. 27 Costs of various adsorbents reported in the literature [73]. (**To take permission from the RSC Adv. for the** https://doi.org/10.1039/c8ra04290j)

on regeneration of adsorbents is very limited or not adequately explored except for the commercial activated carbons.

The exhausted adsorbents can be regenerated by using a number of techniques such as the bioregeneration, chemical treatment, electrochemical, supercritical extraction, thermal, microwave regeneration, ultrasound, and photocatalytic methods [73]. Functional adsorbents are those that are very effective and economical, and the costs of the adsorbents can be lowered through the process of recycling without significant loss of the active sites and removal efficiencies [145].

The cost (in USD currency) of various reported adsorbents for dye removals is shown in Fig. 27. From the figure, it can be learned that the adsorption process by using chitosan-based materials can be regarded as costly, and the regeneration of such bio-based materials would be very crucial in the control of water pollution.

And, the regeneration and possible reuse of chitosan-based films are not yet adequately being explored or discussed in the majority of the reported literature. Thus, this leaves a wide research gap which is to be investigated by researchers in the field of environmental and remediation of wastewater. Some few data that reported the regeneration and reusability studies of chitosan-based films can be found available and they are discussed herein with the clear focus on the chemistry of the desorption process.

The amaranth (Fig. 14) and tartrazine dyes (Fig. 15) removed by the adsorption on chitosan films were desorbed over 2 cycles after 5 min and by using 0.50 M NaOH as eluent. Three adsorption–desorption cycles were run by the authors, and after the first two cycles, the adsorbent maintained its physical nature and maximum

adsorption capacity. They had described that the desorption phenomenon of the dyes was due to the occurrence of an electrostatic attraction [129].

Chitosan/GO composite membrane was regenerated by using a mixture of dilute HCl and ethanol solution at 1:1 v/v ratio. The adsorbed MB dye was desorbed over 3 cycles, and the removal efficacy exceeded 80% after these three consecutive cycles [70]. The result was presented well by the authors and is shown in Fig. 28. The authors had further described that after every desorption process, the adsorbent was dried at 313 K for 24 h before another adsorption cycle was carried out. They concluded that the advantage of the Chitosan/GO composite membrane (cross-linked adsorbent) was its facile separation process and its capability to be regenerated over multiple adsorptions–desorption cycles as depicted in Fig. 28.

The chitosan/CNF composite was regenerated by soaking it in 0.10 M of KOH solution under constant stirring, and the recovered adsorbent was used for another 6 cycles [102]. Intense competition between the $-OH^-$ ions in the KOH solution and the adsorbed MO dye promoted the elution of the dye which leads to the regeneration of the chitosan/CNF composite [146]. The composite was easily affected by the pH change; hence, the process of desorption was quickly completed by rinsing it in the KOH solution.

The adsorbent, Chitosan-g-PAA/Rice Husk hydrogel composite for the MB removal, was subjected to the 5 cycles of adsorption–desorption process [153]. Its dye adsorption showed only a slight decrease after the last cycle, which proved its reusability feature for the practical application in the wastewater treatment. Moreover, the reported chitosan/Magnetic β-CD has a reuse capability for up to the 5 cycles with a high dye desorption behavior. According to the authors, the dye desorption process of this magnetic adsorbent was performed by using organic solvent (ethanol

Fig. 28 Adsorption–desorption cycles of **a** Graphene oxide, GO (orange) and **b** chitosan/GO film, GO-LCTS (blue) [70]. LCTS stands for low molecular weight chitosan and GO graphene oxide. (**To take permission from ACS Omega for** https://doi.org/10.1021/acsomega.8b01871)
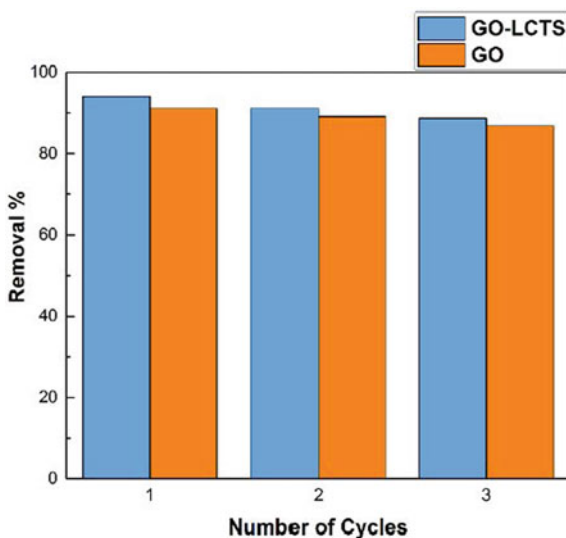
in 0.1 M NaOH), since its dye adsorption was driven through the inclusion type of mechanism. There is also a low decrease of the dye uptake after a fifth cycle.

6.3 Review on Comparative Study

The performances of various adsorbent materials are expressed in the literature by comparing their respective adsorption capabilities. The adsorption can be further expressed in terms of the adsorption or removal efficiency, R (%), or the equilibrium adsorption capacity, Q_e or q (mg g^{-1}). These two distinct terms are mathematically defined by the following two expressions:

$$R (\%) = [(C_o - C_e)/C_o] * 100 \tag{6}$$

$$Q_e(\text{mg g}^{-1}) = [(C_o - C_e)/W] * V \tag{7}$$

where C_o and C_e are the initial and equilibrium concentrations (expressed in mg L^{-1}), W is the weight of the adsorbent (in gram), and V is the volume of the solution in liter [102]. These terms that are described above are usually determined from the experimental data as widely being reported by various researchers.

In the present section, the performance of the chitosan-based adsorptive membranes would be compared with other similar bio-based adsorbents that are being reported recently in the scientific literature. In order to avoid any kind of confusion that may flash on the minds of the respective readers, the term Q_{max}, the maximum or monolayer adsorption capacity, would be taken as the term to differentiate the adsorption performance of each of the adsorbent that are to be discussed herein. The monolayer adsorption capacity, Q_{max}, is calculated value and is determined from the Langmuir isotherm plot; it expressed the maximum amount of the dye adsorbed per active site in the material. Table 2 shows a comprehensive review on comparison of the monolayer adsorption capacities (Q_{max}) among the different chitosan-based adsorbents such as the chitosan films, chitosan composite films, and so on.

The reported adsorption results were entirely different depending on the type and nature of the adsorbent, and the experimental conditions such as the initial concentrations, adsorbent dosage, contact time, and the pH of the solution. In the case for the chitosan-based adsorbents, the origin of chitosan and the degree of the deacetylation (DD) might bring about the difference in the adsorption capacities. For instance, chitosan beads have superior specific surface area than the corresponding chitosan flake-type, chitosan beads obtained from the sources such as the crab, lobster, and shrimp wastes were reported to have difference in their surface areas and dye adsorption capacities in the following order crab>lobster>shrimp, respectively [149].

The comparison about the adsorption of the dyes on the chitosan-based adsorbents could be difficult as the adsorption studies were performed for different dyes under

Table 2 Comparison of the maximum dye adsorption capacity of chitosan-based adsorbents

S./no.	Chitosan films (Adsorbents)	Adsorbate or dye	Conditions: initial conc., dosage, contact time, and pH	Adsorption capacity, Q_m (mg g^{-1})	Literature citations
1	Chitosan film	Congo red	20 mg L^{-1}, 0.1 g, 4 h, and pH 4–6	40.65	[42]
2	Chitosan film	Acid red 18	20–100 mg L^{-1}, 500 mg L^{-1}, 8 h, and pH 7	194.60	[34]
3	Chitosan film	FD&C blue no. 2 dye	20–100 mg L^{-1}, 500 mg L^{-1}, 8 h, and pH 7	154.80	[34]
4	Chitosan film	Amaranth	200 mg L^{-1}, 0.1 g L^{-1}, 2 h, and pH 2	278.30	[129]
5	Chitosan film	Tartrazine	200 mg L^{-1}, 0.1 g L^{-1}, 0.5 h, and pH 2	413.80	[129]
6	Chitosan film	FD&C red 2	50–300 mg L^{-1}, 8 h, and pH 2	494.13	[144]
7	Chitosan film	FD&C yellow 5	50–300 mg L^{-1}, 8 h, and pH 2	480.00	[144]
Chitosan composite films					
1	CS-m-GMCNTs	Congo red	10–1000 mg L^{-1}, 0.05 g, 1–3 h, and pH 6.3	263.3	[49, 64]
2	Chitosan/zeolite A	Bezactive Orange 16	30–80 mg L^{-1}, 0.015 g, 50 h, and pH 6	305.8	[30]
3	Chitosan/GO	Methylene blue dye	100–1000 μM, 0.05 g, 24 h, and pH 7	402.6	[70]
4	Chitosan/cellulose acetate	Acid orange 7	10 mg L^{-1}, 0.25 g, 17 h, and pH 3.6	Q = 9.98 mg g^{-1}	[131]
5	Chitosan/cellulose acetate	Brilliant yellow	10 mg L^{-1}, 0.25 g, 17 h, and pH 3.6	Q = 9.38 mg g^{-1}	[131]

Table 2 (continued)

S./no.	Chitosan films (Adsorbents)	Adsorbate or dye	Conditions: initial conc., dosage, contact time, and pH	Adsorption capacity, Q_m (mg g^{-1})	Literature citations
6	Chitosan/saponin-bentonite	Methyl orange	20–180 mg L^{-1}, 0.5 g, 2.5 h, and pH 4.80–5.30	641.99	[79]
7	Chitosan/MgO	Reactive blue 19	100–700 mg L^{-1}, 0.14 g, 24 h, and pH 7	512.82	[83]
8	Chitosan/CNF	Methyl orange	10–500 mg L^{-1}, 0.1 g, and pH 5	655.23	[102]
9	Chitosan/magnetic maghemite	Methyl orange	10–60 mg L^{-1}, 0.5 g, and pH 2.91	29.41	[147]
10	Chitosan/polyvinyl alcohol/zeolite	Methyl orange	100–500 mg L^{-1}, 0.05 g, 6 min, and pH 4	153	[148]
Other biopolymer adsorbents					
1	Chitosan beads from crab	Reactive red no. 222	0–600 mg L^{-1}, 0.1 g, and 5 days	1106	[149]
2	Chitosan beads from lobster	Reactive red no. 222	0–600 mg L^{-1}, 0.1 g, and 5 days	1037	[149]
3	Chitosan beads from shrimp wastes	Reactive red no. 222	0–600 mg L^{-1}, 0.1 g, and 5 days	1026	[149]
4	Chitosan from crab shells	Acid green no. 25	0–69 mg L^{-1}, 0.2 g, 24 h, and pH 4	645.10	[150]
5	Chitosan from crab shells	Acid orange no.10,	0–69 mg L^{-1}, 0.2 g, 24 h, and pH 4	922.90	[150]
6	Chitosan from crab shells	Acid red no.12	0–69 mg L^{-1}, 0.2 g, 24 h, and pH 4	973.30	[150]
7	Chitosan	FD&C red no. 40	0–250 mg L^{-1}, 0.05 g, 8 h, and pH 6.6	529	[124]

<div align="right">(continued)</div>

Table 2 (continued)

S./no.	Chitosan films (Adsorbents)	Adsorbate or dye	Conditions: initial conc., dosage, contact time, and pH	Adsorption capacity, Q_m (mg g^{-1})	Literature citations
8	Chitosan/GO	Reactive black 5	0–1000 mg L^{-1}, 0.02 g, 24 h, and pH 2	277	[32, 65]
9	Chitosan/magnetic β-CD	Methyl blue dye	1500–6000 mg L^{-1}, 0.03 g, 50 min, and pH 5	2780	[151]
10	Chitosan/modified Ball Clay	Methylene blue	30–300 mg L^{-1}, 0.1 g, and pH 12	142	[135]
11	Chitosan beads/activated carbon	Crystal violet	0–14 mg L^{-1}, 0.4 g, 40 min, and pH 9	12.50	[152]
12	Chitosan-g-PAA/Rice Husk hydrogel	Methylene blue	1500–2500 mg L^{-1}, 0.05 g, 1 h, and pH 5	1952	[153]
13	Chitosan/polyamide nanofibers	Reactive black 5	0–150 mg L^{-1}, 0.2 g L^{-1}, and pH 1	456.90	[154]
14	Chitosan/polyamide nanofibers	Ponceau 4R	0–150 mg L^{-1}, 0.2 g L^{-1}, and pH 1	502.40	[154]
15	Cross-linked Chitosan/AC	Thionine dye	10–100 mg L^{-1}, 0.18 g, 6–8 h, and pH 7	60.90	[155]
16	Chitosan/glutaraldehyde Beads	Reactive black 5	5–65 mg L^{-1}, 0.4 g, 48 h, and pH 3	1.56	[156]

AC = Activated charcoal; CD = cyclodextrin; CNF = cellulose nanofibers; GO = graphene oxide; PAA = polyacrylic acid; FD&C = Food, Drugs, and Cosmetics; CS-m-GMCNTs = chitosan/magnetic graphitized multi-walled carbon nanotubes; Q_{max} = maximum or monolayer adsorption capacity

different experimental conditions. Although the dye removal capacity of most of the adsorbents showed good adsorption except for the Chitosan/Glutaraldehyde Beads which exhibited the least adsorption capacity ($Q_{max} = 1.56$ mg g^{-1}) [156]. The reason was described by the authors that the higher adsorbent dosage could had triggered the overlap of the active sites, hence decreasing the active surface area and the adsorption capacity as well.

The adsorptions of the dyes on chitosan/magnetic β-CD composite and chitosan beads were superior to the adsorptions on chitosan, chitosan films, and chitosan

composite membranes. The chitosan/magnetic β-CD composite showed an adsorption of 2780 mg g^{-1}, which is superior to the entire adsorbents that are presented in Table 2. Such remarkable adsorption behavior of the composite was due to its higher chemical stability, higher surface area due to its spherical nature, ability to form the inclusion complex for the adsorption of the MB dye through the prominent host–guest interactions mechanism, and the absence of the internal diffusion resistance [151].

However, for the removal of more than one type of dye using the same adsorbent, their comparison can be made easier. For instance, chitosan film adsorbed 194.60 mg g^{-1} of AR 18 dye higher than the adsorption of FD&C blue no. 2 dye (154.80 mg g^{-1}) [34]. The two dyes differed in their molecular sizes, the smaller dye, in this case of the AR 18 diffused faster than the other dye. Similarly, the difference in the adsorptions of the Amaranth and Tartrazine dyes onto the chitosan film was due to the same reason. It was noted that the dyes are not of the same structures and molecular sizes, hence this reflected that the diffusion of the dyes into the internal pore structure of the chitosan could be entirely different, hence there might be difference in the adsorption capacities as observed.

From Table 2, it was understood that the adsorptions for some of the chitosan composite membranes or films were said to possess comparatively superior adsorption than for some of the chitosan films. For instance, the chitosan/CNF and Chitosan/saponin-bentonite films adsorbed 655.23 mg g^{-1} and 641.99 mg g^{-1} of dyes, respectively, than all of the chitosan films that are shown in the table. It can be expected that there was strong attractions between the chitosan composite films and the dyes compared to the chitosan films alone [102].

The adsorptions for both the AO 7 ($Q_e = 9.98$ mg g^{-1}) and BY ($Q_e = 9.38$ mg g^{-1}) dyes were reported to be very similar due to the fact that they have same sulfonate groups in their chemical structures [131]. The adsorptions of the respective dyes were experimentally determined by the authors by applying Eq. 7. Here, the Q_e values do not represent the actual maximum adsorption capacities of the composite membrane because the authors did not discuss the Langmuir isotherm model in their adsorption study.

It could be clearly observed from the table that the adsorptions for many of the reviewed dyes occurred under the acidic medium ($1 \leq pH \leq 7$), thus indicating many of the dyes to be anionic in nature or negatively charged compounds. Since most of the chitosan-based adsorbents have positive charges on their structures, the adsorption between the chitosan-based materials and such anionic dyes could be through the electrostatic interactions [151]. The positive charge on chitosan is increased in acidic solutions by the protonation of its amino groups. However, for the cationic dyes, such as the MB and crystal violet, their adsorptions occurred under near neutral and or alkaline conditions, i.e., $pH \geq 7$ as shown in Table 2. Thus, the surface of the chitosan-based adsorbents became negative which got interacted with the positively charged dyes [152].

The influence of the contact time on the dye adsorption and or simply the kinetics of the adsorptions had been well investigated in most of the reported research works.

The faster dye removal rate is a requirement for industrial water pollution application of adsorbents [148]. Hence, in order to design effective adsorbents, the material should have faster adsorption rate. As depicted from Table 2, most of the reported adsorbents, even the ones having the superior adsorption capacities, have slower adsorption rates, because they took longer contact times to complete or for the adsorption to reach the equilibrium stage. For example, the chitosan beads from the crab shells adsorbed around 1106 mg g^{-1} of dye over 5 days [149].

Similarly, the Chitosan/Polyvinyl Alcohol/Zeolite adsorbed 153 mg g^{-1} of MO dye over 6 min contact time [148]. Moreover, the chitosan/Magnetic β-CD adsorbed 2780 mg g^{-1} of the methyl blue dye within 50 min contact time. Hence, these adsorbents have the superior adsorption rates due to the absence of the internal diffusion resistance. The adsorption rate of the Chitosan-g-PAA/Rice husk hydrogel was also satisfactory [153]. The Chitosan/Polyvinyl Alcohol/Zeolite suffered from the lower adsorption compared to the later adsorbent or chitosan composite membranes. The adsorption rate for chitosan/CNF film was not indicated in the previous report, although it possessed a good adsorption, regenerative, and recycling capacities [102].

In order to lower the costs of the production for the effective adsorbents, the regeneration and reusability studies are very important for sustainable application. We have gone deeper into the reported publications and reviewed them accordingly. [129] reported chitosan film can be regenerated and reused for over 2 cycles. The reported chitosan/GO composite membrane exhibited the adsorption–desorption capacity for 3 different cycles [70]. The Chitosan/Magnetic β-CD could be recycled for 5 times in mixed solvents containing sodium hydroxide and ethanol solution [151]. Chitosan-g-PAA/Rice husk hydrogel was subjected also to a 5 adsorption–desorption cycles and the dye adsorption was only decreased slightly [153]. Chitosan/CNF film can be desorbed and reused for up to 6 consecutive cycles [102]. The recovery and reuse study for chitosan beads had not been reported by the scientists [149].

Therefore, effective adsorbent should possess high adsorption capacity, faster adsorption rate; it could be easily recovered/or regenerated and reused for several number of adsorption–desorption cycles. Hence, some of the chitosan films and chitosan/CNF composite film can be subjected to further study in order to improve their sorption characteristics and adsorption rates. Also, Chitosan/Magnetic β-CD and Chitosan-g-PAA/Rice husk hydrogel are excellent and reusable adsorbents which could be considered to develop other chitosan composite films.

We reviewed the performance of chitosan films and chitosan composite membranes towards the dye removals by adsorption phenomenon. The dye removals affinity is significantly affected by the pH of aqueous solution. The adsorption rates of most sorbents are slower due to the diffusion resistance influence except in the case of chitosan/Magnetic β-CD. The reviewed results are compared with those of other similar adsorbents that are found in the literature. There are limitations on recovery and reuse studies for most of the adsorbents.

7   Conclusion and Remarks

Discharge of persistent dye pollutants into the environment is a global major concern, as the dyes can harm plants, animals, and humans; dyes are also very difficult to be treated due to their recalcitrant and complex structural natures. In addition to the existent governmental and organizational policies on water pollution control, the treatment of wastewater containing dyes is a necessary phenomenon to the academia and industrial sectors. Nowadays, it has become a top priority to treat wastewater before being discharged into the surroundings, because the presence of the bulk of polluted water is growing rapidly plus the huge demands for dye-free water globally. Different treatment procedures have been studied and reported by many researchers around the world. However, water pollution by dyes is being best treated by adsorption process using various classes of adsorbents. Also, the adsorption is being widely accepted not only for the lab-scale but for the industrial scale in the removal of different pollutants from water.

The use of the biopolymers as sorbents for the removal of dyes is a green alternative in the water pollution control because biopolymers are renewable, inexpensive, biodegradable, and biocompatible in the living bodies. Chitosan is a good example of the biopolymers, and the chitosan is derived essentially from chitineous materials obtained mostly from the fishery industries. Chitosan has current industrial application in food processing and is also being applied as adsorbent for the removal of dyes.

Chitosan may be converted in the form of flake, beads, films, composite films, and hydrogels. However, in the present chapter, the preparation and structural characteristics of the chitosan have been overviewed; the classification and methods of the preparation of different types of chitosan membranes have been well reviewed with the support of state-of-the-art publications. This chapter has comprehensively presented the recent advancement in the characterization of chitosan composite membranes produced by casting technology for application as adsorptive membrane systems as reported from some literature. Some of the chitosan-based composite membranes that have been focused and reviewed accordingly in the chapter are (1) chitosan/activated carbon; (2) chitosan/carbon nanotubes; (3) chitosan/graphene oxide; (4) chitosan/nano clay; (5) chitosan/Magnesium oxide; (6) chitosan/zeolite A; (7) chitosan/zinc oxide; (8) chitosan/cellulose nanocrystals; and (9) chitosan/cellulose nanofibers.

Recent publications on chitosan-based adsorbents for dye removals have been well reviewed and presented in the current chapter with a view to find the present overall status or progress in the development and application of such greener materials. This chapter has highlighted that the study about the syntheses, physicochemical properties, and water control or dye removal application of chitosan films and chitosan composite membrane systems are very limited as found from the reviewed number of literature reports. Although, there is significant improvement in the chemical and mechanical properties of the chitosan composite membrane systems, such as the chitosan/saponin-bentonite, chitosan/cellulose nanofibers, chitosan/MgO,

chitosan/zeolite A, in particular, than some of the chitosan films and other reported adsorbents.

But, according to the fair comparative review, the chitosan, chitosan films, and chitosan composite membrane systems exhibited good dye adsorptions than other reviewed adsorbents such as the chitosan beads/activated carbons, cross-linked chitosan/activated carbons, chitosan/glutaraldehyde, and chitosan/modified ball clay. In contrast, the Chitosan/magnetic β-cyclodextrin was reviewed to possess excellent adsorption towards the removal of dye owing to its enhanced and superior chemical stability, higher surface area due to its spherical nature, ability to form the inclusion complex with the dye compounds, and the absence of the internal diffusion resistance as against other adsorbents which have slower dye adsorption rates as highlighted in the reviewed Table 2.

The chapter has reviewed that the attractions of the dyes on reported adsorbents is by electrostatic interactions between the dyes and the adsorbents; anionic dyes are preferably adsorbed on chitosan-based adsorbents at a pH ≤ 7, the adsorbent surfaces become positively charged, e.g., in the adsorption of MO dye on the Chitosan/CNF at pH = 5; while the cationic dyes are adsorbed at a pH ≥ 7, in contrast, here the surfaces of the adsorbents are negatively charged, e.g., in the adsorption of MB dye on Chitosan/Modified Ball Clay at pH = 12.

The adsorption–desorption cycles are studied by researchers to find out whether a given or particular adsorbent can be recovered and reused after some several cycles of adsorption and desorption procedures. Since the pH is a factor that has significant effect on the adsorption of dyes, so, the adsorbed dye compounds can be eluted or washed out from the adsorbent's surface by simply washing it with some suitable solvents under different pH. But, in the present chapter, few of the adsorbents have been reported to exhibit the regeneration and reuse capabilities. Chitosan film reported by [129] has a reuse capability for about 2 cycles. Both the composite membranes of chitosan/GO and that of the chitosan/CNF can be run for over 3 and 6 cycles of adsorption–desorption, respectively. Also, the adsorbents, Chitosan-g-PAA/Rice Husk hydrogel and chitosan/Magnetic β-CD are recyclable for five consecutive cycles with some slight decrease in the dye uptake by the adsorbents.

Therefore, the present chapter examines the classification, methods of preparation, physicochemical properties, dye removal application and mechanism, recovery and regeneration capabilities of different classes of the chitosan composite membranes. The chapter also highlights how chitosan films, chitosan composite membranes, and other similar reported chitosan-based materials can be applied as greener adsorbents for the dye removal application from wastewater. Although, very few of the chitosan-based adsorbents have been reported to have some remarkable adsorption and regeneration capacities; there application for the removal of dyes from the industrial effluents is subject to the further intensive study in order to investigate other new systems based on the chitosan adsorptive membranes with additional superior adsorption capacities, adsorption rates, and regeneration and reuse behaviors.

This may open a new approach in the development and application of the chitosan-based membranes in the area of water pollution control, especially the dye removal. Hence, the following remarks can be undertaken for further research works with the

sole intention to develop newly designed magnetic chitosan composite membranes with enhanced adsorption and recycling properties to be applied as adsorptive systems towards the removal of dye compounds from water:

- To develop by optimization some new chitosan or cross-linked chitosan/cyclodextrin (CD) composite membranes from broad sources by incorporation with the magnetic Fe_3O_4 nanoparticles; the advantage of such adsorbents or the membrane may include strong chemical stabilities, high specific surface areas, and absence of the internal diffusion resistance. Moreover, such adsorptive membranes can be easily recovered after the removal of the dyes from wastewater by bar magnet.
- The adsorption capacity of membrane is reportedly said to be directly proportional to the surface area of active site on membrane surface. Therefore, the knowledge on the specific surface area of the adsorptive membranes is highly recommended in this chapter to be obtained by utilizing the Brunauer–Emmett–Teller (BET) surface area analyzer using the N_2 adsorption–desorption measurements. As observed from many of the available publications, this crucial study is entirely missing or not reported.
- The mechanism of the removal of dyes by the adsorption on chitosan-based membranes shall be investigated thoroughly by studying the properties of the adsorptive membranes before and after adsorption of the dyes from aqueous solutions. This would provide an insight or a better understanding on how the dyes interact with the membranes.
- An industrial effluent may contain more than one class of dyes in it. Most of the reported chitosan-based adsorbents have selective adsorption characteristics, i.e., they selectively adsorbed one class of dye more than the other at a given pH value, e.g., chitosan/CNF film adsorbed higher amount of MO dye than MB at pH $= 5$. So, therefore, the development of the nonselective adsorbents should be encouraged in future studies towards the removal of dyes in both single and binary systems.
- The future magnetic adsorbents based on chitosan membranes shall be well focused to possess the capabilities to be recycled for number of adsorption–desorption cycles, in order to make them more economically viable ones.

References

1. Ngah WW, Teong L, Hanafiah M (2011) Adsorption of dyes and heavy metal ions by chitosan composites: a review. Carbohydr Polym 83(4):1446–1456. https://doi.org/10.1016/j.carbpol.2010.11.004

2. Aliabadi M, Irani M, Ismaeili J, Najafzadeh S (2014) Design and evaluation of chitosan/hydroxyapatite composite nanofiber membrane for the removal of heavy metal ions from aqueous solution. J Taiwan Inst Chem Eng 45(2):518–526. https://doi.org/10.1016/j.jtice.2013.04.016

3. Karim Z, Mathew AP, Grahn M, Mouzon J, Oksman K (2014) Nanoporous membranes with cellulose nanocrystals as functional entity in chitosan: removal of dyes from water. Carbohydr Polym 112:668–676. https://doi.org/10.1016/j.carbpol.2014.06.048

4. de Azevedo ACN, Vaz MG, Gomes RF, Pereira AGB, Fajardo AR, Rodrigues FHA (2017) Starch/rice husk ash based superabsorbent composite: high methylene blue removal efficiency. Iran Polym J 26:93–105. https://doi.org/10.1007/s13726-016-0500-2

5. Salleh MAM, Mahmoud DK, Abdul Karim WAW, Idris A (2011) Cationic and anionic dye adsorption by agricultural solid wastes: a comprehensive review. Desalination 280:1–13. https://doi.org/10.1016/j.desal.2011.07.019

6. Mijinyawa AH, Mishra A, Durga G (2020) Cationic dye removal using a newer material fabricated by Taro Mucilage-g-PLA and Organobentonite clay, Mater Today: proceedings (Available online 27 January 2020). https://doi.org/10.1016/j.matpr.2019.12.345

7. Bhatnagar A, Sillanpää M (2010) Utilization of agro-industrial and municipal waste materials as potential adsorbents for water treatment—a review. Chem Eng J 157:277–296. https://doi.org/10.1016/j.cej.2010.01.007

8. Singh A, Sidhu GK, Singh H (2017) Removal of methylene blue dye using activated carbon prepared from biowaste precursor. Indian Chem Eng 61:28–39. https://doi.org/10.1080/00194506.2017.1408431

9. Abolhassani M, Griggs CS, Gurtowski LA, Mattei-Sosa JA, Nevins M, Medina VF, Morgan TA, Greenlee LF (2017) Scalable chitosan-graphene oxide membranes: the effect of GO size on properties and cross-flow filtration performance. ACS Omega 2:8751–8759. https://doi.org/10.1021/acsomega.7b01266

10. Zinadini S, Zinatizadeh AA, Rahimi M, Vatanpour V, Zangeneh H, Beygzadeh M (2014) Novel high flux antifouling nanofiltration membranes for dye removal containing carboxymethyl chitosan coated Fe_3O_4 nanoparticles. Desalination 349:145–154. https://doi.org/10.1016/j.desal.2014.07.007

11. Salehi E, Daraei P, Shamsabadi AA (2016) A review on chitosan-based adsorptive membrane. Carbohydr Polym 152:419–432. https://doi.org/10.1016/j.carbpol.2016.07.033

12. Islam S, Bhuiyan MAR, Islam MN (2017) Chitin and chitosan: structure, properties and applications in biomedical engineering. J Polym Environ 25:854–866. https://doi.org/10.1007/s10924-016-0865-5

13. Kumar GY, Atul GS, Yadav AV (2013) Chitosan and its applications: a review of literature. Int J Res Pharm Biomed Sci 4:312–331

14. Agarwal M, Agarwal MK, Shrivastav N, Pandey S, Gaur P (2018) A simple and effective method for preparation of chitosan from chitin. Int J Life Sci Sci Res 4(2):1721–1728. https://doi.org/10.21276/ijlssr.2018.4.2.18

15. Kasaai MR (2009) Various methods for determination of the degree of N-acetylation of chitin and chitosan: a review. J Agric Food Chem 57(5):1667–1676

16. Aranaz I, Mengíbar M, Harris R, Paños I, Miralles B, Acosta N, Galed G, Heras Á (2009) Functional characterization of chitin and chitosan. Curr Chem Biol 3(2):203–230

17. Olivera S, Muralidhara HB, Venkatesh K, Guna VK, Gopalakrishna K, Kumar Y (2016) Potential applications of cellulose and chitosan nanoparticles/composites in wastewater treatment: a review. Carbohydr Polym 153:600–618. https://doi.org/10.1016/j.carbpol.2016.08.017

18. Chandrasekharan A, Hwang YJ, Seong K, Park S, Kim S, Yang SY (2019) Acid-treated water-soluble chitosan suitable for microneedle-assisted intracutaneous drug delivery. Pharmaceutics 11:209. https://doi.org/10.3390/pharmaceutics11050209

19. Cui L, Gao S, Song X, Huang L, Dong H, Liu J, Chena F, Yu S (2018) Preparation and characterization of chitosan membranes. RSC Adv 8:28433. https://doi.org/10.1039/c8ra05526b

20. Chen P, Huang Y, Kuo T, Liu F, Lai J, Hsieh H (2007) Improvement in the properties of chitosan membranes using natural organic acid solutions as solvents for chitosan dissolution. J Med Biol Eng 27(1):23–28

21. Sun XF, Tian QQ, Xue ZM, Zhang YW, Mu TC (2014) The dissolution behaviour of chitosan in acetate-based ionic liquids and their interactions: from experimental evidence to density functional theory analysis. RSC Adv 4(57):30282–30291. https://doi.org/10.1039/C4RA02594F

22. Crini G, Badot P.-M. (2008) Application of chitosan, a natural aminopolysaccharide, for dye removal from aqueous solutions by adsorption processes using batch studies: a review of recent literature. Prog Polym Sci 33(4), 399–447. https://doi.org/10.1016/j.progpolymsci.2007.11.001

23. Galiano F, Briceño K, Marino T, Molino A, Christensen KV, Figoli A (2018) Advances in biopolymer-based membrane preparation and applications. J Membr Sci 564:562–586. https://doi.org/10.1016/j.memsci.2018.07.059

24. Hassan ME, Bai J, Dou D (2019) Biopolymers: definition, classification and applications. Egypt J Chem 62 (9):1725–1737. https://doi.org/10.21608/ejchem.2019.6967.1580

25. Correia CO, Caridade SG, Mano JF (2014) Chitosan membranes exhibiting shape memory capability by the action of controlled hydration. Polymers 6:1178–1186. https://doi.org/10.3390/polym6041178

26. Govindan V, Hussiensyah S, Leng TP, Amri F (2014) Preparation and characterization of regenerated cellulose using ionic liquid. Adv Environ Biol 8(8):2620–2625

27. Liu ZH, Sun XF, Hao MY, Huang CY, Xue ZM, Mu TC (2015) Preparation and characterization of regenerated cellulose from ionic liquid using different methods. Carbohydr Polym 117:99–105. https://doi.org/10.1016/j.carbpol.2014.09.053

28. Sakai Y, Hayano K, Yoshioka H, Yoshioka H (2001) A novel method of dissolving chitosan in water for industrial application. Polym J 33(8):640–642. https://doi.org/10.1295/polymj.33.640

29. Wan NWS, Teong LC, Hanafiah MAKM (2011) Adsorption of dyes and heavy metal ion by chitosan films: a review. Carbohydr Polym 83:1446–1456. https://doi.org/10.1016/j.carbpol.2010.11.004

30. Nešić AR, Veličković SJ, Antonović DG (2013) Modification of chitosan by zeolite A and adsorption of Bezactive Orange 16 from aqueous solution. Compos Part B 53:145–151. https://doi.org/10.1016/j.compositesb.2013.04.053

31. Xiao DD, Wang Q, Yan H, Qin A, Lv XG, Zhao Y, Zhang M, Zhou Z, Xu JP, Hu QL, Lu MJ (2017) Comparison of morphological and functional restoration between asymmetric bilayer chitosan and bladder acellular matrix graft for bladder augmentation in a rat model. RSC Adv 7(67):42579–42589. https://doi.org/10.1039/C7RA07601K

32. Travlou NA, Kyzas GZ, Lazaridis NK, Deliyanni EA (2012) Graphite oxide/chitosan composite for reactive dye removal. Chem Eng J 217:256–265. https://doi.org/10.1016/j.cej.2012.12.008

33. Mirmohseni A, Dorraji MSS, Figoli A, Tasselli F (2012) Chitosan hollow fibers as effective biosorbent toward dye: preparation and modeling. Bioresour Technol 121(2012):212–220. https://doi.org/10.1016/j.biortech.2012.06.067

34. Dotto GL, Moura JM, Cadaval TRS, Pinto LAA (2013) Application of chitosan films for the removal of food dyes from aqueous solutions by adsorption. Chem Eng J 214:8–16. https://doi.org/10.1016/j.cej.2012.10.027

35. Fajardo AR, Lopes LC, Rubira AF, Muniz EC (2012) Development and application of chitosan/poly (vinyl alcohol) films for removal and recovery of Pb (II). Chem Eng J 183:253–260. https://doi.org/10.1016/j.cej.2011.12.071

36. Wang X, Lou T, Zhao W, Song G (2016) Preparation of pure chitosan film using ternary solvents and its super absorbency. Carbohydr Polym. https://doi.org/10.1016/j.carbpol.2016.07.081

37. Lee SJ, Heo DN, Moon JH, Ko WK, Lee JB, Bae MS, Park SW, Kim JE, Lee DH, Kim EC, Lee CH, Kwon IK (2014) Electrospun chitosan nanofibers with controlled levels of silver nanoparticles: preparation, characterization and antibacterial activity. Carbohydr Polym 111:530–537. https://doi.org/10.1016/j.carbpol.2014.04.026

38. Ji Y-L, An Q-F, Zhao F-Y, Gao C-J (2015) Fabrication of chitosan/PDMCHEA blend positively charged membranes with improved mechanical properties and high nanofiltration performances. Desalination 357:8–15. https://doi.org/10.1016/j.desal.2014.11.005

39. Hasegawa M, Isogai A, Kuga S, Onabe F (1994) Preparation of cellulose-chitosan blend film using chloral/dimethylformamide. Polymer (Guildf) 35:983–987. https://doi.org/10.1016/0032-3861(94)90942-3

40. Dufresne A, Cavaillé J-Y, Dupeyre D et al (1999) Morphology, phase continuity and mechanical behaviour of polyamide 6/chitosan blends. Polymer (Guildf) 40:1657–1666. https://doi.org/10.1016/S0032-3861(98)00335-8

41. Gopi S, Pius A, Karg R, Kleinschek KS, Thomas S (2019) Fabrication of cellulose acetate/chitosan blend films as efficient adsorbent for anionic water pollutants. Polym Bull https://doi.org/10.1007/s00289-018-2467-y

42. Feng T, Xiong S, Zhang F (2013) Application of cross-linked porous chitosan films for Congo red adsorption from aqueous solution. Desalination Water Treat. https://doi.org/10.1080/19443994.2013.870715

43. Trotta F, Biasizzo M, Caldera F (2012) Molecularly imprinted membranes. Membranes 2(3):440–477. https://doi.org/10.3390/membranes2030440

44. Ahmed MA, Abdelbar NM, Mohamed AA (2018) Molecular imprinted chitosan-TiO_2 nanocomposite for the selective removal of Rose Bengal from wastewater. Int J Biol Macromol 107:1046–1053. https://doi.org/10.1016/j.ijbiomac.2017.09.082

45. Xu L, Huang Y-A, Zhu Q-J, Ye C (2015) Chitosan in molecularly-imprinted polymers: current and future prospects. Int J Mol sci 16(8):18328–18347. https://doi.org/10.3390/ijms160818328

46. Tang Y, Hu X, Zhang X, Guo D, Zhang J, Kong F (2016) Chitosan/titanium dioxide nanocomposite coatings: rheological behavior and surface application to cellulosic paper. Carbohydr Polym 151:752–759. https://doi.org/10.1016/j.carbpol.2016.06.023

47. Yin J, Deng B (2015) Polymer-matrix nanocomposite membranes for water treatment. J Membr Sci 479:256–275. https://doi.org/10.1016/j.memsci.2014.11.019

48. Auta M, Hameed BH (2013) Coalesced chitosan activated carbon composite for batch and fixed-bed adsorption of cationic and anionic dyes. Colloids Surf B Biointerfaces 105:199–206. https://doi.org/10.1016/j.colsurfb.2012.12.021

49. Zhu H, Fu Y, Jiang R, Yao J, Liu L, Chen Y, Xiao L, Zeng G (2013) Preparation, characterization and adsorption properties of chitosan modified magnetic graphitized multi-walled carbon nanotubes for highly effective removal of a carcinogenic dye from aqueous solution. Appl Surf Sci 285:865–873. https://doi.org/10.1016/j.apsusc.2013.09.003

50. Nesic AR, Velickovic SJ, Antonovic DG (2012) Characterization of chitosan/montmorillonite membranes as adsorbents for Bezactiv Orange V-3R dye. J Hazard Mater 209–210:256–263. https://doi.org/10.1016/j.jhazmat.2012.01.020

51. Salehi R, Arami M, Mahmoodi NM, Bahrami H, Khorramfar S (2010) Novel biocompatible composite (Chitosan–zinc oxide nanoparticle): Preparation, characterization and dye adsorption properties. Colloids Surf B Biointerfaces 80:86–93. https://doi.org/10.1016/j.colsurfb.2010.05.039

52. Gupta VK (2009) Application of low-cost adsorbents for dye removal–a review. J Environ Manag 90:2313–2342https://doi.org/10.1016/j.jenvman.2008.11.017

53. Auta M, Hameed BH (2011) Preparation of waste tea activated carbon using potassium acetate as an activating agent for adsorption of Acid Blue 25 dye. Chem Eng J 171:502. https://doi.org/10.1016/j.cej.2011.04.017

54. Carrott PJM, Carrott MMLR, Roberts RA (1991) Physical adsorption of gases by microporous carbons. Colloids Surf 58:385–400. https://doi.org/10.1016/0166-6622(91)80217-C
55. Lelifajri R, Nurfatimah R (2018) Preparation of polyethylene glycol diglycidyl ether (PEDGE) crosslinked chitosan/activated carbon composite film for Cd^{2+} removal. Carbohyd Polym. https://doi.org/10.1016/j.carbpol.2018.07.051
56. Mousavi SR, Asghari M, Mahmoodi NM (2020) Chitosan-wrapped multiwalled carbon nanotube as filler within PEBA thin film nanocomposite (TFN) membrane to improve dye removal. Carbohyd Polym 237:116128. https://doi.org/10.1016/j.carbpol.2020.116128
57. Iijima S (1991) Helical microtubes of graphitic carbon. Nature 354:56–58. https://doi.org/10.1038/354056a0
58. Das R, Ali ME, Hamid SBA, Ramakrishna S, Chowdhury ZZ (2014) Carbon nanotube membranes for water purification: a bright future in water desalination. Desalination 336:97–109. https://doi.org/10.1016/j.desal.2013.12.026
59. Wong KC, Goh PS, Taniguchi T, Ismail AF, Zahri K (2019) The role of geometrically different carbon-based fillers on the formation and gas separation performance of nanocomposite membrane. Carbon 149:33–44. https://doi.org/10.1016/j.carbon.2019.04.031
60. Vatanpour V, Haghighat N (2019) Improvement of polyvinyl chloride nanofiltration membranes by incorporation of multiwalled carbon nanotubes modified with triethylenetetramine to use in treatment of dye wastewater. J Environ Manage 242:90–97. https://doi.org/10.1016/j.jenvman.2019.04.060
61. Gong JL, Wang B, Zeng GM, Yang CP, Niu CG, Niu QY, Zhou WJ, Liang Y (2009) Removal of cationic dyes from aqueous solution using magnetic multi-wallcarbon nanotube nanocomposite as adsorbent. J Hazard Mater 164:1517–1522https://doi.org/10.1016/j.jhazmat.2008.09.072
62. Chen C, Hu J, Shao D, Li J, Wang X (2009) Adsorption behavior of multiwall carbon nanotube/iron oxide magnetic composites for Ni(II) and Sr(II). J Hazard Mater 164:923–928. https://doi.org/10.1016/j.jhazmat.2008.08.089
63. Chang PR, Zheng P, Liu B, Anderson DP, Yu J, Ma X (2011) Characterization of magnetic soluble starch-functionalized carbon nanotubes and its application for the adsorption of the dyes. J Hazard Mater 186:2144–2150. https://doi.org/10.1016/j.jhazmat.2010.12.119
64. Zhu HY, Fu YQ, Jiang R, Yao J, Liu L, Chen YW, Xiao L, Zeng GM (2013) Preparation, characterization and adsorption properties of chitosan modified magnetic graphitized multi-walled carbon nanotubes for highly effective removal of a carcinogenic dye from aqueous solution. Appl Surf Sci 285(Part B):865–873. https://doi.org/10.1016/j.apsusc.2013.09.003
65. Travlou NE, Kyzas GZ, Lazaridis NK, Deliyanni EA (2012) Graphite oxide/chitosan composite for reactive dye removal. Chem Eng J. https://doi.org/10.1016/j.cej.2012.12.008
66. Hummers WS Jr, Offeman RE (1958) Preparation of graphitic oxide. J Am Chem Soc 80:1339. https://doi.org/10.1021/ja01539a017
67. Ramesha GK, Kumara AV, Muralidhara HB, Sampath S (2011) Graphene and graphene oxide as effective adsorbents toward anionic and cationic dyes. J Colloid Interface Sci 361:270–277. https://doi.org/10.1016/j.jcis.2011.05.050
68. Zhang W, Zhou C, Zhou W, Lei A, Zhang Q, Wan Q (2011) Zou B (2011) Fast and considerable adsorption of methylene blue dye onto graphene oxide. Bull Environ Contam Toxicol 87:86–90. https://doi.org/10.1007/s00128-011-0304-1
69. Yang X, Tu Y, Li L, Shang S, Tao X-m (2010) Well-dispersed chitosan/graphene oxide nanocomposites. ACS Appl Mater Interfaces 2:1707–1713. https://doi.org/10.1021/am100222m
70. Sabzevari M, Cree DE, Wilson LD (2018) Graphene oxide−chitosan composite material for treatment of a model dye effluent. ACS Omega 3:13045–13054. https://doi.org/10.1021/acsomega.8b01871
71. Ngulube T, Gumbo JR, Masindi V, Maity A (2017) An update on synthetic dyes adsorption onto clay based minerals: a state-of-art review. J Environ Manage 191:35–57. https://doi.org/10.1016/j.jenvman.2016.12.031

72. Huang R, Wang B, Yang B, Zheng D, Zhang Z (2011) Equilibrium, kinetic and thermodynamic studies of adsorption of Cd (II) from aqueous solution onto HACC-bentonite. Desalination 280:297–304. https://doi.org/10.1016/j.desal.2011.07.033

73. Shahadat MM, Isamil S (2018) Regeneration performance of clay-based adsorbents for the removal of industrial dyes: a review. RSC Adv 8:24571.https://doi.org/10.1039/c8ra04290j

74. Shaban M, Abukhadra MR, Shahien MG, Ibrahim SS (2018) Novel bentonite/zeolite-NaP composite efficiently removes methylene blue and Congo red dyes. Environ Chem Lett 16:275–280. https://doi.org/10.1007/s10311-017-0658-7

75. Elmoubarki R, Mahjoubi FZ, Tounsadi H, Moustadraf J, Abdennouri M, Zouhri A, ElAlban A, Barka N (2015) Adsorption of textile dyes on raw and decanted Moroccan clays: kinetics, equilibrium and thermodynamics. Water Resour Ind 9:16–29. https://doi.org/10.1016/j.wri.2014.11.001

76. Rasouli F, Aber S, Salari D, Khataee AR (2014) Optimized removal of Reactive Navy Blue SP-BR by organo-montmorillonite based adsorbents through central composite design. Appl Clay Sci 87:228–234. https://doi.org/10.1016/j.clay.2013.11.010

77. Zhang L, Hu P, Wang J, Huang R (2016) Cross-linked quaternized chitosan/bentonite composite for the removal of Amino black 10B from aqueous solutions. Int J Biol Macromol. https://doi.org/10.1016/j.ijbiomac.2016.08.018

78. Choudhari SK, Kariduraganavar MY (2009) Development of novel composite using quaternized chitosan and Na+-MMT clay for the pervaporation dehydration of isopropanol. J Colloid Interface Sci 338:111–120. https://doi.org/10.1016/j.jcis.2009.05.071

79. Laysandra L, Ondang IJ, Ju Y-H, Ariandini BH, Mariska A, Soetaredjo FE, Putro JN, Santoso SP, Darsono FL (2019) Ismadji S (2019) Highly adsorptive chitosan/saponin-bentonite composite film for removal of methyl orange and Cr(VI). Environ Sci Pollut Res 26:5020–5037. https://doi.org/10.1007/s11356-018-4035-2

80. Kurniawan A, Sutiono H, Ju YH, Soetaredjo FE, Ayucitra A, Yudha A, Ismadji S (2011) Utilization of rarasaponin natural surfactant for organo-bentonite preparation: application for methylene blue removal from aqueous effluent. Microporous Mesoporous Mater 142:184–193

81. Kumar THV, Sivasankar V, Fayoud N, Oualid HA, Sundramoorthy AK (2018) Synthesis and characterization of coral-like hierarchical MgO incorporated fly ash composite for the effective adsorption of azo dye from aqueous solution. Appl Surf Sci 449:719–728. https://doi.org/10.1016/j.apsusc.2018.01.060

82. Nga NK, Hong PTT, Lam TD, Huy TQ (2013) A facile synthesis of nanostructured magnesium oxide particles for enhanced adsorption performance in reactive blue 19 removal. J Colloid Interface Sci 398(2013):210–216. https://doi.org/10.1016/j.jcis.2013.02.018

83. Nga NK, Chau NTT, Viet PH (2020) Preparation and characterization of a chitosan/MgO composite for the effective removal of reactive blue 19 dye from aqueous solution. J Sci Adv Mater Devices 5(2020):65–72. https://doi.org/10.1016/j.jsamd.2020.01.009

84. Ngah WSW, Teong LC, Wong CS, Hanafiah MAKM (2012) Preparation and characterization of chitosan-zeolite composites. J Appl Polym Sci 125:2417–2425. https://doi.org/10.1002/app.36503

85. Metin AÜ, ÇiftçI H, Alver E (2013) Efficient removal of acidic dye using low-cost biocomposite beads. Ind Eng Chem Res 52:10569−10581. https://doi.org/10.1021/ie400480s

86. Saravanan R, Joicy S, Gupta VK, Narayanan V, Stephen A (2013) Visible light induced degradation of methylene blue using CeO_2/V_2O_5 and CeO_2/CuO catalysts. Mater Sci Eng C 33:4725–4731. https://doi.org/10.1016/j.msec.2013.07.034

87. Khoshhesab ZM, Souhani S (2018) Adsorptive removal of reactive dyes from aqueous solutions using zinc oxide nanoparticles. J Chin Chem Soc, 1–9https://doi.org/10.1002/jccs.201700477

88. Srivastava V, Gusain D, Sharma YC (2013) Synthesis, characterization and application of zinc oxide nanoparticles. Ceram Int 39(8):9803–9808. https://doi.org/10.1016/j.ceramint.2013.04.110

89. Velmurugan R, Selvam K, Krishnakumar B, Swaminathan M (2011) An efficient reusable and antiphotocorrosive nano ZnO for the mineralization of Reactive Orange 4 under UV-A light. Sep Purif Technol 80:119–124. https://doi.org/10.1016/j.seppur.2011.04.018

90. Khoshhesab ZM, Gonbadi K, Behbehani GR (2015) Removal of reactive black 8 dye from aqueous solutions using zinc oxide nanoparticles: investigation of adsorption parameters. Desalin Water Treat 56:1558. https://doi.org/10.1080/19443994.2014.967304

91. Li Z, Yang RR, Yu M, Bai F, Li C, Wang ZL (2008) Cellular level biocompatibility and biosafety of ZnO nanowires. J Phys Chem C 112:20114–20117. https://doi.org/10.1021/jp808878p

92. Muinde VM, Onyari JM, Wamalwa B, Wabomba JN (2020) Adsorption of malachite green dye from aqueous solutions using mesoporous chitosan–zinc oxide composite material. Environmental Chemistry and Ecotoxicology 2:115–125. https://doi.org/10.1016/j.enceco.2020.07.005

93. Qiu B, Xu X-F, Deng R-H, Xia G-Q, Shang X-F, Zhou P-H (2019) Construction of chitosan/ZnO nanocomposite film by in situ precipitation. Int J Biol Macromol 122:82–87

94. Liu Z, Sun X, Hao M, Huang C, Xueb Z, Mu T (2015) Preparation and characterization of regenerated cellulose from ionic liquid using different methods. Carbohyd Polym 117:99–105 https://doi.org/10.1016/j.carbpol.2014.09.053

95. Miller SA (2013). Sustainable polymers: opportunities for the next decade. ACS Macro Lett 2:550–554. https://doi.org/10.1021/mz400207g

96. Swatloski RP, Spear SK, Holbrey JD, Rogers RD (2002) Dissolution of cellulose with ionic liquids. J Am Chem Soc 124:4974–4975. https://doi.org/10.1021/ja025790m

97. Xu AR, Wang JJ, Wang HY (2010) Effects of anionic structure and lithium salts addition on the dissolution of cellulose in 1-butyl-3-methylimidazolium-basedionic liquid solvent systems. Green Chem 12:268–275. https://doi.org/10.1039/B916882F

98. Andanson J-M, Bordes E, Devemy J, Leroux F, Padua AA, Gomes MFC (2014). Understanding the role of co-solvents in the dissolution of cellulose in ionic liquids. Green Chem 16:2528–2538. https://doi.org/10.1039/C3GC42244E

99. Ma H, Burher C, Hsiao BS, Chu B (2011) Ultrafine polysaccharide nanofibrous membrane for water purification. Biomacromolecules 12:970–976. https://doi.org/10.1021/bm1013316

100. Ibrahim H, Sazali N, Ibrahim IN, Sharip MS (2019) Nano-structured cellulose as green adsorbents for water purification: a mini review. J Appl Membr Sci Technol 23(2):45–56. https://doi.org/10.11113/amst.v23n2.154

101. Abdul Khalil HPS, Saurabh CK, Adnan AS, Fazita MN, Syakir MI, Davoudpour Y et al (2016). A review on chitosan-cellulose blends and nanocellulose reinforced chitosan biocomposites: properties and their applications. Carbohyd Polym 150:216–226https://doi.org/10.1016/j.carbpol.2016.05.028

102. Huo M-X, Jin Y-L, Sun Z-F, Ren F, Pei L, Ren P-G (2021) Facile synthesis of chitosan-based acid-resistant composite films for efficient selective adsorption properties towards anionic dyes. Carbohyd Polym 254:117473. https://doi.org/10.1016/j.carbpol.2020.117473

103. Tomoda BT, Yassue-Cordeiro PH, Ernesto JV, Lopes PS, Peres LO, Ferreira da Silva C, Agostini de Moraes M (2020) Chapter 3-characterization of biopolymer membranes and films: physicochemical, mechanical, barrier, and biological properties. Biopolym Membr Films, 67–95. https://doi.org/10.1016/B978-0-12-818134-8.00003-1

104. Barbosa GP, Debone HS, Severino P, Souto EB, da Silva CF (2016) Design and characterization of chitosan/zeolite composite films—effect of zeolite type and zeolite dose on the film properties. Mater Sci Eng C 60:246–254. https://doi.org/10.1016/j.msec.2015.11.034

105. Murtey MD, Ramasamy P (2016) Sample preparations for scanning electron microscopy–life sciences. In: Modern electron microscopy in physical and life sciences, IntechOpen. https://doi.org/10.5772/61720

106. de Oliveira Jr O, Ferreira L, Marystela G, de Lima Leite F, Da Róz AL (eds) (2017) Nanocharacterization Techniques. William Andrew

107. Sanmugam A, Vikraman D, Park HJ, Kim H (2017) One-pot facile methodology to synthesize chitosan-ZnO-graphene oxide hybrid composites for better dye adsorption and antibacterial activity. Nanomaterials 7:363. https://doi.org/10.3390/nano7110363

108. Lawrence BD, Omenetto F, Chui K, Kaplan DL (2008) Processing methods to control silk fibroin film biomaterial features. J Mater Sci 43(21):6967–6985. https://doi.org/10.1007/s10853-008-2961-y

109. Chalmers JM (2013) Infrared spectroscopy: sample presentation. In: reference module in chemistry, molecular sciences and chemical engineering. https://doi.org/10.1016/B978-0-12-409547-2.00254-7

110. Callister W, Rethwisch D (2007) Materials science and engineering: an introduction. In: Materials science and engineering, 7th ed. Wiley

111. ASTM D882-18 (2018) Standard test method for tensile properties of thin plastic sheeting

112. ASTM D638-14 (2014) Standard test method for tensile properties of plastics

113. Saurabh CK, Gupta S, Bahadur J, Mazumder S, Variyar PS, Sharma A (2013) Radiation dose dependent change in physiochemical, mechanical and barrier properties of guar gum based films. Carbohydr Polym 98(2):1610–1617. https://doi.org/10.1016/j.carbpol.2013.07.041

114. Shao W, Wu J, Liu H, Ye S, Jiang L, Liu X (2017) Novel bioactive surface functionalization of bacterial cellulose membrane. Carbohydr Polym 178:270–276. https://doi.org/10.1016/j.carbpol.2017.09.045

115. Palacio L, Calvo JI, Pradanos P, Hernandez A, Väisänen P, Nyström M (1999) Contact angles and external protein adsorption onto UF membranes. J Membr Sci 152:189–201. https://doi.org/10.1016/S0376-7388(98)00203-8

116. Gebald C, Wurzbacher JA, Tingaut P, Zimmermann T, Steinfeld A (2011) Amines-based nanofibrillated cellulose as adsorbent for CO_2 capture. Environ Sci Technol 45:9101–9108. https://doi.org/10.1021/es202223p

117. Ma H, Burger C, Hsiao BS, Chu B (2012) Nanofibrous microfiltration membrane based on cellulose nanowhiskers. Biomacromol 13:180–186. https://doi.org/10.1021/bm201421g

118. Crini G, Lichtfouse E, Wilson LD, Morin-Crini N (2019) Conventional and non-conventional adsorbents for wastewater treatment. Environ Chem Lett 17:195–213. https://doi.org/10.1007/s10311-018-0786-8

119. Crini G (2010) Wastewater treatment by sorption. In: Crini G, Badot PM (Eds) Sorption processes and pollution, chap 2. PUFC, Besançon, pp 39–78

120. Gadd GM (1990) Biosorption. Chem Ind 13:421–426

121. Nekouei F, Nekouei S, Tayagi IJ, Gupta VK (2015) Kinetic, thermodynamic and isotherm studies for acid blue 129 removal from liquids using copper oxide nanoparticle- modified activated carbon as a novel adsorbent. J Mol Liq 201:124–133. https://doi.org/10.1016/j.molliq.2014.09.027

122. Chattopadhyay DP (2011) Chapter 4–chemistry of dyeing. In: Handbook of textile and industrial dyeing, principle, processes and types of dyes, volume 1 in wood publishing series in textiles, pp 150–183

123. Gaffar MA, EI-Rafie SM, EI-Tahlawy KF (2005) Preparation and utilization of ionic exchange resin via graft copolymerization of β-CD itaconate with chitosan. Carbohyd Polym 56:387–396. https://doi.org/10.1016/j.carbpol.2004.01.007

124. Piccin JS, Vieira MLG, Gonçalves JO, Dotto GL, Pinto LAA (2009) Adsorption of FD&C red no. 40 by chitosan: isotherms analysis. J Food Eng 95:16–20. https://doi.org/10.1016/j.jfoodeng.2009.03.017

125. Koprivanac N, Kusic H (2008) Hazardous organic pollutants in colored wastewaters. New Science Publishers, New York

126. Shirmardi M, Mesdaghinia A, Mahvi AH, Nasseri S, Nabizadeh R (2012) Kinetics and equilibrium studies on adsorption of acid red 18 (Azo-Dye) using multiwall carbon nanotubes (MWCNTs) from aqueous solution. E-J Chem 4:2371–2383. https://doi.org/10.1155/2012/541909

127. Giles CH, MacEwan TH, Nakhwa SN, Smith D (1960) Studies in adsorption part XI: a system of classification of solution adsorption isotherms and its use in diagnosis of adsorption mechanisms and in measurement of specific surface areas of solids. J Chem Soc 3973–3993. https://doi.org/10.1039/JR9600003973

128. Martin DF, Alessio RJ, McCane CH (2013) Removal of synthetic food dyes in aqueous solution by Octolig®. . J Environ Sci Health Part A Tox/Hazard Subst Environ Eng 48(5):495–500. https://doi.org/10.1080/10934529.2013.730413

129. Rêgo TV, Cadaval Jr TRS, Dotto GL, Pinto LAA (2013) Statistical optimization, interaction analysis and desorption studies for the azo dyes adsorption onto chitosan films. J Colloid Interface Sci 411:27–33. https://doi.org/10.1016/j.jcis.2013.08.051

130. Esquerdo VM, Cadaval TRS Jr, Dotto GL, Pinto LAA (2014) Chitosan scaffold as an alternative adsorbent for the removal of hazardous food dyes from aqueous solutions. J Colloid Interface Sci 424(2014):7–15. https://doi.org/10.1016/j.jcis.2014.02.028

131. Gopi S, Pius A, Kargl R, Kleinschek KS, Thomas S (2018) Fabrication of cellulose acetate/chitosan blend films as efficient adsorbent for anionic water pollutants. Polym Bull. https://doi.org/10.1007/s00289-018-2467-y

132. Gao Z, Bandosz TJ, Zhao Z, Han M, Qiu J (2009) Investigation of factors affecting adsorption of transition metals on oxidized carbon nanotubes. J Hazard Mater 167:357–365. https://doi.org/10.1016/j.jhazmat.2009.01.050

133. Ren Y, Abbood HA, He F, Peng H, Huang K (2013) Magnetic EDTA-modified chitosan/SiO_2/Fe_3O_4 adsorbent: preparation, characterization, and application in heavy metal adsorption. Chem Eng J 226:300–311. https://doi.org/10.1016/j.cej.2013.04.059

134. Zuo P-P, Feng H-F, Xu Z-Z, Zhang L-F, Zhang Y-L, Xia W, Zhang W-Q (2013) Fabrication of biocompatible and mechanically reinforced graphene oxide-chitosan nanocomposite films. Chem Cent J 7:39–40. https://doi.org/10.1186/1752-153X-7-39

135. Auta M, Hameed BH (2014) Chitosan–clay composite as highly effective and low-cost adsorbent for batch and fixed-bed adsorption of methylene blue. Chem Eng J 237:352–361. https://doi.org/10.1016/j.cej.2013.09.066

136. Chen J-T, Fu Y-J, An Q-F, Lo S-C, Huang S-H, Hung W-S, Hu C-C, Lee K-R, Lai J-Y (2013) Tuning nanostructure of graphene oxide/polyelectrolyte LbL assemblies by controlling pH of GO suspension to fabricate transparent and super gas barrier films. Nanoscale 5:9081−9088. https://doi.org/10.1039/C3NR02845C

137. Khosla E, Kaur S, Dave PN (2013) Mechanistic study of adsorption of acid orange-7 over aluminum oxide nanoparticles. J Eng 2013, 8. Article ID 593534. https://doi.org/10.1155/2013/593534

138. Wang S, Wei J, Lv S, Guo Z, Jiang F (2013) Removal of organic dyes in environmental water onto magnetic-sulfonic graphene nanocomposite. Clean Soil Air Water 41(10):992–1001. https://doi.org/10.1002/clen.201200460

139. Gok O, Ozcan AS, Ozcan A (2010) Adsorption behavior of a textile dye of Reactive Blue 19 from aqueous solutions onto modified bentonite. Appl Surf Sci 256:5439–5443. https://doi.org/10.1016/j.apsusc.2009.12.134

140. Malakootian M, Mansoorian HJ, Hosseini A, Khanjani N (2015) Evaluating the efficacy of alumina/carbon nanotube hybrid adsorbents in removing Azo Reactive Red 198 and Blue 19 dyes from aqueous solutions. Process Saf Environ Protect 96:125–137. https://doi.org/10.1016/j.psep.2015.05.002

141. Moussavi G, Mahmoudi M (2009) Removal of azo and anthraquinone reactive dyes from industrial wastewaters using MgO nanoparticles. J Hazard Mater 168:806–812. https://doi.org/10.1016/j.jhazmat.2009.02.097

142. Khan MAN, Siddique M, Wahid F, Khan R (2015) Removal of reactive blue 19 dye by sono, photo and sonophotocatalytic oxidation using visible light. Ultrason Sonochem 26:370–377. https://doi.org/10.1016/j.ultsonch.2015.04.012

143. Shahadat MM, Isamil S (2018) Regeneration performance of clay-based adsorbents for the removal of industrial dyes: a review. RSC Adv 8:24571. https://doi.org/10.1039/c8ra04290j

144. Cadaval Jr TRS, Dotto GL, Pinto LAA (2014) Equilibrium isotherms, thermodynamics and kinetic studies for the adsorption of food azo dyes onto chitosan films. Chem Eng Commun. https://doi.org/10.1080/00986445.2014.934449

145. Tang S, Xia D, Yao Y, Chen T, Sun J, Yin Y et al. (2019) Dye adsorption by self- recoverable, adjustable amphiphilic graphene aerogel. J Colloid Interface Science 554:682–691. https://doi.org/10.1016/j.jcis.2019.07.041

146. Lai KC, Hiew BYZ, Lee LY, Gan S, Thangalazhy-Gopakumar S, Chiu WS, *et al.* (2019) Ice-templated graphene oxide/chitosan aerogel as an effective adsorbent for sequestration of

metanil yellow dye. Bioresour Technol 274:134–144. https://doi.org/10.1016/j.biortech.2018.11.048

147. Jiang R, Fu Y-Q, Zhu H-Y, Yao J, Xiao L (2012) Removal of methyl orange from aqueous solutions by magnetic maghemite/chitosan nanocomposite films: adsorption kinetics and equilibrium. J Appl Polym Sci 125:E540–E549. https://doi.org/10.1002/app.37003

148. Habiba U, Siddique TA, Lee JJL, Joo TC, Ang BC, Afifi AM (2018) Adsorption study of methyl orange by chitosan/polyvinyl alcohol/zeolite electrospun composite nanofibrous membrane. Carbohyd Polym. https://doi.org/10.1016/j.carbpol.2018.02.081

149. Wu FC, Tseng RL, Juang RS (2000) Comparative adsorption of metal and dye on flake- and bead-types of chitosans prepared from fishery wastes. J Hazard Mater B73:63–75. https://doi.org/10.1016/s0304-3894(99)00168-5

150. Wong YC, Szeto YS, Cheung WH, McKay G (2004) Adsorption of acid dyes on chitosan–equilibrium isotherm analyses. Process Biochem 39(6):695–704. https://doi.org/10.1016/S0032-9592(03)00152-3

151. Fan L, Zhang Y, Luo C, Lu F, Qiu H, Sun M (2012) Synthesis and characterization of magnetic β-cyclodextrin-chitosan nanoparticles as nano-adsorbents for removal of methyl blue. Int J Biol Macromol 50:444–450. https://doi.org/10.1016/j.ijbiomac.2011.12.016

152. Kumari HJ, Krishnamoorthy P, Arumugam TK, Radhakrishnan S, Vasudevan D (2016) An efficient removal of crystal violet dye from waste water by adsorption onto TLAC/Chitosan composite: a novel low cost adsorbent. Int J Biol Macromol. https://doi.org/10.1016/j.ijbiomac.2016.11.077

153. Vaz MG, Pereira AGB, Fajardo AR, Azevedo ACN, Rodrigues FHA (2017) Methylene blue adsorption on chitosan-g-poly(acrylic acid)/rice husk ash superabsorbent composite: kinetics, equilibrium, and thermodynamics. Water Air Soil Pollut 228:14. https://doi.org/10.1007/s11270-016-3185-4

154. Dotto GL, Santos JMN, Tanabe EH, Bertuol DA, Foletto EL, Lima EC, Pavan FA (2017) Chitosan/polyamide nanofibers prepared by Forcespinning technology: a new adsorbent to remove anionic dyes from aqueous solutions. J Clean Prod 144:120–129. https://doi.org/10.1016/j.jclepro.2017.01.004

155. Jawad AH, Abdulhameed AS, Mastuli MS (2020) Mesoporous cross-linked chitosan/activated charcoal composite for the removal of thionine cationic dye: comprehensive adsorption and mechanism study. J Polym Environ 28:1095–1105. https://doi.org/10.1007/s10924-020-01671-5

156. Galan J, Trilleras J, Zapata PA, Arana VA, Grande-Tovar CD (2021) Optimization of chitosan glutaraldehyde-crosslinked beads for reactive blue 4 anionic dye removal using a surface response methodology. Life 11:85. https://doi.org/10.3390/life11020085

Lignin-Based Membrane for Dye Removal

Moises Bustamante-Torres, Belén Arcentales-Vera, Sofía Abad-Sojos, Odalys Torres-Constante, Frida Ruiz-Rubio, and Emilio Bucio

Abstract Urbanization, industrial activities, and the rapid increase in major pollutants have led to serious environmental concerns. Dye wastewaters are poor degradable and toxic compounds with serious damage for the life. The demand for a clean environment for pollutants such as dyes has increased. Biodegradation of dyes is important to decrease the amount of dyes as a result of industrial processes. Adsorption is one of the main processes, and fruitful results have been achieved in terms of cost, availability, and efficacy. It is a solution to old traditional methods such as chemistry or biology. Due to the adsorption properties, many polymers have been studied, but lignin has become a potential material for dye removal. Lignin is a multifunctional polymer with great properties such as usable, non-toxic, antibacterial, dye-absorbing, anti-cancer, etc. Therefore, lignin-based materials have arisen for different applications. Besides, lignin-degrading enzymes have been shown potential results in the treatment of dye removal. The dye removal depends on a cooperative process of the main enzymes followed by several accessory enzymes and the reducing substrates or mediators in the catalytic cycle.

M. Bustamante-Torres (✉)
Biomedical Engineering Department, School of Biological and Engineering,
Yachay Tech University, Urcuqui City, Ecuador
e-mail: moises.bustamante@yachaytech.edu.ec

B. Arcentales-Vera
Chemistry Department, School of Chemical and Engineering, Yachay Tech University,
Urcuqui City, Ecuador
e-mail: maria.arcentales@yachaytech.edu.ec

S. Abad-Sojos · O. Torres-Constante
Institute of Biology, ELTE Eötvös Loránd University, Pázmány P. Sétány 1/C, H-1117 Budapest,
Hungary

M. Bustamante-Torres · F. Ruiz-Rubio · E. Bucio (✉)
Department of Radiation Chemistry and Radiochemistry, Institute of Nuclear Sciences, National
Autonomous University of Mexico, Mexico City 04510, Mexico
e-mail: ebucio@nucleares.unam.mx

Keywords Lignin · Lignin-based materials · Biodegradability · Pollutants · Dyes · Environment · Adsorption

1 Introduction

1.1 Overview of Dye Removal

Dyes are used to provide color in different industries such as textile, cosmetic, and food. These dyes are employed by their suitable properties. Practically, a dye can be defined as a molecule with two chemical groups: the chromophore provides color and the auxochrome is required to fix the dye molecule on the tissue [35]. The dye is commonly a soluble substance that is easy to bond with the substrate to which is applied.

In contrast, several industries commonly produce pollution to the environment by the use of dyes. Usually, dyes present adverse effects. Dyes are toxic to aquatic species and may cause severe damage to different human organs such as kidney, reproductive system, liver, brain, central nervous system [54], and skin inflammation. Besides, dyes are knowing to cause mutagenesis, chromosomal fractures, carcinogenesis, and respiratory toxicity [131]. Besides, dyes have a high molecular weight, complex chemical structure, and low biodegradability level [40].

Lignin is an abundant biopolymer. It has potential properties that have attracted attention in recent years. A recent research reports that the annual output of lignin is around 50–70 million tons as a residual product [9]. Besides, lignin is usually discarded instead of being used as a raw material for developing new technologies. Some microorganisms produce lignocellulolytic enzymes. Therefore, researchers have been introduced a cheap and eco-friendly biological treatment, involving microorganisms or enzymes acquired from a biomolecule called lignin.

Therefore, for the purpose of using lignin, some investigations have been conducted, and its effectiveness has been proven in various applications, such as antimicrobial agents, prebiotics and antioxidants, fuel production, etc. The multiple function groups make lignin being a potential polymer for its adsorption capacity. This allows them to bond with certain dyes, thereby removing the dye. In addition, several investigations have reported the production of lignin-based materials to remove dyes [77, 111]. Modified lignin products have useful applications in many areas: concrete admixtures, oil exploration, dispersing of dyes, controlled-release fertilizer, and synthetic wood [118].

1.2 Environment Concerns

In recent years, the increment of human and industrial activities has caused an increase in various types of pollutants on water systems. One type of these pollutants is dye wastewaters that are mainly derived from textile, leather, paper, dyeing, tannery, and paint industries. The textile industry uses approximately 10 000 tons of dyes per year worldwide and represents 60% of dye consumption in the world [1, 59]. Dye wastewaters are poor degradable and toxic compounds that must be passing through treatment before release into water systems due to their severe impact on the environment [25, 80].

However, dyes degradation is important to decrease the amount of dyes as a result of industrial processes. Dyes and their intermediates are biodegradable low-organic compounds and are considered to be one of the main pollutants in aqueous environment. These compounds are highly water soluble but complex to be removed by ordinary techniques. Although many strategies have been developed to remove dyes, some of these methods may cause secondary pollution, or are inefficient, time-consuming, or even costly. The biodegradation is a low-cost technique that can eliminate harmful components in polluted wastewater [70]. Biodegradation employs usually natural enzymes produced from microorganisms because they can carry out a reaction, which is difficult to achieve through organic synthesis to decompose dye molecules. Adsorption is considered as an alternative mechanism to remove dyes in wastewaters using novelty chemical and biological methods [93].

1.3 Lignin as Solution

Lignin shows a fundamental role in woody plant tissues. Besides, lignin exhibits high adsorption capacities for heavy metal ions and can be a good adsorbent for pollutants over wide concentration ranges [119, 125]. Lignin production can be a potential platform for the bioproduction of renewable high-performance materials.

Lignin can be obtained as a byproduct of industrial and agricultural production. A huge amount of lignin is produced every year as a waste in the production of fuel or paper causing an environmental issue [66]. It is a biopolymer characterized by its industrial availability, low cost, the capacity of adsorption of pollutants, strong dye-binding capacity, biodegradability, and non-toxicity. These lignin characteristics make this material considered a viable candidate to treat dye wastewaters and at the same time solve two problems in an environmentally friendly manner. The adsorption of dyes using lignin and lignin-based materials is mainly mediated through π interactions, hydrogen bonds, and electrostatic interactions that drive the adsorption process [77, 108].

1.4 Azo Dyes

Azo dyes contain –N = N – groups in their structure. They are representing the 60–70% of commercially available dyes in the world. Azo dyes are employed in several industries as food, pharmaceutical, cosmetic, textile, and leather. In the 1930s, some azo derivatives such as 4-dimethyl and o-amino- azotoluene showed carcinogenic effects to the liver and bladder after feeding. These adverse effects were developed in workers during the manufacture of particular dyes. The dyes involved were fuchsine, auramine, benzidine, and 2-naphthylamine 1 [16] as shown in Fig. 1.

Fig. 1 Examples of chemical structure from dyes. **a** Fuchsine, **b** Auromine, **c** Benzidine, and **d** 2-Naphthylamine
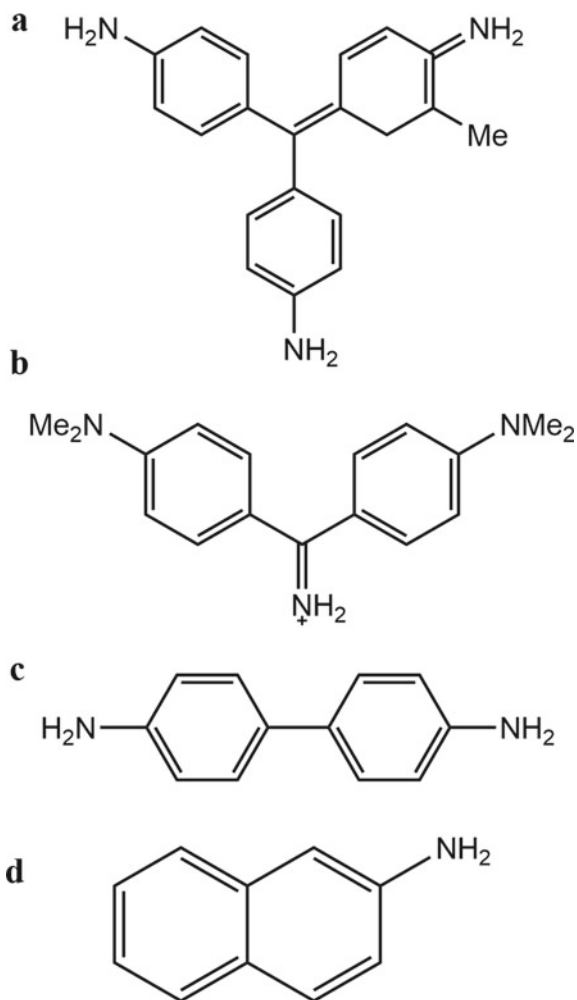
As we mentioned previously, dyes present negative side effects such as carcinogenic, DNA damage, etc. Azo dye toxicity is taken into account during the manufacture in several industries. For instance, genotoxicity is a significant problem for human health. Therefore, azo dye consequences are highly studied [16]. Some of the complex azo dyes are Direct Black 38 or Direct Blue 6 release the aromatic amine, benzidine [85].

2 Lignin

Lignin is an important polymer with important properties and promising applications. It is the second most available polymer in nature, representing approximately up to 10–25% of lignocellulosic biomass [124]. Lignin is a natural polymer with a high molecular weight and a three-dimensional cross-linked structure consisting of phenyl propane monomers. Regarding the solubility of lignin, it depends on the treatment method used for its isolation. However, in most cases, lignin is insoluble in most solvents [13]. As shown in Fig. 2, lignin structure presents carbonyl, carboxyl, and hydroxyl groups, which are functional groups of great interest for several applications.

Lignin possesses interesting physical and chemical properties. Because of its aromatic structure, availability, versatility, biocompatibility, and low cost, it is
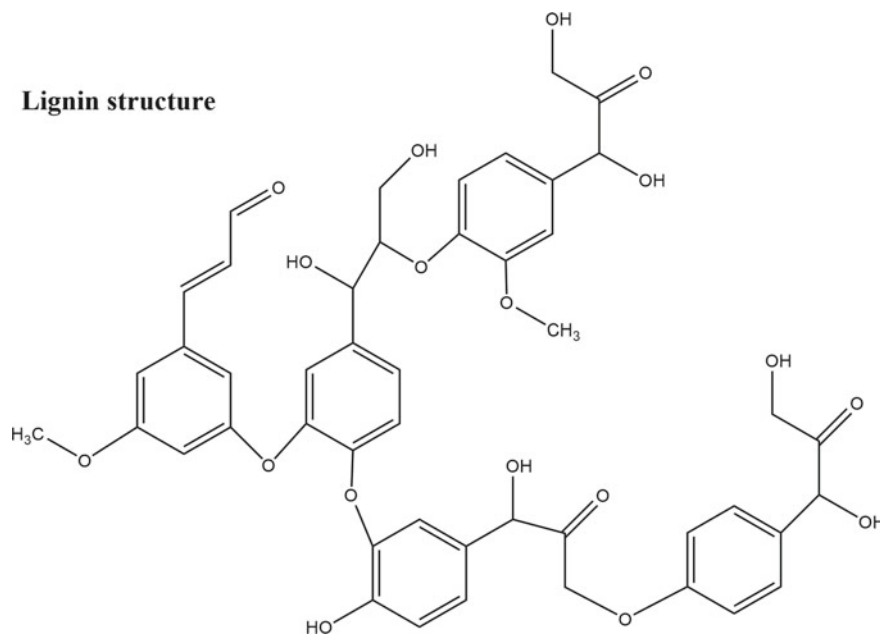
Fig. 2 General structure of lignin
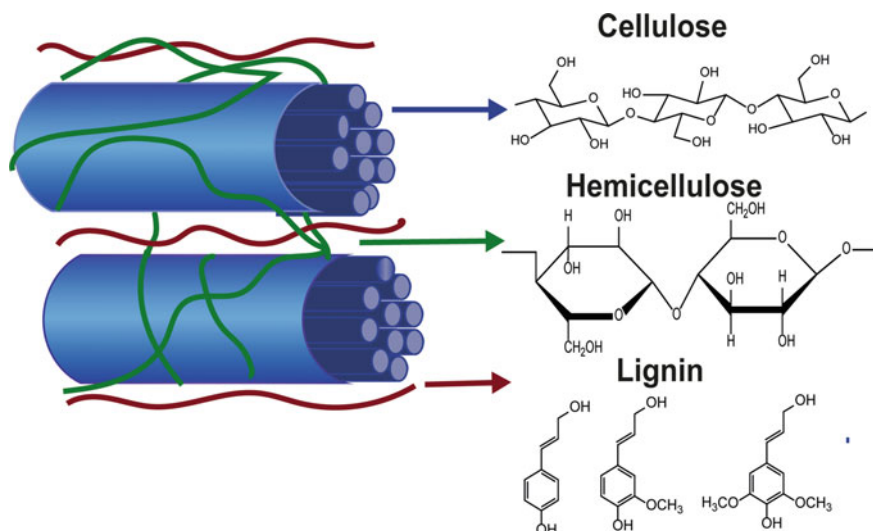
Fig. 3 Schematic representation of the main components of plant fibers: lignin, hemicellulose, and cellulose

considered a promising material [133]. New materials containing lignin polymer and other biomolecules are mainly produced from plant fiber. These biomolecules provide mechanical strength and stability in plants [53]. Biomass also contains small percentages of compounds such as inorganic minerals, pectins, extractives, etc.

This complex polymer exists in plant cell wall, mainly within the secondary wall. Lignin is connected to hemicellulose through covalent and non-covalent bonds [87], forming a covering around the cellulose fibers, as shown in Fig. 3. In addition, lignin acts as a "glue" connecting the cellulose and hemicellulose [56]. In plants, lignin has a variety of functions, including increasing the rigidity of the cell walls, enhancing the transport of minerals and water as well as protective barrier against by microbial and fungal invasion. Besides, lignin is hydrophobic, which can effectively transport water and increase the impermeability of cell walls.

2.1 Lignin Structure

Lignin has a branched structure of aliphatic and aromatic chains [34]. Its entire structure is based on three types of phenylpropanoid units (called mono-lignols). These monomers include coniferyl, sinapyl, and p-coumaryl alcohols, which vary with the degree of methylation. The monomers undergo polymerization reactions to produce structural units called guaiacyl (G), syringyl (S), and p-hydroxyphenyl (H) residues. A scheme of the structures of mono-lignols building blocks is shown in Fig. 4. The polymerization of monomers proceeds through the dehydrogenation
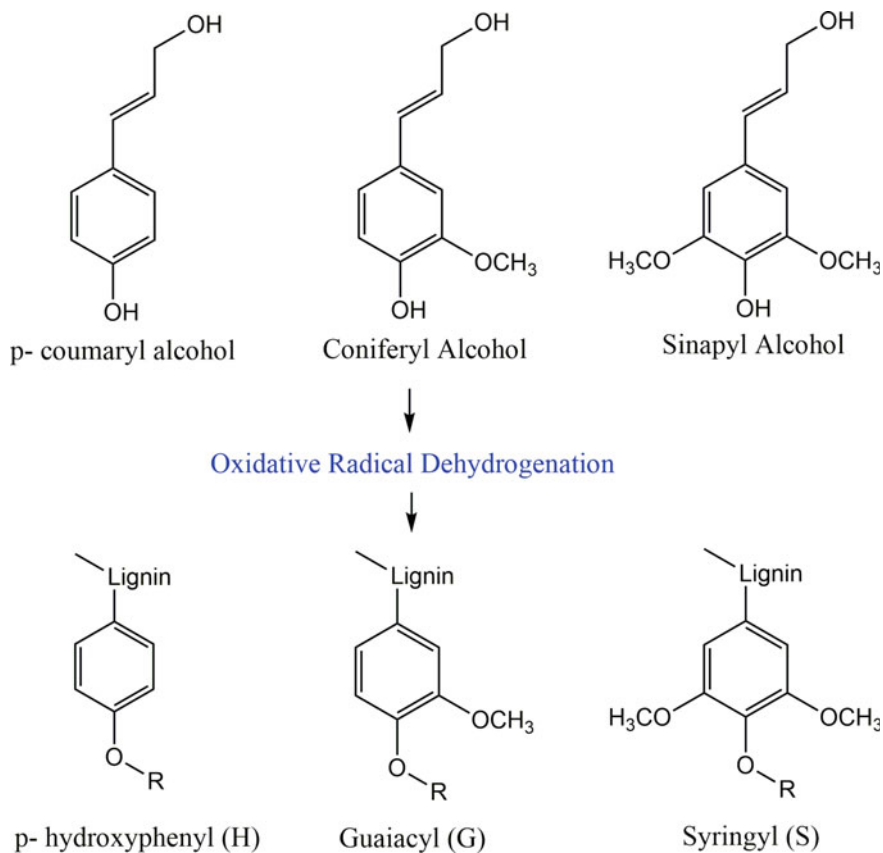
Fig. 4 Structure of lignin monolignols and their corresponding building blocks

reaction of oxidative free radicals [13], thereby forming three-dimensional lignin macromolecules involving carbon–carbon and ether bonds.

The ratio of monomer precursors varies with different factors; such as plant species [114], ecological conditions [112], and pretreatment methods used [116]. Therefore, lignin can be obtained from softwood, hardwood, and grass, usually present diverse compositions.

Besides, the lignin structure contains several functional groups, which are essential in determining the properties and characteristics of polymer [46]. The structure of lignin contains several carbon–carbon (C–O) and carbon–oxygen (C–O) bonds. However, the most predominant bond is the β-O-4 ether linkage as shown in Fig. 5, which represents approximately 50% of the bonds in lignin [13].

Fig. 5 Representation of the β-O-4 ether bond from lignin
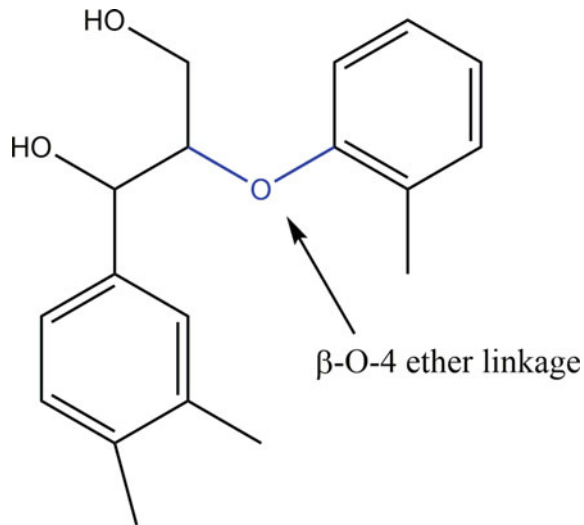
2.2   *Properties of Lignin*

Due to the variable composition and heterogeneity in the lignin structure, some biological activities can be distinguished such as antimicrobial, antioxidant, UV absorption, adsorbent, and other properties. It is known that lignin has strong properties against microbes and microorganisms. This property is derived from the high content of phenolic and methoxy hydroxyl groups in the lignin structure, which inhibits the activities of dangerous species [4]. Lignin-based materials have been evaluated for several applications, including the antimicrobial activity. Some of these applications include food packaging [4] and biomedical applications [27]. Moreover, lignin is an important source of antioxidants. Due to its phenol hydroxyl content, lignin acts by scavenging free radicals [11].

Lignin is used as natural antioxidant involves cosmetic, pharmaceuticals, and polymers [41]. Another characteristic of lignin is its ultraviolet light absorption capacity due to its aromatic structure, which contains chromophores that absorb that light. These absorbing groups include conjugated carbonyl (e.g. α-carbonyl groups and quinones), aromatic rings, and carbon–carbon double bonds [102]. Like the other properties, ultraviolet light absorption will vary depending on composition (lignin source). This property gives lignin the characteristic of natural sunscreen and has even been tested to improve the ultraviolet protection of commercial products [127].

Additionally, one of the most remarkable properties is its adsorption ability by the multiple functional groups. Researches have reported the importance of lignin for the electrostatic and hydrophobic interaction between lignin and dyes for dye adsorption [77]. Due to this adsorption property, lignin has shown a potential efficiency to remove Methylene Blue (MB) dye from aqueous media. Figure 6 illustrates the chemical structure of this dye.
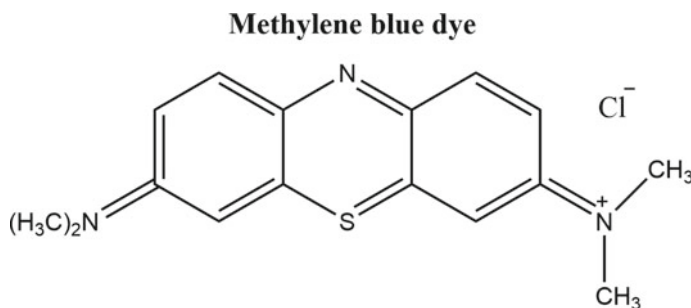
Fig. 6 Chemical structure of Methylene Blue Dye

2.3 Types of Lignin

Lignin is normally present in the epidermal and occasionally hypodermal cell wall of plants [2]. This biopolymer can be classified into different types according to its natural plant species and extraction methods. Today, there is no method that can quantitatively separate lignin without the risk of structural modification. Paper industry is the main source of lignin, where lignin is chemically, enzymatically, and mechanically processed. A brief description of the classification and the different types of lignin is given below.

2.3.1 Based on Plant Source

Lignin structures will depend on the type of plant from which it originates. Generally, lignin is divided into three categories: softwood, hardwood, and grass lignin.

Lignin from Softwood

Softwoods are gymnosperm, such as pines and spruces, with a total lignin content of 25–35% [68]. Softwood lignin comprises mainly guaiacyl (G) units, which derive from coniferyl monomer, and only a small amount of p-hydroxyphenyl (H) units (Fig. 4). Therefore, the structure of softwood lignin does not change much among different species.

Lignin from Hardwood

Hardwood plants are called also angiosperms and are trees characterized by broad leaves. Examples of these species are eucalyptus and acacias. The content of lignin in hardwood plants varies from 15 to 30% of the entire composition. Hardwood lignin contains guaiacyl (G) and syringyl (S) units derived from coniferyl and sinapyl

Table 1 Amounts of building blocks in softwood, hardwood, and grass lignin

Building blocks	Softwood (%)	Hardwood	Grass lignin (%)
Guaiacyl (G)	90–95	25−50%	25−50
Syringyl (S)	0–1	50−75%	25−50
p-hydroxyphenyl (H)	0.5–3.5	Trace	10−25

alcohol, respectively (see Fig. 4). That is, hardwood is characterized by the S/G ratio [88]. However, the ratio and proportion of both components vary widely among different species, and consequently, the structure is also different.

Lignin from Grass

This category includes perennial and annual grass such as corn stalks, sugar cane bagasse, and straws. Lignin structure in grasses comprises the similar amount of guaiacyl (G) and syringyl (S) units (see Fig. 4). However, unlike hardwood and softwood, grass lignin contains a higher proportion of p-hydroxyphenyl (H) units. Table 1 shows the percentage ranges of each building block in different plant sources.

2.3.2   Based on Extraction Method

Lignin can be separated from different sources by two main extraction methods: sulfur-containing lignin and sulfur-free lignin. The resulting lignin is also called industrial lignin, and its structure, degree, and properties are different.

Sulfur-Containing Lignin Methods

These processes are commonly employed by the paper and pulp industry. It includes kraft lignin and lignosulfonates.

Kraft Lignin:

Sulfate/kraft is the most commonly used ligning separation method in the world, accounting for about 85% of total production [17]. The elemental and bounded forms of kraft lignin (such as thiol) have sulfur content as low as 1–2wt%. In this process, the lignin is broken down into smaller fragments of different sizes. Kraft lignin increases the phenolic hydroxyl group content as a result of the cleavage of the β-aryl ether bonds [117]. Then, a large amount of ash is present in lignin structure by the high sodium and sulfur content [103]. Therefore, impurities must be removed with subsequent processing.

Lignosulfonates:

This type of modified lignin is obtained from sulfite pulp, where delignification is achieved through HSO_3^- and SO_3^- ions [85]. Lignin is greatly degraded due to the breaking of ether bonds in sulfite pulp. Unlike kraft lignin, lignosulfonates have a higher degree of sulfur content (4–8 wt%) [104] and therefore a higher degree of sulfonation, which means that the hydroxyl groups are replaced by a sulfonate group. These sulfonate groups make the lignin soluble, which is suitable for many industrial applications [117].

Sulfur-Free Lignin Methods

These types of methods are used to produce bioethanol. The sulfur-free process includes alkaline and organosolv lignin. Sulfur-free lignin is characterized by its high purity and chemical composition close to native lignin, compared to other lignins since it does not contain sulfur.

Soda lignin/Alkali lignin:

It is recovered from soda cooking or soda-anthraquinone pulping process. Most of the soda lignin comes from non-wood sources such as annual plants and agricultural residues. Due to hydrolytic cleavage, the sodium ligninis decomposed into smaller fragments, which are soluble in alkaline cooking liquor. A special feature of lignin obtained from non-woody materials is its high content of silicate and nitrogen [117]. Furthermore, the sodium lignin is very similar to natural lignin, that is, it does not contain sulfur. Therefore, it is widely used in many applications [20].

Organosolv lignin (OL):

This technical lignin is usually produced for research purposes [43]. It is derived from an organosolv pulping process, that is, through the use of organic solvents. Some characteristics of OL are: low molecular weight, high purity, and high quality. In addition, OL is highly soluble in organic solvents but hydrophobic in water. One of the disadvantages of this type of lignin is the high cost and complicated process required to obtain it [69]. Table 2 summarizes the classification, types, and different sources of lignin.

Organosolv pulping uses organic solvents for lignin solubilization. Acetic acid, formic acid, methanol, glycol, ethanol, etc. are solvents used in this technique. This treatment includes the cleavage of the α-aryl-ether and lignin-carbohydrate linkages, while the lower extent β-aryl-ether linkages are degraded [51]. Organosolv pulping causes the fragments to dissolve in the solvent. Table 2 summarizes the types of technical lignin based on extraction processes.

Table 2 Types of technical lignin based on extraction processes

Extraction process	Types	Extraction methods	Potential applications	References
Sulfur-bearing processes	Kraft lignin	Sulfate cooking process	Fertilizers, pesticides, carbon fibers, binders, and resins	[9]
	Lignosulfonates	Sulfite cooking process	Colloidal suspensions, stabilizers, dispersants, and plasticizers	
Sulfur-free processes	Soda/alkali lignin	Soda/soda-anthraquinone pulping process	Phenolic resins, polymers synthesis, dispersants, and animal nutrition	[33]
	Organosolv lignin	Organosolv pulping process, i.e by using organic solvents	Additives of inks, vanishes, and paints	[10]

2.4 Extraction Methods of Lignin

Several lignin extraction and separation methods have been developed such as alkaline, acidic, organosoly, hydrothermal, steam explosion, super critical CO_2, etc. Alkalinity and acidity are widely used methods to hydrolyze lignocellulosic biomass. Alkali treatments are carried out using NaOH, KOH, $Mg(OH)_2$ and $Ca(OH)_2$, while for acidic hydrolysis, some of the most commonly used reagents are HCl, H_2SO_4, and HNO_3 [42]. Alkaline method can break the ester bonds between lignin and other components such as celluloses and hemicelluloses. The focus of the acid treatment is the degradation of hemicellulose and cellulose parts, thereby producing lignin as a residual product.

In addition, there are other conventional and advanced extraction methods for lignocellulosic material such as ionic liquids, eutectic solvents, and supercritical CO_2. It is important to consider different criteria for choosing the most suitable lignin extraction method. These criteria include efficiency, costs, possible biological products, and environmental impact [63].

3 Lignin-Based Materials

Lignin is abundant in the plant kingdom and is the only biopolymer with polyarene content, which makes it unique for several applications. As a result of the paper-making process, high economic value was wasted, leading people to focus on sustainable economics. Lignin is a compound that lends itself to synthesize polymers from biomass, because of its low-cost production, high biocompatibility, and biodegradability, being a good substitute for petroleum-derived polymers.

3.1 Adsorption of Cationic Dyes

OL obtained from the delignification of rice straw has demonstrated strong adsorption of MB dye. The adsorption of OL is pH dependent at pH levels ranging from 5 and 9 [135]. A lignin-based activated carbon (LAC) obtained from black liquor of paper mill has demonstrated MB dye removal using aqueous media [39]. Phenolated sulfuric acid lignin (Ph-SAL) extracted from spent coffee grounds was assessed as a dye removal for wastewater purification. The efficiency of removal of Ph-SAL could reach 99.62% for MB dye at 100 mg/L of concentration [112]. Alkali-extracted lignin (AEL) obtained from corn stalks and posteriorly immersed in alkali solution demonstrates significant values of MB removal using pH 5 [38].

Activated carbon is known for its high adsorption capacity. Unfortunately, from the perspective of dye removal, this material causes some problems such as high cost, difficulty in separating the adsorbent and dye, and failure to regenerate the adsorbent. The production of phosphoric acid-activated carbon prepared from natural lignin at 500 °C seems to be the solution to avoid these problems in dye wastewater treatments. The magnetic lignin spheres (MLS) are composed of organosolv lignin, maleic anhydride, and tetrahydrofuran-Fe_3O_4 nanoparticles. MLS exhibits 31.23 mg/g and 17.62 mg/g of adsorption capacity for the removal of the dyes MB and Rhodamine B, respectively [67].

3.1.1 Adsorption of Anionic Dyes

Softwood kraft lignin using glycidyl trimethylammonium chloride (GTMAC) is used as a flocculant under alkaline aqueous conditions and is capable enhance the property of dye-containing wastewater treatment for removing anionic dyes. At optimal conditions of 70 °C, 1% lignin concentration, and GTMAC/lignin molar ratio 2/1, the lignin cationic part produces hydrophobic interactions with dye segments. The maximum percentage of dye removal of lignin-GTMAC is 87%, 95%, and 95% for the dyes Remazol Brillant Violet, Reactive Black, and Direct Yellow, respectively, in 100 mg/L of dye solution [62].

A copolymer containing lignin, dimethylamine, acetone, and formaldehyde (L-DAF) with a high cationicity of 2.55 mmol/g and molecular weight of 6143 g/mol was capable to remove three anionic dyes: Acid Black 1, Reactive Red 2, and Direct Red 23 with concentrations of 75, 50, and 35 mg/L from wastewater. These dyes were removed with an efficacy close to 100% using this cationic flocculant at pH 6.5 [37]. L-DAF follows two mechanisms for dye removal: flocculation by bridging and coagulation by charge neutralization, this last one is the predominant mechanism.

Lignin amination using Mannich reaction. This aminated lignin presents effective anionic dye adsorption. The Direct Blue 1 dye demonstrating a maximum adsorption capacity of 502.7 mg/g with a concentration of 50 mg/L [77].

Lignin polymerization immersed in acidic aqueous solution with [2-(methacryloyloxy) ethyl] trimethylammonium chloride (METAC) showed high molecular weight cationic lignin-METAC. The flocculation capacity for dye removal was studied in this lignin-based polymer. As a result, lignin-METAC was able to remove 98% and 94% (120 and 105 mg/L) of Reactive Black 5 (RB5) and Reactive Orange 16 (RO16), respectively [120].

Carbon composite lignin-based adsorbent material synthesized from glucose, calcium lignophosphate, and triethylene tetramide through a hydrothermal method was able to adsorb the dyes Congo red and Eriochrome blue black R. The removal capacity of this lignin-based adsorbent reaches 99% in 40 mg/L concentration of the dyes' solution [120].

Magnetic lignin-based adsorbent called Fe_3O_4/C-ACLS is an organic–inorganic composite capable to adsorb and remove dyes with high efficacy. Fe_3O_4/C-ACLS was able to remove 98% of Congo red, 92% of Titan yellow, and 99% of Eriochrome blue black R. Additionally, the lignin-based adsorbent material can have a good removal performance in a range of pH 5 to pH 9 and after five cycles of use, this adsorbent has a regeneration efficiency over 80% [52].

A bifunctional biosorbent of chitin/lignin was produced to treat dye wastewaters with the presence of Direct Blue 71 in aqueous solutions. This biosorbent presents 91% of removal efficiency and 40 mg/g of adsorption capacity at pH 8.4 [125]. Cationic and anionic dyes are also treated with lignin-based materials. Adsorption method is the main technology used, as shown in Fig. 7. Besides, Table 3 summarizes information about cationic and anionic dyes.

3.2   Lignin-Based Hydrogels

As a functionalized material, it can be used in wastewater decontamination processes, in this case, the removal of stains through the lignin hydrogels. Currently, a great amount of technique has been developed for lignin-based hydrogels. These hydrogels can be applied not only to the medical field but also for water bioremediation processes of pollutants such as dyes [99].

Polymeric matrix known as hydrogel is prepared from the association of multiple monomer bonds to form long chains of polymers that can to uptake large amounts
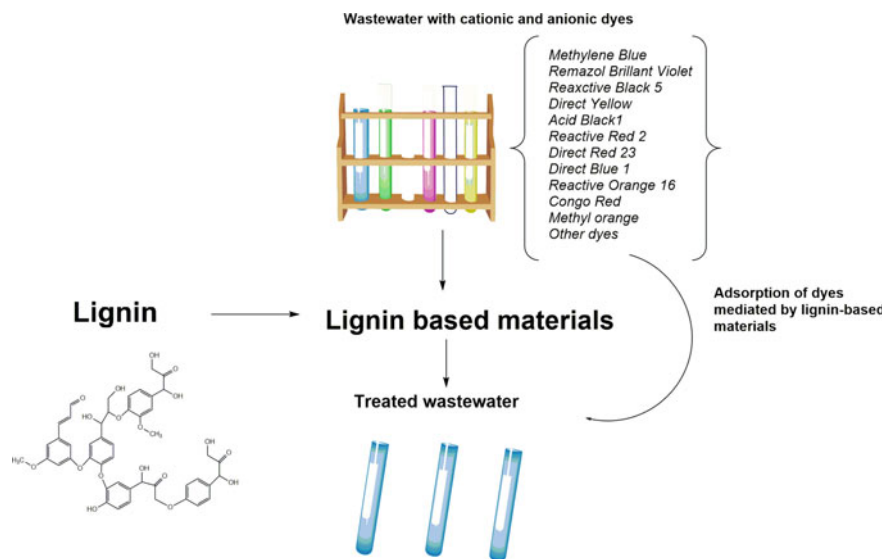
Fig. 7 Lignin-based materials applied to wastewater

of water. These can be of two types, chemical and physical depending on their interactions [44]. Chemical hydrogels build cross-linked networks from covalent bonds; here, the hydrophobic monomers become hydrophilic polymers. On the contrary, physical hydrogels resort to ionic and hydrophobic forces, hydrogen bonds, and Van der Walls interactions to maintain their structure. Its application ranges from tissue engineering, food packaging drug delivery systems to more specific applications in water management such as water retention in sandy soils in areas affected by droughts [90]. Hydrogels have been primarily synthesized from petroleum derivatives. Besides the high availability of lignin appears as an eco-friendly, low-cost option to produce hydrogels.

Dye wastewater contamination from the textile industry and other major industries into water tributaries represents a significant part of the environmental and energy crisis. Most dyes have high chromaticity and organic content, but more importantly azole groups and complex aromatic structures, the latter are difficult to degrade and as a result, they generate a serious problem of environmental pollution. Its high toxicity facilitates transfer to water, so the problem can worsen, affecting all living creatures including humans [100, 106]. Approximately 2% of the chemicals used in the industry are directly discharged into water sources [30, 129]. This situation affects directly aquatic life and the food chain with toxic dyes whose effects become carcinogenic and mutagenic even in small quantities [18, 75].

There are diverse techniques currently used for wastewater dye removal (Almasia et al. 2015). Nowadays, the technique most used due to its low-cost effects on water decolorization, with a simple design and operation, is adsorption. However, the process of obtaining adsorbents is complex and can be very expensive in energy,

Table 3 Lignin-based materials for adsorption of cationic and anionic dyes

Target dye to remove	Lignin-base adsorbent	Adsorption capacity/removal efficiency	pH	References
Cationic dyes				
Methylene blue	Organosolv lignin	40.02 mg/g	5.0–9.0	[135]
Methylene blue	Lignin-based activated carbon (LAC)	92.51 mg/g	–	[39]
Methylene blue	Phenolated sulfuric acid lignin (Ph-SAL)	93.45 mg/g 99.62%	–	[112]
Methylene blue	Alkali extracted lignin (AEL)	121.20 mg/g	5.0	[38]
Methylene blue	Tunisian activated lignin	147 mg/g	11	[64]
Methylene blue Rhodamine	Magnetic lignin spheres (MLS)	31.23 mg/g 17.62 mg/g	–	[67]
Anionic dyes				
Remazol brillant violet 5R (V5) Reactive black 5 (B5) Direct yellow 50 (Y50)	Lignin-GTMAC	87% 95% 95%	–	[62]
Acid black 1 Reactive red 2 Direct red 23	L-DAF	97.1% 98.3% 99.5%	6.5	[37]
Direct blue 1	Aminated CELF lignin	502.7 mg/g	–	[77]
Reactive black 5 (RB5) Reactive orange 16 (RO16)	cationic lignin-METAC	98% 94%	pH-independent	[121]
Congo red Eriochrome blue black R	Carbon composite lignin-based adsorbent	Reach 99%	7	[120]
Congo red Titan yellow Eriochrome blue black R	Fe3O4/C-ACLS	98% 92% 99%	5.0–9.0	[52]
Methyl orange	Lignin-based magnetic carbon nanoparticles	113 mg/g	5.0–9.0	

Table 3 (continued)

Target dye to remove	Lignin-base adsorbent	Adsorption capacity/removal efficiency	pH	References
Direct Blue 71	Chitin/lignin	40 mg/g 91%	8.4	[125]
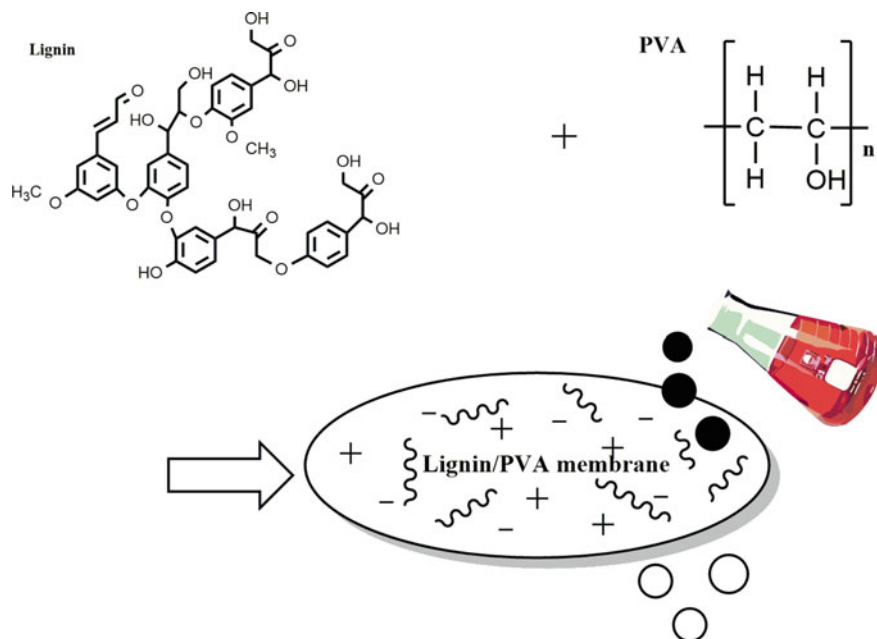
Fig. 8 Process of wastewater treatment by dye removal through lignin/PVA membrane

their high production costs have inclined the search toward a cheaper, green, and sustainable alternative. Lignin is a non-toxic biodegradable natural polymer option, from which hydrogels can be obtained [122].

Hydrogels from natural sources are currently made taking advantage of their biocompatibility and biodegradability [90]. The natural-based hydrogel now spreads to different types of industries such as biomedical implants, pharmaceuticals, food, and even the cosmetic industry. However, only lignin is an aromatic polymer capable of playing an adequate role in functional hydrogels [65, 98, 130].

3.2.1 Lignin Functionalization for Hydrogel Structures

Lignin composition is important because its functional groups represent active sites available to be chemically modified to improve the optimization of the lignin [21, 31,

84]. Under process conditions called biorefining, the addition of atypical components promotes the recovery and chemical conversion of lignin. One of the characteristics of monomeric lignin in improving its extraction efficiency is its flexibility; improving this characteristic through genetic manipulation of biosynthesis pathways or for crops has generated lignin feedstocks whose properties are favorable for hydrogels and product development [95].

The Preparation Procedure of Lignin Hydrogels

Functionalization to improve the performance of lignin for practical applications through chemical modification has been performed previously. Regardless of the monomers selected to compose a hydrogel, the formation of this material is a polymerization reaction that begins due to an initiating agent. This initiator agent triggers the polymerization. When at least two different monomers are used, the reaction is a copolymerization. When it occurs in the block, an initiator and a cross-linking agent are added to the monomers. On the other hand, by dissolution, adding solvents for subsequent precipitation and cross-linking of monomers, cross-linking agents or a solvated gel can also be used [60].

Polymerization Process and Interpenetrating Polymer Network (IPNs)

IPNs are a combination of two or more polymers in networks where a partial interlacing on the molecular scale is present in the matrix [57]. Lignin is used in new hydrogels to improve its functionality, being synthesized by interpenetration and or semi-interpenetration [91]. The fundamental mechanism for its synthesis corresponds to free radical polymerization. The initiator helps the formation of radicals from the phenolic hydroxyl groups of lignin, which subsequently react with the monomer chains and/or polymers chains that are part of the grafted structure [83].

Grafted Lignin Monomers

The synthesis of lignin-based hydrogels uses IPN and cross-linking techniques. Some examples of recently synthesized structures are as follows: Hydrogels with an IPN structure were synthesized from graft copolymerization technique, employing monomers as starch, acrylamide, and lignin/peat, with H_2O_2 as initiator, in the presence of N, N'-methylene-bisacrylamide (MBAAm) as a cross-linker. This hydrogel was used for simulated contaminated water with metal ions. Xanthan gum widely used in the food industry has also been used in conjunction with lignin to form xanthan/lignin hydrogels. This superabsorbent was made from a microbial polysaccharide and varieties of lignin from epoxy-modified resin, aspen Wood, and annual fiber crops using epichloridrine as a crossing agent [97].

Other technologies at the nanocomposite level enhance the adsorption capacity of lignin-based hydrogels in the function of their changing cation exchange capacity. The cavitation process was used during their synthesis [3, 7]. The nano-clay Montmorillonite (MMT), with a layer of aluminum silicate, is one of the most used due to its OH- reactive groups and exchangeable cations. Many studies suggested the incorporation of this clay into a matrix of hydrogels to verify the remarkable efficiency of clay–polymer composites. Acrylamide and N-isopropyl acrylamide were synthesized onto lignin to form a lignin-g-p (AM-co-NIPAM)/MMT hydrogel through free radical polymerization for MB removal. Compared with the matrix without lignin, this hydrogel has greater properties and a high degree of MB removal rate at neutral pH [123].

Today, highly ecological processes are developed. Lignocellulose and N-methyl morpholine-N-oxide (NMMO) have been cross-linked to form Si–O-C cross-links over the fibrils of lignocellulose. This one reported antiultraviolet weathering and biocompatibility and biodegradability advantages over previously reported adsorbents, some of the hydrogels [133]. Besides, the synthesis of cross-linked hydrogel called poly (methyl vinyl ether-co-maleic acid) uses a thermal method through a process without non-organic solvents, or potentially toxic reagents. Besides, they report better absorption than other hydrogels and a greater MB retention capacity, reason by which they can be applied as superabsorbent materials. Lignin will undoubtedly enhance the hydrogel's characteristics [28].

3.2.2 Properties of Lignin-Based Hydrogels

Mechanical Properties

Rheological properties: The Dynamic Storage Modulus (G') represents the stiffness and Loss Modulus (G") the energy dissipation of the hydrogel. The lignin content is proportional to storage modulus, and loss modulus as well [81, 113]. These two parameters will vary according to the structure of the lignin. The hydrogel rheological properties are measured at room temperature. The cross-linking degree increases the rigidness of the lignin structure. This characteristic leads to heat dissipation, which gives way to the movement of a segment of the lignin chain. Consequently, G" increases as the lignin content increases in the hydrogel [78]. Those copolymers that have a thermal response have small G' and G" values at low temperatures. When G' has a value much lower than G", the copolymer is in a liquid state. When the copolymer reaches a crossover temperature G' is higher than G", at this temperature which is usually between 31.5 and 33 C°, the hydrogel is already formed [26].

Tensile strength: Hydrogels containing lignin possess the best tensile strength. Lignin can be associated as a structure similar to nanoparticle, precipitating into a rigid structure when it is part of a network of lignocellulose hydrogels. Similarly, intermolecular hydrogen bonds are formed [81].

Porosity and Morphology

When the hydrogels show a rough structure on the surface, a sheet-like structure; the porosity increases to the maximum of the lignin content, and after that, the pores of the hydrogel disappear completely. Therefore, the porosity will depend on lignin concentration in hydrogel. Any gel at 5% (w/w) or higher exhibits compact, and irregular pores. These pores will cause problems in the texture of the hydrogel [82, 110]. More uniform, smaller pores and, therefore, larger surface area can be seen in hydrogels formed with lignin and cellulose compared with lignin-free hydrogels [134].

Water Retention and Absorption

Both water absorption and retention depend on the structure, size, and morphology of the surface. The swelling capacity varies depending on the hydroxyl, carboxyl chemical groups, and the size of the pores. Therefore, the larger the pores, the higher the swelling ratios. In cellulose and lignin/cellulose hydrogels, the less cellulose the less the diffusion resistance [55, 134]. The primary structure of the lignin also influences the hydrogel structure. The grafting lignosulphonate can encapsulate more drugs because it increases the active sites and the porosity of the three-dimensional hydrogel structure [121].

Biodegradability

Lignin is an abundant organic compound nature that can be easily used to improve soil quality. Different properties of the hydrogels were tested, by resulting that clay and moisture content were reduced due to the loss of the hydrogel during burial period. On the other hand, the phenolic substructures present in the hydrogels were reduced due to the attack of ligninolytic fungi. Therefore, the use of hydrogel can protect the plant from these fungi [71, 90, 132].

3.3 Lignin Membranes

Lignin membrane is a new concept of scientific development. It has previously been demonstrated that lignin can interact with various polymers, including synthetics and biopolymers, forming more stable polymer-based structures [23]. Due to the availability of this compound, the use of lignin-based membrane to remove des has many advantages.

3.3.1   Poly Vinyl Alcohol (PVA) Membrane and Lignin

Polyvinyl alcohol is a water-soluble polymer with great hydrophobicity and chemical stability. It has been proven to have good film-forming ability. The problem is its high solubility in water. Hybridization with lignin improves the conditions of both compounds and promotes the formation of nanomaterials employed to remove dyes in wastewaters [45, 115]. This time instead of focusing on increasing adsorption capacities, the focus is on desorption and its recycling performance. Therefore, the membrane can be used more than once after drying in a vacuum oven [133].

This lignin/PVA membrane prepared by electrospinning is cost-efficient and has high adsorption performance in water bioremediation. PVA as a co-spinning polymer can improve spinning stability and nanofiber quality. In the composition of the nanofiber membrane, the structure was very strong. The adsorption capacity is not significantly reduced in five cycles (80% of the capacity is remained), so the membrane can be recycled, and has high performance for water purification [133] as shows Fig. 8.

3.3.2   Lignin Sulfonate/Cellulose Functionalized Nanofiltration Membrane

The researchers created an NF270 nanofiltration membrane with an area of 40 cm^2 on a circular metal cell in the shape of an O-ring. The aqueous solution of lignin sulfonate was spread over the surface of the nanomembrane, enough to cover the surface of the membrane. Subsequently, it was placed in the oven at 90 °C for about 2 h. Then, the functionalized lignin film is extracted from the circular metal cell, rinsed with deionized water to remove lignin residues. The presence of lignin in the membrane is observable due to the appearance of a faint brown color on the surface of the membrane. After the second rinse cycle, they showed 90% of the initial water flow. Besides, this membrane showed potential antifouling surface applications [22]. Finally, there is still a lot of work to be done for the structure using green technology, membranes, hydrogels, and eco-friendly, low-cost, biocompatible, and biodegradable solutions.

4   Dyes Degraded by Lignin Decomposing Enzymes

In recent years, due to the high redox potential and prospective industrial application of lignin decomposing enzymes, microorganisms can degrade a mixture of several heterogeneous organic compounds as dyes. Each dye can be removed based on the microorganisms selected. One of the main concerns regarding dye removal may be due to the inclusion of sulfonation, carboxylation, and -N = N- functional groups with different chemical bonds [69]. The most commonly used microorganisms are bacteria and fungi.

Pseudomonas, *Aeromonas*, *Bacillus* bacteria have been commonly reported to decolorize bacteria under anaerobic and aerobic conditions [89]. *Enterococcus* and *Enterobacteriaceae* bacteria such as *Citrobacter*, *Klebsiella*, and *Enterobacter* are used to remove reactive dyes [133]. However, even if bacteria can eliminate azo dyes, they can produce harmful and carcinogenic aromatic aryl amine during anaerobic phase [96]. Many studies have combined anaerobic-aerobic treatment, producing mineralization and reduction of azo dyes. This is carried out in two steps: rapid formation of anionic radicals and subsequently the production of the stable dianion component. Nevertheless, if the aromatic amines formed in the anaerobic phase are not rapidly metabolized during the aerobic phase, they will form colored recalcitrant compounds [69, 89].

In the aerobic phase against organic compounds, oxygen is introduced into the aromatic ring because of the catalytic action of enzymes [29]. The direct coupling of oxygen is accomplished by reduced flavin, but the electron donor is NADH or NADPH [74]. Therefore, the importance lies in the use of enzymes to cleave reactive bonds, thereby interrupting the aromatic chain through the redox process of these complex dyes. In addition, it is reported that bacteria (such as *Proteus mirabilis*) under static conditions have a higher decolorization rate than under shaking conditions [73], which is due to the presence of excessive oxygen. The oxygen is preferred for the electrons instead of the azo dyes.

On the other hand, fungi have been found to be the main microorganism that can degrade and mineralize azo dyes. This type of microorganism has a high tolerance to the toxicity of dyes as well as a strong ability to mineralize various persistent organic pollutants in water and non-aqueous media and has the ability to produce non-specific and non-stereoselective oxidases enzymes [96]. Fungi are divided into three categories according to their morphology: white, brown, and mild degradation fungi [61]. Fungi are knowing to degrade lignocellulosic substrates, effectuated by the ligninolytic enzymes such as laccase, manganese peroxidase, and lignin peroxidase.

4.1 Lignin-Degrading Enzymes

White-rot fungi belong to basidiomycetes class, which mineralize lignin as a result of the oxidative enzymes produced [36]. White-rot fungi produce lignin-decomposing enzymes in their secondary metabolism, because the required energy cannot be obtained during lignin oxidation [126]. The expansion enhanced the substrate of ligninolytic enzymes and process electron movement, white-rot fungi produce and release redox mediators [96]. Redox mediators are compounds that have the ability to accept and donate electrons.

Veratryl alcohol stimulates the oxidation of different substrates and is produced as a secondary metabolite of white-rot fungi. Examples of relevant species of white-rot fungi are *Ganoderma lucidum*, *Phanerochaete chryrosporium*, *Pleurotus ostreatus,* and *Irpex lacteus* [96, 128]. As shown in Table 4, white-rot fungi are classified into four categories: the composition and secretion of lignin decomposing enzymes [12].

Table 4 Groups of enzymes from white-rot fungi

Group	White rot fungi	Ligninolytic enzyme	References
A	*Pleurotus ostreatus* and *Pleurotus eryngii, Trametes versicolor, Ganoderma lucidum,* and *Schyzophylum commune*	Lignin peroxidase , manganese peroxidase, and laccase	[5, 6, 48, 92]
B	*Pycnoporus cinnabarinus* and *Phlebia radiata*	Manganese peroxidase and laccase	[5, 109]
C	*Phanerochaete chrysosporium*	Lignin peroxidase and manganese peroxidase	[5, 24]
D	*Dichomitus squalens*	Lignin peroxidase and laccase	[5, 39]

A key to increase white-rot fungi thrive is the production of enzymes. Basidiomycetes is one of these enzymes that can grow in lignocellulosic biomass such as rice straw, banana waste, corn cobs, sugarcane bagasse, sawdust, and wheat straw. Some characteristics, such as strain, substrate composition, ion concentration, and fungi culture conditions, are strongly related with lignin decomposing enzyme production increase [32]. To enhance fungi thrive, there is a process known as submerged fermentation. It is defined as fermentation in the presence of excess water [107], which leads to adequate contact and supply of nutrients for white-rot fungi.

Lignin-degrading enzymes have been classified into lignin peroxidase, manganese peroxidase, and laccase [50]. As part of the phenol oxidase, laccase was found. On other hand, heme peroxidase includes lignin peroxidase, manganese peroxidase (MnP), versatile peroxidase, and dyP-type peroxidases. These enzymes are followed by synergistic effect of several auxiliary enzymes that produce hydrogen peroxide (H_2O_2) required by the peroxidases [36] to further enhance the process, including veratryl alcohol oxidase, glucose 1-oxidase, cellobiose dehydrogenase, among others [128].

4.1.1 Ligninase

Lignin peroxidase also referred as ligninase was discovered in 1983 from the white-rot fungi, known as *P. chrysosporium* [86]. It possesses a pH 3–4.5, which is capable to degrade a significant number of aromatic structures and high redox potential. Ligninase usually employs a catalytic mechanism for which H_2O_2 is required [86]. Besides, high redox compounds can be oxidized using lignin peroxidase [94].

Lignin peroxidase can remain inactive during the oxidation reaction of phenolic compounds, thereby reducing its enzyme activity quickly. On the other hand, the oxidation process of veratryl as shown in Fig. 9 will act as a protector of lignin peroxidase from the inactivation, potentially makes enzymes more active.
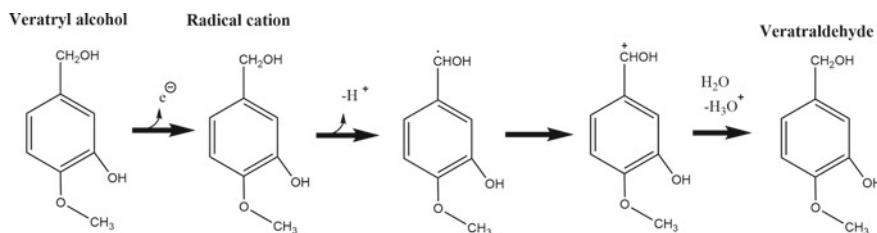
Fig. 9 Decay of veratryl alcohol radical cation by deprotonation

Similarly, the free radical cations of veratryl alcohol can act as an oxidation mediator for secondary substrates that are not normally oxidized using ligninase [128]. Veratryl alcohol radical cation intermediate lifetime is very important to consider it as a redox mediator. Only free radical cation with a sufficient lifetime can diffuse out of the enzyme to induce the oxidation of the lignin polymer [8]. The free radical cations of veratryl alcohol are decomposed by deprotonation at Cα, which is considered to be the reaction of alkyl aromatic radical cations, to form veratraldehyde. Lignin peroxidase activity can be measured at 310 nm during the process shown in Fig. 9 [128].

In general, laccase removes azo dyes with a radical free mechanism that forms phenolic compounds [15]. First, the phenolic group in the azo dye is oxidized, generating phenoxy radical, sequentially followed by oxidation to a carbonium ion [136]. Then, water makes a nucleophilic attack (NuA) on the phenolic ring carbon next to the azo group, generating two compounds, one of which is phenyldiazene and the other is quinone. The free radicals formed in the first step react with quinone instead of being oxidized producing other compounds containing azo groups.

Lignin peroxidase is a mechanism for removing azo dyes similar to phenol oxidase. The mechanism of peroxidase begins with two consecutive one-electron oxidations of the phenolic ring by the H_2O_2-oxidized form of lignin peroxidase to produce carbonium ions. The NuA of water occurs on the carbon with an azo bond and forms the same type of compounds as the laccase mechanism. Many studies have shown that the O_2 and H_2O_2 forms of peroxidase can oxidize phenyldiazene to produce the corresponding radical [19]. Phenyldiazenyl is unstable and expels the diazonium bonds in the form of molecular nitrogen generating a phenyl radical. It is proposed to use oxygen to scavenge phenyl radicals to obtain the corresponding phenyl hydroperoxides. The H_2O_2 in the degradation mechanism of lignin peroxidase is crucial for the biodegradation with peroxidases enzymes. If the H_2O_2 concentration also increases, the degradation rate of the dye will increase until the optimal H_2O_2 concentration is reached.

However, the lignin peroxidases and laccases despite are considered effective catalysts for many compounds [14], one strategy to increase the dye degradation is the cell immobilization. This technique offers a high maintenance biomass concentration, protection from the toxic effects, and can be reused multiple times [89], and it is possible to perform reactions in some reactive dyes. Some studies reported that the

growth of fungi can be inhibited despite the presence of a nutrient medium. The presence of lignin into the medium slightly increased the growth rate [79]. Another important factor for fungal growth is the pH. Low pH values of fungal biomass produce a positive charge, where the anionic groups can be attached [105].

4.1.2 Manganese Peroxidase (MnP)

In 1984, Kuwahara was the first to found MnP in *P. chrysosporium* [94]. It is a glycoprotein with a molecular mass between 38 and 62.5 kDa, composed of 330–370 amino acids, and contains a leader peptide of 21–29 amino acids [49]. MnP has five disulfide bridges, of which one of those bridges is the bonding site of manganese. The catalytic cycle is similar to lignin peroxidase and requires H_2O_2 [86]. The structure of manganese peroxidase contains a single pair of domains with the heme group in the middle such as lignin peroxidase. MnP has been studied in dye removal property against R. Orange 16, M. Blue 13, M. Yellow 3, A. Blue 129, A. Green 27, A. Red 6 and others, was reported [58].

4.1.3 Versatile Peroxidase (VP)

VP has interesting characteristics due to the strong compatibility with Mn and dyes [80]. At first, the *Pleurotus* versatile peroxidase isoenzymes were described as manganese peroxidases isoenzymes but then were recognized as new peroxidase type [101]. These enzymes have properties of lignin peroxidase and manganese peroxidase, designated as "hybrid enzymes" [61]. Besides, VP enzymes have been employed against several dyes. It showed a significant result against many azo dyes such as Evans blue, Amido black 10B, and Guinea Green B [47].

4.1.4 Laccase

Laccase has been studied for long time [72]. The *Rhus vernicifera* tree was the first raw material to extract laccases [94]. Laccases present in their active site, three types as shown in Table 5.

In comparison to lignin peroxidase, laccase does not require H_2O_2 in its catalytic cycle, this enzyme employs oxygen as an oxidizing agent. In general, laccase generates four $1e^-$ oxidations of substrate followed by two $2e^-$ reduction of oxygen to H_2O. Several investigations have determined that laccase can remove dyes such as Reactive Black 5, Orange II, Tartrazine, Indigo Carmine, and Cresol Red [12].

Table 5 Copper atoms in the Laccase structure

Type	Copper (Cu) atoms per molecule	Spectroscopic and/or magnetic properties	References
I	1	Paramagnetic blue Cu with A = 600-610 nm in the oxidized form	[76, 94]
II	1	Paramagnetic normal copper with absorbance in the visible region	
III	2	Diamagnetic spin-coupled Cu–Cu pair with A = 330 nm in the oxidized form	

5   Conclusions

As a solution for dye wastewater treatment, novel technologies have been developed. Lignin-based materials have adsorption and desorption capabilities, recyclability, biodegradability, and non-toxic properties, so they can be used in a variety of ways. These materials represent an environmentally friendly method to remove dyes using aqueous solutions, monolayers, membranes, and hydrogels. The variability of the lignin structure is a priority for the industry due to the economic cost and the high capacity to produce new effective dye removal technologies. Besides, chemical groups from lignin structure make it, an ideal candidate to form bonds with another compound, enhancing its performance. The lignin/PVA membrane is a clear example of synergy, which shows great results, reducing the wastewater due to its adsorption capacity and high recyclable property. In addition, lignin-degrading enzymes are a kind of fungi, which has a lot of attention in order to minimize environmental damage caused by dyes. However, due to environmental factors, the difficulty of this biological treatment lies in the discovery of industrial-scale production of enzymes, and environmental factors are considered to be critical to microorganisms.

References

1. Abdelhamid HN, Zou X (2018) Template-free and room temperature synthesis of hierarchical porous zeolitic imidazolate framework nanoparticles and their dye and CO2 sorption. Green Chem 20:1074–1084. https://doi.org/10.1039/c7gc03805d
2. Agrios GN (2005) How pathogens attack plants. Plant Pathol 175–205.https://doi.org/10.1016/b978-0-08-047378-9.50011-7
3. Alamri H, Low IM (2012) Effect of water absorption on the mechanical properties of nano-filler reinforced epoxy nanocomposites. Mater Des 42:214–222
4. Alzagameem A, Klein SE, Bergs M et al (2019) Antimicrobial activity of lignin and lignin-derived cellulose and chitosan composites against selected pathogenic and spoilage microorganisms. Polymers (Basel) 11:670. https://doi.org/10.3390/polym11040670
5. Asgher M, Shahid M, Kamal S, Iqbal HMN (2014) Recent trends and valorization of immobilization strategies and ligninolytic enzymes by industrial biotechnology. J Mol Catal B Enzym 101:56–66. https://doi.org/10.1016/j.molcatb.2013.12.016

6. Asgher M, Sharif Y, Bhatti HN (2010) Enhanced production of ligninolytic enzymes by *Ganoderma lucidum IBL-06* using lignocellulosic agricultural wastes. Int J Chem Reactor Eng 8:1–17. https://doi.org/10.2202/1542-6580.2203

7. Azeez AA, Rhee KY, Park SJ, Hui D (2013) Epoxy clay nanocomposites –processing, properties, and applications: a review. Compos Part B-Eng 45:308–320

8. Baciocchi E, Bietti M, Francesca Gerini M, Lanzalunga O (2002) The mediation of veratryl alcohol in oxidations promoted by lignin peroxidase: the lifetime of veratryl alcohol radical cation. Biochem Biophys Res Commun 293:832–835. https://doi.org/10.1016/s0006-291x(02)00306-6

9. Bajwa DS, Pourhashem G, Ullah AH, Bajwa SG (2019) A concise review of current lignin production, applications, products and their environment impact. Ind Crops Prod 139:111526. https://doi.org/10.1016/j.indcrop.2019.111526

10. Bhat R, Khalil HPSA, Karim AA (2009) Exploring the antioxidant potential of lignin isolated from black liquor of oil palm waste. Comptes Rendus - Biol 332:827–831. https://doi.org/10.1016/j.crvi.2009.05.004

11. Bilal M, Asgher M, Parra-Saldivar R, Hu H, Wang W, Zhang X, Iqbal HMN (2017) Immobilized ligninolytic enzymes: an innovative and environmental responsive technology to tackle dye-based industrial pollutants – a review. Sci Total Environ 576:646–659. https://doi.org/10.1016/j.scitotenv.2016.10.137

12. Blánquez A, Rodríguez J, Brissos V, Mendes S, Martins LO, Ball AS, Arias ME, Hernández M (2018) Decolorization and detoxification of textile dyes using a versatile Streptomyces laccase-natural mediator system. Saudi J Biol Sci 26(5):913–920. https://doi.org/10.1016/j.sjbs.2018.05.020

13. Brzonova I (2017) Biodegradation and biomodification of lignocellulose with a main focus on lignin. Theses and dissertations, 2180

14. Chacko TJ, Subramaniam K (2011) Enzymatic degradation of Azo dyes – a review. Int J Environ Sci 1:1250–1260

15. Chavan RB (2011) Environmentally friendly dyes. In: Handbook of textile and industrial dyeing, pp 515–561.https://doi.org/10.1533/9780857093974.2.515

16. Chen H (2015) Lignocellulose biorefinery feedstock engineering. In: Lignocellulose Biorefinery Engineering. Elsevier, pp 37–86

17. Cheng H, Feng Q, Liao C, Liu Y, Wu D, Wang Q (2016) Removal of MB with hemicellulose/clay hybrid hydrogels. Chinese J Polym Sci 34:709–719

18. Chivukula M, Spadaro JT, Renganathan V (1995) Lignin peroxidase-catalyzed oxidation of sulfonated Azo dyes generates novel sulfophenyl hydroperoxides. Biochemistry 34:7765–7772. https://doi.org/10.1021/bi00023a024

19. Chung H, Washburn NR (2016) Extraction and types of lignin. In: Lignin in polymer composites. Elsevier, pp 13–25

20. Ciolacu D, Cazacu G (2018) New green hydrogels based on lignin. J Nanosci Nanotechnol 18:2811–2822

21. Colburn A, Vogler RJ, Patel A, Bezold M, Craven J, Liu C, Bhattacharyya D (2019) Composite membranes derived from cellulose and lignin sulfonate for selective separations and antifouling aspects. Nanomaterials (Basel) 9(6):867. https://doi.org/10.3390/nano9060867.PMID:31181627;PMCID:PMC6630825

22. Collins MN, Nechifor M, Tanas MZ, F, McLoughlin A, Stró (2019) Valorization of lignin in polymer and composite systems for advanced engineering applications-a review. Int J Biol Macromol 131:828–849

23. Da Re V, Papinutti L, Forchiassin F, Levin L (2010) Biobleaching of loblolly pine kraft pulp with *Trametes trogii* culture fluids followed by a peroxide stage. Application of Doehlert experimental design to evaluate process parameters. Enzyme Microb Technol 46:281–286. https://doi.org/10.1016/j.enzmictec.2009.12.006

24. De Gisi S, Lofrano G, Grassi M, Notarnicola M (2016) Characteristics and adsorption capacities of low-cost sorbents for wastewater treatment: a review. Sustain Mater Technol 9:10–40. https://doi.org/10.1016/j.susmat.2016.06.002

25. Diao B, Zhang Z, Zhu J, Li J (2014) Biomass-based thermogelling copolymers consisting of lignin and grafted poly(N-isopropyl acrylamide), poly(ethylene glycol), and poly(propylene glycol). RSC Adv 4:42996–43003

26. Domínguez-Robles J, Larrañeta E, Fong ML et al (2020) Lignin/poly(butylene succinate) composites with antioxidant and antibacterial properties for potential biomedical applications. Int J Biol Macromol 145:92–99. https://doi.org/10.1016/j.ijbiomac.2019.12.146

27. Domínguez-Robles J, Peresin MS, Tamminen T, Rodríguez A, Larrañeta E, Jääskeläinen AS (2017) Lignin based hydrogels with "super-swelling" capacities for dye removal. Int J Biol Macromol 115:1249–1259. https://doi.org/10.1016/j.ijbiomac.2018.04.044 Epub 2018 Apr 12 PMID: 29655884

28. Dos Santos AB, Cervantes FJ, Van Lier JB (2007) Review paper on current technologies for decolourisation of textile wastewaters: Perspectives for anaerobic biotechnology. Biores Technol 98:2369–2385. https://doi.org/10.1016/j.biortech.2006.11.013RAJH

29. Dou X, Li P, Zhang D, Feng CL (2012) C2-symmetric benzene-based hydrogels with unique layered structures for controllable organic dye adsorption. Soft Matter 8:3231–3238

30. Duval A, Lawoko M (2014) A review on lignin-based polymeric, micro-and nanostructured materials. React Funct Polym 85:78–96

31. Elisashvili V, Penninckx M, Kachlishvili E, Tsiklauri N, Metreveli E, Kharziani T, Kvesitadze G (2008) *Lentinus edodes* and *Pleurotus species* lignocellulolytic enzymes activity in submerged and solid-state fermentation of lignocellulosic wastes of different composition. Biores Technol 99:457–462. https://doi.org/10.1016/j.biortech.2007.01.011

32. Eloy de Souza R, José Borges Gomes F, Oliveira Brito E et al (2020) A review on lignin sources and uses. https://doi.org/10.15406/jabb.2020.07.00222

33. Elseify LA, Midani M, Shihata LA, El-Mously H (2019) Review on cellulosic fibers extracted from date palms (Phoenix Dactylifera L.) and their applications. Cellulose 26:2209–2232. https://doi.org/10.1007/s10570-019-02259-6

34. Exbrayat JM (2016) Microscopy: light microscopy and histochemical methods. In: Encyclopedia of food and health (pp 715–723). https://doi.org/10.1016/B978-0-12-384947-2.00460-8

35. Falade AO, Nwodo UU, Iweriebor BC, Green E, Mabinya LV, Okoh AI (2016) Lignin peroxidase functionalities and prospective applications. Microbiology Open 6:1–14. https://doi.org/10.1002/mbo3.394

36. Fang R, Cheng X, Xu X (2010) Synthesis of lignin-base cationic flocculant and its application in removing anionic azo-dyes from simulated wastewater. Biores Technol 101(19):7323–7329. https://doi.org/10.1016/j.biortech.2010.04.094

37. Feng Q, Cheng H, Li J, Wang P, Xie Y (2014) Adsorption behavior of basic dye from aqueous solution onto alkali extracted lignin. BioResources 9(2):3602–3612. https://doi.org/10.15376/biores.9.2.3602-3612

38. Fu K, Yue Q, Gao B, Sun Y, Zhu L (2013) Preparation, characterization and application of lignin-based activated carbon from black liquor lignin by steam activation. Chem Eng J 228:1074–1082. https://doi.org/10.1016/j.cej.2013.05.028

39. Garmaroody ER, Resalati H, Fardim P, Hosseini SZ, Rahnama K, Saraeeyan AR, Mirshokraee SA (2011) The effects of fungi pre-treatment of poplar chips on the kraft fiber properties. Biores Technol 102:4165–4170. https://doi.org/10.1016/j.biortech.2010.12.054

40. Gordobil O, Herrera R, Yahyaoui M, İ S, Kaya M, Labidi J (2018) Potential use of kraft and organosolv lignins as a natural additive for healthcare products. RSC Adv 8:24525–24533. https://doi.org/10.1039/c8ra02255k

41. Guangyin Z, Youcai Z (2017) Harvest of bioenergy from sewage sludge by anaerobic digestion. In: Pollution control and resource recovery. Elsevier, pp 181–273

42. Hashmi SF, Meriö-Talvio H, Hakonen KJ, Ruuttunen K, Sixta H (2017) Hydrothermolysis of organosolv lignin for the production of bio-oil rich in monoaromatic phenolic compounds. Fuel Process Technol 168:74–83. https://doi.org/10.1016/j.fuproc.2017.09.005

43. Hoffman AS (2002) Hydrogels for biomedical applications. Adv Drug Deliv Rev 2002:18–23

44. Hu XQ, Ye DZ, Tang JB, Zhang LJ (2016) From waste to functional additives: thermal stabilizing and toughening PVA with lignin. RSC Adv 6:3797–13802

45. Huang J, Shiyu F, Gan L (2019) Structure and characteristics of lignin. In: Lignin chemistry and applications. Elsevier, pp 25–50. https://doi.org/10.1016/b978-0-12-813941-7.00002-3

46. Ilić Đurđić K, Ostafe R, Đurđević Đelmaš A, Popović N, Schillberg S, Fischer R, Prodanović R (2020) Saturation mutagenesis to improve the degradation of azo dyes by versatile peroxidase and application in form of VP-coated yeast cell walls. Enzyme Microb Technol 109509. https://doi.org/10.1016/j.enzmictec.2020.109509

47. Iqbal HMN, Asgher M, Bhatti HN (2011) Optimization of physical and nutritional factors for synthesis of lignin degrading enzymes by a novel strain of *Trametes versicolor*. BioResources 6:1273–1287

48. Janusz G, Kucharzyk KH, Pawlik A, Staszczak M, Paszczynski AJ (2013) Fungal laccase, manganese peroxidase and lignin peroxidase: gene expression and regulation. Enzyme Microb Technol 52:1–12. https://doi.org/10.1016/j.enzmictec.2012.10.003

49. Janusz G, Pawlik A, Sulej J, Ś U, Jarosz-Wilko A, Paszczy A (2017) Lignin degradation: microorganisms, enzymes involved, genomes analysis and evolution. FEMS Microbiol Rev 41(6):941–962. https://doi.org/10.1093/femsre/fux049

50. Jasiukaityt E, Huš M, Grilc M, Likozar B (2020) Acid-catalysed α-O-4 aryl-ether bond cleavage in methanol/(aqueous) ethanol: understanding depolymerisation of a lignin model compound during organosolv pretreatment. Sci Rep 10:1–12. https://doi.org/10.1038/s41598-020-67787-9

51. Jiang C, Wang X, Qin D, Da W, Hou B, Hao C, Wu J (2019) Construction of magnetic lignin-based adsorbent and its adsorption properties for dyes. J Hazard Mater 369:50–61. https://doi.org/10.1016/j.jhazmat.2019.02.021

52. Johansen KS (2016) Lytic polysaccharide monooxygenases: the microbial power tool for lignocellulose degradation. Trends Plant Sci 21:926–936. https://doi.org/10.1016/j.tplants.2016.07.012

53. Kadirvelu K, Kavipriya M, Karthika C, Radhika M, Vennilamani N, Pattabhi S (2003) Utilization of various agricultural wastes for activated carbon preparation and application for the removal of dyes and metal ions from aqueous solutions. Biores Tech 87:129–132. https://doi.org/10.1016/s0960-8524(02)00201-8

54. Kalinoski RM, Shi J (2019) Hydrogels derived from lignocellulosic compounds: evaluation of the compositional, structural, mechanical, and antimicrobial properties. Ind Crop Prod 128:323–330

55. Kang X, Kirui A, Dickwella Widanage MC, Mentink-Vigier F, Cosgrove DJ, Wang T (2019) Lignin-polysaccharide interactions in plant secondary cell walls revealed by solid-state NMR. Nat Commun 10:1–9. https://doi.org/10.1038/s41467-018-08252-0

56. Karak N (2012) Fundamentals of polymers. In: Vegetable oil-based polymers. Elsevier, pp 1–30. https://doi.org/10.1533/9780857097149.1.

57. Kariminiaae-Hamedaani H-R, Sakurai A, Sakakibara M (2007) Decolorization of synthetic dyes by a new manganese peroxidase-producing white rot fungus. Dyes Pigm 72(2):157–162. https://doi.org/10.1016/j.dyepig.2005.08.010

58. Katheresan V, Kansedo J, Lau SY (2018) Efficiency of various recent wastewater dye removal methods: a review. J Environ Chem Eng 6(4):4676–4697. https://doi.org/10.1016/j.jece.2018.06.060

59. Katime D, Katime O, Katime I (2004). The intelligent materials of this millennium: macromolecular hydrogels: synthesis, properties, and applications. Bilbao, Servicio Editorial de la Universidad del País Vasco (UPV/EHU) 1:8483736373

60. Kist CP, Scherer CE, Soares M, Rodrigues MB (2020) Biodegradation of nitroaromatic compounds in Red Water by white rot fungi *Pleurotus ostreatus* and *floridae*. Ambiente & Água - Interdiscip J Appl Sci 15. https://doi.org/10.4136/ambi-agua.2594

61. Knop D, Levinson D, Makovitzki A, Agami A, Lerer E, Mimran A, Yarden O, Hadar Y (2016) Limits of versatility of versatile peroxidase. Appl Environ Microbiol 82:4070–4080. https://doi.org/10.1128/aem.00743-16

62. Kopecek J (2007) Hydrogel biomaterials: a smart future? Biomaterials 28:5185–5192
63. Kumar S, Mohanty AK, Erickson L, Misra M (2009) Lignin and its applications with polymers. J Biobased Mater Bioenergy 3(1):1–24. https://doi.org/10.1166/jbmb.2009.1001
64. Kumar AK, Sharma S (2017) Recent updates on different methods of pretreatment of lignocel-lulosic feedstocks: a review. Bioresour Bioprocess 4:7. https://doi.org/10.1186/s40643-017-0137-9
65. Li Y, Wu M, Wang B, Wu Y, Ma M, Zhang X (2016) Synthesis of magnetic lignin-based hollow microspheres: a highly adsorptive and reusable adsorbent derived from renewable resources. ACS Sustain Chem Eng 4(10):5523–5532. https://doi.org/10.1021/acssuschemeng.6b01244
66. Li C, Zhao X, Wang A, Huber GW, Zhang T (2015) Catalytic transformation of lignin for the production of chemicals and fuels. Chem Rev 115:11559–11624. https://doi.org/10.1021/acs.chemrev.5b00155
67. Lourenço A, Pereira H (2018) Compositional variability of lignin in biomass. lignin - trends and applications. InTech. https://doi.org/10.5772/intechopen.71208
68. Luo H, Abu-Omar MM (2017) Chemicals from lignin. In: Encyclopedia of sustainable technologies. Elsevier, pp 573–585.
69. M-Ridha MJ, Hussein SI, Alismaeel ZT, Atiya MA, Aziz GM, (2020) Biodegradation of reactive dyes by some bacteria using response surface methodology as an optimization technique. Alex Eng J 59:3551–3563. https://doi.org/10.1016/j.aej.2020.06.001
70. Ma Y, Sun Y, Fu Y, Fang G, Yan X, Guo Z, (2016) Swelling behaviors of porous lignin-based poly (acrylic acid), Chemosphere 163–610–619
71. Madhavi V, Lele S (2009) Laccase: properties and applications. BioResources 4:1694–1717
72. Madhushika HG, Ariyadasa TU, Gunawardena SHP (2018) Decolourization of reactive red EXF dye by isolated strain proteus mirabilis. In: Moratuwa engineering research conference (MERCon) 2018:231–234. https://doi.org/10.1109/mercon.2018.8421983
73. Madigan MT, Martinko JM, Bender KS, Buckley DH, Stahl DA (2012) Brock biology of microorganisms, 13th edn. Pearson Education Inc., Benjamin Cummings, San Francisco
74. Mahmoodi NM, Najafi F, Khorramfar S, Amini F, Arami M (2011) Synthesis, character-ization, and dye removal ability of high-capacity polymeric adsorbent: Polyaminoimide homopolymer. J Hazard Mater 198:87–94
75. Matera I, Gullotto A, Tilli S, Ferraroni M, Scozzafava A, Briganti F (2008) Crystal structure of the blue multicopper oxidase from the white-rot fungus Trametes trogii complexed with p-toluate. Inorg Chim Acta 361:4129–4137. https://doi.org/10.1016/j.ica.2008.03.091
76. Meng X, Scheidemantle B, Li M, Wang YY, Zhao X, Toro-González M, ... Ragauskas AJ (2020) Synthesis, characterization, and utilization of a lignin-based adsorbent for effective removal of azo dye from aqueous solution. ACS omega 5(6):2865-2877. https://doi.org/10.1021/acsomega.9b03717
77. Meng Y, Lu J, Cheng Y, Li Q, Wang H (2019) Lignin-based hydrogels: a review of preparation, properties, and application. International Journal of Biological Macromolecules 135:1006–1019. https://doi.org/10.1016/j.ijbiomac.2019.05.198.
78. Mester T, Tien M (2000) Oxidation mechanism of ligninolytic enzymes involved in the degra-dation of environmental pollutants. Int Biodeterior Biodegradation 46:51–59. https://doi.org/10.1016/s0964-8305(00)00071-8
79. Mojsov KD, Andronikov D, Janevski A, Kuzelov A, Gaber S (2016) The application of enzymes for the removal of dyes from textile effluents. Adv Technol 5(1):81–86. https://doi.org/10.5937/savteh1601081M
80. Moreira PR, Duez C, Dehareng D, Antunes A, Almeida-Vara E, Frère JM, Malcata FX, Duarte JC (2005) Molecular characterization of a versatile peroxidase from a Bjerkandera strain. J Biotechnol 118:339–352. https://doi.org/10.1016/j.jbiotec.2005.05.014
81. Musilova L, Mracek A, Kovalcik A, Smolka P, Minarik A, Humpolicek P, Vicha R, Ponizil P (2018) Hyaluronan hydrogels modified by glycinated Kraft lignin: morphology, swelling, viscoelastic properties, and biocompatibility. Carbohydr Polym 181:394–403
82. Naficy S, Spinks GM, Wallace GG (2014) Thin, tough, pH-sensitive hydrogel films with rapid load recovery. ACS Appl Mater Interfaces 6:4109–4114

83. Naseem A, Tabasum S, Zia KM, Zuber M, Ali M, Noreen A (2016) Lignin-derivatives based polymers, blends, and composites: a review. Int J Biol Macromol 93:296–313

84. Naseer A, Jamshaid A, Hamid A et al (2019) Lignin and lignin based materials for the removal of heavy metals from waste water-an overview. Zeitschrift für Phys Chemie 233:315–345. https://doi.org/10.1515/zpch-2018-1209

85. Nikfar S, Jaberidoost M (2014) Dyes and colorants. Encyclopedia Toxicol 2:252–261. https://doi.org/10.1016/b978-0-12-386454-3.00602-3

86. Nishimura H, Kamiya A, Nagata T et al (2018) Direct evidence for α ether linkage between lignin and carbohydrates in wood cell walls. Sci Rep 8:6538. https://doi.org/10.1038/s41598-018-24328-9

87. Novaes E, Kirst M, Chiang V et al (2010) Lignin and biomass: a negative correlation for wood formation and lignin content in trees. Plant Physiol 154:555–561. https://doi.org/10.1104/pp.110.161281

88. Pandey K, Saha P, Rao KVB (2019) A study on the utility of immobilized cells of indigenous bacteria for biodegradation of reactive azo dyes. Prep Biochem Biotechnol 50:317–329. https://doi.org/10.1080/10826068.2019.1692219

89. Passauer L, Halles T, Baeucker E, Ciesielski G, Lebioda S, Hamer U (2015) Biodegradation of hydrogels from oxyethylated lignins in model soils. ACS Sustain Chem Eng 3:1955–1964

90. Penaranda JE, Sabino MA (2010) Effect of the presence of lignin or peat in IPN hydrogels on the sorption of heavy metals. Polym Bull 65:495–508

91. Peng N, Hu D, Zeng J, Li Y, Liang L, Chang C (2016) Superabsorbent cellulose–clay nanocomposite hydrogels for highly efficient removal of dye in water. ACS Sustain Chem Eng 4(12):7217–7224. https://doi.org/10.1021/acssuschemeng.6b02178

92. Plácido J, Capareda S (2015) Ligninolytic enzymes: a biotechnological alternative for bioethanol production. Bioresour Bioprocess 2:1–12. https://doi.org/10.1186/s40643-015-0049-5

93. Périé FH, Reddy GVB, Blackburn NJ, Gold MH (1998) Purification and characterization of laccases from the white-rot basidiomycete dichomitus squalens. Arch Biochem Biophys 353:349–355. https://doi.org/10.1006/abbi.1998.0625

94. Ragauskas AJ, Beckham GT, Biddy MJ, Chandra R, Chen F, Davis MF, Davison BH, Dixon RA, Gilna P, Keller M, Langan P, Naskar AK, Saddler JN, Tschaplinski TJ, Tuskan GA, Wyman CE (2014) Lignin valorization: improving lignin processing in the biorefinery. Science 344:1246843

95. Rajhans G, Sen SK, Barik A, Raut S (2020) Ligninolytic enzyme system of white-rot fungi: a natural approach to bioremediation and detoxification of azo dyes in textile wastewater. Environ Eng Manag J 19:1983–2002

96. Raschip IE, Hitruc EG, Vasile C (2011) Semi-interpenetrating polymer networks containing polysaccharides. II. Xanthan/lignin networks: a spectral and thermal characterization. High Perform Polym 23:219–229

97. Raschip IE, Hitruc GE, Vasile C, Popescu MC (2013) Effect of the lignin type on the morphology and thermal properties of the xanthan/lignin hydrogels. Int J Biol Macromol 54:230–237

98. Rico-García D, Ruiz-Rubio L, Pérez-Alvarez L, Hernández-Olmos SL, Guerrero-Ramírez GL, Vilas-Vilela JL (2020) Lignin-based hydrogels: synthesis and applications. Polymers 12(1):81. MDPI AG. https://doi.org/10.3390/polym12010081

99. Robinson T, Mcmullan G, Marchant R (2001) Remediation of dyes in textile effluent: a critical review on current treatment technologies with a proposed alternative. Bioresour Technol 77:247–255

100. Ruiz-Dueñas FJ, Morales M, García E, Miki Y, Martínez MJ, Martínez AT (2009) Substrate oxidation sites in versatile peroxidase and other basidiomycete peroxidases. J Exp Bot 60:441–452. https://doi.org/10.1093/jxb/ern261

101. Ruwoldt J (2020) A critical review of the physicochemical properties of lignosulfonates: chemical structure and behavior in aqueous solution, at surfaces and interfaces. Surfaces 3:622–648. https://doi.org/10.3390/surfaces3040042

102. Sameni J, Krigstin S, Santos Rosa DD et al (2013) Thermal characteristics of lignin residue from industrial processes. BioResources 9:725–737. https://doi.org/10.15376/biores.9.1.725-737
103. Schutyser W, Renders T, Van den Bosch S et al (2018) Chemicals from lignin: an interplay of lignocellulose fractionation, depolymerisation, and upgrading. Chem Soc Rev 47:852–908. https://doi.org/10.1039/C7CS00566K
104. Sen SK, Raut S, Bandyopadhyay P, Raut S (2016) Fungal decolouration and degradation of azo dyes: a review. Fungal Biol Rev 30:112–133. https://doi.org/10.1016/j.fbr.2016.06.003
105. Shi CM, Tao FR, Cui YZ (2018) Evaluation of nitriloacetic acid modified cellulose film on adsorption of methylene blue. Int J Biol Macromol 114(2018):400–407
106. Singhania RR, Sukumaran RK, Patel AK, Larroche C, Pandey A (2010) Advancement and comparative profiles in the production technologies using solid-state and submerged fermentation for microbial cellulases. Enzyme Microb Technol 46:541–549. https://doi.org/10.1016/j.enzmictec.2010.03.010
107. Sohni S, Hashim R, Nidaullah H, Lamaming J, Sulaiman O (2019) Chitosan/nano-lignin based composite as a new sorbent for enhanced removal of dye pollution from aqueous solutions. Int J Biol Macromol 132:1304–1317. https://doi.org/10.1016/j.ijbiomac.2019.03.151
108. Stewart P, Cullen D (1999) Organization and differential regulation of a cluster of lignin peroxidase genes of *Phanerochaete chrysosporium*. J Bacteriol 181:3427–3432. https://doi.org/10.1128/JB.181.11.3427-3432.1999
109. Sun Y, Ma Y, Fang G, Ren S, Fu Y (2016) Controlled pesticide release from porous composite hydrogels based on lignin and polyacrylic acid. BioResources 11:2361–2371
110. Suteu D, Zaharia C (2012) Application of lignin materials for dye removal by sorption processes. Lignin Prop Appl Biotechnol Bioenergy 477–488.
111. Taleb F, Ammar M, ben Mosbah M, ben Salem R, Moussaoui Y, (2020) Chemical modification of lignin derived from spent coffee grounds for methylene blue adsorption. Sci Rep 10(1):1–13. https://doi.org/10.1038/s41598-020-68047-6
112. Teng X, Xu H, Song W, Shi J, Xin J, Hiscox WC, Zhang J (2017) Preparation and properties of hydrogels based on PEGylated lignosulfonate amine. ACS Omega 2:251–259
113. Tobimatsu Y, Schuetz M (2019) Lignin polymerization: how do plants manage the chemistry so well? Curr Opin Biotechnol 56:75–81. https://doi.org/10.1016/j.copbio.2018.10.001
114. Uddin MJ, Alaboina PK, Zhang L, Cho SJ (2017) A low-cost, environment-friendly lignin polyvinyl alcohol nanofiber separator using a water-based method for safer and faster lithium-ion batteries. Mat Sci Eng B 223:84–90
115. Velmurugan B, Narra M, Rudakiya DM, Madamwar D (2019) Sweet sorghum: a potential resource for bioenergy production. In: Refining biomass residues for sustainable energy and bioproducts: technology, advances, life cycle assessment, and economics. Elsevier, pp 215–242.
116. Vishtal A, Kraslawski A (2011) Challenges in industrial applications of technical lignins. BioResources 6:3547–3568. https://doi.org/10.15376/biores.6.3.3547-3568
117. Wang S, Chen F, Song X (2015) Preparation and characterization of lignin-based membrane material. BioRes 10:5596–5606. https://doi.org/10.15376/biores.10.3.5596-5606
118. Wang S, Kong F, Fatehi P, Hou Q (2018) Cationic high molecular weight lignin polymer: a flocculant for the removal of anionic azo-dyes from simulated wastewater. Molecules 23(8):2005. https://doi.org/10.3390/molecules23082005
119. Wang X, Jiang C, Hou B, Wang Y, Hao C, Wu J (2018) Carbon composite lignin-based adsorbents for the adsorption of dyes. Chemosphere 206:587–596. https://doi.org/10.1016/j.chemosphere.2018.04.183
120. Wang X, Zhou Z, Guo X, He Q, Hao C, Ge C (2016) Ultrasonic-assisted synthesis of sodium lignosulfonate-grafted poly(acrylic acid-co-poly(vinyl pyrrolidone)) hydrogel for drug delivery. RSC Adv 6:35550–35558
121. Wang Y, Xiong Y, Wang J, Zhang X (2017) Ultrasonicassisted fabrication of montmorillonite-lignin hybrid hydrogel: highly efficient swelling behaviors and super-sorbent for dye removal from wastewater. Colloids Surf A: Physicochem Eng Aspects 520:903–913. https://doi.org/10.1016/j.colsurfa.2017.02.050

122. Wang YX, Zhang CY, Zhao LY, Meng GH, Wu JN, Liu ZY (2017) Cellulose-based porous adsorbents with high capacity for methylene blue adsorption from aqueous solutions. Fiber Polym. 18:891–899
123. Watkins D, Nuruddin M, Hosur M, Tcherbi-Narteh A, Jeelani S (2015) Extraction and characterization of lignin from different biomass resources. J Mater Res Technol 4:26–32. https://doi.org/10.1016/j.jmrt.2014.10.009
124. Wawrzkiewicz M, Bartczak P, Jesionowski T (2017) Enhanced removal of hazardous dye form aqueous solutions and real textile wastewater using bifunctional chitin/lignin biosorbent. Int J Biol Macromol 99:754–764. https://doi.org/10.1016/j.ijbiomac.2017.03.023
125. Welinder KG (1992) Superfamily of plant, fungal and bacterial peroxidases. Curr Opin Struct Biol 2:388–393. https://doi.org/10.1016/0959-440x(92)90230-5
126. Widsten P, Tamminen T, Liitiä T (2020) Natural sunscreens based on nanoparticles of modified Kraft Lignin (CatLignin). ACS Omega 5:13438–13446. https://doi.org/10.1021/acsomega.0c01742
127. Wong DWS (2008) Structure and action mechanism of ligninolytic enzymes. Appl Biochem Biotechnol 157:174–209. https://doi.org/10.1007/s12010-008-8279-z
128. Xu D, Hein S, Loo LS, Wang K (2011) Modified chitosan hydrogels for the removal of acid dyes at high ph: modification and regeneration. Ind Eng Chem Res 50:6343–6346
129. Xue BL, Wen JL, Sun RC (2015) Ethanol organosolv lignin as a reactive filler for acrylamide-based hydrogels. J Appl Polym Sci 132:42638–42645
130. Yagub MT, Sen TK, Afroze S, Ang HM (2014) Dye and its removal from aqueous solution by adsorption: a review. Adv Coll Interface Sci 209:172–184. https://doi.org/10.1016/j.cis.2014.04.002
131. Yamamoto H, Amaike M, Saitoh H, Sano Y (2000) Gel formation of lignin and biodegradation of the lignin gels by microorganisms. Mater Sci Eng C 7:143–147
132. Ying-zhi M, Da-feng Z, Zhen-ye M, Rui-jing D, Xue-qing Q (2018) Magnetic lignin-based carbon nanoparticles and the adsorption for removal of methyl orange. Colloids Surf A 559:226–234. https://doi.org/10.1016/j.colsurfa.2018.09.054
133. Zhang LL, Lu HL, Yu J, Fan YM, Yang YQ, Ma JX, Wang ZG (2018) Synthesis of the lignocellulose-based composite hydrogel as a novel biosorbent for Cu2+ removal. Cellulose 25:7315–7328
134. Zhang S, Wang Z, Zhang Y, Pan H, Tao L (2016) Adsorption of methylene blue on organosolv lignin from rice straw. Procedia Environ Sci 31:3–11. https://doi.org/10.1016/j.proenv.2016.02.001
135. Zhang W, Yang P, Li X, Zhu Z, Chen M, Zhou X (2019) Electrospun lignin-based composite nanofiber membrane as a high-performance adsorbent for water purification. Int J Biol Macromol 141:747–755. https://doi.org/10.1016/j.ijbiomac.2019.08.221
136. Zille A, Gornacka B, Rehorek A, Cavaco-Paulo A (2005) Degradation of Azo Dyes by *Trametes villosa* laccase over long periods of oxidative conditions. Appl Environ Microbiol 71:6711–6718. https://doi.org/10.1128/aem.71.11.6711-6718.2005

Metal–Organic Frameworks Membranes

Faiza Ilyas, Umme Ammara, Munazza Shahid, Manzar Sohail, Muhammad Sher, Muhammad Altaf, and Raja Shahid Ashraf

Abstract   Recently, membrane technology is a promising strategy to remove organic dyes from industrial (textile, paint, leather, and dyeing) wastewater. Dyes are important organic pollutants that have been increasing continuously in wastewater and recognized for their hazardous effects on the ecosystem. Wastewater before discharge into main streams must be treated carefully to minimize the harmful effects of dyes on aquatic life and humans. Development in technology and science has directed to advance techniques for dye removal from industrial effluents. Current studies have reviewed the potential dye removal application of metal–organic frameworks boosted membranes (MOFs boosted membranes). MOF-based membranes have been applied extensively in nanofiltration (NF), Forward Osmosis (FO), ultrafiltration (UF), and reverse osmosis (RO) techniques. This chapter discusses various methods for dye removal, MOF adsorbents, and MOF-based membranes. MOF-based membranes design strategies and key features of MOF-based membranes are also described briefly. In addition, MOF boosted membranes solution, challenges and future prospects are summarized.

Keywords MOF boosted membranes · Dye removal · Membrane technology · MOF adsorbent

F. Ilyas · U. Ammara · M. Altaf (✉) · R. S. Ashraf
Department of Chemistry, GC University Lahore, Lahore 54000, Pakistan
e-mail: muhammad.altaf@gcu.edu.pk

M. Shahid (✉)
University of Education, Bank Road Campus, Lahore 54000, Pakistan
e-mail: munazza.shahid@eu.edu.pk

M. Sohail
Department of Chemistry, School of Natural Sciences, National University of Sciences and Technology, Islamabad 44000, Pakistan

M. Sher
Department of Chemistry, Allama Iqbal Open University, Sector H-8, Islamabad 44000, Pakistan

215

Abbreviations

RO   Reverse osmosis
MF   Microfiltration
UF   Ultrafiltration
NF   Nanofiltration
MOFs   Metal organic frameworks
MMMs   Mixed matrix membranes
COD   Chemical oxygen demand
TFN   Thin film nanocomposite
TMC   Trimesoyl chloride
PSS   Polystyrene sulfonate
PSF   Polysulfone
PA   Polymeric amide
MPD   Methyl-2,4-pentanediol

1 Introduction

Clean water is the global concern of time. It is assumed that the availability of water would be insufficient for the people living in the desert. A higher amount of wastewater is being discharged into freshwater resources [9]. Unplanned urbanization and an uncontrolled increase in the human population have significantly increased the demand for freshwater all over the world. There is a dire need for sustainable technologies to eliminate this worldwide burden. Accumulation of dyes into freshwater has rapidly increased due to its high use in the printing, textile, food, and leather industry [8]. Dyes are not only non-biodegradable elements with higher stability to light and oxidants but also extremely toxic and carcinogenic to humans and all other living bodies [72]. The presence of complex aromatic molecules in synthetic dyes makes them more stable and complex compounds that reduce their degradation. The chemical structure of dyes tends to enhance the resistance against water, light, and other chemicals. Several types of dyes including diazo, azo, basic, disperse, acidic, anthraquinone, and complex metal dyes exist [5]. A temperature of 200 °C is needed to degrade the synthetic dyes [3]. Table 1 Give a list of the main industries that release dyes [26].

A rapid increase in the utilization of dyes has degraded the quality of water and thus the removal of these pollutants is very important. Various wastewater treatment techniques with frequent improvements are underuse. Recently, coagulation [62], flocculation, sedimentation, and adsorption [70, 74] are the primary techniques used in the removal of organic and inorganic pollutants. Primary treatments have the potential to remove 65% of oil and grease and 50% of organic matter from municipal sewage. This general waste removal trend is not feasible for contaminated water coming from the textile industry. Chemical or biological oxidation for the removal of

Table 1 % dye release from different industries

Industry	% release dye
Textile	54
Dyeing	21
Paper and pulp	10
Paint and leather	8
Dye manufacturing	7

biodegradable, colloidal, and dissolved organic matter is obtained in the secondary treatment of water. Chlorine forms carcinogenic chloride and chlorinated intermediates when it is used as a chemical oxidizing agent [69]. Hydrogen peroxide, ozone, Fenton reagent, and photo-assisted oxidation are some of the advanced oxidation processes [38], effective for dye removal. Many electrochemical methods have been stated, i.e., electro-oxidation, electro flotation, photo-assisted which are suitable for the removal of organic impurities. The economic feasibility of advanced oxidation processes is yet to be determined at an industrial scale. Textile effluents with a high concentration of contaminants can be removed with biological oxidants. Currently, tertiary wastewater treatment involves an adsorption column made up of biological treatment. Membrane filtration is regarded as the most feasible technique with no chemical additives. Commonly, four types of membranes including microfiltration (MF) (Jianxin [43], nanofiltration (NF) [40], ultrafiltration (UF) [50] and reverse osmosis (RO) [41] are used. Membrane fouling is the main constraint need to be considered for economic viability [37]. Biodegradable products and large particles are removed by MF and UF [11]. RO has a significant role in the removal of inorganic and organic contaminants present in water [6]. Nano pores present in the nanofiltration membrane isolate salt solution from the dye. High-temperature membrane distillation is also practiced for dye removal, part of the zero liquid discharge strategy [22].

Easy fabrication and low economic cost of polymeric membranes have gained more popularity at an industrial scale. Polymeric membranes are very sensitive to a high temperature which is a major constraint in their applicability [85]. Whereas inorganic ceramic membranes are more stable at high temperatures and they have been frequently used at a larger scale with some progress on chemical and mechanical levels [27]. Ceramic membranes are generally expensive than polymeric membranes but their long life span and high stability make them the best option to opt for. The separation ability of membrane filtration is mainly based upon two factors, i.e., selectivity and permeability [27]. In a porous membrane, the separation process generally depends upon the size-exclusion mechanism [66]. Consequently, in membrane filtration uniform pores and high porosity will increase the permeability and decrease selectivity simultaneously. Some amendments such as adsorption, charge repel, adsorption, and hydrophilic interaction in the separation mechanism enhance the permeability and selectivity of the membrane. For wastewater treatment, membrane fouling is a major issue for membrane filtration [95].

To increase separation ability various types of materials can be integrated into conventional membranes. In recent times, MOFs have gained popularity because of their exceptional porous structures. The metal center is coordinated with organic ligands in MOFs. In wastewater purification [33], MOFs can be used as absorbents [2], membranes, and catalysts [10] due to their large surface area, high porosity, and changeable pore size. At present, various types of water-stable MOFs [33] have been reported, i.e., UiO-66 series zirconium/pyrazole-based MOFs [52] and MIL family [68]. The aforementioned water-stable MOFs have high steric hindrance which can protect their coordinate metal–ligand bonds in the presence of moisture [47]. MOFs-based material incorporated with membrane enhances the separation ability compared to conventional membrane filtration processes. Multiple active sites present at the microporous MOFs increase the extent and the separation efficiency of traditional membranes. Porous MOFs transport water molecules effectively which ultimately expands water permeability. Surface properties and porous structures of MOFs can be used to tune the antifouling attributes, selectivity, and permeability of the filtration membrane [84]. The highly stable structures of MOFs effectively increase accessible surface area and inhibit aggregation. For the adsorptive removal of different pollutants, Mon et al. have identified recent methodologies of MOFs [64]. MOF is an interdisciplinary technology linked with chemical engineering and environmental engineering [33].

This chapter focuses on the applications of MOFs as membranes and adsorbents for the removal of dye effluents. It presents approaches for the design of MOFs boosted membranes. In addition, it also explains key properties, challenges and future prospects of MOFs boosted membranes.

2 Methods for Dye Removal

In the 90s, there were no tunable dye removal methods [77]. Effective dye removal methods were introduced after the permissible release of dye effluent (i.e., activated sludge processes and dye degrading filter beds) [1, 75]. Currently, various dye removal techniques coagulations, microbial degradation, membrane separation, and electrochemical degradation are used. These existing methods can be categorized into chemical, biological, and physical treatments. Few methods are implemented these days in industries due to the limitations possessed by the majority of methods. The general method for the treatment of dye effluents is given in Fig. 1 [26, 71, 80].

2.1 Biological Methods for Dye Removal

The biological method is one of the most widely used dye removal processes in most countries for the treatment of wastewater. Generally, this method is very cheap and conventional in which aerobic or anaerobic degradation of microbes takes place
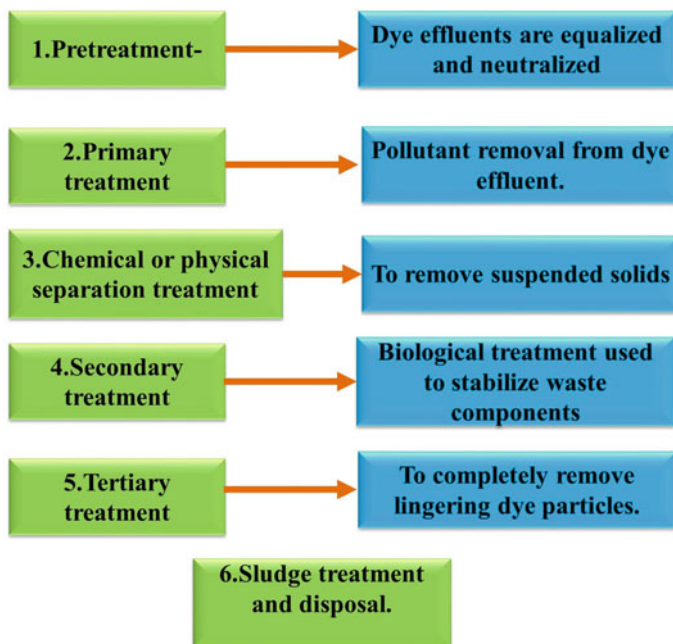
Fig. 1 General method for the treatment of dye effluent

before the dye molecules are released in the environment [4, 75]. Although this conventional method is not much effective to make the water toxic dye-free because it does not treat the hazardous particles present in textile water, it only treats the (COD) in water. Biological methods are integrated by some living organisms such as algae degradation, microbial biomass adsorption, fungal and microbial cultures, and enzyme degradation. Nowadays enzyme degradation is becoming famous however this method also has some limitations such as system instability because it depends on the living things' growth rate [65, 78]. Table 2 Give a brief description of some commonly used biological methods [34].

2.2 Chemical Methods for Dye Removal

This method involves chemistry and its theories to treat wastewater. Conventionally, it consists of electrochemical destruction, oxidation process, ozonation, Fenton reaction, and ultraviolet irradiation [63]. This method is cost-effective compared to physical and biological dye removal methods as it requires electrical energy and specific instruments or reactors for dye removal. Another limitation of this method is that the chemicals and reagents consume at a large scale, also generate secondary pollution particles which pollute the environment. Table 3 Give a brief description of various chemically used methods [34].

Table 2 Brief description of various biologically used dye removal methods

Methods	Configuration	Advantages	Drawbacks
Microbial biomass adsorption	Organic living organism mixture used to adsorb dye molecules	Excellent affinity showed by dyes for microbial biomass	Not efficient for all dyes
Fungal cultures	Fungus use dye molecules for self-growth	Flexible method for the elimination of various dyes	Extensive growth phase and unstable system
Algal degradation	Algae use dyes molecule for the development	Cheap easily computable and environment friendly	Unsteady system
Enzymatic degradation	Specific enzymes used for the degradation of dyes	Non-toxic, cheap and highly efficient	Enzyme production unreliable

Table 3 A brief description of various chemically used dye removal methods

Methods	Configuration	Advantages	Drawbacks
Electrochemical destruction	Electro-coagulation used to digest dye particles	The fairly suitable method, chemicals not get consumed	High cost, less efficient method
Fenton reactions	Fenton's reagent used for wastewater treatment	'Fairly suitable, also remove toxic materials	Long time reaction, not suitable for vat and disperse dyes
Ozonation	Ozone gas used to remove dye particles	Quick reaction, effective method, can also be used in the gaseous state	Expensive, short half-life, unstable method
Oxidation	Oxidizing agents used for dye removal	Degrade dyes, short-time reaction	Costly involves catalyst for dye treatment, difficult to activate
UV irradiation	Use of UV rays to degrade dye particles	absorb bad odors, no sludge production	Costly, energy lessening process
Advanced oxidation method	Oxidation processes used to remove dyes	A good method for dye and toxic material removal	Expensive, Production of side products, not flexible
Photochemical	Fenton reaction integrated with UV light to remove dyes	Efficient method,	Expensive

Table 4 Brief description of various physically used dye removal methods

Methods	Configuration	Advantages	Drawbacks
Ion exchange	Reversible chemical ion-exchange method	Good method, produce high-quality water	Not suitable for all types of dyes
Adsorption	Adsorbents used to remove dye molecules	Excellent method, regenerate adsorbents	Expensive
Membrane filtration	Separation membranes used for dye removal	Effective method	High cost, less suitable for dye removal
RO	Pressure driven method, the water passed from a thin membrane leaving behind the impurities	Effective for decoloring	Expensive requires high pressure
NF/UF	Dye wastewater passed through thin porous membranes	Suitable for all types of dyes	Short life span, high cost, consume high energy
Flocculation/Coagulation	Flocculation/Coagulation agents used for dye removal	Cheap, suitable for dispersing, vat dyes	Not suitable for acidic, basic, azo dyes

2.3 Physical Methods for Dye Removal

These methods are integrated by mass transfer mechanism and conventionally include coagulation, ion exchange, ultrafiltration, adsorption, membrane filtration, and reverse osmosis. Generally, these methods are simple and easy to use as compare to other methods of dye removal and also require fewer amounts of chemicals Table 4 Give a brief description of various physically used dye removal methods [35].

2.4 Adsorption Process as a Dye Removal Method

Adsorption is a physical method and more feasible for the treatment of drinkable water or industrial wastewater. It is one of the ideal techniques to remove the synthetic dyes from wastewater that cannot be removed by using other conventional methods (biological and chemical methods) [30, 60]. Generally, it's an equilibrium separation and mass transfer process in which elements are gathered on the interface of similar or different phases (i.e., gas–liquid, liquid–liquid, and gas–solid). In this process, a solid surface is condensed with the substance the surface is known as the adsorbent while the substance that gets adsorbed is known as the adsorbate. Generally, two types of adsorbents are used, i.e., natural adsorbents and synthetic adsorbents. Natural adsorbents are gained from animals and plants while the synthetics adsorbents are made with zeolites, MOFs, and activated carbon through chemical reactions

Table 5 Various categories of hydrophilic/hydrophobic MOFs-based material

Ligands	Metal center	MOF	Hydrophobic/ hydrophilic nature	Window size (A˚)	Application in liquid separation
(O_2C)–C_6H_4–(CO_2)	Al	MIL-53(Al)	Hydrophobic	8.5	Pervaporation organic solvent nanofiltration water treatment
(O_2C)–C_6H_4–(CO_2)	Cr	MIL-101(Cr)	Hydrophilic	16, 12	Organic solvent nanofiltration Water treatment
(O_2C)–C_6H_4–(CO_2)	Cr	MIL-53(Cr)	Hydrophobic	8.5	Organic solvent nanofiltration
1,3,5-Benzenetricarboxylate	Cu	HKUST-1	Hydrophilic	6.9, 4.1	Pervaporation Organic solvent nanofiltration water treatment
2-Carboxaldehyde imidazolate	Zn	ZIF-90	Slightly hydrophobic	3.5	Pervaporation
4,5-Dichloroimidazole	Zn	ZIF-71	Superhydrophobic	4.2	Water treatment Pervaporation
2-Methylimidazolate	Zn	ZIF-8	Hydrophobic	3.4	Water treatment Pervaporation organic solvent nanofiltration
Benzimidazole	Zn	ZIF-7	Hydrophobic	3.0	Pervaporation
2-Ethylimidazolate	Zn	MAF-6	Highly hydrophobic	18.4	Pervaporation
(O_2C)–C_6H_4–(CO_2)	Zr	UiO-66	Hydrophilic	6	Water treatment; Pervaporation

[12–14]. This technique is becoming popular in recent years due to its efficiency and economic feasibility. The process of adsorption is accomplished in two types of mechanisms, e.g., chemisorption (when the interaction between adsorbent and adsorbate is strong) and physisorption (when there is a weak interface between the adsorbate and adsorbent) [2, 7].

2.4.1 MOFs as Adsorbent

MOFs are the permeable crystalline materials that are made with the integration of metal ions and organic linkers [82]. These porous materials show a lot of applications in chemical separation, catalysis, gas storage, and drug delivery due to their changeable pore size, adjustable internal properties, and ultra-high surface areas [15]. Removal of dye effluents is very essential because they influenced the water quality and are very stable, i.e., too light and oxidation processes. For this purpose, MOFs are the best choice because the adsorption properties of MOFs are much higher than any other chemical adsorbent [20]. Mostly for adsorption MOFs are used in powder form for gas separation or membranes for liquid separation. Encouragingly, various water-stable MOFs are reported in recent year, e.g., Zirconium and pyrazole-based MOFs were used for the treatment of water. The covalent bond between these MOFs is very strong that stops the degradation of metal–ligand bond in the presence of water [2, 29].

3 MOF Boosted Membrane Technology

MOF-based membrane boosted technology is the collaboration of metal–organic framework material and separation membrane [2]. Firstly the separation efficiency is enhanced by the use of crystalline MOFs. Secondly, the MOF-based membranes facilitate the filtration process and water permeability. Thirdly the modification of filtration membranes and antifouling properties was done by operating the surface properties of MOFs. MOF boosted membranes technology is applied in various fields, e.g., chemical engineering, environmental engineering, and material sciences. Conventionally, various configurations of membranes have been used such as sheets, hollow fibers, tubes, and fibrous membranes [57, 64]. Plate membranes are widely used, hollow fiber membranes containing large surface area and low footprint while fibrous membranes also possess large surface area, high porosity, low cost, and high adsorption properties. Figure 2 Shows the arrangement of various MOF-based membranes. Generally, by considering the configuration of membranes, MOF-based membrane technology has been divided into four categories, i.e., [56]

- *(MOF-plus) membrane technology.
- (MOF-as) membrane technology.
- *(MOF-in) membrane technology.
- (MOF-on) membrane technology.

3.1 (MOF-Plus) Membranes

Various filtration membranes reverse osmosis (RO), ultrafiltration (UF), and nanofiltration (NF), are used for the treatment of water. (NF) and (RO) membranes are
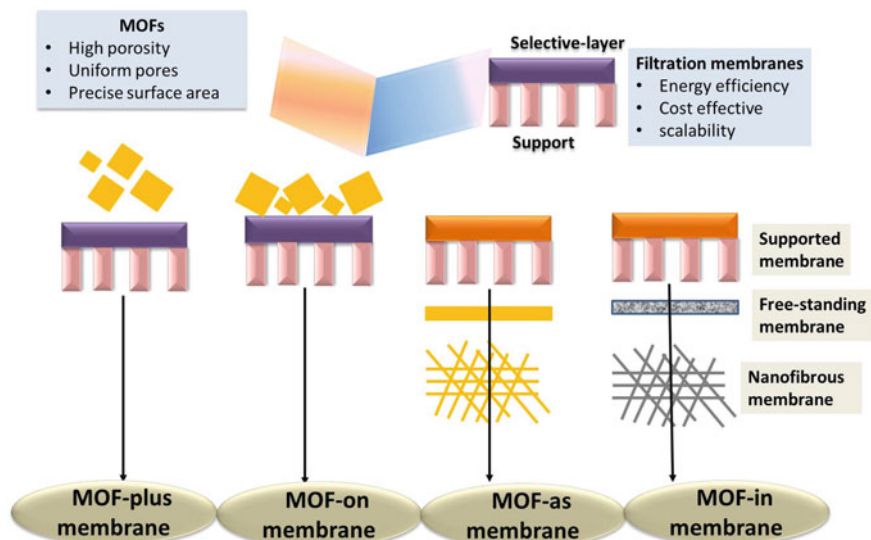
Fig. 2 Arrangement of various MOF boosted membranes
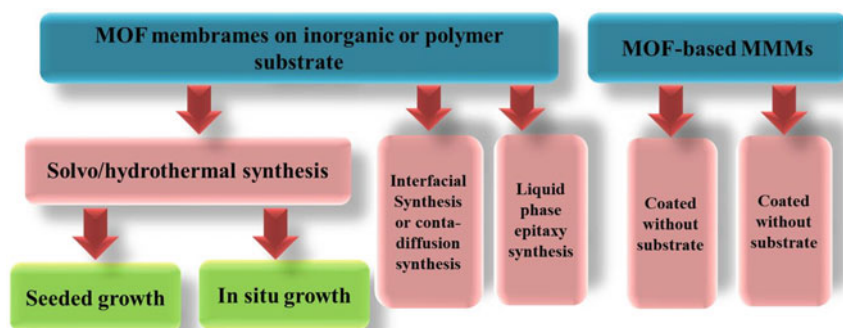
Fig. 3 Designing methods of MOF-based membranes

used for small-sized molecules while UF/MF membranes are used for the macro and bacterial species [93]. The absorbent properties of MOF membranes make them good adsorbent to remove dyes and heavy metal ions, i.e., Pb(II), Cu(II), Hg(II), Cd(II), and Cr(VI). Good adsorptive MOFs integrated with UF membrane which is known as MOF adsorption membrane that is widely used for wastewater treatment. Yin et al. reported the combination method of MOF and filtration membrane for the removal of Pd(II). The adsorption efficiency can be enhanced by the combination of filtration membrane and MOF adsorbent, by this method MOF-plus membrane permeability is significantly improved up to ($1400 \ 1 \ m^{-2} \ h^{-1}$). That is higher than the free MOF membranes [53, 89].

3.2 (MOF-As) Membranes

(MOF-as) membranes are referred to as MOF layers which exhibit uniform pore size. They are categorized into two forms free-standing and supporting MOF membranes. Encouragingly, various strategies are used to fabricate the free-standing membranes, i.e., solution casting, interfacial synthesis, and template method. These membranes show excellent selectivity and adsorption properties [31]. However, free-standing membranes have poor mechanical strength which makes them unfeasible for practical use. Their mechanical strength can be improved by using a macroporous substrate to form a supported MOF membrane. The supported membranes can be designed by using in situ growth and post-assembly method. In the post-assembly method, MOF materials are prepared and set down on the polymeric support. The post assembly process is more facile and also enhances the interfacial adhesion. In the solvothermal growth, the substrate is absorbed with the metal salt ion and organic linker solution. After that MOFs will be produced by the heating process [42, 55].

3.3 (MOF-On) Membranes

(MOF-as) membranes are poles apart from the (MOF-as) membranes, MOF particles are alternatively settled on the surface to improve the membrane efficiency. Their process of fabrication is similar to the (MOF-as) membranes process however in this arrangement MOF particles act as functional additives [31]. By this addition, the antibacterial, adsorption properties, and selectivity of (MOF-on) membranes will be upgraded. The combination of Ag-MOFs and TFC membrane increases the antibacterial activity of the membrane by 100%. Despite these, the fabrication of membranes with MOFs also decreases the pure water fluidity by blocking the effect. These MOF boosted membranes to enhance the adhesion power, so there is a need to pay special attention to the geometry of substrate [21, 51, 67].

3.4 (MOF-In) Membranes

Currently, three kinds of methods can be useful for the fabrication of MOFs with membranes, e.g., in situ growth, blending, and binder-assisted binding. In these processes, Mechanical blending is the more facile way to fabricate the MOFs in membranes. However, the resulted membrane is suffered from aggregation and low mass loading due to the absence of nucleation sites. Although the binder-assisted method increases the mass loading it becomes the reason for pore-clogging. Encouragingly, in situ growth method gives an efficient mode to increase the MOFs loading and also enhance their activity. MOFs are also widely combined with polymeric membranes to form (TFN) and (MMMs) [28]. Generally, most of the MOFs are

obtained in powder form, firstly the MOFs powder is immersed with polymer solution then it is cast into the membrane. While the TFN membranes can be designed by the interfacial polymerization method in which the polymerization between the MPD solution and TMC solution takes place. In the in situ growth process, the MOF particles are strongly attached to the polymer so it's a reliable process to fabricate the membranes as compared to other processes. When TFN nanocomposite membranes are made by using MOFs the properties and structure is related to the MOFs used. Zhao et al. reported the combination of different water-stable MOFs with TFN membranes, i.e., "MIL-53", "ZIF-8" and "NH_2-UiO-66". They investigated that the MOFs increase the thickness, selectivity, surface negative charges, and surface roughness [46, 81].

4 Key Features for MOF Boosted Membranes

The separation process of MOF boosted membranes is greatly influenced by the structural and physical characteristics of MOFs. There are some important properties of an ideal MOF-based membrane such as long-term operation capability; acceptable component stability and efficient separation ability. Similarly, its fabrication process should be economical and sustainable and environmentally friendly. In various liquid separation methods, standard MOFs should exploit their configurational ascendency for effective membranes. Additionally, their hydrophilicity/hydrophobicity, dispersibility, and stability should be considered deliberately.

4.1 Dispersibility

In a polymer, dispersion of MOFs influences the performance of matrix mixed membrane (MMM) and interfacial defects. The dispersion of higher concentration of MOF during solvent evaporation, phase separation, and interfacial polymerization may be made aggregates that embedded in the polymer layer. In a long-term process, MOF aggregates may cause the decline performance of membranes due to swelling and flux rejection (disposal of non-selective matter from the liquid environment) or a decrease in flux enhancement. While an unwanted interfacial defect formation can reduce by choosing compatible MOF and polymer. Thus, a key factor to design MOF boosted membranes with an excellent separation performance is maximum loading and uniform MOF dispersion in a polymer.

Several approaches were described to accomplish a uniform MOFs dispersion in a hybrid system:

- Pre-dispersion: It is very difficult to form a homogeneous membrane and uniform MOF by dispersing MOFs direct in a solution of polymer (e.g., the polymer in N, N-dimethylformamide (DMF) or N-methyl pyrrolidone (NMP)) [94]. Hence, first

of all, MOFs are dispersed in isooctane solvent and then added polymer solution into it.

- Novel fabrication techniques: Self-assembly is a new in-situ approach to develop MOF-based membranes for liquid separation [76]. In this strategy coordination of organic ligands and metal ions takes place at the support interfacial surface as a result newly formed MOFs are dispersed homogeneously. By inspiring this method, two more strategies, layer-by-layer self-assembly [83] and spray self-assembly [24], were established to confine MOFs aggregation in MMMs effectively.

- Surface modification of MOFs: Flexible and diverse structural framework of MOFs assists uniform dispersion of MOFs in a hybrid membrane approach.

MIL-101 MOF family, for instance, having amine groups was used for MOF/chitosan nanofiltration membranes synthesis that removes multivalent cations efficiently [58]. NH_2-MIL-101 maintains the vital structural properties of MIL-101, whereas, amine group addition intensifies the positive charge and makes its dispersion easy in the chitosan polymeric matrix containing $–NH_2$ groups. Above all discussion declare that the polymer should not penetrate into the porous structure of MOFs because penetration would block filler porosity partially and result in a decrease in flux.

4.2 Hydrophobicity/Hydrophilicity

Primarily, MOFs hydrophilicity/hydrophobicity is dependent upon the porosity of metal and types of ligands as their rational choice influences the nature of target MOF boosted membranes in the separation of an aqueous solution. For the removal of organic pollutants from water hydrophobic MOFs are commonly used through pervaporation and display considerable adsorption selectivity. ZIF-71 shows intrinsic hydrophobic properties with 0.42 nm apertures variably have an RHO topology. As ZIF-71 crystals could be adsorbed selectively ethanol and methanol from a mixture of alcohol-water particularly under low pressures. Dong et al. formed a ZIF-71 membrane for the first time for the separation of dimethyl carbonate-methanol mixture and alcohol-water mixture by pervaporation [23]. It has been stated that ZIF-71nanocrystals are promising membrane materials for the separation of aqueous-organic and organic-organic mixtures. The hydrophobic MOFs behavior uses to made advanced MOF-based membranes to improve the organic pollutants removal from aqueous solution by the pervaporation. Nevertheless, hydrophobic MOF-based membranes are not applicable for water treatment. Particularly, most of the hydrophobic MOFs adversely influence the whole action (e.g., water permeability and membrane antifouling) of such MOF membranes hybrid strategy.

For instance, effective dye rejection, the intensive hydrophilic surfaces, and the ordered porous structure are necessary [73]. Additionally, hydrophobic MOFs for the assembly of interfacial polymerization with MOF boosted membranes may result in

their nonappearance from an aqueous oil interface, however, into the polyamide layer weak entrapments may occur that will lead a large MOFs loss. According to this approach in wastewater purification, the performance of MOF membranes is enhanced by improving hydrophilicity with the help of selective hydrophilic MOFs. An innovative idea of thin-film nanocomposite membranes (TFN) was reported on the hydrophilic MOFs modification [97]. The hydrophilicity of ZIF-8 nanocrystals can be increased using water-soluble Poly(sodium 4-styrenesulfonate) (PSS) polymer as a modifier. When modified MOFs combine with polyamide layer as a result membranes with higher hydrophilicity would obtain. This process was revealed through reduced contact angle. As compared to other mZIF content, the 0.10% w/v suspension of mZIF gives the highest water permeable (14.9 L m^{-2} h^{-1} bar^{-1}) TFN membranes. Table 5 Explain various categories of hydrophilic/hydrophobic MOFs-based materials.

The nanoporous mZIF integration induced a relatively loose PA layer and high surface hydrophilicity that is responsible for the highest permeability. Furthermore, MOFs hydrophilicity can also be used for the organic solvents dehydration through pervaporation. Liu et al. used a controlled method of solvothermal synthesis to form UiO-66 polycrystalline hydrophilic membranes for wastewater treatment. The structural framework of UiO-66 hydrophilic membranes contains a large number of hydroxyl groups as a result hydrophilic adsorption sites are found [54]. These hydrophilic adsorption sites purify typical biochemical, biofuels, and organic compounds with great efficacy.

4.3 Stability

Most of the early stated MOFs are water-sensitive owing to the weak metal–ligand bonds. However, the water instability of these MOFs has significantly limited their commercialization and advanced applications as moisture/water content is present in liquid separation. Structural characteristics of water-stable MOFS normally have substantial steric hindrance and stronger coordination bonds that forbid weak metal–ligand bond impairment and unfavorable hydrolysis reaction [16].

Mainly, MOFs with good water stability have been classified into three categories:

(1) Common metal carboxylates family contains generally high valent metal ions. According to the soft/hard acid–base concept, a high valence metal ion forms a stronger coordination bond with organic ligand while the entire coordination environment remains constant. This trend was observed by MOF material scientists. Similarly, metal units with higher charge density form a firm structure that makes the metal sites water stable.

(2) Many metal-azolate MOFs have N-donor organic linkers. Many molecules of ligands, i.e., tetrazolates imidazolates, pyrazolate, and triazolates are also water-stable complexes. These organic ligands are soft and give stronger MOF structures when they coordinate with soft divalent metal ions. For example, the most common metal-azolate MOFs are ZIFs which are prepared by the

reaction of Zn^{2+}/Co^{2+} with imidazolate to generate zeolite topology analogous variety of stable crystals.

(3) MOFs connected with blocked metal ions or hydrophobic pore surfaces that exactly functionalized the steric hindrance to retain bond strength in an aqueous solution. Thus, water molecules cannot be approached the lattice and attacking the structures of MOFs. With this process, post-synthesis methods such as metal or ligand exchange reactions and ligand modification can be used to enhance the water stability of MOFs.

5 Important Factors for MOFs in Membrane-Based Aqueous Solution Separations

Some factors can be considered for the effective designing of membranes.

- Solute rejection and high flux
- Membrane materials choice
- Configuration of module
- Thermal/ mechanical/chemical stability
- Design of system at industrial scale with processability
- Cost-effectiveness for operating conditions

The application of MOFs in a real liquid separation membrane is mainly based on both the separation properties of MOFs and the abovementioned factors. In the meantime, the screening for characteristic-oriented applications also emphasizes the rational selection of MOFs for separation. Furthermore, another measure involves the types of MOF-based membrane filtration in the screening of MOFs. In liquid filtration, a positive pressure is applied to the feed for separations. According to this mechanism, the larger species than pore diameter are rejected while the smaller species are membrane-permeable. The selective permeability result in true molecular sieving as the MOFs nature is crystalline. Regardless of the above-described characteristics of MOFs, i.e., stability, dispersibility, and hydrophilicity/hydrophobicity some other important following features of MOFs should be considered for liquid separation membranes.

Synthesis conditions: As compared to other porous materials, most of the MOFs are synthesized at lower activation energy. For example, different room temperature preparation techniques have been reported for the synthesis of MOFs such as HKUST-1 and ZIF-71 [86, 98]. More often, both of these techniques are used to form MOFs-based liquid separation membranes. There are many advantages of this methodology, i.e., economical and easy equipment, low energy cost, and a short reaction time that offer energy-saving procedures to fabricate MOF-based membranes.

Particle size: Particle size also exhibits an imperative role in MOF membrane synthesis. Reduction in particle size is directly related to enhancing intrinsic characteristics manifestation. MOF particles, with improved accessibility toward internal as well as external specific surface area, have shown a substantial amendment in aqueous

solution separation. For instance, the sub-micrometer-sized ZIF-71 nanocrystals of the range of 140, 290, or 430 nm have been recognized as ideal fillers to make smooth, thin, and uniform membranes. Moreover, MM membranes have an outstanding filler dispersion character for the refinement of the bioethanol with the help of pervaporation at high loading up to 40 w.t %. The remarkable influence of ZIF-71 nanocrystals for considerable separation factor and increase of flux is due to the advanced MOF adsorption process.

6 MOF-Based Membranes Design Strategies

The rational design of the fabrication membrane is the key to fulfill the demand for fast and precise liquid separation. The principle of fabrication for membranes is "design-for-purpose" for high efficiency. The fabrication processes of MOF-based membranes are attaining more improvements from the past decades and are environment friendly. Two main fabrication procedures are usable for the designing of liquid separation membranes that are continuous growth of MOF-based membranes and mixed matrix MOF-based membranes. By considering the rational designs several strategies are used to assemble the MOF-based membranes, i.e., (i) in situ preparation path, (ii) blending, and (iii) interfacial polymerization method. Figure 3 shows the designing methods of MOF-based membranes [61, 90].

6.1 Continuous Method

In this method of continuous growth pure MOF layer is fabricated on the substrate. The microcrystalline powder of MOFs is added to a solution to make a polymer dope which is molded into a membrane. The resulted in pure MOF exhibits chemical properties that only depend on the MOFs themselves. There are many strategies for the continuous growth of MOF-based membranes, e.g., in situ growth, seeded growth, or liquid-phase synthesis. Figure 4 shows the various methods of MOF-based membranes designing [25, 32, 88]. In the in situ growth method, a substrate is immersed with the growth solution. A polycrystalline structure is formed by heating metal salt and organic ligand solution followed by the addition of a substrate. The intergrowth and nucleation growth of crystals takes place in the fabrication step. The limitations of the method are cracks and film defects in the growth of polycrystalline structures. Firstly, a ZIF-8 immersed with the (PSf) ultrafiltration membrane followed by the in situ development of ZIF. After that, a (PA) was layered on (ZIF-8) by interfacial polymerization. The (ZIF-8) crystals work as seeds for the surface of the membrane, the absolute (ZIF-8-PSf) sheath gives a constant (ZIF-8) layer [18, 96].

Secondary growth is the method in which already prepared seed crystals are used for membrane growth, it is also a continuous MOFs membranes strategy followed by in situ preparation route. However, secondary growth is rather a complex method as
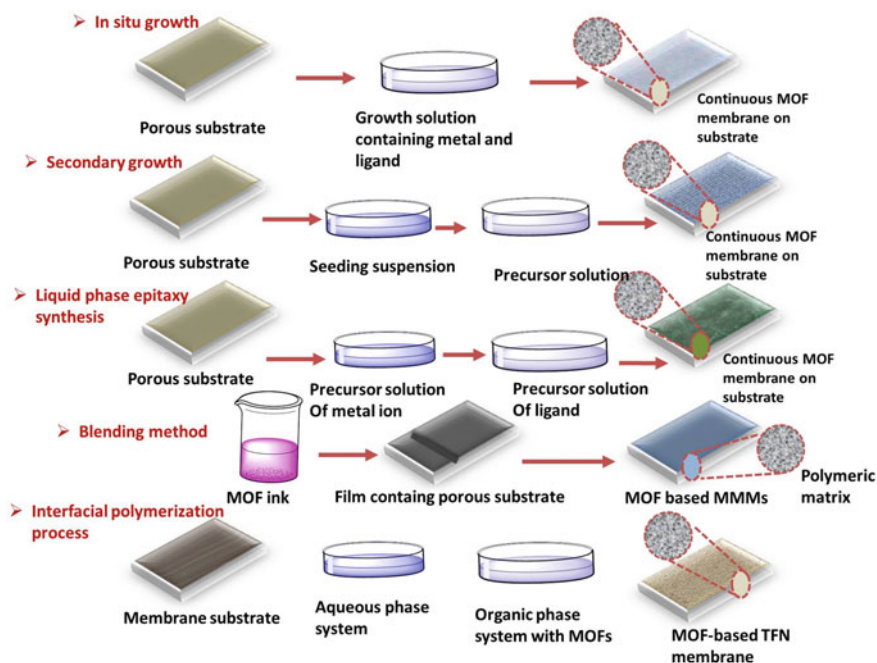
Fig. 4 Various methods of MOF-based membrane designing

compared to in situ growth method. Secondary growth is moderately good to regulate the final alignment and for obtaining thick, crack-free continuous membranes. In 2012, by using the secondary growth ZIF-8 was designed on ($\grave{\alpha}$-Al$_2$O$_3$) microfiltration membranes. Similarly, a reactive seeding process was established for the preparation of MIL-based MOFs membranes, in which the porous surface is the inorganic while an organic linker grows a seeding layer [45, 59]. A ZnO substrate was used for the fabrication of a (ZIF-71) membrane that was usable to separate the, i.e., dimethyl carbonate–methanol and alcohol-water mixtures [91, 92].

The liquid stage epitaxy synthesis method is used to design continuous MOFs-based membranes. In this method, the substrate is recycled with intermediate washing steps, immersed with (only metal and ligand solutions), and followed by the synthesis of continuous MOF layers. Typically this procedure is appropriate to synthesize MOF thin layers and research scale MOFs-based membranes with low limitations. These films are good due to affordable use and having fewer defects while other processes are time taking, non-trivial and difficult to scale up [39, 87].

In the interfacial diffusion method, the opposite surfaces of the substrate are protected by metal and ligand-only solution, these two components combine to form a MOFs membrane. The major advantage of this method is self-repairing as compare to layer by layer process. This method is greatly promoted to MOFs membrane fabrication [44].

6.2 Composite System

MOF-based (MMMs) types of membrane are prepared by the combination of MOFs (micro- or nanoparticles) and a polymer matrix. In this method, a pure MOFs layer is fabricated on the substrate. The microcrystalline powder of MOFs is added to a solution that results in a polymer dope then it is cast into membranes. MOF-based MMMs exhibit high porosity and feasible processability of polymers. The mixed matrix membrane synthesis needs a supporting substrate, which gives free-standing membranes rather than MOF synthetic conditions. Although for enhancing the properties of polymeric membranes small MOFs loading in (MMMs) plays a supportive role. However, the increased amount of MOFs in (MMMs) than the polymer can control the MMMs properties, in this situation polymer works as a binder. Despite these MOFs-based MMMs also possess some limitations, e.g., the non-porous nature of various polymers reduces the permeability as compared to pure MOFs. To overcome this limitation high loading of MOFs was used which converts the MMMs toward MOF dominant [17, 52].

To design MOF-based MMMs blending is another significant method it may be substrate-based blending or substrate-free blending. Substrate-based blending is used to prepare the thin MOF-based membranes for pervaporation [99]. For this purpose, various porous polymeric membranes are used to improve the stability and strength of MMMs. This process involved three major steps (i) mixing of polymer and MOFs (ii) casting of the solution on the membrane (iii) Drying off the solvent. Furthermore in a novel blending strategy through electrostatic attraction, a polymeric membrane is used to support a MOF precursor. After those metal–organic frameworks are produced, throughout this process production of metal–organic frameworks and fabrication of membranes are assimilated in one system that provides benefits of low cost and high separation potential. The substrate-free blending method is effective and flexible; there is no need for polymeric support for liquid separation. This method faces MOF particle agglomeration problem which is resolved by the post-synthetic polymerization of organic oligomer [49, 79].

Interfacial polymerization is a classic method for the designing of the membrane. MOFs are also widely combined with polymeric membranes to form (TFN) and (MMMs). Generally, most of the MOFs are obtained in powder form, firstly the MOFs powder is immersed with polymeric solution then it is cast into the membrane. While the TFN membranes can be designed by the interfacial polymerization method in which the polymerization between the MPD solution and TMC solution takes place [48, 61].

7 MOF Boosted Membranes Solution, Challenges, and Future Prospects

In a short time, due to large surface area, structural variety, tunability, and high porosity, MOF boosted membranes have been drawn increasing consideration in environmental and water applications. A suitable combination of filtration membranes is used to enhance the worthwhile application of MOFs.

Instead of direct use of MOF powder/monolith, MOFs combined with filtration membranes can be used. There have been substantial advancements in permeability, antifouling, and selectivity in membrane filtration. MOF boosted membranes such as adsorptive, antifouling, high permeable, and catalytic membranes are also observed for a similar trend. Specifically, the action of MOF-modified RO/NF/FO/UF membranes have importantly built by qualifying the following properties of the membrane:

1. MOF-based membranes have various properties including; variable porosity, excessive channels, and approachable great surface areas, which enhance the transport of water across the membranes; and
2. These MOFs are hydrophilic and have great susceptibility to harvester-specific functionalities/species quite easily without ever-changing the MO-framework topology.

This preferential intensifies selectivity of membrane and membrane antifouling owing to electrostatic repulsion of charges and steric omission. Furthermore, the modification of industrial application on a large scale with the use of selected MOFs in NF/RO/FO/UF membranes thus amended the stability and crudeness of membranes significantly. Nevertheless, the practical applications of MOF modified membrane were limited to small-scale short endeavors and selected solutes (including heavy metals, NaCl & organic dyes), under limited water and operative parameters. Consequently, an extensive evaluation of different MOF-boosted membranes for various materials under specific operational conditions and for different concentrations of water is crucial mainly: to evaluate the effect of various MOFs on film production and their properties based on their porosity, hydrophilicity, and surface texture. It is quite stimulating to determine the uniform dispersion of MOFs in numerous solvents, the combination of MOFs and model compounds or the use of streamlined integrated techniques, and post-treatment techniques to lessen the insufficiency of PMs. A "trade-off" in terms of removal of salts, as well as water permeability for RO, UF, NF, FO, and MOF-based film, is also studied to determine the MMMs transport performances in the presence of natural organic pollutants and various ions concentrations and to reproduce natural waters [19]. For practical liquid separation application, principally hydrolytic and chemically stable MOFs combined with membrane are considered. In particular, during membrane filtration, the specific pH of the solution might cause simple MOF structure degradation. It may change or damage the distinctive phase as a result of a loss of filtration capacity.

For water sustainability, great struggles were devoted to them and stimulate worldwide interest from prototype development, academic research, and practical applications at large scale are some of the promising results that have been demonstrated.

There are still many challenges to be addressed. The biggest challenge is poor water stability. Most of the MOFs are unstable in moisture environments apart from a few MOFs, i.e., UiO-66, MIL, and ZIF series and cause a difficult recovery and second pollution. Hydrophobic modification is a well-adapted method to enhance the hydrolytic stability of MOFs while they are not applicable in wastewater treatment.

Continuous efforts for water-stable MOFs should be devoted to exploring the new approaches without scarifying the hydrophilicity. To prepare water-stable MOFs, new methods are rapidly needed. The increased adhesion between substrates and MOFs is also required. For example, for the advanced self-clean and antifouling membranes in wastewater treatment, add photocatalytic MOFs into filtration membranes. To improve efficiency and engineering strategy in traditional photocatalysts can be adopted. Modified MOFs with organic ligands and metal-oxoclusters can be prepared to achieve higher stability, a larger surface area, boasted photocatalytic action, and a stronger light response at a large scale. The best MOFs would be able to degrade contaminants into sustainable substances. The compounds after the photocatalytic process such as non-aqueous gas can remove from the liquid system automatically. Water sustainability as photo-thermal are and water captures some new applications of simple MOFs. Scientists must target to advance widespread applications of MOFs such as easy eco-friendly recycling or regeneration practices, environmentally friendly disposal options for the waste materials, and cost-minimization of the final product [36, 57]. To make MOFs widely acceptable membranes in water purification, there is a need for the systematic evolution of MOFs toward better stability and efficiency.

8 Conclusion

Water safety is becoming a challenging situation globally. Many hazardous materials, e.g., pharmaceutical products, organic pollutants (organic dyes) heavy metals, and polyaromatic compounds are discharged in the water without any treatment. In environmental water bodies, the presence of dye effluents is one of the big problems to produce pollution. To overcome this problem various methods, e.g., biological, physical, chemical, MOFs, and MOFs-based membranes used for the processing of wastewater. Conventionally, used dye removal methods possess some limitations such as the production of secondary pollutants, less efficiency, and high cost. Among all the dye removal methods the use of MOFs and MOFs-based membranes is reliable because MOFs are crystalline materials showing high porosity and large surface area. The integration of MOFs with filtration membranes (NF, RO, FO, and UF) is also a great deal. Numerous studies significantly showed the improvement in water flux,

selectivity, and antifouling by using the combination of MOFs with various MOFs-based membranes. The performance of MOFs-based membranes can be enhanced by increasing the different properties, i.e., MOFs-based MMMs have great porosities, large surface area and the hydrophilic MOFs prevent the membranes from fouling. The incorporation of MOFs with filtration membranes increases the durability of membranes, their roughness and also makes them feasible for large-scale applications. However, studies are limited to a few MOFs so there is a need for comprehensive evaluations on MOFs-based membranes to determine the effect of different MOFs on membrane fabrication. Despite these new fabrication methods are needed which focusing on practical applications, increase durability and are inexpensive.

References

1. Adegoke KA, Bello OS (2015) Dye sequestration using agricultural wastes as adsorbents. Water Resour Industry 12:8–24. https://doi.org/10.1016/j.wri.2015.09.002
2. Adeyemo AA, Adeoye IO, Bello OS (2012) Metal organic frameworks as adsorbents for dye adsorption: overview, prospects and future challenges. Toxicol Environ Chem 94(10):1846–1863. https://doi.org/10.1080/02772248.2012.744023
3. Akbari A, Remigy JC, Aptel P (2002) Treatment of textile dye effluent using a polyamide-based nanofiltration membrane. Chem Eng Process 41(7):601–609. https://doi.org/10.1016/S0255-2701(01)00181-7
4. Al-Alwani MA, Ludin NA, Mohamad AB, Kadhum AAH, Mukhlus A (2018) Application of dyes extracted from Alternanthera dentata leaves and Musa acuminata bracts as natural sensitizers for dye-sensitized solar cells. Spectrochim Acta Part A Mol Biomol Spectrosc 192:487–498. https://doi.org/10.1016/j.saa.2017.11.018
5. Al-Aseeri M, Bu-Ali Q, Haji S, Al-Bastaki N (2007) Removal of acid red and sodium chloride mixtures from aqueous solutions using nanofiltration. Desalination 206(1):407–413. https://doi.org/10.1016/j.desal.2006.03.575
6. Al-Bastaki N (2004) Removal of methyl orange dye and Na2SO4 salt from synthetic waste water using reverse osmosis. Chem Eng Process Process Intensif 43(12):1561–1567. https://doi.org/10.1016/j.cep.2004.03.001
7. Allen S, Koumanova B (2005) Decolourisation of water/wastewater using adsorption. J Univ Chem Technol Metall 40(3):175–192
8. Amini M, Arami M, Mahmoodi NM, Akbari A (2011) Dye removal from colored textile wastewater using acrylic grafted nanomembrane. Desalination 267(1):107–113. https://doi.org/10.1016/j.desal.2010.09.014
9. Anjum M, Miandad R, Waqas M, Gehany F, Barakat MA (2019) Remediation of wastewater using various nano-materials. Arab J Chem 12(8):4897–4919. https://doi.org/10.1016/j.arabjc.2016.10.004
10. Araya T, Jia M, Yang J, Zhao P, Cai K, Ma W, Huang Y (2017) Resin modified MIL-53 (Fe) MOF for improvement of photocatalytic performance. Appl Catal B 203:768–777. https://doi.org/10.1016/j.apcatb.2016.10.072
11. Badani Z, Ait-Amar H, Si-Salah A, Brik M, Fuchs W (2005) Treatment of textile waste water by membrane bioreactor and reuse. Desalination 185(1):411–417. https://doi.org/10.1016/j.desal.2005.03.088
12. Baek S-W, Kim J-R, Ihm S-K (2004) Design of dual functional adsorbent/catalyst system for the control of VOC's by using metal-loaded hydrophobic Y-zeolites. Catal Today 93:575–581. https://doi.org/10.1016/j.cattod.2004.06.107

13. Ballav N, Das R, Giri S, Muliwa AM, Pillay K, Maity A (2018) L-cysteine doped polypyrrole (PPy@ L-Cyst): a super adsorbent for the rapid removal of Hg+ 2 and efficient catalytic activity of the spent adsorbent for reuse. Chem Eng J 345:621–630. https://doi.org/10.1016/j.cej.2018.01.093

14. Bello O, Ahmad M (2012) Preparation and characterization of activated carbon derived from rubber seed coat. Chem Bulg J Sci Edu 21:389–395. https://doi.org/10.1007/s13201-015-0345-4

15. Britt D, Tranchemontagne D, Yaghi OM (2008) Metal-organic frameworks with high capacity and selectivity for harmful gases. Proc Natl Acad Sci 105(33):11623–11627. https://doi.org/10.1073/pnas.0804900105

16. Burtch NC, Jasuja H, Walton KS (2014) Water stability and adsorption in metal-organic frameworks. Chem Rev 114(20):10575–10612. https://doi.org/10.1021/cr5002589

17. Campbell J, Davies RP, Braddock DC, Livingston AG (2015) Improving the permeance of hybrid polymer/metal–organic framework (MOF) membranes for organic solvent nanofiltration (OSN) – development of MOF thin films via interfacial synthesis. J Mater Chem A 3(18):9668–9674. https://doi.org/10.1039/C5TA01315A

18. Campbell J, Székely G, Davies RP, Braddock DC, Livingston AG (2014) Fabrication of hybrid polymer/metal organic framework membranes: mixed matrix membranes versus in situ growth. J Mater Chem A 2(24):9260–9271. https://doi.org/10.1039/C4TA00628C

19. Carson CG, Hardcastle K, Schwartz J, Liu X, Hoffmann C, Gerhardt RA, Tannenbaum R (2009) Synthesis and structure characterization of copper terephthalate metal-organic frameworks. Eur J Inorg Chem 2009(16):2338–2343. https://doi.org/10.1002/ejic.200801224

20. Chen S, Zhang J, Zhang C, Yue Q, Li Y, Li C (2010) Equilibrium and kinetic studies of methyl orange and methyl violet adsorption on activated carbon derived from Phragmites australis. Desalination 252(1–3):149–156. https://doi.org/10.1016/j.desal.2009.10.010

21. Chen Y, Zhang S, Cao S, Li S, Chen F, Yuan S, Wang B (2017) Roll-to-Roll production of metal-organic framework coatings for particulate matter removal. Adv Mater 29(15). https://doi.org/10.1002/adma.201606221

22. Criscuoli A, Zhong J, Figoli A, Carnevale MC, Huang R, Drioli E (2008) Treatment of dye solutions by vacuum membrane distillation. Water Res 42(20):5031–5037. https://doi.org/10.1016/j.watres.2008.09.014

23. Dong X, Lin YS (2013) Synthesis of an organophilic ZIF-71 membrane for pervaporation solvent separation. Chem Commun 49(12):1196–1198. https://doi.org/10.1039/C2CC38512K

24. Fan H, Wang N, Ji S, Yan H, Zhang G (2014) Nanodisperse ZIF-8/PDMS hybrid membranes for biobutanol permselective pervaporation. J Mater Chem A 2(48):20947–20957. https://doi.org/10.1039/C4TA04114C

25. Fan H, Xie Y, Li J, Zhang L, Zheng Q, Zhang G (2018) Ultra-high selectivity COF-based membranes for biobutanol production. J Mater Chem A 6(36):17602–17611. https://doi.org/10.1039/C8TA06902F

26. De Gisi S, Lofrano G, Grassi M, Notarnicola M (2016) Characteristics and adsorption capacities of low-cost sorbents for wastewater treatment: a review. Sustain Mater Technol 9:10–40. https://doi.org/10.1016/j.susmat.2016.06.002

27. Goh PS, Ismail AF (2018) A review on inorganic membranes for desalination and wastewater treatment. Desalination 434:60–80. https://doi.org/10.1016/j.desal.2017.07.023

28. Gu Q, Ng HY, Zhao D, Wang J (2020) Metal–organic frameworks (MOFs)-boosted filtration membrane technology for water sustainability. APL Mater 8(4):040902. https://doi.org/10.1063/5.0002905

29. Haque E, Khan NA, Park JH, Jhung SH (2010) Synthesis of a metal–organic framework material, iron terephthalate, by ultrasound, microwave, and conventional electric heating: a kinetic study. Chem Europ J 16(3):1046–1052. https://doi.org/10.1002/chem.200902382

30. Hethnawi A, Nassar NN, Manasrah AD, Vitale G (2017) Polyethylenimine-functionalized pyroxene nanoparticles embedded on Diatomite for adsorptive removal of dye from textile wastewater in a fixed-bed column. Chem Eng J 320:389–404. https://doi.org/10.1016/j.cej.2017.03.057

31. Hu Y, Dong X, Nan J, Jin W, Ren X, Xu N, Lee YM (2011) Metal–organic framework membranes fabricated via reactive seeding. Chem Commun 47(2):737–739. https://doi.org/10.1039/C0CC03927F

32. Jun B-M, Al-Hamadani YAJ, Son A, Park CM, Jang M, Jang A, Yoon Y (2020) Applications of metal-organic framework based membranes in water purification: a review. Sep Purifi Technol 247:116947. https://doi.org/10.1016/j.seppur.2020.116947

33. Kadhom M, Deng B (2018) Metal-organic frameworks (MOFs) in water filtration membranes for desalination and other applications. Appl Mater Today 11:219–230. https://doi.org/10.1016/j.apmt.2018.02.008

34. Katheresan V, Kansedo J, Lau SY (2018) Efficiency of various recent wastewater dye removal methods: a review. J Environ Chem Eng 6(4):4676–4697. https://doi.org/10.1016/j.jece.2018.06.060

35. Khan NA, Bhadra BN, Jhung SH (2018) Heteropoly acid-loaded ionic liquid@ metal-organic frameworks: Effective and reusable adsorbents for the desulfurization of a liquid model fuel. Chem Eng J 334:2215–2221. https://www.cheric.org/research/tech/periodicals/doi.php?art_seq=1593550

36. Kim H, Rao SR, Kapustin EA, Zhao L, Yang S, Yaghi OM, Wang EN (2018) Adsorption-based atmospheric water harvesting device for arid climates. Nat Commun 9(1):1191. https://doi.org/10.1038/s41467-018-03162-7

37. Le-Clech P, Chen V, Fane TAG (2006) Fouling in membrane bioreactors used in wastewater treatment. J Membr Sci 284(1):17–53. https://doi.org/10.1016/j.memsci.2006.08.019

38. Ledakowicz S, Solecka M, Zylla R (2001) Biodegradation, decolourisation and detoxification of textile wastewater enhanced by advanced oxidation processes. J Biotechnol 89(2):175–184. https://doi.org/10.1016/S0168-1656(01)00296-6

39. Lee D-J, Li Q, Kim H, Lee K (2012) Preparation of Ni-MOF-74 membrane for CO2 separation by layer-by-layer seeding technique. Microporous Mesoporous Mater 163:169–177. https://doi.org/10.1016/j.micromeso.2012.07.008

40. Li Q, Elimelech M (2004) Organic fouling and chemical cleaning of nanofiltration membranes: measurements and mechanisms. Environ Sci Technol 38(17):4683–4693. https://doi.org/10.1021/es0354162

41. Li H, Lin Y, Luo Y, Yu P, Hou L (2011) Relating organic fouling of reverse osmosis membranes to adsorption during the reclamation of secondary effluents containing methylene blue and rhodamine B. J Hazard Mater 192(2):490–499. https://doi.org/10.1016/j.jhazmat.2011.05.044

42. Li X, Liu Y, Wang J, Gascon J, Li J, Van der Bruggen B (2017) Metal–organic frameworks based membranes for liquid separation. Chem Soc Rev 46(23):7124–7144. https://doi.org/10.1039/C7CS00575J

43. Li J, Sanderson RD (2002) In situ measurement of particle deposition and its removal in microfiltration by ultrasonic time-domain reflectometry. Desalination 146(1):169–175. https://doi.org/10.1016/S0011-9164(02)00521-0

44. Li Y, Wee LH, Volodin A, Martens JA, Vankelecom IFJ (2015) Polymer supported ZIF-8 membranes prepared via an interfacial synthesis method. Chem Commun 51(5):918–920. https://doi.org/10.1039/C4CC06699E

45. Li W, Zhang Y, Li Q, Zhang G (2015) Metal−organic framework composite membranes: synthesis and separation applications. Chem Eng Sci 135:232–257. https://doi.org/10.1016/j.ces.2015.04.011

46. Li Z, Zhou G, Dai H, Yang M, Fu Y, Ying Y, Li Y (2018) Biomineralization-mimetic preparation of hybrid membranes with ultra-high loading of pristine metal–organic frameworks grown on silk nanofibers for hazard collection in water. J Mater Chem A 6(8):3402–3413. https://doi.org/10.1039/C7TA06924C

47. Li J, Wang H, Yuan X, Zhang J, Chew JW (2020) Metal-organic framework membranes for wastewater treatment and water regeneration. Coord Chem Rev 404:213116. https://doi.org/10.1016/j.ccr.2019.213116

48. Lin R, Ge L, Hou L, Strounina E, Rudolph V, Zhu Z (2014) Mixed matrix membranes with strengthened MOFs/Polymer interfacial interaction and improved membrane performance. ACS Appl Mater Interfaces 6(8):5609–5618. https://doi.org/10.1021/am500081e

49. Lin R, Villacorta Hernandez B, Ge L, Zhu Z (2018) Metal organic framework based mixed matrix membranes: an overview on filler/polymer interfaces. J Mater Chem A 6(2):293–312. https://doi.org/10.1039/C7TA07294E

50. Lindau J, Jönsson AS, Bottino A (1998) Flux reduction of ultrafiltration membranes with different cut-off due to adsorption of a low-molecular-weight hydrophobic solute-correlation between flux decline and pore size. J Membr Sci 149(1):11–20. https://doi.org/10.1016/S0376-7388(98)00161-6

51. Liu J, Choi HJ, Meng LY (2018) A review of approaches for the design of high-performance metal/ graphene electrocatalysts for fuel cell applications. J Ind Eng Chem 64:1–15. https://doi.org/10.1016/j.jiec.2018.02.021

52. Liu X, Demir NK, Wu Z, Li K (2015) Highly water-stable zirconium metal-organic framework UiO-66 membranes supported on alumina hollow fibers for desalination. J Am Chem Soc 137(22):6999–7002. https://doi.org/10.1021/jacs.5b02276

53. Liu R, Sui Y, Wang X (2019) Metal–organic framework-based ultrafiltration membrane separation with capacitive-type for enhanced phosphate removal. Chem Eng J 371:903–913. https://doi.org/10.1016/j.cej.2019.04.136

54. Liu X, Wang C, Wang B, Li K (2017) Novel organic-dehydration membranes prepared from zirconium metal-organic frameworks. Adv Func Mater 27(3):1604311. https://doi.org/10.1002/adfm.201604311

55. Liu J, Wöll C (2017) Surface-supported metal–organic framework thin films: fabrication methods, applications, and challenges. Chem Soc Rev 46(19):5730–5770. https://doi.org/10.1039/C7CS00315C

56. Liu X, Zhang L, Wang J (2021) Design strategies for MOF-derived porous functional materials: preserving surfaces and nurturing pores. J Materiomics 7(3):440–459. https://doi.org/10.1016/j.jmat.2020.10.008

57. Ma X, Chai Y, Li P, Wang B (2019) Metal-organic framework films and their potential applications in environmental pollution control. Acc Chem Res 52(5):1461–1470. https://doi.org/10.1021/acs.accounts.9b00113

58. Ma X-H, Yang Z, Yao Z-K, Xu Z-L, Tang CY (2017) A facile preparation of novel positively charged MOF/chitosan nanofiltration membranes. J Membr Sci 525:269–276. https://doi.org/10.1016/j.memsci.2016.11.015

59. Ma X, Li Y, Huang A (2020) Synthesis of nano-sheets seeds for secondary growth of highly hydrogen permselective ZIF-95 membranes. J Mbr Sci 597:117629. https://doi.org/10.1016/j.memsci.2019.117629

60. Maleki A, Hamesadeghi U, Daraei H, Hayati B, Najafi F, McKay G, Rezaee R (2017) Amine functionalized multi-walled carbon nanotubes: single and binary systems for high capacity dye removal. Chem Eng J 313:826–835

61. Matsumoto M, Valentino L, Stiehl GM, Balch HB, Corcos AR, Wang F, Dichtel WR (2018) Lewis-acid-catalyzed interfacial polymerization of covalent organic framework films. Chem 4(2):308–317. https://doi.org/10.1016/j.chempr.2017.12.011

62. Merzouk B, Gourich B, Madani K, Vial C, Sekki A (2011) Removal of a disperse red dye from synthetic wastewater by chemical coagulation and continuous electrocoagulation a comparative study. Desalination 272(1):246–253. https://doi.org/10.1016/j.desal.2011.01.029

63. Mezohegyi G, van der Zee FP, Font J, Fortuny A, Fabregat A (2012) Towards advanced aqueous dye removal processes: a short review on the versatile role of activated carbon. J Environ Manage 102:148–164. https://doi.org/10.1016/j.jenvman.2012.02.021

64. Mon M, Bruno R, Ferrando-Soria J, Armentano D, Pardo E (2018) Metal–organic framework technologies for water remediation: towards a sustainable ecosystem. J Mater Chem A 6(12):4912–4947. https://doi.org/10.1039/C8TA00264A

65. Özacar M, Şengil İA (2006) A two stage batch adsorber design for methylene blue removal to minimize contact time. J Environ Manage 80(4):372–379. https://doi.org/10.1016/j.jenvman.2005.10.004

66. Park HB, Kamcev J, Robeson LM, Elimelech M, Freeman BD (2017) Maximizing the right stuff: The trade-off between membrane permeability and selectivity. Science 356(6343):eaab0530. https://doi.org/10.1126/science.aab0530

67. Puthiaraj P, Cho S-M, Lee Y-R, Ahn W-S (2015) Microporous covalent triazine polymers: efficient friedel-crafts synthesis and adsorption/storage of CO2 and CH4. J Mater Chem A 3(13):6792–6797. https://doi.org/10.1039/C5TA00665A

68. Qian X, Yadian B, Wu R, Long Y, Zhou K, Zhu B, Huang Y (2013) Structure stability of metal-organic framework MIL-53 (Al) in aqueous solutions. Int J Hydrogen Energy 38(36):16710–16715. https://doi.org/10.1016/j.ijhydene.2013.07.054

69. Quader AA (2010) Treatment of textile wastewater with chlorine: an effective method. Chem Eng Res Bull 14(1):59–63. https://doi.org/10.3329/cerb.v14i1.3206

70. Rafatullah M, Sulaiman O, Hashim R, Ahmad A (2010) Adsorption of methylene blue on low-cost adsorbents: a review. J Hazard Mater 177(1):70–80. https://doi.org/10.1016/j.jhazmat.2009.12.047

71. Raffatulah M, Sulaiman O, Hashim R, Ahmad A (2010) Adsorption of methylene blue on low-cost adsorbent: a review. J Chem Eng 177: 7080. https://doi.org/10.20885/ijcr.vol2.iss1.art6

72. Rashed M, El-Amin A (2007) Photocatalytic degradation of methyl orange in aqueous TiO2 under different solar irradiation sources. Int J Phys Sci 2(3):73–81. https://doi.org/10.5897/IJPS.9000436

73. Ruan H, Guo C, Yu H, Shen J, Gao C, Sotto A, Van der Bruggen B (2016) Fabrication of a MIL-53(Al) nanocomposite membrane and potential application in desalination of dye solutions. Ind Eng Chem Res 55(46):12099–12110. https://doi.org/10.1021/acs.iecr.6b03201

74. Safa Y, Bhatti HN (2011) Adsorptive removal of direct textile dyes by low cost agricultural waste: application of factorial design analysis. Chem Eng J 167(1):35–41. https://doi.org/10.1016/j.cej.2010.11.103

75. Sarro M, Gule NP, Laurenti E, Gamberini R, Cristina M, Mallon PE, Calza P ZnO-based materials and enzymes hybrid systems as highly e ffi cient catalysts for recalcitrant pollutants abatement G RA PHICAL AB STRACT. https://doi.org/10.1016/j.cej.2017.11.146

76. Shu L, Wang N, Zhao C, Meng Y, Ji S, Li J-R (2019) Facile fabrication of high performance nanofiltration membranes by using molecular coordination complexes as pore-forming agents. ACS Sustain Chem Eng 7(2):2728–2738. https://doi.org/10.1021/acssuschemeng.8b05817

77. Simpson DL, Brooks CL (1999) Tailoring the structural integrity process to meet the challenges of aging aircraft. Int J Fatigue 21:S1–S14. https://doi.org/10.1016/S0142-1123(99)00052-3

78. Solis-Oba MM, Solís A, Pérez HI, Manjarrez N, Flores M (2012) Microbial decolouration of azo dyes. Process Biochem 47(12):1723–1748. https://doi.org/10.1016/j.procbio.2012.08.014

79. Sun J, Li Q, Chen G, Duan J, Liu G, Jin W (2019) MOF-801 incorporated PEBA mixed-matrix composite membranes for CO2 capture. Sep Purif Technol 217:229–239. https://doi.org/10.1016/j.seppur.2019.02.036

80. Tang L, Yu J, Pang Y, Zeng G, Deng Y, Wang J, Feng H (2018) Sustainable efficient adsorbent: alkali-acid modified magnetic biochar derived from sewage sludge for aqueous organic contaminant removal. Chem Eng J 336:160–169. https://doi.org/10.1016/j.cej.2017.11.048

81. Tian W, Sun H, Duan X, Zhang H, Ren Y, Wang S (2020) Biomass-derived functional porous carbons for adsorption and catalytic degradation of binary micropollutants in water. J Hazard Mater 389:121881. https://doi.org/10.1016/j.jhazmat.2019.121881

82. Valizadeh B, Nguyen TN, Stylianou KC (2018) Shape engineering of metal–organic frameworks. Polyhedron 145:1–15. https://doi.org/10.1016/j.poly.2018.01.004

83. Wang L, Fang M, Liu J, He J, Li J, Lei J (2015) Layer-by-layer fabrication of high-performance polyamide/ZIF-8 Nanocomposite membrane for nanofiltration applications. ACS Appl Mater Interfaces 7(43):24082–24093. https://doi.org/10.1021/acsami.5b07128

84. Wang C, Liu X, Chen JP, Li K (2015) Superior removal of arsenic from water with zirconium metal-organic framework UiO-66. Sci Rep 5(1):16613. https://doi.org/10.1038/srep16613

85. Warsinger DM, Chakraborty S, Tow EW, Plumlee MH, Bellona C, Loutatidou S, Lienhard JH (2018) A review of polymeric membranes and processes for potable water reuse. Prog Polym Sci 81:209–237. https://doi.org/10.1016/j.progpolymsci.2018.01.004

86. Wee LH, Li Y, Zhang K, Davit P, Bordiga S, Jiang J, Martens JA (2015) Submicrometer-Sized ZIF-71 filled organophilic membranes for improved bioethanol recovery: mechanistic insights by monte carlo simulation and FTIR spectroscopy. Adv Func Mater 25(4):516–525. https://doi.org/10.1002/adfm.201402972

87. Xiang F, Marti AM, Hopkinson DP (2018) Layer-by-layer assembled polymer/MOF membrane for H2/CO2 separation. J Membr Sci 556:146–153. https://doi.org/10.1016/j.memsci.2018.03.081

88. Yang H, Cheng X, Cheng X, Pan F, Wu H, Liu G, Jiang Z (2018) Highly water-selective membranes based on hollow covalent organic frameworks with fast transport pathways. J Membr Sci 565:331–341. https://doi.org/10.1016/j.memsci.2018.08.043

89. Yang L, Wang Z, Zhang J (2017) Zeolite imidazolate framework hybrid nanofiltration (NF) membranes with enhanced permselectivity for dye removal. J Membr Sci 532:76–86. https://doi.org/10.1016/j.memsci.2017.03.014

90. Yang H, Wu H, Pan F, Li Z, Ding H, Liu G, Wang B (2016) Highly water-permeable and stable hybrid membrane with asymmetric covalent organic framework distribution. J Membr Sci 520:583–595. https://doi.org/10.1016/j.memsci.2016.08.022

91. Yin Y, Li Z, Yang X, Cao L, Wang C, Zhang B, Jiang Z (2016) Enhanced proton conductivity of Nafion composite membrane by incorporating phosphoric acid-loaded covalent organic framework. J Power Sources 332:265–273. https://doi.org/10.1016/j.jpowsour.2016.09.135

92. Yoo Y, Lai Z, Jeong H-K (2009) Fabrication of MOF-5 membranes using microwave-induced rapid seeding and solvothermal secondary growth. Microporous Mesoporous Mater 123(1):100–106. https://doi.org/10.1016/j.micromeso.2009.03.036

93. Zacher D, Shekhah O, Wöll C, Fischer RA (2009) Thin films of metal–organic frameworks. Chem Soc Rev 38(5):1418–1429. https://doi.org/10.1039/B805038B

94. Zhang X, Liu Y, Li S, Kong L, Liu H, Li Y, Qiu J (2014) New membrane architecture with high performance: ZIF-8 membrane supported on vertically aligned ZnO nanorods for gas permeation and separation. Chem Mater 26(5):1975–1981. https://doi.org/10.1021/cm500269e

95. Zhao X, Zhang R, Liu Y, He M, Su Y, Gao C, Jiang Z (2018) Antifouling membrane surface construction: chemistry plays a critical role. J Membr Sci 551:145–171. https://doi.org/10.1016/j.memsci.2018.01.039

96. Zhou S, Wei Y, Zhuang L, Ding L-X, Wang H (2017) Introduction of metal precursors by electrodeposition for the in situ growth of metal–organic framework membranes on porous metal substrates. J Mater Chem A 5(5):1948–1951. https://doi.org/10.1039/C6TA09469D

97. Zhu J, Qin L, Uliana A, Hou J, Wang J, Zhang Y, Van der Bruggen B (2017) Elevated performance of thin film nanocomposite membranes enabled by modified hydrophilic MOFs for nanofiltration. ACS Appl Mater Interfaces 9(2):1975–1986. https://doi.org/10.1021/acsami.6b14412

98. Zhuang J-L, Ceglarek D, Pethuraj S, Terfort A (2011) Rapid room-temperature synthesis of metal-organic framework HKUST-1 crystals in bulk and as oriented and patterned thin films. Adv Func Mater 21(8):1442–1447. https://doi.org/10.1002/adfm.201002529

99. Zornoza B, Tellez C, Coronas J, Gascon J, Kapteijn F (2013) Metal organic framework based mixed matrix membranes: an increasingly important field of research with a large application potential. Microporous Mesoporous Mater 166:67–78. https://doi.org/10.1016/j.micromeso.2012.03.012

Polyethersulfone and Its Derivatives as Membrane Materials for Dye Removal from Water

Swarnalatha Venkatanarasimhan, Durgadevi Nagarajan, and Thilagavathy Palanisamy

Abstract Water contamination by industrial dye effluents is a critical issue faced on a global level over the past few decades and the problem only seems to rise day by day. Dye-polluted water on its consumption, adversely affects human lives and aquatic lives thus creating an imbalance in the ecosystem. Diverse methods are available to treat dye-contaminated water and membrane technology is established as an emerging one among them. Membrane separation has garnered more attention owing to the salient features such as ease of implementation, low cost, and reduction of waste generation. Polyethersulfone (PES) membranes are extensively used for this purpose as they possess high thermal and mechanical stability over other polymeric membrane materials. The key objective of this book chapter is to consolidate the recent advances made in the usage of PES-based membranes for the removal of dye contaminants. Native PES membranes are highly prone to undergo fouling. The hydrophobic nature associated with PES also reduces the separation efficiency. To overcome these drawbacks and also to render higher dye separation efficiency, several organic and inorganic modifications have been carried out to get custom-modified PES membranes. The modifications and the resultant improvements made in PES membranes have been elaborately reviewed in this book chapter.

Keywords Dye wastewater treatment · Dye removal · Dye separation · Membranes · Membrane filtration · Polyethersulfone · Dye rejection · Hydrophilicity of membranes · Water flux · Phase inversion method

S. Venkatanarasimhan (✉) · D. Nagarajan · T. Palanisamy
Department of Sciences, Amrita School of Engineering, Amrita Vishwa Vidyapeetham, Coimbatore, India
e-mail: v_swarnalatha@cb.amrita.edu

T. Palanisamy
e-mail: p_thilagavathy@cb.amrita.edu

1 Membrane Filtration Technology in Dye Wastewater Treatment

Remedial methods suggested for treating dye-contaminated wastewater are plenty in number and adsorption, reverse osmosis, ion exchange, and membrane filtration are few to be named among them [38]. Even though there is no single ideal treatment methodology available for wastewater treatment, membrane filtration technology is demonstrated to be a promising treatment process due to ease of implementation, simple operation, low cost, high separation efficiency, long-term use, low energy consumption, and low environmental impact [41]. In the membrane filtration technique, thin layers of semi-permeable materials specifically known as membranes are put to use, for the permeation of selected components from a feed stream through the membrane [17]. A membrane filtration process can exercise microfiltration, ultrafiltration, nanofiltration, or reverse osmosis membranes, depending on the size of the materials to be removed. The pore sizes of the membranes decrease in the order: microfiltration > ultrafiltration > nanofiltration > reverse osmosis membranes [9]. All these membrane filtration techniques rely on pressure-driven membrane separation, in which the pressure gradient developed across the membrane acts as a driving force for the selective filtration.

Appertaining to the sources of the materials used, membranes can be polymeric, inorganic, or biological in nature. Also, these membranes can be either natural or artificial. For wastewater treatment processes, the use of artificial (synthetic) membranes is in common practice, since natural membranes are limited in number. Despite the availability of diverse types of artificial membrane materials, polymers are found to be irreplaceable membrane materials. Membranes used in labs and industries are mostly synthetic polymer-based membranes owing to the ease with which the barrier structures and properties can be tuned in accordance with the design of polymer. Low-cost, superior mechanical, chemical, and thermal stabilities provided by synthetic polymers also make them ideal materials for membrane fabrication.

With the global industrialization surging in the recent few decades, environmental pollution of all kinds has substantially escalated including water pollution by dyes. The negative effects of these dyes on the ecosystem necessitate for their eradication from water before its consumption. Water purification processes become intricate when a contaminated water sample contains various polluters like colorants, toxic cations, anions, pesticides, microbes, and radioactive wastes [50]. Based on the target pollutants present in the contaminated water, membrane materials are carefully chosen, developed, and used. Furthermore, optimizing parameters such as pore size, permeation flux, water flux, and separation factor of the membrane are crucial in a membrane filtration technique.

Polymers used in the membrane fabrication are desired to have features such as low affinity toward the separated molecules, low cost and competence to resist harsh conditions during operation and cleaning. Thus far, a majority of polymeric materials have been reported for dye removal from contaminated water. Few examples are polyacrylonitrile [18], polyvinylidene fluoride [6], cellulose acetate [14],

polyethersulfone [19], polypropylene [49], and polyvinyl chloride [4]. They vary from each other in their strength, pH tolerance, surface charge, flexibility, and affinity to water. Among them, polyethersulfone-based membranes are prevailingly used in wastewater treatment processes, particularly in dye removal.

In this chapter, an overview of the latest scientific papers reporting on the applications of PES-based membranes in dye removal from water is presented. The chapter has been divided based on the types of materials employed to modify PES membranes and literature works dedicated toward achieving improved PES membrane performance and dye separation efficiency have been collected and included in an organized manner. The chapter highlights preparative methods, advantages, improvements made, and demerits in all of the reported PES-based membranes in dye removal with suitable figures and tables.

1.1 Polyethersulfone as Membrane Material for Dye Removal

Polyethersulfone is an amorphous high-performance thermoplastic polymer that belongs to polysulfone family. The chemical structure of polyethersulfone is presented in Fig. 1. Apart from its application in water treatment plants, PES is also used in numerous other fields such as electrical industry, automotive industry, and medicine.

1.1.1 Advantages of PES-Based Membranes

In spite of a variety of polymeric membranes recommended for wastewater treatment, PES is the most preferred choice as a commercial membrane material. Excellent thermal and oxidative stability, wide pH tolerance, and good biological stability are the reasons behind the predominant use of PES as a membrane material. PES undergoes glass transition at a temperature as high as 225 ˚C [43]. On top of that, PES suffers a mass loss of only 1% at an elevated temperature of 400 ˚C in air [34]. The observation highlights the enhanced temperature resistance possessed by PES in comparison to its counterpart polymers. PES is even preferred over polyvinylidene fluoride, the other common polymer used in membrane preparation since PES is more hydrophilic and highly stable toward alkaline solutions including sodium
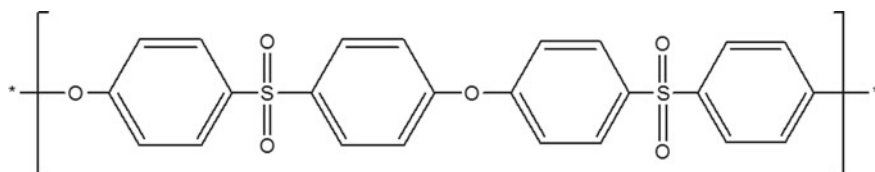

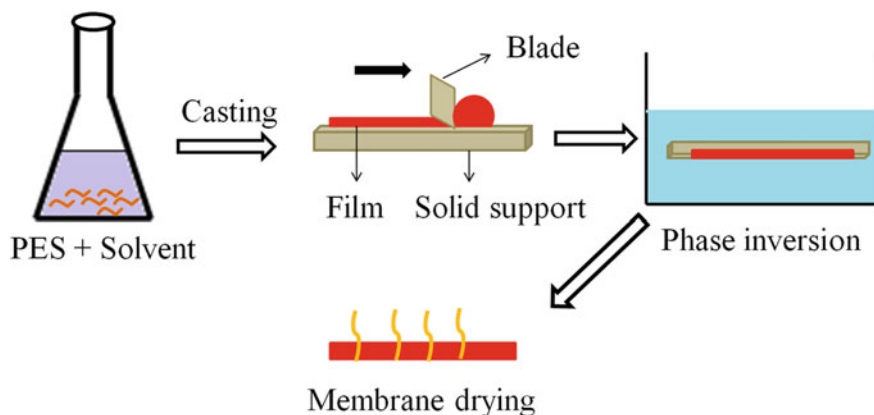
Fig. 1 Chemical structure of PES

Fig. 2 Pictorial representation for the fabrication of PES via the classical phase inversion method (Adapted and redrawn from [16])

hypochlorite [7, 34]. PES is also characterized by exceptional mechanical strength and high rigidity [5]. PES membranes are majorly fabricated via the classical phase inversion method, which is the most convenient and standard technique exercised for membrane preparation.

In a typical phase inversion membrane preparation, a stable polymer solution is converted into a solid in a controlled manner followed by liquid–liquid demixing. The phase with a higher polymer concentration results in gelation/crystallization, whereas the lower polymer concentration phase leads to pore formation on the solid membrane matrix. Liquid–liquid demixing can be carried out by immersion precipitation, controlled evaporation, thermal precipitation, and precipitation from the vapor phase. In literature, most of the studies have adopted the immersion precipitation method for preparing PES membranes, using N-methyl-2-pyrrolidone as a solvent and water as a non-solvent. Structural morphology can be satisfactorily tuned by optimizing the parameters like solution concentration, time of exposure before adding in the coagulation bath, temperature of the bath, and harshness of the precipitation bath [2, 11].

A pictorial illustration of a typical phase inversion procedure for preparing PES membranes is provided in Fig. 2.

1.1.2   Limitations in the Usage of PES Membranes

Though there are numerous positive aspects listed for the utilization of PES in membrane separation, PES is not free of few shortcomings. The major setback in employing pure PES membranes is derived from its hydrophobic nature. The hydrophobicity of PES membrane may create concentration polarization in which the non-permeating dye molecules are carried toward the membrane through convective flux and remains there, thus reducing the performance of the membrane. However,

it is a reversible phenomenon and can be controlled by adjusting the flow of the filtrant. Another major challenge faced while using PES membranes is that PES has a tendency to readily undergo fouling. Membrane fouling is the deposition of contaminating substances on the membrane surface or the blockage of the membrane pores. The common factors causing the fouling of PES membranes are microbial growth, deposition of macroparticles, slime formation, and colloidal deposition. All these factors in turn minimize the permeation flux of the membrane and membrane separation efficiency.

1.1.3 Need for Modification in PES Membranes

While employing pure PES membranes in dye removal from aqueous solutions, the users must deal with the issues caused by the hydrophobicity and fouling. Literature reports therefore suggest the usage of modified PES membranes for dye removal so as to reach improved membrane performance. Researchers have proposed various approaches to upgrade the hydrophilic properties and the antifouling tendency of PES membranes such as coating the PES surface with hydrophilic polymer [13], grafting hydrophilic brushes on the PES surface by surface-initiated atom transfer radical polymerization [55], blending PES with hydrophilic materials [21], and enzyme-catalyzed modification [37]. Detailed review papers exploring various modification methods adopted on PES membranes are available [5, 56]. Other than the specified protocols, bulk modification of PES membranes also can be performed by means of introducing hydrophilic functional groups such as hydroxyl, carboxylic acid, amino, and sulfonic acid groups to the PES main chain [5]. PES modification via additive blending is found to be more prevalent in literature studies. A meticulous compilation of all the additives used for PES modification has been done by Otitoju et al. [39]. PES membranes find applications in a number of fields as evident from numerous research reports. However, in this book chapter, PES membranes and modified PES membranes fabricated for the purpose of removing dyes alone have been discussed. Based on the nature of the modifiers used on PES membranes, this section has been divided into four subsections as follows:

(1) Modification of PES membranes by organic/polymeric molecules.
(2) Modification of PES membranes by inorganic molecules.
(3) Modification of PES membranes by polymeric and inorganic molecules.
(4) Modification of PES membranes by carbonaceous nanomaterials.

2 Modification of PES Membranes

2.1 Modification of PES Membranes by Organic/Polymeric Molecules

Versatile organic molecules have been employed as modifiers of PES toward dye removal. Native polyethersulfone can be subjected to organic functionalization with either polymer or small molecules in line with the target properties desired in the final product.

An initial work done with such theme was reported by Min et al., in which the PES/polyethyleneimine nanofiltration membrane had been developed for the removal of a variety of anionic dyes [33]. The micro-nanostructured nanofibrous affinity membrane containing PES blended with polyethyleneimine was prepared via electrospinning process followed by crosslinking reaction with glutaraldehyde. The average diameter of the electrospun fibers was 350 nm whereas the polyethyleneimine spherules had an average size of 200 nm. Given the fact that amine groups could be used to remove both anionic and cationic species from water based on the working pH conditions, the PEI-modified PES membrane not only helped in removing anionic dyes such as sunset yellow FCF, fast green FCF, and amaranth, but also in the removal of cations like Cu(II), Pb(II), and Cd(II) making it more noteworthy for treating water with multiple pollutants. The interactions between anionic dyes and functional groups on the modified membranes have been depicted in Fig. 3.

In a later work, PES hollow fiber nanofiltration membranes were fabricated by a single-step spinning process for the removal of dyes [53]. With the intention to
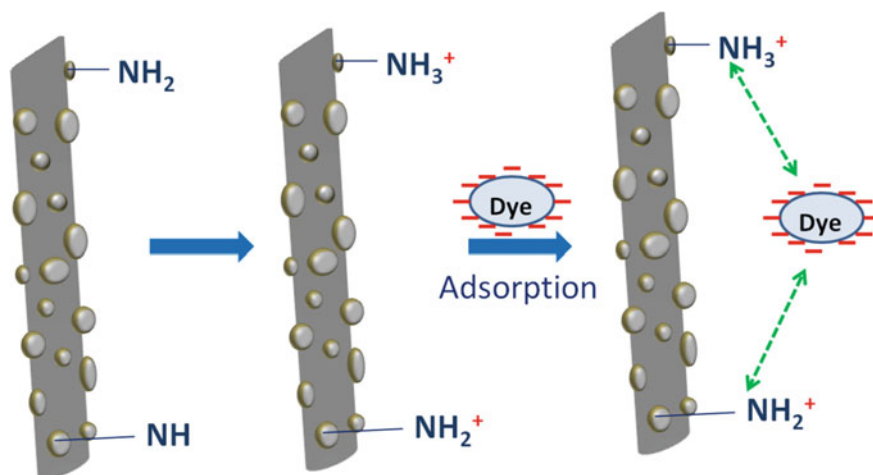

Fig. 3 Possible adsorption mechanism of anionic dyes on PES/PEI nanofibrous membranes (redrawn from [33])

achieve improved hydrophilicity and negatively charged membrane surface, a small amount of sulfonated polysulfone was added as a dopant to PES before subjecting to electrospinning. Hollow fiber membranes thus created by using lithium bromide as a pore former had improved water flux. Besides, the developed membranes owned an outer selective layer as opposed to an inner selective layer to gain more surface area. The separation efficiency of the fabricated membrane had been tested for the removal of reactive black 5, brilliant blue R, remazol brilliant blue R, and indigo carmine dyes, among which the removal efficiency was the maximum for indigo carmine dye.

Polyethylene glycol is another important polymeric additive used to improve the PES membranes [24]. Following these studies, Hassan et al. had reported the usage of PES nanofiltration membranes with polyethylene glycol in the removal of methylene blue, methyl violet, and acid orange [22]. The membrane displayed better pore formation and 99.8% dye rejection was achieved for methylene blue dye.

In another work, ultrafiltration membranes made up of polyphenylsulfone–PES polymer blends were analyzed for the removal of acid black 210 from wastewater [3]. Unlike the other reports mentioned here, in this work, the base membrane material considered was polyphenylsulfone, to which PES was added as a blend material. From the experiments, it was observed that the addition of PES led to an increase in the porosity of the polyphenylsulfone membrane and in turn the dye removal efficiency. In a considerably similar work, polyphenylsulfone/PES ultrafiltration membranes were prepared with different PES compositions in comparison to the previous work. The fabricated membranes also were employed for the removal of acid black 210 [19].

In a recent research paper, the dye removal potency of tetrathioterephthalate-coated aniline oligomers functionalized PES membranes had been explored by using direct red 16 and methylene blue as dyes [35]. The surface functionalization thus done benefitted to improve the hydrophilicity and the fouling resistance of the PES membranes. Likewise, relative to the pristine PES membranes, the pure water flux and the flux recovery ratio of the functionalized membranes were ascertained to rise by about 500.30% and 175.06%, respectively. Additionally, the fabricated membranes were evidenced to exhibit high rejection for Cu(II) and Pb(II) ions.

Suhaimi et al. had carried out the plasma polymerization by using hepty-lamine as a precursor to affect the surface modification of PES membranes, with varying deposition period [52]. The purpose of the modification was to improve the hydrophilicity and antifouling nature of the PES membranes. Plasma polymerization is an ecofriendly method which does not generate any secondary wastes. Modified PES membranes with 5 min of deposition time possessed 58% increase in pure water flux with 63% reduction in fouling than pristine PES membranes. Thus, in turn, there was an increase in the Congo red rejection by 10% by the modified membranes in comparison to pure PES membranes.

Aside from utilizing various synthetic polymers listed above, natural polymers also have been used applied in the modification of PES membranes. Natural polymers hold a number of benefits such as non-toxicity, easy availability, biocompatibility, and presence of functional groups. Cellulose derivatives are major polymeric materials

Table 1 Dye removal efficiencies of various organically modified PES membranes—a comparison

S. No	Membrane materials used	Dyes studied	Dye removal efficiency (%)	Reference
1	Poly(ethersulfone)/poly (ethyleneimine)	Sunset yellow FCF, fast green FCF, and Amaranth	–	[33]
2	PES/sulfonatedpolysulfone	Indigo Carmine	94.9	[53]
3	PES/polyethylene glycol	Methyl blue, Methyl violet Acid orange	99.8 81 95.7	[22]
4	Polyphenylsulfone/PES	Acid black 210	99.65	[3]
5	Polyphenylsulfone/PES	Drupel black NT	96.62	[19]
6	Tetrathioterephthalate-coated aniline oligomers functionalized PES	Direct red 16 and Methylene blue	99.52 98.89	[35]
7	Plasma polymerized heptylamine/PES	Congo red	95	[52]
8	PES/cellulose nanocrystal	Direct red 80	95.8	[10]

applied to modify PES membranes and few cases have been discussed in the following paragraphs.

Novel nanocomposite membranes of multiple compositions were produced from PES and cellulose nanocrystals, via classical phase inversion technique to be further applied for the removal of direct red 80 from water [10]. The introduction of cellulose nanocrystals resulted in a substantial increase in the solvent permeation, hydrophilicity, and antifouling characteristics in comparison to that in untreated PES membranes. Especially on mixing 0.5% additive, the water flux was mounted by 75% than pristine PES membranes. Using the nanocomposite membranes with 0.5% and 1% of cellulose nanocrystals, respectively, 95.8% and 93.6% rejection power was reached. Nonetheless, as the authors stated, its application in a major scale might be difficult due to the use of cost-intensive cellulose nanocrystals (Table 1).

2.2 Modification of PES Membranes by Inorganic Molecules

A wide variety of inorganic materials have been suggested for the effective modification of PES membranes to be used toward dye removal. Studies involving only inorganic materials for modifying PES membranes have been described here.

Hematite nanoparticles-incorporated PES membranes were prepared by the phase inversion method for their utility in removing reactive black 5 from water [40]. These membranes showed higher water flux and good dye rejection tendency. Nevertheless, a flux reduction was noticed beyond a certain dose of iron oxide nanoparticles due to

their agglomeration. It could be noted that in this work, the iron oxide nanoparticles were synthesized without any external stabilizers.

Another iron-based nanofiller used in the preparation of PES mixed matrix membrane was nano-goethite [42]. Like in other studies, the surface hydroxyl groups present in α-FeO(OH) aided to improve the antifouling property and hydrophilicity of the PES membranes. With direct red 16 as a model dye, the goethite/PES membranes exhibited an increased dye rejection tendency by 10% compared to the unmodified PES membranes. It was also inferred that the high dye rejection obtained was a result of the adsorption of dye molecules by the modified membranes used.

Iron-doped titania nanotubes and silver-doped titania nanotubes had been employed as modifiers to get PES mixed matrix membranes by Lukku Thuyavan et al. [30]. Upon modifying the PES membranes, superior hydrophilicity and surface free energy were attained. Between the two dopants, the separation performance was relatively better for iron-doped titanium oxide modified membranes than silver-doped titanium oxide modified membranes. The adsorptive hollow membranes thus developed exhibited 97% rejection efficiency for rhodamine B at acidic pH conditions.

PES photocatalytic membranes have a unique feature that they are capable of degrading organic dyes besides their removal, contrary to regular PES membranes. Pure PES membranes are made photocatalytically active by means of adding a well-known photocatalyst like nanotitania. For example, photocatalytic PES membranes were fabricated by incorporating titania and silver oxide of various dosages to PES membranes via phase inversion technique [44]. The degradation trials carried out validated the photocatalytic degradation of methylene blue in the presence of ultra-violet light and the developed membranes, with the acquirement of a maximum of 85% degradation by one of the prepared sample membranes. In a relatively newer study, hyperbranched polyethyleneimine/titanium oxide nanocomposite-embedded PES membranes were prepared as photocatalytically active membranes [32]. The addition of titania assisted in the photocatalytic degradation of methyl orange while the presence of amine groups from hyperbranched polyethyleneimine conferred enhanced hydrophilicity to the PES membranes. Dye degradation analyses showed that these membranes could degrade methyl orange under the influence of UV light at all pH conditions.

Hitherto, a number of diverse inorganic nanofillers modified PES membranes and their usage in dye wastewater treatment has been discussed. Not only nanofillers, but inorganic compounds that are not nano-sized also have been used to modify PES membranes. The usage of barium chloride as an additive to PES ultrafiltration membranes had been independently reported in two research studies, where the modified membranes were corroborated for removing synthetic dyes from water [8, 46]. In both the studies, the hydrophilicity and the water flux of PES membranes were demonstrated to increase significantly, after the addition of barium chloride. The influence of the composition of barium chloride by weight % on the water contact angle and porosity of the membranes is graphically shown in Fig. 4 [8].

In Table 2, the compilation of the PES membranes modified with inorganic fillers with its dye rejection efficiency values is presented.
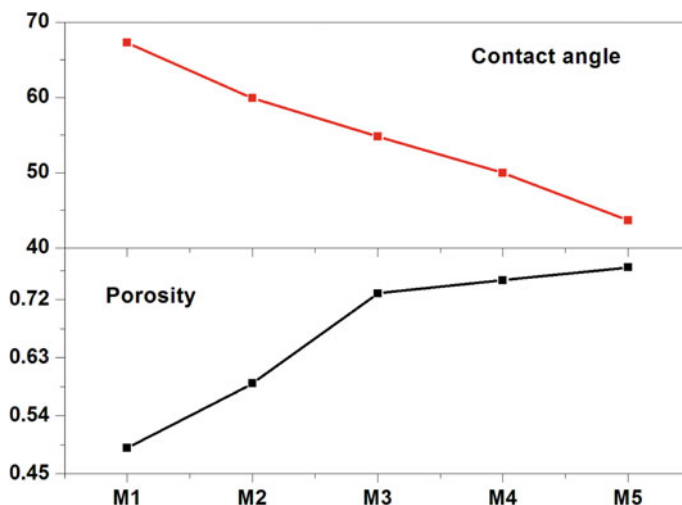
Fig. 4 Water contact angle and porosity of various barium chloride modified membranes (PES—20% in all the cases; M1—0%; M2—1%; M3—2%; M4—3%, and M5—4% barium chloride)(redrawn from [8])

Table 2 Dye removal efficiencies of various inorganically modified PES membranes

S. No.	Membrane process	Membrane material	Dyes studied	Dye removal efficiency (%)	References
1	Nanofiltration	PES/iron oxide (Fe_2O_3)	Reactive black 5	98	[40]
2	Nanofiltration	Goethite/PES	Direct red 16	99	[42]
3	Ultrafiltration	Fe-doped TiO_2 nanotubes/PES	Rhodamine B	97	[30]
4	Photocatalytic membrane	TiO_2-Ag_2O/PES	Methylene blue	85	[44]
5	Ultrafiltration	PES/$BaCl_2$	Congo red Orange II	<90 <70	[46]
6	Ultrafiltration	PES/$BaCl_2$	Orange G Methylene blue	85 91	[8]

2.3 Modification of PES Membranes by Polymeric and Inorganic Molecules

In addition to using organic/polymeric molecules and inorganic molecules, there are also literature reports available emphasizing the use of a combination of these

two classes of compounds. Inorganic molecules and polymeric/organic molecules have been used altogether to get enhanced properties and the following paragraphs highlight few examples.

Zinadini et al. reported the use of O-carboxymethyl chitosan-coated magnetite core–shell nanoparticles as nanofillers and polyvinylpyrrolidone as a pore former to PES nanofiltration membranes [58]. The compositions of the nanoparticles in the casting solutions were altered and the membrane properties of all the samples prepared were studied, including direct red 16 rejection efficiency. The inclusion of the nanofillers boosted the hydrophilic character and the antifouling stability of the PES membranes. The induced negative charge on the membrane surface contributed by the additive also facilitated improved dye rejection. Dye retention performance exhibited by the modified membranes has been presented in Fig. 5.

PES hybrid nanofiltration membranes blended with sulfonated and highly cross-linked halloysite nanotubes were developed and their separation performance was evaluated for reactive black 5 and reactive red 49 [54]. Through distillation–precipitation polymerization procedure, styrene grafted halloysite nanotubes were prepared which were further sulfonated to form highly cross-linked nanofillers. These nanofillers were blended with PES membranes. The introduction of the nanofillers caused a remarkable rise in the water flux and the dye rejection tendency. Additionally, the hybrid membranes could be used for the desalting process since a low retention of salt solutions was witnessed during the tests.

PES ultrafiltration membranes blended with polyethylene glycol and iron oxide nanoparticles had been developed with enhanced hydrophilicity, porosity, and thermal stability, which were subsequently utilized for the removal of orange II
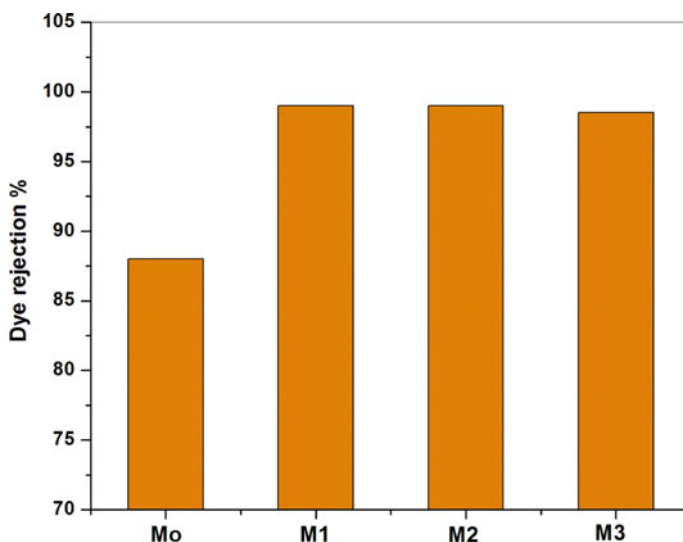

Fig. 5 Dye retention performance of the modified membranes (PES—20% in all the cases; M0—0%; M1—0.1%; M2—0.5%, and M3—1% carboxymethyl coated iron oxide nanoparticles) [58]

and Congo red [29]. Experimental results revealed a fourfold increment in the pure water flux for the modified membranes as against the pristine PES membranes. Despite this observation, both unfilled and modified membranes exhibited almost the same dye separation efficiency. In a recent study, (3-aminopropyl)triethoxysilane and melamine-based dendrimer amine groups functionalized iron oxide nanoparticles of different dosages had been embedded into PES membrane matrices to provide more hydrophilicity and permeation [27]. There was a notable improvement in the pure water flux permeability and antifouling property of the membrane after the modification, as expected. Also, there were greater dye rejections by these modified membranes compared to that by pure PES membranes, while using reactive green 19 as a representative dye. In a similar fashion as in the previous case, (3-aminopropyl)trimethoxysilane-coated iron oxide nanoparticles of various concentrations were used as nanofillers to fabricate modified PES membranes to be eventually tested for the removal of methyl red [26]. The membranes were also successful in removing Cd(II) ions in addition to methyl red.

Another bulk inorganic additive utilized for the modification of PES membranes is calcium chloride. Poly(vinylpyrrolidone) blended PES membranes and polyethylene glycol blended PES membranes to remove various synthetic dyes were synthesized using calcium chloride as an additive [45, 47]. Detailed studies carried out implied that the membrane properties such as porosity, permeability, antifouling behavior, and dye removal capability of these modified membranes were superior to the unfilled PES membranes.

Various PES membranes modified with polymer containing inorganic fillers have been given in Table 3 with their dye rejection rates.

2.4 Modification of PES Membranes by Carbonaceous Nanomaterials

In the last decade, graphene is undoubtedly the most popularly used nanomaterial in multiple fields of science and technology. The utility of graphene-based materials has been extended to membrane filtration as well to treat dye wastewater. For modifying PES membranes, graphene oxide (GO), which is an oxidized form of graphene has been frequently employed. Functional groups possessed by graphene oxide such as hydroxyl (–OH), carboxyl (–COOH), and epoxy (C–O–C) groups enable GO to readily bind with the organic pollutants present in water [15, 51]. Furthermore, the presence of these functional groups improves the PES membrane properties especially hydrophilicity. In consequence, the modified PES membranes are regarded to display efficient dye rejection. In the following paragraphs, example studies with the use of GO-modified PES membranes for dye removal have been elaborated.

Mixed matrix PES nanofiltration membranes embedded with GO nanoplates of various loading were prepared to enhance the antifouling property of the pristine PES membranes [59]. GO nanoplates were synthesized from natural graphite via

Table 3 Dye removal efficiencies of PES membranes modified with polymer containing inorganic fillers

S. No	Membrane process	Membrane material	Dyes studied	Dye removal efficiency (%)	References
1	Nanofiltration	O-carboxymethyl chitosan/Fe_3O_4 nanoparticles blended PES	Direct red 16	99	[58]
2	Nanofiltration	Sulfonatedhalloysite nanotubes/PES	Reactive black 5 Reactive red 49	<90 80–90	[54]
3	Ultrafiltration	Polyethylene glycol and iron oxide nanoparticles blended PES	Congo red	92	[29]
4	Nanofiltration	Melamine-based dendrimer amine functionalized Fe_3O_4 blended PES	Reactive green 19	<96	[27]
5	Nanofiltration	Fe_3O_4@SiO_2-NH_2 embedded PES	Methyl red	97	[26]
6	Photocatalytic membrane	PES/hyper branched polyethyleneimine/TiO_2	Methyl orange	70	[32]
7	Ultrafiltration	Poly (vinylpyrrolidone) blended PES/$CaCl_2$	Congo red	85	[47]
8	Nanofiltration	Polyethylene glycol blended PES/nanoporous $CaCl_2$	Congo red	<90	[45]

Hummer's method. The prepared membranes had higher water flux than the pure PES membranes due to the increased hydrophilic character of the membranes post-modification. For evaluating the nanofiltration performance, direct red 16 was chosen as a dye. Studies revealed that a dye rejection of 99% had been obtained for the GO/PES nanofiltration membranes in contrast to a 90% rejection rate shown by unfilled PES membranes.

Zhou et al. demonstrated the usage of GO-PES composite nanoparticles with three different PES shells for the uptake of a cationic dye [57]. The three different PES shells suggested were unmodified PES (PES@GO), PES modified with poly-acrylic acid (PES/PAA@GO), and PES blended with GO (PES/GO@GO). GO served as the core in all the cases. From the experiments, it was concluded that the hydrophilicity of the core–shell particles with modified PES shells was improved. The maximum methylene blue adsorption capacity values calculated for GO-based core–shell particles ranged from 328.95 and 425.53 mg/g. It was also illustrated that the dye adsorption rates could be improved by adding hydrophilic fillers to PES shells.

The utilization of PES microfiltration membranes modified with GO for the removal of methylene blue was examined in another research work [23]. The GO nanosheets were prepared by adopting the modified Hummer's method. The surface modification of the PES membranes was carried out by treating them with sulfuric acid first followed by the permeation of GO nanosheets, to get PES/H_2SO_4 + GO microfiltration membranes. The dye rejection rates of the modified and commercial PES membranes were determined to be 92.1% and 50.1%, respectively. Shaabani et al. made use of sodium dodecyl sulfate as an anionic surfactant for the uniform incorporation of GO, while modifying the PES membranes [48]. Embedding graphene oxide and sodium dodecyl sulfate to PES membranes resulted in improved hydrophilicity, pure water flux, and fouling resistance. The results showed a near 100% dye removal from algal wastewater, upon using the modified membranes.

Magnetic graphene-based PES composite membrane was developed by using metformin/graphene oxide/magnetite hybrid as nanofiller. Metformin/graphene oxide/magnetite hybrid was synthesized in the first step and in the second step, different doses were incorporated into PES nanofiltration membranes [1]. The mixing of GO-based hybrid filler accounted for the improved pure water flux and hydrophilicity of the modified membranes. The dye rejection of the filled PES membranes was about 99%, whereas the dye rejection of bare PES membranes was only 91%, using direct red 16. The repulsive interactions between the negative charges present on the membrane surface and negative charges of the dye molecules were the cause for the high value obtained for dye rejection. Hydrogen bond or π-π interactions formed between the functional groups present in the membranes and the dye molecules also led to an effective adsorption, thereby stopping the permeation of dye molecules through the membranes. A pictorial representation of the possible interactions between the dye molecules and the GO-modified membrane is presented in Fig. 6. The modified membrane was also effective in the removal of copper(II) ions.
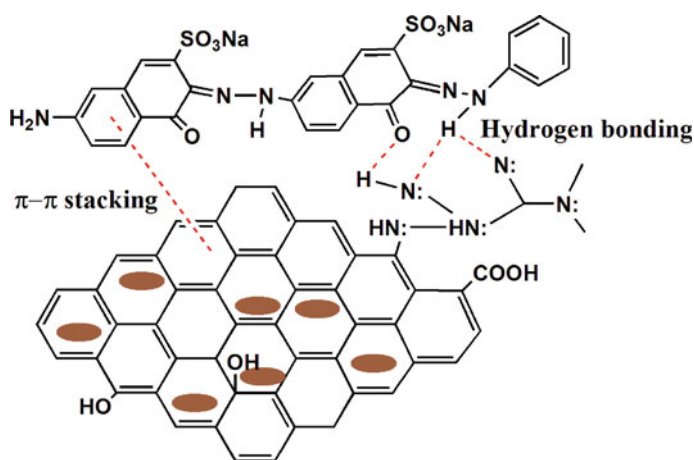

Fig. 6 Possible interactions between dye and GO-modified membrane (redrawn from [1])

Efficacy toward removing methyl orange and methylene blue from aqueous solutions was examined for GO nanoparticles-incorporated PES nanocomposite membranes, which had been prepared via phase inversion procedure [31]. The GO-filled membranes showed considerable improvement in water flux, water absorption, hydrophilicity, and antifouling properties. Studies conducted revealed that a higher rejection was noticed for methyl orange than methylene blue dye irrespective of the loading percentage of GO. The membrane separation performance in removing copper(II) ions from water also was ascertained by using the modified PES membrane.

The application of novel photocatalytic mixed matrix PES membranes in dye removal was proposed by making use of GO and zinc oxide nanoparticles as modifiers [12]. Sulfonated GO, zinc oxide nanoparticles, and sulfonated GO/ zinc oxide-incorporated PES membranes were prepared with upgraded antifouling and hydrophilic properties and the rejection efficiency of crystal violet was studied. Among the sample membranes, mixed matrix membranes containing both SGO/ZnO were found to serve as better photocatalysts for the degradation of crystal violet in the presence of UV irradiation. The addition of GO to a prominent photocatalyst (zinc oxide nanoparticle) was done with the aim of improving its photocatalytic activity, as GO could act as an electron acceptor during the photocatalytic reaction. In a latest study, GO nanoparticles-modified ultrafiltration PES membranes were exploited for the removal of acid black and rose Bengal, where the rejection rates were measured to be greater than 99% for both the dyes [25].

Another notable carbon nanomaterial used in modifying PES membranes for the dye removal is carbon nanotube. Multi-walled carbon nanotubes (MWCNTs) and poly(sodium 4-styrenesulfonate)-wrapped CNTs were utilized to fabricate PES mixed matrix membranes and their dye separation efficiency was compared with that of pure PES membranes [20]. PES membranes modified by poly(sodium 4-styrenesulfonate)-wrapped MWCNTs had improved permeation flux and acid orange 7 removal efficiency. A mathematical model (D model) was constructed for conducting statistical analysis of permeate flux and dye removal efficiency. The observed removal for the considered parameters like pH, dye solution concentration, and membranes was close to the predicted removal thereby validating the suggested model. The results from the analytical model indicated that the addition of nanofillers to PES increased dye removal ability of the membrane.

Mousavi et al. proposed the fabrication of ultraporous PES membrane coated with a thin layer of polyether block amide/chitosan-wrapped MWCNT [36]. Initially, MWCNTs had been functionalized with chitosan and different loadings of the chitosan functionalized MWCNTs were embedded into the polyether block amide. In the following step, CNT-modified PES membranes were developed via phase inversion method. Polyether block amide is a hydrophilic polymer with micro-biphasic structures where soft polyether and hard amide segments constitute the polymer main chain. When PES membranes are coated with polyether block amide, they are expected to exhibit less fouling and higher water flux. The results obtained were in consistency with the aim of the modification since antifouling property and water flux

Fig. 7 Nanofiltration setup designed for the effective dye removal (redrawn from [36])
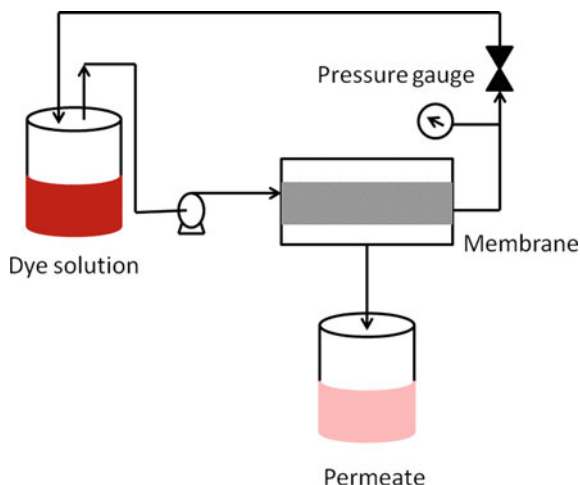
were improved after the modification. All the membranes were capable of showing greater than 95% rejection of malachite green. A simple illustration describing the nanofiltration setup used in the study is depicted in Fig. 7.

A latest addition to the list of carbon-based nanomaterials is carbon dots and Koulivand et al. prepared carbon dots-modified PES nanofiltration membranes by non-solvent-induced phase inversion technique [28]. Carbon dots were synthesized using citrate precursor. The developed membrane was tested for the membrane permeability, antifouling property, dye, and salt rejection. A twofold rise in the pure water flux and a significant improvement in the antifouling property were noticed. The carbon dots-modified PES membrane exhibited a dye rejection of about 99% for reactive red 198. Additionally, the modified membranes exhibited high salt rejections.

In Table 4, the dye removal efficiency values exhibited by different PES membranes modified using carbon-based nanomaterials are listed.

3 Conclusion and Future Perspectives

Membrane separation is considered as a convenient way to treat dye-contaminated water. Polyethersulfone membranes are the prominent membranes used in the area of wastewater treatment. PES membranes not only possess so many benefits but also few serious limitations. Hydrophobicity and fouling are the issues raised while using pure PES membranes and hence several modification procedures have been prescribed by scientists. Different approaches adopted in improving the PES membrane performance in removing dyes from aqueous solutions have been compiled and discussed in this book chapter. The prime aim of all these studies has been improving hydrophilic property, fouling resistance, pure water flux, and dye rejection efficiency. Toward

Table 4 Carbonaceous nanomaterials-modified PES membranes and their dye removal tendency

S. No.	Membrane process	Membrane material	Dyes studied	Dye removal efficiency (%)	Reference
1	Nanofiltration	PES/GO nanoplates	Direct red 16	99	[59]
2	–	PES/GO@GO core–shell	Methylene blue	–	[57]
3	Microfiltration	PES/H$_2$SO$_4$ + GO	Methylene blue	92.1	[23]
4	Nanofiltration	GO and sodium dodecyl sulfate-embedded PES	Algal waste dye	100	[48]
5	Nanofiltration	Metformin/graphene oxide/magnetite hybrid-incorporated PES	Direct red 16	99	[1]
6	Nanocomposite	PES/GO	Methyl orange Methylene blue	<80 ~70	[31]
7	Nanocomposite	Sulfonated GO/ZnO-incorporated PES	Crystal violet	92.3	[12]
8	Ultrafiltration	PES/GO	Acid black Rose Bengal	99 99	[25]
9	Nanofiltration	Poly(sodium 4-styrenesulfonate)-wrapped CNTs/PES	Acid orange 7	–	[20]
10	Ultrafiltration	Polyether block amide/chitosan-wrapped MWCNT embedded PES	Malachite green	<95	[36]
11	Nanofiltration	Carbon dots-modified PES	Reactive red 198	99	[28]

attaining these objectives, many more research studies are still being done and in the future, and there is a broad scope for further development in the modification of PES membranes to yield better separation efficiency and stability.

References

1. Abdi G, Alizadeh A, Zinadini S, Moradi G (2018) Removal of dye and heavy metal ion using a novel synthetic polyethersulfone nanofiltration membrane modified by magnetic graphene oxide/metformin hybrid. J Mem Sci 552:326–335. https://doi.org/10.1016/j.memsci.2018.02.018

2. Hołda AK, IFJV (2015) Understanding and guiding the phase inversion process for synthesis of solvent resistant nanofiltration membranes. J Appl Polym Sci 42130:1–17. https://doi.org/10.1002/APP.42130

3. Al-Ani DM, Al-Ani FH, Alsalhy QF, Ibrahim SS (2019) Preparation and characterization of ultrafiltration membranes from PPSU-PES polymer blend for dye removal. Chem Eng Commun 0:1–19. https://doi.org/10.1080/00986445.2019.1683546

4. Alardhia SM, Alrubaye JM, Albayati TM (2020) Hollow fiber ultrafiltration membrane for methyl green dye removal. Eng Technol J 38:1077–1083. https://doi.org/10.30684/etj.v38i7A.653

5. Alenazi NA, Hussein MA, Alamry KA, Asiri AM (2017) Modified polyether-sulfone membrane: a mini review. Des Monomers Polym 20:532–546. https://doi.org/10.1080/15685551.2017.1398208

6. Alyarnezhad S, Marino T, Parsa JB et al (2020) Polyvinylidene fluoride-graphene oxide membranes for dye removal under visible light irradiation. Polymers 12:1–19. https://doi.org/10.3390/polym12071509

7. Arahman N, Nursidik M et al (2015) The stability of poly(ether sulfone) membranes treated in hot water and hypochlorite solution. Procedia Chem 16:709–715. https://doi.org/10.1016/j.proche.2015.12.017

8. Ashok Kumar S, Srinivasan G, Govindaradjane S (2019) Development of a new blended polyethersulfone membrane for dye removal from synthetic wastewater. Environ Nanotechnol Monit Manag 12:100238. https://doi.org/10.1016/j.enmm.2019.100238

9. Bajpai P (2016) Chapter 11-emerging technologies. In: Bajpai PBT-P and PI (ed) Pulp and Paper Industry. Elsevier, Amsterdam, pp 189–251

10. Balcik-Canbolat C, Van der Bruggen B (2020) Efficient removal of dyes from aqueous solution: the potential of cellulose nanocrystals to enhance PES nanocomposite membranes. Cellulose 27:5255–5266. https://doi.org/10.1007/s10570-020-03157-y

11. Bazargan AM, Gholamvand Z, Naghavi M et al (2009) Phase inversion preparation and morphological study of polyvinylidene fluoride ultrafiltration membrane modified by nano-sized alumina. Funct Mater Lett 2:113–119. https://doi.org/10.1142/S1793604709000648

12. Boopathy G, Gangasalam A, Mahalingam A (2020) Photocatalytic removal of organic pollutants and self-cleaning performance of PES membrane incorporated sulfonated graphene oxide/ZnO nanocomposite. J ChemTech Biotech 95:3012–3023. https://doi.org/10.1002/jctb.6462

13. Cheng C, Li S, Zhao W et al (2012) The hydrodynamic permeability and surface property of polyethersulfone ultrafiltration membranes with mussel-inspired polydopamine coatings. J MemSci 417–418:228–236. https://doi.org/10.1016/j.memsci.2012.06.045

14. Cheng J, Zhan C, Wu J et al (2020) Highly efficient removal of methylene blue dye from an aqueous solution using cellulose acetate nanofibrous membranes modified by polydopamine. ACS Omega 5:5389–5400. https://doi.org/10.1021/acsomega.9b04425

15. Dikin DA, Stankovich S, Zimney EJ et al (2007) Preparation and characterization of graphene oxide paper. Nature 448:457–460. https://doi.org/10.1038/nature06016

16. Dong X, Al-Jumaily A, Escobar IC (2018) Investigation of the use of a bio-derived solvent for non-solvent-induced phase separation (NIPS) fabrication of polysulfone membranes. Membranes 8(2):23. https://doi.org/10.3390/membranes8020023

17. Ezugbe EO, Rathilal S (2020) Membrane technologies in wastewater treatment: a review. Membranes 10:1–28. https://doi.org/10.3390/membranes10050089

18. Foroozmehr F, Borhani S, Hosseini SA (2016) Removal of reactive dyes from wastewater using cyclodextrin functionalized polyacrylonitrile nanofibrous membranes. J Text Polym 4:45–52

19. Ghadhban MY, Majdi HS, Rashid KT et al (2020) Removal of dye from a leather tanning factory by flat-sheet blend ultrafiltration (UF) membrane. Membranes 10(3):47. https://doi.org/10.3390/membranes10030047

20. Ghaemi N, Madaeni SS, Daraei P et al (2015) PES mixed matrix nanofiltration membrane embedded with polymer wrapped MWCNT: fabrication and performance optimization in dye removal by RSM. J Hazard Mat 298:111–121. https://doi.org/10.1016/j.jhazmat.2015.05.018

21. Gohari B, Abu-Zahra N (2018) Polyethersulfone membranes prepared with 3-aminopropyltriethoxysilane modified alumina nanoparticles for Cu(II) removal from water. ACS Omega 3:10154–10162. https://doi.org/10.1021/acsomega.8b01024

22. Hassan AR, Rozali S, Safari NHM, Besar BH (2018) The roles of polyethersulfone and polyethylene glycol additive on nanofiltration of dyes and membrane morphologies. Environ Eng Res 23:316–322. https://doi.org/10.4491/eer.2018.023

23. Homem NC, Yamaguchi NU, Vieira MF et al (2017) Surface modification of microfiltration membrane with GO nanosheets for dyes removal from aqueous solutions. Chem Eng Trans 60:259–264. https://doi.org/10.3303/CET1760044

24. Idris A, Mat Zain N, Noordin MY (2007) Synthesis, characterization and performance of asymmetric polyethersulfone (PES) ultrafiltration membranes with polyethylene glycol of different molecular weights as additives. Desalination 207:324–339. https://doi.org/10.1016/j.desal.2006.08.008

25. Kadhim RJ, Al-Ani FH, Al-Shaeli M et al (2020) Removal of dyes using graphene oxide (Go) mixed matrix membranes. Membranes 10:1–24. https://doi.org/10.3390/membranes10120366

26. Kamari S, Shahbazi A (2020) Biocompatible Fe3O4@SiO2-NH2 nanocomposite as a green nanofiller embedded in PES–nanofiltration membrane matrix for salts, heavy metal ion and dye removal: Long–term operation and reusability tests. Chemosphere 243:125282. https://doi.org/10.1016/j.chemosphere.2019.125282

27. Koulivand H, Shahbazi A, Vatanpour V (2019) Fabrication and characterization of a high-flux and antifouling polyethersulfone membrane for dye removal by embedding Fe3O4-MDA nanoparticles. Chem Eng Res Des 145:64–75. https://doi.org/10.1016/j.cherd.2019.03.003

28. Koulivand H, Shahbazi A, Vatanpour V, Rahmandoust M (2020) Development of carbon dot-modified polyethersulfone membranes for enhancement of nanofiltration, permeation and antifouling performance. Sep Purif Technol 230. https://doi.org/10.1016/j.seppur.2019.115895

29. Krishnamoorthy R, Sagadevan V (2015) Polyethylene glycol and iron oxide nanoparticles blended polyethersulfone ultrafiltration membrane for enhanced performance in dye removal studies. E-Polymers 15:151–159. https://doi.org/10.1515/epoly-2014-0214

30. Lukka Thuyavan Y, Arthanareeswaran G, Ismail AF et al (2020) Treatment of synthetic textile dye effluent using hybrid adsorptive ultrafiltration mixed matrix membranes. Chem Eng Res Des 159:92–104. https://doi.org/10.1016/j.cherd.2020.04.005

31. Marjani A, Nakhjiri AT, Adimi M et al (2020) Effect of graphene oxide on modifying polyethersulfone membrane performance and its application in wastewater treatment. Sci Rep 10:1–11. https://doi.org/10.1038/s41598-020-58472-y

32. Mathumba P, Maziya K, Kuvarega AT et al (2020) Photocatalytic degradation of a basic dye in water by nanostructured HPEI/TiO2 containing membranes. Water SA 46:500–505. https://doi.org/10.17159/wsa/2020.v46.i3.8660

33. Min M, Shen L, Hong G et al (2012) Micro-nano structure poly(ether sulfones)/poly(ethyleneimine) nanofibrous affinity membranes for adsorption of anionic dyes and heavy metal ions in aqueous solution. Chem Eng J 197:88–100. https://doi.org/10.1016/j.cej.2012.05.021

34. Mohammad AW, Teow YH, Chong WC, Ho KC (2019) Chapter 13 - Hybrid Processes: Membrane Bioreactor. In: Ismail AF, Rahman MA, Othman MHD, Matsuura TBT-MSP and A (eds) Handbooks in Separation Science. Elsevier, pp 401–470

35. Moradi G, Rahimi M, Zinadini S (2021) Antifouling nanofiltration membrane via tetrathioterephthalate coating on aniline oligomers-grafted polyethersulfone for efficient dye and heavy metal ion removal. J Environ Chem Eng 9:104717. https://doi.org/10.1016/j.jece.2020.104717

36. Mousavi SR, Asghari M, Mahmoodi NM (2020) Chitosan-wrapped multiwalled carbon nanotube as filler within PEBA thin film nanocomposite (TFN) membrane to improve dye removal. Carbohydrate Poly 237:116128. https://doi.org/10.1016/j.carbpol.2020.116128

37. Nady N, Schroën K, Franssen MCR et al (2011) Mild and highly flexible enzyme-catalyzed modification of poly(ethersulfone) membranes. ACS Appl Mater Interfaces 3:801–810. https://doi.org/10.1021/am101155e

38. Nagarajan D, Venkatanarasimhan S (2019) Copper(II) oxide nanoparticles coated cellulose sponge—an effective heterogeneous catalyst for the reduction of toxic organic dyes. Environ Sci Pollut Res 26:22958–22970. https://doi.org/10.1007/s11356-019-05419-0
39. Otitoju TA, Ahmad AL, Ooi BS (2018) Recent advances in hydrophilic modification and performance of polyethersulfone (PES) membrane via additive blending. RSC Adv 8:22710–22728. https://doi.org/10.1039/c8ra03296c
40. Patil H, Shanmugam V, Marathe K (2020) Studies in synthesis and modification of PES membrane and its application for removal of reactive black 5 dye. Indian Chem Eng 0:1–10. https://doi.org/10.1080/00194506.2020.1822761
41. Quist-Jensen CA, Macedonio F, Drioli E (2015) Membrane technology for water production in agriculture: desalination and wastewater reuse. Desalination 364:17–32. https://doi.org/10.1016/j.desal.2015.03.001
42. Rahimi M, Zinadini S, Zinatizadeh AA et al (2016) Hydrophilic goethite nanoparticle as a novel antifouling agent in fabrication of nanocomposite polyethersulfone membrane. J Appl Polym Sci 133:1–13. https://doi.org/10.1002/app.43592
43. Rahimpour A, Madaeni SS, Mehdipour-Ataei S (2008) Synthesis of a novel poly(amide-imide) (PAI) and preparation and characterization of PAI blended polyethersulfone (PES) membranes. J Mem Sci 311:349–359. https://doi.org/10.1016/j.memsci.2007.12.038
44. Rajis Z, Azmi NFAN, Makhtar SNNM et al (2017) Preparation, characterization and performances of photocatalytic TiO2-Ag2O/PESf membrane for methylene blue removal. J Appl Membrane Sci Technol 23:83–97. https://doi.org/10.11113/amst.v23n2.160
45. Rambabu K, Bharath G, Monash P et al (2019) Effective treatment of dye polluted wastewater using nanoporous CaCl2 modified polyethersulfone membrane. Process Saf Environ Prot 124:266–278. https://doi.org/10.1016/j.psep.2019.02.015
46. Rambabu K, Srivatsan N, Gurumoorthy AVP (2017) Polyethersulfone-barium chloride blend ultrafiltration membranes for dye removal studies. IOP Conf Ser Mat Sci Eng 263:0–9. https://doi.org/10.1088/1757-899X/263/3/032027
47. Rambabu K, Velu S (2016) Improved performance of CaCl2 incorporated polyethersulfone ultrafiltration membranes. Periodica Polytech Chem Eng 60:181–191. https://doi.org/10.3311/PPch.8482
48. Shaabani N, Zinadini S, Zinatizadeh AA (2018) Preparation and characterization of PES nanofiltration membrane embedded with modified graphene oxide for dye removal from algal wastewater. Journal of Applied Research in Water and Wastewater 9:407–410
49. Shao H, Qi Y, Liang S et al (2019) Polypropylene composite hollow fiber ultrafiltration membranes with an acrylic hydrogel surface by in situ ultrasonic wave-assisted polymerization for dye removal. J Appl Polym Sci 136:1–10. https://doi.org/10.1002/app.47099
50. Sharma S, Bhattacharya A (2017) Drinking water contamination and treatment techniques. Appl Water Sci 7:1043–1067. https://doi.org/10.1007/s13201-016-0455-7
51. Shin DS, Kim HG, Ahn HS et al (2017) Distribution of oxygen functional groups of graphene oxide obtained from low-temperature atomic layer deposition of titanium oxide. RSC Adv 7:13979–13984. https://doi.org/10.1039/C7RA00114B
52. Suhaimi A, Mahmoudi E, Siow KS et al (2020) Nitrogen incorporation by plasma polymerization of heptylamine on PES membrane for removal of anionic dye (Congo red). Int J Environ Sci Technol 1–10. https://doi.org/10.1007/s13762-020-02879-7
53. Thong Z, Gao J, Lim JXZ et al (2018) Fabrication of loose outer-selective nanofiltration (NF) polyethersulfone (PES) hollow fibers via single-step spinning process for dye removal. Sep Purif Technol 192:483–490. https://doi.org/10.1016/j.seppur.2017.10.031
54. Wang Y, Zhu J, Dong G et al (2015) Sulfonated halloysite nanotubes/polyethersulfone nanocomposite membrane for efficient dye purification. Sep Purif Technol 150:243–251. https://doi.org/10.1016/j.seppur.2015.07.005
55. Xiang T, Yue WW, Wang R et al (2013) Surface hydrophilic modification of polyethersulfone membranes by surface-initiated ATRP with enhanced blood compatibility. Colloids Surf, B 110:15–21. https://doi.org/10.1016/j.colsurfb.2013.04.034

56. Zhao C, Xue J, Ran F, Sun S (2013) Modification of polyethersulfone membranes - A review of methods. Prog Mater Sci 58:76–150. https://doi.org/10.1016/j.pmatsci.2012.07.002
57. Zhou J, Chen S, Xu S et al (2016) Graphene oxide-based polyethersulfone core-shell particles for dye uptake. RSC Adv 6:102389–102397. https://doi.org/10.1039/c6ra18950d
58. Zinadini S, Zinatizadeh AA, Rahimi M et al (2014) Novel high flux antifouling nanofiltration membranes for dye removal containing carboxymethyl chitosan coated Fe3O4 nanoparticles. Desalination 349:145–154. https://doi.org/10.1016/j.desal.2014.07.007
59. Zinadini S, Zinatizadeh AA, Rahimi M et al (2014) Preparation of a novel antifouling mixed matrix PES membrane by embedding graphene oxide nanoplates. J Mem Sci 453:292–301. https://doi.org/10.1016/j.memsci.2013.10.070

Cross-Linked Polymer-Based Adsorbents and Membranes for Dye Removal

Marlene A. Velazco-Medel, Luis A. Camacho-Cruz, José C. Lugo-González, and Emilio Bucio

Abstract Contamination of water is a problem that severely affects the equilibrium of ecosystems and human health. Through the years, various techniques have been implemented for the elimination of colorants from the water discarded by the textile industry; nevertheless, some of the wastes obtained are hard to treat and toxic. Polymers can be used as an adsorbent membrane, a coagulant, or a flocculant, and the inclusion of them has been a promising strategy used for the versatility, effectivity, and low toxicity of some polymers. Organic polymers have demonstrated good ability for the elimination of colorants by the adsorption mechanism, and they have been useful for the preparation of membranes for nanofiltration. Synthetic and natural polymers mixed with other materials have improved the performance of membranes without altering the permeation and flux. The cross-linking has allowed the formation of polymeric networks with pores, which aid to the dye retention assisted by the functional groups in the polymer chains; additionally, this cross-linking is useful for the incorporation of other compounds such as nanomaterials of magnetic nanoparticles to improve the cleaning of wastewater. The control of the charge density in the polymer, the physical properties of the dispersed medium, the chemical structure of the dye, and cross-linked polymers for adsorption and coagulation are some of the aspects to review in this chapter.

Keywords Cross-linked · Polymers · Dye · Nanofiltration · Adsorption · Coagulation · Membrane · Wastewater

M. A. Velazco-Medel · L. A. Camacho-Cruz · E. Bucio (✉)
Departamento de Química de Radiaciones y Radioquímica, Instituto de Ciencias Nucleares, Universidad Nacional Autónoma de México, Ciudad Universitaria, Circuito Exterior, México City CDMX 04510, México
e-mail: ebucio@nucleares.unam.mx

J. C. Lugo-González
Facultad de Química, Universidad Nacional Autónoma de México, 04510 México City, México

1 Introduction

Contamination of water is a problem that generates several conflicts in human life. The excess of dyes and heavy metals in water from textile industries has attracted the attention of scientists in previous years, mainly for the cities with high production of textiles. Several of these dyes are highly toxic to animals and humans, and they render the residual water useless. The removal of dyes from wastewater is important to ensure human health; however, the elimination of them is hindered due to some limitations, e.g., the concentration of the dye, the chemical auxiliaries, and other aspects [1, 2].

For dye removal, several factors affect the colored wastewater, first, factors that only depend on the rest of pollutants from the dye industry and the physicochemical properties of the water, and second, the factors that depend on the dye. Generally, for any removal process, some of these factors are pH, ionic strength, temperature, among others. This is due to the destabilization process involved in the elimination of the dye, which is closely related to a complexation reaction or to other chemical interactions [3, 4]. Additionally, as it was mentioned, the chemical structure of the dye plays an important role in the process because the functionalities allow the interaction between the coagulant, flocculant, or adsorbent membrane. It is important to mention additionally that colorants present two main parts on their structures, the chromophore, and the auxochrome; which are responsible for the absorption–emission of light, and directly, the color.

On the one hand, the chromophore in a molecule is the conjugated double bond moiety (π bonds), which present adsorption in the visible region on the electromagnetic spectrum, that is the reason why almost all colorants present aromatic rings in their structure, connected to an auxochrome. On the other hand, an auxochrome is a functional group attached to the chromophore, which modifies the ability of the chromophore to absorb light. For this portion, acidic and basic groups are commonly used, the protonation or deprotonation of a group can extend the conjugation of a molecule and change the wavelength or intensity of the absorption. In this way, dyes are classified as cationic, anionic, or non-ionic, and this charge density is important for eliminate them from water.

One of the most employed strategies for wastewater treatment is the coagulation/flocculation (C/F) method. C/F is a two-stage technique that consists of the destabilization of dispersed solid particles in water. For the effect of the coagulants, the charged particles get to gather and for bigger particles. Coagulation is the first step in the process and is always accompanied by rapid mixing of the coagulant and the water to be treated. In this step, the coagulant is added, and the mixing favors the accumulation of molecules and the formation of flocs. In the flocculation stage, the speed of mixing is decreased, and the flocs aggregate to form bigger flocs. The use of metals and polymers is common for the destabilization of dye molecules to subsequently eliminate them by precipitation or filtration [5].

The use of inorganic coagulants is a strategy usually used; however, the waste is toxic to human health and the environment [6, 7] such as the residues of aluminum

salts. Another disadvantage of using metal salts for water treatment is that the precipitate and the sludge produced are difficult to treat after the dye removal. For that reason, other alternatives have been employed, including, organic materials (e.g., polymers). An advantage of these materials is that they can be mixed with metals or other compounds to get a dual coagulant/flocculant or adsorbents, obtaining greener, cleaner, and more effective materials [8, 9].

Water-soluble polymers are the most used for C/F method; some natural and synthetic polymers have been explored [9–11]. As it was mentioned above, the chemical structure of the dye affects the way it is removed, the destabilization of the colloids dispersed in the medium influences the polymer used and the technique desired. In the case of C/F, the dyes are trapped by the effect of the charged groups in their structure-forming bigger structures, or by the anchoring of other functional groups similar to a host–guest chemistry.

Natural polymers have attracted attention in recent years because they are easy to get from plants or animals, and they are non-toxic to humans or animals. Biopolymers such as gums, chitosan, or cellulose are vastly used as adsorbents or coagulants; nevertheless, the disadvantage is that the molecular weights of these polymers cannot be controlled. Although synthetic polymers can be more toxic than natural polymers, the process of synthesis offers control in the chemical structure of chains, the functional groups, charge density, molecular weight, and microstructure. Moreover, ionic groups can be added to the polymer, i.e., polyelectrolytes, and this is important for the type of dye to remove from water. Hence cationic, anionic, and non-ionic polymers are used for dye removal. Amine- and carboxylic-functionalized polymers are extensively used. Additionally, acrylates, imines, acrylamide, polyguanidines, and other acid or basic groups are added to polymer chains.

Polymeric materials have been explored as alternatives to conventional inorganic alum or toxic metal coagulants. Depending on the chemical structure of the dye and polymer, polymers can act as both coagulant and flocculant, they trigger the destabilization of the dye molecules dispersed in the medium, which forms aggregates and flocs, with subsequent precipitation or sedimentation. To reach the formation of the flocs or micelle-type structures, the dosage, charge, and the size of the polymer are important factors to control; as well as agitation of the system since it can break the formed aggregates, very fast agitation is important to reduce the repulsive forces between the colloids before charge neutralization, and thus the formation of aggregates is favored [12, 13].

The pre-treatment of wastewater with coagulant/flocculant process followed by nanofiltration has allowed the water reusability, and the polymeric materials are easier to treat after the first stage. Otherwise, some studies have shown that the use of metallic coagulants, e.g., aluminum salts, as coagulant induces the formation of foulants hard to treat and that are highly toxic, such as aluminum hydroxide or aluminum derivatives [14, 15]. In contrast, iron and polymeric coagulants are easier to remove by other cleaning techniques, they are biodegradable or can be reused for various cycles of filtration.

The mechanism of dye removal involving polymers can be divided into four types: (1) electrical double-layer compression; (2) charge neutralization; (3) sweeping; and (4) adsorption [11, 16]. Table 1 summarizes these four mechanisms.

Furthermore, another way to remove dyes is by the retention in the polymeric matrix, the binding and attachment of dyes to the polymer depend on the chemical interactions between them. All the processes depend on electrostatic and non-covalent interactions such as hydrophobic interaction, hydrogen bonding, or the formation of complexes. For this reason, synthetic polyelectrolytes and natural polysaccharides are suitably used for water treatment, since they possess hydroxyl groups and can be manipulated to get charged groups [17, 18]. The selected polymer is dependent on the dye and they can either be cationic (e.g., quaternary amines), anionic (e.g., anionic polyacrylamide), or non-ionic (e.g., cellulose).

Adsorption has also been used as a wastewater cleaning method, nanomaterials made of organic ligands or dye receptors (based on the chemical structure of the desired dye) [19]. The adsorption mechanism is common for polymers as coagulants

Table 1 Mechanisms of dye removal from wastewater

	Mechanism	Description
Coagulation/Flocculation	Electrical double-layer compression	For this mechanism, highly charged ionic coagulants are used. They disturb the stability of colloids by changing the ionic strength in the media, thus the double layer around the particle collapses, which conduct to the formation of aggregates by electrostatic interactions
	Charge neutralization	In the case of neutralization, coagulants with different charges are added to de dispersion. The surface of colloids binds to the coagulant by the opposite electrostatic force and it drives to the neutralization of charges
	Sweeping	The sweeping is when the dispersed particles are captured into the matrix of the insoluble metal hydroxide (e.g., aluminum or ferric hydroxides) formed from the hydrolysis of the metal coagulant. These hydroxides are formed when alum or ferric coagulants are added to water
Filtration	Adsorption	This mechanism is the most common for polymeric coagulants. The polymer captures the dye assisted by the functional groups and forms a bridge between the molecules. In consequence, bigger aggregates and settleable flocs are obtained

and flocculants; polyaniline and other cationic polymers are useful for the elimination of colorants from water [20]. The adsorption process is used for the development of membranes for micro- and nanofiltration, for that, the polymer can be disposed of in bulk or packed in a column to carry out the absorption process. The physicochemical properties of the medium such as pH, ionic strength, and the nature of dye are important to select the method.

Several natural and synthetic polymers are used as adsorbents for the removal of different dyes; natural carbohydrate-based polymers such as cellulose, chitosan, and starch work with this mechanism. For example, membranes based on polysaccharides such as chitosan or cellulose have been prepared. The chemical structure of these biopolymers allows the retention of dyes in a large scale of pH since they have acid or basic groups [21–24]. The chitosan has been used for the adsorption and coagulation of several dyes, even sulfonic dyes [25], and it has been grafted with other polymers to obtain good adsorbents [26, 27].

Conveniently, some low molecular weight polypeptides from animals, plants, and seeds have demonstrated good ability to remove colorants by adsorption, due to their amphiphilic behavior. Moreover, this type of biomaterials is non-toxic, easy to treat after the cleaning process, and eco-friendly adsorbents. There are several reviews and summaries about the use of biopolymers for wastewater treatment [18, 28]. For example, the aqueous extract of the seed of *Moringa oleifera* has been tested as coagulant and adsorbent for the removal of dyes [29] such as azo-dyes [30, 31], indigoid dyes [32], and anthraquinonic dyes [33]. Even, this extract has shown better results for dye removal than metallic coagulants, e.g., polyaluminum chloride [34]. Other polymers are obtained from *Cassia angustifolia* seed, *Cassia javahikai* seed gum, mesquite bean, *Cactus latifaria*, chestnut, and acorn [29, 35–37].

It is worthy of note of not only the chemical interactions the dye keeps anchored to the matrix but also this retention in the polymeric matrix can also be enhanced by a porous system, working similar to size exclusion chromatography. Polymeric membranes in a 3D arrangement are achieved by the addition of cross-linking agents, to form a network with a reduced free volume between the polymer chains and pores. Those pores avoid the release of big molecules, thus they are trapped in the sludge or the waste from polymer, this approach is used for nanofiltration.

The cross-linking of polymers for this purpose has allowed the incorporation of other useful species to the polymer network, and it can be by supramolecular or covalent cross-linking. This approach, like the grafting technique, has been used to combine or add properties of two different polymers to a final material; for example, natural polymers have been mixed with synthetic ones, ionic liquids with polymers, organic–inorganic polymers [20], and magnetic nanoparticles with polymers [38, 39]. These types of 3D polymers, hydrogels, and membranes are vastly used for filtration and nanofiltration as well as for fractionation of salts and dyes.

Nanofiltration (NF) is defined as a pressure-driven method that allows the separation of solutes from liquid matrixes by size exclusion and charges repulsion (Donnan exclusion) throughout a semipermeable membrane. The term NF arises from the scale of separations (0.5–2 nm) that depends on the membrane pore dimensions.

Commonly, there have been two approaches for NF design, those based on polymeric matrixes (e.g., cross-linked polymers or polymeric hollow fiber membranes) and those based on ceramic membranes. For our purposes, we are going to deal with the former one, those based on cross-linked polymers, their design, and performance concerning the removal of dyes from wastewater processing.

Technologies based on polymeric nanofiltration membranes were developed at the end of the 1980´s decade with a broad spectrum of applications, e.g., water processing [40], plasma pool clarification virus, biomolecules removal [41], or petrochemical industries. Recently, it has been documented a growing number of publications concerning water processing using NF, almost 18% of nanofiltrations concerns with wastewater processing, replacing reverse osmosis, which has the advantage of operating at lower pressures [40]. NF employs membranes with a smaller pore dimension than micro- or ultrafiltration but bigger than in reverse osmosis (RO) with pore dimension about 0.1 nm. Additionally, NF requires higher pressures (4–10 bar) than RO and it is effective for solutes with molecular weights of about 100–5000 Da.

Among more important factors to get low-operating costs are the pre-treating processes to prevent membrane fouling as well as the need of housing them into appropriate modules that provide porous support for large-scale applications [42]. Membrane performance is characterized by quantifying the key aspects of their separation mechanisms such as solute rejection, pore dimensions, and permeate flux, which is related to applied pressure. These factors interplay a compromise between selectivity and efficiency.

It is worthy of note that in the literature, solute rejection is also taken by the rejection of total dissolved solids (TDS) or salt rejection, depending on the application or solute that is being removed. NF is useful for the removal of divalent or polyvalent ions (e.g., $CaSO_4$) while monovalent ions such as Na^+ and Cl^- commonly pass through.

Concerning wastewater from the textile industry, removal of azoic and basic dyes is an important application in the research to get membranes with high dye rejection that enables recycling the wastewater effluents. In aqueous media, azoic dyes (coming mainly from textile industries where they are applied to fibers) are generally anionic because of the strong acidity of the sulfonic group (pK_a values <0), so they are completely ionized and belong to the acid-dyes class. On the other hand, basic dyes (coming from cosmetic, food, and paper industries) are cationic species in aqueous media, e.g., methyl blue, crystal violet, safranin, etc. The differential chemistry of the solutes pointed out the importance of selectivity properties in NF membrane design.

Although it is possible to calculate performance parameters theoretically like dye rejection and permeate flux (the flux that passes through the membrane as a measure of the rate of the process) with a known membrane morphology, it is still more common to test membrane performance at the lab scale using relative ease accessible membranes based on cross-linked polymers.

Polyetherimide (PEI) is a thermoplastic with strong absorption properties has been the base of several cross-linked membranes for NF in water media. Their cross-linked structure with *m*-phenylenediamine (MPD) has been obtained for which the studied parameters were doped solution composition and cross-linking time as

well as dye concentration upon membrane performance, resulting in increased dye rejection when the acetone concentration in dope solution was maximized. The best performance was reached with cross-linked membrane composition PEI: 15, acetone: 20 wt%, and 10 min of cross-linking time. This membrane showed 98% of dye rejection of Reactive Red 120 at 1500 ppm with an operating pressure of 4 bar. The increasing membrane performance with acetone content in the dope solution was related to a tighter membrane [43]. Figure 1 shows a typical procedure for testing membrane dye removal by NF.

Interestingly, PEI also has been used to make composite membranes by interfacial cross-linking with nylon for selective removal of anionic dyes. As an example, an inspired membrane inspired on thin-film composite (TFC) for RO and NF has been reported by amidation of PEI with trimesoyl chloride over nylon support. This composite membrane works selectively at pH = 3 by electrostatic interactions between positively charged PEI chains and anionic dye Sunset Yellow. The membrane can be regenerated at alkaline pH values and works at very low pressures compared with NF (only 0.01 bar) affording to permeate flux of about 10 L/m² h bar [44].

Fig. 1 Schematic setup for nanofiltration of dye aqueous solution
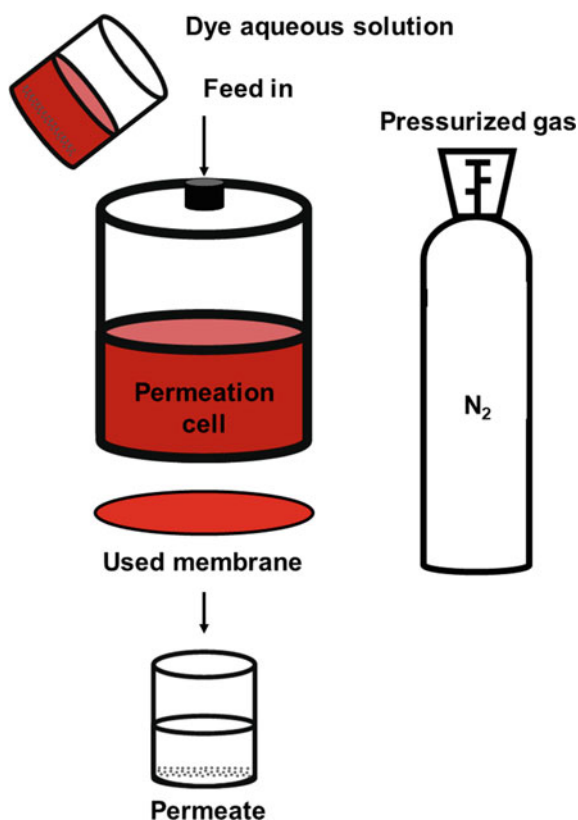
As shown above, the mechanism for dye rejection can be driven not only by size exclusion but also by electrostatic partitioning also known as Donnan exclusion. Thus, the design of positively charged membranes has played emergent attention given cationic charged solutes. In this regard, composite NF membranes have been obtained using PEI for cross-linking polyimide (PI). The resulting NF membranes have ortho-diamide groups with free amine groups available for protonation even at neutral pH values [45, 46]. However, cross-linking conditions are difficult to optimize in view that mechanical properties of the membranes can be damaged, which has driven to the cross-linking only at the surfaces of flat-sheet membranes efforts.

In this concern, substituting PI with Torlon® polyamide-imide (PAI) has shown advantages due to its superior mechanical properties as well as its pH stability. This NF membrane showed good dye rejection performance (>95%) toward basic dyes (Methylene Blue, Janus green B, methyl green, Alcian Blue 8GX) with a molecular weight ranging from 319 to 1300 Da [47]. Regarding synthetic details, it was found that stirring speed (500 rpm) at 70 °C for 80 min in cross-linker solution played a key role in successful surface functionalization. The cross-linked membrane showed a marked decrease in molecular weight cut-off (MWCO, defined as the lowest molecular weight retained at 90% by the membrane) from 17,520 Da in the parent non-cross-linked PAI to 458 Da in the cross-linked membrane, as well as a change from anionic to the cationic character.

More recently, ethylenediamine (ED) has been used as a cross-linking agent in PEI-based membranes. The resulting cross-linked membrane was obtained as a flat-sheet membrane by phase immersion method from dope solutions with 20% of acetone. Afterward, the membranes were submerged in ED 2.5% (v/v) methanolic solution by 30 min. The best performance was obtained when using PEI at 16% in dope solution (if raised to 17% the water permeation results too low to be practical). At 2.8 bar pressure and using the model azoic dye Reactive Red 120 (RR120), 98% of rejection was achieved compared with 84% for the pristine membrane. This work has underlined the sensitivity of the performance to polymer content in dope solutions, being significant variations even at 1% [48].

Li et al. prepared another loose nanofiltration membrane by coating onto a conventional ultrafiltration membrane made of polyethersulfone (PES); the mixture solution for coating was obtained by aqueous cross-linking between tannic acid (TA) and PEI. The resulting modified membrane (PEI-TA/PES) demonstrated good efficiency for the fractionation of inorganic salts and Congo Red. Moreover, it showed high permeability (40.6 LMH·bar^{-1} for 0.1 g/L Congo Red), high rejection to dye (99.8%) as well as low rejection toward NaCl and Na$_2$SO$_4$ (below 10%). The salts passed through the membrane and it allowed the good separation of those inorganic salts and the dye [49].

Another approach to get composite membranes has been developed by grafting cross-linked polymers on porous supports of polysulfones (PSf). In this approach, interfacial polymerization using piperazine (PIP) and trimesoyl chloride (TMC) has been the monomers to get the polyamides (PA). Interestingly, PSf supports have a MWCO of about 30,000 Da, this was reduced to 500 Da after coating it with cross-linked PA, which produces good NF performance in dye rejection toward Direct Red

81, Direct Yellow 8, and Direct Yellow 27. However, this method based on coating of porous PSf showed a disadvantage of membrane fouling, thus, pre-treatment with coagulant agents like ferric chloride of the dye solutions is necessary [50].

Regarding NF, polyvinyl chloride (PVC)-based membranes have received less attention compared with PEI, PI, or PAI-based membranes due to their flexible chains and their putative low resistance to high pressures used in NF. However, it has been reported the synthesis of the copolymer with of PVC and poly(*N,N*-dimethylaminoethyl methacrylate (PDMA, 31.1 wt%), resulting in a PVC-*graft*-PDMA in which ulterior cross-linking with XDC/*n*-heptane (2 wt%) yielded a positively charged membrane with a quaternization degree of 27.8%. Despite the lack of tests of dye rejection tests in this study, this membrane showed excellent salt rejection of $MgCl_2$ by Donnan exclusion mechanisms, which make cross-linked PVC-based membranes promissory for NF [51].
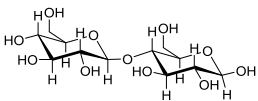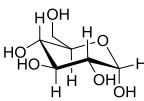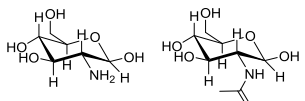
2 Cross-Linked Polymers Based on Natural and Synthetic Polysaccharides: Starch, Chitosan, Cellulose, and Cyclodextrins

The utilization of synthetic polymers and other systems such as composites including carbon nanomaterials and solid-state materials for the absorption of dyes is often very effective and represents many advantages in favor of other purification methods for the elimination of dye and related pollutants from the pigment and printing industries. Nevertheless, these systems have a series of disadvantages, which include a high cost of production and implementation, synthetic procedures that are also polluting, and the difficulty of disposal of the purification systems once they have been used (since they may not degrade easily and cause secondary contamination). For the aforementioned, systems for dye substrates removal based on natural resources have been developed which can be effective dye removal substrates, but also come from natural sources. One of the most popular choices for such substrates is the system based on polysaccharides [52–55].

Starch, chitosan, and cellulose are the three most abundant polysaccharides derived from natural sources, their abundance due to their presence in many biological systems such as plants and animals. The structures of these three natural polysaccharides are shown in Table 2. As a reference to the reader, the key characteristics and differences in the structures of these polysaccharides are presented in this table [52, 53, 56].

Even when these polymers are very abundant, the derivatization of these systems is not a trivial task, mainly due to synthetic limitations such as solubility. These polysaccharides are not readily soluble in most solvents used in polymer synthesis because of their rigid structures with high crystallinities (due to hydrogen bonds); therefore modification and cross-linking reactions often need to be carried out on unconventional solvents or solvent mixtures that may interact with these hydrogen

Table 2 Characteristics of the three most common natural polysaccharides used as cross-linked dye removal systems

Polysaccharide	Cellulose	Starch	Chitosan
Chemical composition	Composed of two repeating units of β-D-glucose bonded between carbons 1 and 4 through an alpha glycosidic bond	Composed of two different polymeric substructures: -Amylose: repeating units of α-D-glucose bonded between carbons 1 and 4 through an alpha glycosidic bond -Amylopectin: repeating units of α-D-glucose bonded between carbons 1 and 4 with branched with α-D-glucose units between carbons 1 and 6 through alpha glycosidic bonds	Composed of randomly organized repeating units of β-D-glucosamine and N-acetyl-D-glucosamine. Chitosan comes from the partial deacetylation of chitin, another natural polysaccharide that is composed of repeating units of β-D-glucosamine bonded between carbons 1 and 4 through a beta glycosidic bond
Repeating unit			
Natural source	Present on the cell wall of all green plants and some algae. Cellulose is the most abundant natural polymer on earth. Cellulose may also be used on derivatized forms such as carboxymethylcellulose (CMC) or hydroxypropyl methylcellulose (HPMC)	Present as an energy storage source for plants and algae. Starch is therefore extensively present on food products	Chitosan comes from the partial deacetylation of chitin. Chitin is the main component of cell walls on fungi, and it is also present in the shells of many crustaceans and insects

bonds such as NaOH/urea and ionic liquids [56, 57]. As such, many of the synthetic procedures for cellulose, starch, or chitosan have strong similarities between them. Mainly, the cross-linking and modification of these polysaccharides are performed by one of the following methods:

- Physical cross-linking through weak interactions (supramolecular forces)
- Chemical cross-linking through chemical reactions with cross-linkers
- Chemical cross-linking and grafting of functional molecules
- Formation of interpenetrated polymeric networks (IPNs) or semi-interpenetrated networks (semi-IPNs).

Despite the great similarity of these polymeric systems these polymeric systems, from the fact that the three are composed of glucose-derived building blocks, to the fact they might be modified with similar synthetic procedures; the key differences between these systems are very crucial in the development of systems for dye absorption. Therefore, in the following subsections, examples of cross-linked systems derived from, consisting of, or containing these polysaccharides will be presented highlighting their key advantages and characteristics.

On the other hand, polymeric cross-linked systems based on cyclodextrins (CDs) also will be discussed. CDs are synthetic cyclic glucose oligomers obtained from starch degradation by hydrolases [58]. They have been used in membrane science as well as in chromatography due to their enzyme-like properties, chirality recognition, their capability to form inclusion complexes as well as the possibility to get modified and cross-linked CDs for membrane design [59].

2.1 Cross-Linked Systems Based on Cellulose

Cellulose is arguably the most important natural polymer for the production of systems for dye removal, probably because cellulose and its derivatives are the most abundant polymers in nature. Research on cross-linked cellulose systems for dye removal started in 1970 where the uptake of dyes cross-linked celluloses was studied as a means of improving the staining of these cross-linked cellulosic materials [60, 61]. However, the utilization of cross-linked cellulose materials for the removal of dyes started being an important topic around 2009, where research on hydrogels of carboxymethyl cellulose (CMC) and hydroxypropyl cellulose (HPC) was performed. One of these examples is presented as a testament to the remarkable advances in this field. In 2009, CMC was cross-linked and functionalized with poly(vinyl alcohol) using ionizing radiation, obtaining a material that was tailored for the absorption of anionic dyes such as Acid Green B, Ismative Violet 2R, and Direct Pink 3B with absorption capacities of around 30 mg/g [60]. After these developments, rapid advances on dye uptake by cross-linked cellulosic materials were performed; therefore, in this subsection, some of these developments are presented.

As a first example in which a cellulose-modified substrate was evaluated against cationic MB is the research performed by Zhou and collaborators in 2011 in which

they investigated the possibility of modifying cellulose with grafts of polyacrylic acid (PAAc) using phosphoric acid as a solvent for cellulose. PAAc was used as a modifier for cellulose as a way of obtaining a superabsorbent hydrogel system based on cellulose. The synthetic procedure involved the dissolution of cellulose on phosphoric acid followed by cross-linking polymerization reaction with *N,N'*-methylenebisacrylamide, and APS as initiator, followed by a grafting polymerization reaction of acrylic acid (AAc). These hydrogels demonstrated the ability. This study demonstrated that the dye-absorption capability of the materials is dependent on the amount of poly(acrylic acid) graft present on the samples, which is probably related to the amount free of carboxylic acid groups on the sample. This was corroborated with adsorption testing in different pH conditions, having poor absorption at low pH as expected (carboxylic acid groups are on their protonated below their pKa value of approximately 4) [62].

Another recent example that is worthy of mentioning is the production of nanocrystalline nanogels formed of cross-linked cellulose for the removal of cationic dyes by Liang and collaborators. In this work, the research group developed a methodology for producing chemically cross-linked aerogels composed of poly(methyl vinyl ether-co-maleic acid), poly(ethylene glycol), and nanocrystals of cellulose through freeze-drying with liquid nitrogen and curing at 90 °C. In this series of studies, the authors evaluated the ability of this system in retaining Methylene Blue (MB) dye determining that these systems can adsorb up to 116.2 mg/g of MB. Additionally, the authors determined that these systems may be reusable up to five cycles of dye removal without losing efficiency [63, 64].

Another example, a system that also profits from the properties of nanocrystalline cellulose while also combining it with the benefits of chitosan (refer to the chitosan subsection) was produced in 2016. To modify nanocrystalline cellulose (NCC), an oxidation reaction with periodate and chlorite ions was performed to yield NCC with carboxylic acid and aldehyde moieties. A representation of this system is shown in Fig. 2. This procedure was followed by a cross-linking reaction via imine formation with carboxymethylated chitosan. In this study, the materials were characterized with a great variety of techniques such as conductimetric titrations, solid-state ^{13}C-NMR, AFM, SEM, porosity measurements, and adsorption isotherms. This system demonstrated excellent capabilities for dye adsorption (785 mg/g of MB) while also maintaining good behavior after several cycles of use [65].

A final recent example was the modification of CMC with a similar methodology in which the cellulosic material was oxidized to form dialdehyde moieties, which could later be cross-linked with gelatin for the removal of dyes such as Rhodamine B and Methyl violet. This system was crafted as an alternative dye-removal substrate, which was only composed of biopolymers and could also be mechanically stable and biodegradable [66].
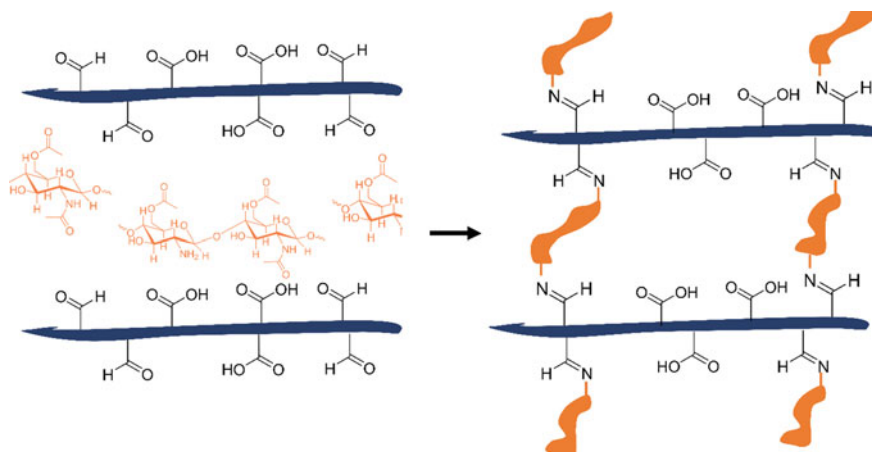
Fig. 2 Cross-linking via Schiff base formation of nanocrystalline cellulose using carboxymethy-lated cellulose [65]

3 Cross-Linked Systems Based on Starch

Similarly, to cellulose, starch is a natural polymer derived from glucose, which is mostly present in plants. However, the difference between cellulose and starch is that the latter is a combination of a linear polysaccharide (amylose) and a branched polysaccharide (amylopectin) while the former is a linear polysaccharide; therefore, the characteristics and behaviors of both polymers in the macroscale differ considerably. Due to the branched structure of starch, its capabilities of adsorbing and retaining chemical compounds are higher than that of cellulose: therefore, the use of cross-linked starches for the removal of dyes predates the use of cellulose [53, 67]. One of the first examples of starch systems for dye removal was developed in 2002, where Delval and collaborators produced a cross-linked starch substrate using epichlorohydrin (Fig. 3) in the presence of ammonium hydroxide as a cross-linker. In this early study, the absorption capabilities of the produced systems were evaluated, and it was verified that dye adsorption is dependent on the number of ammonium groups present on the polymer [68]. It is important to mention that epichlorohydrin is a very important cross-linker for the production of starch and even chitosan systems,
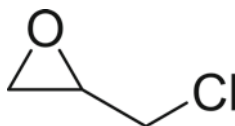

Fig. 3 Chemical structure of epichlorohydrin, a very important cross-linker for starch and chitosan-based systems

and as such, the original protocol described by Simkovic et al. is presented here as a reference to the reader [69].

A more recent example of starch-based materials for the removal of dyes, a 2006 study reported the behavior of a specially crafted cross-linked starch-containing both carboxylate groups and quaternary ammonium ions in its structure for the adsorption of both cationic and anionic dyes (Acid Red G, acid Light Yellow 2G, methyl green, and methyl violet). In this study, the effect of pH, times, concentration of dyes were evaluated allowing to obtain adsorption isotherms and kinetic parameters [70].

In 2019, Zhang Hao and collaborators developed a cross-linked starch system that was cross-linked using epichlorohydrin and containing γ-cyclodextrin by immobilization by esterification. This system was evaluated as an alternative for adsorption of MB, methyl purple (MP), and congo red (CR) as model anionic and cationic dyes in complicated matrices intended to emulate real conditions of adsorption (referred by the authors by dyestuff). The materials showed improved absorption of these three dyes compared with both cross-linked starch, and other absorbents such as diatomite and zeolite. Additionally, cyclodextrin containing starch showed improved stability to biodegradation; therefore, improving the durability of the material while not compromising its biodegradability [71].

A final example in which starch was modified to improve its capabilities of removing dyes was the research by Janaki and collaborators. In this work, maize starch was modified with polyaniline produced in situ by the oxidative polymerization of aniline with ammonium peroxydisulfate forming a cross-linked material due to hydrogen bonds (Fig. 4). In this study, the removal of dyes such as Reactive Black 5 and Reactive Violet 4 was studied in different conditions, in particular, it was interesting that the uptake of these dyes was possible at low pH, this is because amine groups of aniline are charged at low pH in contrast to carboxylic acid-based
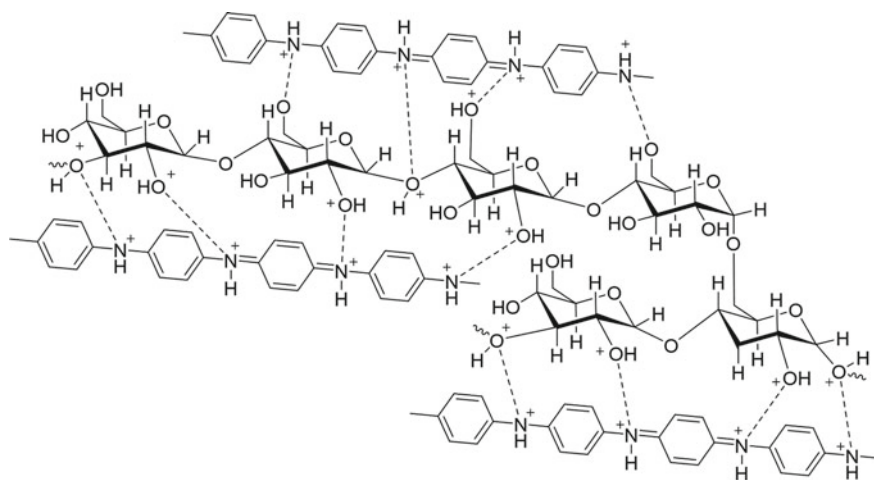

Fig. 4 Starch cross-linked with polyaniline via hydrogen–bond interactions

adsorption, which occurs at higher pH values with high effectiveness. Additional to this, the authors of this study verified that the adsorption of the dyes was due to ionic interactions [72].

It is important to mention that although these selected examples present an overview of the chemistry of cross-linked starch, there are many examples of functionalization and cross-linking of starch to obtain materials capable of dye absorption and other applications, as a reference to the reader, some of these works as well as some extensive reviews are presented as a conclusion to this subsection [53, 73–78].

4 Cross-Linked Systems Based on Chitosan

As it may be notable, chitosan is the only of these three polymeric systems (and cyclodextrins for that matter) that is not composed of repeating units of glucose; in contrast, the remarkable functional group present in chitosan is the amine group of glucosamine. The presence of this functional group in particular because, due to its acid–base properties, it has a positive charge at neutral pH (the amine group becomes an ammonium group below its pKa of around 9); therefore, in most conditions, chitosan is a positively charged polymer. With this in mind, chitosan systems are particularly effective with the adsorption of negatively charged species like anionic dyes [56, 79–82].

The first interesting example is a 2003 paper by M. S. Chiou and H. Y. Li in which they first produced chitosan beads that were then cross-linked using epichlorohydrin and NaOH or glutaraldehyde in aqueous conditions. The adsorption capabilities of this substrate were evaluated by batch adsorption assays against reactive red 189 and by evaluating the effect of pH and temperature on the absorption of this dye [83].

In another important example of chitosan modification, an interpenetrated network composed of chitosan chains and polymerized acrylamide. This material is interesting because it profits from the adsorption capabilities and abundance of chitosan as a polysaccharide, while also providing rigidity to the matrix by forming the interpenetrated network with poly(acrylamide). This interpenetrated network was formed by cross-linking acrylamide with *N,N'*-methylenebisacrylamide, and glutaraldehyde as cross-linkers (Fig. 5). This material arranged in cylinders was demonstrated to be an effective substrate for the absorption of EY-4GL Yellow and S-Blue in complicated matrixes [84].

In a recent example a combination system in which chitosan was integrated onto activated carbon and cross-linked with epichlorohydrin. This composite system was synthesized by dissolving chitosan into acetic acid and mixed with activated carbon and then cross-linking with epichlorohydrin and NaOH. In this work, the surface area of the materials was characterized by N_2 adsorption and desorption, the crystallinity was evaluated using X-ray diffraction. Additionally, SEM was used to visualize the materials before and after adsorption, FTIR to verify the presence of certain functional groups. As in other studies, the adsorption capabilities of this polymer against thionine were evaluated concerning pH, temperature, and contact time [85].
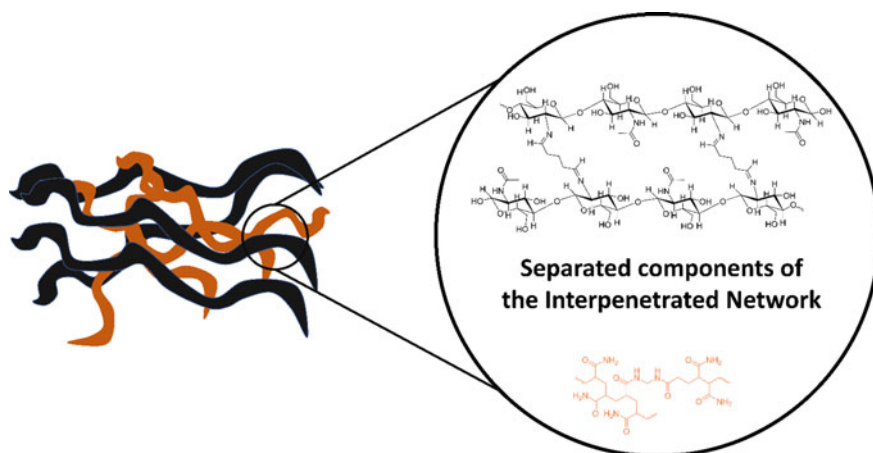
Fig. 5 Chitosan-polyacrylamide interpenetrated network

A final example of chitosan as a cross-linked matrix is a 2017 paper by Martina Salzano de Luna and collaborators. In this work, the authors wanted to investigate if the inherent absorption capabilities of chitosan could be enhanced by producing porous hyper cross-linked polymer particles that could entrap cationic and anionic dye molecules onto its pores. These substrates were produced by the hyper cross-linking reaction in which poly(VBC-DVB) is synthesized as a cross-linking precursor with the capability of cross-linking several times through Friedel Crafts reactions to form a hyper cross-linked resin, which was then mixed with chitosan to form a hydrogel. These materials were shown to be effective in dye adsorbing with different chemical structures such as Indigo Carmine, Rhodamine 6G, and Sunset Yellow even after several adsorption–desorption cycles while having improved mechanical performance when compared with chitosan and good and thermal stability [86].

5 Cross-Linked Systems Based on Cyclodextrins (CDs)

CDs have been known for more than 100 years but until the 1980s when the first applications in the food and pharmaceutical industry scale-up CDs research and production at industry levels. This led to the synthesis of pure native CDs, which are cyclic oligomers of glucose bonded by α-1,4 glycosidic bonds. They are called α-CD, β-CD, and γ-CD depending on the number of bonded glucose units (Fig. 6) and have characteristic toroidal shapes with hydrophobic central nanocavities capable to host small molecules due to their cage-type shape. CDs' surface shows hydrophilic properties surface due to the pointing outside OH groups.
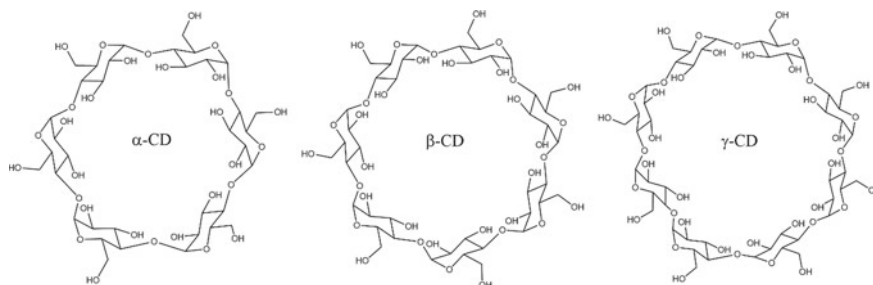
Fig. 6 Native CDs form starch degradation, α-CD (six glucose units), β-CD (seven glucose units), and γ-CD (nine glucose units)

Concerning materials with dye removal applications, cross-linked CDs have been implemented in membranes and adsorbents materials. The formers have the advantage of high dye removal properties when implemented in nanofiltration, as well as high regeneration capacities, but they are not always suitable from the cost operation point of view. On the other hand, adsorbent materials have arisen as an alternative due to their low cost of production and operation. However, typically adsorbent materials show either lower regeneration capabilities or lower dye removal capacity than membranes for nanofiltration (NF) [87]. Both will be discussed here with representative examples.

Among the most used methods to get flat sheet and hollow fiber membranes base on cross-linked CDs is phase inversion followed by cross-linking process and interfacial cross-linking [88]. For example, composite porous membrane based on β-CD and supported on a microfiltration nylon membrane (average pore size = 0.45 μm) has been reported to take advantage of mass transport in porous support without the need for high pressures. Nylon porous membrane was submerged in alkaline aqueous solution containing β-CD (0–0.14%) to get dip-coated membrane. After drying by evaporation, the cross-linking process was achieved by the addition of trimesoyl chloride (TMC, 0–2%) in hexane at 60 °C. The composite membrane showed rejection of bisphenol (BPA, a waste reagent in dye and plastic industry) with a feed solution of 10 mg L^{-1} and permeation flux of 80 L m^{-2} h $^{-1}$. The N element content on the pristine composite membrane was 11.3%, while a marked drop to 0.9% in N composition was confirmed by XPS surface analysis after cross-linking process [89].

The use of ceramic membranes (Al_2O_3) to support polymeric systems has also been reported concerning water purification from monocyclic aromatic hydrocarbons by sorption. For example, sylation of β-CD (60–70%) and subsequent sol–gel reaction yielded cross-linked triethoxysilylated cyclodextrins on the ceramic Al_2O_3 surface. Subsequent hydrolysis to silanols and thermic treatment yielded a siloxane network on the surface of the organic–inorganic filter. This membrane showed a higher affinity toward lipophilic pollutants than ceramic materials and high rejection of organic pollutants of low molecular weight, like those proceeding from textile finishing industries, i.e., dye color fixation process. [90].

Cyclodextrin solute complexation often improves the absorbency properties of the membranes. Poly(vinyl alcohol)/glutaraldehyde membranes have been modified by embedded β-CD to obtain membranes with high sorption of methyl orange, and Methylene Blue (MB) dyes. The β-CD is not covalently bonded to PVA but mixed into matrix polymer. With 8% β-CD, a maximum of adsorption capacity was obtained. Also, the swelling ratio increased from 58 in PVA/GA to 100% in PVA/GA/ β-CD, which indicates the more hydrophilic character of the modified membrane and their capability to promote interaction of non-polar MB with the nanocavity of β-CD. Additionally, the pH value controls the adsorption process since the surface charge of the polymer resulted in a pH function. In this case, the MB adsorption process is favored in an acid medium in which the PVA/GA/ β-CD membrane is stable and also shows regeneration capacities after one cycle of use [91].

Interestingly, the use of CDs in cross-linked polymers has also been applied to obtain insoluble nanofibrous membranes. β-CD functionalized with polyvinyl pyrrolidone (PVP) has been cross-linked using glutaraldehyde, an excellent cross-linking agent for CDs, by electrospinning preparation. The sorption experiments showed methyl orange adsorption (39.82 mg per gram of membrane) providing an alternative to traditional filtration technologies for dye removal from wastewater [92].

Recently, a gelatin/β-CD composite fiber has been reported. Gelatin is a type of protein produced by the hydrolysis of collagen, and its composites typically show excellent mechanical strength. The gelatin/β-CD composite was cross-linked with glutaraldehyde showed high removal capacity of MB, Basic Fuchsin, Brilliant Blue R, and Malachite Green dyes. After nine cycles of use, the fibers showed high adsorption efficiency. Figure 7 shows a schematic representation of the Gelatin/β-CD composite fiber in which is clear that the cross-linking agent can bind CDs units and gelatine polymer as well as gelatine chains [93].

Concerning the design and synthesis of polymers for sorption of anionic azo dyes, CDs and starch have been cross-linked with hexamethylene diisocyanate (HMDI), yielding insoluble resins. Host–guest interaction involving inclusion complex between β-CD and the azo dyes plays a key role in the mechanism of
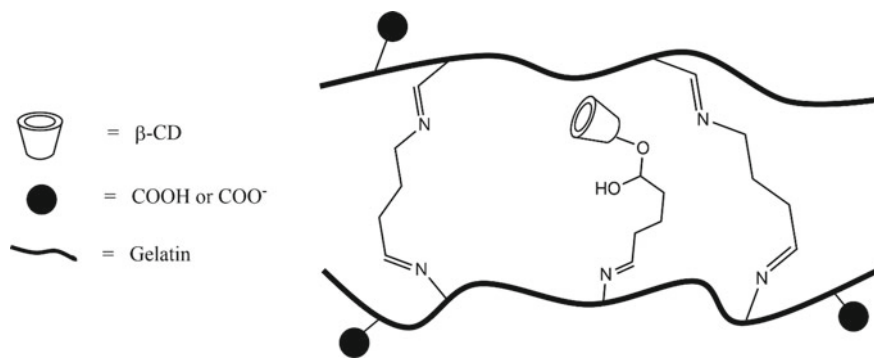

Fig. 7 Gelatin/β-CD composite fiber

dye removal from wastewater. These resins showed a high capacity for the removal of azo dyes, e.g., Direct Violet 51, Tropaeolin 000 (Orange II), and methyl orange [94].

More recently, a porous β-CD polymer containing carboxylic acid groups was obtained and tested as a sorbent of cationic MB, obtaining a dye removal of 672 mg per g of material. The results were interpreted in terms of triple effects in the mechanism of sorption; inclusion complex with β-CD, the porous network of the cross-linked polymers, and the electrostatic attraction between the cationic dye and the negative carboxylate groups of the polymer [95].

6   Polymeric Composites and Synthetic Polymers

On the other side, some blends, composites, and mixes are used as an alternative for the preparation of adsorbent membranes. Some of the most common are the polymer–metal coagulants, which have been demonstrated to be efficient as adsorbents in the cleaning water process, with a remotion of almost 90% of dyes in a solution [13]. Additionally, the combination or modification of these components allows the decreasing of the dosage of the metal coagulant reducing toxicity. Other hybrid materials and composites have been prepared for dye removal [39, 96], the combination of carbon nanomaterials, inorganic polymers [49], magnetic particles [39], and natural compounds has been tested. Carbon nanotubes and graphene oxide (GO) have demonstrated good performance for dye removal [97], and magnetic nanoparticles aid in the elimination of heavy metals and anionic dyes by coagulation [98].

In the case of carbon nanomaterials, GO has been mixed with natural or synthetic polymers to obtain adsorbents for dyes. Abdi et al. modified conventional PES membranes with magnetic graphene oxide sheets. They prepared a hybrid material based on magnetite (Fe_3O_4), metformin, and GO (metformin/GO/Fe_3O_4), and then it was introduced into the PES. The resulting material was able to remove copper ions by the interaction of Cu^{2+} with the primary and secondary amines in the metformin; and the azo dye, Direct Red 16, was retained by supramolecular interactions, π–π stacking with GO phenolic groups, and hydrogen bonding between carbonyl and amine groups. The membrane performance was not been affected, it maintains the water flux and the removal capacity with the addition of only 0.5 wt% of the hybrid material (metformin/GO/Fe_3O_4) [99].

Besides, polysaccharides have been mixed with GO for the removal of dyes; for example, Song et al. prepared a composite made of phosphorylated chitosan (PCS) PCS-GO by grafting deposited onto polyacrylonitrile (PAN) membranes (PSC-GO/PAN). By covalent immobilization of the chitosan derivative onto the GO surface, the separation performance for anionic dyes including Direct Black 38, Ponceau S, Xylenol Orange, NaCl, and Na_2SO_4, was successful. Additionally, the PSC-GO/PAN NF membrane showed a good technique for the treatment of salty anionic dye solutions with antifouling performance [100].

For crystal violet removal (cationic dye), a composite made of GO and polysaccharide hydrogels were tested for [101]. The GO was functionalized with a macroinitiator to obtain free vinyl groups on the surface of GO, subsequently, the hydrogel was cross-linked using the modified GO as a cross-linking agent. The final cross-linked hydrogel was synthesized by mixing (Acrylic Acid)-*co*-(2-acrylamido-2-methylpropane sulfonic acid) poly(AAc-*co*-AMPSA) and *xanthan gum* (anionic polysaccharide) with the previously modified GO. The cross-linked hydrogel was disposed of as a column for filtration with a successful separation of CV, by hydrogen bonding and π–π stacking with the hydrogel and the GO sheets. Additionally, the material demonstrated good performance by eliminating almost 99% of the dye at neutral pH, and good reusability (useful for 20 adsorption–desorption cycles) [101].

The grafting approach has allowed the incorporation of virtually any material onto a surface, the last examples used this technique to enhance the versatility and performance of membranes for filtration and separation of salts and dyes. AAc has been employed to remove cationic dyes by complexation with the carboxylate groups. Gamma radiation has been used to achieve cross-linked polymeric matrixes, and to modify surfaces; hence, it allowed the fabrication of hydrogels and membranes for dye removal. Dafader et al. made the modification of cotton (cellulose) with AAc (AAc-*g*-cotton) in aqueous media by grafting technique, the final material was tested for the adsorption of a cationic dye, MB. The authors suggested that the retention of the dye is due to electrostatic (ionic) interaction between the cationic group of MB and the anionic group (COO^-) of AAc-*g*-cotton. It is also found that dye adsorption increases with increased concentration of dye in aqueous solution, the material showed an adsorption capacity of 16.89 mg/g at room temperature [102].

Additionally, hydrogels have shown good adsorbent behavior through colorants and pollutants from textile water. PAAc has demonstrated ability to remove cationic dyes, since the carboxylate groups. Another hydrogel prepared by gamma radiation showed high adsorption of MB when the contact time with the colored water and the adsorbent dosage is increased. The poly(vinyl alcohol)/acrylic acid/poly-4-styrene sulphonic acid hydrogel (PVA/AAc/PSSa) exhibited a removal efficiency at neutral pH condition and it showed a reusability of four cycles [103].

As well as other polysaccharides, pectin has been combined with AAc to synthesize hydrogels for MB removal. Abdullah et al. used gamma and microwave (MW) radiation to obtain pectin-based hydrogels. The pectin was extracted from the dragon fruit peel waste (*Hylocereus polyrhizus*), and two different hydrogels were obtained, the first using MW polymerization and the second by gamma rays. Both hydrogels exhibited excellent performance in absorbing aqueous solution (tested by swelling) and MB in alkaline medium, although, the hydrogels prepared using gamma radiation showed better performance with about 45% of absorbency with 20 mg of the sample [104].

Also, azo dyes can be removed using hydrogels, it totally depends on de-chemical structure of the polymer and dye. Methacrylates, similar to acrylates, have been used to prepare adsorbent hydrogels. Hydrogels from 2-hydroxyethylmethacrylate (HEMA), methacrylate derivatives, and PVA were synthesized by Gupta and Sadegh

group in 2015 as an adsorbent for the removal of Malachite green and Congo Red at pH 9 [105].

As a final example of synthetic polymers being used for this mean, a 2018 paper by Hernandez–Martinez and collaborators dealt with the synthesis of a cross-linked system using *N,N*-dimethylacrylamide and 2-hydroxyethyl methacrylate using AIBN as a polymerization initiator in an inert atmosphere. This work measured the swelling capabilities of these materials obtaining outstanding swelling in a couple of hours and uptakes of MB up to 30–40 mg/g at high concentration of dye on the initial solution [106].

7 Conclusion

The extensive use of dyes in a variety of industries and their incorrect disposal pose a serious threat to both the environment and human health due to concerns about the safety of the dyes once they entered water sources. The solution for this effect has, in recent years, developed from a handful of techniques, which, although effective, were costly, not as effective, or even generating secondary pollution. Nowadays, there exist the possibility of designing functional polymeric systems for removing dyes and related pollutants from water sources through cleaner and more effective methods profiting from the chemical composition of novel polymer systems, which are both derived from classical chemical synthesis and the derivatization of existing natural polymers. In the future, the utilization of more advanced systems that combine mechanisms like size exclusion, supramolecular interaction, and electrostatic forces will probably arise as means of effective wastewater purification for both dyes and many other pollutants.

References

1. Bhatia D, Sharma NR, Singh J, Kanwar RS (2017) Biological methods for textile dye removal from wastewater: a review. Crit Rev Environ Sci Technol 47(19):1836–1876
2. Katheresan V, Kansedo J, Lau SY (2018) Efficiency of various recent wastewater dye removal methods: a review. J Environ Chem Eng 6(4):4676–4697
3. Hynes NRJ, Kumar JS, Kamyab H, Sujana JAJ, Al-Khashman OA, Kuslu Y, et al (2020) Modern enabling techniques and adsorbents based dye removal with sustainability concerns in textile industrial sector–a comprehensive review. J Clean Prod 272:122636
4. Kabdaşlı I, Ölmez T, Tünay O (2002) Factors affecting colour removal from reactive dye bath by ozonation. Water Sci Technol 45(12):261–270

5. Sher F, Malik A, Liu H (2013) Industrial polymer effluent treatment by chemical coagulation and flocculation. J Environ Chem Eng 1(4):684–689
6. Xiao Y, De AC, Sze CC, Stuckey DC (2015) Toxicity measurement in biological wastewater treatment processes: a review. J Hazard Mater 286:15–29
7. Kim Y, Farnazo DM (2017) Toxicity characteristics of sewage treatment effluents and potential contribution of micropollutant residuals. J Ecol Environ 41(1):39
8. Zhou Y, Lu J, Zhou Y, Liu Y (2019) Recent advances for dyes removal using novel adsorbents: a review. Environ Pollut 252:352–365
9. Abiola ON (2019) Polymers for coagulation and flocculation in water treatment. In: Polymeric materials for clean water. p 77–92
10. Fleischmann C, Lievenbrück M, Ritter H (2015) Polymers and dyes: developments and applications. Polymers 7(4):717–746
11. Aldás Sandoval MB, Buenaño Bautista BB, Vera Calle ER (2019) Study of coagulating/flocculating characteristics of organic polymers extracted from biowaste for water treatment. Ing e Investig 39(1)
12. Arafat HA (2007) Simple physical treatment for the reuse of wastewater from textile industry in the Middle East. J Environ Eng Sci 6(1):115–122
13. Zahrim AY, Tizaoui C, Hilal N (2011) Coagulation with polymers for nanofiltration pretreatment of highly concentrated dyes: a review. Desalination 266(1–3):1–16
14. Bennett GF (1989) Impact of toxic chemicals on local wastewater treatment plant and the environment. Environ Geol Water Sci 13(3):201–212
15. Comber SDW, Gardner MJ, Churchley J (2005) Aluminium speciation: implications of wastewater effluent dosing on river water quality. Chem Speciat Bioavailab 17(3):117–128
16. Ghernaout D, Ghernaout B (2012) Sweep flocculation as a second form of charge neutralisation—a review. Desalin Water Treat 44(1–3):15–28
17. Suopajärvi T, Liimatainen H, Hormi O, Niinimäki J (2013) Coagulation–flocculation treatment of municipal wastewater based on anionized nanocelluloses. Chem Eng J 231:59–67
18. Sarode S, Upadhyay P, Khosa MA, Mak T, Shakir A, Song S et al (2019) Overview of wastewater treatment methods with special focus on biopolymer chitin-chitosan. Int J Biol Macromol 121:1086–1100
19. Yagub MT, Sen TK, Afroze S, Ang HM (2014) Dye and its removal from aqueous solution by adsorption: a review. Adv Colloid Interface Sci 209:172–184
20. Nasar A, Mashkoor F (2019) Application of polyaniline-based adsorbents for dye removal from water and wastewater—a review. Environ Sci Pollut Res 26(6):5333–5356
21. Munjur H, Hasan MN, Awual MR, Islam MM, Shenashen MA, Iqbal J (2020) Biodegradable natural carbohydrate polymeric sustainable adsorbents for efficient toxic dye removal from wastewater. J Mol Liq 319:114356
22. Vakili M, Rafatullah M, Salamatinia B, Abdullah AZ, Ibrahim MH, Tan KB et al (2014) Application of chitosan and its derivatives as adsorbents for dye removal from water and wastewater: a review. Carbohydr Polym 113:115–130
23. Varaprasad K, Jayaramudu T, Sadiku ER (2017) Removal of dye by carboxymethyl cellulose, acrylamide and graphene oxide via a free radical polymerization process. Carbohydr Polym 164:186–194
24. Wan Ngah WS, Teong LC, Hanafiah MAKM (2011) Adsorption of dyes and heavy metal ions by chitosan composites: a review. Carbohydr Polym 83(4):1446–1456
25. Szyguła A, Guibal E, Palacín MA, Ruiz M, Sastre AM (2009) Removal of an anionic dye (Acid Blue 92) by coagulation–flocculation using chitosan. J Environ Manage 90(10):2979–2986
26. Sadeghi-Kiakhani M, Arami M, Gharanjig K (2013) Preparation of chitosan-ethyl acrylate as a biopolymer adsorbent for basic dyes removal from colored solutions. J Environ Chem Eng 1(3):406–415
27. Jiang Y, Liu B, Xu J, Pan K, Hou H, Hu J et al (2018) Cross-linked chitosan/β-cyclodextrin composite for selective removal of methyl orange: adsorption performance and mechanism. Carbohydr Polym 182:106–114

28. Kanmani P, Aravind J, Kamaraj M, Sureshbabu P, Karthikeyan S (2017) Environmental applications of chitosan and cellulosic biopolymers: a comprehensive outlook. Bioresour Technol 242:295–303

29. Vieira AMS, Vieira MF, Silva GF, Araújo ÁA, Fagundes-Klen MR, Veit MT et al (2010) Use of Moringa oleifera seed as a natural adsorbent for wastewater treatment. Water Air Soil Pollut 206(1–4):273–281

30. Beltrán-Heredia J, Sánchez MJ (2008) Azo dye removal by Moringa oleifera seed extract coagulation. Color Technol 124(5):310–317

31. Jabar JM, Odusote YA, Alabi KA, Ahmed IB (2020) Kinetics and mechanisms of congo-red dye removal from aqueous solution using activated Moringa oleifera seed coat as adsorbent. Appl Water Sci 10(6):136

32. Beltrán-Heredia J, Sánchez-Martín J, Delgado-Regalado A (2009) Removal of carmine indigo dye with Moringa oleifera seed extract. Ind Eng Chem Res 48(14):6512–6520

33. Beltrán-Heredia J, Sánchez-Martĭn J, Delgado-Regalado A (2009) Removal of dyes by Moringa oleifera seed extract. Study through response surface methodology. J Chem Technol Biotechnol 84(11):1653–1659

34. Tie J, Jiang M, Li H, Zhang S, Zhang X (2015) A comparison between Moringa oleifera seed presscake extract and polyaluminum chloride in the removal of direct black 19 from synthetic wastewater. Ind Crops Prod 74:530–534

35. Janoš P, Coskun S, Pilařová V, Rejnek J (2009) Removal of basic (Methylene Blue) and acid (Egacid Orange) dyes from waters by sorption on chemically treated wood shavings. Bioresour Technol 100(3):1450–1453

36. Sanghi R, Bhattacharya B, Singh V (2006) Use of Cassia javahikai seed gum and gum-g-polyacrylamide as coagulant aid for the decolorization of textile dye solutions. Bioresour Technol 97(10):1259–1264

37. Lau Y-Y, Wong Y-S, Teng T-T, Morad N, Rafatullah M, Ong S-A (2014) Coagulation-flocculation of azo dye acid orange 7 with green refined laterite soil. Chem Eng J 246:383–390

38. Luo X, Zhan Y, Huang Y, Yang L, Tu X, Luo S (2011) Removal of water-soluble acid dyes from water environment using a novel magnetic molecularly imprinted polymer. J Hazard Mater 187(1–3):274–282

39. Huang L, He M, Chen B, Cheng Q, Hu B (2017) Facile green synthesis of magnetic porous organic polymers for rapid removal and separation of methylene blue. ACS Sustain Chem Eng. 5(5):4050–4055

40. Oatley-Radcliffe DL, Walters M, Ainscough TJ, Williams PM, Mohammad AW, Hilal N (2017) Nanofiltration membranes and processes: a review of research trends over the past decade. J Water Process Eng 19:164–71

41. Shokri Doodeji M, Zerafat M, Mahdi Zerafat M (2018) A review on the applications of nanofiltration in virus removal and pharmaceutical industries. Glob J Nanomed 3

42. Lau WJ, Ismail AF (2009) Polymeric nanofiltration membranes for textile dye wastewater treatment: preparation, performance evaluation, transport modelling, and fouling control–a review. Desalination 245(1–3):321–348

43. Gunawan FM, Mangindaan D, Khoiruddin K, Wenten IG (2019) Nanofiltration membrane cross-linked by m-phenylenediamine for dye removal from textile wastewater. Polym Adv Technol 30(2):360–367

44. Liu C, Cheng L, Zhao Y, Zhu L (2017) Interfacially crosslinked composite porous membranes for ultrafast removal of anionic dyes from water through permeating adsorption. J Hazard Mater 337:217–225

45. Ba C, Langer J, Economy J (2009) Chemical modification of P84 copolyimide membranes by polyethylenimine for nanofiltration. J Memb Sci. 327(1–2):49–58

46. Zhao S, Ba C, Yao Y, Zheng W, Economy J, Wang P (2018) Removal of antibiotics using polyethylenimine cross-linked nanofiltration membranes: relating membrane performance to surface charge characteristics. Chem Eng J 335:101–109

47. Wang X, Ju X, Jia TZ, Xia QC, Guo JL, Wang C et al (2018) New surface cross-linking method to fabricate positively charged nanofiltration membranes for dye removal. J Chem Technol Biotechnol 93(8):2281–2291

48. Mangindaan D, Kasih TP (2020) Diaminoethane-crosslinked polyetherimide nanofiltration membrane for textile wastewater dye removal. IOP Conf Ser Earth Environ Sci 426(1):012112

49. Li Q, Liao Z, Fang X, Wang D, Xie J, Sun X et al (2019) Tannic acid-polyethyleneimine crosslinked loose nanofiltration membrane for dye/salt mixture separation. J Memb Sci. 584:324–332

50. Mo JH, Lee YH, Kim J, Jeong JY, Jegal J (2008) Treatment of dye aqueous solutions using nanofiltration polyamide composite membranes for the dye wastewater reuse. Dye Pigment 76(2):429–434

51. Fang LF, Zhou MY, Cheng L, Zhu BK, Matsuyama H, Zhao S (2019) Positively charged nanofiltration membrane based on cross-linked polyvinyl chloride copolymer. J Memb Sci 572:28–37

52. Qureshi MA, Nishat N, Jadoun S, Ansari MZ (2020) Polysaccharide based superabsorbent hydrogels and their methods of synthesis: a review. Carbohydr Polym Technol Appl 1:100014. https://doi.org/10.1016/j.carpta.2020.100014

53. Crini G, Badot PM (2010) Starch-based biosorbents for dyes in textile wastewater treatment. Int J Environ Technol Manag 12(2–4):129–150

54. Panic V, Seslija S, Nesic A, Velickovic S (2013) Adsorption of azo dyes on polymer materials. Hem Ind 67(6):881–900. http://www.doiserbia.nb.rs/Article.aspx?ID=0367-598X1300020P

55. Tan KB, Vakili M, Horri BA, Poh PE, Abdullah AZ, Salamatinia B (2015) Adsorption of dyes by nanomaterials: recent developments and adsorption mechanisms. Sep Purif Technol 150:229–242. https://doi.org/10.1016/j.seppur.2015.07.009

56. Qamar SA, Ashiq M, Jahangeer M, Riasat A, Bilal M (2020) Chitosan-based hybrid materials as adsorbents for textile dyes–a review. Case Stud Chem Environ Eng 2:100021. https://doi.org/10.1016/j.cscee.2020.100021

57. Zainal SH, Mohd NH, Suhaili N, Anuar FH, Lazim AM, Othaman R (2021) Preparation of cellulose-based hydrogel: a review. J Mater Res Technol 10:935–952. https://doi.org/10.1016/j.jmrt.2020.12.012

58. Crini G (2014) Review: a history of cyclodextrins. Chemical Reviews 114:10940–10975

59. Davis ME, Brewster ME (2004) Cyclodextrin-based pharmaceutics: past, present and future. Nat Rev Drug Disc 3:1023–1035

60. Taleb MFA, El-Mohdy HLA, El-Rehim HAA (2009) Radiation preparation of PVA/CMC copolymers and their application in removal of dyes. J Hazard Mater 168(1):68–75

61. Yan L, Shuai Q, Gong X, Gu Q, Yu H (2009) Synthesis of microporous cationic hydrogel of hydroxypropyl cellulose (HPC) and its application on anionic dye removal. Clean Soil Air Water 37(4–5):392–8. https://doi.org/10.1002/clen.200900006

62. Zhou Y, Fu S, Liu H, Yang S, Zhan H (2011) Removal of methylene blue dyes from wastewater using cellulose-based superadsorbent hydrogels. Polym Eng Sci 51(12):2417–24. https://doi.org/10.1002/pen.22020

63. Liang L, Zhang S, Goenaga GA, Meng X, Zawodzinski TA, Ragauskas AJ (2020) Chemically cross-linked cellulose nanocrystal aerogels for effective removal of cation dye. Front Chem 8:1–9

64. Liang L, Huang C, Hao N, Ragauskas AJ (2019) Cross-linked poly(methyl vinyl ether-co-maleic acid)/poly(ethylene glycol)/nanocellulosics foams via directional freezing. Carbohydr Polym 213:346–351. https://doi.org/10.1016/j.carbpol.2019.02.073

65. Yang H, Sheikhi A, Van De Ven TGM (2016) Reusable green aerogels from cross-linked hairy nanocrystalline cellulose and modified chitosan for dye removal. Langmuir 32(45):11771–11779

66. Sethi S, Kaith BS, Kaur M, Sharma N, Khullar S (2020) A hydrogel based on dialdehyde carboxymethyl cellulose–gelatin and its utilization as a bio adsorbent. J Chem Sci 132(1). https://doi.org/10.1007/s12039-019-1700-z

67. Delval F, Crini G, Bertini S, Filiatre C, Torri G (2005) Preparation, characterization and sorption properties of crosslinked starch-based exchangers. Carbohydr Polym 60(1):67–75
68. Delval F, Crini G, Morin N, Vebrel J, Bertini S, Torri G (2002) The sorption of several types of dye on crosslinked polysaccharides derivatives. Dye Pigment 53(1):79–92
69. Šimkovic I, Laszlo JA, Thompson AR (1996) Preparation of a weakly basic ion exchanger by crosslinking starch with epichlorohydrin in the presence of NH4OH1. Carbohydr Polym 30(1):25–30
70. Xu S, Wang J, Wu R, Wang J, Li H (2006) Adsorption behaviors of acid and basic dyes on crosslinked amphoteric starch. Chem Eng J 117(2):161–167
71. Hao Z, Yi Z, Bowen C, Yaxing L, Sheng Z (2019) Preparing γ-cyclodextrin-immobilized starch and the study of its removal properties to dyestuff from wastewater. Polish J Environ Stud. 28(3):1701–1711
72. Janaki V, Vijayaraghavan K, Oh B, Lee K, Muthuchelian K, Ramasamy AK, et al (2012) Starch/polyaniline nanocomposite for enhanced removal of reactive dyes from synthetic effluent. Carbohydr Polym 90(4):1437–44. https://linkinghub.elsevier.com/retrieve/pii/S0144861712006686
73. Guo J, Wang J, Zheng G (2019) Synthesis of cross-linking cationic starch and its adsorption properties for reactive dyes. IOP Conf Ser Earth Environ Sci 227(6)
74. Mandal B, Ray SK (2015) Synthesis, characterization, swelling and dye adsorption properties of starch incorporated acrylic gels. Int J Biol Macromol 81:847–57. https://doi.org/10.1016/j.ijbiomac.2015.08.050
75. Xing G, Liu S, Xu Q, Liu Q (2012) Preparation and adsorption behavior for brilliant blue X-BR of the cost-effective cationic starch intercalated clay composite matrix. Carbohydr Polym 87(2):1447–1452. https://doi.org/10.1016/j.carbpol.2011.09.038
76. Xu H, Canisag H, Mu B, Yang Y (2015) Robust and flexible films from 100% starch cross-linked by biobased disaccharide derivative. ACS Sustain Chem Eng 3(11):2631–2639
77. Phoothong F, Boonmahitthisud A, Tanpichai S (2019) Using borax as a cross-linking agent in cellulose-based hydrogels. IOP Conf Ser Mater Sci Eng 600(1)
78. Feng K, Wen G (2017) Absorbed Pb2+ and Cd2+ ions in water by cross-linked starch xanthate. Int J Polym Sci 2017
79. Crini G (2006) Non-conventional low-cost adsorbents for dye removal: a review. Bioresour Technol 97(9):1061–85. https://linkinghub.elsevier.com/retrieve/pii/S0960852405002452
80. Dhiman N, Shukla SP, Kisku GC (2017) Statistical optimization of process parameters for removal of dyes from wastewater on chitosan cenospheres nanocomposite using response surface methodology. J Clean Prod 149:597–606. https://doi.org/10.1016/j.jclepro.2017.02.078
81. Barik B, Nayak PS, Achary LSK, Kumar A, Dash P (2019) Synthesis of alumina-based cross-linked chitosan-HPMC biocomposite film: an efficient and user-friendly adsorbent for multipurpose water purification. New J Chem 44(2):322–337
82. Zhao F, Repo E, Yin D, Chen L, Kalliola S, Tang J et al (2017) One-pot synthesis of trifunctional chitosan-EDTA-β-cyclodextrin polymer for simultaneous removal of metals and organic micropollutants /. Sci Rep 7(1):1–14
83. Chiou MS, Li HY (2003) Adsorption behavior of reactive dye in aqueous solution on chemical cross-linked chitosan beads. Chemosphere 50(8):1095–1105
84. Ekici S, Güntekin G, Saraydin D (2011) The removal of textile dyes with cross-linked chitosan-poly(acrylamide) adsorbent hydrogels. Polym–Plast Technol Eng 50(12):1247–1255
85. Jawad AH, Abdulhameed AS, Mastuli MS (2020) Mesoporous crosslinked chitosan-activated charcoal composite for the removal of thionine cationic dye: comprehensive adsorption and mechanism study. J Polym Environ 28(3):1095–105. https://doi.org/10.1007/s10924-020-01671-5

86. Salzano de Luna M, Castaldo R, Altobelli R, Gioiella L, Filippone G, Gentile G, et al (2017) Chitosan hydrogels embedding hyper-crosslinked polymer particles as reusable broad-spectrum adsorbents for dye removal. Carbohydr Polym 177:347–54. https://doi.org/10.1016/j.carbpol.2017.09.006

87. Wang J, Cheng G, Lu J, Chen H, Zhou Y (2020) PDA-cross-linked beta-cyclodextrin: a novel adsorbent for the removal of BPA and cationic dyes. Water Sci Technol 81(11):2337–2350

88. Trotta F (2016) Cyclodextrin in membranes. In: Encyclopedia of membranes. Springer Berlin Heidelberg, Berlin, Heidelberg, pp 505–507

89. Wang Z, Guo S, Zhang B, Fang J, Zhu L (2020) Interfacially crosslinked β-cyclodextrin polymer composite porous membranes for fast removal of organic micropollutants from water by flow-through adsorption. J Hazard Mater 384:121187

90. Allabashi R, Arkas M, Hörmann G, Tsiourvas D (2007) Removal of some organic pollutants in water employing ceramic membranes impregnated with cross-linked silylated dendritic and cyclodextrin polymers. Water Res 41(2):476–486

91. Ghemati D, Aliouche D (2014) Dye adsorption behavior of polyvinyl alcohol/glutaraldehyde/β-cyclodextrin polymer membranes. J Appl Spectrosc 81(2):257–263

92. Meng N, Zhou NL, Zhang SQ, Shen J (2009) Synthesis and antifungal activities of polymer/montmorillonite-terbinafine hydrochloride nanocomposite films. Appl Clay Sci 46(2):136–140

93. Chen Y, Ma Y, Lu W, Guo Y, Zhu Y, Lu H, et al (2018) Environmentally friendly gelatin/β-cyclodextrin composite fiber adsorbents for the efficient removal of dyes from wastewater. Molecules 23(10)

94. Ozmen EY, Sezgin M, Yilmaz A, Yilmaz M (2008) Synthesis of β-cyclodextrin and starch based polymers for sorption of azo dyes from aqueous solutions. Bioresour Technol 99(3):526–531

95. Jiang HL, Lin JC, Hai W, Tan HW, Luo YW, Xie XL et al (2019) A novel crosslinked β-cyclodextrin-based polymer for removing methylene blue from water with high efficiency. Coll Surf A Physicochem Eng Asp 560:59–68

96. Pei R, Fan L, Zhao F, Xiao J, Yang Y, Lai A, et al (2020) 3D-Printed metal-organic frameworks within biocompatible polymers as excellent adsorbents for organic dyes removal. J Hazard Mater 384:121418

97. Shabaan OA, Jahin HS, Mohamed GG (2020) Removal of anionic and cationic dyes from wastewater by adsorption using multiwall carbon nanotubes. Arab J Chem 13(3):4797–4810

98. Bober P, Minisy IM, Acharya U, Pfleger J, Babayan V, Kazantseva N, et al (2020) Conducting polymer composite aerogel with magnetic properties for organic dye removal. Synth Met 260:116266

99. Abdi G, Alizadeh A, Zinadini S, Moradi G (2018) Removal of dye and heavy metal ion using a novel synthetic polyethersulfone nanofiltration membrane modified by magnetic graphene oxide/metformin hybrid. J Memb Sci 552:326–335

100. Song Y, Sun Y, Chen M, Huang P, Li T, Zhang X, et al (2020) Efficient removal and fouling-resistant of anionic dyes by nanofiltration membrane with phosphorylated chitosan modified graphene oxide nanosheets incorporated selective layer. J Water Process Eng 34:101086

101. Mittal H, Al Alili A, Morajkar PP, Alhassan SM (2021) Graphene oxide crosslinked hydrogel nanocomposites of xanthan gum for the adsorption of crystal violet dye. J Mol Liq 323:115034

102. Dafader NC, Rahman N, Alam MF (2014) Study on grafting of acrylic acid onto cotton using gamma radiation and its application as dye adsorbent. 2(1):37–40

103. Azady MAR, Alam MS, Paul SC, Rahaman MS, Sultana S, Hasnine SMM et al (2021) Preparation and Characterization Of Gamma Radiation Assisted Poly-Vinyl Alcohol/Acrylic Acid/Poly-4-Styrene Sulphonic Acid Based Hydrogel: Application For Textile Dye Removal. J Polym Environ 29(2):520–537

104. Abdullah MF, Azfaralariff A, Lazim AM (2018) Methylene blue removal by using pectin-based hydrogels extracted from dragon fruit peel waste using gamma and microwave radiation polymerization techniques. J Biomater Sci Polym Ed 29(14):1745–1763

105. Gupta VK, Tyagi I, Agarwal S, Sadegh H, Shahryari-ghoshekandi R, Yari M et al (2015) Experimental study of surfaces of hydrogel polymers HEMA, HEMA–EEMA–MA, and PVA as adsorbent for removal of azo dyes from liquid phase. J Mol Liq 206:129–136

106. Hernandez-Martínez AR, Lujan-Montelongo JA, Silva-Cuevas C, Mota-Morales JD, Cortez-Valadez M, Ruíz-Baltazar Á de J, et al (2018) Swelling and methylene blue adsorption of poly(N,N-dimethylacrylamide-co-2-hydroxyethyl methacrylate) hydrogel. React Funct Polym 122:75–84. https://doi.org/10.1016/j.reactfunctpolym.2017.11.008

Ceramic Nanocomposite Membranes for Dye Removal

Nhamo Chaukura, Alfred Riet, Dumiso Mithi, and Munyaradzi Manjoro

Abstract Due to their complex aromatic molecular structure, dyes persist in the aquatic environment and pose severe environmental and human health risks. To reduce the risks, it is important to treat dye-contaminated wastewater before it is discharged into waterways. A number of treatment methods have been used for dye removal from wastewater. Most of these processes produce large quantities of toxic sludge and are expensive. In this regard, membrane separation processes represent an alternative process for the treatment of dye-contaminated wastewater. Because of their low energy demand and low environmental footprint, membrane separation has been widely used in wastewater treatment. Membrane processes such as microfiltration, nanofiltration, reverse osmosis and ultrafiltration are efficient in wastewater treatment. Although polymeric membranes are more widely used, ceramic membranes can extend the scope of application to address challenges such as chemical and mechanical stabilities, fouling and lifespan. Specifically, ceramic membranes possess good chemical stability, exceptional mechanical properties, thermal stability and a long lifespan. The major disadvantage of membrane separation technologies is fouling, which results in variations in selectivity and a decrease in permeate flux. Consequently, the efficiency of the separation process declines. To mitigate membrane fouling, several mechanical and/or chemical cleaning strategies are frequently used. These cleaning procedures are, however, likely to damage the membrane structure, particularly in polymeric membranes. For this and other reasons, the interest on the application of inorganic and, specifically, ceramic membranes has increased. This chapter summarizes: (1) the synthesis and fabrication of ceramic membranes, (2) their structure and properties and (3) their subsequent application in dye removal.

Keywords Environmental pollution · Nanomaterials · Remediation · Wastewater

N. Chaukura (✉) · A. Riet · D. Mithi · M. Manjoro
Department of Physical and Earth Sciences, Sol Plaatje University, Kimberley, South Africa
e-mail: nhamo.chaukura@spu.ac.za

1   Introduction

Aquatic systems are polluted by a range of geogenic and anthropogenic chemical compounds that include toxic metals, a variety of organic compounds, pathogens and dyes. Dyes are particularly problematic due to their capacity to cause aesthetic pollution even at low concentrations. In addition, they reduce the penetration of sunlight into water, resulting in reduced photosynthetic activity by aquatic plants. This in turn reduces the oxygen concentration of water, and can result in stress and ultimately death of biota. The human health and environmental hazards associated with organic dyes in wastewater such as allergies, carcinogenic and mutagenic effects and phototoxicity have been widely studied [1]. One major source of dyes into aquatic systems is the textile industry. Textile dyeing processes pose an environmental risk due to the large volumes of water used and the subsequent discharge of dye- and chemical-laden effluent [2]. In addition, the composition of textile effluents varies widely owing to the changing characteristics of the textile products and the various processes involved, making its treatment challenging (Alventosa-deLara et al. 2014). Due to increasingly strict regulations on the pollutant concentrations in industrial wastewater, it is essential to remove the pollutants from wastewater before emitting it into the environment [3].

Several remediation strategies for dyes such as conventional water treatment, adsorption, biological treatment, and other methods such as advanced oxidation processes or electrocoagulation have been reported, but most are limited by high costs, poor decolourization efficiencies at large-scale operation and the generation of toxic sludge [2, 4]. Besides these disadvantages, the use of chemicals potentially generates carcinogens and toxicants. Moreover, conventional water treatment techniques cannot efficiently remove dyes, while advanced treatment technologies are complex. In view of this, there is a need for more cost-effective, efficient and effective water treatment methods that use simple and inexpensive technologies.

The discharge of dyes into waterways can be reduced through cleaner production strategies such as membrane separation, which can be used to recycle dye wastewater as a useful resource [4]. Membrane technologies, such as nanofiltration (NF), reverse osmosis (RO) and ultrafiltration (UF), have been successfully used to decolourize dye effluents, and are cost-effective while reducing water demand through water recovery [2]. Furthermore, because they possess high separation efficiency, membranes have been widely applied in food industry, gas separation, petrochemical industry, pharmaceutical industry and wastewater treatment [5]. However, most membranes lack the necessary durability or performance upon exposure to solutions of organic compounds. The development of membranes designed for use in such severe environments has been stimulated by interest from industry and research [6].

Membrane installation requires process stability, reduced pretreatment and minimal maintenance [3]. Compared to polymeric membranes, ceramic membranes can meet this demand owing to their superior chemical, mechanical and thermal properties, making them suitable for harsh operating environments. In this regard, interests in ceramic membranes for the treatment of dye effluents are rapidly growing

[1]. Ceramic membranes are mechanically, thermally and chemically robust, and can be applied in various configurations as stand-alone units, or integrated with other techniques to enhance removal. Moreover, these membranes produce a permeate of high quality, can use steam sterilization and back flushing, high abrasion resistance, high flux, bacterial resistance, can potentially be regenerated and stored under dry conditions following cleaning and has a smaller environmental footprint [3]. However, stand-alone membrane processes may not adequately remove organic pollutants. Further, the occurrence of membrane fouling reduces the flux and lifespan of the membrane, and strategies for its reduction deserve further research [1].

The major precursors for the fabrication of ceramic membranes are clay or related metal oxides and pore-forming sacrificial fugitive materials. A range of processes have been used to fabricate ceramic membranes and high-performance membranes, which provide for submicron filtration of polluted water in delicate aquatic systems. Other studies have reported the use of nanocomposite ceramic membranes, and photocatalytic ceramic membranes with varying dye removal efficiencies. This chapter summarizes: (1) the synthesis and fabrication of ceramic membranes and (2) their subsequent application in dye removal.

2 Membrane Technologies

Membrane processes are environmental friendly and efficient as the separation is primarily based on size exclusion, the phenomenon that makes membrane separation suited to treating a wide range of industrial effluents. Further, membrane separation is relatively cost-effective, mainly due to a low requirement of chemicals and a low energy demand Mouiya et al. [7]; [8]. Pressure-driven membrane separation processes such as microfiltration (MF), nanofiltration (NF), reverse osmosis (RO) and ultrafiltration (UF) are extensively applied in textile wastewater treatment [1, 9–11]. Owing to high separation efficiency, low operating cost and simplicity, UF membranes are widely used for removing dyes from wastewater [1, 3, 9]. Other notable membrane separation processes include electrodialysis, membrane bioreactor and vacuum membrane distillation [8].

Despite polymeric membranes being more common, ceramic membranes have also been used [11]. Ceramic membranes have advantages of high chemical, mechanical and thermal stabilities, well-defined porosity and a high flux [12–14]. Such properties make them particularly suitable for the treatment of dye-contaminated wastewater, which is usually alkaline and is at a high temperature [12]. Ceramic membranes are usually used in MF and UF processes, and occasionally in RO and NF configurations [11].

The major disadvantage of membrane separation technologies is fouling, which results in variations in selectivity and a decrease in permeate flux. Consequently, the efficiency of the separation process declines [2, 15]. To mitigate membrane fouling, several strategies of aggressive mechanical and/or chemical cleaning are usually

used. These cleaning procedures are, however, likely to damage the membrane structure, particularly in polymeric membranes. For this and other reasons, the interest on the application of inorganic and, specifically, ceramic membranes has increased [16]. Membrane fouling can be reduced to enhance performance through membrane modification, pretreatment and cleaning. The emerging nanotechnology has opened new avenues for functionalization of UF membranes with nanomaterials to produce membranes with antifouling properties, improved permeate flux, and synergistic pollutant degradation and self-cleaning [15].

3 Ceramic Membranes

3.1 Structure and Properties of Ceramic Membranes

Typically, the microstructure of ceramic membranes is multi-layered, and the layers are IUPAC categorized as microporous (<2 nm), mesoporous (2–50 nm) and macroporous (>50 nm) according to the pore sizes [6, 7]. In general, a macroporous substrate layer provides structural strength to a denser and thinner, selective, meso- or microporous layer [11]. The active layer is crucial in the separation process, and the support provides mechanical strength to the membrane. Occasionally, intermediate layers are incorporated to modify the porous structure, and mechanical strength [11]. In addition to the chemical nature, the topology and fabrication process of the membrane determine the durability and resistance to severe conditions like alkaline and acidic environments [17].

Ceramic membranes provide resistance to chemical attack, antioxidation and thermal stability. Moreover, metal and metal oxide catalysts can be attached onto a ceramic membrane through calcination, providing conductivity because of metal and metal oxides anchored on the surface of the membrane [4]. As dye is removed from wastewater, dye molecules adsorbed on the surface of the membrane are degraded by catalysts. This decreases membrane fouling and enhances performance. For example, because of its chemical structure and stability, SnO_2 can function as a catalyst in wastewater treatment [4].

3.2 Fabrication of Ceramic Membranes

Feedstock materials used in preparing membranes determine membrane properties and performance [11]. The choice of the feedstock ceramic materials is guided by properties such as chemical, mechanical and thermal stabilities, hydrophobicity and microstructure. Moreover, the cost-effectiveness should be taken into consideration. The frequently used ceramic materials for membrane fabrication include alumina, silica, titania, zeolites and zirconia [11].

Commercial ceramic membranes are fabricated from metal oxides such as silica, alumina, titania or a combination of these [18]. These materials are expensive and require higher firing temperatures. To address the challenge of high cost, two main strategies have been proposed: (1) use of low-cost feedstock and (2) reducing energy consumption during the firing process [9, 19, 20]; Mouiya et al. [7]. Ceramic membranes derived from cheap natural materials together with other materials generally considered as waste have been widely studied. These materials have the benefit of low cost relative to commonly used materials. Natural clays are widely available, require lower sintering temperatures and are more durable relative to metal oxides Buoazizi et al. [21]; [17]; Mouiya et al. [7]. Recently, there has been a growing interest in fabricating ceramic MF membranes from cheaper natural feedstock such as geomaterials. In this regard, locally available clays have been widely used to fabricate ceramic membranes with both flat and tubular geometries [5]. For instance, bentonite clay was used to fabricate an UF membrane from colloidal solution via spin coating [8]. Another study used kaolin clay and aluminium through extrusion, sintering and slip coating [17]. Relative to flat-sheet membranes, tubular membranes have a higher surface-to-volume ratio, and have therefore attracted interest [11]. Both configurations could be applied in dye removal from wastewater.

Ceramic membranes can be fabricated through compaction, extrusion, spin coating, hydrothermal methods and sol–gel techniques. Of these, compaction, however, is the commonly used method, and depends on the integration of a pore-forming sacrificial phase (porogen) [19]. These ceramic supports afford adequate strength and high porosity, thus permitting high fluxes of effluent to filter through [7]. The fabrication of more selective membranes such as UF and NF membranes using natural clays is still limited by the presence of concomitants like amorphous silicate, calcite, dolomite, organic matter and quartz [18]. Although the existence of carbonate and organic matter in the feedstock enhances membrane porosity and permeability, excessive amounts generate large pores and defects, particularly in the fabrication of thin membrane layers that are more sensitive to high temperatures. Further, amorphous silicates suffer from vitrification at low temperatures before membrane sintering, resulting in pore closure and a reduction in porosity [22]. Consequently, the membrane permeability declines remarkably. To avoid this, it is essential to purify natural clay prior to membrane fabrication. This can potentially result in the improvement of pore size and selectivity of the resulting membrane.

Usually the substrates for the ceramic membranes are prepared from silicon carbides or aluminium oxides [3]. These materials possess high mechanical and thermal stabilities. The substrates can be made for a single channel or multi-channels, and a few microns thickness of the membrane layer is deposited on the inner side of the channel [3]. Membrane layers are commonly formed through dip coating, slip casting, spin coating and spray coating [11, 23, 7]. Normally, mono- or multi-layers are coated onto ceramic substrates to provide asymmetric structures comprising of a pore size gradient. Nevertheless, it is desirable to fabricate asymmetric membranes, where the same material is used to prepare the homogeneous membrane thin layer and the substrate [7]. The fabrication process influences the cost of the ceramic membrane. For instance, the wet pathway uses chemical additives such as binders and

plasticizers to achieve an extrudable paste, and requires extra energy for drying [11]. However, dry pressing is an appropriate technique that reduces the membrane cost. Moreover, dry pressing is a rapid and simple process, which produces membranes with no defects. Of note, it is possible to fabricate self-supported MF membranes via a single sintering step contrary to techniques such as dip coating and slip coating that require double sintering stages for the substrate and the active layers, respectively [7].

With the emergence of novel techniques, ceramic membranes with tailored properties can be produced. For example, the 3D printing technique was used to fabricate UF ceramic membranes [23]. The major benefit of 3D printing is that it provides more control over the designs.

3.3 Hybrid Ceramic Membranes

A number of strategies have been used to prepare ceramic membranes composed of different materials. For instance, composite membranes have been fabricated using a ceramic substrate and organic layer [9]. The advantages of this approach include high mechanical strength and chemical resistance. Owing to the large number of oxygen-carrying functional groups such as OH, carbonyl and carboxyl groups on graphene oxide, it has been used to modify polymeric membranes [15]. Such membranes have enhanced antifouling properties, permeate flux and selectivity. In contrast, graphene oxide-modified ceramic membranes have been less investigated and are gradually gaining attention [6]. Thus, efforts to integrate the benefits of ceramic materials with the tunability of organic polymers have resulted in the development of a new class of membranes. Modification of a ceramic support with an organic compound can considerably improve the properties of ceramic membranes.

The development of nanomaterials has opened opportunities for synthesis and modification of a wide range of materials with improved performance. Specifically, nanomaterials offer a plethora of desirable properties to be incorporated into ceramic membranes for the selective removal of dyes from wastewater [24, 25]. Such nanomaterials include $BiFeO_3$, BiOBr, Bi_3O_4Br, Fe_2O_3, Fe-$ZnIn_2S_4$, TiO_2 and ZnO, which are integrated into the membrane active layer to enhance fouling resistance, permeability, permeate quality and roughness [25]. Another new technology is charged ceramic membrane separation [26]. Separation by these membranes is based on physical screening and electrical interaction. The introduction of charged moieties results in improved membrane hydrophilicity, reduces solution osmotic pressure and increases flux. This consequently reduces the operation costs. A summary of membrane fabrication methods is provided in Table 1.

Table 1 Synthesis and fabrication of ceramic membranes

Membrane	Precursors	Processing	References
Polysulfone (PSf)/ polyetherimide (PEI) UF membrane	Granular PSf and PEI polymers	PSf/PEI layer deposited on pozzolan support via spin/spray coating	[9]
Inside ceram UF ceramic membrane	Tubular ZrO_2/TiO_2 layer	Membranes modified through transmembrane pressure and cross-flow velocity	[2]
Bentonite UF membrane	Bentonite clay	Spin coating from colloidal solutions	[8]
TiO_2-anodized aluminium oxide (TiO_2-AAO)	TiO_2 and aluminium oxide	Membrane prepared via atomic layer deposition	[10]
TiO_2 composite UF membrane	Np-TiO_2 Natural bentonite micronized phosphate	Spin coating	[27]
Positively charged SiO_2 membrane	SiO_2 $YCl_3.6H_2O$ urea	Dip coating and thermal decomposition	[26]
UF membrane derived from Moroccan clay	Clay A (smooth) Clay B (rough)	Spin coating	[18]
Clay–alumina UF membrane	Powder Kaolin clay, Aluminium	Extrusion, sintering and slip coating	[17]
Bismuth–stibium–tin dioxide ceramic membrane	Bismuth–stibium Tin dioxide	Dip coating	[4]
Metal-oxide-coated ceramic UF membrane	MnO_2 Fe_2O_3 Co_3O_4 CuO Mn_3O_4	Dip coating method, silane modification, calcination	[28]
Nanosilica ceramic membrane	Rice husk, HNO_3	Dry pressing a mixture of nanosilica obtained from rice husk by hydrothermal technique at sub-critical water conditions	[24]
Polyacrylonitrile (PAN)-ethanolamine (ETA) UF membrane	PAN-DMSO ETA	Solution casting	[29]

Table 1 (continued)

Membrane	Precursors	Processing	References
Polyamide-based NF membrane	4.4'-diaminodiphenylmethane 1,3,5-Benzenetricarbonyl trichloride	Membrane prepared by interfacial polymerization	[30]
Polyvinylidene fluoride (PVDF)/Polytetrafluoride ethylene (PTFE) nanocomposite membrane	Powdered PVDF PTFE	Thermally induced solvent evaporation process	[31]

4 Membrane Processes

Integrating membrane filtration with ozonation holds great promise for wastewater treatment. Ozone is a powerful oxidizing agent, and can reduce membrane fouling [32]. Due to their high thermal, chemical and mechanical stabilities, ceramic membranes can resist degradation by ozonation and have longer lifespans than polymeric membranes.

Ceramic membranes can be integrated into membrane bioreactors. A study used a flat ceramic membrane element in an anaerobic flat-sheet ceramic membrane bioreactor for treating dye effluent [33]. Other membrane separation processes have used MF, UF, RO or NF, which are able to recover, concentrate or purify dye compounds for reuse [16, 26]. Owing to its effective salt transmission and high flux, UF processes are attractive in dye separation and reuse [34, 35]. However, the UF process is limited by flux decrease due to fouling and concentration polarization [15]. Using strong acids and hydrodynamic and physical cleaning methods can be useful in reducing flux decline [13, 35]. NF processes are effective in the separation and purification of mixtures of dye and NaCl. The large NF membrane pores allow the movement of the monovalent NaCl, which considerably reduces the feed and permeate osmotic pressure gradient, and thus enhances the flux. Moreover, NF membranes usually possess high rejection for dyes through the synergistic effect of molecular sieving and electrostatic interactions, which separate the dye and NaCl mixtures [34]. The NF set-up is thus frequently used for dye desalting and purification. Yet, the major disadvantages of this technique are high cost and low flow rate [26].

5 Application of Ceramic Membranes in Dye Removal

Owing to their desirable properties, ceramic membranes have been used for the remediation of dye-contaminated wastewater. One study used a membrane fabricated through the atomic layer deposition of TiO_2 on anodized Al_2O_3 membranes and achieved up to 80% methylene blue removal [10]. The mechanism of removal was primarily photocatalytic degradation. Another study used an MF flat-tubular

membrane made from alumina, and Congo Red dye removals were 10% at pH 6, and more than 90% at pH 4.5 [1]. Similarly, over 99% removal of Eriochrome black T dye was achieved using a porous multi-channel tubular membrane with TiO_2 and α-Al_2O_3 as active layer and substrate, respectively [13]. Yet a separate study applied a ceramic membrane coated with electropositive nano-Y_2O_3 to remove up to 99.6% Titan Yellow [26]. An asymmetric tubular UF ceramic membrane composed of a TiO_2 support layer with a ZrO_2-TiO_2 active layer removed 93% Reactive Black 5 [36]. In these separation processes, the primary mechanism is based on size exclusion, while electrostatic interactions and degradation occur more predominantly in membranes that are modified with specific functional groups and catalysts, respectively Mouiya et al. [7]; [8]. Table 2 provides a summary of dye removals by selected ceramic membranes. Although most of these studies were performed at laboratory scale, ceramic membranes of different structure and configuration have demonstrated good performance in dye removal from wastewater.

6 Conclusion and Future Outlook

Majority of the dyes used in textile processes are recalcitrant to degradation by ultraviolet light, and are non-biodegradable. Moreover, they are also stable to aerobic digestion, making dyes persistent in the aquatic environment. To ameliorate the environmental risk associated with dye pollution, dye effluents should be treated before discharge into waterways. A number of techniques have been reported for dye separation from wastewater, but membrane filtration has proved the most efficient.

Generally, polymeric membranes have superior retention and permeability for polar organic compounds. However, non-polar molecules are challenging, likely to either chemically degrade the membrane or physically alter the membrane geometry. These challenges can be circumvented by using ceramic membranes [6, 11]. Ceramic membranes represent a clean technology capable of withstanding harsh operating conditions. Owing to the existence of OH group, most ceramic membranes exhibit high hydrophilicity [19]. Consequently, the modification of hydrophilic into superhydrophobic ceramic membranes has attracted interests for a range of applications. Superhydrophobic membranes themselves have antibacterial, antifouling and self-cleaning properties.

The need to combine the best properties of each material has led to the development of hybrid materials. These hybrid materials can minimize the challenges affecting polymeric membranes. However, mixed matrix membranes are plagued by instability of dispersed inorganic particles, reduced selectivity caused by large pores, reduced permeability at high pressure and compromised thermal stability [6].

In summary, this chapter has demonstrated that ceramic membranes: (1) are useful in dye separation processes that require high mechanical strength, chemical resistance and high temperature conditions; (2) can be fabricated through a variety of methods, and the use of natural clays and biomass as a porogen significantly reduces the cost of the membrane; (3) membrane fouling can be reduced by incorporating nanomaterials

Table 2 Summary of dye removals by various ceramic membranes

Dye	Ceramic membrane	%Removal	References
Methylene blue	Atomic layer deposited TiO_2 on anodized Al_2O_3 membranes	≤80%	[10]
Coloured effluent from printing baths	UF and NF membranes	83.5%	[14]
Congo Red	Alumina-derived MF flat-tubular membrane	10% at pH 6, ≥90% at pH 4.5	[1]
Phthalates	Ceramic UF membrane derived from CuO/TiO_2 ultrafine particles	>99%	[37]
Eriochrome black T	Porous multi-channel tubular membrane with TiO_2 and α-Al_2O_3 as active layer and substrate, respectively	>99%	[13]
Titan yellow	Porous ceramic membrane coated with electropositive nano-Y_2O_3	≤99.6%	[26]
Red 80	Ceramic UF membranes from natural Moroccan clay	97–99%	[18]
Alizarin red	Asymmetric UF ceramic membrane with single disconnected TiO_2 nanoparticles layer	99%	[17]
Rhodamine B	Ceramic perlite aid coated with UF bentonite membrane	≤80.1%	[8]
Direct orange S	Bismuth/stibium–tin dioxide membrane anchored on a ceramic support	≤99%	[4]
Methyl orange	Ceramic tubular UF membrane with a polyamide selective barrier	42.8%	[38]
Alcian Blue 8GX	Metal-oxide-coated ceramic membrane	increased by 10.2–47.6%	[28]
Reactive Black 5	Asymmetric tubular UF ceramic membrane with TiO_2 support layer and ZrO_2-TiO_2 active layer	93%	[36]

that have antifouling and self-cleaning properties; (4) can be used in a range of configurations, although UF ceramic membranes are commonly used and (5) have high dye removal performance.

Future research should focus on: (1) the use of 3D printing technique for fabricating ceramic membranes as this technique provides more control over various designs; (2) increasing membrane performance and reduce fouling and (3) studies on the fabrication and application of charged ceramic membranes in dye removal from wastewater.

Overall, as ceramic membranes are largely more expensive compared to polymeric membranes, their use should mainly focus on applications that require higher thermal or chemical resistance.[5, 25]

References

1. Ahmad R, Guo J, Kim J (2019) Structural characteristics of hazardous organic dyes and relationship between membrane fouling and organic removal efficiency in fluidized ceramic membrane reactor. J Clean Prod 232:608–616
2. Alventosa-deLara E, Barredo-Damas S, Alcaina-Miranda MI, Iborra-Clar MI (2012) Ultrafiltration technology with a ceramic membrane for reactive dye removal: optimization of membrane performance. J Hazard Mater 209–210:492–500
3. Majewska-Nowak KM (2010) Application of ceramic membranes for the separation of dye particles. Desalination 254:185–191
4. Wang Z-B, Ni D, Shang Y-L, Guan Y-J (2019) Recycling of dye from wastewater using a ceramic membrane modified with bismuth/stibium co-doped tin dioxide. J Clean Prod 213:192–198
5. Manni A, Achiou B, Karim A, Harrati A, Sadik C, Ouammou M, Younssi SA, El Bouari A (2020) New low-cost ceramic microfiltration membrane made from natural magnesite for industrial wastewater treatment. J Environ Chem Eng 8:103906
6. Merlet RB, Pizzoccaro-Zilamy M-A, Nijmeijer A, Winnubst L (2020) Hybrid ceramic membranes for organic solvent nanofiltration: State-of-the-art and challenges. J Memb Sci 599:117839
7. Mouiya M, Bouazizi A, Abourrich A, Benhammou A, El Hafiane Y, Ouammou M, Abouliatim Y, Younssi SA, Smithe A, Hannache H (2019) Fabrication and characterization of a ceramic membrane from clay and banana peel powder: application to industrial wastewater treatment. Mater Chem Phys 227:291–301
8. Saja S, Bouazizi A, Achiou B, Ouaddari H, Karim A, Ouammou M, Aaddane A, Bennazh J, Younssi SA (2020) Fabrication of low-cost ceramic ultrafiltration membrane made from bentonite clay and its application for soluble dyes removal. J Eur Ceram Soc 40:2453–2462
9. Benkhaya S, Achiou B, Ouammou M, Bennazh J, Younssi SA, M'rabet S, El Harfi A (2019) Preparation of low-cost composite membrane made of polysulfone/polyetherimide ultrafiltration layer and ceramic pozzolan support for dyes removal Mater Today Commun 19:212–219
10. Berger TE, Regmi C, Sch€afer AI, Richards BS (2020) Photocatalytic degradation of organic dye via atomic layer deposited TiO_2 on ceramic membranes in single-pass flow-through operation. J Memb Sci 604:118015
11. He Z, Lyu Z, Gu Q, Zhang L, Wang J (2019) Ceramic-based membranes for water and wastewater treatment. Coll Surf A 578:123513

12. Alventosa-deLara E, Barredo-Damas S, Zuriaga-Agustí E, Alcaina-Miranda MI, Iborra-Clar MI (2014) Ultrafiltration ceramic membrane performance during the treatment of model solutions containing dye and salt. Sep Purif Methods 129:96–105

13. Chen P, Ma X, Zhong Z, Zhang F, Xing W, Fan Y (2017) Performance of ceramic nanofiltration membrane for desalination of dye solutions containing NaCl and Na_2SO_4. Desalination 404:102–111

14. Agtas M̧ Yılmaz O, Dilaver M, Alp K, Koyuncu I (2020) Hot water recovery and reuse in textile sector with pilot scale ceramic ultrafiltration/nanofiltration membrane system. J Clean Prod 256:120359

15. Li C, Sun W, Lu Z, Ao X, Yang C, Li S (2019) Systematic evaluation of TiO_2-GO-modified ceramic membranes for water treatment: retention properties and fouling mechanisms. Chem Eng J 378:122138

16. Palacio L, Bouzerdi Y, Ouammou M, Albizane A, Bennazh J, Hernández A, Calvo JI (2009) Ceramic membranes from Moroccan natural clay and phosphate for industrial water treatment. Desalination 245:501–507

17. Oun A, Tahri N, Mahouche-Chergui S, Carbonnier B, Majumdar S, Sarkar S, Sahoo GC, Amar RB (2017) Tubular ultrafiltration ceramic membrane based on titania nanoparticles immobilized on macroporous clay-alumina support: elaboration, characterization and application to dye removal. Sep Purif Technol 188:126–133

18. Ouaddari H, Karim A, Achiou B, Saja S, Aaddane A, Bennazh J, El Hassani IEA, Ouammou M, Albizane A (2019) New low-cost ultrafiltration membrane made from purified natural clays for direct Red 80 dye removal. J Environ Chem Eng 7:103268

19. Hubadillah SK, Othman MHD, Jamalludin MR, Naim R, Kadir SHSA, Puteh MH, Pauzan MAB, Sobri FAM (2020) Fabrication and characterisation of superhydrophobic bio-ceramic hollow fibre membranes prepared from cow bone waste. Ceram Int. https://doi.org/10.1016/j.ceramint.2020.09.295

20. Mouratib R, Achiou B, El Krati M, Younssi SA, Tahiri S (2020) Low-cost ceramic membrane made from alumina- and silica-rich water treatment sludge and its application to wastewater filtration. J Eur Ceram Soc 40:5942–5950

21. Bouazizi A, Breida M, Karim A, Achiou B, Ouammou M, Calvo JI, Aaddane A, Khiata K, Younssi AA (2017) Development of a new TiO2 ultrafiltration membrane on flat ceramic support made from natural bentonite and micronized phosphate and applied for dye removal. Ceram Int 43:1479–1487

22. Chaukura N, Chiworeso R, Gwenzi W, Motsa MM, Munzeiwa W, Moyo W, Chikurunhe I, Nkambule TTI (2020) A new generation low-cost biochar-clay composite 'biscuit' ceramic filter for point-of-use water treatment. Appl Clay Sci 185C:105409

23. Ray SS, Dommati H, Wang J-C, Chen S-S (2020) Solvent based slurry stereolithography 3D printed hydrophilic ceramic membrane for ultrafiltration application. Ceram Int 46:12480–12488

24. Tolba GMK, Bastaweesy AM, Ashour EA, Abdelmoez W, Khalil KA, Barakat NAM (2016) Effective and highly recyclable ceramic membrane based on amorphous nanosilica for dye removal from the aqueous solutions. Arab J Chem 9:287–296

25. Sheikh M, Pazirofteh M, Dehghani M, Asghari M, Rezakazemi M, Valderrama C, Cortin J-L (2020) Application of ZnO nanostructures in ceramic and polymeric membranes for water and wastewater technologies: a review. Chem Eng J 391:123475

26. Cheng X, Li N, Zhu M, Zhang L, Deng Y, Deng C (2016) Positively charged microporous ceramic membrane for the removal of Titan Yellow through electrostatic adsorption. J Environ 44:204–212

27. Bouazizi A, Breida M, Karim A, Achiou B, Ouammou M, Calvo JI, Aaddane A, Khiat K, Younssi SA (2017) Development of a new TiO_2 ultrafiltration membrane on flat ceramic support made from natural bentonite and micronized phosphate and applied for dye removal. Ceram Int 43:1479–1487

28. Zhao Q, Lu D, Jiang H, Zhao Y, Sun Y, Li Z, Yang M, Wang P, Ma J (2019) Peroxymonosulfate-based cleaning technology for metal oxide-coated ceramic ultrafiltration membrane polluted

by Alcian Blue 8GX dye: radical and non-radical oxidation cleaning mechanism. J Membr Sci 573:210–217

29. Yun J, Wang Y, Liu Z, Li Y, Yang H, Xu Z-L (2020) High efficient dye removal with hydrolyzed ethanolamine-polyacrylonitrile UF membrane: rejection of anionic dye and selective adsorption of cationic dye. Chemosphere 259:127390

30. Yang C, Xu W, Nan Y, Wang Y, Chen X (2020) Novel negatively charged nanofiltration membrane based on 4,4′-diaminodiphenylmethane for dye removal. Sep Purif Technol 248:117089

31. Khumalo NP, Nthunya LN, De Canck E, Derese S, Verliefde AR, Kuvarega AT, Mamba BB, Mhlanga SD, Dlamini DS (2019) Congo red dye removal by direct membrane distillation using PVDF/PTFE membrane. Sep Purif Technol 211:578–586

32. Song Z, Li Y, Wang Z, Wang M, Wang Z, Zhang Y, Sun J, Liu C, Liu Y, Xu B, Qi F (2020) Effect of the coupling modes on EfOM degradation and fouling mitigation in ozonation-ceramic membrane filtration. Chem Eng J 394:124935

33. Zhang W, Liu F, Wang D, Jin Y (2018) Impact of reactor configuration on treatment performance and microbial diversity in treating high-strength dyeing wastewater: anaerobic flat-sheet ceramic membrane bioreactor versus upflow anaerobic sludge blanket reactor. Biores Technol 269:269–275

34. Jiang M, Ye K, Lin J, Zhang X, Ye W, Zhao S, Van der Bruggen B (2018) Effective dye purification using tight ceramic ultrafiltration membrane. J Membr Sci 566:151–160

35. Kim H-G, Park C, Yang J, Lee B, Kim S-S, Kim S (2007) Optimization of backflushing conditions for ceramic ultrafiltration membrane of disperse dye solutions. Desalination 202:150–155

36. Zuriaga-Agustı E, Alventosa-deLar E, Barredo-Damas S, Alcaina-Miranda MI, Iborra-Clar MI, Mendoza-Roca JA (2014) Performance of ceramic ultrafiltration membranes and fouling behavior of a dye-polysaccharide binary system. Water Res 54:199–210

37. Bhattacharya P, Mukherjee D, Deb N, Swarnakar S, Banerjee S (2021) Indigenously developed CuO/TiO_2 coated ceramic ultrafiltration membrane for removal of emerging contaminants like phthalates and parabens: toxicity evaluation in PA-1 cell line. Mater Chem Phys 258:123920

38. Xia L, Ren J, Wey M, McCutcheon JR (2018) Ceramic-supported thin film composite membrane for organic solvent nanofiltration. J Membr Sci 563:857–863